frontiers | Research Topics

Women in pediatric oncology: 2021

Edited by
Sarah K. Tasian, Yong-mi Kim and Paraskevi Panagopoulou

Published in
Frontiers in Oncology

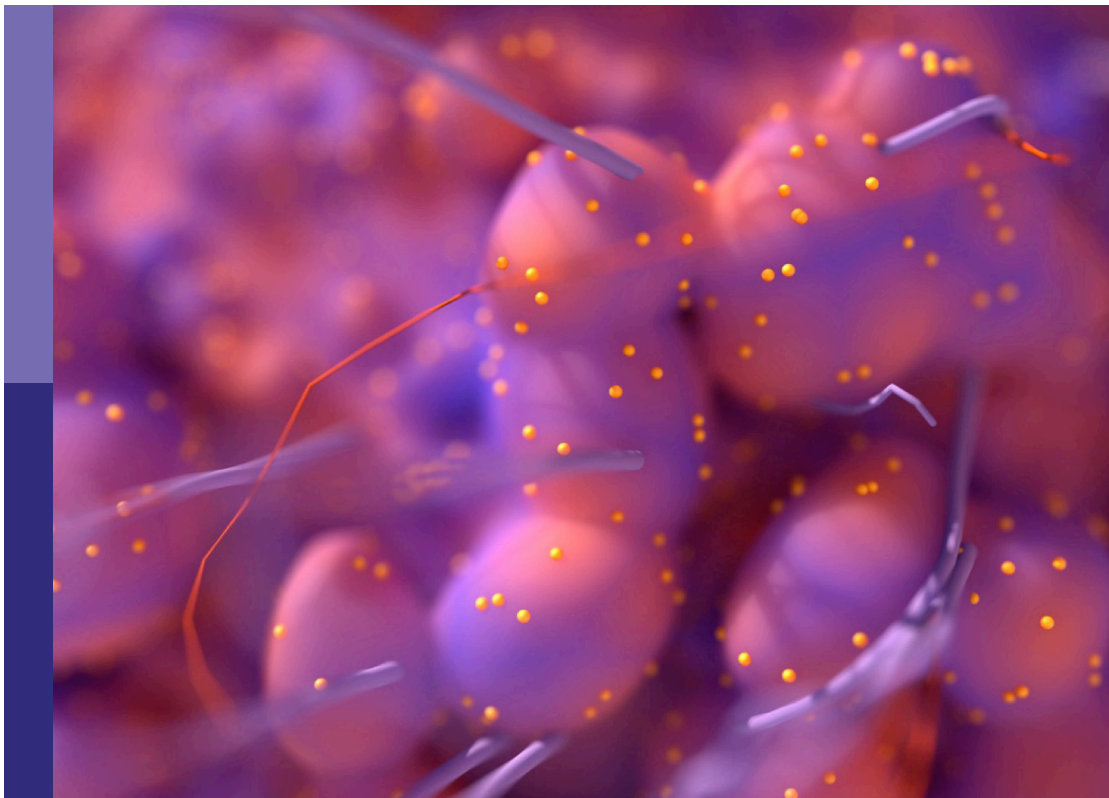

ISSN 1664-8714
ISBN 978-2-83251-087-2
DOI 10.3389/978-2-83251-087-2

About Frontiers

Frontiers is more than just an open access publisher of scholarly articles: it is a pioneering approach to the world of academia, radically improving the way scholarly research is managed. The grand vision of Frontiers is a world where all people have an equal opportunity to seek, share and generate knowledge. Frontiers provides immediate and permanent online open access to all its publications, but this alone is not enough to realize our grand goals.

Frontiers journal series

The Frontiers journal series is a multi-tier and interdisciplinary set of open-access, online journals, promising a paradigm shift from the current review, selection and dissemination processes in academic publishing. All Frontiers journals are driven by researchers for researchers; therefore, they constitute a service to the scholarly community. At the same time, the *Frontiers journal series* operates on a revolutionary invention, the tiered publishing system, initially addressing specific communities of scholars, and gradually climbing up to broader public understanding, thus serving the interests of the lay society, too.

Dedication to quality

Each Frontiers article is a landmark of the highest quality, thanks to genuinely collaborative interactions between authors and review editors, who include some of the world's best academicians. Research must be certified by peers before entering a stream of knowledge that may eventually reach the public - and shape society; therefore, Frontiers only applies the most rigorous and unbiased reviews. Frontiers revolutionizes research publishing by freely delivering the most outstanding research, evaluated with no bias from both the academic and social point of view. By applying the most advanced information technologies, Frontiers is catapulting scholarly publishing into a new generation.

What are Frontiers Research Topics?

Frontiers Research Topics are very popular trademarks of the *Frontiers journals series*: they are collections of at least ten articles, all centered on a particular subject. With their unique mix of varied contributions from Original Research to Review Articles, Frontiers Research Topics unify the most influential researchers, the latest key findings and historical advances in a hot research area.

Find out more on how to host your own Frontiers Research Topic or contribute to one as an author by contacting the Frontiers editorial office: frontiersin.org/about/contact

Women in pediatric oncology: 2021

Topic editors

Sarah K. Tasian — Children's Hospital of Philadelphia, United States

Yong-mi Kim — Children's Hospital of Los Angeles, United States

Paraskevi Panagopoulou — Aristotle University of Thessaloniki, Greece

Citation

Tasian, S. K., Kim, Y.-m., Panagopoulou, P., eds. (2023). *Women in pediatric oncology: 2021*. Lausanne: Frontiers Media SA. doi: 10.3389/978-2-83251-087-2

Table of contents

frontiers in Oncology

REVIEW
published: 01 April 2021
doi: 10.3389/fonc.2021.662209

Radiosensitization in Pediatric High-Grade Glioma: Targets, Resistance and Developments

Dennis S. Metselaar[1,2†], Aimée du Chatinier[1†], Iris Stuiver[2], Gertjan J. L. Kaspers[1,2] and Esther Hulleman[1]*

[1] Department of Neuro-oncology, Princess Máxima Center for Pediatric Oncology, Utrecht, Netherlands, [2] Emma Children's Hospital, Amsterdam UMC, Vrije Universiteit Amsterdam, Pediatric Oncology, Cancer Center Amsterdam, Amsterdam, Netherlands

Pediatric high-grade gliomas (pHGG) are the leading cause of cancer-related death in children. These epigenetically dysregulated tumors often harbor mutations in genes encoding *histone 3*, which contributes to a stem cell-like, therapy-resistant phenotype. Furthermore, pHGG are characterized by a diffuse growth pattern, which, together with their delicate location, makes complete surgical resection often impossible. Radiation therapy (RT) is part of the standard therapy against pHGG and generally the only modality, apart from surgery, to provide symptom relief and a delay in tumor progression. However, as a single treatment modality, RT still offers no chance for a cure. As with most therapeutic approaches, irradiated cancer cells often acquire resistance mechanisms that permit survival or stimulate regrowth after treatment, thereby limiting the efficacy of RT. Various preclinical studies have investigated radiosensitizers in pHGG models, without leading to an improved clinical outcome for these patients. However, our recently improved molecular understanding of pHGG generates new opportunities to (re-) evaluate radiosensitizers in these malignancies. Furthermore, the use of radio-enhancing agents has several benefits in pHGG compared to other cancers, which will be discussed here. This review provides an overview and a critical evaluation of the radiosensitization strategies that have been studied to date in pHGG, thereby providing a framework for improving radiosensitivity of these rapidly fatal brain tumors.

Keywords: pediatric high-grade glioma (pHGG), radiotherapy, glioma, radio-enhancement, radiosensitizer, radioresistance

OPEN ACCESS

Edited by:
Yong-mi Kim,
Children's Hospital of Los Angeles, United States

Reviewed by:
Joshua John Breunig,
Cedars Sinai Medical Center, United States
Rintaro Hashizume,
Northwestern University, United States

****Correspondence:***
Esther Hulleman
e.hulleman@prinsesmaximacentrum.nl

[†]These authors have contributed equally to this work

Specialty section:
This article was submitted to Pediatric Oncology, a section of the journal Frontiers in Oncology

Received: *31 January 2021*
Accepted: *17 March 2021*
Published: *01 April 2021*

Citation:
Metselaar DS, du Chatinier A, Stuiver I, Kaspers GJL and Hulleman E (2021) Radiosensitization in Pediatric High-Grade Glioma: Targets, Resistance and Developments. Front. Oncol. 11:662209. doi: 10.3389/fonc.2021.662209

INTRODUCTION

Cancer is one of the leading causes of death among children in developed countries. Among pediatric cancers, central nervous system (CNS) tumors represent the second-most common and the most lethal group, accounting for around 40 percent of cancer-related deaths (1). While the prognosis of children with almost all types of cancer has improved over the past decades, this improvement is minimal in children with CNS tumors (2). This dismal prognosis is mainly caused by pediatric high-grade gliomas (pHGG); aggressive tumors that often originate from glial progenitor cells in the CNS (3–5). pHGG comprise all pediatric glioma lesions that are classified as 'grade III' or 'grade IV' by the World Health Organization (WHO) (6). A subset of pHGG,

referred to as diffuse midline glioma (DMG) (formerly known as diffuse intrinsic pontine glioma or DIPG), arise in the midline of the brain and carry a particularly grim prognosis (5, 7). Children with DMG have a median survival of 11 months, with less than 1 percent surviving past 5 years after diagnosis (8, 9). Glioblastoma (formerly known as glioblastoma multiforme) are the most common subset of pHGG and have a reported 5-year survival rate of less than 20 percent (10).

In recent years, distinct pHGG entities have been identified based on recurrent mutations affecting the epigenome. One entity is characterized by a missense lysine-to-methionine substitution at amino acid 27 of the tail of histone H3.1 or H3.3 (H3-K27M) (11). Another pHGG subgroup is characterized by glycine-to-arginine/valine substitutions at amino acid 34 in histone H3.3 (H3-G34R/V) and has recently been described as the first identified pHGG with a neuronal rather than glial precursor cell of origin (11–14). These epigenetically mutated entities have a distinct neuroanatomical predilection. K27M mutations occur exclusively in the midline of the brain, while G34R/V mutations occur exclusively in the cerebral cortex (11). Notably, these mutations represent a hallmark characteristic for pediatric versus adult HGG (aHGG), defining ~50 percent of pediatric cases compared to less than 1 percent of adults, emphasizing the necessity to research them independently (15).

pHGG are characterized by a diffuse and infiltrative growth pattern, often in delicate and difficult to reach parts of the brain, which makes complete surgical removal often not an option (3, 16). Gross total resection of diffuse tumors in the midline of the brain is particularly not possible as these tumors are intricately woven into areas of normal neural tissue that control vital functions, such as heart rate and breathing. The standard of care for most midline tumors, except for infants, is fractionated radiation therapy (RT) (7). Although this treatment modality provides temporary symptom relief, a minor delay in tumor progression, and a three-month survival benefit on average, it offers no chance for a cure (3, 16, 17). For diffuse tumors in the cerebral cortex, partial surgical resection is often performed, followed by RT and chemotherapy (4, 16). In addition to the surgical difficulties, pHGG often gain resistance to the applied chemotherapy or the therapy does not reach the tumor at all due to inadequate penetration of the blood-brain barrier (BBB) (18). As a result, pHGG are still among the most lethal tumors in children and improved therapeutic options are desperately needed.

Ionizing radiation essentially impairs tumor growth by evoking DNA damage, either directly or through reactive oxygen species (ROS). In response to DNA damage, cell cycle checkpoint kinases are alerted to initiate DNA damage response (DDR) in which cell cycle progression is halted and the DNA-repair machinery is activated (19). The ability of DDR proteins to sense DNA damage and activate repair pathways play an essential role in regulating radiation sensitivity, because the amount of DNA damage is a critical factor for the therapeutic efficacy of RT (20). As a resistance mechanism, irradiated cancer cells often increase their DNA-repair efficiency by enhancing the expression of DDR components (21). In addition, as with tissue injury at large, RT-induced cytotoxicity typically activates mitogenic signaling pathways, resulting in an enhanced proliferation rate and repopulation of the tumor volume (21). To improve the sensitivity of tumor cells to radiation, various studies have investigated compounds that can counteract these resistance mechanisms or enhance the radiation effect in a different manner. These compounds are referred to as radiosensitizers and are defined as "*compounds that, when combined with radiation, achieve greater tumor inactivation than would have been expected from the additive effect of each modality*" (22).

This concept of radiosensitization is of particular interest in pHGG, where radiosensitizers may increase the efficacy of RT and thereby allow the use of lower radiation doses to achieve a similar anti-tumor effect, while sparing healthy brain tissue. As such, this could reduce the chance of long-term toxicity and late effects such as neurocognitive dysfunction, growth impairment, and secondary malignancies. Moreover, the risk of added toxicity of such combination therapies is lower, given that the cytotoxic effect of a good radiosensitizer is mainly exploited within the irradiated tumor area. Furthermore, the advantage of drug synergism with RT, instead of drug-to-drug- synergism, is that at least half of the combination is not obstructed by the BBB, thus essentially requiring only one drug to pass this barrier. Finally, radiosensitizers can relatively easily be combined with standard clinical care, as it makes use of the already applied RT. Together, this makes for a broadly applicable approach, and exploring its full potential can contribute considerably to the improvement of current therapy (**Figure 1**).

In this review, we summarize the molecular determinants of radiosensitivity identified in pHGG and provide a critical evaluation of the radiosensitization strategies, and their underlying mechanisms, studied to date. These strategies can be divided into targeting TP53 and protein phosphatase 1D (PPM1D), DNA damage repair, ROS, mitogen-activated protein kinase (MAPK) and phosphoinositide 3-kinase (PI3K) signal transduction pathways, the cell cycle, cancer stem cells (CSCs), and the epigenome. We summarize and discuss the current knowledge on radiosensitization in pHGG and aim to provide researchers and clinicians with leads to further develop (pre) clinical therapy for these rapidly fatal brain tumors.

All preclinical and clinical studies that will be discussed in this review are summarized in **Tables 1** and **2** respectively.

TP53 AND PPM1D

As with most cancers, the response to RT is not uniform among pHGG patients and appears to be associated with the tumor's mutational status. Initially, response to RT in H3-K27M pHGG correlates with the type of histone H3 mutation, with patients carrying a *H3F3A* (H3.3) mutation having a significantly worse clinical and radiological response and earlier relapse than those with *HIST1H3B* (H3.1) mutations (70, 71). In contrast, Werbrouck et al. demonstrated that radioresistance is not correlated to the type of H3-K27M mutation but rather driven

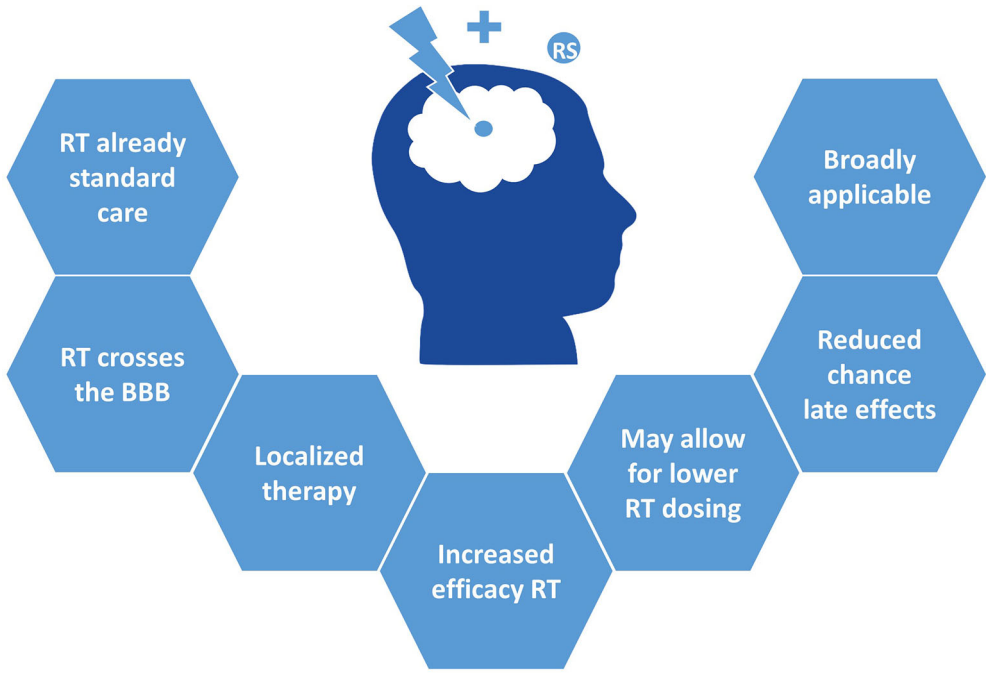

FIGURE 1 | Clinical advantages of radiosensitizers in pHGG.

by alterations of the tumor suppressor TP53, which is a critical component of the DDR downstream of checkpoint kinases (25). The discrepancy between these studies likely stems from the confounding factor that most H3.3-K27M tumors are also TP53-mutant, whereas H3.1-K27M tumors rarely are (72). In order to account for this confounding factor, the latter study performed a multivariate analysis adjusted for age at diagnosis, TP53, and histone H3 mutational status and demonstrated that there was no difference in clinical or radiological response to RT when comparing patients according to H3 mutational status. In contrast, patients carrying a TP53 mutation had a significantly worse clinical and radiological response to RT. At the same time, the type of H3-K27M mutation appeared to be a stronger predictor of post-irradiation relapse and overall survival, whereas TP53 alterations were only marginally associated with survival. As such, these studies suggest that short-term response to RT is driven by TP53 mutations, whereas long-term prognosis after RT is mainly determined by the type of H3-K27M mutation. Since Werbrouck et al. analyzed various other determinants of radiosensitivity on a preclinical and clinical level, the study will be discussed on multiple occasions throughout this review in relation to the corresponding topics.

Although the majority of H3.3-K27M tumors harbor a TP53 mutation, a subset of H3.3-K27M, TP53-wildtype tumors contain a gain-of-function mutation in the gene *PPM1D* instead (73). PPM1D encodes the protein wildtype p53-induced phosphatase 1 (WIP1), which dephosphorylates and inactivates p53 (23). Loss-of-function TP53 and gain-of-function PPM1D mutations are mutually exclusive and often considered to be functionally equivalent (73). However, while TP53 alterations are associated with overt radioresistance, PPM1D-mutant tumors appear to have an intermediate radiosensitive phenotype compared to TP53-mutant and -wildtype tumors (23, 25). As a potential explanation for this intermediate phenotype, PPM1D has been shown to affect the DDR independent of its effect on p53 (24). For example, PPM1D inactivates the checkpoint kinases ATM, ATR, and CHK1/2 and consequently impairs the initiation of the DDR after RT (**Figure 2**) (24). Moreover, PPM1D dephosphorylates the protein H2AX and therewith prevents the repair of damaged DNA directly (24). Thus, the enhanced activity of PPM1D that is associated with gain-of-function PPM1D mutations may both reduce radiosensitivity by inhibiting p53 and increase radiosensitivity by reducing the activity of other DDR components.

Though PPM1D-mutant tumors appear to be relatively susceptible to irradiation already, Akamandisa et al. demonstrated that the PPM1D inhibitor GSK2830371 could increase radiosensitivity of PPM1D-mutant tumors even further *in vitro* and *in vivo*, supposedly by restoring the activation of p53 (23). Corroborating these findings, inhibition of PPM1D has been reported to increase radiosensitivity of PPM1D-mutant cells by impairing the HDR DNA-repair pathway through reactivation of p53 (24).

The studies discussed above imply that loss of p53 activity, either directly through somatic mutations or indirectly through enhanced activity of the negative regulator PPM1D, confers radioresistance by relieving the p53-mediated brake on homology-directed repair (HDR) activity. In contrast, it has

TABLE 1 | Overview preclinical radiosensitization studies addressed in this review.

Target	*In vitro* efficacy	*In vivo* efficacy	pHGG model	Remarks	References
PPM1D	+	+	H3.3-K27M DIPG	PPM1D-mutant cells more sensitive than PPM1D-WT cells	23
	+	n/a	H3.3-K27M DIPG	Synergy with PARP inhibition PPM1D-mutant cells more sensitive than PPM1D-WT cells	24
CHK1	+	n/a	H3.1-K27M DIPG H3.3-K27M DIPG	TP53-mutant cells more sensitive than TP53-WT cells	25
ATM	+	n/a	H3.3-K27M anaplastic astrocytoma H3-WT GBM		26
	+	+	H3.3-K27M anaplastic astrocytoma		27
	n/a	+	PDGF-B driven TP53-deficient BSG mouse model	TP53-mutant cells more sensitive than TP53-WT cells	28
WEE1	+	+	H3.3-K27M DIPG		29
	+	+	H3-WT GBM H3-G34R GBM H3.3-K27M DIPG		30
PLK1	+	n/a	H3.1-K27M DIPG H3.3-K27M DIPG		31
BUB1/BUBR1	+	n/a	H3-WT GBM		32
CDK4/6	n/a	+	PDGF-B driven Ink4a-ARF-deficient BSG mouse model		33
Notch	+	n/a	H3.3-K27M DIPG		34
PARP	+	n/a	H3-G34R GBM		35
	+	+	H3-WT HGA H3-G34R HGA H3.3-K27M DIPG		36
MTH1	+	n/a	H3-WT GBM H3-G34R GBM	Synergy with PARP inhibition	37
IGF-1R	+	n/a	H3-WT GBM H3-G34R GBM		38
mTOR	+	n/a	H3.3-K27M DIPG		39
	+	n/a	H3.3-K27M DIPG		40
PI3K/mTOR	+	n/a	H3-WT GBM		41
JMJD3	+	+	H3.3-K27M DIPG	H3-K27M-mutant cells more sensitive than H3-WT cells	42
	+	n/a	H3.3-K27M DIPG	Synergy with mutant-p53 inhibition	43
HDAC	+	n/a	H3-WT GBM H3-G34R GBM		44
	+	n/a	H3.3-K27M DIPG	Synergy with AXL inhibition	45
PI3K/HDAC	+	+	H3-WT GBM H3-G34R GBM H3.1-K27M DIPG H3.3-K27M DIPG		46
BRD4	+	+	H3-K27M DIPG		47

GBM, glioblastoma multiforme; DIPG, diffuse intrinsic pontine glioma; HGA, high-grade astrocytoma; BSG, brainstem glioma; n/a, data not available.

been hypothesized that radioresistance in TP53-mutant cells could be caused by RT-activated G1/S checkpoint escape rather than increased DNA-repair efficiency, an effect that may sensitize these tumors to cell cycle checkpoint inhibitors and is addressed in the following section (25). Alternatively, Deland et al. argued that the inherent radioresistance of TP53-mutant pHGG is mediated by hyperactivation of the nuclear factor erythroid 2–related factor 2 (NRF2) pathway, a key regulator of the cellular response to oxidative stress (28). Given that p53 has been reported to repress transcription of NRF2 targets, loss of p53 and subsequent activation of antioxidant pathways is likely to alter to the response to RT by reducing the level of intracellular ROS (28). Apart from the loss of function of p53, mutations in the p53 protein have been hypothesized to contribute directly to radioresistance by gain-of-function variants. For instance, knockdown or inhibition of mutant p53 has been reported to increase radiosensitivity of TP53-mutant cells (25, 43). Of note, any putative correlation in these studies between radiosensitivity and TP53 mutations may be confounded by co-occurring mutations. For instance, H3-K27M pHGG cells that, besides a TP53 mutation, harbor a mutation in the SWI/SNF chromatin-remodeling protein ATRX were shown to have an intermediate radiosensitivity with respect to other TP53-mutant and -wildtype cells (25). Indeed, loss of function ATRX mutations impair the NHEJ DNA-repair pathway, which likely reduces the repair efficiency of RT-induced DSBs (74). As research on this topic is conflicting, the exact interplay between TP53- and PPM1D mutations and radiosensitivity remains to be elucidated. Nonetheless, TP53 and PPM1D alterations appear to affect radiosensitivity differently, thereby emphasizing the necessity to distinguish between TP53- and PPM1D-mutant tumors in preclinical and clinical studies that use RT.

TABLE 2 | Overview clinical radiosensitization studies addressed in this review.

Target	Drug(s)	Population	Study	References
PARP	Veliparib	Newly diagnosed DIPG	Phase 1/2	48
Glutathione S-transferase	Etanidazole	DIPG	Phase 1	49
Thioredoxin and ribonucleotide	Motexafin gadolinium	DIPG	Phase 1	50
reductases	Motexafin gadolinium	DIPG	Phase 2	51
EGFR	Erlotinib	HGG	Phase 1	52
	Erlotinib	Brainstem glioma	Phase 1	53
	Gefitinib	Newly diagnosed brain stem gliomas or supratentorial malignant gliomas	Phase 1	54
	Gefitinib	Newly diagnosed brainstem gliomas	Phase 2	55
	Cetuximab	Newly diagnosed DIPG and HGA	Phase 2	56
	Nimotuzumab	DIPG	Phase 2	57
	Nimotuzumab	Newly diagnosed DIPG	Phase 3	58
VEGF	Bevacizumab	DIPG/HGG	Retrospective analysis	59
	Bevacizumab	Newly diagnosed DIPG/HGG		60
	Bevacizumab	Newly diagnosed HGG	Phase 2	61
various RTKs	Vandetanib	DIPG	Phase 1	62
	Vandetanib and Dasatinib	Newly diagnosed DIPG	Phase 1	63
	Imatinib	Newly diagnosed brainstem and recurrent malignant gliomas	Phase 1	64
HDAC	Panobinostat	Progressive DIPG	Case study	65
	Valproic acid	HGG	Retrospective analysis	66
	Valproic acid	DIPG	Retrospective analysis	67
	Valproic acid	Newly diagnosed DIPG or HGG	Phase 2	68
	Vorinostat	Newly diagnosed HGG	Phase 2	69

DIPG, diffuse intrinsic pontine glioma; HGA, high-grade astrocytoma; HGG, high-grade glioma; n/a, data not available.

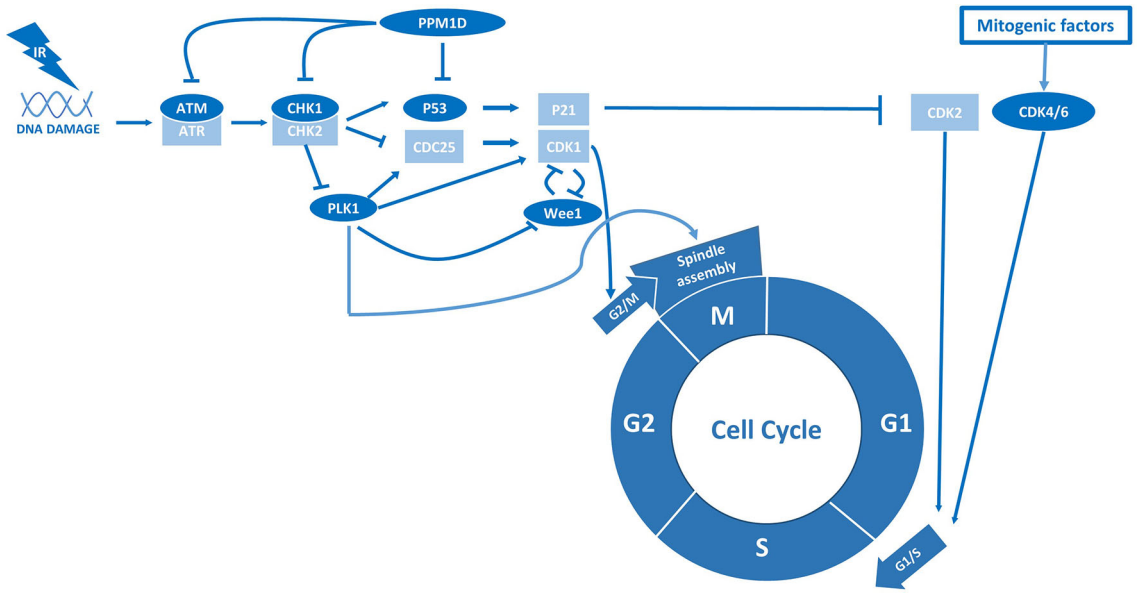

FIGURE 2 | p53 and PPM1D are central regulators of radiation sensitivity in pHGG.

CELL CYCLE AND GSCs

Cell cycle checkpoints play a critical role in sensing DNA damage and consequently mobilizing DNA-repair proteins, as well as halting cell cycle progression to allow time for DNA-repair (75). In general, the absence of these checkpoint kinases or downstream components causes continued cell division in the presence of DNA damage, typically leading to mitotic catastrophe and cell death (75). To improve radiosensitivity in tumor cells, researchers have tried to mimic such events by abrogating cell cycle checkpoint activity as a possible therapeutic strategy in various cancer types, including pHGG (25–32). Of note, this strategy may be of particular interest in pHGG that already possess aberrations in cell cycle checkpoints, such as TP53 mutations, as these tumor cells heavily rely on the remaining checkpoints to repair RT-induced DNA damage (19, 75). Furthermore, various studies indicate that pHGGs contain a considerable number of quiescent glioma stem cells (GSCs) intrinsically resistant to RT due to constitutive activation of cell cycle checkpoints and associated high DNA-repair efficiency (76, 77). Therefore, checkpoint inhibitors are also hypothesized to improve the efficacy of RT in pHGG by promoting re-entry of quiescent GSCs into the cell cycle (26, 78, 79). Importantly, this would not only improve the response to RT but also prevent repopulation of the tumor volume after cessation of treatment. Using patient-derived H3-K27M GSCs, one study revealed that this radiosensitization strategy is indeed specifically effective in a TP53-mutant background by demonstrating that shRNA-mediated inhibition of the checkpoint kinases ATM and CHK1 is synthetic lethal with RT in TP53-mutant but not TP53-wildtype cells (25). This synergistic anti-tumor effect with RT could also be achieved with the CHK1 inhibitor prexasertib. Inhibition of CHK1 in the absence of p53 simultaneously abrogated RT-activated G1/S and G2/M checkpoints, thereby enforcing replication in the presence of DNA damage. In contrast, TP53-wildtype cells could not be sensitized to RT by CHK1 inhibition as they remained blocked in G1. Corroborating these findings, deletion of the ATM locus has been reported to increase survival of genetically engineered mice with TP53-deficient but not TP53-wildtype brainstem gliomas following RT (28). Thus, although TP53 alterations appear to be correlated with radioresistance, they seem to evoke a specific vulnerability to the combination of RT and ATM/CHK1 inhibitors, which increase radiosensitivity by abrogating RT-induced cell cycle arrest (**Figure 2**).

In addition to the vulnerability of TP53-mutant glioma cells to ATM/CHK1 inhibitors, Werbrouck *et al.* identified a synthetic lethal interaction between RT and knockdown of the checkpoint kinases WEE1 and polo-like kinase 1 (PLK1) in TP53-mutant H3-K27M cells (25). In pHGG, both WEE1 and PLK1 are attractive therapeutic targets that are specifically overexpressed in these tumors (77). WEE1 is a checkpoint kinase that is activated by CHK1/2 and executes the cell cycle arrest at G2/M following DNA damage (75). Corresponding to this function, various studies reported that inhibition of WEE1 by the small molecule inhibitor adavosertib (MK1775/AZD1775) attenuates RT-induced cell cycle arrest and impairs repair of RT-induced DNA damage prior to entering mitosis, resulting in increased cell death *in vitro* and *in vivo* (29, 30). Of note, these effects were observed in H3-wildtype, H3-K27M, and H3-G34R/V tumors. In contrast to the preferential sensitivity of TP53-mutant cells mentioned above, Mueller et al. noticed no difference in the degree of radiosensitization based on TP53 mutational status (30). To explain this discrepancy, the authors argued that inhibition of WEE1 may directly increase DNA damage irrespective of its effect on the cell cycle, although the mechanism behind this is yet unclear (30).

Corroborating the synthetic lethality of PLK1 inhibition, Amani et al. demonstrated the radio-enhancing effect of inhibiting PLK1 in H3-K27M pHGG cells with the small molecule inhibitor volasertib (31). PLK1 is a checkpoint kinase that is inactivated by CHK1/2 following DNA damage and so inhibition of PLK1 typically leads to cell cycle arrest (80). These observations suggest that inhibition of PLK1 is associated with a different radiosensitizing mechanism than described for CHK1 and WEE1. Since PLK1 also regulates the separation of chromosomes during mitosis, it may be hypothesized that inhibition of PLK1 increases radiosensitivity evoking mitotic catastrophe. Other checkpoint kinases that regulate chromosome segregation and have also been discovered as potential radio-enhancing targets are BUB1 and BUBR1, which are part of the Budding Uninhibited by Benzimidazole (BUB) and the Mitotic Arrest Deficient (MAD) gene families of mitotic spindle checkpoints (32). In this study, inhibition of BUB1 and BUBR1 was associated with an increased formation of micronuclei, which reflects the presence of chromosomal damage, suggesting that the absence of mitotic spindle checkpoints may indeed evoke catastrophic mitotic events following RT.

The radiosensitizing abilities of volasertib may also be explained by the difference in radiosensitivity between cell cycle phases, with cells being most sensitive in G2 and M, less sensitive in G1, and least sensitive in S-phase (20). Radioresistance in the S-phase is associated with an elevated level of DNA synthesis, repair enzymes and antioxidants (20). Cells in the G2/M phase are known to be more sensitive to irradiation because there is less time for repair before chromosome segregation takes place (20). Therefore, agents that can maintain cells in radiosensitive phases (i.e., PLK1 inhibitors) or eliminate those cells in radioresistant phases are likely to cooperate with RT for enhanced efficacy (21). Surprisingly, Barton et al. demonstrated that radiosensitivity could be increased by arresting pHGG cells in G1 phase with the cyclin-dependent kinases 4 and 6 (CDK4/6) inhibitor palbociclib (**Figure 2**) (33). Notably, CDK4/6 inhibitors may be particularly effective in pHGG, which frequently harbor amplified CDK4/6 loci. Also, the expression of the cyclin-dependent kinase inhibitor p16 is typically repressed in H3-K27M tumors, which has been shown to confer susceptibility to CDK4/6 inhibition (77, 81). However, the mouse DMG models used by Barton et al. contain a genomic deletion of the Ink4-ARF locus, which are not found in DMG patients and may cause a specific susceptibility to CDK4/6 inhibitors (33).

Finally, in addition to the indirect targeting of GSCs through cell cycle checkpoints, others suggest that radiosensitivity can also be increased by directly inhibiting the stem cell-like

phenotype of pHGG. For instance, inhibition of the NOTCH pathway, which is essential for maintaining stem cell-ness, with the γ-secretase inhibitor MRK003 has been shown to enhance RT-induced apoptotic cell death of H3-K27M pHGG cells (34). This study also demonstrated increased NOTCH pathway activity in primary pHGG samples and *in vitro* models, signifying NOTCH as a potential therapeutic target and suggesting that inhibiting this pathway may selectively radiosensitize the GSCs without impacting the radiosensitivity of adjacent normal tissue. Taken together, interfering with the cell cycle has yielded promising results on a preclinical level. However, it remains unclear to what extent either stimulation or abrogation of cell cycle progression is needed to maximize radiosensitivity.

DNA DAMAGE REPAIR AND ROS

While the previous sections argue for the indirect targeting of DNA damage repair activity through cell cycle checkpoints, others indicate that radiosensitivity can be increased by directly blocking DNA damage repair (35, 36, 82). Tumors characterized by a high prevalence of defects in DNA-repair pathways, like pHGG, are thought to be particularly sensitive to DNA-repair inhibitors following RT, since they have become highly dependent on a few remaining DNA-repair systems (19, 75, 77). The poly ADP-ribose polymerase (PARP) enzymes, which are essential for recruiting the DNA-repair machinery to RT-induced DNA strand breaks (**Figure 3**), are especially interesting therapeutic targets as they are often overexpressed in pHGG and are thought to be predictive for prognosis (77). Several preclinical studies reported that radiosensitivity of pHGG could be increased *in vitro* and *in vivo* by inhibiting PARP activity (35, 36). These studies also demonstrated that inhibition of PARP enhances radiosensitivity by causing persistence of RT-induced DNA damage. Again, these effects were observed in H3-wildtype, H3-K27M, and H3-G34R/V tumors. The combined treatment of RT and the PARP inhibitor veliparib has also been tested in a phase I/II clinical trial; however, in contrast to the preclinical success, this study did not demonstrate a clinical benefit compared to RT alone (48). Of note, Chornenkyy et al. compared the PARP inhibitors olaparib, niraparib, and veliparib *in vitro* and demonstrated that only olaparib, niraparib, but not veliparib, were able to reduce tumor cell growth, while all inhibitors effectively inhibited PARP activity (36). Niraparib and olaparib, but not veliparib, have a dual mechanism of action by both inhibiting PARP activity and inducing the formation of cytotoxic PARP1–DNA damage complexes, suggesting a possible explanation for the low efficacy of veliparib in the clinic (36). However, limited BBB penetration of these compounds might be the main limiting factor toward clinical efficacy, which is often overlooked.

As an alternative explanation for the poor efficacy of veliparib, Versano et al. demonstrated that veliparib increases Mut-T homolog 1 (MTH1) expression, an antioxidant that protects against oxidative stress and DNA damage by hydrolyzing oxidized nucleotides (37). Consistent with this protective effect, inhibition of MTH1 by siRNAs or the small molecule inhibitor TH588 was shown to increase the anti-tumor effect of veliparib in both H3-wildtype and H3-G34R/V pHGG cells. These results imply that the potency of PARP inhibitors can be enhanced by neutralizing antioxidants and through sufficient oxidative stress. In agreement with these observations, Versano et al. further demonstrated that histone deacetylase (HDAC) inhibitors, which are known to promote oxidative stress, increase the anti-tumor effect of veliparib. Moreover, they demonstrated that MTH1 inhibition enhances radiosensitivity by exacerbating DNA damage, suggesting that neutralizing antioxidants may not only improve the efficacy of veliparib as monotherapy but also as a radiosensitizer. Others suggest that the efficacy of veliparib as a radiosensitizer may also be enhanced by blocking additional DNA-repair pathways. For example, Wang et al. demonstrated that inhibition of PPM1D sensitizes PPM1D-mutant (H3-K27M) pHGG cells to PARP inhibitors by synergistically impairing DSB repair, which also enhanced sensitivity to RT (24). Taken together, these observations imply that PARP inhibitors should not be disregarded despite the initial discouraging results of veliparib in clinical trials and that re-evaluation may be warranted. Moreover, the latter study would advocate for using a particular combination of radiosensitizers in a specific subgroup (i.e., PPM1D-mutant pHGG) rather than using a single radiosensitizer in an unstratified group of patients, as has been the case in clinical trials at large.

The studies described above suggest that other antioxidant inhibitors may also function as radiosensitizers (**Figure 3**). In pHGG, this proposition has been studied in phase I and II clinical trials with motexafin gadolinium, an inhibitor of thioredoxin and ribonucleotide reductases, and etanidazole, an inhibitor of glutathione S-transferase (49–51). Although these compounds could be safely administered in combination with RT, these trials did not advance further than phase II due to a lack of superior efficacy over RT. Nonetheless, as indicated above, these inhibitors may still boost the radiosensitizing effect of other strategies, suggesting that the full potential of exploiting oxidative stress as a radiosensitizing strategy is yet to be uncovered. Taken together, although compounds targeting DNA-repair and ROS pathways have not yet proven to be successful as radiosensitizers in pediatric glioma patients thus far, using these compounds in the right combination may be a promising radiosensitizing strategy against certain pHGG subgroups.

MAPK/PI3K

As for most cancers, mitogenic MAPK and PI3K signaling pathways are often constitutively active in pHGG due to mutations or gene amplification in core components or upstream proteins, such as receptor tyrosine kinases (RTKs) (77). When tissue injury and cell loss occurs following radiation, these mitogenic signaling pathways are usually further activated, which leads to an enhanced proliferation rate and repopulation of the tumor volume after treatment (19). Moreover, these pathways stimulate the repair of RT-induced DNA damage by

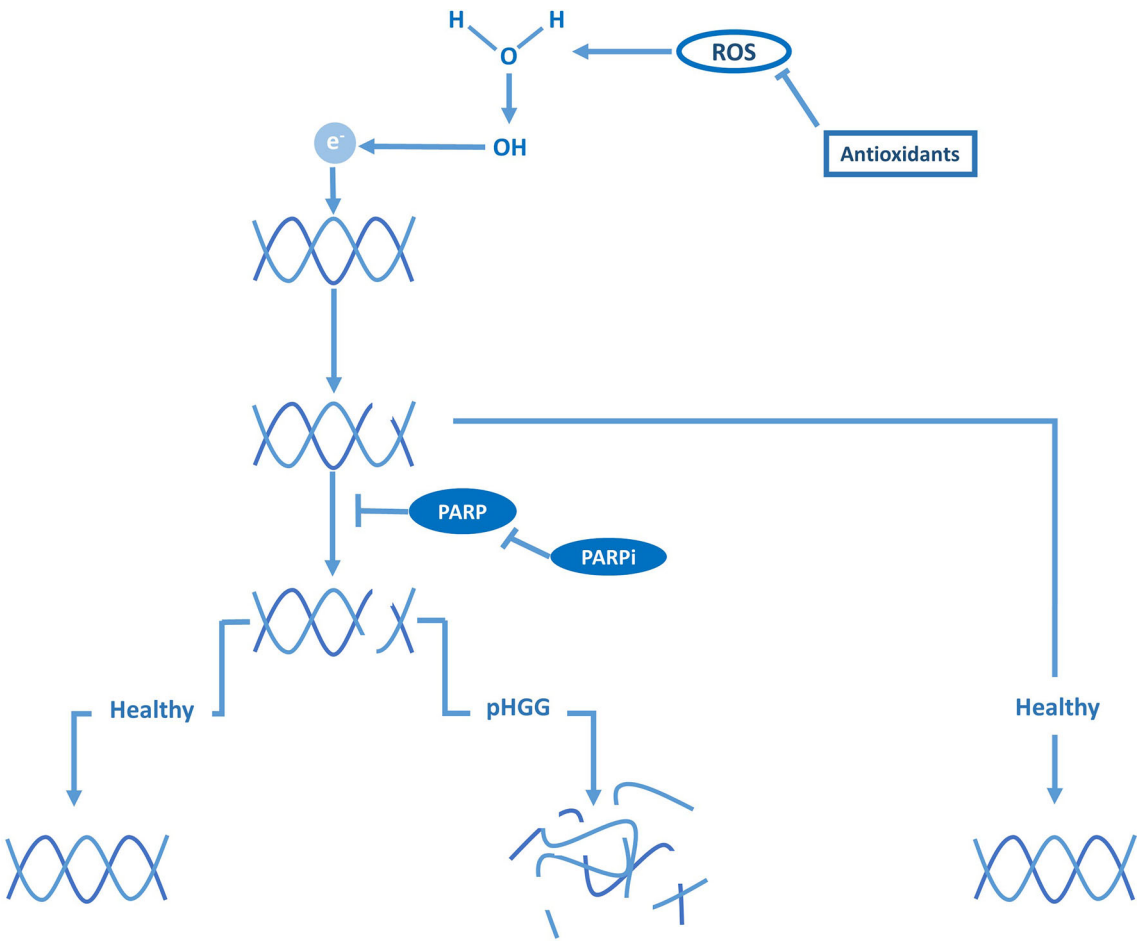

FIGURE 3 | DNA damage repair and PARP are vital against ROS-induced DNA breaks in pHGG.

regulating the expression of DDR components (19). As such, hyperactive MAPK and PI3K pathways typically elevate the baseline DNA damage repair capacity of pHGG tumors and thereby contribute to their radioresistant phenotype (**Figure 4**). To reduce both DNA-repair efficacy and repopulation following radiotherapy, various studies have investigated inhibiting upstream or downstream MAPK and PI3K components in combination with irradiation (38–41). One study demonstrated that radioresistance in pHGG correlates to overexpression of the RTK insulin-like growth factor receptor (IGF-1R), which, in turn, correlates with a worse prognosis in pHGG patients (38). Furthermore, they demonstrated that inhibition of IGF-1R with the small molecule inhibitor BMS-754807 enhances radiosensitivity of H3-wildtype and H3-G34R/V pHGG cells by impairing the repair of RT-induced DNA damage. Likewise, several studies demonstrated that inhibition of the mammalian target of rapamycin (mTOR) complex, a downstream effector of IGF-1R, increases radiosensitivity of H3-wildtype and H3-K27M pHGG cells (39–41). However, although mTOR acts downstream of IGF-1R, these mTOR inhibitors did not appear to recapitulate the increase in DNA damage that was observed for IGF-1R inhibition. Miyahara et al. demonstrated that the radiosensitizing effects of mTOR kinase inhibitor TAK228 was instead due to a downregulation of anti-apoptotic proteins (39). In contrast, Agliano et al. reported that the PI3K/mTOR inhibitor NVP-BEZ235 increases radiosensitivity by abrogating RT-induced G2/M arrest rather than affecting apoptosis or DNA-repair efficiency (41). Therefore, further studies are required to elucidate whether shared or unique radiosensitizing mechanisms underlie these observations and which target or mechanism in these pathways is critical for improving radiosensitivity.

Although targeting MAPK and PI3K through inhibition of RTKs appears a promising radiosensitization strategy on a preclinical level (**Figure 4**), the RTK inhibitors tested to date in pHGG clinical trials uniformly failed to improve prognosis over RT alone (52–64). As many small molecules developed as anti-cancer drugs have historically been selected for their inability to pass the BBB to minimalize neurological side effects, the failure of these inhibitors in pHGG patients may be attributed to inadequate drug delivery. In this regard, it is worth noting that clinical trials nowadays increasingly incorporate compounds or vehicles with good brain penetration and

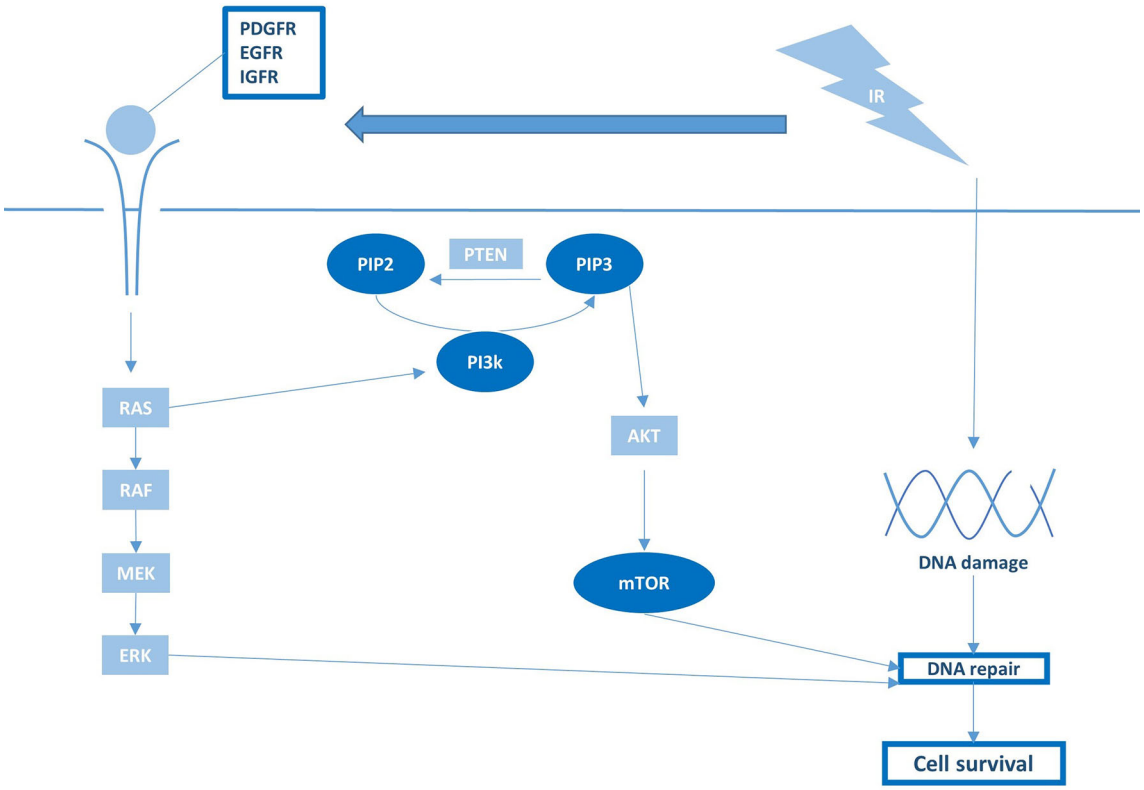

FIGURE 4 | Growth factor receptor activation and downstream PI3K/mTOR signaling are pivotal regulators of RT sensitivity and pHGG survival.

distribution. As one example, a phase I trial has recently been initiated with a novel brain-penetrant PI3K/mTOR inhibitor GDC-0084 in newly diagnosed DMG (NCT03696355). While awaiting the results of these studies, the true clinical feasibility and efficacy of this radiosensitization strategy remain elusive.

EPIGENOME

Based on the high prevalence of histone H3 mutations in pHGG, and their consequences for chromatin remodeling and gene transcription, reversing the aberrant methylation/acetylation balance in these tumors using epigenetic modifiers has been extensively investigated over the last decade as a possible therapeutic strategy (1). One strategy has been directed at restoring di- and trimethylation of H3-K27 (H3-K27me2/3) in H3-K27M tumors by inhibiting the lysine 27-specific histone demethylase jumonji domain containing-3 (JMJD3). While JMJD3 inhibitors show promising anti-tumor effects as monotherapy, the JMJD3 inhibitor GSK-J4 has also been reported to increase radiosensitivity *in vitro* and *in vivo*, specifically in H3-K27M tumors (42). In those tumors, GSK-J4 treatment impaired the repair of RT-induced DNA damage by reducing the expression of DNA-repair genes (**Figure 5**). Furthermore, GSK-J4 was shown to block DNA-repair by arresting the cell cycle in early S phase and, consequently, excluding the HDR pathway that is only active in late S/G2. In contrast, GSK-J4 did not affect the expression of repair genes and did not improve radiosensitivity in H3-wildtype tumors (42). Nikolaev et al. corroborated these findings in H3-K27M pHGG and demonstrated that the radiosensitizing effect of GSK-J4 could be enhanced in TP53-mutant cells by adding APR-246, an agent that forms covalent bonds with mutant p53 and neutralizes the protein (43). Since GSK-J4 treatment restores H3-K27me2/3, these findings indicate that reversing the hypomethylation phenotype of H3-K27M tumors is not only cytotoxic but may also improve the response to RT.

Another consequence of H3-K27M mutations is an increase in H3-K27 acetylation (H3-K27ac), resulting in an open chromatin structure and subsequent transcriptional activation at these genomic loci (77). Although it seems counterintuitive, a therapeutic strategy that has been investigated is to aggravate this hyperacetylation state using HDAC inhibitors (77). By increasing histone acetylation, these inhibitors appear to rescue the hypomethylation phenotype indirectly and, as a result, reduce tumor growth (**Figure 5**) (77). HDAC inhibitors have even been proposed to "detoxify" H3-K27M-induced inhibition of PRC2, but whether this is clinically relevant remains to be determined as various studies indicate that the response to HDAC inhibition is unrelated to histone mutational status

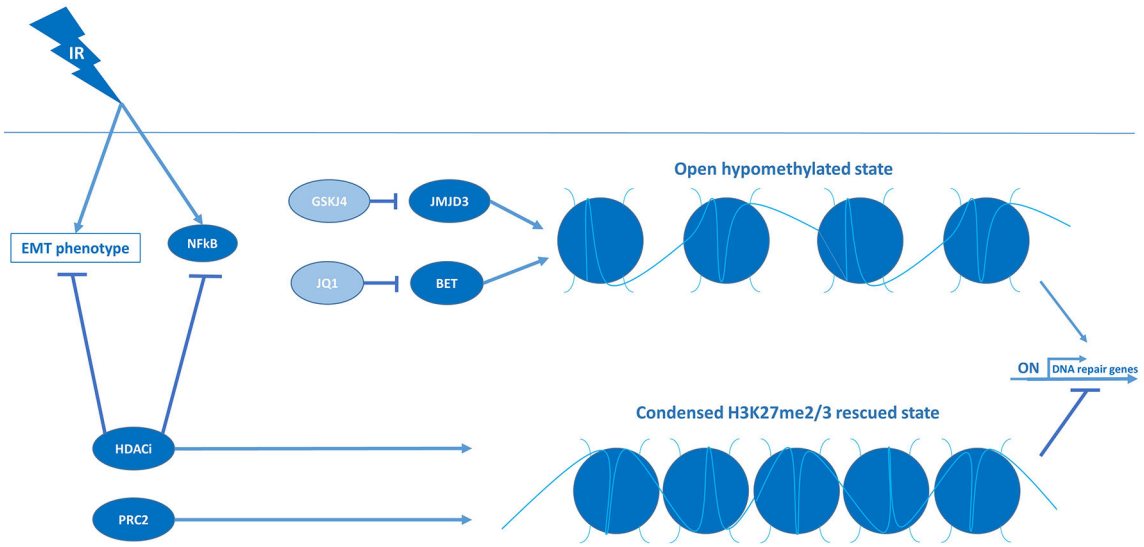

FIGURE 5 | Condensed chromatin structures suppress DNA-repair machineries and induce RT sensitivity in pHGG.

(1, 83). Concerning radiosensitivity, HDAC inhibitors have been reported to reduce the expression of checkpoint kinases and DNA-repair genes and, as such, have been proposed to also function as radiosensitizers. For instance, Pal et al. showed that a dual inhibitor of HDAC and PI3K, fimepinostat, sensitized a large panel of *in vitro* and *in vivo* pHGG models to irradiation by downregulating the checkpoint kinases WEE1 and CHK1 (46). Like checkpoint inhibition, the reduced expression of WEE1 and CHK1 resulted in abrogation of RT-induced G2/M arrest and enforced replication in the presence of DNA damage. Additionally, they demonstrated that fimepinostat induces G1 arrest, which, similar to GSK-J4, is known to inhibit the repair of DNA damage by excluding the HDR pathway. Fimepinostat was also shown to block the repair of RT-induced DNA damage by downregulating genes essential for HDR and NHEJ. To explain these observations on a mechanistic level, Pal et al. further demonstrated that fimepinostat blocks RT-induced expression and nuclear localization of the nuclear factor kappa-B (NFkB) transcription factors, thereby impairing gene expression of this vital NFkB survival mechanism (**Figure 5**). In line with this observation, knockdown of NFkB recapitulated the radiosensitizing effect of fimepinostat, suggesting that NFkB inhibitors may also be of value in combination with RT in pHGG. Furthermore, it is worth noting that these effects were observed in both H3-wildtype, H3-K27M, and H3-G34R/V tumors, suggesting that at least some of the radiosensitizing effect of HDAC inhibition is unrelated to histone mutational status. In line with these findings, the HDAC inhibitor abexinostat has been shown to increase radiosensitivity of H3-wildtype and H3-G34R/V cells by reducing the expression of genes essential for HDR and NHEJ (44). Taken together, these findings advocate for the use of HDAC inhibitors as radiosensitizers and the broad applicability of these compounds.

In addition to their effects on DNA-repair, HDAC inhibitors are of interest in pHGG due to their ability to reverse epithelial-to-mesenchymal transition (EMT), a process in which epithelial cells adopt a mesenchymal phenotype by loss of cell-cell adhesion and acquisition of migratory properties (16). This migratory phenotype, which is stimulated by RT, is hypothesized to allow the tumor cells to escape from the irradiated area, thereby evading the treatment (9, 16). This transition is also believed to be responsible for the induction and maintenance of stem cell characteristics and, consequently, a higher radioresistant phenotype (16). Recently, we demonstrated that the HDAC inhibitor panobinostat can reverse the EMT phenotype and that this effect can be enhanced by simultaneously inhibiting the growth factor receptor AXL, a putative driver of EMT (45). They further demonstrated that combined treatment with the AXL inhibitor BGB324 and panobinostat downregulates the expression of genes associated with stem cell maintenance and DNA-repair. This reversal of the mesenchymal, stem cell-like, therapy-resistant phenotype of H3-K27M pHGG cells resulted in a synergistic anti-tumor effect and a robust sensitization to RT *in vitro*. Notably, while panobinostat was observed to function as a radiosensitizer alone, it could not prevent tumor regrowth. However, the addition of BGB324, having no significant radiosensitizing effect on its own, produced robust triple synergy in combination with panobinostat and RT and completely abolished tumor growth. These findings suggest that a combinatory approach may be necessary to improve radiosensitivity sufficiently. In line with this hypothesis, the HDAC inhibitors tested in combination with RT in clinical studies, demonstrated encouraging response rates but have not been able to significantly improve survival compared to conventional treatment (65–69). Taken together, HDAC inhibitors may considerably enhance the response to RT by

reversing EMT, although a combinatory approach may be necessary to achieve a significant effect.

Another therapeutic approach related to the H3-K27-dependent increase in histone acetylation is directed at the occupancy of the H3-K27ac sites by bromodomain and extra-terminal (BET) proteins, reader proteins that associate with acetylated histones and recruit the transcriptional machinery to initiate expression (11, 84). Displacement of BET proteins from acetylated histones is known to disrupt RNA polymerase II-mediated transcription, thereby reducing the high-level expression of oncogenes associated with H3-K27M mutations (1). Regarding radiosensitivity, inhibition of the BET protein family member bromodomain-containing protein 4 (BRD4) with the small molecule inhibitor JQ1 has been shown to markedly reduce the expression of DNA-repair genes and sustain high levels of RT-induced DNA damage in H3-K27M cells, leading to an enhanced RT effect *in vitro* and *in vivo* (47). Altogether, by affecting cell cycle checkpoints, DNA-repair, and EMT, targeting the epigenome combined with RT holds great potential for improving radiosensitivity of pHGG tumors.

DISCUSSION

Until a decade ago, pre-clinical research to understand the molecular characteristics of pHGG was virtually absent due to a lack of representative culture and xenograft models. Furthermore, to this day clinical treatment protocols in pHGG are often derived from trials in adult patients, and effective therapeutic options remain scarce. With the implementation of biopsy and autopsy protocols for collecting biological pHGG material, preclinical research is expanding rapidly, and our understanding of the pathobiology of these malignancies has improved tremendously. One of the most vital discoveries from these recent preclinical studies encompasses the identification of H3 mutations in about 50% of all pHGG, in major contrast to aHGG, including its correlation with age of onset, aggressiveness, and location of the tumor (15). The epigenetic deregulated nature of these tumors has been discovered to contribute to a stem cell-like, therapy-resistant phenotype, which further sets these tumors apart from their adult counterparts (9). These differences also result in a strong differential RT response between pediatric and adult glioma (85). Now that adequate pHGG *in vitro* and *in vivo* models are available and increasingly used in research, re-evaluation of radiosensitization may prove valuable for improving the standard of care for these fatal childhood brain tumors, for which this review serves as a guide.

The studies discussed in this review draw the image of an intricate balance between radiosensitivity and radioresistance in pHGG based on the mutational status of each tumor. For instance, mutations in upstream or downstream regulators within the same pathway do not necessarily phenocopy the level of radiosensitivity, as illustrated by p53 and PPM1D mutations. Furthermore, some combinations of co-occurring mutations alter the response to RT, as shown by the intermediate radiosensitivity of TP53- and ATRX-mutant cells with respect to other TP53-mutant and TP53-wildtype cells. As discussed in this review, several studies also show that the mutational status of pHGG evokes vulnerabilities to specific radiosensitizing agents. For example, checkpoint inhibitors are overall better radiosensitizers in TP53-mutant than TP53-wildtype tumors, and PPM1D inhibitors specifically radiosensitize PPM1D-mutant tumors. However, radiosensitivity is often a more complicated matter, as sufficient oxidative stress or DNA damage are often required to induce the desired RT-enhancing effect of radiosensitizers, as shown with combined antioxidant and PARP inhibitor treatment. Furthermore, sometimes drug-synergy is only effective in a specific mutational background, as with combined PPM1D and PARP inhibition in PPM1D-mutant tumors. These observations emphasize the necessity for a personalized and stratified approach (**Figure 6**) rather than applying a single radiosensitizer to an unstratified group of patients, as has been the case in the majority of clinical trials to date.

Pediatric gliomas are hallmarked by epigenetic dysregulation, often caused by H3 mutations, which widely impact tumor-behavior and emphasizes the necessity of a treatment strategy tailored to a histone-mutant or -wildtype background. However, this concept has thus far only been demonstrated with JMJD3 inhibitors in H3-K27M pHGG, possibly because epigenetic dysregulation in cancer is a relatively new field of research and still poorly understood. Since abnormal histone functioning is associated with genomic instability (especially with G34R/V mutations), compounds that impair DNA-repair or checkpoint kinases may specifically improve radiosensitivity in these

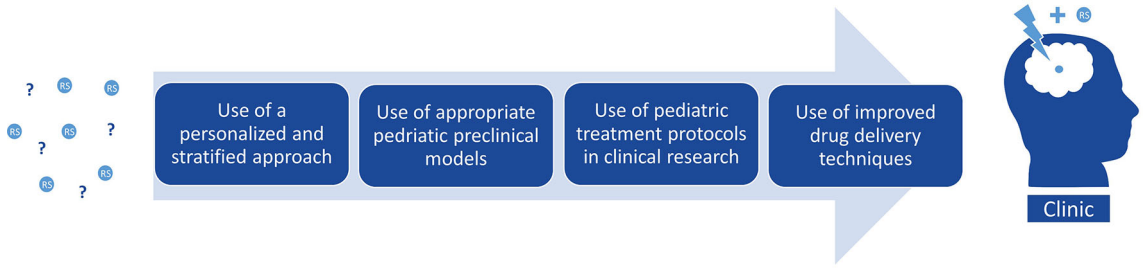

FIGURE 6 | Considerations for improved clinical translation of pre-clinical radiosensitizers in pHGG.

histone-mutant tumors by causing an overload of DNA damage. Although most studies discussed in this review did include different histone H3-mutant and -wildtype models, differential sensitivity was not assessed in the majority of these studies, warranting further investigation.

Although representative pediatric models are pivotal in the search for effective therapy against pHGG, results from studies in adult patients or models may still be relevant. An important query that has been studied in aHGG is the relation between radiobiology and the immune system. Here it was shown that irradiation activates the immunosuppressive "cold" environment in brain tumors and triggers an abscopal effect: a phenomenon in which RT initiates an immune response that eliminates cancer cells distant from the irradiated volume (86). Given the diffuse growth characteristics of pHGG, this may represent a promising radiosensitization strategy. Immunotherapy for pediatric brain tumors is an area that is relatively unexplored in preclinical research, mainly due to the lack of immunocompetent *in vivo* models. The development of these models would allow us to study the interactions between immune cells and radiotherapy in patient-derived pHGG models *in vivo*, which may revolutionize the field of radiosensitization in pediatric brain tumors. Fortunately, novel methods have recently been published that describe the generation of spontaneous murine HGG models with or without histone 3 mutations, accompanied by somatic mutations of choice (87–89). When used within a similar mouse strain, cells from these spontaneous models can easily be used to generate xenografts in immunocompetent mice, allowing us to study the interaction between tumor-microenvironment, immune system and treatment. Furthermore, these models resemble a more realistic pathophysiology compared to many of the older inducible cancer models, which are often generated in the presence of mutations that are rarely found in those tumors.

Despite the promising radio-enhancing effects of the agents addressed in this review, a recurrent problem with small molecule inhibitors remains the limited distribution through the brain due to their inability to cross the BBB. Although the BBB is often disrupted in aHGG, the integrity of this barrier in pHGG is often more intact, especially in DMG, but also appears to have a heterogeneous representation (90). Regardless of BBB integrity within the tumor, the ability to penetrate the brain remains a prerequisite for any compound used in these diffusely growing brain tumors as tumor cells can migrate into regions of the brain with an intact BBB. In this regard, promising innovations emerged in recent years to disrupt or circumvent the BBB, like convection-enhanced delivery (CED) and sonoporation using high-intensity focused ultrasound (HIFU) combined with microbubbles (90–92). These novel strategies have only recently been developed for clinical use and will be of vital importance for the efficacy of radiosensitizers in patients (**Figure 6**). Furthermore, with the help of these brain penetrating strategies, we might want to reconsider some of the many potential RT-enhancing agents that have failed translation to the clinic since the mid-1980s.

CONCLUSIONS

pHGGs are highly malignant brain tumors with a devastating prognosis, causing the most cancer-related deaths in children. Radiotherapy is part of the standard therapy against pHGG and often the only option to provide temporary symptom relief and a delay in tumor progression. Various preclinical and clinical studies have evaluated the potential of improving sensitivity to radiotherapy by targeting key survival or radioresistance mechanisms combined with irradiation. Although these strategies appear promising at a preclinical level, the radiosensitizers tested to date in clinical trials have not yet significantly improved survival. Nonetheless, the last decade has taught us much about the behavior, vulnerabilities, molecular characteristics, and modeling methods of pHGG. With this knowledge and access to a plethora of target-specific small molecule inhibitors, a variety of clinically relevant possibilities towards pHGG-specific radiosensitization can now be explored. Especially with the increasing availability of biological material and adequate *in vitro* and *in vivo* models, as well as the development of novel brain-penetrant agents, designing an effective radiosensitizing strategy for these fatal childhood brain tumors is at an apparent reach.

AUTHOR CONTRIBUTIONS

DM and AC conceived and designed this review. DM and AC have written the manuscript. DM and IS designed and created illustrations. GK and EH acquired funding and provided supervision.

All authors have reviewed the manuscript. All authors contributed to the article and approved the submitted version.

REFERENCES

1. Hashizume R. Epigenetic Targeted Therapy for Diffuse Intrinsic Pontine Glioma. *Neurol Med Chir (Tokyo)* (2017) 57(7):331–42. doi: 10.2176/nmc.ra.2017-0018
2. Smith MA, Seibel NL, Altekruse SF, Ries LA, Melbert DL, O'Leary M, et al. Outcomes for children and adolescents with cancer: challenges for the twenty-first century. *J Clin Oncol Off J Am Soc Clin Oncol* (2010) 28(15):2625–34. doi: 10.1200/JCO.2009.27.0421
3. Lulla RR, Saratsis AM, Hashizume R. Mutations in chromatin machinery and pediatric high-grade glioma. *Sci Adv* (2016) 2(3):e1501354. doi: 10.1126/sciadv.1501354
4. Sturm D, Pfister SM, Jones DTW. Pediatric Gliomas: Current Concepts on Diagnosis, Biology, and Clinical Management. *J Clin Oncol* (2017) 35 (21):2370–7. doi: 10.1200/JCO.2017.73.0242
5. Jones C, Baker SJ. Unique genetic and epigenetic mechanisms driving paediatric diffuse high-grade glioma. *Nat Rev Cancer* (2014) 14 (10):10.1038/nrc3811. doi: 10.1038/nrc3811
6. Louis DN, Perry A, Reifenberger G, von Deimling A, Figarella-Branger D, Cavenee WK, et al. The 2016 World Health Organization Classification of Tumors of the Central Nervous System: a summary. *Acta Neuropathol* (2016) 131(6):803–20. doi: 10.1007/s00401-016-1545-1
7. Wierzbicki K, Ravi K, Franson A, Bruzek A, Cantor E, Harris M, et al. Targeting and Therapeutic Monitoring of H3K27M-Mutant Glioma. *Curr Oncol Rep* (2020) 22(2):19. doi: 10.1007/s11912-020-0877-0

8. Bailey CP, Figueroa M, Mohiuddin S, Zaky W, Chandra J. Cutting Edge Therapeutic Insights Derived from Molecular Biology of Pediatric High-Grade Glioma and Diffuse Intrinsic Pontine Glioma (DIPG). *Bioeng (Basel)* (2018) 5(4):88. doi: 10.3390/bioengineering5040088
9. Kluiver TA, Alieva M, van Vuurden DG, Wehrens EJ, Rios AC. Invaders Exposed: Understanding and Targeting Tumor Cell Invasion in Diffuse Intrinsic Pontine Glioma. *Front Oncol* (2020) 10:92. doi: 10.3389/fonc.2020.00092
10. Das KK, Kumar R. Pediatric Glioblastoma. In: S De Vleeschouwer, editor. *Glioblastoma*. Brisbane, AU: Codon Publications Copyright: The Authors (2017).
11. Vanan MI, Underhill DA, Eisenstat DD. Targeting Epigenetic Pathways in the Treatment of Pediatric Diffuse (High Grade) Gliomas. *Neurotherapeutics* (2017) 14(2):274–83. doi: 10.1007/s13311-017-0514-2
12. Chen CCL, Deshmukh S, Jessa S, Hadjadj D, Lisi V, Andrade AF, et al. Histone H3.3G34-Mutant Interneuron Progenitors Co-opt PDGFRA for Gliomagenesis. *Cell* (2020) 183(6):1617–33.e22. doi: 10.1016/j.cell.2020.11.012
13. Funato K, Smith RC, Saito Y, Tabar V. Dissecting the impact of regional identity and the oncogenic role of human-specific NOTCH2NL in an hESC model of H3.3G34R-mutant glioma. *Cell Stem Cell* (2021) S1934-5909(21)00053-9. doi: 10.1016/j.stem.2021.02.003
14. Bressan RB, Southgate B, Ferguson KM, Blin C, Grant V, Alfazema N, et al. Regional identity of human neural stem cells determines oncogenic responses to histone H3.3 mutants. *Cell Stem Cell* (2021) S1934-5909(21)00016-3. doi: 10.1016/j.stem.2021.01.016
15. Kasper LH, Baker SJ. Invited Review: Emerging functions of histone H3 mutations in paediatric diffuse high-grade gliomas. *Neuropathol Appl Neurobiol* (2019) 46(1):73–85. doi: 10.1111/nan.12591
16. Meel MH, Schaper SA, Kaspers GJL, Hulleman E. Signaling pathways and mesenchymal transition in pediatric high-grade glioma. *Cell Mol Life Sci* (2018) 75(5):871–87. doi: 10.1007/s00018-017-2714-7
17. Aziz-Bose R, Monje M. Diffuse intrinsic pontine glioma: molecular landscape and emerging therapeutic targets. *Curr Opin Oncol* (2019) 31(6):522–30. doi: 10.1097/CCO.0000000000000577
18. Hennika T, Becher OJ. Diffuse Intrinsic Pontine Glioma: Time for Cautious Optimism. *J Child Neurol* (2016) 31(12):1377–85. doi: 10.1177/0883073815601495
19. Toulany M. Targeting DNA Double-Strand Break Repair Pathways to Improve Radiotherapy Response. *Genes (Basel)* (2019) 10(1):25. doi: 10.3390/genes10010025
20. Sharda N, Yang C-R, Kinsella T, Boothman D. Radiation Resistance. In: JR Bertino, editor. *Encyclopedia of Cancer*, *2nd ed.* New York: Academic Press (2002). p. 1–11.
21. Willey CD, Yang ES-H, Bonner JA. Chapter 4 - Interaction of Chemotherapy and Radiation. In: LL Gunderson, JE Tepper, editors. *Clinical Radiation Oncology*, *4th ed.* Philadelphia: Elsevier (2016). p. 63–79.e4.
22. Koch CJ, Parliament MB, Brown JM, Urtasun RC. 4 - Chemical Modifiers of Radiation Response. In: RT Hoppe, TL Phillips, M Roach, editors. *Leibel and Phillips Textbook of Radiation Oncology*, *3rd ed.* Philadelphia: W.B. Saunders (2010). p. 55–68.
23. Akamandisa MP, Nie K, Nahta R, Hambardzumyan D, Castellino RC. Inhibition of mutant PPM1D enhances DNA damage response and growth suppressive effects of ionizing radiation in diffuse intrinsic pontine glioma. *Neuro Oncol* (2019) 21(6):786–99. doi: 10.1093/neuonc/noz053
24. Wang Z, Xu C, Diplas BH, Moure CJ, Chen CJ, Chen LH, et al. Targeting Mutant PPM1D Sensitizes Diffuse Intrinsic Pontine Glioma Cells to the PARP Inhibitor Olaparib. *Mol Cancer Res MCR* (2020) 18(7):968–80. doi: 10.1158/1541-7786.MCR-19-0507
25. Werbrouck C, Evangelista CCS, Lobon-Iglesias MJ, Barret E, Le Teuff G, Merlevede J, et al. TP53 Pathway Alterations Drive Radioresistance in Diffuse Intrinsic Pontine Gliomas (DIPG). *Clin Cancer Res* (2019) 25(22):6788–800. doi: 10.1158/1078-0432.CCR-19-0126
26. Vecchio D, Daga A, Carra E, Marubbi D, Raso A, Mascelli S, et al. Pharmacokinetics, pharmacodynamics and efficacy on pediatric tumors of the glioma radiosensitizer KU60019. *Int J Cancer* (2015) 136(6):1445–57. doi: 10.1002/ijc.29121
27. Frosina G, Ravetti JL, Corvo R, Fella M, Garre ML, Levrero F, et al. Faithful animal modelling of human glioma by using primary initiating cells and its implications for radiosensitization therapy [ARRIVE 1]. *Sci Rep* (2018) 8(1):14191. doi: 10.1038/s41598-018-32578-w
28. Deland K, Starr BF, Mercer JS, Byemerwa J, Crabtree DM, Williams NT, et al. Tumor genotype dictates radiosensitization after Atm deletion in primary brainstem glioma models. *J Clin Invest* (2020) 131(1):e142158. doi: 10.1101/2020.08.24.262642
29. Caretti V, Hiddingh L, Lagerweij T, Schellen P, Koken PW, Hulleman E, et al. WEE1 kinase inhibition enhances the radiation response of diffuse intrinsic pontine gliomas. *Mol Cancer Ther* (2013) 12(2):141–50. doi: 10.1158/1535-7163.MCT-12-0735
30. Mueller S, Hashizume R, Yang X, Kolkowitz I, Olow AK, Phillips J, et al. Targeting Wee1 for the treatment of pediatric high-grade gliomas. *Neuro Oncol* (2014) 16(3):352–60. doi: 10.1093/neuonc/not220
31. Amani V, Prince EW, Alimova I, Balakrishnan I, Birks D, Donson AM, et al. Polo-like Kinase 1 as a potential therapeutic target in Diffuse Intrinsic Pontine Glioma. *BMC Cancer* (2016) 16:647. doi: 10.1186/s12885-016-2690-6
32. Morales AG, Pezuk JA, Brassesco MS, de Oliveira JC, de Paula Queiroz RG, Machado HR, et al. BUB1 and BUBR1 inhibition decreases proliferation and colony formation, and enhances radiation sensitivity in pediatric glioblastoma cells. *Childs Nerv Syst* (2013) 29(12):2241–8. doi: 10.1007/s00381-013-2175-8
33. Barton KL, Misuraca K, Cordero F, Dobrikova E, Min HD, Gromeier M, et al. PD-0332991, a CDK4/6 inhibitor, significantly prolongs survival in a genetically engineered mouse model of brainstem glioma. *PloS One* (2013) 8(10):e77639. doi: 10.1371/journal.pone.0077639
34. Taylor IC, Hutt-Cabezas M, Brandt WD, Kambhampati M, Nazarian J, Chang HT, et al. Disrupting NOTCH Slows Diffuse Intrinsic Pontine Glioma Growth, Enhances Radiation Sensitivity, and Shows Combinatorial Efficacy With Bromodomain Inhibition. *J Neuropathol Exp Neurol* (2015) 74(8):778–90. doi: 10.1097/NEN.0000000000000216
35. van Vuurden DG, Hulleman E, Meijer OL, Wedekind LE, Kool M, Witt H, et al. PARP inhibition sensitizes childhood high grade glioma, medulloblastoma and ependymoma to radiation. *Oncotarget* (2011) 2(12):984–96. doi: 10.18632/oncotarget.362
36. Chornenkyy Y, Agnihotri S, Yu M, Buczkowicz P, Rakopoulos P, Golbourn B, et al. Poly-ADP-Ribose Polymerase as a Therapeutic Target in Pediatric Diffuse Intrinsic Pontine Glioma and Pediatric High-Grade Astrocytoma. *Mol Cancer Ther* (2015) 14(11):2560–8. doi: 10.1158/1535-7163.MCT-15-0282
37. Versano Z, Shany E, Freedman S, Tuval-Kochen L, Leitner M, Paglin S, et al. MutT homolog 1 counteracts the effect of anti-neoplastic treatments in adult and pediatric glioblastoma cells. *Oncotarget* (2018) 9(44):27547–63. doi: 10.18632/oncotarget.25547
38. Simpson AD, Soo YWJ, Rieunier G, Aleksic T, Ansorge O, Jones C, et al. Type 1 IGF receptor associates with adverse outcome and cellular radioresistance in paediatric high-grade glioma. *Br J Cancer* (2020) 122(5):624–9. doi: 10.1038/s41416-019-0677-1
39. Miyahara H, Yadavilli S, Natsumeda M, Rubens JA, Rodgers L, Kambhampati M, et al. The dual mTOR kinase inhibitor TAK228 inhibits tumorigenicity and enhances radiosensitization in diffuse intrinsic pontine glioma. *Cancer Lett* (2017) 400:110–6. doi: 10.1016/j.canlet.2017.04.019
40. Flannery PC, DeSisto JA, Amani V, Venkataraman S, Lemma RT, Prince EW, et al. Preclinical analysis of MTOR complex 1/2 inhibition in diffuse intrinsic pontine glioma. *Oncol Rep* (2018) 39(2):455–64. doi: 10.3892/or.2017.6122
41. Agliano A, Balarajah G, Ciobota DM, Sidhu J, Clarke PA, Jones C, et al. Pediatric and adult glioblastoma radiosensitization induced by PI3K/mTOR inhibition causes early metabolic alterations detected by nuclear magnetic resonance spectroscopy. *Oncotarget* (2017) 8(29):47969–83. doi: 10.18632/oncotarget.18206
42. Katagi H, Louis N, Unruh D, Sasaki T, He X, Zhang A, et al. Radiosensitization by Histone H3 Demethylase Inhibition in Diffuse Intrinsic Pontine Glioma. *Clin Cancer Res* (2019) 25(18):5572–83. doi: 10.1158/1078-0432.CCR-18-3890
43. Nikolaev A, Fiveash JB, Yang ES. Combined Targeting of Mutant p53 and Jumonji Family Histone Demethylase Augments Therapeutic Efficacy of Radiation in H3K27M DIPG. *Int J Mol Sci* (2020) 21(2):490. doi: 10.3390/ijms21020490
44. de Andrade PV, Andrade AF, de Paula Queiroz RG, Scrideli CA, Tone LG, Valera ET. The histone deacetylase inhibitor PCI-24781 as a putative

radiosensitizer in pediatric glioblastoma cell lines. *Cancer Cell Int* (2016) 16:31. doi: 10.1186/s12935-016-0306-5

45. Meel MH, de Gooijer MC, Metselaar DS, Sewing ACP, Zwaan K, Waranecki P, et al. Combined therapy of AXL and HDAC inhibition reverses mesenchymal transition in diffuse intrinsic pontine glioma. *Clin Cancer Res* (2020) 26(13):3319–32. doi: 10.1158/1078-0432.CCR-19-3538
46. Pal S, Kozono D, Yang X, Fendler W, Fitts W, Ni J, et al. and PI3K Inhibition Abrogates NFkappaB- and FOXM1-Mediated DNA Damage Response to Radiosensitize Pediatric High-Grade Gliomas. *Cancer Res* (2018) 78 (14):4007–21. doi: 10.1158/0008-5472.CAN-17-3691
47. Sasaki T, Katagi H, Unruh D, Goldman S, Zou L, Shilatifard A, et al. PDTM-34. Radiosensitization By BRD4 Inhibition In Diffuse Intrinsic Pontine Glioma. *Neuro-oncology* (2019) 21(Supplement_6):vi194–vi5. doi: 10.1093/neuonc/noz175.810
48. Baxter P, Su J, Li X-n, Thomas AO, Billups C, Thompson P, et al. EPT-15: A phase1/2 clinical trial of veliparib (abt-888) and radiation followed by maintenance therapy with veliparib and temozolomide (tmz) in patients with newly diagnosed diffuse intrinsic pontine glioma (dipg): a pediatric brain tumor consortium interim report of phase ii study. *Neuro-Oncology* (2016) 18(Suppl 3):iii27–iii. doi: 10.1093/neuonc/now069.14
49. Marcus KJ, Dutton SC, Barnes P, Coleman CN, Pomeroy SL, Goumnerova L, et al. A phase I trial of etanidazole and hyperfractionated radiotherapy in children with diffuse brainstem glioma. *Int J Radiat Oncol Biol Phys* (2003) 55 (5):1182–5. doi: 10.1016/S0360-3016(02)04391-2
50. Bradley KA, Pollack IF, Reid JM, Adamson PC, Ames MM, Vezina G, et al. Motexafin gadolinium and involved field radiation therapy for intrinsic pontine glioma of childhood: a Children's Oncology Group phase I study. *Neuro-oncology* (2008) 10(5):752–8. doi: 10.1215/15228517-2008-043
51. Bradley KA, Zhou T, McNall-Knapp RY, Jakacki RI, Levy AS, Vezina G, et al. Motexafin-gadolinium and involved field radiation therapy for intrinsic pontine glioma of childhood: a children's oncology group phase 2 study. *Int J Radiat Oncol Biol Phys* (2013) 85(1):e55–60. doi: 10.1016/j.ijrobp.2012.09.004
52. Broniscer A, Baker SJ, Stewart CF, Merchant TE, Laningham FH, Schaiquevich P, et al. Phase I and pharmacokinetic studies of erlotinib administered concurrently with radiotherapy for children, adolescents, and young adults with high-grade glioma. *Clin Cancer Res an Off J Am Assoc Cancer Res* (2009) 15(2):701–7. doi: 10.1158/1078-0432.CCR-08-1923
53. Geoerger B, Hargrave D, Thomas F, Ndiaye A, Frappaz D, Andreiuolo F, et al. Innovative Therapies for Children with Cancer pediatric phase I study of erlotinib in brainstem glioma and relapsing/refractory brain tumors. *Neuro-oncology* (2011) 13(1):109–18. doi: 10.1093/neuonc/noq141
54. Geyer JR, Stewart CF, Kocak M, Broniscer A, Phillips P, Douglas JG, et al. A phase I and biology study of gefitinib and radiation in children with newly diagnosed brain stem gliomas or supratentorial malignant gliomas. *Eur J Cancer* (2010) 46(18):3287–93. doi: 10.1016/j.ejca.2010.07.005
55. Pollack IF, Stewart CF, Kocak M, Poussaint TY, Broniscer A, Banerjee A, et al. A phase II study of gefitinib and irradiation in children with newly diagnosed brainstem gliomas: a report from the Pediatric Brain Tumor Consortium. *Neuro Oncol* (2011) 13(3):290–7. doi: 10.1093/neuonc/noq199
56. Macy ME, Kieran MW, Chi SN, Cohen KJ, MacDonald TJ, Smith AA, et al. A pediatric trial of radiation/cetuximab followed by irinotecan/cetuximab in newly diagnosed diffuse pontine gliomas and high-grade astrocytomas: A Pediatric Oncology Experimental Therapeutics Investigators' Consortium study. *Pediatr Blood Cancer* (2017) 64(11):10.1002/pbc.26621. doi: 10.1002/pbc.26621
57. Massimino M, Biassoni V, Miceli R, Schiavello E, Warmuth-Metz M, Modena P, et al. Results of nimotuzumab and vinorelbine, radiation and re-irradiation for diffuse pontine glioma in childhood. *J Neuro-Oncol* (2014) 118(2):305–12. doi: 10.1007/s11060-014-1428-z
58. Fleischhack G, Massimino M, Warmuth-Metz M, Khuhlaeva E, Janssen G, Graf N, et al. Nimotuzumab and radiotherapy for treatment of newly diagnosed diffuse intrinsic pontine glioma (DIPG): a phase III clinical study. *J Neurooncol* (2019) 143(1):107–13. doi: 10.1007/s11060-019-03140-z
59. Salloum R, DeWire M, Lane A, Goldman S, Hummel T, Chow L, et al. Patterns of progression in pediatric patients with high-grade glioma or diffuse intrinsic pontine glioma treated with Bevacizumab-based therapy at diagnosis. *J Neuro-Oncol* (2015) 121(3):591–8. doi: 10.1007/s11060-014-1671-3
60. Hummel TR, Salloum R, Drissi R, Kumar S, Sobo M, Goldman S, et al. A pilot study of bevacizumab-based therapy in patients with newly diagnosed high-grade gliomas and diffuse intrinsic pontine gliomas. *J Neuro-Oncol* (2016) 127 (1):53–61. doi: 10.1007/s11060-015-2008-6
61. Grill J, Massimino M, Bouffet E, Azizi AA, McCowage G, Cañete A, et al. Phase II, Open-Label, Randomized, Multicenter Trial (HERBY) of Bevacizumab in Pediatric Patients With Newly Diagnosed High-Grade Glioma. *J Clin Oncol Off J Am Soc Clin Oncol* (2018) 36(10):951–8. doi: 10.1200/JCO.2017.76.0611
62. Broniscer A, Baker JN, Tagen M, Onar-Thomas A, Gilbertson RJ, Davidoff AM, et al. Phase I study of vandetanib during and after radiotherapy in children with diffuse intrinsic pontine glioma. *J Clin Oncol Off J Am Soc Clin Oncol* (2010) 28(31):4762–8. doi: 10.1200/JCO.2010.30.3545
63. Broniscer A, Baker SD, Wetmore C, Pai Panandiker AS, Huang J, Davidoff AM, et al. Phase I trial, pharmacokinetics, and pharmacodynamics of vandetanib and dasatinib in children with newly diagnosed diffuse intrinsic pontine glioma. *Clin Cancer Res an Off J Am Assoc Cancer Res* (2013) 19 (11):3050–8. doi: 10.1158/1078-0432.CCR-13-0306
64. Pollack IF, Jakacki RI, Blaney SM, Hancock ML, Kieran MW, Phillips P, et al. Phase I trial of imatinib in children with newly diagnosed brainstem and recurrent malignant gliomas: a Pediatric Brain Tumor Consortium report. *Neuro-oncology* (2007) 9(2):145–60. doi: 10.1215/15228517-2006-031
65. Wang ZJ, Ge Y, Altinok D, Poulik J, Sood S, Taub JW, et al. Concomitant Use of Panobinostat and Reirradiation in Progressive DIPG: Report of 2 Cases. *J Pediatr Hematol Oncol* (2017) 39(6):e332–e5. doi: 10.1097/MPH.0000000000000806
66. Masoudi A, Elopre M, Amini E, Nagel ME, Ater JL, Gopalakrishnan V, et al. Influence of valproic acid on outcome of high-grade gliomas in children. *Anticancer Res* (2008) 28(4c):2437–42.
67. Felix FH, de Araujo OL, da Trindade KM, Trompieri NM, Fontenele JB. Retrospective evaluation of the outcomes of children with diffuse intrinsic pontine glioma treated with radiochemotherapy and valproic acid in a single center. *J Neurooncol* (2014) 116(2):261–6. doi: 10.1007/s11060-013-1280-6
68. Su JM, Murray JC, McNall-Knapp RY, Bowers DC, Shah S, Adesina AM, et al. A phase 2 study of valproic acid and radiation, followed by maintenance valproic acid and bevacizumab in children with newly diagnosed diffuse intrinsic pontine glioma or high-grade glioma. *Pediatr Blood Cancer* (2020) 67 (6):e28283. doi: 10.1002/pbc.28283
69. Hoffman LM, Geller J, Leach J, Boue D, Drissi R, Chen L, et al. TR-14: A feasibility and randomized phase ii study of vorinostat, bevacizumab, or temozolomide during radiation followed by maintenance chemotherapy in newly-diagnosed pediatric high-grade glioma: children's oncology group study acns0822. *Neuro-Oncology* (2015) 17(Suppl 3):iii39–40. doi: 10.1093/neuonc/nov061.159
70. Castel D, Grill J, Debily MA. Histone H3 genotyping refines clinico-radiological diagnostic and prognostic criteria in DIPG. *Acta Neuropathol* (2016) 131(5):795–6. doi: 10.1007/s00401-016-1568-7
71. Castel D, Philippe C, Calmon R, Le Dret L, Truffaux N, Boddaert N, et al. Histone H3F3A and HIST1H3B K27M mutations define two subgroups of diffuse intrinsic pontine gliomas with different prognosis and phenotypes. *Acta Neuropathol* (2015) 130(6):815–27. doi: 10.1007/s00401-015-1478-0
72. Mackay A, Burford A, Carvalho D, Izquierdo E, Fazal-Salom J, Taylor KR, et al. Integrated Molecular Meta-Analysis of 1,000 Pediatric High-Grade and Diffuse Intrinsic Pontine Glioma. *Cancer Cell* (2017) 32(4):520–37.e5. doi: 10.1016/j.ccell.2017.08.017
73. Buczkowicz P, Hawkins C. Pathology, Molecular Genetics, and Epigenetics of Diffuse Intrinsic Pontine Glioma. *Front Oncol* (2015) 5:147. doi: 10.3389/fonc.2015.00147
74. Koschmann C, Calinescu AA, Nunez FJ, Mackay A, Fazal-Salom J, Thomas D, et al. ATRX loss promotes tumor growth and impairs nonhomologous end joining DNA repair in glioma. *Sci Trans Med* (2016) 8(328):328ra28. doi: 10.1126/scitranslmed.aac8228
75. Pedersen H, Schmiegelow K, Hamerlik P. Radio-Resistance and DNA Repair in Pediatric Diffuse Midline Gliomas. *Cancers* (2020) 12(10):2813. doi: 10.3390/cancers12102813
76. Bao S, Wu Q, McLendon RE, Hao Y, Shi Q, Hjelmeland AB, et al. Glioma stem cells promote radioresistance by preferential activation of the DNA damage response. *Nature* (2006) 444(7120):756–60. doi: 10.1038/nature05236

77. Meel MH, Kaspers GJL, Hulleman E. Preclinical therapeutic targets in diffuse midline glioma. *Drug Resist Updat* (2019) 44:15–25. doi: 10.1016/j.drup.2019.06.001
78. Raso A, Vecchio D, Cappelli E, Ropolo M, Poggi A, Nozza P, et al. Characterization of glioma stem cells through multiple stem cell markers and their specific sensitization to double-strand break-inducing agents by pharmacological inhibition of ataxia telangiectasia mutated protein. *Brain Pathol* (2012) 22(5):677–88. doi: 10.1111/j.1750-3639.2012.00566.x
79. Vecchio D, Daga A, Carra E, Marubbi D, Baio G, Neumaier CE, et al. Predictability, efficacy and safety of radiosensitization of glioblastoma-initiating cells by the ATM inhibitor KU-60019. *Int J Cancer* (2014) 135 (2):479–91. doi: 10.1002/ijc.28680
80. Pezuk JA, Brassesco MS, Morales AG, de Oliveira JC, de Oliveira HF, Scrideli CA, et al. Inhibition of polo-like kinase 1 induces cell cycle arrest and sensitizes glioblastoma cells to ionizing radiation. *Cancer Biother Radiopharm* (2013) 28(7):516–22. doi: 10.1089/cbr.2012.1415
81. Cordero FJ, Huang Z, Grenier C, He X, Hu G, McLendon RE, et al. Histone H3.3K27M Represses p16 to Accelerate Gliomagenesis in a Murine Model of DIPG. *Mol Cancer Res* (2017) 15(9):1243–54. doi: 10.1158/1541-7786.MCR-16-0389
82. King AR, Corso CD, Chen EM, Song E, Bongiorni P, Chen Z, et al. Local DNA Repair Inhibition for Sustained Radiosensitization of High-Grade Gliomas. *Mol Cancer Ther* (2017) 16(8):1456–69. doi: 10.1158/1535-7163.MCT-16-0788
83. Maury E, Hashizume R. Epigenetic modification in chromatin machinery and its deregulation in pediatric brain tumors: Insight into epigenetic therapies. *Epigenetics* (2017) 12(5):353–69. doi: 10.1080/15592294.2016.1278095
84. Piunti A, Hashizume R, Morgan MA, Bartom ET, Horbinski CM, Marshall SA, et al. Therapeutic targeting of polycomb and BET bromodomain proteins in diffuse intrinsic pontine gliomas. *Nat Med* (2017) 23(4):493–500. doi: 10.1038/nm.4296
85. Merchant TE, Pollack IF, Loeffler JS. Brain tumors across the age spectrum: biology, therapy, and late effectsSeminars in radiation oncology. *Semin Radiat Oncol* (2010) 20:(1):58–66. doi: 10.1016/j.semradonc.2009.09.005
86. Ene CI, Kreuser SA, Jung M, Zhang H, Arora S, White Moyes K, et al. Anti-PD-L1 antibody direct activation of macrophages contributes to a radiation-induced abscopal response in glioblastoma. *Neuro-oncology* (2020) 22(5):639–51. doi: 10.1093/neuonc/noz226
87. Pathania M, De Jay N, Maestro N, Harutyunyan AS, Nitarska J, Pahlavan P, et al. H3.3(K27M) Cooperates with Trp53 Loss and PDGFRA Gain in Mouse Embryonic Neural Progenitor Cells to Induce Invasive High-Grade Gliomas. *Cancer Cell* (2017) 32(5):684–700.e9. doi: 10.1016/j.ccell.2017.09.014
88. Kim GB, Rincon Fernandez Pacheco D, Saxon D, Yang A, Sabet S, Dutra-Clarke M, et al. Rapid Generation of Somatic Mouse Mosaics with Locus-Specific, Stably Integrated Transgenic Elements. *Cell* (2019) 179(1):251–67.e24. doi: 10.1016/j.cell.2019.08.013
89. Patel SK, Hartley RM, Wei X, Furnish R, Escobar-Riquelme F, Bear H, et al. Generation of diffuse intrinsic pontine glioma mouse models by brainstem-targeted in utero electroporation. *Neuro Oncol* (2020) 22(3):381–92. doi: 10.1093/neuonc/noz197
90. Haumann R, Videira JC, Kaspers GJL, van Vuurden DG, Hulleman E. Overview of Current Drug Delivery Methods Across the Blood-Brain Barrier for the Treatment of Primary Brain Tumors. *CNS Drugs* (2020) 34 (11):1121–31. doi: 10.1007/s40263-020-00766-w
91. Sasaki T, Katagi H, Goldman S, Becher OJ, Hashizume R. Convection-Enhanced Delivery of Enhancer of Zeste Homolog-2 (EZH2) Inhibitor for the Treatment of Diffuse Intrinsic Pontine Glioma. *Neurosurgery* (2020) 87(6): E680–8. doi: 10.1093/neuonc/noz175.390
92. Louis N, Liu S, He X, Drummond DC, Noble CO, Goldman S, et al. New therapeutic approaches for brainstem tumors: a comparison of delivery routes using nanoliposomal irinotecan in an animal model. *J Neurooncol* (2018) 136 (3):475–84. doi: 10.1007/s11060-017-2681-8

Conflict of Interest: The authors declare that the research was conducted in the absence of any commercial or financial relationships that could be construed as a potential conflict of interest.

frontiers in Oncology

ORIGINAL RESEARCH
published: 27 April 2021
doi: 10.3389/fonc.2021.664928

Extracorporeal Membrane Oxygenation in Children With Cancer or Hematopoietic Cell Transplantation: Single-Center Experience in 20 Consecutive Patients

Jenny C. Potratz[1], Sarah Guddorf[1], Martina Ahlmann[2], Maria Tekaat[1], Claudia Rossig[2], Heymut Omran[1], Katja Masjosthusmann[1] and Andreas H. Groll[2]*

[1] Department of General Pediatrics, University Children's Hospital Münster, Münster, Germany, [2] Department of Pediatric Hematology and Oncology, University Children's Hospital Münster, Münster, Germany

OPEN ACCESS

Edited by:
Graeme MacLaren, National University Hospital, Singapore

Reviewed by:
Warwick Wolf Butt, Royal Children's Hospital, Australia
Thomas Vincent Brogan, Seattle Children's Hospital, United States

***Correspondence:**
Jenny C. Potratz
jenny.potratz@ukmuenster.de

Specialty section:
This article was submitted to Pediatric Oncology, a section of the journal Frontiers in Oncology

Received: *06 February 2021*
Accepted: *06 April 2021*
Published: *27 April 2021*

Citation:
Potratz JC, Guddorf S, Ahlmann M, Tekaat M, Rossig C, Omran H, Masjosthusmann K and Groll AH (2021) Extracorporeal Membrane Oxygenation in Children With Cancer or Hematopoietic Cell Transplantation: Single-Center Experience in 20 Consecutive Patients. Front. Oncol. 11:664928. doi: 10.3389/fonc.2021.664928

Extracorporeal membrane oxygenation (ECMO) is a rescue therapy for severe respiratory and/or circulatory failure. Few data exist on the potential benefit of ECMO in immunocompromised pediatric patients with cancer and/or hematopoietic cell transplantation (HCT). Over a period of 12 years, eleven (1.9%) of 572 patients with new diagnosis of leukemia/lymphoma and nine (3.5%) of 257 patients post allogeneic HCT underwent ECMO at our center. Five (45%) and two (22%) patients, respectively, survived to hospital discharge with a median event-free survival of 4.2 years. Experiences and outcomes in this cohort may aid clinicians and families when considering ECMO for individual patients.

Keywords: extracorporeal membrane oxygenation, leukemia, cancer, transplantation, immunosuppression, children, respiratory failure, infection

INTRODUCTION

Extracorporeal membrane oxygenation (ECMO) technology can provide temporary life support for children with severe respiratory and/or cardiac failure (1). With growing expertise and survival rates of between 40 and 60% overall (1, 2), ECMO has been expanded to children with relevant non-respiratory and non-cardiac co-morbidities (3, 4). Despite an increased risk of life-threatening infections or bleeding due to granulocytopenia and low platelet count, most centers now offer ECMO to children with cancer, and large registries report in-hospital survival rates of 30 to 40% (2–4). In contrast, given the often prolonged and severe immunodeficiency after allogeneic hematopoietic cell transplantation (HCT) with reported in-hospital survival rates of 0 to 20% (4–6), HCT frequently is considered a relative contraindication. Data-driven decision-making to offer or withhold ECMO in patients with cancer or HCT remains difficult, because both groups are extraordinarily heterogeneous and factors predictive of each patients' relative risk or benefit are currently lacking. Recently, detailed oncological characteristics such as interval from diagnosis,

remission status, granulocytopenia and platelet count at ECMO initiation were reported from two large ECMO centers in Europe for nine (7) and twelve (8) patients with hematologic malignancies. Such data may be useful for evaluating patients in the context of decision making for ECMO.

The main objectives of this study were to describe the utilization and outcome of ECMO in children with cancer or HCT at a large pediatric cancer center, and to provide further analyses on indications, co-morbidities, immunodeficiencies and complications in this special population for use in daily practice and future clinical research.

PATIENTS AND METHODS

This single center, retrospective cohort study included all patients (<18 years) who were newly diagnosed with a cancer or had received allogeneic HCT at the Department of Pediatric Hematology and Oncology of the University Children's Hospital Münster between January 2007 (the start of the pediatric intensive care ECMO program) and December 2018. The center's referral patterns and admission data have been reported recently (9). Patients who had received ECMO were identified through Medical Controlling. ECMO indications followed institutional standards that are based on international guidelines by the Extracorporeal Life Support Organization (available at www.elso.org). Indications were a potentially reversible cause of respiratory and/or circulatory failure, with persistent inadequate gas exchange (such as oxygenation index of >30-40, respiratory acidosis with pH <7.1, harmful ventilator settings, imminent right ventricular failure secondary to pulmonary pressures) and/or high need of vasoactive inotrope medication, together resulting in a mortality risk estimated at ≥80% by an interdisciplinary team of pediatric intensivists and oncologists that assessed ECMO indications and contraindications on a case-by-case basis. All patient-related data was captured by a standardized case report form and entered in pseudonymized form into an electronic database. The study was reviewed and approved by the joint ethics committee of the Westfälische Wilhelms-University of Münster and the Chamber of Physicians Westfalen-Lippe (document 2019-225-f-S).

RESULTS

During the 12-years study period, 11 of 572 patients with a new diagnosis of leukemia/lymphoma (1.9%; leukemia, 8; lymphoma, 3) and nine of 257 patients post allogeneic HCT (3.5%; MDS/leukemia, 6; non-malignant disorders, 3) underwent ECMO at our center. No single case was identified among patients receiving treatment for solid tumors or brain tumors and among non-transplanted patients with non-malignant hematological disorders. Demographics, key clinical characteristics and outcome of the 20 patients (median age: 11.2 years; r, 0.2-17.8) are summarized in **Table 1**.

The median time from the start of the last treatment (chemotherapy or conditioning prior to HCT) to ECMO was 28.2 days (r, -1-492). Six patients had co-morbidities (Down syndrome, 1; chronic graft-versus-host disease (GvHD), 2; mediastinal mass syndrome, 1; leukostasis, 1; other, 3). Six patients had received glucocorticosteroids within the last two weeks before ECMO, four according to the respective chemotherapy protocol (median prednisolone equivalent 2.4 mg/kg/day, median duration of administration 14 days) and two for treatment of chronic GvHD (prednisolone equivalent 0.5 and 1 mg/kg/day for >3 months). Nine patients were granulocytopenic (absolute neutrophil count < 500 cells/μL) at the start of ECMO. All 20 patients required ECMO for respiratory failure, three of them also for concurrent circulatory failure. Acute respiratory failure was due to pulmonary (10) or non-pulmonary (2) infection in 15 patients, and due to the underlying malignancy (2) or HCT-associated inflammatory conditions (3; peri-engraftment respiratory distress syndrome/idiopathic pneumonia syndrome) in the remaining five patients. Ten patients received glucocorticosteroids to treat inflammation in the context of acute respiratory failure (median prednisolone equivalent 2.8 mg/kg/day for a median of three days with a median taper of 18 days).

The median duration of ECMO support was 12.2 days (r, 1-48). With the exception of one patient (pt.15, multiple smaller cerebral infarctions, no residual neurologic deficit), complications during ECMO were uniformly associated with death. In two patients, ECMO support was withdrawn within less than 48 hours due to cerebral mass bleeding or leukostasis, respectively. In the remaining 10 non-survivors, ECMO was stopped after a median of 21.4 days (r, 2-48) due to secondary infection (1), pulmonary hemorrhage (1), persistent isolated pulmonary failure (2) and multi-organ failure (6). In the two non-survivors with persistent isolated pulmonary failure, lung damage was considered irreversible on the basis of progressive pulmonary fibrosis and pulmonary hypertension (pt. 8), and diffuse alveolar hemorrhage probably associated with pre-existing sickle cell-associated lung damage underestimated at ECMO indication (pt. 20). One patient died three days after weaning off ECMO from septic shock due to a secondary infection. Seven patients (35%) survived to hospital discharge and are long-term survivors with a median follow-up of 4.2 years (r, 1.9-7.5) (**Figure 1**).

Supplementary Table 1 shows selected clinical data and scores at baseline and during ECMO tabulated for the entire cohort and according to HCT status. Due to the small number of patients enrolled, no obvious signal for meaningful differences relative to HCT status can be seen. Comparison of survivors and non-survivors, in contrast, shows a trend towards a lower vasoactive inotrope score at ECMO initiation, and shorter duration of granulocytopenia, absence of infectious or bleeding complications, and absence of non-pulmonary organ failures during ECMO in surviving patients (**Supplementary Table 2**).

DISCUSSION

In this single-center cohort study, the utilization of ECMO in children diagnosed with hematologic malignancies was 1.9%, which is comparable to the 1.3% reported by the Swedish childhood cancer registry (8). With 45% survival to hospital discharge, outcome in our series was similar to the 44% and 50%

TABLE 1 | Clinical characteristics of 20 consecutive ECMO patients.

Pt. No.	Year	Age (years) gender (m/f)	Underlying disease	Treatment/ protocol prior to ECMO (days post HCT)	Time since diagnosis/ start of last treatment (days)	Relevant co-morbidities	Steroid[a] treatment of disease or co-morbidity	Granulocytopenia at start of ECMO	Type of ECMO support	Indication for ECMO	Steroid[b] treatment of ECMO indication	Duration of ECMO (days)	ECMO-related complications	Outcome and cause of death
1	2008	8.4 m	ALL (CR1)	Protocol II, ALL-BFM 2000	206/39	None	No	No	R, VV	Pneumonia (Influenza B)	No	21	Infection (sepsis of unknown etiology)	Dead (ECMO withdrawal: secondary sepsis)
2	2010	10.7 f	FA, MDS	HCT (d+483), n/a	983/492	GvHD, BOOP	Yes	No	R, VV	Pneumonia (Influenza A)	No	1	Hemorrhage (cerebral)	Dead (ECMO withdrawal: cerebral hemorrhage)
3	2013	0.6 f	AML M6 (CR1)	ADxE induction, AML-BFM 2012	27/25	None	No	Yes	R, VA	Pneumonia (RSV A)	Yes	9	–	Alive; follow-up: 90 months
4	2014	2.1 f	AML M7 (CR1)	AIE induction, ML-DS 2006	30/29	Trisomy 21	No	Yes	R, VA	Pneumonia (RSV B)	Yes	11	–	Alive; follow-up: 74 months
5	2014	17.7 m	ALL (CR1)	HCT (d+65), ALL SZT-BFM 2003	267/73	AKI	No	No	R, VV	Pneumonia (CMV)	Yes	21	Infection (VRE sepsis), RRT	Dead (ECMO withdrawal: MOF, hypoxic cardiac failure)
6	2014	16.2 m	HD	OEPA, GPOH HD registry	68/19	None	Yes	No	R, VV	Sepsis (*E. coli*), ARDS, pulmonary hemorrhage	No	13	Hemorrhage (pulmonary), RRT	Dead (ECMO withdrawal: MOF, pulmonary failure)
7	2014	1.1 f	AML M2 (CR2)	HCT (d+4), AML SCT-BFM 2007	259/12	None	No	Yes	R, VA	Pneumonia (PIV-3)	Yes	11	Hemorrhage (mucosal, cannula), RRT	Dead (ECMO withdrawal: MOF, abdom. compartment)
8	2015	17.4 f	CHH	HCT (d+32), n/a	253/40	CLD	No	No	R, VV	IPS	Yes	24	Hemorrhage (mucosal), RRT	Dead (ECMO withdrawal: pulmonary fibrosis with PH)
9	2015	15.6 m	ALL (CR1)	HR3, AIEOP ALL-BFM 2009	169/20	None	Yes	Yes	R, VV	Pneumonia (PIV-3), pulmonary hemorrhage	No	15	Infection (*Aspergillus niger*), RRT	Dead (septic shock 3 days after ECMO)
10	2015	11.9 f	ALL (CR1)	Protocol IIIb, AIEOP ALL-BFM 2009	353/9	None	No	Yes	R, VV	Pneumonia (unknown etiology)	No	17	–	Alive; follow-up: 53 months
11	2016	15.3 f	ALL (CR2)	HCT (d+15), ALL SCT 2012 FORUM	582/21	None	No	Yes	R, VV	Pneumonia (HMPV; *Aspergillus fumigatus*)	Yes	34	Infection (*Enterobacter cloacae* sepsis)	Dead (ECMO withdrawal: MOF, pulmonary failure)

(Continued)

TABLE 1 | Continued

Pt. No.	Year	Age (years) gender (m/f)	Underlying disease	Treatment/ protocol prior to ECMO (days post HCT)	Time since diagnosis/ start of last treatment (days)	Relevant co-morbidities	Steroid[a] treatment of disease or co-morbidity	Granulocytopenia at start of ECMO	Type of ECMO support	Indication for ECMO	Steroid[b] treatment of ECMO indication	Duration of ECMO (days)	ECMO-related complications	Outcome and cause of death
12	2016	14.6 m	ALL (CR2)	HCT (d+21), ALL SZT-BFM 2003	904/28	Hepatitis C	No	Yes	R, VV	PERDS	Yes	4	–	Alive; follow-up: 51 months
13	2016	11.6 f	ALL (diagnosis)	n/a	0/n/a	None	No	Yes	R, VV	Pneumonia (*S. aureus*), pulmonary hemorrhage, sepsis	No	48	Infection (SMA), RRT, Hemorrhage (surgery)	Dead (ECMO withdrawal: MOF, pulmonary abscesses)
14	2016	17.8 m	ALL (CR1)	HCT (d+237), ALL SZT-BFM 2003	420/239	GvHD	Yes	Yes	R, VV	Sepsis (3MRGN *E. coli*, SMA), ARDS	No	2	Hemorrhage (pulmonary), RRT	Dead (ECMO withdrawal: pulmonary hemorrhage)
15	2017	15.8 m	LBL (diagnosis)	n/a	0/n/a	Mediastinal mass	No	No	R + C, VA	Mediastinal compression syndrome	No	2	Neurologic (embolic cerebral infarctions)	Alive; follow-up: 33 months
16	2018	0.2 f	Familial HLH	HCT (+19), n/a	93/29	None	No	No	R, VA	IPS	Yes	10	–	Alive; follow-up: 26 months
17	2018	1.7 m	AML M5 (diagnosis)	Prephase, AML-BFM registry	1/1	Leukostasis	No	No	R + C, VA	Pulmonary leukostasis	No	1	Neurologic (infarction)	Dead (ECMO withdrawal: leukostasis)
18	2018	9.8 m	ALL (CR2)	SCA1, IntReALL SR 2010	1350/37	None	Yes	No	R, VV	PERDS, Pneumonia (*Aspergillus fumigatus*)	Yes	27	Infection (CMV), hemorrhage (intestinal)	Dead (on ECMO: MOF, secondary HLH)
19	2018	3.2 m	LBL (CR1)	Protocol II/a, NHL-BFM registry	209/29	None	Yes	No	R + C, VA	Sepsis (Coag. neg. *Staph*), ARDS (Coronavirus OC43)	No	6	–	Alive; follow-up: 23 months
20	2018	5.9 m	SCD	HCT (d+41), n/a	893/48	None	No	No	R, VV	Pneumonia (Bocavirus), diffuse alveolar hemorrhage	Yes	48	–	Dead (ECMO withdrawal: persistent pulmonary failure)

ECMO, extracorporeal membrane oxygenation; HCT, hematopoietic stem cell transplantation; n/a, not applicable; underlying disease: ALL, acute lymphoblastic leukemia; FA, Fanconi anemia; MDS, myelodysplastic syndrome; AML, acute myeloblastic leukemia; HD, Hodgkin disease; CHH, cartilage-hair hypoplasia; LBL, lymphoblastic lymphoma; HLH, hemophagocytic lymphohistiocytosis; SCD, sickle cell disease; CR, complete remission; co-morbidities: GvHD, graft-versus-host-disease; BOOP, bronchiolitis obliterans organizing pneumonia; AKI, acute kidney injury; CLD, chronic lung disease; ECMO support: R, respiratory; C, circulatory; VV, veno-venous cannulation; VA, veno-arterial cannulation; ECMO indication: ARDS, acute respiratory distress syndrome; IPS, idiopathic pneumonia syndrome; PERDS, peri-engraftment respiratory failure; pathogens: RSV, respiratory syncytial virus; CMV, cytomegalovirus; PIV-3, Parainfluenza virus 3; HMPV, human metapneumovirus; MRGN, multidrug-resistant Gram-negative; SMA, Stenotrophomonas maltophilia; Staph, Staphylococcus; VRE, vancomycin-resistant Enterococcus; complications: RRT, renal replacement therapy; cause of death: MOF, multi-organ failure; PH, pulmonary arterial hypertension.

[a]*Treatment with glucocorticosteroids within two weeks prior to ECMO.*

[b]*Glucocorticosteroids for treatment of acute illness leading to ECMO.*

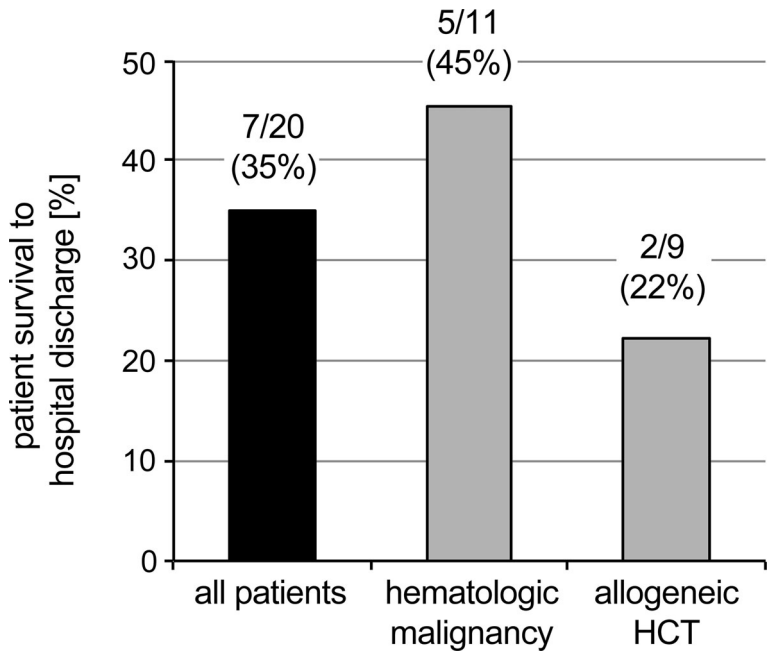

FIGURE 1 | Survival status of ECMO patients. Solid bar: Survival status of the entire cohort. Shaded bars: Survival of patients without allogeneic HCT (left) compared to patients with status post allogeneic HCT (right).

recently reported from two European high-volume ECMO centers (7, 8). These survival rates are comparable to other high-risk ECMO settings such as for pertussis, cardiopulmonary resuscitation or neonatal cardiac failure (1). A summary of selected studies reporting ECMO outcomes in children with hematologic malignancies or allogeneic HCT is provided in **Supplementary Table 3**. In patients post allogeneic HCT, the use of ECMO at our center was approximately two-fold higher than in patients with hematological malignancies (3.5%). Two of nine patients (22%) survived to discharge, which is within the range of data from the U.S. Pediatric Health Information System database and the Extracorporeal Life Support Organization (ELSO) registry (4, 6, 11). The fact that all seven patients surviving to discharge also are long-term survivors is notable considering the high rates of mortality reported within the first 90 days post ECMO treatment (12, 13).

While, despite signals for improved survival of ECMO in more recent years (10, 11), status post allogeneic HCT, a diagnosis of leukemia, and granulocytopenia remain to be generally associated with higher odds of mortality relative to non-immunocompromised patients (4), clinical variables in our patients at initiation and during ECMO do not show any evidence for additional differences between patients post allogeneic HCT and those receiving chemotherapy for hematological malignancies. Indeed, although not reaching statistical significance, exploration of differences between survivors and non-survivors suggest a low vasoactive inotrope score (VIS) at initiation of ECMO, shorter duration of granulocytopenia, absence of emerging infections and bleeding complications, and absence of non-pulmonary organ failure during ECMO as being associated with survival.

Existing scores that incorporate cancer as global high-risk diagnosis when estimating mortality at ICU admission or ECMO initiation, such as PIM3 (14), P-PREP (15) or Ped-RESCUERS (16), did not distinguish survivors and non-survivors in our cohort. To better predict chances of survival, scores capturing information that is more relevant to the status of patients with hematological malignancies and allogeneic HCT in the context of intensive care support and ECMO would be highly desirable, and well-established Pediatric Oncology databases and study groups may be able to contribute detailed and robust data, specifically on pre-ECMO variables. At present, consistent with our experience, the development of new infections, major hemorrhage, and organ complications while on ECMO seem to be the main variables associated with unfavorable outcome (2, 7, 8, 17), and multi-organ failure is a leading cause of ECMO withdrawal and death (2, 6, 7). In this context, the systematic use of scores [e.g. daily PELOD-2 (18)] could help to identify and compare guidance for stopping of ECMO across centers.

Obvious limitations of the current analysis include its retrospective, single-center format with analysis of a small cohort of inhomogeneous patients that precludes robust statistical analyses of unfavorable outcome; and the absence of detailed data on functional, cognitive, behavioral and quality of life outcomes in the surviving patients. Despite these limitations, the analysis of this cohort of unselected, consecutive patients supports the notion that ECMO can offer a chance for survival to children with hematological malignancies or allogeneic HCT who are treated in curative intention and develop respiratory and/or cardiovascular failure due to a presumably reversible acute disease process. Nevertheless, morbidity and mortality of

this invasive rescue therapy remain high. As recently stated (19), to offer or withhold ECMO in immunocompromised children with potentially reversible respiratory or cardiorespiratory failure should therefore remain a careful patient- and family-centered decision made with the support of a multidisciplinary expert team.

DATA AVAILABILITY STATEMENT

The raw data supporting the conclusions of this article will be made available by the authors, without undue reservation.

ETHICS STATEMENT

The studies involving human participants were reviewed and approved by the ethics committee of the Westfälische Wilhelms-University of Münster and the Chamber of Physicians Westfalen-Lippe (document 2019-225-f-S). Written informed consent from the participants' legal guardian/next of kin was not required to participate in this study in accordance with the national legislation and the institutional requirements.

AUTHOR CONTRIBUTIONS

JP, KM, and AG contributed to conception and design of the study. JP, SG, MA, MT, CR, and HO acquired data. JP, SG, and AG analyzed the data. JP performed the statistical analysis. JP, SG, KM, and AG interpreted the data. JP, KM, and AG supervised the project. JP and AG wrote the manuscript. All authors contributed to manuscript revision, read, and approved the submitted version.

ACKNOWLEDGMENTS

The authors would like to acknowledge the contributions of the patients described in this study and those of the medical staff caring for them. The authors also thank the members of the Clinical Research Unit of the Department of Pediatric Hematology and Oncology for their invaluable support.

SUPPLEMENTARY MATERIAL

The Supplementary Material for this article can be found online at: https://www.frontiersin.org/articles/10.3389/fonc.2021.664928/full#supplementary-material

REFERENCES

1. Barbaro RP, Paden ML, Guner YS, Raman L, Ryerson LM, Alexander P, et al. Pediatric Extracorporeal Life Support Organization Registry International Report 2016. *ASAIO J* (2017) 63:456–63. doi: 10.1097/MAT.0000000000000603
2. Gow KW, Heiss KF, Wulkan ML, Katzenstein HM, Rosenberg ES, Heard ML, et al. Extracorporeal Life Support for Support of Children With Malignancy and Respiratory or Cardiac Failure: The Extracorporeal Life Support Experience. *Crit Care Med* (2009) 37:1308–16. doi: 10.1097/CCM.0b013e31819cf01a
3. Zabrocki LA, Brogan TV, Statler KD, Poss WB, Rollins MD, Bratton SL. Extracorporeal Membrane Oxygenation for Pediatric Respiratory Failure: Survival and Predictors of Mortality. *Crit Care Med* (2011) 39:364–70. doi: 10.1097/CCM.0b013e3181fb7b35
4. Coleman RD, Goldman J, Moffett B, Guffey D, Loftis L, Thomas J, et al. Extracorporeal Membrane Oxygenation Mortality in High-Risk Populations: An Analysis of the Pediatric Health Information System Database. *ASAIO J* (2020) 66:327–31. doi: 10.1097/MAT.0000000000001002
5. Gupta M, Shanley TP, Moler FW. Extracorporeal Life Support for Severe Respiratory Failure in Children With Immune Compromised Conditions. *Pediatr Crit Care Med* (2008) 9:380–5. doi: 10.1097/PCC.0b013e318172d54d
6. Di Nardo M, Locatelli F, Palmer K, Amodeo A, Lorusso R, Belliato M, et al. Extracorporeal Membrane Oxygenation in Pediatric Recipients of Hematopoietic Stem Cell Transplantation: An Updated Analysis of the Extracorporeal Life Support Organization Experience. *Intensive Care Med* (2014) 40:754–6. doi: 10.1007/s00134-014-3240-9
7. Cortina G, Neu N, Kropshofer G, Meister B, Klingkowski U, Crazzolara R. Extracorporeal Membrane Oxygenation Offers Long-Term Survival in Childhood Leukemia and Acute Respiratory Failure. *Crit Care* (2018) 22:222. doi: 10.1186/s13054-018-2134-6
8. Ranta S, Kalzén H, Nilsson A, Schewelov von K, Broman LM, Berner J, et al. Extracorporeal Membrane Oxygenation Support in Children With Hematological Malignancies in Sweden. *J Pediatr Hematol Oncol* (2020) 43: e272–75. doi: 10.1097/MPH.0000000000001808
9. Barking CTMM, Masjosthusmann K, Rellensmann G, Ehlert K, Zöllner S, Jocham S, et al. Treatment of Children With Cancer and/or Hematopoietic Stem Cell Transplantation in the Intensive Care Unit: Experience At a Large European Pediatric Cancer Center. *J Pediatr Hematol Oncol* (2020) 42:e583–8. doi: 10.1097/MPH.0000000000001718
10. Steppan DA, Coleman RD, Viamonte HK, Hanson SJ, Carroll MK, Klein OR, et al. Outcomes of Pediatric Patients With Oncologic Disease or Following Hematopoietic Stem Cell Transplant Supported on Extracorporeal Membrane Oxygenation: The PEDECOR Experience. *Pediatr Blood Cancer* (2020) 67: e28403. doi: 10.1002/pbc.28403
11. Olson TL, O'Neil ER, Kurtz KJ, MacLaren G, Anders MM. Improving Outcomes for Children Requiring Extracorporeal Membrane Oxygenation Therapy Following Hematopoietic Stem Cell Transplantation. *Crit Care Med* (2021) 49:e381–93. doi: 10.1097/CCM.0000000000004850
12. Bahr von V, Hultman J, Eksborg S, Gerleman R, Enstad Ø, Frenckner B, et al. Long-Term Survival and Causes of Late Death in Children Treated With Extracorporeal Membrane Oxygenation. *Pediatr Crit Care Med* (2017) 18:272–80. doi: 10.1097/PCC.0000000000001069
13. Smith S, Butt W, Best D, MacLaren G. Long-Term Survival After Extracorporeal Life Support in Children With Neutropenic Sepsis. *Intensive Care Med* (2016) 42:942–3. doi: 10.1007/s00134-015-4163-9
14. Straney L, Clements A, Parslow RC, Pearson G, Shann F, Alexander J, et al. Anzics Paediatric Study Group and the Paediatric Intensive Care Audit Network. Paediatric Index of Mortality 3: An Updated Model for Predicting Mortality in Pediatric Intensive Care*. *Pediatr Crit Care Med* (2013) 14:673–81. doi: 10.1097/PCC.0b013e31829760cf
15. Bailly DK, Reeder RW, Zabrocki LA, Hubbard AM, Wilkes J, Bratton SL, et al. Extracorporeal Life Support Organization Member Centers. Development and Validation of a Score to Predict Mortality in Children Undergoing Extracorporeal Membrane Oxygenation for Respiratory Failure: Pediatric Pulmonary Rescue With Extracorporeal Membrane Oxygenation Prediction Score. *Crit Care Med* (2017) 45:e58–66. doi: 10.1097/CCM.0000000000002019
16. Barbaro RP, Boonstra PS, Paden ML, Roberts LA, Annich GM, Bartlett RH, et al. Development and Validation of the Pediatric Risk Estimate Score for Children Using Extracorporeal Respiratory Support (Ped-RESCUERS). *Intensive Care Med* (2016) 42:879–88. doi: 10.1007/s00134-016-4285-8

17. Gow KW, Wulkan ML, Heiss KF, Haight AE, Heard ML, Rycus P, et al. Extracorporeal Membrane Oxygenation for Support of Children After Hematopoietic Stem Cell Transplantation: The Extracorporeal Life Support Organization Experience. *J Pediatr Surg* (2006) 41:662–7. doi: 10.1016/j.jpedsurg.2005.12.006
18. Leteurtre S, Duhamel A, Deken V, Lacroix J, Leclerc F. Groupe Francophone De Réanimation Et Urgences Pédiatriques. Daily Estimation of the Severity of Organ Dysfunctions in Critically Ill Children by Using the PELOD-2 Score. *Crit Care* (2015) 19:324–6. doi: 10.1186/s13054-015-1054-y
19. Alexander PMA, Thiagarajan RR. Pediatric oncology-The Final Frontier for Extracorporeal Membrane Oxygenation in Children? *Pediatr Blood Cancer* (2020) 67:e28521. doi: 10.1002/pbc.28521

Conflict of Interest: The authors declare that the research was conducted in the absence of any commercial or financial relationships that could be construed as a potential conflict of interest.

frontiers in Oncology

ORIGINAL RESEARCH
published: 08 June 2021
doi: 10.3389/fonc.2021.660892

Phase 2 Study of Pomalidomide (CC-4047) Monotherapy for Children and Young Adults With Recurrent or Progressive Primary Brain Tumors

Jason Fangusaro[1], Maria Giuseppina Cefalo[2], Maria Luisa Garré[3], Lynley V. Marshall[4], Maura Massimino[5], Bouchra Benettaib[6], Noha Biserna[6], Jennifer Poon[6], Jackie Quan[6], Erin Conlin[6], John Lewandowski[6], Mathew Simcock[7], Neelum Jeste[6], Darren R. Hargrave[8], François Doz[9‡] and Katherine E. Warren[10†‡]*

[1] Department of Pediatrics, Children's Healthcare of Atlanta and Aflac Cancer Center at Emory University Medical School, Atlanta, GA, United States, [2] Department of Hematology/Oncology and Stem Cell Transplantation, IRCCS Bambino Gesù Children's Hospital, Rome, Italy, [3] Neuro-Oncology Unit, Istituto Giannina Gaslini, Genoa, Italy, [4] Children and Young People's Unit, The Royal Marsden Hospital and The Institute of Cancer Research, London, United Kingdom, [5] Pediatric Oncology Unit, Fondazione IRCCS Istituto Nazionale dei Tumori, Milan, Italy, [6] Bristol Myers Squibb, Princeton, NJ, United States, [7] Celgene Corporation, Uxbridge, United Kingdom, [8] Pediatric Oncology Unit, UCL Great Ormond Street Hospital for Children, London, United Kingdom, [9] Department of Pediatric Oncology, Institut Curie and University of Paris, Paris, France, [10] National Cancer Institute, National Institutes of Health, Bethesda, MD, United States

Introduction: Treatment of recurrent primary pediatric brain tumors remains a major challenge, with most children succumbing to their disease. We conducted a prospective phase 2 study investigating the safety and efficacy of pomalidomide (POM) in children and young adults with recurrent and progressive primary brain tumors.

Methods: Patients with recurrent and progressive high-grade glioma (HGG), diffuse intrinsic pontine glioma (DIPG), ependymoma, or medulloblastoma received POM 2.6 mg/m^2/day (the recommended phase 2 dose [RP2D]) on days 1-21 of a 28-day cycle. A Simon's Optimal 2-stage design was used to determine efficacy. Primary endpoints included objective response (OR) and long-term stable disease (LTSD) rates. Secondary endpoints included duration of response, progression-free survival (PFS), overall survival (OS), and safety.

Results: 46 patients were evaluable for response (HGG, n = 19; DIPG, ependymoma, and medulloblastoma, n = 9 each). Two patients with HGG achieved OR or LTSD (10.5% [95% CI, 1.3%-33.1%]; 1 partial response and 1 LTSD) and 1 patient with ependymoma had LTSD (11.1% [95% CI, 0.3%-48.2%]). There were no ORs or LTSD in the DIPG or medulloblastoma cohorts. The median PFS for patients with HGG, DIPG, ependymoma, and medulloblastoma was 7.86, 11.29, 8.43, and 8.43 weeks, respectively. Median OS was 5.06, 3.78, 12.02, and 11.60 months, respectively. Neutropenia was the most common grade 3/4 adverse event.

Conclusions: Treatment with POM monotherapy did not meet the primary measure of success in any cohort. Future studies are needed to evaluate if POM would show efficacy in tumors with specific molecular signatures or in combination with other anticancer agents.

OPEN ACCESS

Edited by:
Jaume Mora, Hospital Sant Joan de Déu Barcelona, Spain

Reviewed by:
Andres E. Morales La Madrid, Hospital Sant Joan de Déu Barcelona, Spain
Stephen C. Mack, Baylor College of Medicine, United States

****Correspondence:***
Jason Fangusaro
jfangus@emory.edu

†Present address:
Katherine E. Warren, Department of Pediatric Oncology, Dana-Farber Cancer Institute, Boston, MA, United States

‡These authors have contributed equally to this work and share senior authorship

Specialty section:
This article was submitted to Pediatric Oncology, a section of the journal Frontiers in Oncology

Received: *29 January 2021*
Accepted: *23 March 2021*
Published: *08 June 2021*

Citation:
Fangusaro J, Cefalo MG, Garré ML, Marshall LV, Massimino M, Benettaib B, Biserna N, Poon J, Quan J, Conlin E, Lewandowski J, Simcock M, Jeste N, Hargrave DR, Doz F and Warren KE (2021) Phase 2 Study of Pomalidomide (CC-4047) Monotherapy for Children and Young Adults With Recurrent or Progressive Primary Brain Tumors. Front. Oncol. 11:660892. doi: 10.3389/fonc.2021.660892

Clinical Trial Registration: ClinicalTrials.gov, identifier NCT03257631; EudraCT, identifier 2016-002903-25.

Keywords: diffuse intrinsic pontine glioma, ependymoma, high-grade glioma, medulloblastoma, pomalidomide, progressive or recurrent disease

INTRODUCTION

Central nervous system (CNS) tumors represent the second most common pediatric cancer and remain the leading cause of childhood cancer-related mortality (1–3). In children and adolescents, high-grade glioma (HGG World Health Organization grades III and IV), diffuse intrinsic pontine glioma (DIPG), medulloblastoma, and ependymoma represent the majority of malignant primary brain and CNS tumors (4–6). The 5-year overall survival (OS) rate for patients with HGG ranges between 10% to 20% while the OS rate for DIPG is less than 10% to 15% (7). In addition, most patients with recurrent medulloblastoma and ependymoma will die from progressive disease despite treatment (5, 6). The need for alternative and efficacious treatment options is further compounded by treatment-associated morbidities with treatments such as radiation and classic cytotoxic chemotherapies, which can impact a child's quality of life and functional outcomes (8–14).

Novel agents with unique mechanisms of action may help to overcome these barriers. Immunomodulatory agents, including pomalidomide (POM), thalidomide, and lenalidomide, have demonstrated anti-inflammatory properties (including T-cell activation and proinflammatory cytokine inhibition), angiogenesis inhibition, and induction of antiproliferative activities (15–23). Furthermore, POM has been shown to penetrate the blood-brain barrier (24). The multimodal mechanism of action and ability to cross the blood-brain barrier suggest that POM may represent a unique approach for addressing the unmet needs in primary pediatric CNS tumors.

A Pediatric Brain Tumor Consortium (PBTC) phase 1 trial of pediatric patients with recurrent, refractory, or progressive primary CNS tumors demonstrated tolerability of lenalidomide at doses exceeding those in adults as well as evidence of activity within the confines of a phase 1 study (25). Myelosuppression was the most common adverse event (AE) during the dose-finding part of the study (25). Another PBTC phase 1 study in children with recurrent, progressive/refractory CNS tumors identified the POM maximum-tolerated dose as 2.6 mg/m^2; diarrhea, thrombocytopenia, and lung infection were dose-limiting toxicities (26). Subsequently, 12 additional patients were enrolled based on age and steroid use, and there was no obvious difference in tolerability observed based on these factors (26). POM exposure increased in a dose-dependent manner, similar to what has been observed in adults (26). In this trial, one patient with an oligodendroglioma achieved long-term stable disease (LTSD) and one patient with an anaplastic pleomorphic xanthoastrocytoma achieved a partial response (PR).

The preliminary safety and efficacy data in this PBTC phase 1 study led to the development of the current phase 2 study where we investigated safety and efficacy of POM in children and young adults with recurrent or progressive primary CNS tumors at the RP2D.

MATERIALS AND METHODS

Study Oversight

The study was approved by the institutional review board or ethics committee at each participating study site prior to initiation. This study was conducted in accordance with the Declaration of Helsinki and Good Clinical Practice Guidelines of the International Council for Harmonisation. Written informed consent (and assent when appropriate) was obtained from each patient and/or their legal guardian prior to study entry. The protocol is included in the **Supplementary Materials**.

Patients

Eligible patients included those aged 1 to < 21 years with a diagnosis of recurrent or progressive primary HGG, DIPG, ependymoma, or medulloblastoma. Patients must have received ≥1 prior standard therapy (or a generally accepted upfront therapy if no standard existed) and have no known curative therapeutic alternative. Other key inclusion criteria were tumor located in the brain, histologic verification at the time of either diagnosis or recurrence (patients with DIPG were exempt from histologic verification if they had typical clinical course and magnetic resonance imaging [MRI] findings of DIPG), and measurable disease (primary brain tumor that was measurable in 2 perpendicular diameters on MRI). Patients were required to have a Lansky or Karnofsky functional performance status score ≥ 50 at screening, as well as adequate renal, hepatic, pulmonary, and bone marrow function. Prior to enrollment, patients must have recovered from any clinically significant acute treatment-related AEs associated with prior therapies and had no significant worsening in clinical status for a minimum of 7 days prior to the first dose of POM.

Treatment

Patients started POM at the RP2D of 2.6 mg/m^2/day once daily on days 1-21 of each 28-day treatment cycle, followed by a 7-day rest period (26). Treatment could continue for up to 24 cycles or until progressive disease, consent withdrawal, treatment intolerance, or death.

Study Design and Power Calculation

This phase 2, multicenter, international, open-label, parallel-group study assessed POM using a Simon's Optimal 2-stage design (**Supplementary Figure 1**). Under Simon's Optimal 2-stage design with a 5% significance level and 90% power,

assuming a lower boundary of interest in the objective response (OR) and long-term stable disease rate of 10% and an upper boundary of interest in the OR and LTSD rate of 40%, a total of 20 patients evaluable for the primary endpoint were required per cohort: 9 in stage 1 and an additional 11 in stage 2.

In stage 1, 9 patients were enrolled for each primary brain tumor type (cohort). During stage 1, if ≥ 2 patients in any given cohort achieved either an OR (complete response or PR) within the first 6 cycles of treatment (first 3 cycles for DIPG) or achieved LTSD (maintained for ≥ 6 cycles [≥ 3 cycles for DIPG]), an additional 11 patients were enrolled for a total of 20 patients per cohort. During stages 1 and 2, if ≥ 5 patients among the 20 in a given cohort achieved either OR or LTSD within the specified time, POM would be considered effective in that disease indication. The study was registered at ClinicalTrials.gov (NCT03257631) and EudraCT (2016–002903–25).

Endpoints

The primary endpoint was the proportion of patients achieving either OR or LTSD. The secondary endpoints were duration of response (DOR), progression-free survival (PFS), and OS (all of which were assessed using Kaplan-Meier curves) as well as safety. POM pharmacokinetics was an exploratory endpoint. Efficacy endpoints were assessed in the response population, which included all enrolled patients who received ≥ 1 cycle of POM or who withdrew prior to completing 1 cycle of POM due to disease progression; patients who withdrew treatment for any reason other than disease progression prior to completing 1 cycle of POM were replaced. Treatment exposure, dose modification, and safety data were assessed in the safety population.

Assessments and Follow-Up

Brain tumor assessments were conducted by standard MRI (with and without contrast) using 3 sequences (T1-weighted pre- and postcontrast, T2-weighted, and fluid-attenuated inversion recovery). Brain MRI assessments were conducted during screening and then on day 1 of cycles 3, 5, 7, 10, 13, 16, 19, and 22; after completion of cycle 24; and as clinically indicated. For patients with DIPG only, post-baseline brain MRI assessments were performed on day 1 of cycles 4, 7, 10, 13, 16, 19, and 22; after completion of cycle 24; and as clinically indicated. Radiographic OR was assessed using the sequence best representative of the tumor in the opinion of the neuroradiologist (the same sequence was used for serial measurements). Patients who did not meet the criteria for response or disease progression by the end of cycle 6 (end of cycle 3 for DIPG) were considered to have LTSD.

Response evaluations were assessed both locally and by an independent central reviewer; the local investigator assessment was used for patient eligibility and treatment decisions. Efficacy-based endpoints incorporating tumor assessments were based on the independent central assessment. For DOR, PFS, and OS, median values and corresponding 95% CIs were estimated using Kaplan-Meier methods.

Adverse events were coded according to the Medical Dictionary for Regulatory Activities. The severity and intensity of AEs were graded based upon patient symptoms according to the National Cancer Institute Common Terminology Criteria for AEs (version 4.03). Laboratory assessments were performed locally and at each scheduled visit.

Whole blood samples were collected for pharmacokinetics analyses at the time of POM administration (pre-dose) and 2 hours following POM administration on days 8 and 15 of cycle 1. Plasma concentrations of POM were summarized by geometric mean and geometric coefficient of variation.

After POM discontinuation, patients were followed every 3 months (± 14 days) from the 28-day post-treatment safety follow-up visit for second primary malignancies (regardless of causal relationship), any drug-related serious AEs, OS, and start of any new anticancer therapies. Follow-up continued for up to 5 years after last patient enrollment unless a patient withdrew consent, was lost to follow-up, or died.

RESULTS

Patient Disposition and Baseline Characteristics

Of 57 patients who were screened for eligibility, 53 were enrolled at 18 institutions in France (n = 5), Italy (n = 3), Spain (n = 2), the United Kingdom (n = 3), and the United States (n = 5). Four patients were screened but not enrolled due to screen failure (n = 3) and death (n = 1). One enrolled patient did not receive study treatment. Patients were treated between August 2017 and March 2019. As of the database cutoff date (March 15, 2019), 2 patients were still on treatment (1 each in the HGG and DIPG cohorts [the patient with DIPG was not part of the response population]). The remaining 50 patients discontinued POM treatment due to progressive disease (84.0%), death (6.0%), withdrawal by parent or guardian (6.0%), or AE (4.0%) (**Figure 1**). The response population consisted of 46 patients (19 patients with HGG; 9 patients each with DIPG, ependymoma, or medulloblastoma).

Baseline characteristics are reported in **Table 1**. The median age was 11.5 years (range, 4-18 years), and most patients were male (63.5%). Overall, patients received a median of 3 (range, 1-17) previous systemic therapies.

Efficacy

The median follow-up time for all patients was 4.86 months (range, 0.6-17.2 months). For the primary analyses (response population), the OR and LTSD rates were 10.5% (1 PR and 1 LTSD) for HGG and 11.1% (1 LTSD) for ependymoma (**Table 2**). All 3 patients with PR or LTSD had received radiation treatment as part of an upfront therapy. No OR or LTSD was recorded in the DIPG or medulloblastoma cohorts.

The independently assessed PFS analysis was based on 17 (89.5%), 9 (100.0%), 9 (100.0%), and 8 (88.9%) events for patients in the response population with HGG, DIPG, ependymoma, and medulloblastoma, respectively (**Table 3**). The median PFS values were 7.86, 11.29, 8.43, and 8.43 weeks, respectively. The OS analysis was based on 12 (63.2%), 7 (77.8%), 5 (55.6%), and 4 (44.4%) events for patients in the response population with HGG,

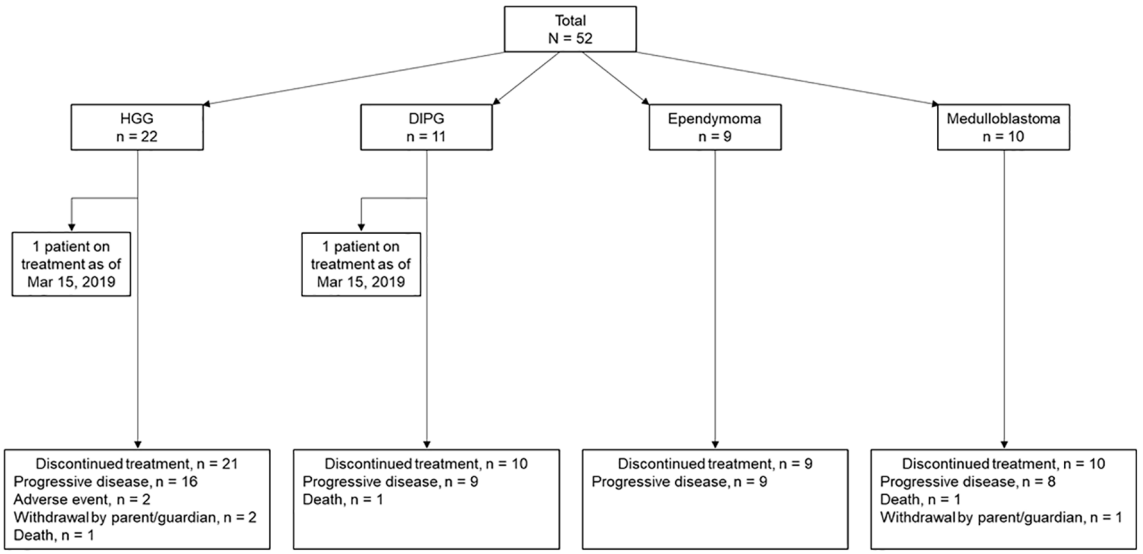

FIGURE 1 | Patient Disposition by Tumor Type (safety population).

TABLE 1 | Demographics and Baseline Characteristics (safety population).

Characteristic	HGG n = 22	DIPG n = 11	Ependymoma n = 9	Medulloblastoma n = 10	Total n = 52
Age, median (range), years	13.5 (5-18)	7.0 (4-12)	12.0 (4-15)	10.0 (4-17)	11.5 (4-18)
≥ 1 to < 6, n (%)	1 (4.5)	1 (9.1)	2 (22.2)	1 (10.0)	5 (9.6)
≥ 6 to < 12, n (%)	5 (22.7)	9 (81.8)	1 (11.1)	6 (60.0)	21 (40.4)
≥ 12, n (%)	16 (72.7)	1 (9.1)	6 (66.7)	3 (30.0)	26 (50.0)
Sex, n (%)					
Male	14 (63.6)	7 (63.6)	5 (55.6)	7 (70.0)	33 (63.5)
Female	8 (36.4)	4 (36.4)	4 (44.4)	3 (30.0)	19 (36.5)
Prior lines of therapy					
Radiation therapy					
n	22	11	9	10	52
Median (range)	1.0 (1-2)	1.0 (1-3)	2.0 (1-4)	1.0 (1-3)	1.0 (1-4)
Surgery					
n	21	5	9	10	45
Median (range)	1.0 (1-4)	1.0 (1-2)	3.0 (1-4)	2.0 (1-5)	2.0 (1-5)
Systemic therapy[a]					
n	20	7	8	10	45
Median (range)	2.0 (1-7)	2.0 (1-4)	4.0 (2-7)	7.0 (3-17)	3.0 (1-17)
Stem cell transplants (autologous)					
n	0	0	0	3	3
Median (range)	NA	NA	NA	1.0 (1-4)	1.0 (1-4)
Lansky performance status score[a]					
n	15	11	9	9	44
Median (range)	80.0 (60-100)	80.0 (50-100)	100.0 (70-100)	90.0 (70-100)	90.0 (50-100)
90-100, n (%)	7 (31.8)	3 (27.3)	7 (77.8)	7 (70.0)	24 (46.2)
70-80, n (%)	5 (22.7)	6 (54.5)	2 (22.2)	2 (20.0)	15 (28.8)
50-60, n (%)	3 (13.6)	2 (18.2)	0	0	5 (9.6)
Karnofsky performance status score[b]					
n	7	0	0	1	8
Median (range)	80.0 (60-100)	NA	NA	90.0 (90-90)	85.0 (60-100)
90-100, n (%)	3 (13.6)	NA	NA	1 (10.0)	4 (7.7)
70-80, n (%)	2 (9.1)	NA	NA	0	2 (3.8)
50-60, n (%)	2 (9.1)	NA	NA	0	2 (3.8)

DIPG, diffuse intrinsic pontine glioma; HGG, high-grade glioma; NA, not applicable.

[a]*Includes anti-epidermal growth factor receptor monoclonal antibody (mAb)/inhibitors, chemotherapy, anti-vascular endothelial growth factor mAbs, mammalian target of rapamycin inhibitors, immunomodulatory agents, immune checkpoint inhibitors, and/or B-Raf inhibitors.*

[b]*Lansky performance status score was collected for patients < 16 years of age; Karnofsky performance status score was collected for patients ≥ 16 years of age.*

TABLE 2 | Objective Response and Long-Term Stable Disease per Independent Central Review (response population).

Parameter	HGG n = 19	DIPG n = 9	Ependymoma n = 9	Medulloblastoma n = 9
Rate of objective response or long-term stable disease[a]				
n (%)	2 (10.5)	0	1 (11.1)	0
95% CI	(1.3-33.1)	(0.0-33.6)	(0.3-48.2)	(0.0-33.6)
Objective response, n (%)	1 (5.3)	0	0	0
Long-term stable disease, n (%)[a]	1 (5.3)	0	1 (11.1)	0
Best overall response, n (%)				
Complete response	0	0	0	0
Partial response	1 (5.3)	0	0	0
Stable disease	1 (5.3)	0	3 (33.3)	1 (11.1)
≥ 3 cycles	1 (5.3)	0	3 (33.3)	1 (11.1)
≥ 6 cycles	1 (5.3)	0	1 (11.1)	0
Disease progression	11 (57.9)	6 (66.7)	6 (66.7)	5 (55.6)
Not evaluable[b]	6 (31.6)	3 (33.3)	0	3 (33.3)

DIPG, diffuse intrinsic pontine glioma; HGG, high-grade glioma.

[a]*Long-term stable disease was defined as stable disease maintained for ≥ 6 cycles (≥ 3 cycles for DIPG).*

[b]*Patients who discontinued study treatment due to disease progression or relapse prior to disease assessment were considered not evaluable with regard to the primary endpoint.*

TABLE 3 | Progression-Free Survival and Overall Survival (response population).

	HGG (n = 19)	DIPG (n = 9)	Ependymoma (n = 9)	Medulloblastoma (n = 9)
Progression-free survival per independent central review				
Events, n (%)	17 (89.5)	9 (100.0)	9 (100.0)	8 (88.9)
Time to event, median (95% CI), weeks[a]	7.86 (5.14-8.14)	11.29 (2.86-12.57)	8.43 (5.57-16.14)	8.43 (7.29-18.00)
Event-free rate, % (SE)				
Week 4	78.9 (9.35)	88.9 (10.48)	100.0	100.0
Week 8	34.0 (11.20)	66.7 (15.71)	66.7 (15.71)	66.7 (15.71)
Week 16	11.3 (7.54)	0	33.3 (15.71)	27.8 (16.17)
Week 24	11.3 (7.54)	—	11.1 (10.48)	0
Week 32	5.7 (5.50)	—	0	—
Overall survival				
Events, n (%)	12 (63.2)	7 (77.8)	5 (55.6)	4 (44.4)
Time to event, median (95% CI), months[a]	5.06 (2.04-11.63)	3.78 (0.66-NA)	12.02 (2.86-NA)	11.60 (1.74-NA)
Event-free rate, % (SE)				
Month 3	65.7 (11.50)	55.6 (16.56)	88.9 (10.48)	88.9 (10.48)
Month 6	44.3 (12.81)	33.3 (15.71)	59.3 (18.48)	63.5 (16.92)
Month 9	35.5 (12.96)	22.2 (13.86)	59.3 (18.48)	63.5 (16.92)
Month 12	11.8 (10.58)	22.2 (13.86)	59.3 (18.48)	42.3 (20.64)

DIPG, diffuse intrinsic pontine glioma; HGG, high-grade glioma; NA, not available; SE, standard error.

[a]*Median time to event based on Kaplan-Meier product-limit estimates.*

DIPG, ependymoma, and medulloblastoma, respectively (**Table 3**); the median OS values were 5.06, 3.78, 12.02, and 11.60 months, respectively.

Treatment Exposure and Dose Modifications

The median treatment durations for patients in the safety population with HGG, DIPG, ependymoma, and medulloblastoma were 40.5 (range, 11-532), 84.0 (range, 7-448), 112.0 (range, 28-252), and 57.0 (range, 28-118) days, respectively. Patients received a median of 2.0 (range, 1-19), 3.0 (range, 1-16), 4.0 (range, 1-9), and 2.0 (range, 1-4) treatment cycles, respectively. Cumulative treatment exposure and dose intensity data are reported in **Supplementary Table 1**.

Four patients had dose reductions (HGG, n = 2; ependymoma, n = 1; and medulloblastoma, n = 1). One patient with HGG required a dose reduction for AEs (febrile neutropenia, pneumonia, and neutropenia). Six patients had dose interruptions (HGG, n = 1; ependymoma, n = 3; and medulloblastoma, n = 2). AEs were the primary reason for dose interruptions (4 of 6 patients; 1 patient each had a dose interruption due to forgetfulness [ependymoma] and forgot/missed dose [medulloblastoma]). The AEs leading to dose interruption were diarrhea and hydrocephalus (2 patients each), anemia, neutropenia, thrombocytopenia, and vomiting (1 patient each).

Safety

Overall, 63.6%, 45.5%, 77.8%, and 80.0% of patients with HGG, DIPG, ependymoma, and medulloblastoma, respectively, experienced a treatment-emergent AE (TEAE) related to POM (**Table 4**); the corresponding rates for grade 3/4 TEAEs related to POM were 45.5%, 27.3%, 22.2%, and 40.0%. The most common grade 3/4 TEAE related to POM was neutropenia. The rates of grade 3/4 neutropenia for patients with HGG, DIPG, ependymoma, and medulloblastoma were similar across

TABLE 4 | Safety (safety population).

Safety parameter, n (%)	HGG n = 22	DIPG n = 11	Ependymoma n = 9	Medulloblastoma n = 10
Patients with ≥ 1 TEAE related to POM	14 (63.6)	5 (45.5)	7 (77.8)	8 (80.0)
Patients with ≥ 1 grade 3/4 TEAE related to POM	10 (45.5)	3 (27.3)	2 (22.2)	4 (40.0)
Patients with ≥ 1 serious TEAE related to POM	6 (27.3)	1 (9.1)	0	0
TEAEs (any grade) related to POM[a]				
Neutropenia	9 (40.9)	3 (27.3)	7 (77.8)	4 (40.0)
Leukopenia	6 (27.3)	3 (27.3)	6 (66.7)	3 (30.0)
Lymphopenia	6 (27.3)	1 (9.1)	5 (55.6)	0
Thrombocytopenia	6 (27.3)	0	3 (33.3)	3 (30.0)
Anemia	5 (22.7)	0	3 (33.3)	2 (20.0)
Alanine aminotransferase level increased	2 (9.1)	1 (9.1)	1 (11.1)	2 (20.0)
Constipation	3 (13.6)	0	1 (11.1)	2 (20.0)
Maculopapular rash	1 (4.5)	0	3 (33.3)	2 (20.0)
Pruritus	0	2 (18.2)	2 (22.2)	1 (10.0)
Fatigue	1 (4.5)	0	1 (11.1)	2 (20.0)
Decreased appetite	0	1 (9.1)	0	2 (20.0)
Dry skin	0	1 (9.1)	2 (22.2)	0
Vomiting	1 (4.5)	0	0	2 (20.0)
Grade 3/4 TEAEs related to POM[b]				
Neutropenia	7 (31.8)	3 (27.3)	2 (22.2)	3 (30.0)
Lymphopenia	2 (9.1)	1 (9.1)	0	0
Febrile neutropenia	2 (9.1)	0	0	0
Leukopenia	1 (4.5)	1 (9.1)	0	0
Thrombocytopenia	2 (9.1)	0	0	0
Hypokalemia	0	0	0	1 (10.0)
Vertigo	0	1 (9.1)	0	0

DIPG, diffuse intrinsic pontine glioma; HGG, high-grade glioma; POM, pomalidomide; TEAE, treatment-emergent adverse event.
[a]*≥ 20% incidence for any tumor type.*
[b]*≥ 5% incidence for any tumor type.*

disease cohorts: 31.8%, 27.3%, 22.2%, and 30.0%, respectively. Other frequent TEAEs related to POM are summarized in **Table 4**. Overall, 6 patients (27.3%) with HGG and 1 (9.1%) with DIPG experienced ≥ 1 serious TEAE related to POM.

Ten patients from the safety population died during the treatment period of the study; 9 of those deaths were due to progressive disease (HGG, n = 5; DIPG, n = 2; ependymoma, n = 1; medulloblastoma, n = 1), and 1 was due to an AE (sepsis; patient with DIPG). The investigator concluded the sepsis (grade 4 and subsequent death) was not treatment-related. During follow-up, 20 additional patients from the safety population died due to progressive disease (HGG, n = 7; DIPG, n = 5; ependymoma, n = 4; medulloblastoma, n = 4).

Pharmacokinetics

Plasma concentrations of POM by tumor type are reported in **Supplementary Table 2**. No clear differences in POM exposure were observed between the different tumor types.

DISCUSSION

The current study did not demonstrate the necessary level of clinically meaningful activity of POM monotherapy based on the original statistical design in children and young adults with recurrent or progressive HGG, DIPG, ependymoma, and medulloblastoma. The HGG cohort met the protocol-defined criteria for advancement to stage 2; however, this was the only cohort to advance to stage 2, and the criteria for reaching a threshold of efficacy interest for POM in the Simon stage 2 were not met. The safety profile of POM was generally consistent with previous findings in adults and children (26), with neutropenia being the most common grade 3/4 TEAE related to POM.

In the current study, 1 patient with progressive HGG at study entry achieved a PR and received treatment for > 1.5 years, and 2 patients (1 with HGG, 1 with ependymoma) experienced LTSD. Despite the overall discouraging findings with POM monotherapy, these data suggest some activity potentially worth further investigation. Identifying patients who could potentially benefit from combining POM with other anticancer agents may enhance the level of activity observed in clinical trials. A phase 1 trial examined the combination of dasatinib, lenalidomide, and temozolomide in pediatric patients with either relapsed or refractory CNS tumors (27). The trial established feasibility of the combination; however, any efficacy data were preliminary, and it remains to be determined whether an efficacy benefit exists. It is also unclear if specific tumor molecular signatures may be more responsive to POM as this was not explored in the current study. The inclusion of molecular testing in ongoing clinical trials may lead to the identification of potential driver mutations of pediatric CNS tumors that can inform therapeutic decisions (28). For example, our current understanding of HGG tumors is that they can be categorized into 4 epigenetic subgroups (29–31), including the common histone 3 K27M mutation that disrupts H3K27 methylation and acetylation, causing widespread gene dysregulation (32). The combination of POM and histone deacetylase inhibitors or H3K27 methyltransferase inhibitors demonstrated antitumor activity in preclinical models of

multiple myeloma (33, 34) and could be considered in pediatric CNS tumors.

Beyond immunomodulatory therapies, additional efforts are ongoing to investigate immune checkpoint inhibitor-based regimens and targeted therapies. For example, the combination of checkpoint inhibitors with low-dose radiotherapy or chemotherapy (e.g., NCT03585465, NCT03690869, NCT02989636) or other types of immunotherapy, such as chimeric antigen receptor T cells and cancer vaccines (e.g., NCT03500991, NCT03638167, NCT04185038 NCT04239040) are being investigated in pediatric patients (34). Additionally, targeted therapies (i.e., BRAF, MEK and TRK inhibitors) have demonstrated promising activity in pediatric brain tumors (35, 36).

The safety profile of POM in the current study was generally consistent with previous findings in adults and children. The grade 3/4 TEAEs related to POM were mainly hematologic in nature, and the most common was neutropenia. Interestingly, the medulloblastoma cohort, a patient population typically treated with craniospinal radiotherapy, had a similar incidence of myelosuppression as that of the cohorts not typically treated with craniospinal radiotherapy. Previously published studies of POM and lenalidomide in pediatric patients with recurrent, refractory, or progressive CNS tumors also reported hematologic AEs (25, 26).

This study is limited by the relatively small sample size; however, the tolerability, safety, and failure to achieve threshold antitumor activity in this setting are generally consistent with previous findings in patients with recurrent or progressive CNS tumors. The lack of clinically meaningful efficacy in this patient population underscores the urgent need for efficacious treatments and a better understanding of the specific antitumor mechanisms of POM. Future efforts should focus on understanding tumor molecular profiles and combination therapy with other cytotoxic, molecular, and immunomodulatory compounds.

DATA AVAILABILITY STATEMENT

Bristol Myers Squibb policy on data sharing may be found at https://www.bms.com/researchers-and-partners/independent-research/data-sharing-request-process.html.

ETHICS STATEMENT

The study was approved by the institutional review board or ethics committee at each participating study site prior to initiation. This study was conducted in accordance with the Declaration of Helsinki and Good Clinical Practice Guidelines of the International Council for Harmonisation. Written informed consent (and assent when appropriate) was obtained from each patient and/or their legal guardian prior to study entry. The protocol is included in the **Supplementary Materials**.

AUTHOR CONTRIBUTIONS

Conception or design of the work [JF, FD, KEW, MS, JL, NB, and BB] or the acquisition, analysis, or interpretation of data for the work [all authors]. Drafting the manuscript or revising it critically for important intellectual content [all authors]. Agreement to be accountable for all aspects of the work in ensuring that questions related to the accuracy or integrity of any part of the work are appropriately investigated and resolved [all authors]. All authors contributed to the article and approved the submitted version.

FUNDING

This study was funded by Bristol Myers Squibb.

ACKNOWLEDGMENTS

The authors thank the patients who participated in the study, as well as their families. Sponsorship of this study and article processing charges were funded by Bristol Myers Squibb. Writing assistance was provided by Aaron Runkle, PhD, of MediTech Media, Ltd, and funded by Bristol Myers Squibb. The authors are fully responsible for all content and editorial decisions for this manuscript.

SUPPLEMENTARY MATERIAL

The Supplementary Material for this article can be found online at: https://www.frontiersin.org/articles/10.3389/fonc.2021.660892/full#supplementary-material

REFERENCES

1. Society TAC. *Key Statistics for Brain and Spinal Cord Tumors in Children* (2018). Available at: https://www.cancer.org/cancer/brain-spinal-cord-tumors-children/about/key-statistics.html (Accessed August 26 2019).
2. Fleming AJ, Chi SN. Brain tumors in children. *Curr Probl Pediatr Adolesc Health Care* (2012) 42(4):80–103. doi: 10.1016/j.cppeds.2011.12.002
3. Ostrom QT, de Blank PM, Kruchko C, Petersen CM, Liao P, Finlay JL, et al. Alex's Lemonade Stand Foundation infant and childhood primary brain and central nervous system tumors diagnosed in the United States in 2007-2011. *Neuro Oncol* (2015) 16(Suppl 10):x1–x36. doi: 10.1093/neuonc/nou327
4. Dolecek TA, Propp JM, Stroup NE, Kruchko C. CBTRUS statistical report: primary brain and central nervous system tumors diagnosed in the United States in 2005-2009. *Neuro Oncol* (2012) 14(Suppl 5):v1–49. doi: 10.1093/neuonc/nos218
5. Dhall G. Medulloblastoma. *J Child Neurol* (2009) 24(11):1418–30. doi: 10.1177/0883073809341668
6. Zacharoulis S, Moreno L. Ependymoma: an update. *J Child Neurol* (2009) 24 (11):1431–8. doi: 10.1177/0883073809339212
7. Fangusaro J. Pediatric high-grade gliomas and diffuse intrinsic pontine gliomas. *J Child Neurol* (2009) 24(11):1409–17. doi: 10.1177/0883073809338960
8. Jussila MP, Remes T, Anttonen J, Harila-Saari A, Niinimaki J, Pokka T, et al. Late vertebral side effects in long-term survivors of irradiated childhood brain tumor. *PloS One* (2018) 13(12):e0209193. doi: 10.1371/journal.pone.0209193
9. Wang SS, Bandopadhayay P, Jenkins MR. Towards immunotherapy for pediatric brain tumors. *Trends Immunol* (2019) 40(8):748–61. doi: 10.1016/j.it.2019.05.009
10. Vinchon M, Baroncini M, Leblond P, Delestret I. Morbidity and tumor-related mortality among adult survivors of pediatric brain tumors: a review. *Childs Nerv Syst* (2011) 27(5):697–704. doi: 10.1007/s00381-010-1385-6

11. Armstrong GT. Long-term survivors of childhood central nervous system malignancies: the experience of the Childhood Cancer Survivor Study. *Eur J Paediatr Neurol* (2010) 14(4):298–303. doi: 10.1016/j.ejpn.2009.12.006
12. Ellenberg L, Liu Q, Gioia G, Yasui Y, Packer RJ, Mertens A, et al. Neurocognitive status in long-term survivors of childhood CNS malignancies: a report from the Childhood Cancer Survivor Study. *Neuropsychology* (2009) 23(6):705–17. doi: 10.1037/a0016674
13. Turner CD, Rey-Casserly C, Liptak CC, Chordas C. Late effects of therapy for pediatric brain tumor survivors. *J Child Neurol* (2009) 24(11):1455–63. doi: 10.1177/0883073809341709
14. Gurney JG, Kadan-Lottick NS, Packer RJ, Neglia JP, Sklar CA, Punyko JA, et al. Endocrine and cardiovascular late effects among adult survivors of childhood brain tumors: Childhood Cancer Survivor Study. *Cancer* (2003) 97 (3):663–73. doi: 10.1002/cncr.11095
15. Li S, Pal R, Monaghan SA, Schafer P, Ouyang H, Mapara M, et al. IMiD immunomodulatory compounds block C/EBP{beta} translation through eIF4E down-regulation resulting in inhibition of MM. *Blood* (2011) 117 (19):5157–65. doi: 10.1182/blood-2010-10-314278
16. Verhelle D, Corral LG, Wong K, Mueller JH, Moutouh-de Parseval L, Jensen-Pergakes K, et al. Lenalidomide and CC-4047 inhibit the proliferation of malignant B cells while expanding normal CD34+ progenitor cells. *Cancer Res* (2007) 67(2):746–55. doi: 10.1158/0008-5472.CAN-06-2317
17. Schafer PH, Gandhi AK, Loveland MA, Chen RS, Man HW, Schnetkamp PP, et al. Enhancement of cytokine production and AP-1 transcriptional activity in T cells by thalidomide-related immunomodulatory drugs. *J Pharmacol Exp Ther* (2003) 305(3):1222–32. doi: 10.1124/jpet.102.048496
18. Gandhi AK, Kang J, Havens CG, Conklin TT, Ning Y, Wu L, et al. Immunomodulatory agents lenalidomide and pomalidomide co-stimulate T cells by inducing degradation of T cell repressors Ikaros and Aiolos via modulation of the E3 ubiquitin ligase complex $CRL4^{CRBN}$. *Br J Haematol* (2014) 164(6):811–21. doi: 10.1111/bjh.12708
19. Corral LG, Haslett PA, Muller GW, Chen R, Wong LM, Ocampo CJ, et al. Differential cytokine modulation and T cell activation by two distinct classes of thalidomide analogues that are potent inhibitors of TNF-alpha. *J Immunol* (1999) 163(1):380–6.
20. Payvandi F, Wu L, Naziruddin SD, Haley M, Parton A, Schafer PH, et al. Immunomodulatory drugs (IMiDs) increase the production of IL-2 from stimulated T cells by increasing PKC-theta activation and enhancing the DNA-binding activity of AP-1 but not NF-kappaB, OCT-1, or NF-AT. *J Interferon Cytokine Res* (2005) 25(10):604–16. doi: 10.1089/jir.2005.25.604
21. Lu L, Payvandi F, Wu L, Zhang L-H, Hariri RJ, Man H-W, et al. The anti-cancer drug lenalidomide inhibits angiogenesis and metastasis via multiple inhibitory effects on endothelial cell function in normoxic and hypoxic conditions. *Microvasc Res* (2009) 77(2):78–86. doi: 10.1016/j.mvr.2008.08.003
22. D'Amato RJ, Loughnan MS, Flynn E, Folkman J. Thalidomide is an inhibitor of angiogenesis. *Proc Natl Acad Sci USA* (1994) 91(9):4082–5. doi: 10.1073/pnas.91.9.4082
23. Lentzsch S, Rogers MS, LeBlanc R, Birsner AE, Shah JH, Treston AM, et al. S-3-Amino-phthalimido-glutarimide inhibits angiogenesis and growth of B-cell neoplasias in mice. *Cancer Res* (2002) 62(8):2300–5.
24. Li Z, Qiu Y, Personett D, Huang P, Edenfield B, Katz J, et al. Pomalidomide shows significant therapeutic activity against CNS lymphoma with a major impact on the tumor microenvironment in murine models. *PloS One* (2013) 8 (8):e71754. doi: 10.1371/journal.pone.0071754
25. Warren KE, Goldman S, Pollack IF, Fangusaro J, Schaiquevich P, Stewart CF, et al. Phase I trial of lenalidomide in pediatric patients with recurrent, refractory, or progressive primary CNS tumors: Pediatric Brain Tumor Consortium study PBTC-018. *J Clin Oncol* (2011) 29(3):324–9. doi: 10.1200/JCO.2010.31.3601
26. Fangusaro J, Mitchell DA, Kocak M, Robinson GW, Baxter PA, Hwang EI, et al. Phase 1 study of pomalidomide in children with recurrent, refractory, and progressive central nervous system tumors: A Pediatric Brain Tumor Consortium trial. *Pediatr Blood Cancer* (2021) 68(2):e28756. doi: 10.1002/pbc.28756
27. Robison NJ, Yeo KK, Berliner AP, Malvar J, Sheard MA, Margol AS, et al. Phase I trial of dasatinib, lenalidomide, and temozolomide in children with relapsed or refractory central nervous system tumors. *J Neurooncol* (2018) 138 (1):199–207. doi: 10.1007/s11060-018-2791-y
28. Terry RL, Meyran D, Ziegler DS, Haber M, Ekert PG, Trapani JA, et al. Immune profiling of pediatric solid tumors. *J Clin Invest* (2020) 130(7):3391–402. doi: 10.1172/JCI137181
29. Lu VM, Alvi MA, McDonald KL, Daniels DJ. Impact of the H3K27M mutation on survival in pediatric high-grade glioma: a systematic review and meta-analysis. *J Neurosurg Pediatr* (2018) 23(3):308–16. doi: 10.3171/2018.9.PEDS18419
30. Sturm D, Witt H, Hovestadt V, Khuong-Quang DA, Jones DT, Konermann C, et al. Hotspot mutations in H3F3A and IDH1 define distinct epigenetic and biological subgroups of glioblastoma. *Cancer Cell* (2012) 22(4):425–37. doi: 10.1016/j.ccr.2012.08.024
31. Kumar R, Liu APY, Orr BA, Northcott PA, Robinson GW. Advances in the classification of pediatric brain tumors through DNA methylation profiling: From research tool to frontline diagnostic. *Cancer* (2018) 124(21):4168–80. doi: 10.1002/cncr.31583
32. Lin GL, Wilson KM, Ceribelli M, et al. Therapeutic strategies for diffuse midline glioma from high-throughput combination drug screening. *Sci Transl Med* (2019) 11(519):eaaw0064. doi: 10.1126/scitranslmed.aaw0064
33. North BJ, Almeciga-Pinto I, Tamang D, Yang M, Jones SS, Quayle SN. Enhancement of pomalidomide anti-tumor response with ACY-241, a selective HDAC6 inhibitor. *PloS One* (2017) 12(3):e0173507. doi: 10.1371/journal.pone.0173507
34. Drew AE, Motwani V, Campbell JE, Tang C, Smith JJ, Chesworth R, et al. Abstract 5060: Activity of the EZH2 inhibitor tazemetostat as a monotherapy and in combination with multiple myeloma therapies in preclinical models. *Cancer Res* (2017) 77(13 Suppl):5060. doi: 10.1158/1538-7445.Am2017-5060
35. Landi DB, Thompson EM, Ashley DM. Immunotherapy for pediatric brain tumors. *Neuroimmunol Neuroinflamm* (2018) 5(7):29. doi: 10.20517/2347-8659.2018.35
36. Fangusaro JR, Onar-Thomas A, Young-Poussaint T. A phase II prospective study of selumetinib in children with recurrent or refractory low-grad glioma (LGG): a pediatric brain tumor consortium (PBTC) study. *J Clin Oncol* (2017) 35(Suppl 15):10504. doi: 10.1200/JCO.2017.35.15_suppl.10504

Conflict of Interest: BB, NB, JP, JQ, EC, JL and NJ were employed by Bristol Myers Squibb. MS is employed by and has stock ownership with Celegne. JF: Related to the work: Celgene (a Bristol-Myers Squibb Company) (advisory board). LM: Honoraria/consulting/advisory boards for Bristol-Myers Squibb, Bayer, Eisai, Tesaro. MM: Bristol-Myers Squibb (advisory boards and travel expenses), Roche (advisory board), Novartis (advisory board), Oncoscience (advisory board). BB, NB, JP, JQ, EC, JL and NJ: Employment and stock ownership with Bristol-Myers Squibb Company. DH: Related to the work: Celgene (a Bristol-Myers Squibb Company) (advisory board). Not related to the work: Consulting, AstraZeneca, Bayer, Boehringer Ingelheim, Novartis, Roche/Genentech; research funding, AstraZeneca; expert testimony, AstraZeneca; travel, Boehringer Ingelheim, Novartis, Roche/Genentech; other, AbbVie, Bristol-Myers Squibb, and Novartis. FD: Related to the work: Celgene (a Bristol-Myers Squibb Company) (advisory board). Not related to the work: Bayer (advisory boards and travel expenses), Bristol-Myers Squibb (advisory boards and travel expenses), Roche (advisory board and travel expenses), Loxo Oncology (advisory board), Novartis (advisory board), Tesaro (advisory board), Servier (advisory boards and consulting). KW: Related to the work: Celgene (a Bristol-Myers Squibb Company) (advisory board). Not related to the work: Celgene (a Bristol-Myers Squibb Company) (clinical trial sponsorship).

The remaining authors declare that the research was conducted in the absence of any commercial or financial relationships that could be construed as a potential conflict of interest.

The authors declare that this study received funding from Bristol Myers Squibb. The sponsor was involved in the study design, collection, analysis, interpretation of data, and funded the writing of this article.

frontiers in Oncology

ORIGINAL RESEARCH
published: 15 June 2021
doi: 10.3389/fonc.2021.664462

Fenretinide Acts as Potent Radiosensitizer for Treatment of Rhabdomyosarcoma Cells

Eva Brack[1,2,3], *Sabine Bender*[4], *Marco Wachtel*[1,2], *Martin Pruschy*[4] *and Beat W. Schäfer*[1,2*]

[1] Department of Oncology, Children's Research Center, University Children's Hospital Zurich, Zurich, Switzerland, [2] Children's Research Center, University Children's Hospital Zurich, Zurich, Switzerland, [3] Pediatric Hematology/Oncology, Department of Pediatrics, Inselspital, Bern University Hospital, University of Bern, Bern, Switzerland, [4] Department of Radiology Biology, University Hospital Zurich, Radio-Oncology, Zurich, Switzerland

Fusion-positive rhabdomyosarcoma (FP-RMS) is a highly aggressive childhood malignancy which is mainly treated by conventional chemotherapy, surgery and radiation therapy. Since radiotherapy is associated with a high burden of late side effects in pediatric patients, addition of radiosensitizers would be beneficial. Here, we thought to assess the role of fenretinide, a potential agent for FP-RMS treatment, as radiosensitizer. Survival of human FP-RMS cells was assessed after combination therapy with fenretinide and ionizing radiation (IR) by cell viability and clonogenicity assays. Indeed, this was found to significantly reduce cell viability compared to single treatments. Mechanistically, this was accompanied by enhanced production of reactive oxygen species, initiation of cell cycle arrest and induction of apoptosis. Interestingly, the combination treatment also triggered a new form of dynamin-dependent macropinocytosis, which was previously described in fenretinide-only treated cells. Our data suggest that fenretinide acts in combination with IR to induce cell death in FP-RMS cells and therefore might represent a novel radiosensitizer for the treatment of this disease.

Keywords: rhabdomyosarcoma, childhood cancer, fenretinide, radiation therapy, radiosensitizer, reactive oxygen species

OPEN ACCESS

Edited by:
Giuseppe Maria Milano, Bambino Gesù Children Hospital (IRCCS), Italy

Reviewed by:
Josep Roma, Vall d'Hebron Research Institute (VHIR), Spain
Julia Chisholm, Royal Marsden Hospital, United Kingdom

***Correspondence:**
Beat W. Schäfer
beat.schaefer@kispi.uzh.ch

Specialty section:
This article was submitted to Pediatric Oncology, a section of the journal Frontiers in Oncology

Received: *05 February 2021*
Accepted: *29 March 2021*
Published: *15 June 2021*

Citation:
Brack E, Bender S, Wachtel M, Pruschy M and Schäfer BW (2021) Fenretinide Acts as Potent Radiosensitizer for Treatment of Rhabdomyosarcoma Cells. Front. Oncol. 11:664462. doi: 10.3389/fonc.2021.664462

INTRODUCTION

Radiation therapy (RT) applying ionizing radiation (IR) is, along with chemotherapy and surgery, part of the standard therapeutic regimen for many malignancies. In the pediatric patient population this treatment is used e.g. in neuroblastoma, medulloblastoma, Ewing and soft tissue sarcomas (1). Rhabdomyosarcoma (RMS) is the most common soft tissue malignancy in children and young adolescents. Especially the fusion-positive rhabdomyosarcoma subgroup (FP-RMS) is associated with a poor outcome due to its aggressiveness and a high risk of relapse (2–5).

The effectiveness of IR is well studied and has direct and indirect effects on cancer cells. As direct action, IR damages DNA, proteins and lipids, which eventually results in genotoxic stress, cell cycle arrest and cell death (6). Indirect effects occur through radiolysis of water and the production of reactive oxygen species (ROS). The unpaired electrons in ROS are highly reactive and can induce

DNA single- and double-strand breaks (7–10). Further, they act as signaling molecules driving cells towards cell death.

On the other hand, IR is also associated with considerable off-target effects and induces damage to non-diseased tissues and organs depending on the absorbed dose. This may cause relevant side effects especially in pediatric patients, which become apparent only later in life, such as growth retardation, reduced neurocognitive development, infertility, and most importantly the risk to develop secondary malignancies (11, 12). One current goal in radiobiology is therefore to minimize these side effects, while at the same time maximizing radiation benefits against tumor cells. Image-guided and intensity-modulated RT for example has led to significant improvements in the field (13, 14).

Another well-recognized option to achieve this goal is the simultaneous administration of radio sensitizers (15). Drugs are defined as radio sensitizing agents when they render cancer cells more vulnerable to radiation therapy. They have been categorized based on their structures into three different categories including small molecules, nanostructures, and macromolecules (16).

Previously, we identified the small molecule fenretinide (retinoic acid p-hydroxyanilide) as a potential additional treatment option for RMS, as it was found to have strong cytotoxic effects on FP-RMS cells (17). Fenretinide is a compound that is well established in the treatment for multiple malignancies during adulthood and that is already in clinical use in children (Clinicaltrials.gov ID NCT02163356) (18, 19). Importantly, its side-effect profile is very favorable with no limiting toxicities (20).

Multiple studies suggest that fenretinide induced cell death occurs mainly through apoptosis in most cell lines studied, either through the production of reactive oxygen species (ROS) or the involvement of lipid second messengers (21–25). In contrast, experiments in RMS showed that the underlying mechanism of cell death also depends on enhanced production of ROS and is accompanied by increased accumulation of cytoplasmic vesicles originating from macropinocytosis pathways (26), characteristics of a recently described new form of cell death (27, 28).

While fenretinide has not been investigated together with RT for the treatment of RMS, this combination is currently under investigation for the treatment of diffuse intrinsic pontine glioma (DIPG), with promising results in mice (29).

In the current study, we therefore elucidate the potential of fenretinide as radio sensitizer in RMS and describe the underlying mechanisms of cell death occurring during combination treatment in more detail. Overall, the study highlights the combination of fenretinide and IR as potential novel treatment option for FP-RMS.

MATERIAL AND METHODS

Gamma Irradiation

Irradiation was performed using an Xstrahl 200 kV X-Ray unit (Ratingen, Germany) at 100 cGy/min. Depending on the question, different intensities of radiation were applied to the cells.

Cell Culture

The fusion-positive rhabdomyosarcoma cell line Rh4 (provided by Peter Houghton, Greehey Children's Cancer Research Institute, San Antonio, Texas, USA) was maintained in high glucose Dulbecco's Modified Eagle Medium (DMEM, Sigma-Aldrich, Buchs, Switzerland), supplemented with 100 U/ml penicillin/streptomycin (Invitrogen, ThermoFisher, Waltham, Massachusetts, USA), 2 mM L-glutamine (BioConcept, Allschwil, Switzerland) or Glutamax (Gibco, ThermoFisher, Waltham, Massachusetts, USA), and 10% fetal bovine serum (FBS, Sigma-Aldrich, Buchs, Switzerland), in 5% CO_2 at 37°C. FP-RMS cell lines were regularly tested for mycoplasma infection, authenticated by short tandem repeat analysis (STR profiling) in 2011/2014 and positively matched with reference data (30).

Cell Viability Assay

8,000 Rh4 cells were seeded in 96 well format (TC-Plate, Standard F, Sarstedt, Nümbrecht, Germany) in 100 µl medium. The studied compounds (see **Supplementary Table 7**) were added for 72 h. For measurement of cell viability, 10 µl WST-1 reagent (Sigma-Aldrich, Buchs, Switzerland) was added. After 30 min incubation at 37°C in the dark, absorbance at 440 and 640 nm were measured with a Synergy™ HT multi-detection microplate reader (BioTek, Winooski, Vermont, USA). The difference of the two values was calculated (delta optical density; ΔOD) and values from pure medium were subtracted as background.

Clonogenic Assays

Clonogenic cell survival was determined by the ability of single cells to form colonies *in vitro* (31). 50,000 cells were seeded per 10 cm dish (TC-Dish, 100, Standard, Sarstedt, Nümbrecht, Germany). The following day, cells were treated with the desired concentration of fenretinide and irradiated with the desired intensity. After 12 days of culturing in 5% CO_2 at 37°C the medium was removed and the cells fixed with glutaraldehyde (6.0%) and stained with crystal violet (CV) (0.5%). For data processing, the images were exported as TIFF files and the mean integrated density was quantified with the image processing program Fiji (53).

Flow Cytometry

For all flow cytometry experiments, 150,000 Rh4 cells were seeded per well in Corning Costar 6-well plates (Sigma-Aldrich, Buchs, Switzerland). After treatments, cells were detached from the plates using trypsin, washed once with PBS and re-suspended in 0.5 ml indicated buffer. Data was acquired with the LSRII Fortessa flow cytometer (BD Biosciences, San Jose, California, USA) or the BD FACS Canto system (BD Biosciences, San Jose, California, USA).

Acquired data was analyzed with FlowJo software, version 9.9.6 (Tree Star Inc., Ashland, Orlando, USA). All used fluorescent stains are listed in **Supplementary Table 8** in **Supplementary Material and Methods.**

Pan ROS Measurement

Cells were seeded and treated with the desired compounds according to **Supplementary Table 7** (in the **Supplementary Material and Methods**). About 4 μM CellRox Deep red (ThermoFisher, Waltham, Massachusetts, USA) solution was simultaneously added to the medium. One hour after drug treatment, cells were irradiated with the desired intensity. After 18 h, cells were detached, washed in PBS and re-suspended in FluoroBrite live cell fluorescence imaging medium DMEM (ThermoFisher, Waltham, Massachusetts, USA). CellRox signal was measured by flow cytometry (50,000 events per sample) with excitation laser 640 nm and emission filter 670/14.

Mitochondrial ROS Measurement

Cells were seeded and treated with the desired compounds according to **Supplementary Table 7** in **Supplementary Material and Methods**.

One hour after drug treatment, cells were irradiated with the desired intensity. After 18 h, cells were detached, washed in PBS and re-suspended in MitoSox (ThermoFisher, Waltham, Massachusetts, USA) solution (10μM MitoSox in PBS) for 30 min at 37°C in the dark. MitoSox signal was measured by flow cytometry (50,000 events per sample) with excitation laser 561 nm, and emission filter 570 LP, 525/50.

Cell Cycle Analysis

Cells were seeded and treated with the indicated concentration of fenretinide. One hour after drug treatment, cells were irradiated with the desired intensity. After 24 and 48 h, cells were collected, washed with PBS and fixed with ice-cold 70% ethanol for 4 h at −20°C. Then cells were washed three times with PBS and incubated for 30 min with 20 mg/ml propidium iodide (PI) (Sigma-Aldrich, Buchs, Switzerland) and 200 mg/ml RNAse A (Qiagen, Hilden, Germany) in 0.1% Triton-X in PBS (Sigma-Aldrich, Buchs, Switzerland). PI signals were quantified by flow cytometry (50,000 events per sample) with excitation laser 488 nm, and emission filter 585/42.

Acridine Orange (AO) Staining

Acridine orange (Sigma-Aldrich, Buchs, Switzerland) (AO) was used to measure fluid-phase endocytic uptake induced by fenretinide treatment and IR after 48 h.

Cells were seeded and treated with the indicated compounds according to **Supplementary Table 7** in **Supplementary Material and Methods**. One hour after drug treatment, cells were irradiated with the desired intensity. After 48 h, AO (2.7 μM) in FluoroBrite DMEM live cell fluorescence imaging medium (ThermoFisher, Waltham, Massachusetts, USA) was added to the cells 4 h prior to their preparation for flow cytometry. Cells were then collected, washed in PBS and re-suspended in PBS. AO signal (50,000 events per sample) were acquired with excitation laser 488 nm and 561, emission filter 505 LP, 530/30 and 635LP, 670/30.

Epifluorescence Microscopy

All images were taken with the Zeiss Axio Observer microscope (Zeiss, Oberkochen, Germany) equipped with a Hamamatsu Orca Flash 4.0 V2, sCMOS cooled fluorescence camera (Hamamatsu, Hamamatsu City, Japan) and an objective with 20× magnification. All fluorescent stains used can be found in **Supplementary Table 2** in **Supplementary Material and Methods**.

For data processing, images were exported as TIFF files and the mean integrated density was quantified with the image processing software Fiji (32). The integrated density value of an image was divided by the number of cells (counted on the phase image). Per treatment, a minimum of four pictures was taken.

Lucifer Yellow Fluorescence Microscopy

Some 50,000 cells per chamber were seeded in Falcon™ chambered cell culture slides (four wells, Corning) (Thermo Scientific, ThermoFisher, Waltham, Massachusetts, USA) and treated with 3 μM fenretinide. One hour after drug treatment, cells were irradiated with the desired intensity. After 48 h, cells were stained with Lucifer Yellow (820 μM) in FluoroBrite DMEM for 4 h at 37°C, 5% CO_2. Afterwards, cells were washed with PBS and fixed with 4% PFA for 15 min at room temperature. After three PBS washes, the chamber was removed and the cells were mounted in Vectashield mounting medium with 4′,6-Diamidin-2-phenylindol (Vector Laboratories, Burlingame, California, USA).

Western Blot

Whole cell extracts were prepared from cells lysed with RIPA buffer (50 mM Tris–Cl (pH 7.5), 150 mM NaCl, 1% NP-40, 0.5% Na-deoxycholate, 1 mM EGTA, 0.1% SDS, 50 mM NaF, 10 mM sodium β-glycerolphosphate, 5 mM sodium pyrophosphate, 1 mM sodium orthovanadate and supplemented with Complete Mini Protease Inhibitor cocktail (all from Sigma Aldrich, Buchs, Switzerland). Proteins were separated using NuPAGE™ Novex™ 4-12% Bis-Tris gels (ThermoFisher, Waltham, Massachusetts, USA) and transferred to nitrocellulose membranes (GE Healthcare Life Sciences). Membranes were blocked with 5% milk in TBS/0.05% Tween and subsequently incubated with primary antibodies overnight at 4°C. After three times washing in TBS-0.05% tween, membranes were incubated with horseradish peroxidase (HRP)-linked secondary antibodies for 1 h at RT.

Following antibodies were used: Rabbit anti-phospho-Histone H2A.X (Ser139) (Cat# 9718), rabbit anti-cleaved-Caspase 7 (Cat# 9491), rabbit anti-cleaved PARP (Cat# 5625), rabbit anti-GAPDH (Cat# 2118) all from Cell Signaling (Cell Signaling Technology, Danvers, Massachusetts, USA). Horseradish peroxidase-conjugated goat anti-rabbit antibody from Cell Signaling (Cat# 7077) were used as secondary antibodies. After three additional washing steps with TBS/0.05% Tween, proteins were detected by chemiluminescence using either the Pierce™ ECL Western blotting substrate (ThermoFisher, Waltham, Massachusetts, USA) or supersignal Western blotting reagent (ThermoFisher, Waltham, Massachusetts, USA) and a ChemiDoc MP (BioRad Laboratories AG, Cressier, Switzerland) imager. The images were analyzed with the software Image Lab Version 6.0. (BioRad Laboratories AG, Cressier, Switzerland).

Statistics

The software GraphPad Prism (La Jolla, California, USA) was used for all statistical analyses. Comparisons of differences between two groups were analyzed by parametric paired t-test. The data were considered significant when $p \leq 0.05$. Radiation/drug synergy was calculated using the Bliss independence model in the free Synergy Finder WebApp (33).

RESULTS

We previously demonstrated that fenretinide efficiently induces a novel dynamin-dependent cell death in FP-RMS cells (26). As RT is part of the FP-RMS standard treatment regimens, we questioned whether fenretinide would enhance the anti-tumor effect of RT on FP-RMS cells. In a first step, we therefore co-treated Rh4 cells with two single doses of radiation (5 and 10 Gy) and two low concentrations of fenretinide (IC10 and IC20, equals to 1.9 and 2.6 μM) and assessed cell viability after 72 h by WST-1 assay. Indeed, for all combination treatments, cell viability decreased, however only significantly for the lower concentration (**Figure 1A**, left panel, **Supplementary Table 1**). We found a dose dependent synergistic effect of fenretinide with IR, with calculated Bliss Scores of 30.275 according to the Bliss independence model [SynergyFinder WebApp (33)], indicating a very high synergistic effect (**Figure 1A**, right panel). Next, we assessed the combinatorial effect on clonogenic cell survival. In this setting, we observed a strong combinatorial effect already at lower concentrations of fenretinide (0.5 μM) together with low radiation doses of 2 Gy (**Figure 1B**, right and left panels).

Next, we investigated the mechanism of cell death that was induced by the combination treatment. Western blot analysis of cleaved Caspase 7 and cleaved PARP revealed induction of apoptosis in single treated cells, which was enhanced by the combination treatment. The addition of Z-vad, a pan-caspase inhibitor abolished both caspase 7 and PARP cleavage (**Figure 1C**). Next, we were interested to see whether the combination would induce enhanced phosphorylation of histone H2AX (γH2AX), a well-established marker for DNA double-strand breaks (34). Western blot analysis and the corresponding band intensity index showed enhanced phosphorylation of γH2AX in the combination treated cells, most prominently after 30 min and rapidly decreasing over the next 4 h (**Figures 1D**, left and right panel). Based on these findings, we further investigated the effect of fenretinide and IR on cell cycle distribution. Fenretinide alone did not change the cell cycle distribution after 24 h. In contrast, single treatment of IR induced a dose-dependent G2/M arrest (**Figure 1E**, left panel) which was further increased in the combination. After 48 h, the G2/M arrest was less prominent, but a Sub-G1 peak became evident indicating induction of cell death after this treatment period (**Figure 1E**, right panel). These data suggest that fenretinide combined with IR enhances a G2/M cell cycle arrest.

Next, we wanted to see whether the combination treatment affected generation of reactive oxygen species (ROS). Indeed, increasing concentrations of fenretinide and to a lower extent also increasing doses of IR enhanced ROS production (pan-ROS) compared to control cells. This was significantly more pronounced in the combination treatment (**Figure 2A** and **Supplementary Table 2**). To confirm specificity, we co-treated cells with the hydrogen-peroxide scavenger N-acetylcysteine (NAC) and observed a significant reduction of ROS production (**Figure 2A** and **Supplementary Table 2**). Since we previously found mitochondria derived ROS to be the main source of ROS under fenretinide treatment, we also analyzed cells with a mitochondria specific ROS staining (MitoSox). We observed a significant dose-dependent increase of mitochondrial ROS upon fenretinide treatment alone, as well as a further increase under combination treatment. Interestingly, radiation alone did not enhance mitochondrial ROS production (**Figure 2B** and **Supplementary Table 3**).

To further characterize and validate the impact of ROS species on cell death, we treated the cells additionally with Vitamin C as a well-recognized pan-ROS scavenger and MitoTempo, a mitochondrial-specific ROS scavenger. We observed an almost complete rescue from cell death by both Vitamin C and MitoTempo (**Figure 2C** and **Supplementary Table 4**).

Taken together, both fenretinide and IR induce the production of ROS whereas mitochondrial derived superoxides are mainly generated by fenretinide.

Previously, we could demonstrate that fenretinide induced the formation of large phase lucent cytoplasmic vesicles, which derive from increased macropinocytosis, an effect that could be efficiently blocked by the dynamin-inhibitor dynasore. Therefore, our next aim was to clarify whether fenretinide would also enhance accumulation of cytoplasmic vesicles when combined with IR. Hence, we co-treated cells with either dynasore, Vitamin C or Z-vad and measured acridine orange (AO) staining to assess endocytosis (**Figures 3A–C** and **Supplementary Figures 1A–C**). These experiments revealed a significant increase in dye uptake in the fenretinide-only treated cells, which was further enhanced by IR treatment. Interestingly, IR treatment alone only minimally affected the uptake of AO. In addition, co-treatment of the cells with Vitamin C and dynasore decreased the dye uptake in treated cells (**Figures 3A, B** and **Supplementary Figures 1 A, B** and **Supplementary Tables 5**, **6**). No change was observed in the IR-only treated cells (**Figures 3A, B**, **Supplementary Figures 1 A, B** and **Supplementary Tables 5**, **6**). As expected, the addition of Z-vad did not change the levels of endocytosis as measured by AO uptake (**Figure 3C**, **Supplementary Figure 1A** and **Supplementary Tables 5**, **6**).

Finally, to validate these findings we used the fluid phase dye Lucifer Yellow and performed fluorescence microscopy. We confirmed a non-significant increase of dye uptake when cells were treated with IR alone, whereas a significant increase was observed in the combination treatments (**Figure 3D**). These findings suggest that the combination of IR with fenretinide significantly enhanced the uptake of fluid phase dyes whereas IR alone does not. Further, enhanced endocytosis might depend on mitochondrial ROS production and involve dynamin GTPases as most likely triggering factors.

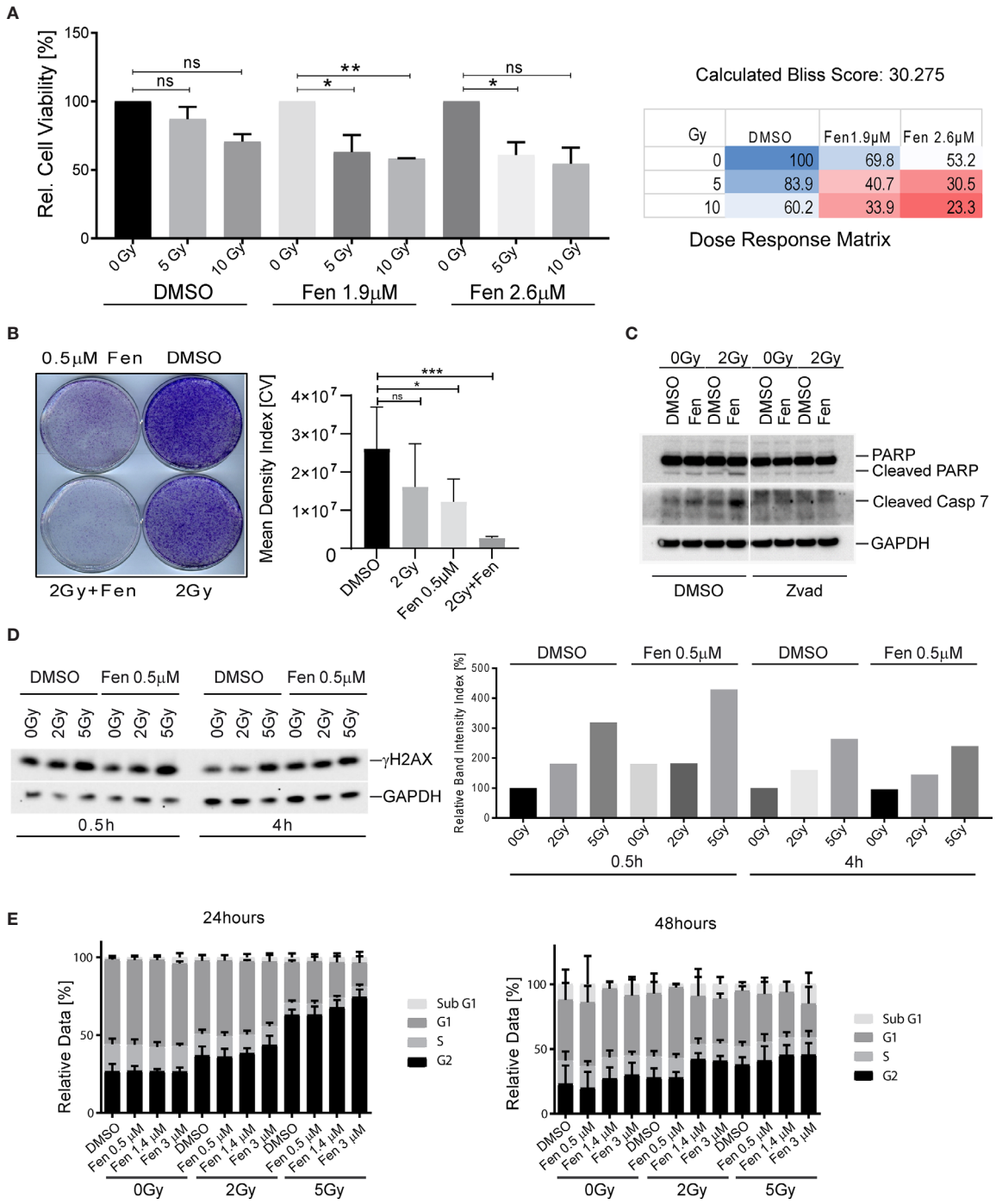

FIGURE 1 | Combinatorial treatment of aRMS cells with fenretinide and ionizing radiation leads to enhanced cell death. **(A)** Cell viability of Rh4 cells treated with fenretinide in combination with ionizing radiation at the indicated concentrations and dosages as determined by WST assay (left panel). Synergy was calculated according to the Bliss independence model using the SynergyFinder WebApp (33) (right panel). ns: $p > 0.05$, *p</=0.05, **p</=0.01. **(B)** Clonogenicity assay with Rh4 cells treated with fenretinide and ionizing radiation at the indicated concentrations and dosages. Cells were grown for 12 days after treatment (left panel). Right panel shows the mean density index of the crystal violet (CV) stainings (n = 3). ns: $p > 0.05$, *p</=0.05, ***p</=0.001. **(C)** Western Blot using whole cell lysates from Rh4 cells treated with 0.5 µM fenretinide and 2 Gy IR. Cleaved PARP, Caspase 7 and GAPDH were detected. **(D)** Western Blot using whole cell lysates from Rh4 cells treated with 0.5 µM fenretinide and either 2 or 5 Gy IR. Phosph-H2AX and GAPDH were detected (left panel). Quantification of individual band intensities assessed by BioRad Software: Depicted are the normalized ratios of γH2AX and GAPDH (right panel). **(E)** Cell cycle analysis determined by flow cytometry of Rh4 cells after 24 and 48 h treatment with fenretinide and IR at the indicated concentrations and dosages. Staining with propidium iodide (20 mg/ml).

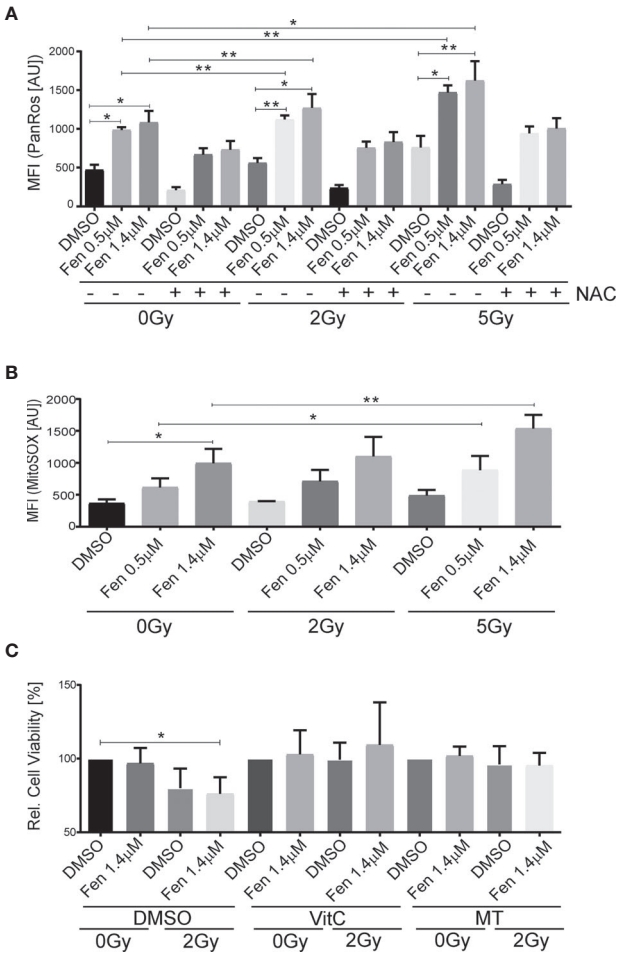

FIGURE 2 | The combination of fenretinide and ionizing radiation enhances the production of reactive oxygen species. **(A, B)** Mean fluorescence index analysis of flow cytometry data of Rh4 cells treated with fenretinide (0.5/1.4 μM) and IR (2/5 Gy), in presence or absence of 15 mM N-acetylcysteine (NAC). Cells were stained with CellRox (4 μM) **(A)** and MitoSox (10 μM) **(B)**. *p</=0.05, **p</=0.01. **(C)** Cell viability of Rh4 cells treated with fenretinide (1.4 μM) and IR (2 Gy) in presence or absence of the mitochondria specific ROS scavenger MitoTempo (300 μM) or Vitamin C (50 μM) as determined by WST assay. *p</=0.05.

DISCUSSION

The aim of this study was to evaluate the potential of fenretinide as radio sensitizer for co-treatment of FP-RMS cells together with IR. In radiation therapy, timing, duration, and dose are crucial factors for effectiveness and prevention of long-term side effects. Therefore, identification of combinations of agents and treatment modalities that act synergistically is highly appreciated. Radiosensitizing agents are capable to broaden the therapeutic window and selectively augment radiation effects in tumor cells while simultaneously sparing the surrounding tissue. Fenretinide combined with IR was studied in the context of diffuse intrinsic pontine glioma (DIPG) and showed promising results in mouse experiments (29). However, up-to-now no other studies exploring this combinatorial effect in additional tumors have been performed.

We already showed that fenretinide has a strong anti-tumour effect in FP-RMS cells through the production of mainly mitochondria derived ROS, which induced a new form of a dynamin-dependent cell death accompanied by accumulation of cytoplasmic vesicles (26). Here, first experiments demonstrated a dose-dependent combinatorial anti-tumor effect of fenretinide together with IR. This enabled us to reduce both treatment dosages with a persisting effect already at 2Gy, which also impaired clonogenic growth.

As underlying cell death mechanism apoptosis was identified in part. However, treatment also led to induction of ROS and subsequent DNA damage. RT is known to induce G2 cell cycle arrest following DNA damage (35), which was confirmed by our findings. It is also known that fenretinide can induce cell cycle arrest (36). Our results showed that impaired cell cycle progression through G2/M is most pronounced upon combination treatment. This is an important finding as one of the hallmarks of cancer is sustained proliferative signaling, even after DNA damage (37), and therefore restoration of a normal physiological response such as induction of cell death is desirable.

Our experiments using a pan-ROS detecting agent further revealed a significant increase of ROS production in irradiated cells. In our previous experiments, we were able to show that fenretinide alone induces mitochondrial derived ROS (26). Here, irradiation mainly induced the production of hydrogen peroxide, which we were able to scavenge with NAC. Hence triggering different ROS species in our combination treatment might be important in the context of resistance development, as cancer cells are known to upregulate antioxidant pathways (38).

To identify the cell death mechanism in more detail, we evaluated whether IR would also trigger dynamin-dependent macropinocytosis as this was found previously to be a relevant mode of action of fenretinide in FP-RMS cells. As shown above, we were able to identify increased macropinocytosis in the co-treated cells. In cells irradiated only, this increase was minimal when assessed by flow cytometry but slightly more prominent when assessed by light microscopy. The discrepancy between flow cytometry and light microscopy might actually be an analysis bias and explained by the fact that ionizing irradiation induces cell cycle arrest and senescence (as observed by microscopy imaging) and subsequently morphological changes of cells. As they become bigger, they might be capable to take up more dye and the analysis will show an increased integrated mean density index per cell. Due to the gating strategy applied in flow cytometry, the cell size is not relevant. However, in contrast to cells treated with fenretinide alone, in cells treated only by IR dye uptake could neither be inhibited with a dynamin inhibitor nor with a ROS-scavenger. Based on these findings it is unlikely that IR induced cell death is the result of increased macropinocytosis. However, this cell death mode can be triggered and enhanced upon co-treatment with fenretinide, most likely through the induction of a distinct population of ROS.

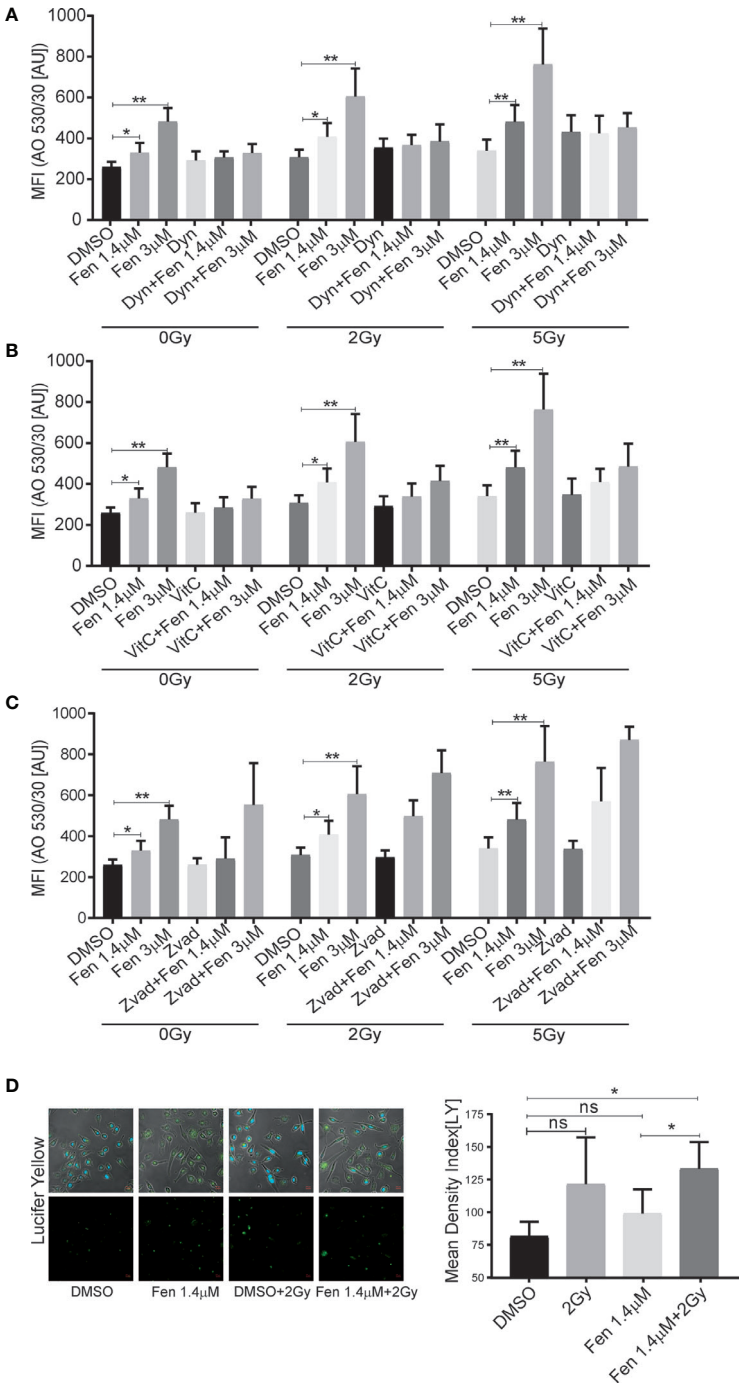

FIGURE 3 | The combinatorial treatment of fenretinide and radiation therapy leads to an enhanced uptake of phase lucent dyes. **(A–C)** Mean fluorescence index analysis of flow cytometry data of fenretinide (1.4/3 µM) and IR (2 Gy/5 Gy) treated Rh4 cells, co-treated with either dynasore (30 µM) **(A)**, Vitamin C (50 µM) **(B)** or Z-vad (100 µM) **(C)** and stained with acridine orange (2.7 µM) using two different bandpass filters, here 530/30 (Bandpass filter 670/30 **Supplementary Figures 1A–C**) *p</=0.05, **p</=0.01. **(D)** Fluorescence microscopy images of Rh4 cells left untreated or treated with fenretinide (1.4 µM), IR (5 Gy) or the combination thereof and stained with Lucifer Yellow (820 µM). Quantification of the relative mean density index was performed with Fiji software: Total integrated density value of an image was divided by the number of cells. ns: p>0.05, **p</=0.01. **Supplementary Figure 1**: The combinatorial treatment of fenretinide and IR therapy leads to an enhanced uptake of phase lucent dyes. **(A–C)** Mean fluorescence index analysis of flow cytometry data of fenretinide (1.4/3 µM) and IR (2Gy/5Gy) treated Rh4 cells in presence or absence of dynasore (30 µM) **(A)**, Vitamin C (50 µM) **(B)** or Z-vad (100 µM) **(C)** and stained with acridine orange (2.7 µM) using two different bandpass filters, here 670/30 (Bandpass filter 530/30 **A–C**). **p</=0.01.

Taken together our findings support the hypothesis that fenretinide acts as a promising radiation sensitizer in co-treatment of FP-RMS cells. Different modes of cell death mechanisms are activated and enhanced by these two treatment modalities. Reactive oxygen species and DNA damage are the main underlying triggering factors, whereas macropinocytosis as induced by fenretinide treatment plays only a minor role in IR-only treated cells. A combinatorial treatment with both modalities however may help to reduce development of resistances and increases the therapeutic window for local treatment. Hence, it might represent a promising treatment regimen in paediatric patients with FP-RMS.

DATA AVAILABILITY STATEMENT

The original contributions presented in the study are included in the article/**Supplementary Material**. Further inquiries can be directed to the corresponding author.

AUTHOR CONTRIBUTIONS

EB performed the experiments and wrote the manuscript. SB assisted her with the experiments. MW, MP, and BS provided the topic, supervised and guided the work, and proofread and edited the manuscript. All authors contributed to the article and approved the submitted version.

FUNDING

This work was funded by Krebsliga Zürich.

SUPPLEMENTARY MATERIAL

The Supplementary Material for this article can be found online at: https://www.frontiersin.org/articles/10.3389/fonc.2021.664462/full#supplementary-material

REFERENCES

1. Koscielniak EKT. *CWS-Guidance for Risk Adapted Treatment of Soft Tissue Sarcoma and Soft Tissue Tumours, in Children, Adolescents, and Young Adults Vol Version 1.6.1*. Stuttgart: Cooperative Weichteilsarkom Studie Group-CWS der GPOH (2014).
2. Brien D, Jacob AG, Qualman SJ, Chandler DS. Advances in Pediatric Rhabdomyosarcoma Characterization and Disease Model Development. *Histol Histopathol* (2012) 27:13–22. doi: 10.14670/hh-27.13
3. Williamson D, Missiaglia E, de Reynies A, Pierron G, Thuille B, Palenzuela G, et al. Fusion Gene-Negative Alveolar Rhabdomyosarcoma is Clinically and Molecularly Indistinguishable From Embryonal Rhabdomyosarcoma. *J Clin Oncol* (2010) 28:2151–8. doi: 10.1200/JCO.2009.26.3814
4. Dantonello TM, Int-Veen C, Schuck A, Seitz G, Leuschner I, Nathrath M, et al. Survival Following Disease Recurrence of Primary Localized Alveolar Rhabdomyosarcoma. *Ped Blood Cancer* (2013) 60:1267–73. doi: 10.1002/pbc.24488
5. Fuchs J, Urla C, Sparber-Sauer M, Schuck A, Leuschner I, Klingebiel T, et al. Treatment and Outcome of Patients With Localized Intrathoracic and Chest Wall Rhabdomyosarcoma: A Report of the Cooperative Weichteilsarkom Studiengruppe (Cws). *J Cancer Res Clin Oncol* (2018) 144:925–34. doi: 10.1007/s00432-018-2603-y
6. Powell S, McMillan TJ. DNA Damage and Repair Following Treatment With Ionizing Radiation. *Radiother Oncol* (1990) 19:95–108. doi: 10.1016/0167-8140(90)90123-E
7. Ward JF. Biochemistry of DNA Lesions. *Radiat Res* (1985) Suppl 8:S103–11. doi: 10.2307/3583517
8. Diehn M, Cho RW, Lobo NA, Kalisky T, Dorie MJ, Kulp AN, et al. Association of Reactive Oxygen Species Levels and Radioresistance in Cancer Stem Cells. *Nature* (2009) 458:780. doi: 10.1038/nature07733
9. Lu L, Dong J, Wang L, Xia Q, Zhang D, Kim H, et al. Activation of STAT3 and Bcl-2 and Reduction of Reactive Oxygen Species (ROS) Promote Radioresistance in Breast Cancer and Overcome of Radioresistance With Niclosamide. *Oncogene* (2018) 37:5292–304. doi: 10.1038/s41388-018-0340-y
10. Hatzi VI, Laskaratou DA, Mavragani IV, Nikitaki Z, Mangelis A, Panayiotidis MI, et al. Non-Targeted Radiation Effects In Vivo: A Critical Glance of the Future in Radiobiology. *Cancer Lett* (2015) 356:34–42. doi: 10.1016/j.canlet.2013.11.018
11. Jaffray DA, Lindsay PE, Brock KK, Deasy JO, Tomé WA. Accurate Accumulation of Dose for Improved Understanding of Radiation Effects in Normal Tissue. *Int J Radiat Oncol Biol. Phys* (2010) 76:S135–9. doi: 10.1016/j.ijrobp.2009.06.093
12. Cèfaro A. *Delineating Organs at Risk in Radiation Therapy*. Milan: Springer Science & Business Media (2013).
13. Raziee H, Moraes FY, Murgic J, Chua MLK, Pintilie M, Chung P, et al. Improved Outcomes With Dose Escalation in Localized Prostate Cancer Treated With Precision Image-Guided Radiotherapy. *Radiother Oncol* (2017) 123:459–65. doi: 10.1016/j.radonc.2017.04.003
14. Kong F, Ying H, Zhai R, Du C, Huang S, Zhou J, et al. Clinical Outcome of Intensity Modulated Radiotherapy for Carcinoma Showing Thymus-Like Differentiation. *Oncotarget* (2016) 7:81899–905. doi: 10.18632/oncotarget.11914
15. Bentzen SM. Preventing or Reducing Late Side Effects of Radiation Therapy: Radiobiology Meets Molecular Pathology. *Nat Rev Cancer* (2006) 6:702–13. doi: 10.1038/nrc1950
16. Wang H, Mu X, He H, Zhang XD. Cancer Radiosensitizers. *Trends Pharmacol Sci* (2018) 39:24–48. doi: 10.1016/j.tips.2017.11.003
17. Herrero Martin D, Boro A, Schafer BW. Cell-Based Small-Molecule Compound Screen Identifies Fenretinide as Potential Therapeutic for Translocation-Positive Rhabdomyosarcoma. *PloS One* (2013) 8:e55072. doi: 10.1371/journal.pone.0055072
18. Maurer BJ, Kang MH, Janeba J, Villablanca JG, Groshen S, Matthay KK, et al. Phase I Trial of Fenretinide Delivered Orally in a Novel Organized Lipid Complex in Patients With Relapsed/Refractory Neuroblastoma: A Report From the New Approaches to Neuroblastoma Therapy (Nant) Consortium. *Ped Blood Cancer* (2013) 60:1801–8. doi: 10.1002/pbc.24643
19. Mohrbacher AM, Yang AS, Groshen S, Kummar S, Gutierrez ME, Kang MH, et al. Phase I Study of Fenretinide Delivered Intravenously in Patients With Relapsed or Refractory Hematologic Malignancies: A California Cancer Consortium Trial. *Clin Cancer Res* (2017) 23:4550–5. doi: 10.1158/1078-0432.CCR-17-0234
20. Garaventa A, Luksch R, Lo Piccolo MS, Cavadini E, Montaldo PG, Pizzitola MR, et al. Phase I Trial and Pharmacokinetics of Fenretinide in Children With Neuroblastoma. *Clin Cancer Res* (2003) 9:2032–9.
21. Chen NE, Maldonado NV, Khankaldyyan V, Shimada H, Song MM, Maurer BJ, et al. Reactive Oxygen Species Mediates the Synergistic Activity of Fenretinide Combined With the Microtubule Inhibitor ABT-751 Against Multidrug-Resistant Recurrent Neuroblastoma Xenografts. *Mol Cancer Ther* (2016) 15:2653–64. doi: 10.1158/1535-7163.MCT-16-0156
22. Suzuki S, Higuchi M, Proske RJ, Oridate N, Hong WK, Lotan R. Implication of Mitochondria-Derived Reactive Oxygen Species, Cytochrome C and Caspase-3 in N-(4-hydroxyphenyl)retinamide-induced Apoptosis in Cervical Carcinoma Cells. *Oncogene* (1999) 18:6380–7. doi: 10.1038/sj.onc.1203024
23. Osone S, Hosoi H, Kuwahara Y, Matsumoto Y, Iehara T, Sugimoto T. Fenretinide Induces Sustained-Activation of JNK/p38 MAPK and Apoptosis in a Reactive Oxygen Species-Dependent Manner in Neuroblastoma Cells. *Int J Cancer* (2004) 112:219–24. doi: 10.1002/ijc.20412

24. Goto H, Takahashi H, Fujii H, Ikuta K. Yokota S. N-(4-Hydroxyphenyl) retinamide (4-HPR) Induces Leukemia Cell Death Via Generation of Reactive Oxygen Species. *Int J Hematol* (2003) 78:219–25. doi: 10.1007/BF02983798
25. Tosetti F, Vene R, Arena G, Morini M, Minghelli S, Noonan DM, et al. N-(4-Hydroxyphenyl)Retinamide Inhibits Retinoblastoma Growth Through Reactive Oxygen Species-Mediated Cell Death. *Mol Pharmcol* (2003) 63 (3):565–73. doi: 10.1124/mol.63.3.565
26. Brack E, Wachtel M, Wolf A, Kaech A, Ziegler U, Schafer BW. Fenretinide Induces a New Form of Dynamin-Dependent Cell Death in Pediatric Sarcoma. *Cell Death Differ* (2020) 8:2500–16. doi: 10.1038/s41418-020-0518-z
27. Maltese WA, Overmeyer JH. Methuosis: Nonapoptotic Cell Death Associated With Vacuolization of Macropinosome and Endosome Compartments. *Am J Pathol* (2014) 184:1630–42. doi: 10.1016/j.ajpath.2014.02.028
28. Overmeyer JH, Kaul A, Johnson EE, Maltese WA. Active Ras Triggers Death in Glioblastoma Cells Through Hyperstimulation of Macropinocytosis. *Mol Cancer Res* (2008) 6:965–77. doi: 10.1158/1541-7786.MCR-07-2036
29. Tsoli M, Yeung N, Valvi S, Joshi S, Franshaw L, Shen H, et al. Dipg-05. Combination of Synthetic Retinoid Fenretinide With Receptor Tyrosine Kinase Inhibitor as a Potential New Approach Against Diffuse Intrinsic Pontine Glimoma. *Neuro Oncol* (2017) 19(Suppl 4):iv5–6. doi: 10.1093/neuonc/nox083.020
30. Hinson AR, Jones R, Crose LE, Belyea BC, Barr FG, Linardic CM. Human Rhabdomyosarcoma Cell Lines for Rhabdomyosarcoma Research: Utility and Pitfalls. *Front Oncol* (2013) 3:183. doi: 10.3389/fonc.2013.00183
31. Franken NAP, Rodermond HM, Stap J, Haveman J, van Bree C. Clonogenic Assay of Cells In Vitro. *Nat Prot* (2006) 1:2315. doi: 10.1038/nprot.2006.339
32. Schindelin J, Arganda-Carreras I, Frise E, Kaynig V, Longair M, Pietzsch T, et al. Fiji: An Open-Source Platform for Biological-Image Analysis. *Nat Meth* (2012) 9:676–82. doi: 10.1038/nmeth.2019
33. Ianevski A, He L, Aittokallio T, Tang J. SynergyFinder: A Web Application for Analyzing Drug Combination Dose-Response Matrix Data. *Bioinformatics* (2017) 33:2413–5. doi: 10.1093/bioinformatics/btx162
34. Bonner WM, Redon CE, Dickey JS, Nakamura AJ, Sedelnikova OA, Solier S, et al. γh2ax and Cancer. *Nat Rev Cancer* (2008) 8:957–67. doi: 10.1038/nrc2523
35. Strasser-Wozak EM, Hartmann BL, Geley S, Sgonc R, Bock G, Santos AJ, et al. Irradiation Induces G2/M Cell Cycle Arrest and Apoptosis in p53-deficient Lymphoblastic Leukemia Cells Without Affecting Bcl-2 and Bax Expression. *Cell Death Differ* (1998) 5:687–93. doi: 10.1038/sj.cdd.4400402
36. Cowan AJ, Frayo SL, Press OW, Palanca-Wessels MC, Pagel JM, Green DJ, et al. Bortezomib and Fenretinide Induce Synergistic Cytotoxicity in Mantle Cell Lymphoma Through Apoptosis, Cell-Cycle Dysregulation, and IkappaBalpha Kinase Downregulation. *Anticancer Drugs* (2015) 26:974–83. doi: 10.1097/CAD.0000000000000274
37. Hanahan D, Weinberg RA. Hallmarks of Cancer: The Next Generation. *Cell* (2011) 144:646–74. doi: 10.1016/j.cell.2011.02.013
38. Schumacker PT. Reactive Oxygen Species in Cancer Cells: Live by the Sword, Die by the Sword. *Cancer Cell* (2006) 10:175–6. doi: 10.1016/j.ccr.2006.08.015

Conflict of Interest: The authors declare that the research was conducted in the absence of any commercial or financial relationships that could be construed as a potential conflict of interest.

frontiers in Oncology

ORIGINAL RESEARCH
published: 28 June 2021
doi: 10.3389/fonc.2021.689833

Whole-Genome Methylation Study of Congenital Lung Malformations in Children

Sara Patrizi[1], *Federica Pederiva*[2*†] *and Adamo Pio d'Adamo*[1,3†]

[1] Medical, Surgical and Health Sciences Department, University of Trieste, Trieste, Italy, [2] Pediatric Surgery, Institute for Maternal and Child Health–IRCCS "Burlo Garofolo", Trieste, Italy, [3] Laboratory of Medical Genetics, Institute for Maternal and Child Health–IRCCS "Burlo Garofolo", Trieste, Italy

OPEN ACCESS

Edited by:
Hongbo Liu,
University of Pennsylvania,
United States

Reviewed by:
Alexandra Avgustinova,
Institute for Research in Biomedicine,
Spain
Julia Krushkal,
National Cancer Institute (NCI),
United States

***Correspondence:**
Federica Pederiva
federica_pederiva@yahoo.it

[†]These authors have contributed equally to this work and share senior authorship

Specialty section:
This article was submitted to Pediatric Oncology, a section of the journal Frontiers in Oncology

Received: 01 April 2021
Accepted: 07 June 2021
Published: 28 June 2021

Citation:
Patrizi S, Pederiva F and d'Adamo AP (2021) Whole-Genome Methylation Study of Congenital Lung Malformations in Children. Front. Oncol. 11:689833. doi: 10.3389/fonc.2021.689833

Background and Objectives: The treatment of asymptomatic patients with congenital pulmonary malformations (CPMs) remains controversial, partially because the relationship between congenital lung malformations and malignancy is still undefined. Change in methylation pattern is a crucial event in human cancer, including lung cancer. We therefore studied all differentially methylated regions (DMRs) in a series of CPMs in an attempt to find methylation anomalies in genes already described in association with malignancy.

Methods: The DNA extracted from resected congenital lung malformations and control lung tissue was screened using Illumina MethylationEPIC arrays. Comparisons between the group of malformed samples or the malformed samples of same histology or each malformed sample and the controls and between a pleuropulmonary blastoma (PPB) and controls were performed. Moreover, each malformed sample was pairwise compared with its respective control. All differentially methylated regions (DMRs) with an adjusted p-value <0,05 were studied.

Results: Every comparison highlighted a number of DMRs closed to genes involved either in cell proliferation or in embryonic development or included in the Cancer Gene Census. Their abnormal methylation had been already described in lung tumors.

Conclusions: Methylation anomalies already described in lung tumors and also shared by the PPB were found in congenital lung malformations, regardless the histology. The presence of methylation abnormalities is suggestive of a correlation between congenital lung malformations and some step of malignant transformation.

Keywords: congenital lung malformation, lung tumor, methylation, whole genome, children

INTRODUCTION

There is a general consensus that symptomatic congenital pulmonary malformations (CPMs) should be removed surgically. However, the treatment of asymptomatic patients remains controversial (1). Some authors recommend prophylactic pulmonary resection to avoid the long-term risk of pulmonary recurrent infections, pneumothorax, or development of lung malignancy (1, 2), while others suggest a conservative approach based on the observation of the patient (1, 3).

The relationship between congenital lung malformations and malignancy remains undefined and continues to be a critical consideration in surgical decision making. Hartman and Stochat reported that 4% of pulmonary malignant tumors were associated with congenital cystic malformations. Tumors developing within these malformations included rhabdomyosarcoma, pleuropulmonary blastoma (PPB), adenocarcinoma, squamous cell carcinoma, and mesenchymoma (4). Later, Ozcan et al. reported 29 cases of primary rhabdomyosarcoma, 15 of which arose in a preexisting congenital lung malformations (5). Nasr et al. (6) found 2% of association between PPB and congenital pulmonary malformations. Recently, in a systematic review (7) we highlighted 168 cases, 76 children and 92 adults, in whom a lung tumor was found in association with a CPM. We concluded that all histological types of CPMs could be associated with malignant lung lesions and that the malignant transformation could happen at any age.

One hallmark of cancer cells is their completely different methylation pattern. In many malignant tumors, the levels of methylation are decreased, while promoter regions of important regulatory and tumor suppressor genes are hypermethylated and therefore silenced. Hypermethylation associated with tumor suppressor genes is uncommon in normal cells. However, it is widely represented in cancer cells (8, 9). Abnormal DNA hypomethylation has been demonstrated to also play an important role in tumor development, both increasing genome instability (10) and activating the transcription of oncogenes that are normally silenced (11).

The aim of this study was to investigate the possible biologic relationship between congenital pulmonary malformations and lung tumors. Using Illumina MethylationEPIC array analysis that is easy to use, time efficient, and cost effective technique (12), we studied all differentially methylated regions (DMRs) in a series of congenital lung malformations in an attempt to find methylation anomalies in genes already described in association with malignancy.

Abbreviations: ccRE, cis-regulatory element; CGC, Cancer Gene Census; CPAM1, 2, 3, congenital pulmonary airway malformation types 1, 2, 3; CPM, congenital pulmonary malformation; DMR, differentially methylated region; DNA, deoxyribonucleic acid; ELS, extralobar sequestration; PPB, pleuropulmonary blastoma; GOI, genes of interest; ILS, intralobar sequestration; MDS, multidimensional scaling; TCGA, The Cancer Genome Atlas; TSS, transcription start site; UTR, untranslated region.

MATERIAL AND METHODS

All congenital lung malformations resected at the Institute for Maternal and Child Health–IRCCS "Burlo Garofolo" (Trieste, Italy) from January 2010 to January 2019 were assessed. After approval by the Institutional Ethical Committee, the medical records of the patients were analyzed.

Lung biopsies from the resected malformed lobes were snap-frozen and stored at −80°C. Samples used as control included biopsies from macroscopically normal lung tissue adjacent to the malformation of seven patients, three with intralobar sequestration (ILS) and four with congenital pulmonary airway malformation type 2 (CPAM2) and from the lung of a patient who was thought to have a congenital malformation until histological analysis proved the tissue to be normal. Lung biopsies from a patient with PPB were also analyzed. We were not able to recruit other patients with the same tumor firstly because of its rarity and, secondly, because it is frequently mistaken with other diagnostic entities and formalin-fixed and paraffin-embedded. This technique of storage could lower the quality of the DNA, and therefore the comparison with higher quality DNA from fresh frozen tissues could generate artifacts. Moreover, pediatric patients with lung malignancies are also absent from public databases such as The Cancer Genome Atlas (TCGA) (13) or ENCODE (14). It is also not possible to compare methylation data from adult lung malignancies to our pediatric malformations because the methylation pattern changes drastically with age (15).

Genomic DNA was extracted from lung tissue samples (16), and its concentration was measured with Qubit dsDNA Broad Range Assay Kit (Thermo Fisher Scientific). Of each DNA sample, 1 μg was bisulfite-converted with EZ DNA Methylation Kit and screened using MethylationEPIC Beadchips according to the manufacturer's instructions (Zymo Research and Illumina Inc. respectively). Raw methylation data were analyzed with R version 3.6.2 (2019-12-12), using package ChAMP (17) (Chip Analysis Methylation Pipeline) version 2.16.1 in Rstudio.

Standard parameters of function champ.load were used to load and filter the dataset. After normalization with BMIQ method, the effect of two confounding variables (age of the samples and beadchip of origin) was removed using function removeBatchEffect from package Limma. All analyses were performed on the corrected dataset.

Significant differentially methylated regions (DMRs) were then calculated using the Bumphunter algorithm applying 1,000 permutations to each comparison, and the p-value was adjusted for multiple testing.

In our first analysis we compared the cohort of malformed samples with controls, looking for changes to the methylation pattern common to all malformations, regardless of histology. Then, we compared groups of the same histology with controls to identify any methylation signatures shared by cases of the same histological profile. Finally, we compared each individual malformed sample with the group of controls for individual differences. For eight samples that had a control tissue from the same patient available, we also performed a pairwise DMR analysis, using the standard parameters of R package

DMRforPairs (18). Furthermore, the methylation profile of the malformed samples was compared with that of the single tumor sample to highlight any similarities.

At each comparison, the identified DMRs were classified according to their location, mapping to either the gene body, the TSS (transcription start site), the 5′ UTR (untranslated region) or the 3′ UTR of protein-coding genes of interest (that we refer to in the manuscript as GOI); or mapping to an intergenic region that according to the ENCODE database contains a candidate cis-regulatory element (ccRE) close to a GOI. These genes were either included in the Cancer Gene Census (CGC, Cosmic (19) or implicated in embryonic development or involved in cell proliferation (both according to the AmiGO 2 database (20), and the overlap between the three groups of genes was also taken into consideration.

Raw data was uploaded to Gene Expression Omnibus as dataset GSE174625.

RESULTS

Eighteen patients, nine girls and nine boys, all Caucasian except for one of African ethnicity, who underwent lung resection for congenital lung malformations, were considered. Thirteen of them had prenatal diagnosis. Ten patients remained asymptomatic, while eight had different degrees of respiratory infection. Six patients had intralobar sequestration (ILS), nine had congenital pulmonary airway malformations (CPAM) associated with extralobar sequestration (ELS) in two cases. Clinical data and histology are summarized in **Table 1**.

No clear separation between the malformed and the control samples was found on a multidimensional scaling (MDS) plot representing the similarity of all samples based on the signal of the top 1,000 most variable probes. They form a homogeneous group (**Figure 1A**) completely separated from the PPB sample (**Figure 1B**).

The comparison between all the malformed samples and the controls identified 10 statistically significant DMRs (with and adjusted p-value < 0,05). Among them, one involved a ccRE located in an intergenic region near exon 1 of the gene ZFP57. In this region the mean methylation beta value was slightly higher in the malformed group than in the control group (**Figure 2**).

We also checked whether samples with the same histology have DMRs in common and that differ from controls. We found 10 significant DMRs in the ILS samples, none of which was close to a GOI. In the other histological type there were no DMRs near genes involved in cancer, but some were close to other GOIs, related to cell proliferation or embryonic development: in particular, seven out of 31 in the ELS samples, four out of 19 in the CPAM1 samples, two out of 14 in the CPAM2 samples, and two out of 20 in the CPAM3 samples (**Figure 3** and **Table 2**).

When each malformed sample was compared with the controls, the number of DMRs ranged from eight, in samples 4 and 18B, to 100 in sample 10B (**Figure 4**). Nine of them were repeated at least three times and were localized close to genes which act in cell proliferation or in embryonic development or are included in the CGC (**Table 3**). The percentage of DMRs that each sample had in common with the PPB sample ranges from 30% in sample 1 to 84% in sample 2 (**Figure 5**).

The pairwise DMR analysis, limited to the samples that had a control tissue from the same patient available, identified statistically significant DMRs in three out of eight samples: 23 in sample 10B, four in sample 12, and two in sample 17. The number of DMRs near the genes of interest was respectively thirteen, two, and one (**Table 4**).

TABLE 1 | Clinical features and histopathology of patients with congenital lung malformations.

Patient n	Sex	Prenatal diagnosis	Age at surgery (months)	Symptoms	Surgical procedure	Histology
1	F	no	21	Respiratory infections	Left lower segmentectomy	ILS
2	F	yes	5	Asymptomatic	Left lower lobectomy	ILS
3	M	no	10	Respiratory infections	Right lower lobectomy	ILS
4	F	yes	5	Respiratory infections	Left upper lobectomy	CPAM 2
5	M	yes	5	Asymptomatic	Right middle lobectomy	CPAM 3
6	F	yes	6	Asymptomatic	Right lower lobectomy	CPAM 3
7	M	yes	60	Respiratory infections	Right middle lobectomy	CPAM 3
8	M	no	108	Right lung pneumonia	Right upper lobectomy	CPAM 1
9	F	yes	57	Respiratory infections	Left lower lobectomy	ILS
10 (A + B)	M	no	120	Pneumonias	Left lower lobectomy + ELS resection	CPAM 2 + ELS
11	F	yes	7	Asymptomatic	Left lower lobectomy	CPAM 2
12	F	yes	9	Asymptomatic	Left lower lobectomy	ILS
13	M	no	140	Pneumonias	Left lower lobectomy	CPAM 2
14	F	yes	14	Asymptomatic	Left lower lobectomy	CPAM 2
15	F	yes	8	Asymptomatic	Right middle lobectomy	CPAM 1
16	M	yes	9	Asymptomatic	Left upper lobectomy	CPAM 2
17	M	yes	9	Asymptomatic	Right lower lobectomy	ILS
18 (A + B)	M	yes	10	Asymptomatic	Right upper lobectomy + ELS resection	CPAM 2 + ELS

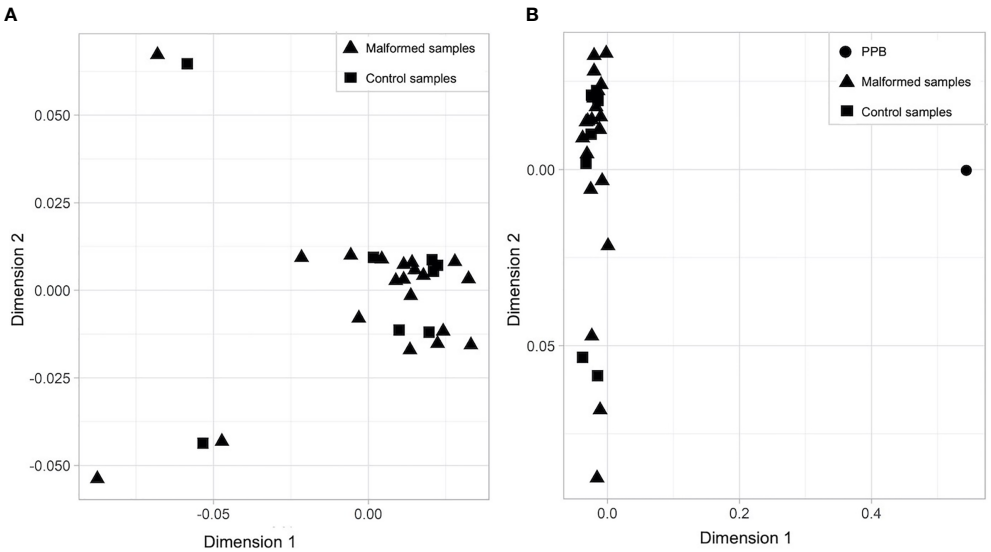

FIGURE 1 | Multidimensional scaling (MDS) plot of **(A)** malformed and control samples; **(B)** malformed, control and pleuropulmonary blastoma samples. In each plot, the X axis represents Dimension 1 and the Y axis Dimension 2 of the MDS statistical analysis, which better expresses the mathematical distance between the samples.

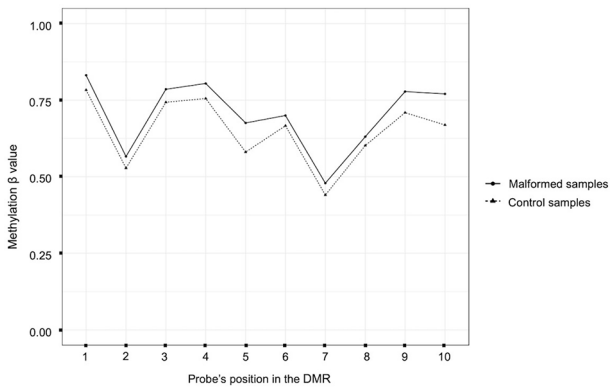

FIGURE 2 | Plot of the beta methylation values (Y axis) of each probe (X axis) of the DMR located near the gene ZFP57. The beta values range from 1 (completely methylated) to 0 (completely unmethylated). The position of the probes inside the DMR is ordered according to their genomic position.

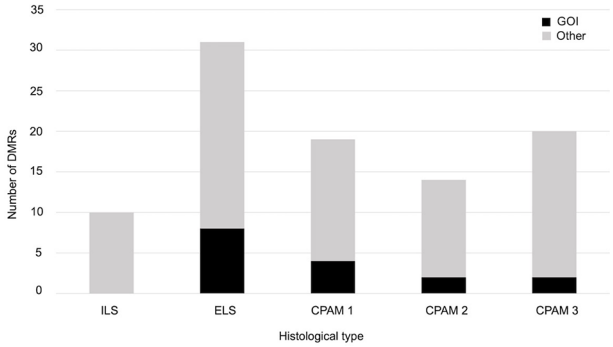

FIGURE 3 | Number of significant DMRs (adjusted p-value < 0,05), close to GOI (black) and to different genes (gray), identified when the cases of same histology were compared with controls.

DISCUSSION

Congenital pulmonary malformations are developmental abnormalities of the lung occurring in approximately one to 4.2 per 10,000 births (21). Postnatal presentation varies from severe respiratory distress to complete lack of symptoms (22). Although all authors agree that surgical resection is the standard of care for symptomatic cases, the management of asymptomatic lesions remains controversial. The main reason for recommending elective surgery is late development of complications, including the highly debated malignancy. The relationship between congenital lung malformations and malignancy remains unknown and continues to be a critical consideration in surgical decision making. Some studies have addressed this issue in an attempt to find premalignant characteristics in congenital lung malformations.

Vargas and colleagues analyzed the karyotype and looked for p53 mutations in congenital cystic adenomatoid malformations. As they did not find cytogenetic abnormalities in congenital cystic adenomatoid malformations by conventional karyotype analysis, they concluded that congenital lung anomalies were non-neoplastic (23). Later, Rossi and colleagues found expression of mucins and K-RAS mutations in mucinogenic proliferations of congenital pulmonary airway malformations and concluded that these findings supported the neoplastic nature of the

TABLE 2 | GOI close to significant DMRs elicited by the comparison between cases of same histology with controls.

Histology	Gene(s) in or near the DMR	GOI
ELS	HOXB1	development
	HOXD4	development
	CTNNA1	proliferation
	NR2F2	proliferation and development
	HSF4	proliferation
	MEIS1	proliferation
	PTN	proliferation
CPAM 1	PLD6	development
	TXNRD1	proliferation and development
	S100A13	proliferation
	MSX2	proliferation and development
CPAM 2	ZFP57	development
	MEIS1	proliferation
CPAM 3	MSX2	proliferation and development
	PITX2, ENPEP	proliferation

TABLE 3 | GOI close to significant DMRs repeated at least three times when each malformed sample was compared to the controls.

Patient n	Gene(s) in or near the DMR	GOI
2	HOXB1	development
	SIX1, SIX4, MNAT1	cancer, proliferation and development
5	ZFP57	development
	IRAK4	proliferation
	MSX2	development
6	ZFP57	development
	MSX2	proliferation and development
7	ZFP57	development
	IRAK4	proliferation
	MSX2	proliferation and development
	NR2F2	proliferation and development
	MEIS1	proliferation
	HOXB1	development
	HOXD4	development
11	ZFP57	development
12	ZFP57	proliferation
	IRAK4	proliferation
13	ZFP57	development
	IRAK4	proliferation
17	ZFP57	development
	MMP2, IRX5	proliferation and development
	HOXD4	development
	MEIS1	proliferation
	IRAK4	proliferation
	SIX1, SIX4, MNAT1	cancer, proliferation and development
16	HOXD4	development
	ZFP57	development
18a	ZFP57	development
	HOXB1	development
	HOXD4	development
	NR2F2	proliferation and development
	MEIS1	proliferation
	MMP2, IRX5	proliferation and development
	SIX1, SIX4, MNAT1	cancer, proliferation and development
18b	ZFP57	development
	HOXD4	development

malformations (24). Recently, Hsu et al. (25) described in the blood of 19 cases of CPAM several damaging variants in genes involved in lung carcinoma.

The aim of this study was to look for further insight into the biologic relationship between congenital pulmonary malformations and lung tumors. As the change in methylation pattern is a pivotal event in human cancer including lung cancer, in this study we focused on DNA methylation in a series of congenital lung malformations.

Firstly, we compared all the malformed samples with the controls identifying, among ten, only one DMR of interest, involving a candidate cis-regulatory element (ccRE) and located near exon 1 of the gene ZFP57, which acts in genome

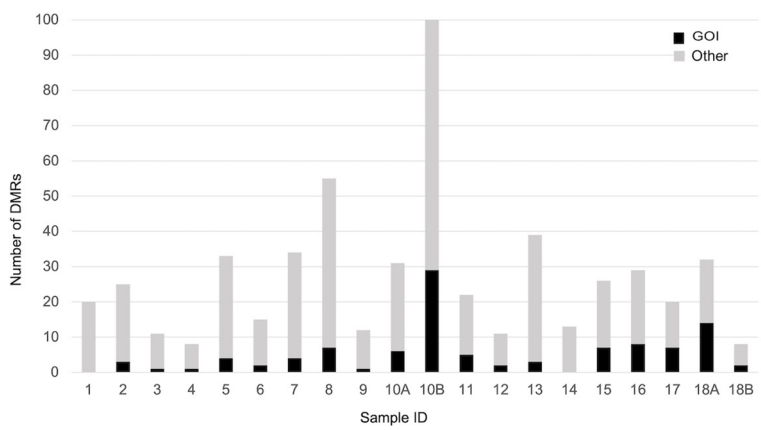

FIGURE 4 | Number of significant DMRs (adjusted p-value < 0,05), close to GOI (black) and to different genes (gray), identified comparing each malformed case with controls.

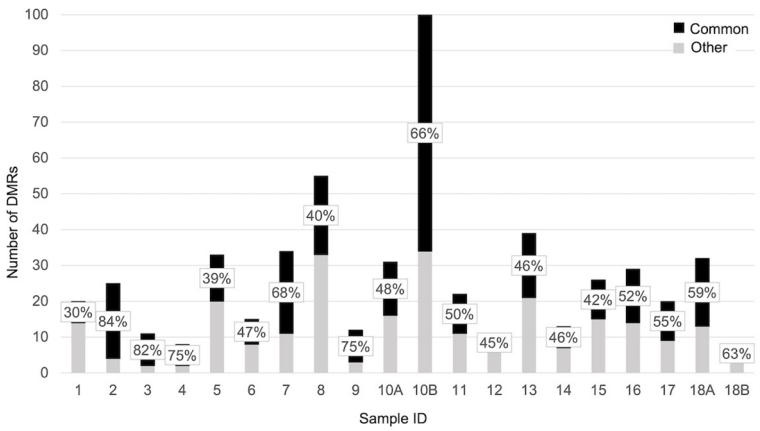

FIGURE 5 | Bar plot representing the percentage of significant DMRs (adjusted p-value < 0,05) shared by each sample with the PPB.

TABLE 4 | GOI close to significant DMRs elicited by the pairwise comparison between each malformed sample and the corresponding control tissue.

Patient n	Gene(s) in or near the DMR	GOI
10B	HOXA3	development
	CTNNA1	proliferation
	CTSZ	proliferation
	NR2F2	proliferation and development
	GPR37L1	proliferation
	IGF2BP1	proliferation
	TGFB1I1	proliferation and development
	HOXC6	development
	TSPAN32	proliferation
	S100A13	proliferation
	BRD2	development
	HOXB1	development
12	SMAD6	proliferation and development
	FOXP1	proliferation and cancer
17	HOXD3–HOXD4	development

imprinting, regulation of gene expression, and cell signaling. It has recently been hypothesized that ZFP57 is a potential susceptibility gene for lung cancer development through the increase of IGF2 expression (26).

The analysis did not uncover a common methylation pattern since the significant DMRs were very few. This was not surprising, as the malformed samples were a very heterogeneous group, and the individual differences in the methylation patterns of each malformed sample, combined with the likely cellular heterogeneity of the samples (that was beyond the control of the investigators), masked the differences between the two groups.

Looking for a common methylation signature among the cases of CPMs, we then compared the cases of same histology with controls. The results highlighted seven DMRs in the ELS close to genes mostly involved in embryonic development (at the TSS of HOXB1, HOXD4) and cell proliferation (at the TSS of CTNNA1, NR2F2, HSF4, MEIS1, and at the gene body of PTN). Both HOXB1 and HOXD4 were abnormally expressed in lung tumors. HOXB1 was described down-regulated in lung cancer tissue (27) and, similarly, we found the DMR close to this gene was hypermethylated. HOXB1 is an anti-tumor gene acting by inhibiting the expression of survival oncogenic genes (28); its decreased expression had been correlated with cell invasion and proliferation and inhibited apoptosis in glioma (29). HOXD4 was reported up-regulated in lung squamous cell carcinoma resulting in more aggressive invasiveness of lung cancer cells (30). In our samples of ELS HOXD4 was hypermethylated in an opposite fashion compared to those in the literature. Either CTNNA1 (31) or NF2F2 (32) has been found significantly down-regulated in lung cancer. The DMR close to CTNNA1 was hypermethylated in our samples in line with previous report of the literature. NF2F2 was also known to play a role in angiogenesis and development and to contribute to transform a non-invasive lung cancer in an invasive one through its expression (33). MEIS1 might limit the proliferation of non-small-cell lung adenocarcinoma (34) and was described methylated in squamous cell carcinomas (35). PTN is highly expressed in embryonic and postnatal development, while it is quite down-regulated in adult life; however, it is strongly expressed in lung tumor and other types of cancer (36). Hypermethylation was found in our samples for the DMR close to MEIS1 and PTN.

Four DMRs were found in CPAM1 cases close to genes related to cell proliferation or embryonic development (at the TSS of PLD6, S100A13; MXS2, and at the 5′ UTR of TXNRD1). S100A13's overexpression was associated with intratumoral angiogenesis and more aggressive invasive phenotype in non-small-cell lung cancer (37). In our samples the DMR was hypermethylated differently from those in the literature. MSX2 is a regulator of embryonic development, and it is involved in pancreatic and breast cancer, but recently it has been found that it plays a role also in lung adenocarcinoma (38). The DMR was hypermethylated in our samples.

We found two DMRs in CPAM2 cases, close to the already discussed intergenic region near ZFP57, acting in embryonic

development, and the gene body of MEIS1, whose closed DMR was hypomethylated differently from the mechanism in literature.

Finally, CPAM3 cases presented two DMRs, one close to the TSS of MSX2 which was this time hypomethylated, and the other in an intergenic region involving a ccRE near two genes involved in proliferation that was hypomethylated as well. The first gene near the second DMR was PITX2, whose low methylation correlated with higher risk of lung cancer progression (39), and the other was ENPEP that was under-expressed in lung adenocarcinoma (40).

One more time, the heterogenicity of the malformed samples likely prevented to highlight a common methylation signature. However, the presence of methylation abnormalities in genes already described in association with malignancy is suggestive, especially considering their role in lung tumors.

Due to the heterogeneity in our malformed samples, we also checked for individual differences by comparing each sample with the control group. It yielded a wide range of DMRs, but nine of them recurring at least three times: three including one ccRE each, near the genes ZFP57, SIX1-SIX4-MNAT1, and MMP2-IRX5; four at the TSS of genes HOXB1, HOXD4, NR2F2 and MSX2; one at the 5′ UTR of IRAK4, and one at the gene body of MEIS1. ZFP57, HOXB1, HOXD4, NR2F2, MEIS1, and MSX2 were already described when the cases of same histology were compared with controls. Interestingly, the DMR close to HOXB1 was found hypomethylated and the one close to HOXD4 hypermethylated, in the opposite way to the literature. SIX1 and SIX4 were associated with increased risk of tumorigenesis when their expression was increased. SIX4 controlled the expression of oncogenes, and it correlated with higher stages of the tumor, poor survival in NSCLC, and worse rate of relapses in lung adenocarcinoma (41). MNAT1 might have a role in promoting the development of NSCLC (42). MMP2 mRNA and protein levels were found increased in NSCLC (43).

The pairwise DMR analysis found statistically significant DMRs in three out of eight samples, when comparing each one of them with the corresponding control tissue from the same patient. The number of DMRs near to genes of interest was 12 out of 23 in one of the ELS (sample 10B), two out of four in an ILS (sample 12), and one out of two in another ILS (sample 17). In the ELS, the DMRs of interest were located at the gene body or the TSS of genes involved in embryo development (HOXA3, HOXC6, HOXB1, TGFB1I1, BRD2), cell proliferation (CTNNA1, CTSZ, GPR37L1, S100A13, TSPAN32, FOXP2), or both processes (IGF2BP1, NR2F2). In one of the ILS (sample 12), one DMR of interest was hypomethylated with respect to the control tissue, and located at the gene body of SMAD6 that has been reported as a "master regulator" of lung adenocarcinoma, for which both oncogenic and tumor suppressing activities have been proposed (44). The second DMR of interest for the same sample was a hypermethylated region at the gene body of FOXP1, a transcription factor involved in cell proliferation and included in the CGC that according to Sheng et al (45), prevented the growth of lung adenocarcinoma cells by the suppression of chemokine signaling pathways. The DMR of interest in the other ILS (sample 17) was located at the TSS of HOXD4, a gene that has been discussed earlier, and it was less methylated in the malformed than in the control tissue, contrarily to our previous findings but in concordance with the literature.

Both types of single sample analyses have strengths and weaknesses. Comparison of one sample to the entire control group allowed the analysis of samples that do not have a control tissue from the same patient, but it could introduce artifacts due to inter-patient variability of the methylation profile. The pairwise analysis, on the other hand, was possible in this case for a smaller number of samples, but it excluded any underlying methylation alterations not strictly related to the malformation, thus producing more specific results.

Finally, we compared the PPB sample with the controls and considered to discuss, among all, the DMRs in common with the malformed samples, mapping to the 3′ UTR of CACNA1C, the 5′ UTR of HOXA5, the TSS of CTSZ, ESRP2, HAND2, HOXA2, HOXA3, MAGI2, TWIST1, ccREs near MMP2, MSX1-OTX1-RUNX1, TBX3–TBX5, and the gene body of SH3PXD2A and WT1).

CACNA1C was found down-regulated in lung cancer (46). CTSZ was involved in promoting NSCLC cell migration and invasion (47). ESRP2 maintained the epithelial phenotype, avoiding the epithelial to mesenchymal transition that contributed to metastases. In NSCLC it was inhibited (48). HAND2 was found either hypermethylated or hypomethylated in different stages of lung adenocarcinoma (49). HOXA2, HOXA3, and HOXA5 have been recognized as target for DNA methylation in lung cancer, and they promoted carcinogenesis, but also acted as tumor-suppressor factors (50). MAGI2 was reported to act as an anti-tumor in hepatocellular cancer and breast cancer; its down-regulation has been demonstrated in NSCLC (51). CpG islands associated with MSX1 and OTX1 were methylated in the majority of lung squamous cell carcinomas, while the ones associated with RUNX1 were methylated in more than 80% of lung adenocarcinomas, being well known that hypermethylation of CpG islands is a signature of malignant progression (35). SH3PXD2A's increased expression in lung adenocarcinoma directly correlated with metastasis and worse prognosis for the patient (52). TBX5 and TBX3 were highly expressed in normal lungs, but significantly suppressed in lung adenocarcinoma (53). TWIST1 expression was found increased in lung cancer tissue (54). WT1 was described as oncogene in lung cancer, among other malignancies (55).

The DMRs of interest were spread throughout the cases, and we were not able to find a recurrent pattern of abnormalities in the different types of congenital lung malformations.

It has been demonstrated that lung cancer develops through the acquisition of alterations in oncogenes and tumor suppressor genes. Prolonged exposure to carcinogens that interact with various genetic susceptibility and/or resistance factors contributes to the accumulation of genomic alterations, including nucleotide substitutions, small insertions and deletions, and chromosomal rearrangements in human lung cancer (56). This mechanism of action may explain the cases of association between congenital pulmonary malformations,

sometimes asymptomatic for many years, and lung tumors described in literature (7), in which the genetic susceptibility together with the progressive exposure to carcinogens might trigger the development of malignancy.

This study has highlighted some key points. First, methylation anomalies already described in lung tumors could be found in samples of congenital lung malformations, regardless the histology, both when compared to the control group and when compared to a specific control tissue. Second, some methylation anomalies of the congenital lung malformations were shared by the PPB. Third, it seems unlikely that the presence of methylation abnormalities, which have been reported in association with lung tumors, could be considered a casual event in congenital lung malformations, in which malignant transformation has been described (7). Pulmonary malformations are essentially due to a dysregulation of cell proliferation which, during organogenesis, creates an abnormal development of some areas of the lower respiratory tract. Our study indicates that, at least in part, this dysregulation is caused by some genes which, due to their role in the cell cycle, are also involved in some stages of tumor development.

Our study, however, had some limits that should be acknowledged, such as the small number of samples of congenital lung malformations included and their heterogenicity. Moreover, the difficulty in finding proper control samples has limited their number. Another limitation is the lack of material from pediatric adenocarcinoma of the lung, which is the second tumor for frequency that has been found in association with CPMs in children (7), and the impossibility to compare the methylation of pediatric CPMs to the available adult adenocarcinoma samples due to the age-related changes in the methylation pattern. To our knowledge, this study represents the first attempt to address the methylation anomalies in pediatric congenital lung malformations using a whole genome approach. We have also described some methylation changes which, in some genes, appeared to have the opposite sign to what is described in the literature regarding their expression. These results, however, should not be discarded, because the relationship between DNA methylation and gene expression could be more complicated than previously understood [for example, it can have different effects according to its position with respect to the gene (57)], and DNA methylation is only one of the factors that regulate the expression of a gene. Thus, since we did not study the gene expression in our samples, we cannot be certain that hypomethylation corresponds to hyperexpression or *vice versa*.

CONCLUSION

Methylation anomalies already described in lung tumors and also shared by the PPB were found in congenital lung malformations, regardless the histology. This is suggestive of a correlation between congenital lung malformations and some step of malignant transformation.

More detailed analysis of genetic and epigenetic interactions as well as functional interactions among genes altered in congenital pulmonary malformations will further provide insights into the molecular mechanism of lung carcinogenesis.

DATA AVAILABILITY STATEMENT

The original contributions presented in the study are publicly available. This data can be found here https://www.ncbi.nlm.nih.gov/geo/query/acc.cgi?acc=GSE174625.

ETHICS STATEMENT

The studies involving human participants were reviewed and approved by IRCCS Burlo Garofolo. Written informed consent to participate in this study was provided by the participants' legal guardian/next of kin.

AUTHOR CONTRIBUTIONS

FP and AD'A conceptualized and designed the study, drafted the initial manuscript, and reviewed and revised the manuscript. SP designed the data collection instruments, collected data, carried out the initial analyses, and reviewed and revised the manuscript. All authors contributed to the article and approved the submitted version.

FUNDING

This study was supported by the IRCCS "Burlo Garofolo" (RC 22/11). The funder/sponsor did not participate in the work.

REFERENCES

1. Lo AY, Jones S. Lack of Consensus Among Canadian Pediatric Surgeons Regarding the Management of Congenital Cystic Adenomatoid Malformation of the Lung. *J Pediatr Surg* (2008) 43:797–9. doi: 10.1016/j.jpedsurg.2007.12.016
2. Laberge JM, Puligandla P, Flageole H. Asymptomatic Congenital Lung Malformations. *Semin Pediatr Surg* (2005) 14:16–33. doi: 10.1053/j.sempedsurg.2004.10.022
3. Aziz D, Langer JC, Tuuha SE, Ryan G, Ein SH, Kim PC. Perinatally Diagnosed Asymptomatic Congenital Cystic Adenomatoid Malformation: to Resect or Not? *J Pediatr Surg* (2004) 39:329–34; discussion 329-34. doi: 10.1016/j.jpedsurg.2003.11.021
4. Hartman GE, Shochat SJ. Primary Pulmonary Neoplasms of Childhood: A Review. *Ann Thorac Surg* (1983) 36:108–19. doi: 10.1016/S0003-4975(10)60664-9
5. Ozcan C, Celik A, Ural Z, Veral A, Kandiloglu G, Balik E. Primary Pulmonary Rhabdomyosarcoma Arising Within Cystic Adenomatoid Malformation: A Case Report and Review of the Literature. *J Pediatr Surg* (2001) 36:1062–5. doi: 10.1053/jpsu.2001.24747
6. Nasr A, Himidan S, Pastor AC, Taylor G, Kim PC. Is Congenital Cystic Adenomatoid Malformation a Premalignant Lesion for Pleuropulmonary Blastoma? *J Pediatr Surg* (2010) 45:1086–9. doi: 10.1016/j.jpedsurg.2010.02.067
7. Casagrande A, Pederiva F. Association Between Congenital Lung Malformations and Lung Tumors in Children and Adults: A Systematic Review. *J Thorac Oncol* (2016) 11:1837–45. doi: 10.1016/j.jtho.2016.06.023

8. Traube FR, Carell T. The Chemistries and Consequences of DNA and RNA Methylation and Demethylation. *RNA Biol* (2017) 14:1099–107. doi: 10.1080/15476286.2017.1318241
9. Liu XR, Zhang RY, Gong H, Rugo HS, Chen LB, Fu Y, et al. Methylome Variation Predicts Exemestane Resistance in Advanced Er(+) Breast Cancer. *Technol Cancer Res Treat* (2020) 19:1533033819896331. doi: 10.1177/1533033819896331
10. Gaudet F, Hodgson JG, Eden A, Jackson-Grusby L, Dausman J, Gray JW, et al. Induction of Tumors in Mice by Genomic Hypomethylation. *Science* (2003) 300:489–92. doi: 10.1126/science.1083558
11. Ehrlich M. DNA Hypomethylation in Cancer Cells. *Epigenomics* (2009) 1:239–59. doi: 10.2217/epi.09.33
12. Pidsley R, Zotenko E, Peters TJ, Lawrence MG, Risbridger GP, Molloy P, et al. Critical Evaluation of the Illumina Methylationepic BeadChip Microarray for Whole-Genome DNA Methylation Profiling. *Genome Biol* (2016) 17:208. doi: 10.1186/s13059-016-1066-1
13. Hutter C, Zenklusen JC. The Cancer Genome Atlas: Creating Lasting Value Beyond Its Data. *Cell* (2018) 173:283–5. doi: 10.1016/j.cell.2018.03.042
14. Davis CA, Hitz BC, Sloan CA, Chan ET, Davidson JM, Gabdank I, et al. The Encyclopedia of DNA Elements (ENCODE): Data Portal Update. *Nucleic Acids Res* (2018) 46:D794–801. doi: 10.1093/nar/gkx1081
15. Johansson A, Enroth S, Gyllensten U. Continuous Aging of the Human DNA Methylome Throughout the Human Lifespan. *PLoS One* (2013) 8:e67378. doi: 10.1371/journal.pone.0067378
16. Miller SA, Dykes DD, Polesky HF. A Simple Salting Out Procedure for Extracting DNA From Human Nucleated Cells. *Nucleic Acids Res* (1988) 16:1215. doi: 10.1093/nar/16.3.1215
17. Tian Y, Morris TJ, Webster AP, Yang Z, Beck S, Feber A, et al. ChAMP: Updated Methylation Analysis Pipeline for Illumina Beadchips. *Bioinformatics* (2017) 33:3982–4. doi: 10.1093/bioinformatics/btx513
18. Rijlaarsdam MA, van der Zwan YG, Dorssers LC, Looijenga LH. DmrforPairs: Identifying Differentially Methylated Regions Between Unique Samples Using Array Based Methylation Profiles. *BMC Bioinf* (2014) 15:141. doi: 10.1186/1471-2105-15-141
19. Sondka Z, Bamford S, Cole CG, Ward SA, Dunham I, Forbes SA. The COSMIC Cancer Gene Census: Describing Genetic Dysfunction Across All Human Cancers. *Nat Rev Cancer* (2018) 18:696–705. doi: 10.1038/s41568-018-0060-1
20. Carbon S, Ireland A, Mungall CJ, Shu S, Marshall B, Lewis S, et al. AmiGO: Online Access to Ontology and Annotation Data. *Bioinformatics* (2009) 25:288–9. doi: 10.1093/bioinformatics/btn615
21. Raychaudhuri P, Pasupati A, James A, Whitehead B, Kumar R. Prospective Study of Antenatally Diagnosed Congenital Cystic Adenomatoid Malformations. *Pediatr Surg Int* (2011) 27:1159–64. doi: 10.1007/s00383-011-2909-1
22. Hammond PJ, Devdas JM, Ray B, Ward-Platt M, Barrett AM, McKean M. The Outcome of Expectant Management of Congenital Cystic Adenomatoid Malformations (CCAM) of the Lung. *Eur J Pediatr Surg* (2010) 20:145–9. doi: 10.1055/s-0030-1249047
23. Vargas SO, Korpershoek E, Kozakewich HP, de Krijger RR, Fletcher JA, Perez-Atayde AR. Cytogenetic and p53 Profiles in Congenital Cystic Adenomatoid Malformation: Insights Into Its Relationship With Pleuropulmonary Blastoma. *Pediatr Dev Pathol* (2006) 9:190–5. doi: 10.2350/06-01-0025.1
24. Rossi G, Gasser B, Sartori G, Migaldi M, Costantini M, Mengoli MC, et al. MUC5AC, Cytokeratin 20 and HER2 Expression and K-RAS Mutations Within Mucinogenic Growth in Congenital Pulmonary Airway Malformations. *Histopathology* (2012) 60:1133–43. doi: 10.1111/j.1365-2559.2011.04170.x
25. Hsu JS, Zhang R, Yeung F, Tang CSM, Wong JKL, So MT, et al. Cancer Gene Mutations in Congenital Pulmonary Airway Malformation Patients. *ERJ Open Res* (2019) 5:00196–2018. doi: 10.1183/23120541.00196-2018
26. Lamontagne M, Joubert P, Timens W, Postma DS, Hao K, Nickle D, et al. Susceptibility Genes for Lung Diseases in the Major Histocompatibility Complex Revealed by Lung Expression Quantitative Trait Loci Analysis. *Eur Respir J* (2016) 48:573–6. doi: 10.1183/13993003.00114-2016
27. Cui F, Zhou Q, Xiao K, Ma S. The MicroRNA Hsa-Let-7g Promotes Proliferation and Inhibits Apoptosis in Lung Cancer by Targeting Hoxb1. *Yonsei Med J* (2020) 61:210–7. doi: 10.3349/ymj.2020.61.3.210
28. Lopez R, Garrido E, Pina P, Hidalgo A, Lazos M, Ochoa R, et al. HOXB Homeobox Gene Expression in Cervical Carcinoma. *Int J Gynecol Cancer* (2006) 16:329–35. doi: 10.1111/j.1525-1438.2006.00350.x
29. Han L, Liu D, Li Z, Tian N, Han Z, Wang G, et al. Hoxb1 Is a Tumor Suppressor Gene Regulated by miR-3175 in Glioma. *PLoS One* (2015) 10: e0142387. doi: 10.1371/journal.pone.0142387
30. Bao L, Zhang Y, Wang J, Wang H, Dong N, Su X, et al. Variations of Chromosome 2 Gene Expressions Among Patients With Lung Cancer or Non-Cancer. *Cell Biol Toxicol* (2016) 32:419–35. doi: 10.1007/s10565-016-9343-z
31. Srivastava M, Khurana P, Sugadev R. Lung Cancer Signature Biomarkers: Tissue Specific Semantic Similarity Based Clustering of Digital Differential Display (DDD) Data. *BMC Res Notes* (2012) 5:617. doi: 10.1186/1756-0500-5-617
32. Ning J, Li P, Zhang B, Han B, Su X, Wang Q, et al. miRNAs Deregulation in Serum of Mice is Associated With Lung Cancer Related Pathway Deregulation Induced by PM2. *5 Environ Pollut* (2019) 254:112875. doi: 10.1016/j.envpol.2019.07.043
33. Navab R, Gonzalez-Santos JM, Johnston MR, Liu J, Brodt P, Tsao MS, et al. Expression of Chicken Ovalbumin Upstream Promoter-Transcription Factor II Enhances Invasiveness of Human Lung Carcinoma Cells. *Cancer Res* (2004) 64:5097–105. doi: 10.1158/0008-5472.CAN-03-1185
34. Li W, Huang K, Guo H, Cui G. Meis1 Regulates Proliferation of Non-Small-Cell Lung Cancer Cells. *J Thorac Dis* (2014) 6:850–5. doi: 10.3978/j.issn.2072-1439.2014.06.03
35. Rauch TA, Wang Z, Wu X, Kernstine KH, Riggs AD, Pfeifer GP. DNA Methylation Biomarkers for Lung Cancer. *Tumour Biol* (2012) 33:287–96. doi: 10.1007/s13277-011-0282-2
36. Zha L, He L, Xie W, Cheng J, Li T, Mohsen MO, et al. Therapeutic Silence of Pleiotrophin by Targeted Delivery of siRNA and Its Effect on the Inhibition of Tumor Growth and Metastasis. *PLoS One* (2017) 12:e0177964. doi: 10.1371/journal.pone.0177964
37. Miao S, Qiu T, Zhao Y, Wang H, Sun X, Wang Y, et al. Overexpression of S100A13 Protein Is Associated With Tumor Angiogenesis and Poor Survival in Patients With Early-Stage Non-Small Cell Lung Cancer. *Thorac Cancer* (2018) 9:1136–44. doi: 10.1111/1759-7714.12797
38. Bidkhori G, Narimani Z, Hosseini Ashtiani S, Moeini A, Nowzari-Dalini A, Masoudi-Nejad A. Reconstruction of an Integrated Genome-Scale Co-Expression Network Reveals Key Modules Involved in Lung Adenocarcinoma. *PLoS One* (2013) 8:e67552. doi: 10.1371/journal.pone.0067552
39. Luo J, Yao Y, Ji S, Sun Q, Xu Y, Liu K, et al. PITX2 Enhances Progression of Lung Adenocarcinoma by Transcriptionally Regulating WNT3A and Activating Wnt/beta-Catenin Signaling Pathway. *Cancer Cell Int* (2019) 19:96. doi: 10.1186/s12935-019-0800-7
40. Goldstein B, Trivedi M, Speth RC. Alterations in Gene Expression of Components of the Renin-Angiotensin System and Its Related Enzymes in Lung Cancer. *Lung Cancer Int* (2017) 2017:6914976. doi: 10.1155/2017/6914976
41. Liu Q, Li A, Tian Y, Liu Y, Li T, Zhang C, et al. The Expression Profile and Clinic Significance of the SIX Family in Non-Small Cell Lung Cancer. *J Hematol Oncol* (2016) 9:119. doi: 10.1186/s13045-016-0339-1
42. Chen Y, Guan JX, Shen H. [MNAT1 Expression in Non-Small Cell Lung Cancer and Its Biological Cellular Impact]. *Zhonghua Bing Li Xue Za Zhi* (2019) 48:626–32. doi: 10.3760/cma.j.issn.0529-5807.2019.08.008
43. Zeng F, Yu N, Han Y, Ainiwaer J. The Long non-Coding RNA Miat/miR-139-5p/MMP2 Axis Regulates Cell Migration and Invasion in Non-Small-Cell Lung Cancer. *J Biosci* (2020) 45:51. doi: 10.1007/s12038-020-0019-8
44. De Bastiani MA, Klamt F. Integrated Transcriptomics Reveals Master Regulators of Lung Adenocarcinoma and Novel Repositioning of Drug Candidates. *Cancer Med* (2019) 8:6717–29. doi: 10.1002/cam4.2493
45. Sheng H, Li X, Xu Y. Knockdown of FOXP1 Promotes the Development of Lung Adenocarcinoma. *Cancer Biol Ther* (2019) 20:537–45. doi: 10.1080/15384047.2018.1537999
46. Phan NN, Wang CY, Chen CF, Sun Z, Lai MD, Lin YC. Voltage-Gated Calcium Channels: Novel Targets for Cancer Therapy. *Oncol Lett* (2017) 14:2059–74. doi: 10.3892/ol.2017.6457
47. Li W, Yu X, Ma X, Xie L, Xia Z, Liu L, et al. Deguelin Attenuates Non-Small Cell Lung Cancer Cell Metastasis Through Inhibiting the CtsZ/FAK Signaling Pathway. *Cell Signal* (2018) 50:131–41. doi: 10.1016/j.cellsig.2018.07.001

48. Gemmill RM, Roche J, Potiron VA, Nasarre P, Mitas M, Coldren CD, et al. ZEB1-Responsive Genes in Non-Small Cell Lung Cancer. *Cancer Lett* (2011) 300:66–78. doi: 10.1016/j.canlet.2010.09.007
49. Pradhan MP, Desai A, Palakal MJ. Systems Biology Approach to Stage-Wise Characterization of Epigenetic Genes in Lung Adenocarcinoma. *BMC Syst Biol* (2013) 7:141. doi: 10.1186/1752-0509-7-141
50. Rauch T, Wang Z, Zhang X, Zhong X, Wu X, Lau SK, et al. Homeobox Gene Methylation in Lung Cancer Studied by Genome-Wide Analysis With a Microarray-Based Methylated CpG Island Recovery Assay. *Proc Natl Acad Sci USA* (2007) 104:5527–32. doi: 10.1073/pnas.0701059104
51. He J, Zhou X, Li L, Han Z. Long Noncoding Magi2-As3 Suppresses Several Cellular Processes of Lung Squamous Cell Carcinoma Cells by Regulating miR-374a/b-5p/CADM2 Axis. *Cancer Manag Res* (2020) 12:289–302. doi: 10.2147/CMAR.S232595
52. Li CM, Chen G, Dayton TL, Kim-Kiselak C, Hoersch S, Whittaker CA, et al. Differential Tks5 Isoform Expression Contributes to Metastatic Invasion of Lung Adenocarcinoma. *Genes Dev* (2013) 27:1557–67. doi: 10.1101/gad.222745.113
53. Khalil A, Dekmak B, Boulos F, Kantrowitz J, Spira A, Fujimoto J, et al. Transcriptomic Alterations in Lung Adenocarcinoma Unveil New Mechanisms Targeted by the TBX2 Subfamily of Tumor Suppressor Genes. *Front Oncol* (2018) 8:482. doi: 10.3389/fonc.2018.00482
54. Pan J, Fang S, Tian H, Zhou C, Zhao X, Tian H, et al. Lncrna JPX/miR-33a-5p/Twist1 Axis Regulates Tumorigenesis and Metastasis of Lung Cancer by Activating Wnt/beta-Catenin Signaling. *Mol Cancer* (2020) 19:9. doi: 10.1186/s12943-020-1133-9
55. Wu C, Wang Y, Xia Y, He S, Wang Z, Chen Y, et al. Wilms' Tumor 1 Enhances Cisplatin-Resistance of Advanced NSCLC. *FEBS Lett* (2014) 588:4566–72. doi: 10.1016/j.febslet.2014.10.026
56. Kohno T, Otsuka A, Girard L, Sato M, Iwakawa R, Ogiwara H, et al. A Catalog of Genes Homozygously Deleted in Human Lung Cancer and the Candidacy of PTPRD as a Tumor Suppressor Gene. *Genes Chromosomes Cancer* (2010) 49:342–52. doi: 10.1002/gcc.20746
57. Spainhour JC, Lim HS, Yi SV, Qiu P. Correlation Patterns Between DNA Methylation and Gene Expression in The Cancer Genome Atlas. *Cancer Inform* (2019) 18:1176935119828776. doi: 10.1177/1176935119828776

Conflict of Interest: The authors declare that the research was conducted in the absence of any commercial or financial relationships that could be construed as a potential conflict of interest.

frontiers in Oncology

ORIGINAL RESEARCH
published: 05 November 2021
doi: 10.3389/fonc.2021.762063

Association Analysis Between the Functional Single Nucleotide Variants in miR-146a, miR-196a-2, miR-499a, and miR-612 With Acute Lymphoblastic Leukemia

Silvia Jiménez-Morales[1], Juan Carlos Núñez-Enríquez[2], Jazmín Cruz-Islas[1], Vilma Carolina Bekker-Méndez[3], Elva Jiménez-Hernández[4], Aurora Medina-Sanson[5], Irma Olarte-Carrillo[6], Adolfo Martínez-Tovar[6], Janet Flores-Lujano[1], Julian Ramírez-Bello[7], María Luisa Pérez-Saldívar[1], Jorge Alfonso Martín-Trejo[8], Héctor Pérez-Lorenzana[9], Raquel Amador-Sánchez[10], Felix Gustavo Mora-Ríos[11], José Gabriel Peñaloza-González[12], David Aldebarán Duarte-Rodríguez[1], José Refugio Torres-Nava[13], Juan Eduardo Flores-Bautista[14], Rosa Martha Espinosa-Elizondo[15], Pedro Francisco Román-Zepeda[16], Luz Victoria Flores-Villegas[17], Edna Liliana Tamez-Gómez[18], Víctor Hugo López-García[18], José Ramón Lara-Ramos[18], Juana Esther González-Ulivarri[19], Sofía Irene Martínez-Silva[20], Gilberto Espinoza-Anrubio[21], Carolina Almeida-Hernández[22], Rosario Ramírez-Colorado[23], Luis Hernández-Mora[24], Luis Ramiro García-López[25], Gabriela Adriana Cruz-Ojeda[26], Arturo Emilio Godoy-Esquivel[27], Iris Contreras-Hernández[28], Abraham Medina-Hernández[29], María Guadalupe López-Caballero[30], Norma Angélica Hernández-Pineda[31], Jorge Granados-Kraulles[31], María Adriana Rodríguez-Vázquez[32], Delfino Torres-Valle[33], Carlos Cortés-Reyes[34], Francisco Medrano-López[35], Jessica Arleet Pérez-Gómez[35], Annel Martínez-Ríos[36], Antonio Aguilar-De-los-Santos[37], Berenice Serafin-Díaz[38], María de Lourdes Gutiérrez-Rivera[39], Laura Elizabeth Merino-Pasaye[20], Gilberto Vargas-Alarcón[40], Minerva Mata-Rocha[41], Omar Alejandro Sepúlveda-Robles[41], Haydeé Rosas-Vargas[41], Alfredo Hidalgo-Miranda[1] and Juan Manuel Mejía-Aranguré[1,41,42]**

[1] Laboratorio de Genómica del Cáncer, Instituto Nacional de Medicina Genómica, Mexico City, Mexico, [2] Unidad de Investigación Médica en Epidemiología Clínica, Unidad Medica de Alta Especialidad (UMAE) Hospital de Pediatría "Dr. Silvestre Frenk Freund", Centro Médico Nacional "Siglo XXI", Instituto Mexicano del Seguro Social (IMSS), Mexico City, Mexico, [3] Unidad de Investigación Médica en Inmunología e Infectología, Hospital de Infectología "Dr. Daniel Méndez Hernández", "La Raza", IMSS, Mexico City, Mexico, [4] Servicio de Hematología Pediátrica, Hospital General "Gaudencio González Garza", Centro Médico Nacional "La Raza", IMSS, Mexico City, Mexico, [5] Departamento de Hemato-Oncología, Hospital Infantil de México Federico Gómez, Mexico City, Mexico, [6] Servicio de Hematología, Departamento de Investigación, Hospital General de México Dr. Eduardo Liceaga, Mexico City, Mexico, [7] Departamento de Endocrinología, Instituto Nacional de Cardiología, Ignacio Chávez, México City, Mexico, [8] Servicio de Hematología Pediátrica Unidad Medica de Alta Especialidad (UMAE) Hospital de Pediatría "Dr. Silvestre Frenk Freund", Centro Médico Nacional "Siglo XXI", IMSS, Mexico City, Mexico, [9] Servicio de Cirugía Pediátrica, Hospital General "Gaudencio González Garza", Centro Médico Nacional (CMN) "La Raza", IMSS, Mexico City, Mexico, [10] Servicio de Hematología Pediátrica, Hospital General Regional "Carlos McGregor Sánchez Navarro", IMSS, Mexico City, Mexico, [11] Cirugía Pediátrica, Hospital Regional "General Ignacio Zaragoza", Instituto de Seguridad y Servicios Sociales de los Trabajadores del Estado (ISSSTE), Mexico City, Mexico, [12] Servicio de Onco-Pediatria, Hospital Juárez de México, Mexico City, Mexico, [13] Servicio de Oncología, Hospital Pediátrico de Moctezuma, Secretaría de Salud de la Ciudad de México (SSCDMX), Mexico City, Mexico, [14] Servicio de Pediatría, Hospital General de Tláhuac, Mexico City, Mexico, [15] Servicio de Hematología Pediátrica, Hospital General de México, Mexico City, Mexico, [16] Coordinación Clínica y Servicio de Cirugía Pediátrica, Hospital General Regional (HGR) No. 1 "Dr. Carlos Mac Gregor Sánchez Navarro", IMSS, Mexico City, Mexico, [17] Servicio de Hematología Pediátrica, Centro Médico Nacional "20 de Noviembre", ISSSTE, Mexico City, Mexico, [18] Servicio de Hemato-Oncología Hospital Infantil de Tamaulipas, Cd. Victoria, Mexico, [19] Jefatura de Enseñanza, Hospital Pediátrico de Iztacalco, SSCDMX, Mexico City, Mexico, [20] Jefatura de Enseñanza, Hospital Pediátrico de Iztapalapa, SSCDMX, Mexico City, Mexico, [21] Servicio de Pediatría, Hospital General Zona

OPEN ACCESS

Edited by:
Yong-Mi Kim, Children's Hospital of Los Angeles, United States

Reviewed by:
Danuta Januszkiewicz-Lewandowska, Poznan University of Medical Sciences, Poland
Adel Abaskharon Guirgis, University of Sadat City, Egypt

***Correspondence:**
Silvia Jiménez-Morales
sjimenez@inmegen.gob.mx
Juan Manuel Mejía-Aranguré
jmejia@inmegen.gob.mx

Specialty section:
This article was submitted to Pediatric Oncology, a section of the journal Frontiers in Oncology

Received: *20 August 2021*
Accepted: *12 October 2021*
Published: *05 November 2021*

(HGZ) No. 8 "Dr. Gilberto Flores Izquierdo" IMSS, Mexico City, Mexico, [22] Jefatura de Enseñanza, Hospital General de Ecatepec "Las Américas", Instituto de Salud del Estado de México (ISEM), Mexico City, Mexico, [23] Jefatura de Enseñanza, Hospital Pediátrico La Villa, SSCDMX, Mexico City, Mexico, [24] Jefatura de Enseñanza, Hospital Pediátrico San Juan de Aragón, Secretaría de Salud (SS), Mexico City, Mexico, [25] Servicio de Pediatría, Hospital Pediátrico de Tacubaya, SSCDMX, Mexico City, Mexico, [26] Coordinación Clínica de Educación e Investigación en Salud, HGZ No. 47, IMSS, Mexico City, Mexico, [27] Servicio de Cirugía Pediátrica, Hospital Pediátrico de Moctezuma, SSCDMX, Mexico City, Mexico, [28] Coordinación de Investigación en Salud, IMSS, Mexico City, Mexico, [29] Pediatría, Hospital Materno-Pediátrico de Xochimilco, SSCDMX, Mexico City, Mexico, [30] Jefatura de Enseñanza, Hospital Pediátrico de Coyoacán, SSCDMX, Mexico City, Mexico, [31] Coordinación Clínica y Pediatría del Hospital General de Zona 76, IMSS, Mexico City, Mexico, [32] Coordinación Clínica y Pediatría del Hospital General de Zona 68, IMSS, Mexico City, Mexico, [33] Coordinación Clínica y Pediatría del Hospital General de Zona 71, IMSS, Mexico City, Mexico, [34] Pediatría, Hospital General Dr. Darío Fernández Fierro, ISSSTE, Mexico City, Mexico, [35] Coordinación Clínica y Servicio de Pediatría, HGR No. 72 "Dr. Vicente Santos Guajardo", IMSS, Mexico City, Mexico, [36] Cirugía Pediátrica del Hospital Regional "General Ignacio Zaragoza", ISSSTE, Mexico City, Mexico, [37] Coordinación Clínica y Pediatría del Hospital General de Zona 98, IMSS, Mexico City, Mexico, [38] Coordinación Clínica y Pediatría del Hospital General de Zona 57, IMSS, Mexico City, Mexico, [39] Servicio de Oncología Pediátrica Unidad Medica de Alta Especialidad (UMAE) Hospital de Pediatría "Dr. Silvestre Frenk Freund", IMSS, Mexico City, Mexico, [40] Departamento of Biología Molecular, Instituto Nacional de Cardiología Ignacio Chávez, Mexico City, Mexico, [41] Unidad de Investigación Médica en Genética Humana, Unidad Medica de Alta Especialidad (UMAE) Hospital de Pediatría "Dr. Silvestre Frenk Freund", Centro Médico Nacional "Siglo XXI", IMSS, Mexico City, Mexico, [42] Facultad de Medicina, Universidad Nacional Autónoma de México, Mexico City, Mexico

Background: Acute lymphoblastic leukemia (ALL) is characterized by an abnormal proliferation of immature lymphocytes, in whose development involves both environmental and genetic factors. It is well known that single nucleotide polymorphisms (SNPs) in coding and noncoding genes contribute to the susceptibility to ALL. This study aims to determine whether SNPs in *miR-146a*, *miR-196a-2*, *miR-499a*, and *miR-612* genes are associated with the risk to ALL in pediatric Mexican population.

Methods: A multicenter case-control study was carried out including patients with *de novo* diagnosis of ALL and healthy subjects as control group. The DNA samples were obtained from saliva and peripheral blood, and the genotyping of rs2910164, rs12803915, rs11614913, and rs3746444 was performed using the 5′exonuclease technique. Gene-gene interaction was evaluated by the multifactor dimensionality reduction (MDR) software.

Results: *miR-499a* rs3746444 showed significant differences among cases and controls. The rs3746444G allele was found as a risk factor to ALL (OR, 1.6 [95% CI, 1.05–2.5]; p = 0.028). The homozygous GG genotype of rs3746444 confers higher risk to ALL than the AA genotype (OR, 5.3 [95% CI, 1.23–23.4]; p = 0.01). Moreover, GG genotype highly increases the risk to ALL in male group (OR, 17.6 [95% CI, 1.04–298.9]; p = 0.00393). In addition, an association in a gender-dependent manner among SNPs located in *miR-146a* and *miR-196a-2* genes and ALL susceptibility was found.

Conclusion: Our findings suggest that SNP located in *miR-499a*, *miR-146a*, and *miR-196a-2* genes confer risk to ALL in Mexican children. Experimental analysis to decipher the role of these SNPs in human hematopoiesis could improve our understanding of the molecular mechanism underlying the development of ALL.

Keywords: acute lymphoblastic leukemia, *mir-146a*, *mir-196a-2*, *miR-499a*, *miR-612*, association study, Mexican population, single nucleotide polymorphism

INTRODUCTION

Acute lymphoblastic leukemia (ALL) is the most common pediatric hematological malignancy around the world, representing over 80% of all cases under 18 years old (1). This entity is highly prevalent in Mexican population, which displays one of the highest rate of relapse and death in comparison with other ethnic groups even after using chemotherapeutic approaches implemented in developed countries (2, 3).

ALL emerges by an abnormal proliferation of immature lymphocytes and their progenitors that replace the hematopoietic elements in the bone marrow and other lymphoid organs. So far, most of the causes of ALL are undeciphered; however, it is well known that an interaction within environmental and genetic factors is needed to develop this malignancy (4–6). Among the identified risk genetic factors to suffer ALL are the single nucleotide polymorphisms (SNP), both, in coding and no coding genes (6–9). No coding genes comprises around 98% of the human-transcribed genome, which is mainly represented by microRNAs (miRNAs) and long noncoding RNAs (lncRNAs) that play a relevant role in LLA and other types of cancer (10). miRNAs are small endogenous RNAs of 19–25 nucleotides that function as posttranscriptional regulators silencing specific mRNAs. miRNAs interact with their targeted mRNAs by complementary base pairing, most of them in the 3′-untranslated region (UTR) of the target mRNA, although interplay in the 5′UTR region has also been documented. Targeted coding mRNAs by specific miRNAs could be either in complete or incomplete fashion (11). Experimental evidences have revealed that miRNA dysfunction contributes to the establishment of diverse human diseases, since miRNA-mRNA-specific interaction makes fine-scale adjustments to protein outputs (8, 12, 13). It has been identified that several SNP located into miRNA gene sequences are closely responsive for their abnormal function by modifying pri-miRNA transcription, pri-miRNA/pre-miRNA processing, or by disrupting miRNA-mRNA interactions (14, 15). The rs2910164 G/C in *miR-146a* gene has been reported as an alterer of the gene expression, then its targeted mRNAs, which are involved in fundamental biological processes (cell differentiation, hematopoyesis, and innate and adaptive immunity, etc.) (16, 17). The rs2910164 has been associated with many types of cancer and several immune-mediated diseases (18–20); however, its association with ALL has shown controversial results (9, 17, 21). Another functional miR-SNP is rs3746444, which results from an A-to-G substitution in the seed region of *miR-499a*, was reported as significantly associated with an increased susceptibility to several human conditions, including cancer (19, 22). To know whether rs2910164 G/C in *miR-146a*, rs11614913 T/C in *miR-196a-2*, rs3746444 A/G in *miR-499a*, and rs12803915 G/A in *miR-612* are associated with ALL in Mexican children, we performed a case control study.

MATERIAL AND METHODS

Subjects

As part of the Mexican Interinstitutional Group for the Identification of the Causes of Childhood Leukemia (MIGICCL), we conducted a case-controls study from August 1, 2014, to July 31, 2016. Participants were younger than 18 years, residents of the Metropolitan Area of Mexico City, and recruited from public hospitals and health institutions from Mexico City, Mexico as was described previously by Medina-Sanzon et al. (6). ALL diagnosis was established by either a hematologist or an oncologist according to clinical characteristics, and bone marrow (BM) aspirate data. Gender, age at diagnosis, white blood cell count (WBC), immunophenotype, and risk classification group were registered from the patients' medical records. We used the National Cancer Institute (NCI) risk criteria for ALL case stratification as follows: (a) standard risk: 1–9.99 years of age or WBC <50 × 10^9/L, and (b) high risk: ≤1 or ≥10 years of age and/or WBC ≥50 × 10^9/L. Patients included in the study were treated with chemotherapy, none of them received HSCT therapy. Relapse was considered when ≥5% leukemic blasts were detected in BM sample during the first 36 months after having achieved complete remission (CR). Early mortality was defined as the patient's death during the first 24 months. Cases with Down syndrome were excluded from the analysis. All institutional committees of Ethics, Research, and Biosecurity of the participant institutions approved this study. Written informed consent was obtained from all participants and the children's parents. Patients ≥8 years old gave their assent (when possible) to be included in the present study. Cases and controls were selected according to criteria described in a previous study (6). Briefly, controls were recruited from second-level hospitals of the same health institution that referred the children with ALL to the third-level care hospitals. Control children were recruited from the departments of ambulatory surgery, pediatrics, and ophthalmology; orthopedic outpatient clinics; and the emergency room of the referred hospitals and have no leukemia, hematological diseases, allergies, infections, and congenital malformations. A set of adult patients was included to test the associated SNP *miR-499a_* rs3746444. The group of adult patients and controls is described in the *Material and Methods* section in the **Supplementary Material**.

DNA Extraction, SNP Selection, and Genotyping

Genomic DNA from saliva or peripheral blood was obtained according to the ORAGENE Purification Kit (DNA Genotek Inc., Kanata, ON, Canada) and the Gentra Kit (Gentra Systems Inc., Minneapolis, MN, USA) according to the manufacturer's instructions. DNA purity and concentration were determined by sypectrofotometry (Nanodrop-1000). The rs2910164 (*miR-146a*), rs11614913 (*miR-196a-2*), rs3746444 (*miR-499a*), and rs12803915 (*miR-612*) were selected base on previous association studies in ALL and other malignancies (8, 9, 13, 17, 21, 23–26). Genotyping was performed using the 5′exonuclease technique and TaqMan MGB chemistry in a QuantStudio 5 system according to the manufacturer's instructions (Thermo Fisher, Foster City, CA, USA). TaqMan probes used were C:15946974_10 (rs2910164), C:31185852_10 (rs11614913), C:_2142612_40 (rs3746444), and C:32062363_10 (rs12803915). PCR reaction contained 25 ng of genomic DNA, 2.5 µl of TaqMan master mix, 0.0625 µl of 40× assay mix, and ddH_2O up to a final volume of 5 µl. The PCR protocol included denaturing at 95°C for 10 min, followed by 40 cycles of denaturing at 95°C for 15 s, and annealing and extension at 60°C for 1 min. Genotypes were assigned automatically by measuring the allele-specific fluorescence by using QuantStudio

Design and Analysis software 5 for allelic discrimination (Applied Biosystems, Foster City, CA, USA). The overall genotype call rate was over 98.0% and 100% concordance of a subset of randomly repeated samples during the genotyping.

Statistical Analyses

Hardy-Weinberg Equilibrium (HWE) test was performed using the FINETTI program (http://ihg.gsf.de/cgicbin/hw/hwa1.pl). Alleles and genotype frequencies were compared among groups by using Chi-square and Fisher's exact tests (when appropriate) implemented in the STATCALC program (Epi Info v.6.02 software, Centers for Disease Control and Prevention, Atlanta, GA). By comparing cases and controls, all SNPs were evaluated under the codominant, dominant, and recessive genetic models using the FINETTI program. Bonferroni correction test was applied. The multifactor dimensionality reduction (MDR) software (V 3.0.2) was used to evaluate gene-gene interactions (27). All p-values ≤ 0.05 were considered statistically significant.

RESULTS

Features of Studied Subjects

The present work included 678 subjects from Mexico City, of which, 423 were children with ALL, and 255 children non-ALL. The ALL children were followed up for at least 3 years (3–7) after initial diagnosis. Males were more frequent than females either in cases (57.9% *vs*. 42.1%, respectively) nor controls (54.7% v/s 45.2%, respectively), but differences were not statistically significant (p = 0.43). The proportion of children under 10 years old were higher in both groups, and a significant difference was detected among cases (62.2%) and controls (71.1%) (p = 0.02). Median age of ALL children was 9.09 (0–18) and 6.4 (0–17) of the control group. Overall, 68.3% had >90% blast in bone marrow; 91.2%, 6.9%, and 1.9% were pre-B, cell-T, and biphenotype, respectively. Available clinical data are shown in **Table 1**.

TABLE 1 | Clinical characteristics of patients with acute lymphoblastic leukemia.

Features	Cases (n = 423)	
	n	%
Gender		
Male	245	57.9
Female	178	42.1
Age group (years)		
<1	9	2.1
1–9	258	61.0
≥10	156	36.9
Age at diagnosis (years)		
Median (min–max)	7.9 (0–18)	
BM blast at diagnosis (%)		
<90	135	31.7
≥90	288	68.3
Median (min–max)	85.3 (20–100)	
Inmunophenotype		
Pre-B Cell	386	91.2
Cell-T	29	6.9
Biphenotype	8	1.9
NCI risk classification		
Standard risk	214	50.6
High risk	209	49.4
Relapse		
No	346	81.8
Yes	77	18.2
Relapse site		
Isolated BM	52	67.5
Isolated CNS	17	22.1
BM and CNS	2	2.6
BM and CNS and eye	1	1.3
CNS and eyes	1	1.3
BM and testis	3	3.9
Ovary	1	1.3
Death		
No	364	86.0
Yes	59	14.0

WBC, whole blood cell count; BM, bone marrow; NCI, National Cancer Institute; CNS, central nervous system.

Association Study

Except for *miR-146a*, the genotypes of *miR-196a-2*, *miR-499a*, and *miR-612* were in HWE in the control population. The association analysis between miRNA SNPs and ALL are described in **Table 2** and **Supplementary Table S1**. Case-control analysis including all children showed a significant association among *miR-499a* rs374644 with ALL (**Table 2**). *miR-499a* rs3746444G alelle observed an OR of 1.6 (95% CI, 1.008–2.5), p = 0.028. However, this significance did not remain after Bonferroni correction test. To note, under codominant model analysis AA *vs*. GG, statistical significance was found: OR, 5.3 (95% CI, 1.23–23.4); p = 0.01 (**Table 1**). Stratification analysis by gender observed that *miR-499a* rs3746444G is associated with ALL in a gender-dependent manner, being a risk factor to males (OR, 2.46 [95% CI, 1.31–4.60]; p = 0.0037) but no to girls (p = 0.95) (**Table 3**). Moreover, in comparison with AA genotype, GG genotype highly increases the risk to ALL (OR, 17.6 [95% CI, 1.04–298.9]; p = 0.00393) in males. Data are shown in **Table 3**.

miR-146a rs2910164, *miR-196a-2* rs11614913, and *miR-612* rs12803915 association analysis including all children with ALL showed differences among cases and controls but were not statistically significant (**Supplementary Table S1**). The analysis stratified by gender revealed that homozygote genotype for the minor allele CC of *miR-146a* rs2910164 was differentially distributed among male ALL cases and male controls (OR, 4.3 (1.60–11.61); p = 0.02). Meanwhile, *miR-196a-2* rs11619413 was associated with ALL in female (C *vs*. T: OR, 1.54 [95% CI, 1.08–2.2]; p = 0.015) (**Supplementary Table S2**).

Association Between *miR-146a*, *miR-196a-2*, *miR-499a*, and *miR-612* SNPs With Clinical Characteristics

To know whether the studied SNPs were associated with clinical and biological ALL features, we performed the case-control analysis into the patients group stratified by gender, age group, immunophenotype, NCI-risk classification, relapse, death, and

TABLE 2 | Association analysis among miR-499 rs3746444 and acute lymphoblastic leukemia.

	Children		OR [CI], *p*-value	Adults		OR [CI], *p*-value	All		OR [CI], *p*-value
	Control (%)	Cases *n* (%)		Control *n* (%)	Cases *n* (%)		Control *n* (%)	Cases *n* (%)	
N	255	416		180	71		435	489	
Genotypes									
AA	229 (89.8)	362 (87.0)		157 (87.2)	59 (83.1)		386 (88.7)	421 (86.1)	
AG	24 (9.4)	39 (9.3)		23 (12.8)	9 (12.7)		47 (10.8)	48 (9.8)	
GG	2 (0.8)	17 (4.8)		0 (0)	3 (4.2)		2 (0.5)	20 (4.1)	
Alelles			1.6 [1.05–2.5], 0.028*			1.7 [0.87–3.34], 0.11			1.58 [1.1–2.2], 0.01*
A	482 (94.5)	763 (91.4)		337 (93.6)	127 (89.4)		819 (94.1)	824 (91.0)	
G	28 (5.5)	73 (8.8)		23 (6.4)	15 (10.6)		51 (5.9)	88 (9.0)	
Codominant AA *vs*. GG			5.3 [1.23–23.4], 0.01*			18.5 [0.94–364], 0.005			9.16 [2.1–39.4], 0.00033*

*OR, odds ratio; CI, confidence interval. *Statistically significant.*

TABLE 3 | Association analysis among miR-499 rs3746444 and acute lymphoblastic leukemia in children stratified by gender.

	Male		OR [CI], *p*-value	Female		OR [CI], *p*-value
	Control (%)	Cases *n* (%)		Control *n* (%)	Cases *n* (%)	
N	255	416		180	71	
Genotypes						
AA	126 (89.8)	207 (87.0)		103 (87.2)	155 (83.1)	
AG	13 (9.4)	25 (9.3)		9 (12.8)	14 (12.7)	
GG	0 (0.8)	14 (4.8)		2 (0)	3 (4.2)	
Alelles			2.46 [1.31–4.60], 0.0037*			1.021 [0.49–2.09], 0.95
A	482 (94.5)	763 (91.4)		337 (93.6)	127 (89.4)	
G	28 (5.5)	73 (8.8)		23 (6.4)	15 (10.6)	
Codominant AA *vs*. GG			17.6, [1.04–298.9], 0.00393*			0.99 [0.16 6.06], 0.99

*OR, odds ratio; CI, confidence interval. *Statistically significant. Genotyping >98%.*

hereditary cancer family history (**Supplementary Table S3**). Significant differences among gender and age were found in the distribution of the *miR-196a-2* rs11614913C allele ($p = 0.02$, $p = 0.02$, respectively). Additionally, analysis comparing infants *versus* children older than 1 year was performed. **Supplementary Table S3** shows the results grouping the patients by age groups: <1 year; 1–9.9 and ≥10 years, considering that it has been reported that adolescents with ALL also have a dismal prognosis in comparison with children below this age and is considered an important prognostic factor. Regarding immunophenotype, NCI risk classification, relapse, death, and hereditary family history, no significant differences were observed (**Supplementary Table S3**). Furthermore, we conducted survival analyses between the SNPs analyzed and the overall survival of pediatric patients with ALL, but no significant associations were observed neither including all cases nor after stratifying by child's sex and age groups.

Gene-Gene Interaction Analysis

To know whether **g**ene-gene interactions among *miR-146a*, *miR-196a-2*, *miR-499*a, and *miR-612* SNPs predict the risk to ALL, a MDR analysis was performed by including cases and controls having complete genotyping data of all evaluated SNPs. No SNP was identified as the best factor model. The multi*locus* model with maximum crossvalidation consistency (CVC) and minimum prediction error is displayed in **Supplementary Table S4**. Four-*locus* genotype combinations associated with the risk of ALL, as well as their distribution among cases (left) and controls (right) is summarizes in **Figure 1A**. This analysis gave evidence of epistasis or gene-gene interaction (**Figures 1B, C**). Entropy data showed that rs3746444 had the larger effect on the susceptibility to develop ALL (0.59%) followed by rs*2910164* (0.49%). Week synergy among *miR-196a-2* and *miR-612* was observed (orange line) (**Figure 1B**). Redundancy was observed among all SNPs (blue and green lines) (**Figures 1B, C**). To note, gene-gene gender interaction observed a strong synergy (red line) among *miR-196a-2* and gender (**Supplementary Figure S1**).

DISCUSSION

Mountain evidence reveals that miRNAs are relevant in the gene regulation contributing to the establishment of human diseases and modifying their treatment response of the patients. For instance, by using miRanda, TargetScan, and miRTarget2, it is predicted that *AKT2* is a potential target of *miR-612*, which has been reported as

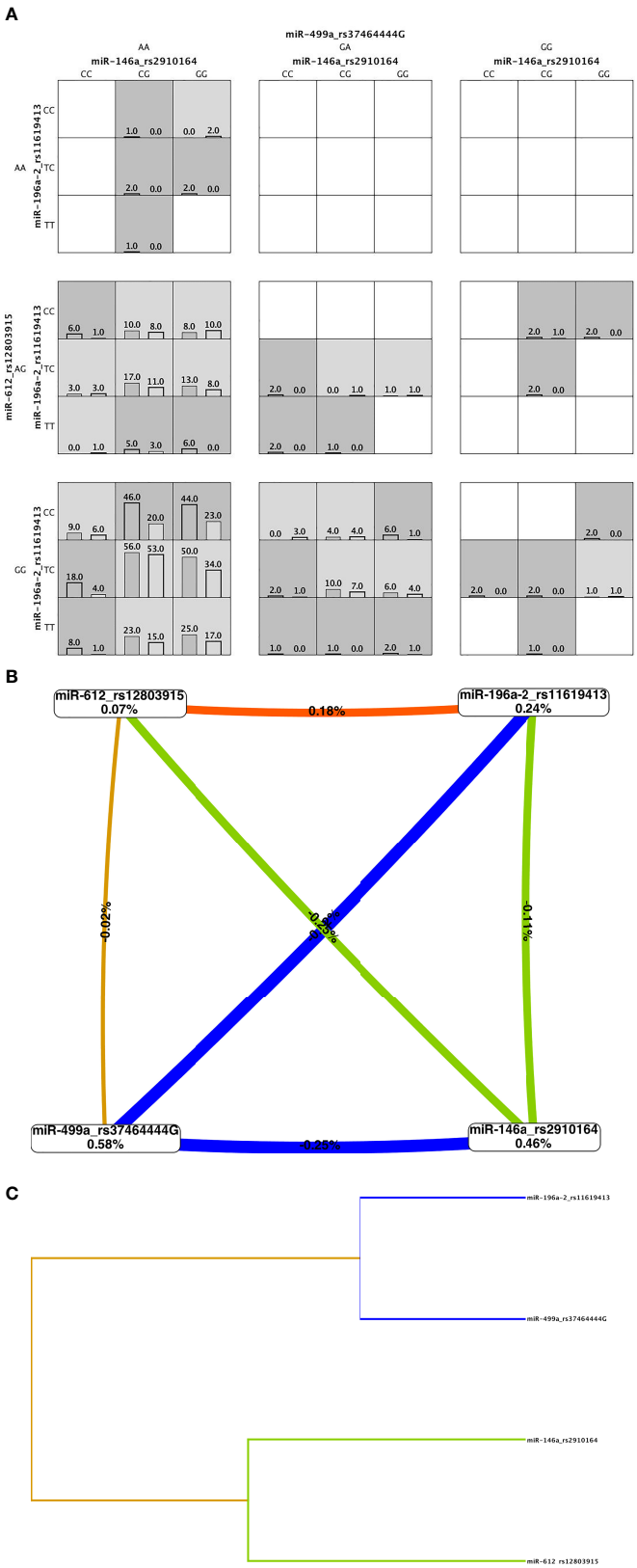

FIGURE 1 | Continued

FIGURE 1 | Multifactor dimensionality reduction (MDR) analysis. **(A)** Four-*locus* MDR model. Genotype combinations with high risk (shaded dark grey) and low risk (shaded light grey) for acute lymphoblastic leukemia (ALL) and their distribution in cases (left bar) and controls (right bar). The patterns of high (shaded and low-risk cells, which differ across each of the different multi locus dimension, means that the influence each genotype on the ALL risk is dependent on the genotypes a each of the other three loci. **(B)** Interaction entropy graph for gene-gene interaction and ALL risk. Graph shows the percent of the entropy in case-control removed by each factor (boxes) and by each pair-wise combination of attributes (lines). Positive value and orange line indicate low degree of synergy and negative values and blue and green lines mean redundancy. Gold line means independency. **(C)** The dendrogram graphic shows the presence, strength, and nature of epistatic effects. The shorter the line connecting two attributes the stronger the interaction. Strength of interaction goes from left to right (gray line).

significantly upregulated in ALL patients. *AKT2* expression in lymphocytes correlates negatively with sensitive to glucocorticoids, and patients have poor prognosis (28–30). For its part, *miR-146a* has been involved in megakaryopoiesis by activating innate immunity targets TIRAP and TRAF6 (31). In addition, experimental data have shown that SNPs in miRNAs could affect cell differentiation, proliferation, and apoptosis conducting cancer development. The SNPs rs2910164 in *miR146a*, rs11614913 in *miR-196a-2*, rs3746444 in *miR-499*a, and rs12803915 in *miR-612* are among the most studied SNPs in cancer. In a case-control study, we did no find association among rs12803915 of *miR-612* but to rs3746444 of *miR-499a* with ALL, as well as, in a gender-dependent manner rs2910164 of *miR146a*, and rs11614913 of *miR-196a-2* were associated with the risk to this disease.

To date, only three studies have explored the association among *miR-499a* rs3746444 and ALL. Our results are in line with the findings of de Souza et al., who studied 100 pediatric ALL patients, and 180 healthy individuals from Brazilian-amazon reported that *miR499a*_rs3746444 increases 17-fold the risk of development of ALL (26). We found that the mutant homozygote rs3746444GG genotype was associated with a 1.6-fold increase in the risk of developing ALL. However, our data are in contrast to those published previously by Gutierrez-Camino et al., who including 213 B-cell ALL pediatric patients and 387 controls from Spain, found a protective role of the G allele on the risk of ALL (8) and by Hasani et al., studying 75 children diagnosed with ALL and 115 children from Iran with no history of any type of cancer (23). To note, we explored whether *miR-499a* rs3746444 has in adults with ALL the same effect as we observed in children by genotyping 71 patients >18 years old with clinical diagnosis of ALL and 180 healthy adults (1:1 female/male). Samples from ALL adults were obtained from the biobank of the Servicio de Hematología, Hospital General de México. Adult control group was obtained from the DNA biobank of the laboratorio de Investigation, Hospital Juárez de México. *miR-499a* rs3746444A allele frequency was very similar among children and adults (cases and controls) and notably, *miR-499a* rs3746444G allele was not detected in no-ALL adults (0%). However, differences among adult cases and adult controls or between children and adults were not statistically significant (**Table 2**). Our study is the first to investigate the role of rs3746444 in the susceptibility to ALL in adults, which has been associated with common adulthood cancer types (22, 32). The rs3746444 is located in pre-*mir-499* gene resulting changes of an A:U to a G:U pairing and mismatching that reduces the stability of the *pre-miR-499* secondary structure (33) and this SNP, located in the seed region of miR-499a could alter the targeted genes. In fact, Yang et al. (34) reported that this SNP potentially recognizes 573 new target genes and lost 5,392 original target genes. Several of these genes are involved in biological processes as cell proliferation and migration (35).

It is known that *mir146a* plays anti-inflammatory functions, has roles as tumor suppressor and commonly shows altered expression levels in human leukemia (32–38). Data from ALL Jurkat cells have shown that *miR-146*a can promote growth of leukemia cells by regulating the expression anti-apoptosis factor Bcl-xL and altering the expression of diverse genes involved in T-cell differentiation (37–39). Recent papers have given evidence that rs2910164 in *miR146* can modify the expression of nuclear factor (NF-κB) through reducing *IRAK1* and *TRAF* gene expression thus, driving inflammation and leukemia progression in myeloid cells (40). Stickel et al. (41) observed that patients with the *miR-146a* polymorphism rs2910164 display higher major histocompatibility complex class II (MHCII) molecule levels on monocytes. In addition, experimental evidences have shown that the rs2910164 in human allogeneic hematopoietic cell transplantation (allo-HCT) recipients significantly increases the risk for acute severe acute graft-*versus*-host disease in patients with hematological malignancies (41). The G to C polymorphism rs2910164 in *miR146a* changes the G:U pair to a C:U mismatch in the stem structure of *miR-146a* precursor, resulting in a reduced level of mature miR146a (36). To note, we found that *miR-146a* rs2910164 GG genotype confer risk to ALL in male. This SNP is widely associated with cancer, but association studies in ALL have reveled conflicting results. On one hand, it has been reported that *miR-146a* rs2910164 is associated with childhood ALL susceptibility in Asian population, including Iranian, Chinese, and Taiwanese (17, 23, 25). On the other hand, studies in Thailand, India, and China failed to replicate these results (9, 21, 42). No published study has reported an association among ALL and rs2910164 in a gene-dependent manner, and considering the higher prevalence of ALL in male than female, these findings should be deeply explored.

Regarding rs11614913 C/T, in the 3p mature miRNA region of *miR-196a2*, leads to a variation from G:T to G:C in the stem region of the *miR-196a2* precursor. Comparing the minimum free energy for optimal secondary structures of the SNP rs11614913 in pre-miR196a2 found that this SNP had no dramatic effect on its secondary structure (43); however, Hoffman et al. (44) already show that rs11614913C may affect the processing of pre-miRNA, modify both, its expression level and function, then alters its interactions with its targeted genes. In fact, various studies have observed a correlation among abnormal expression of *miR-196a2* and genes involved in cancer (45, 46). Studies in several types of cancer suggest that the common rs11614913 variant may play a role in the development of malignancies in an ethnic-dependent manner (43, 47, 48). For instance, a meta-analysis including 41,673 cases and 49,570 controls from 111 studies revealed that *mir-196a-2* rs11614913 T allele was significantly associated with

cancer risk only in Asians but not Caucasians (47). As for hematological malignancies, association data are scarce. Findings in Non-Hodgkin's lymphoma suggest that the *miR-196a-2* polymorphism may increase the risk of the disease by altering the expression of mature *miR-196a* (48). In ALL, two studies have published that rs11614913C allele contributes to an increased risk of this disease in Thailand, and China, but another one found no association results in Taiwanese ALL cases (13, 24, 49). Comparing the minimum free energy for optimal secondary structures of the SNP rs11614913 in *pre-miR196a-2* found no dramatic effect on its secondary structure (47). We found an association among this SNP with ALL risk in females, but whether this SNP is playing a role in ALL susceptibility remains unknown.

Regarding rs12803915 in *mir-612*, experimental studies reveal that rs12803915 SNP affects mature *mir-612* expression in a cell-type-specific manner. As example, Kim et al. observed that rs12803915A allele increases and decreases mature *mir-612* expression in prostate cancer and colon cancer cell lines, respectively (50). In ALL, two studies have explored this SNP (8, 51). On one hand, the rs12803915 in *mir-612* was associated with ALL in patients from Spain (8). On the other hand, in 100 B-ALL cases and 105 controls from Iran, no association was observed (51).

To know whether there is a gene-gene interaction among the evaluated SNPs in the risk to ALL, we employed a MDR analysis. We observed that *miR-499a* is the main casual factor for ALL, a strong redundancy interaction effect of this SNP and *miR-196a-2* and *miR-146a* on ALL risk, and a low synergism with *miR-612*; thus, this analysis gave evidence of epistasis. Both genes have already been shown to be associated with cancer risk in various populations, but no data regarding their interaction has been published. To note, both SNPs have been found as susceptibility factors to ALL in a Spanish population (8).

The discrepancies on the association findings among the present work and other populations may be related to the sample selection, and the genetic background of the populations, since the linkage disequilibrium complex structure of the populations could mask the causal SNP (51). In addition, differences in the genetic background of cases and control could bias the association results. To note, our control group and a subset of the ALL cases belong to a genotyped cohort using 32 informative ancestry markers. As we published previously, ALL cases and controls are Mexican-Mestizo (6). However, to clarify the effect of miRNA polymorphism on ALL risk, studies including patients from different ethnicities and larger sample sizes are needed. Experimental analysis could also add data to decipher the role of *miR-499* in ALL.

In conclusion, our analysis revealed that *miR-499* rs3746444 confers risk to ALL and there is a gender-dependent association among *miR-146a* and *miR-196a-2* and ALL in Mexican children. Studies are needed to evaluate the potential molecular mechanisms underlying the contribution of these SNPs in ALL susceptibility.

DATA AVAILABILITY STATEMENT

The original contributions presented in the study are included in the article/**Supplementary Material**. Further inquiries can be directed to the corresponding authors.

ETHICS STATEMENT

The studies involving human participants were reviewed and approved by the Ethics and National Committee of Scientific Research of the Instituto Mexicano del Seguro Social with number R-2013-785-062. Written informed consent to participate in this study was provided by the participants' legal guardian/next of kin.

AUTHOR CONTRIBUTIONS

SJ-M: conceptualization. SJ-M, JN-E, JC-I, and JR-B: methodology. SJ-M, JN-E, JC-I, and JR-B: formal analysis. SJ-M: investigation. JN-E, VB-M, EJ-H, AM-S, IO-C, AM-T, JF-L, MP-S, JM-T, HP-L, RA-S, FM-R, JP-G, DD-R, JT-N, JF-B, RE-E, PR-Z, LF-V, ET-G, VL-G, JL-R, JG-U, SM-S, GE-A, CA-H, RR-C, LH-M, LG-L, GC-O, AG-E, IC-H, AM-H, ML-C, NH-P, JG-K, MR-V, DT-V, CC-R, FM-L, JP-G, AM-R, AA-S, BS-D, MG-R, LM-P, GV-A, MM-R, OS-R, HR-V, JR-B, and AH-M: resources. SJ-M: writing—original draft preparation. SJ-M, AH-M, and JM-A: writing—review and editing and supervision. SJ-M, JC-E, and JM-A: funding acquisition. All authors reviewed the final manuscript and read and approved the submitted version.

FUNDING

This work was supported by the Consejo Nacional de Ciencia y Tecnología (CONACyT), Investigación en Fronteras de la Ciencia (IFC)-2016-01-2119, PDCPN2013-01-215726, CB-2015-1-258042, FIS/IMSS/PROT/1548, FONCICYT/37/2018, FIS/IMSS/PROT/1782, and FORDECYT-PRONACES-377883-2020. We also thank the financial support from the National Institute of Genomic Medicine (01/2018/I, 19/2019/I).

ACKNOWLEDGMENTS

We thank to Dr. Catherine Metayer from the California, Berkeley School of Public Health, USA, because of their donation of saliva kits used to perform this project. We thank all patients and people from the institutions involved in the clinical management of our cases.

SUPPLEMENTARY MATERIAL

The Supplementary Material for this article can be found online at: https://www.frontiersin.org/articles/10.3389/fonc.2021.762063/full#supplementary-material

REFERENCES

1. Pérez-Saldivar ML, Fajardo-Gutiérrez A, Bernáldez-Ríos R, Martínez-Avalos A, Medina-Sanson A, Espinosa-Hernández L, et al. Childhood Acute Leukemias are Frequent in Mexico City: Descriptive Epidemiology. *BMC Cancer* (2011) 11:355. doi: 10.1186/1471-2407-11-355
2. Jiménez-Hernández E, Jaimes-Reyes EZ, Arellano-Galindo J, García-Jiménez X, Tiznado-García HM, Dueñas-González MT, et al. Survival of Mexican Children With Acute Lymphoblastic Leukaemia Under Treatment With the Protocol From the Dana-Farber Cancer Institute 00-01. *BioMed Res Int* (2015) 2015:576950. doi: 10.1155/2015/576950
3. Martín-Trejo JA, Núñez-Enríquez JC, Fajardo-Gutiérrez A, Medina-Sansón A, Flores-Lujano J, Jiménez-Hernández E, et al. Early Mortality in Children With Acute Lymphoblastic Leukemia in a Developing Country: The Role of Malnutrition at Diagnosis. A Multicenter Cohort MIGICCL Study. *Leuk Lymphoma* (2017) 58(4):898–908. doi: 10.1080/10428194.2016.1219904
4. Hunger SP, Mullighan CG. Acute Lymphoblastic Leukemia in Children. *N Engl J Med* (2015) 373(16):1541–52. doi: 10.1056/NEJMra1400972
5. Jiménez-Hernández E, Duarte-Rodríguez DA, Núñez-Enriquez JC, Flores-Lujano J, Martín-Trejo JA, Espinoza-Hernández LE, et al. Maternal and Paternal Ages at Conception of Index Child and Risk of Childhood Acute Leukaemia: A Multicentre Case-Control Study in Greater Mexico City. *Cancer Epidemiol* (2020) 67:101731. doi: 10.1016/j.canep.2020.101731
6. Medina-Sanson A, Núñez-Enríquez JC, Hurtado-Cordova E, Pérez-Saldivar ML, Martínez-García A, Jiménez-Hernández E, et al. Genotype-Environment Interaction Analysis of NQO1, CYP2E1, and NAT2 Polymorphisms and the Risk of Childhood Acute Lymphoblastic Leukemia: A Report From the Mexican Interinstitutional Group for the Identification of the Causes of Childhood Leukemia. *Front Oncol* (2020) 10:571869. doi: 10.3389/fonc.2020.571869
7. Xu H, Cheng C, Devidas M, Pei D, Fan Y, Yang W, et al. ARID5B Genetic Polymorphisms Contribute to Racial Disparities in the Incidence and Treatment Outcome of Childhood Acute Lymphoblastic Leukemia. *J Clin Oncol* (2012) 30(7):751–7. doi: 10.1200/JCO.2011.38.0345
8. Gutierrez-Camino A, Lopez-Lopez E, Martin-Guerrero I, Piñan MA, Garcia-Miguel P, Sanchez-Toledo J, et al. Noncoding RNA-Related Polymorphisms in Pediatric Acute Lymphoblastic Leukemia Susceptibility. *Pediatr Res* (2014) 75(6):767–73. doi: 10.1038/pr.2014.43
9. Jemimah Devanandan H, Venkatesan V, Scott JX, Magatha LS, Durairaj Paul SF, Koshy T. MicroRNA 146a Polymorphisms and Expression in Indian Children With Acute Lymphoblastic Leukemia. *Lab Med* (2019) 50(3):249–53. doi: 10.1093/labmed/lmy074
10. James AR, Schroeder MP, Neumann M, Bastian L, Eckert C, Gökbuget N, et al. Long non-Coding RNAs Defining Major Subtypes of B Cell Precursor Acute Lymphoblastic Leukemia. *J Hematol Oncol* (2019) 12(1):8. doi: 10.1186/s13045-018-0692-3
11. Liu B, Li J, Cairns MJ. Identifying miRNAs, Targets and Functions. *Brief Bioinform* (2014) 15(1):1–19. doi: 10.1093/bib/bbs075
12. Dzikiewicz-Krawczyk A, Macieja A, Mały E, Januszkiewicz-Lewandowska D, Mosor M, Fichna M, et al. Polymorphisms in microRNA Target Sites Modulate Risk of Lymphoblastic and Myeloid Leukemias and Affect microRNA Binding. *J Hematol Oncol* (2014) 7:43. doi: 10.1186/1756-8722-7-43
13. Rakmanee S, Pakakasama S, Hongeng S, Sanguansin S, Thongmee A, Pongstaporn W. Increased Risk of Thai Childhood Acute Lymphoblastic Leukemia With the MiR196a2 T>C Polymorphism. *Asian Pac J Cancer Prev* (2017) 18(4):1117–20. doi: 10.22034/APJCP.2017.18.4.1117
14. Duan R, Pak C, Jin P. Single Nucleotide Polymorphism Associated With Mature miR-125a Alters the Processing of pri-miRNA. *Hum Mol Genet* (2007) 16(9):1124–31. doi: 10.1093/hmg/ddm062
15. Sun G, Yan J, Noltner K, Feng J, Li H, Sarkis DA, et al. SNPs in Human miRNA Genes Affect Biogenesis and Function. *RNA* (2009) 15(9):1640–51. doi: 10.1261/rna.1560209
16. Duyu M, Durmaz B, Gunduz C, Vergin C, Yilmaz Karapinar D, Aksoylar S, et al. Prospective Evaluation of Whole Genome microRNA Expression Profiling in Childhood Acute Lymphoblastic Leukemia. *BioMed Res Int* (2014) 2014:967585. doi: 10.1155/2014/967585
17. Zou D, Yin J, Ye Z, Zeng Q, Tian C, Wang Y, et al. Association Between the *miR-146a* Rs2910164 Polymorphism and Childhood Acute Lymphoblastic Leukemia Susceptibility in an Asian Population. *Front Genet* (2020) 11:886. doi: 10.3389/fgene.2020.00886
18. Lian H, Wang L, Zhang J. Increased Risk of Breast Cancer Associated With CC Genotype of Has-miR-146a Rs2910164 Polymorphism in Europeans. *PloS One* (2012) 7(2):e31615. doi: 10.1371/journal.pone.0031615
19. Alemán-Ávila I, Jiménez-Morales M, Beltrán-Ramírez O, Barbosa-Cobos RE, Jiménez-Morales S, Sánchez-Muñoz F, et al. Functional Polymorphisms in *Pre-Mir146a* and *Pre-Mir499* are Associated With Systemic Lupus Erythematosus But Not With Rheumatoid Arthritis or Graves' Disease in Mexican Patients. *Oncotarget* (2017) 8(54):91876–86. doi: 10.18632/oncotarget.19621
20. Mi Y, Ren K, Zou J, Bai Y, Zhang L, Zuo L, et al. The Association Between Three Genetic Variants in MicroRNAs (Rs11614913, Rs2910164, Rs3746444) and Prostate Cancer Risk. *Cell Physiol Biochem* (2018) 48(1):149–57. doi: 10.1159/000491671
21. Chansing K, Pakakasama S, Hongeng S, Thongmee A, Pongstaporn W. Lack of Association Between the MiR146a Polymorphism and Susceptibility to Thai Childhood Acute Lymphoblastic Leukemia. *Asian Pac J Cancer Prev* (2016) 17(5):2435–8.
22. Yang X, Li X, Zhou B. A Meta-Analysis of miR-499 Rs3746444 Polymorphism for Cancer Risk of Different Systems: Evidence From 65 Case-Control Studies. *Front Physiol* (2018) 9:737. doi: 10.3389/fphys.2018.00737
23. Hasani SS, Hashemi M, Eskandari-Nasab E, Naderi M, Omrani M, Sheybani-Nasab M. A Functional Polymorphism in the miR-146a Gene is Associated With the Risk of Childhood Acute Lymphoblastic Leukemia: A Preliminary Report. *Tumour Biol* (2014) 35(1):219–25. doi: 10.1007/s13277-013-1027-1
24. Tong N, Xu B, Shi D, Du M, Li X, Sheng X, et al. Hsa-miR-196a2 Polymorphism Increases the Risk of Acute Lymphoblastic Leukemia in Chinese Children. *Mutat Res* (2014) 759:16–21. doi: 10.1016/j.mrfmmm.2013.11.004
25. Pei JS, Chang WS, Hsu PC, Chen CC, Chin YT, Huang TL, et al. Significant Association Between the MiR146a Genotypes and Susceptibility to Childhood Acute Lymphoblastic Leukemia in Taiwan. *Cancer Genomics Proteomics* (2020) 17(2):175–80. doi: 10.21873/cgp.20178
26. de Souza TP, de Carvalho DC, Wanderley AV, Fernandes SM, Rodrigues JCG, Cohen-Paes A, et al. Influence of Variants of the *Drosha*, *Mir499a*, and *Mir938* Genes on Susceptibility to Acute Lymphoblastic Leukemia in an Admixed Population From the Brazilian Amazon. *Am J Transl Res* (2020) 12(12):8216–24.
27. Moore JH, Gilbert JC, Tsai CT, Chiang FT, Holden T, Barney N, et al. A Flexible Computational Framework for Detecting, Characterizing, and Interpreting Statistical Patterns of Epistasis in Genetic Studies of Human Disease Susceptibility. *J Theor Biol* (2006) 241(2):252–61. doi: 10.1016/j.jtbi.2005.11.036
28. Chen C, Yan Y , Liu X. microRNA-612 Is Downregulated by Platelet-Derived Growth Factor-BB Treatment and has Inhibitory Effects on Vascular Smooth Muscle Cell Proliferation and Migration *via* Directly Targeting AKT2. *Exp Ther Med* (2018) 15(1):159–65. doi: 10.3892/etm.2017.5428
29. Xie M, Yang A, Ma J, Wu M, Xu H, Wu K, et al. Akt2 Mediates Glucocorticoid Resistance in Lymphoid Malignancies Through FoxO3a/Bim Axis and Serves as a Direct Target for Resistance Reversal. *Cell Death Dis* (2019) 9(10):1013. doi: 10.1038/s41419-018-1043-6
30. Liu Y, Lu LL, Wen D, Liu DL, Dong LL, Gao DM, et al. MiR-612 Regulates Invadopodia of Hepatocellular Carcinoma by HADHA-Mediated Lipid Reprogramming. *J Hematol Oncol* (2020) 13(1):12. doi: 10.1186/s13045-019-0841-3
31. Taganov KD, Boldin MP, Chang KJ, Baltimore D. NF-kappaB-Dependent Induction of microRNA miR-146, an Inhibitor Targeted to Signaling Proteins of Innate Immune Responses. *Proc Natl Acad Sci U S A* (2006) 103(33):12481–6. doi: 10.1073/pnas.0605298103
32. Yan W, Gao X, Zhang S. Association of miR-196a2 Rs11614913 and miR-499 Rs3746444 Polymorphisms With Cancer Risk: A Meta-Analysis. *Oncotarget* (2017) 8(69):114344–59. doi: 10.18632/oncotarget.22547
33. Hu Z, Liang J, Wang Z, Tian T, Zhou X, Chen J, et al. Common Genetic Variants in pre-microRNAs Were Associated With Increased Risk of Breast Cancer in Chinese Women. *Hum Mutat* (2009) 30(1):79–84. doi: 10.1002/humu.20837
34. Yang S, Zheng Y, Zhou L, Jin J, Deng Y, Yao J, et al. miR-499 Rs3746444 and miR-196a-2 Rs11614913 Are Associated With the Risk of Glioma, But Not the Prognosis. *Mol Ther Nucleic Acids* (2020) 22:340–51. doi: 10.1016/j.omtn.2020.08.038

35. He S, Li Z, Yu Y, Zeng Q, Cheng Y, Ji W, et al. Exosomal miR-499a-5p Promotes Cell Proliferation, Migration and EMT *via* mTOR Signaling Pathway in Lung Adenocarcinoma. *Exp Cell Res* (2019) 379(2):203–13. doi: 10.1016/j.yexcr.2019.03.035
36. Shen J, Ambrosone CB, DiCioccio RA, Odunsi K, Lele SB, Zhao H. A Functional Polymorphism in the miR-146a Gene and Age of Familial Breast/Ovarian Cancer Diagnosis. *Carcinogenesis* (2008) 29(10):1963–6. doi: 10.1093/carcin/bgn172
37. Saki N, Abroun S, Soleimani M, Mortazavi Y, Kaviani S, Arefian E. The Roles of miR-146a in the Differentiation of Jurkat T-Lymphoblasts. *Hematology* (2014) 19(3):141–7. doi: 10.1179/1607845413Y.0000000105
38. Yan W, Guo H, Suo F, Han C, Zheng H, Chen T. The Effect of miR-146a on STAT1 Expression and Apoptosis in Acute Lymphoblastic Leukemia Jurkat Cells. *Oncol Lett* (2017) 13(1):151–4. doi: 10.3892/ol.2016.5395
39. Wang L, Zhang H, Lei D. microRNA-146a Promotes Growth of Acute Leukemia Cells by Downregulating Ciliary Neurotrophic Factor Receptor and Activating JAK2/STAT3 Signaling. *Yonsei Med J* (2019) 60(10):924–34. doi: 10.3349/ymj.2019.60.10.924
40. Su YL, Wang X, Mann M, Adamus TP, Wang D, Moreira DF, et al. Myeloid Cell-Targeted miR-146a Mimic Inhibits NF-κb-Driven Inflammation and Leukemia Progression *In Vivo*. *Blood* (2020) 135(3):167–80. doi: 10.1182/blood.2019002045
41. Stickel N, Hanke K, Marschner D, Prinz G, Köhler M, Melchinger W, et al. MicroRNA-146a Reduces MHC-II Expression *via* Targeting JAK/STAT Signaling in Dendritic Cells After Stem Cell Transplantation. *Leukemia* (2017) 31(12):2732–41. doi: 10.1038/leu.2017.137
42. Xue Y, Yang X, Hu S, Kang M, Chen J, Fang Y. A Genetic Variant in miR-100 is a Protective Factor of Childhood Acute Lymphoblastic Leukemia. *Cancer Med* (2019) 8(5):2553–60. doi: 10.1002/cam4.2082
43. Martin-Guerrero I, Gutierrez-Camino A, Lopez-Lopez E, Bilbao-Aldaiturriaga N, Pombar-Gomez M, Ardanaz M, et al. Genetic Variants in miRNA Processing Genes and pre-miRNAs are Associated With the Risk of Chronic Lymphocytic Leukemia. *PloS One* (2015) 10(3):e0118905. doi: 10.1371/journal.pone.0118905
44. Hoffman AE, Zheng T, Yi C, Leaderer D, Weidhaas J, Slack F, et al. microRNA miR-196a-2 and Breast Cancer: A Genetic and Epigenetic Association Study and Functional Analysis. *Cancer Res* (2009) 69(14):5970–7. doi: 10.1158/0008-5472.CAN-09-0236
45. Luthra R, Singh RR, Luthra MG, Li YX, Hannah C, Romans AM, et al. MicroRNA-196a Targets Annexin A1: A microRNA-Mediated Mechanism of Annexin A1 Downregulation in Cancers. *Oncogene* (2008) 27(52):6667–78. doi: 10.1038/onc.2008.256
46. Zhao H, Xu J, Zhao D, Geng M, Ge H, Fu L, et al. Somatic Mutation of the SNP Rs11614913 and Its Association With Increased MIR 196a2 Expression in Breast Cancer. *DNA Cell Biol* (2016) 35(2):81–7. doi: 10.1089/dna.2014.2785
47. Choupani J, Nariman-Saleh-Fam Z, Saadatian Z, Ouladsahebmadarek E, Masotti A, Bastami M. Association of Mir-196a-2 Rs11614913 and Mir-149 Rs2292832 Polymorphisms With Risk of Cancer: An Updated Meta-Analysis. *Front Genet* (2019) 10:186. doi: 10.3389/fgene.2019.00186
48. Li T, Niu L, Wu L, Gao X, Li M, Liu W, et al. A Functional Polymorphism in microRNA-196a2 is Associated With Increased Susceptibility to non-Hodgkin Lymphoma. *Tumour Biol* (2015) 36(5):3279–84. doi: 10.1007/s13277-014-2957-y
49. Chen CC, Hsu PC, Shih LC, Hsu YN, Kuo CC, Chao CY, et al. MiR-196a-2 Genotypes Determine the Susceptibility and Early Onset of Childhood Acute Lymphoblastic. *Leukemia Anticancer Res* (2020) 40(8):4465–9. doi: 10.21873/anticanres.14451
50. Kim HK, Prokunina-Olsson L, Chanock SJ. Common Genetic Variants in miR-1206 (8q24.2) and miR-612 (11q13.3) Affect Biogenesis of Mature miRNA Forms. *PloS One* (2012) 7(10):e47454. doi: 10.1371/journal.pone.0047454
51. Siyadat P, Ayatollahi H, Barati M, Sheikhi M, Shahidi M. High Resolution Melting Analysis for Evaluation of Mir-612 (Rs12803915) Genetic Variant With Susceptibility to Pediatric Acute Lymphoblastic Leukemia. *Rep Biochem Mol Biol* (2021) 9(4):385–93. doi: 10.52547/rbmb.9.4.385

Conflict of Interest: The authors declare that the research was conducted in the absence of any commercial or financial relationships that could be construed as a potential conflict of interest.

Publisher's Note: All claims expressed in this article are solely those of the authors and do not necessarily represent those of their affiliated organizations, or those of the publisher, the editors and the reviewers. Any product that may be evaluated in this article, or claim that may be made by its manufacturer, is not guaranteed or endorsed by the publisher.

Citation: *Jiménez-Morales S, Núñez-Enríquez JC, Cruz-Islas J, Bekker-Méndez VC, Jiménez-Hernández E, Medina-Sanson A, Olarte-Carrillo I, Martínez-Tovar A, Flores-Lujano J, Ramírez-Bello J, Pérez-Saldívar ML, Martín-Trejo JA, Pérez-Lorenzana H, Amador-Sánchez R, Mora-Ríos FG, Peñaloza-González JG, Duarte-Rodríguez DA, Torres-Nava JR, Flores-Bautista JE, Espinosa-Elizondo RM, Román-Zepeda PF, Flores-Villegas LV, Tamez-Gómez EL, López-García VH, Lara-Ramos JR, González-Ulivarri JE, Martínez-Silva SI, Espinoza-Anrubio G, Almeida-Hernández C, Ramírez-Colorado R, Hernández-Mora L, García-López LR, Cruz-Ojeda GA, Godoy-Esquivel AE, Contreras-Hernández I, Medina-Hernández A, López-Caballero MG, Hernández-Pineda NA, Granados-Kraulles J, Rodríguez-Vázquez MA, Torres-Valle D, Cortés-Reyes C, Medrano-López F, Pérez-Gómez JA, Martínez-Ríos A, Aguilar-De-los-Santos A, Serafin-Díaz B, Gutiérrez-Rivera ML, Merino-Pasaye LE, Vargas-Alarcón G, Mata-Rocha M, Sepúlveda-Robles OA, Rosas-Vargas H, Hidalgo-Miranda A and Mejía-Aranguré JM (2021) Association Analysis Between the Functional Single Nucleotide Variants in miR-146a, miR-196a-2, miR-499a, and miR-612 With Acute Lymphoblastic Leukemia.*
Front. Oncol. 11:762063. doi: 10.3389/fonc.2021.762063

frontiers in Oncology

ORIGINAL RESEARCH
published: 23 November 2021
doi: 10.3389/fonc.2021.756025

Defining the Spectrum, Treatment and Outcome of Patients With Genetically Confirmed Gorlin Syndrome From the HIT-MED Cohort

Katja Kloth[1], Denise Obrecht[1], Dominik Sturm[2,3,4], Torsten Pietsch[5], Monika Warmuth-Metz[6], Brigitte Bison[7], Martin Mynarek[1] and Stefan Rutkowski[1]*

[1] Department of Pediatric Hematology and Oncology, University Medical Center Hamburg-Eppendorf, Hamburg, Germany, [2] Hopp Children's Cancer Center (KiTZ) Heidelberg, Heidelberg, Germany, [3] Division of Pediatric Glioma Research, German Cancer Research Center (DKFZ) Heidelberg, Heidelberg, Germany, [4] Department of Pediatric Oncology, Hematology, and Immunology, Heidelberg University Hospital, Heidelberg, Germany, [5] Department of Neuropathology, Deutsche Gesellschaft für Neuropathologie und Neuroanatomie (DGNN) Brain Tumor Reference Center, Bonn, Germany, [6] Institute of Diagnostic and Interventional Neuroradiology, University Hospital Wuerzburg, Wuerzburg, Germany, [7] Department of Diagnostic and Interventional Neuroradiology, University Hospital Augsburg, Augsburg, Germany

OPEN ACCESS

Edited by:
Pasqualino De Antonellis, Hospital for Sick Children, Canada

Reviewed by:
Angela Mastronuzzi, Bambino Gesù Children Hospital (IRCCS), Italy
Ana Guerreiro Stücklin, University Children's Hospital Zurich, Switzerland

***Correspondence:**
Katja Kloth
k.kloth-stachnau@uke.de

Specialty section:
This article was submitted to Pediatric Oncology, a section of the journal Frontiers in Oncology

Received: *09 August 2021*
Accepted: *04 November 2021*
Published: *23 November 2021*

Citation:
Kloth K, Obrecht D, Sturm D, Pietsch T, Warmuth-Metz M, Bison B, Mynarek M and Rutkowski S (2021) Defining the Spectrum, Treatment and Outcome of Patients With Genetically Confirmed Gorlin Syndrome From the HIT-MED Cohort. Front. Oncol. 11:756025. doi: 10.3389/fonc.2021.756025

Gorlin syndrome is a genetic condition associated with the occurrence of SHH activated medulloblastoma, basal cell carcinoma, macrocephaly and other congenital anomalies. It is caused by heterozygous pathogenic variants in *PTCH1* or *SUFU*. In this study we included 16 patients from the HIT2000, HIT2000interim, I-HIT-MED, observation registry and older registries such as HIT-SKK87, HIT-SKK92 (1987 – 2020) with genetically confirmed Gorlin syndrome, harboring 10 *PTCH1* and 6 *SUFU* mutations. Nine patients presented with desmoplastic medulloblastomas (DMB), 6 with medulloblastomas with extensive nodularity (MBEN) and one patient with classic medulloblastoma (CMB); all tumors affected the cerebellum, vermis or the fourth ventricle. SHH activation was present in all investigated tumors (14/16); DNA methylation analysis (when available) classified 3 tumors as iSHH-I and 4 tumors as iSHH-II. Age at diagnosis ranged from 0.65 to 3.41 years. All but one patient received chemotherapy according to the HIT-SKK protocol. Ten patients were in complete remission after completion of primary therapy; four subsequently presented with PD. No patient received radiotherapy during initial treatment. Five patients acquired additional neoplasms, namely basal cell carcinomas, odontogenic tumors, ovarian fibromas and meningioma. Developmental delay was documented in 5/16 patients. Overall survival (OS) and progression-free survival (PFS) between patients with *PTCH1* or *SUFU* mutations did not differ statistically (10y-OS 90% *vs*. 100%, p=0.414; 5y-PFS 88.9% ± 10.5% *vs*. 41.7% ± 22.2%, p=0.139). Comparing the Gorlin patients to all young, SHH activated MBs in the registries (10y-OS 93.3% ± 6.4% *vs*. 92.5% ± 3.3%, p=0.738; 10y-PFS 64.9%+-16.7% *vs*. 83.8%+-4.5%, p=0.228) as well as comparing Gorlin M0 SKK-treated patients to all young, SHH activated, M0, SKK-treated MBs in the HIT-MED database did not reveal significantly different clinical outcomes (10y-OS 88.9% ± 10.5% *vs*. 88% ± 4%, p=0.812; 5y-PFS 87.5% ± 11.7% *vs*.

77.7% ± 5.1%, p=0.746). Gorlin syndrome should be considered in young children with SHH activated medulloblastoma, especially DMB and MBEN but cannot be ruled out for CMB. Survival did not differ to patients with SHH-activated medulloblastoma with unknown germline status or between *PTCH1* and *SUFU* mutated patients. Additional neoplasms, especially basal cell carcinomas, need to be expected and screened for. Genetic counselling should be provided for families with young medulloblastoma patients with SHH activation.

Keywords: Gorlin, *PTCH1*, *SUFU*, medulloblastoma, childhood cancer predisposition syndrome

INTRODUCTION

Tumor predisposition syndromes are hereditary diseases causing a higher risk to develop certain benign or malignant neoplasms in adults and children (1, 2). In adults, the percentage of malignancies attributed to causative genetic alterations is said to be 5-10% (1, 3). In childhood, there is an overlapping but different spectrum of syndromes associated with tumor predisposition, like Li-Fraumeni syndrome, Gorlin syndrome, Fanconi anemia, tuberous sclerosis, neurofibromatosis, Cowden syndrome, APC related adenomatous polyposis, Beckwith-Wiedemann syndrome, etc (1, 4, 5).

Genetic cancer predisposition rates for children have lately been reanalyzed after the discovery of now more than 100 associated genes, and causative germline variants were identified in up to 8.5% of affected individuals (6–8), most of them presenting with an unremarkable family history (8). However, certain entities are more frequently assessed and directed towards genetic testing, making the diagnosis of a hereditary tumor syndrome more likely, e.g. in younger women diagnosed with breast or ovarian cancer or very young children with Wilms or adrenal cortical tumors in (1, 3).

Gorlin, Li-Fraumeni and rhabdoid tumor predisposition syndrome (RTPS) as well as neurofibromatosis type 1 and 2, von Hippel-Lindau syndrome and tuberous sclerosis complex (TSC) are some of the syndromes associated with an increased risk for childhood-onset brain tumors (9, 10). Brain tumors are the most common solid malignancies in childhood with medulloblastomas being the second most frequent entity constituting nearly 20% of all pediatric brain tumors (11–13). Medulloblastomas arise from the cerebellum, vermis or fourth ventricle/posterior fossa and split up in 4 different molecular subgroups: wingless (WNT)-activated (TP53wt), wingless (WNT)-activated (TP53mut), sonic hedgehog (SHH)-activated (TP53wt), MB without WNT/SHH activation (Group 3 or Group 4 (G3/4)) as defined in the 2021 WHO classification (14, 15). They are further characterized by their varying origins, molecular drivers, demographics and clinical outcomes (16, 17).

SHH-activated medulloblastomas (SHH-MB) account for approximately 25% of all medulloblastomas. Almost all SHH-MB contain at least one driver event, most frequently affecting *PTCH1, SUFU, TP53* or *SMO, KMT2D/2C, HAT, GPR161* and *ELP1;* with germline mutations in *TP53* and *ELP1* mostly identified in older pediatric medulloblastoma patients (16, 18–20). The number of damaging germline mutations identified is highest in this subgroup; *MYC* or *MYCN* genes are also regularly amplified (16, 21).

SHH-MB occur at two age peaks, in infancy/young childhood and adulthood - with 50% of the affected children being diagnosed before the age of 5 years. At the time of diagnosis 30-40% of patients present with metastatic disease; the 5 year overall survival for this group is only 66% with many long term survivors facing treatment-related neurological adverse effects (22, 23). Median survival time for relapsed disease is still less than 1 year (24).

Patients under the age of 3 will preferably be treated by systemic interval chemotherapy after gross resection of the tumor. Depending on the risk stratification, irradiation can be omitted during initial therapy or delayed until the child is older (or a relapse occurs) (25). Delaying or omitting craniospinal radiotherapy is especially successful in children with non-metastatic disease presenting with desmoplastic or extensive nodular histology which is a strong independent favorable prognostic factor compared to classical MB (26–29). A chemotherapy-only approach (e.g. HIT-SKK regime) is especially favorable in young Gorlin patients where a radiotherapy-sparing treatment option is important to prevent the occurrence of secondary neoplasms like basal cell carcinomas (BCC) (26, 27, 30–34). In line with this, the choice of the primary treatment with the highest possible chance to avoid relapse and consecutively radiotherapy is key (26, 27, 35, 36).

Tumor predisposition syndromes - like *PTCH1* or *SUFU* associated Gorlin and *TP53* associated Li-Fraumeni syndrome - affect approximately 7-8% of children with childhood/adolescent cancers and 5-6% of medulloblastoma patients with the highest prevalence of 14-20% for germline mutations in the SHH-MB subgroup (16, 19, 30, 37). Gorlin syndrome is diagnosed at a prevalence of approximately 1:30.000 - 60.000 (38, 39).

The risk for developing a medulloblastoma in Gorlin patients is estimated at 2-5% with a male predominance of approximately 3:1, usually occurring in the first 3 years of life (16, 30). The syndrome was first described in 1960 by Gorlin and Goltz. They initially described a subgroup of patients with basal cell carcinomas, jaw cysts and congenital rib anomalies (40). Subsequently, causative mutations in the genes *PTCH1* and *SUFU* were identified (9, 41). Recently, potentially disease causing heterozygous *PTCH2* variants have been identified in patients with a milder Gorlin associated phenotype and

controversially discussed but this gene has not yet been included in routine testing for Gorlin syndrome (42, 43). Smoothened (*SMO*) is another candidate gene frequently harboring somatic mutations in medulloblastoma tumors but also affecting the germline in adult medulloblastoma patients, potentially opening the door for target therapies such as SMO inhibitors (31, 44).

The *PTCH1* or *SUFU* associated Gorlin syndrome follows an autosomal dominant inheritance pattern; up to 80% of the mutations seem to be familial with a sporadic *de novo* event occurring in 20-30% (38, 39). Offspring of an affected individual will inherit the pathogenic variant in 50%. Penetrance is described to be almost 100% with a highly variable expression (32, 39).

Approximately 60% of Gorlin patients present with typical phenotypic features such as macrocephaly, frontal bossing, coarse facial features, palmar/plantar pits and/or skeletal abnormalities, e.g. of the ribs and vertebrae. Some degree of motor delay is often described, although this is almost always temporary. Global developmental delay is not routinely associated with Gorlin syndrome (33).

Neoplasms in patients with Gorlin syndrome include the typical basal cell nevi/carcinomas (90-100%), jaw keratocysts (90%), cardiac and/or ovarian fibromas (2-20%) and medulloblastomas (5%); most commonly the desmoplastic subtype.

Medulloblastomas occur significantly more often in patients with pathogenic *SUFU* variants (33%) than in those harboring *PTCH1* variants (<2%) (45, 46). Additionally, the risk for radiation-induced meningioma is significantly higher in *SUFU* mutated patients (47). General life expectancy is not reduced in Gorlin patients (33).

MATERIALS AND METHODS

The international HIT-SKK87, HIT-SKK92, HIT2000interim, HIT2000, I-HIT-MED and observation registries were retrospectively screened for patients with suspected or genetically confirmed Gorlin syndrome. A prospective screening for Gorlin syndrome was not part of this study. 2232 patients (0 – 18y) with medulloblastomas were diagnosed between 1987and 2020 and included in one of the registries mentioned above. Out of those 2232 patients, 323 were histologically classified as DMB (0.2y – 17.8y) or MBEN (0.2 – 4.1y) and 1779 as CMB (0.0 – 17.9y) by local pathologists and/or central neuropathological review since 1994 at the Brain Tumor Reference Center of the DGNN at the Institute of Neuropathology, University of Bonn Medical Center, Germany (n=1475). Patients were included in this study if the diagnosis of Gorlin syndrome was genetically confirmed by germline genetic testing and defined as the Gorlin Cohort.

SHH activation was tested by immunohistochemistry or DNA methylation analysis as described previously (48–50).

To form the Comparative Cohort all patients from the existing registries (see above) were screened for age < 3.5 years at the time of diagnosis and SHH activation. To form the M0 Comparative Cohort the patients were screened for M0 status at the time of diagnosis. Gorlin syndrome was not ruled out systematically by genetic testing in all of these patients.

Progression-free survival (PFS) was defined as the time from surgery to first progression (progression or relapse) or date of last follow-up. Overall survival (OS) was defined as the time from surgery to reported date of death or until a certain point in time within the follow-up for a specific patient, e.g. 3 year-OS or 5 year-OS. Survival of patient groups was compared by log-rank test and Kaplan-Meier curves were constructed.

All examinations were carried out on the basis and according to the legal requirements of the revised Declaration of Helsinki of the World Medical Association in 1983. Informed consent was given at study inclusion by the parents or adolescent patients themselves. Corresponding demographic and clinical data were extracted from the existing registry database (see above).

RESULTS

Patients' Characteristics

As of November 2020 there were 2232 patients <18y with medulloblastoma registered in the current and former HIT registries, namely I-HIT-MED (NCT02417324), HIT2000 interim registry (NCT02238899), HIT2000 (NCT00303810), HIT-SKK87 and HIT-SKK92 (26, 27). 323 of these patients were diagnosed with desmoplastic medulloblastoma (DMB) or medulloblastomas with extensive nodularity (MBEN). For 147 patients SHH activation was observed by molecular neuropathological assessment. 162 patients in this cohort were diagnosed when 3.5 years old or younger. 94 of those presented with SHH activation; SHH activation was not assessed in the remaining patients. A total of 1779 patients presented with CMB. Out of the 640 that underwent DNA methylation analysis, 24 patients presented with SHH activation. 8 of these were diagnosed aged 3.5 years or younger (see **Figure 1**).

Gorlin Cohort

From our above mentioned registries, we obtained genetic confirmation of Gorlin syndrome for 16 patients. There were 8 affected females and males, respectively. In 10 patients *PTCH1* mutations were identified, while 6 patients presented with pathogenic or likely pathogenic *SUFU* variants. *PTCH1* mutations were detected in 4 females and 6 males each, *SUFU* mutations were identified in 4 females and 2 males.

Family history was positive for Gorlin syndrome in 5/16 of patients (31.3%): In one family identical twins were affected, in one family the mother and one sister were affected, in one family two cousins were affected (the parents of the patients or their siblings were not mentioned) and in another family the father was also affected. All patients with a positive family history carried *PTCH1* variants, except for the two affected cousins harboring *SUFU* mutations.

Histologically, 9 patients presented with desmoplastic medulloblastoma (DMB), 6 patients with medulloblastomas with extensive nodularity (MBEN) and 1 patient with a classic

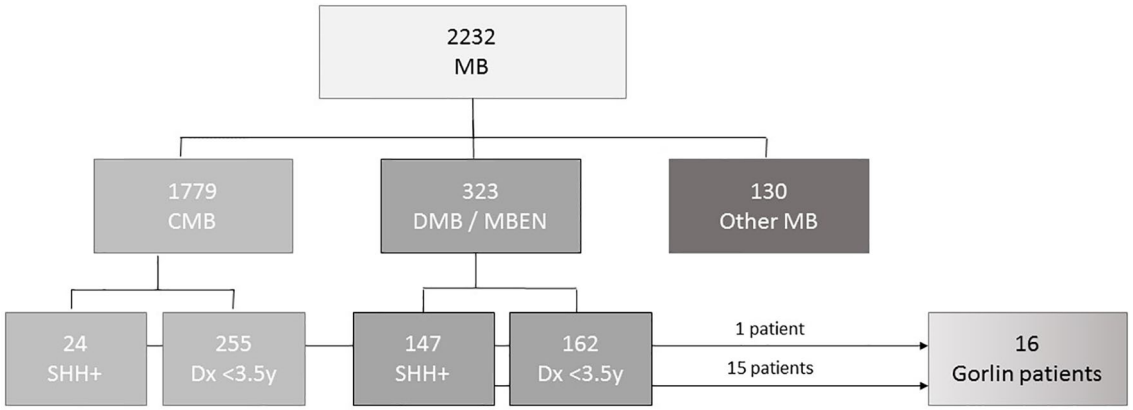

FIGURE 1 | CONSORT diagram of the cohorts' patient characterics.

medulloblastoma (CMB). 12 were localized in the cerebellum, vermis and/or the 4th ventricle while 4 were located in the cerebellar hemispheres (see **Table 1**).

Age at diagnosis ranged from 0.65 to 3.41 years with a median age of 0.97 years. Median age at diagnosis in the *PTCH1* mutated group was 0.9 years *vs.* 2.12 years in the *SUFU* mutated group.

Biological workup was completed in 10 patients who showed no amplification of *MYC* or *MYCN*; SHH activation was shown in 14/16 patients (8 DMBs, 5 MBENs, 1 CMB). The remainder of the patients was not screened for *MYC/MYCN* amplification or SHH activation. 4/16 patients presented with M+ status at initial diagnosis (see **Table 1**).

DNA methylation profiles were available for 8 of these patients and were further subclassified by *t*-distributed stochastic neighbor embedding (*t*-SNE) to differentiate between iSHH-I and iSHH-II (28, 35, 51, 52). It revealed SHH-I in 3 patients, SHH-II in 4 patients and 1 unclear result. Copy-number variation (CNV) analysis revealed varying chromosomal anomalies. Findings in the *PTCH1* group included loss of chromosome 9 in 2 patients and loss of 2qtel and a small deletion in 8q. Results in the *SUFU* group showed loss of chromosome 10 or 10q in 2 patients, loss of 16q, gain of chromosome 3, 4, 9, 13 and 15, gain of 3q, gain of 19q and a flat genome in 3 patients. Due to the small number of analyses, no statistically relevant differences could be detected between *PTCH1* and *SUFU* mutated patients.

4 patients were included in the MNP2.0 study which included screening for somatic and/or germline variants *via* next generation sequencing (NGS) (36): 1 patient`s somatic workup was unremarkable, 1 patient presented with a somatic *SUFU* and *KMT2D* variant, 1 patient presented with 2 somatic *SUFU* variants, 1 *PIK3CA* and 1 *GSE1* variant and in another patient a somatic *PTEN* variant was identified. 3 of these patients showed remarkable findings in the germline in the study and subsequently underwent routine germline genetic testing after genetic counseling. The patient whose somatic workup was unremarkable subsequently underwent NGS germline testing which revealed a pathogenic *SUFU* variant. The patient with the somatic *PTEN* variant subsequently underwent targeted germline testing which revealed a pathogenic *SUFU* variant.

TABLE 1 | Patient characteristics for the Gorlin cohort (all genetically diagnosed *PTCH1* and *SUFU* associated Gorlin syndrome patients) *vs.* the Comparative cohort (all DMB/MBEN, SHH+, <3.5y).

	Gorlin cohort (all genetically confirmed Gorlin patients) n = 16	Comparative cohort (all DMB/MBEN, SHH+, <3.5y) n = 92
Age [years]	0.65 – 3.41	0.2 – 3.5
Sex		
Male	8	87
Female	8	63
Histology		
DMB/MBEN	9	60
MBEN	6	32
CMB	1	n/a
Staging		
M0	13	63
M+	3	23
n/a	0	5
R0 (no rest, <1.5cm^2)	11	64
R+ (>1.5cm^2)	5	24
n/a	0	4
Initial Treatment		
SKK therapy	15	54
Intensified Induction	0	14
Other	1	23
Trial		
HIT-SKK'92	1	3
HIT2000 Interim Registry	2	9
HIT2000	3	42
I-HIT-MED	8	36
Observation registry	2	2

Dysmorphism/Accompanying Clinical Features

11 patients presented with dysmorphic or congenital anomalies at the age of diagnosis of medulloblastoma: 8 patients presented with macrocephaly; in all 11 patients other abnormalities like

thoracic, vertebral or rib malformations, hypertelorism, hydrocephalus, turricephalus, craniosynostosis, strabismus, frontal bossing, hemangioma, palmoplantar pits/dents, scapula alata, pectus carinatum, optic atrophy, short stature and/or scoliosis were documented. 7 out of 10 *PTCH1* (70%) mutated patients showed phenotypic anomalies, while 4/6 patients (66.7%) with *SUFU* mutations presented with signs of dysmorphism. 2 dysmorphic patients had been diagnosed with developmental delay prior to their diagnosis of MB; 1 of them carried a *PTCH1* and the other a *SUFU* mutation. A detailed neuropsychological evaluation was not available for these patients. 5 patients showed no dysmorphic features or anomalies at the time of diagnosis of the MB, making the medulloblastoma the first symptom of the syndrome.

Therapy

All 16 patients received adjuvant chemotherapy following resection. 15/16 patients received the standardized HIT-SKK regime depending on the currently applicable study protocol; e.g. 3 cycles of SKK or 3 SKK cycles followed by 2 modified SKK cycles (26, 28, 53). One patient received a modified chemotherapy regime in his home country (TOT1 (CPM/VCR; CPM/VCR; CDDP/Eto), followed by 1x CPM/VCR without MTX). 13/15 patients received 3 SKK cycles, 1 patient received 4 cycles and 1 patient discontinued treatment after a resuscitation under chemotherapy resulting in hypoxic brain damage. Outcome after completion of initial treatment was CR in 10 patients, PR in 4 patients and SD in one patient (see **Figure 2**). Outcome at the last follow up (FU) was CR in 11 patients, PD in one patient and PR or SD in 2 patients. One patient had died, and one patient was lost to follow-up (LFU).

One patient with PD underwent another round of modified SKK (see **Table 1** and **Figure 2**).

Intraventricular methotrexate (26, 28) was administered in at least 12/16 patients (75%). 9 patients received the full or at least 75% of the target dosage. 3 patients received a significantly reduced amount.

0/16 patients received radiotherapy during initial treatment. 2 patients received radiotherapy because of PD or relapse: 1 patient received radiotherapy following a relapse under salvage chemotherapy after initially declining CSI. CSI was administered following resection of the recurrence and stem cell transplantation but was discontinued after 15 Gy due to the diagnosis of the pathogenic *SUFU* mutation (see **Figure 2**, patient G-SUFU-5). The second patient received local radiotherapy with 54 Gy because of PD of his residual tumor mass (initially R+) upon completing the 2nd cycle of modified SKK. He progressed to M2/M3 under local radiotherapy and was started on a modified MEMMAT protocol (54). Since he showed no response, this was terminated and he is scheduled for palliative, salvage spinal radiation of the largest metastases (see **Figure 2**, patient G-SUFU-6).

Radiotherapy as a second line treatment was considered for at least one other patient due to persistence of residual tumor and metastases after the 1st cycle of adjuvant SKK chemotherapy but was not administered because of the diagnosis of Gorlin syndrome.

Relapse/Recurrence

Recurrence of the disease occurred in 4 out of 16 patients with Gorlin syndrome: 1 presented with local PD early after completion of chemotherapy (see **Figure 2**, patient G-PTCH1-1). 1 patient developed a local relapse/PD after initially presenting with PR following initial therapy (see **Figure 2**, patient G-SUFU-3). 1 patient presented with spinal metastases after initially presenting with PR following initial therapy (see **Figure 2**, patient G-SUFU-5). 1 patient presented with local PD under local radiotherapy after initially presenting with SD upon completion of primary therapy. This patient later additionally developed spinal metastases (see **Figure 2**, patient G-SUFU-6). All patients who relapsed presented with residual tumor after their initial surgery. 3 out of the 4 patients presented with metastatic disease at initial diagnosis. 3/4 of the relapsed Gorlin patients harbored *SUFU* mutations.

Follow Up

Severe global developmental delay or developmental delay/cognitive deficits were documented in 3 patients; 2 of them carried *PTCH1* mutations, 1 patient carried a *SUFU* variant. In 3 patients motor development delay/motor deficits were documented. 2 additional patients had been diagnosed with developmental delay prior to their diagnosis of MB. In 2 patients leukencephalopathy grade I (LEP I) and neurotoxicity grade II were reported following treatment; detailed information on consecutive deficits was not available.

At the last follow up, 15 patients were recorded as active and alive. 1 patient with a *PTCH1* mutation had died of complications of hypoxic brain damage resulting from a resuscitation under chemotherapy.

Additional Neoplasms

Additional neoplasms were reported in 5/16 patients (31.3%) from the Gorlin Cohort: one had a meningioma (M) 13 years and multiple basal cell carcinomas on head and sternum 15 years after diagnosis, one presented with multiple basal cell carcinomas of the face 9 years after treatment, odontogenic cysts at the age of 10 years and multiple ovarian fibromas (OF) on both sides at the age of 16 years, one patient had a ovarian fibroma that was operated on 11 years after initial diagnosis of the medulloblastoma and two other patients developed multiple odontogenic cysts/tumors (OC) (see **Figure 3**). All 5 patients with these additional tumors harbored *PTCH1* mutations. In comparison, all medulloblastoma patients from our current and former registries combined present with a cumulative incidence for additional/secondary neoplasms of 5.05%.

Survival

10y-OS for the entire Gorlin cohort was 93.3% ± 6.4%. 1/16 patients died during the follow up period (6.2%) (see **Figure 4.1**). 10y-PFS was 69.3% ± 13% (see **Figure 4.2**).

10y-OS in the *PTCH1* cohort was 90%, whereas it was 100% in the *SUFU* mutated cohort (p=0.414) (see **Figure 5**). However, the subset of patients with *PTCH1* mutations showed a median follow up of 12.1 years, while the median follow up in patients with *SUFU* mutations was 2.58 years.

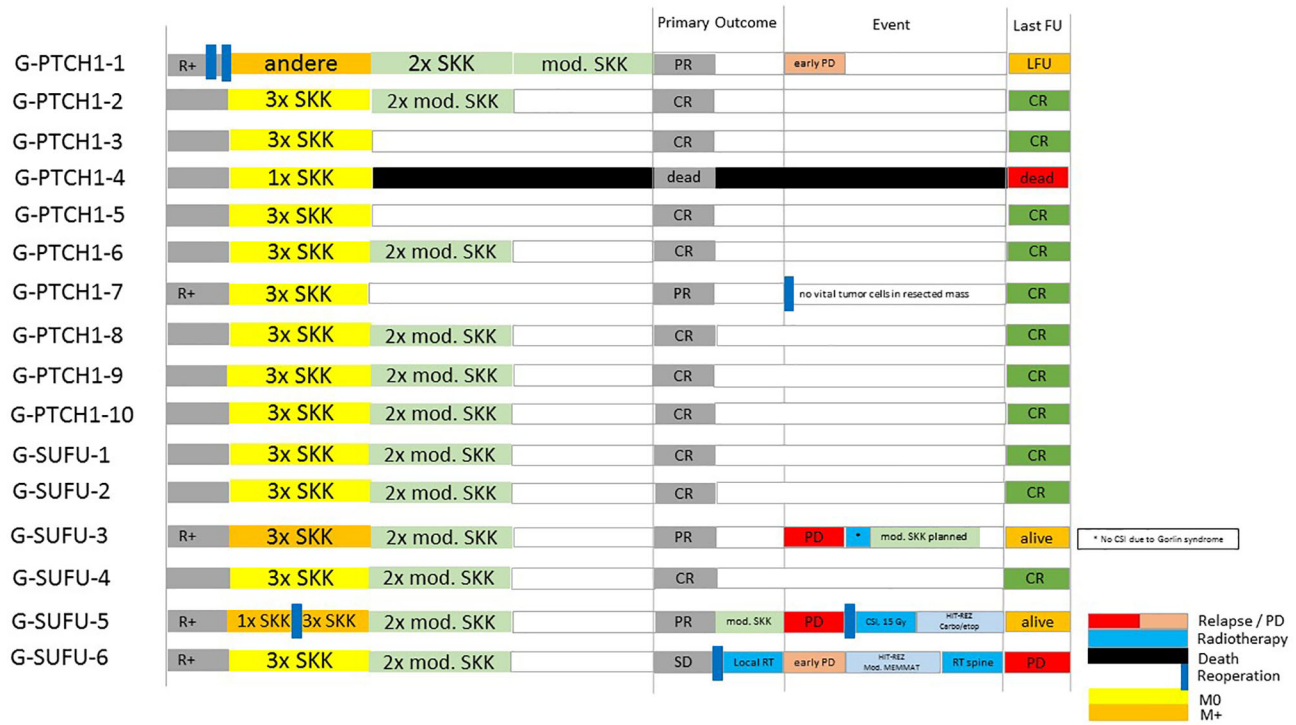

FIGURE 2 | Clinical courses of patients from the Gorlin cohort.

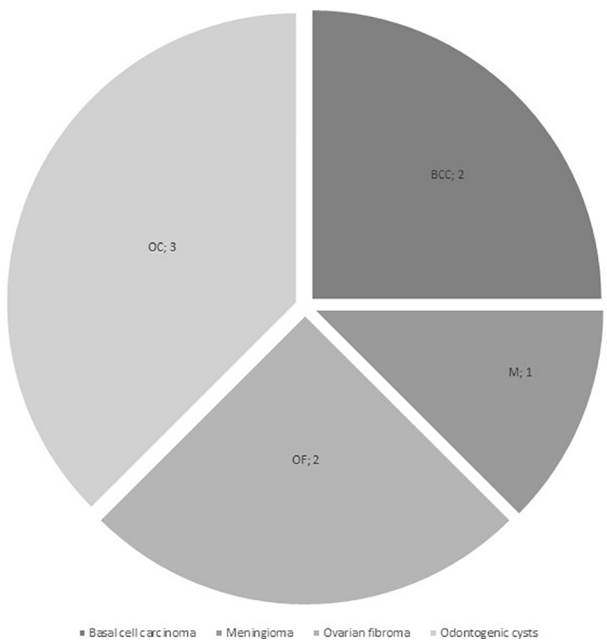

FIGURE 3 | Additional neoplasms in the Gorlin Cohort (BCC, basal cell carcinoma; M, meningioma; OC, odontogenic cysts / tumors; OF, ovarian fibroma).

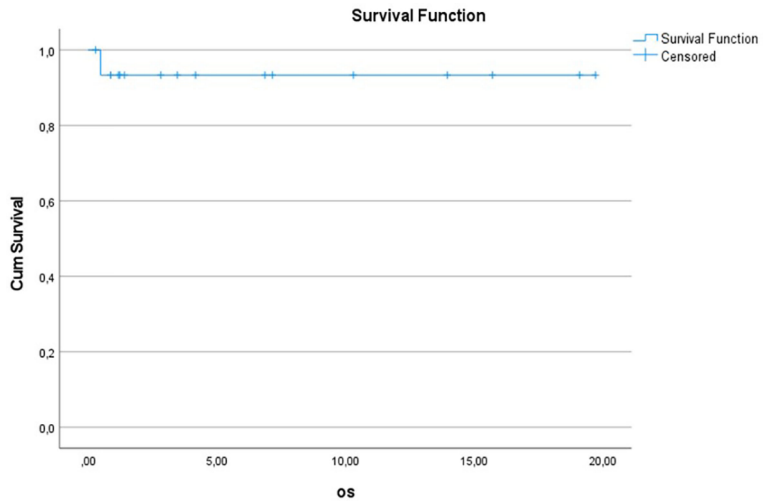

FIGURE 4.1 | Kaplan-Meier plot of OS for all patients with Gorlin syndrome (n=16).

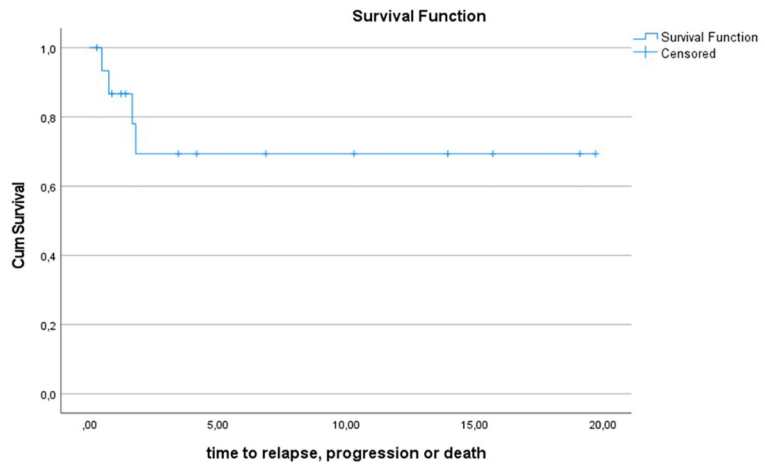

FIGURE 4.2 | Kaplan-Meier plot PFS for all patients with Gorlin syndrome (n=16).

The 5y-PFS in the *PTCH1* mutated cohort was 88.9% ± 10.5%; the 5y-PFS in the *SUFU* mutated cohort was 41.7% ± 22.2% (p=0.139) (see **Figure 6**).

Comparing survival of the Gorlin patients with the Comparative Cohort consisting of all patients from the registries with MBEN or DMB, diagnosed at 3.5y or younger, presenting with SHH activation, there was no significant difference in terms of OS (p=0.738) or PFS (p=0.228): 10y-OS in the Gorlin Cohort was 93.3% ± 6.4% *vs.* 92.5% ± 3.3% in the Comparative Cohort (p=0.738) (see **Figure 7.1**). 10y-PFS in the Gorlin Cohort was 64.9%+-16.7% *vs.* 83.8%+-4.5% in the Comparative Cohort (p=0.228) (see **Figures 7.2**, **8**, **9**).

Comparing survival of the genetically diagnosed Gorlin patients with M0 status (n=13) to the previously published SHH-activated, M0 infant medulloblastomas (n=51) (compare to (28)) (see **Table 2**), there was no significant difference in terms of OS (p=0.812): Median follow up time in the Comparative M0 cohort was 7.04 years. 10y-OS in the Gorlin M0 Cohort was 88.9% ± 10.5% *vs.* 88% ± 4% for the Comparative M0 Cohort (p=0.812) (see **Figure 10**).

DISCUSSION

Genetic testing for childhood cancer predisposition syndromes is a rapidly evolving field with significant consequences for the patient himself, the treatment regime and the prognosticated outcome as well as the affected family. Thus, whom to test and when to test will

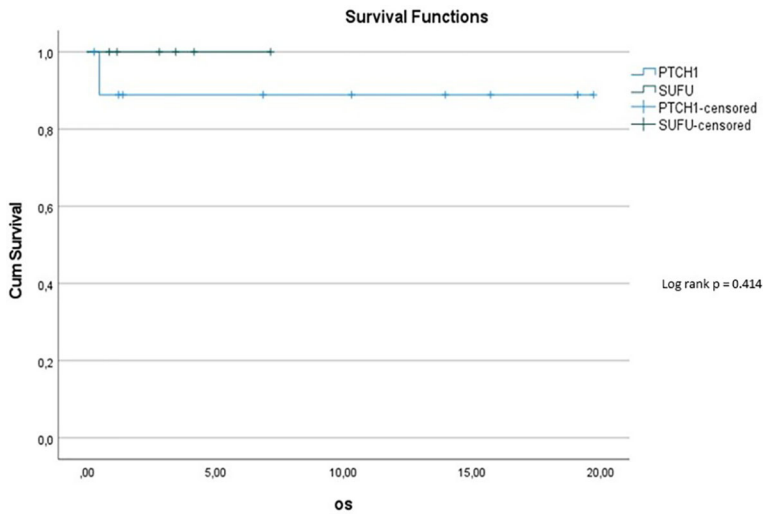

FIGURE 5 | Kaplan-Meier plot for OS for patients depending on mutational status (blue = *PTCH1* mutated patients; green = *SUFU* mutated patients).

be more relevant now than ever, especially when an oncological diagnosis is first made, and a treatment plan is mapped out. To facilitate these decisions in the future we decided to retrospectively reassess the genetically diagnosed Gorlin patients in our HIT-MED database as well as look at the different patient characteristics such as age at diagnosis, histology, molecular subgroups, residual disease, staging, treatment regimens and clinical outcomes.

As shown in previous studies (55, 56), the age at diagnosis in our cohort was younger than 3.5 years with a range from 0.65 to 3.41 years. Again in line with previous publications (9, 39, 55, 56), all but one patient in our Gorlin cohort presented with medulloblastomas that were histologically classified as DMB (62.5%) or MBEN (37.5%).

In line with recommendations from other groups, nowadays we routinely suggest genetic testing for Gorlin syndrome in patients who are less than 4 years of age at the time of diagnosis and present with an SHH-activated medulloblastoma (9, 37, 57). Retrospectively, in around 1/3 (34/92 patients) of SHH-activated young MBs Gorlin syndrome was reportedly suspected and recommended to the supervising clinician. 16/34 patients (47.1%) were diagnosed with pathogenic *PTCH1* (10/16 patients) or *SUFU* variants (6/16 patients).

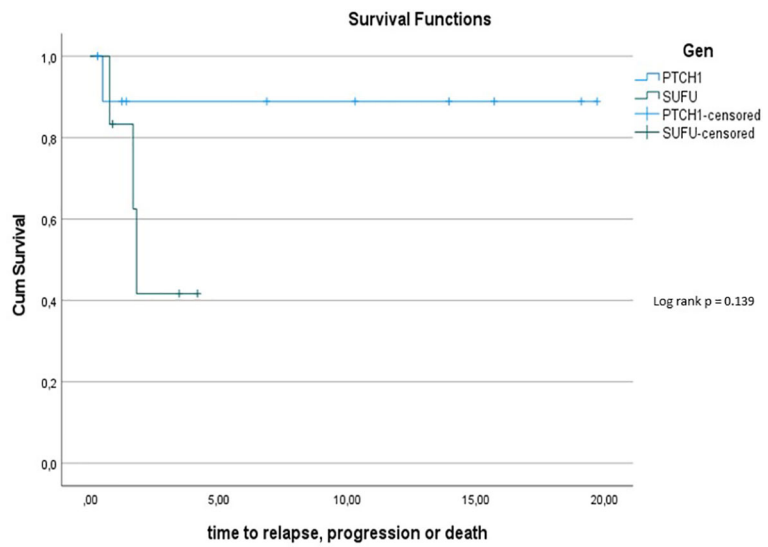

FIGURE 6 | Kaplan-Meier plot for PFs for all patients depending on mutational status (blue = *PTCH1* mutated patients; green = *SUFU* mutated patients).

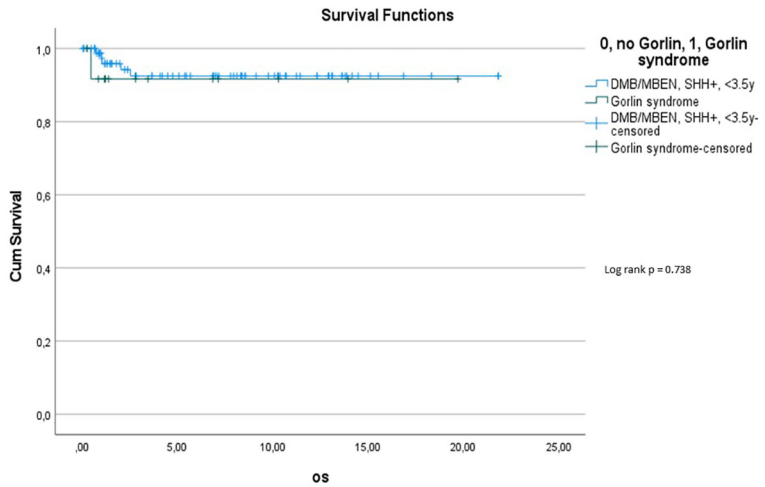

FIGURE 7.1 | OS for all SHH +, MBEN/DMB, <3.5 *vs*. all Gorlin patients.

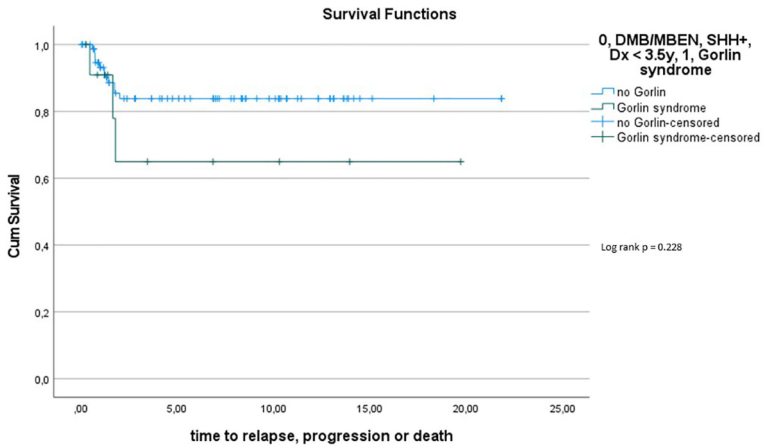

FIGURE 7.2 | PFS for all SHH +, MBEN/DMB, <3.5 *vs*. all Gorlin patients.

Since testing for SHH activation was not available for all 16 Gorlin patients (8/16 patients), we can only assume that SHH activation was present in all of them. Looking at those patients who presented with an SHH activated medulloblastoma aged 3.5 years and younger as well as assuming SHH activation for all our Gorlin patients, approximately 17% of them would have tested positive for a pathogenic *PTCH1* or *SUFU* mutation.

Since genetic testing was not conducted in all patients in our cohort, we unfortunately cannot evaluate the cumulative incidence of Gorlin syndrome. Taking into account that 16 out of 2187 patients from our cohort of patients with medulloblastomas were genetically diagnosed with Gorlin syndrome, we can only attest for these 0.7%. Judging by the low number of genetic analysis conducted within this cohort, e.g. only 4/16 cases (25%) were screened for germline variants by the MNP 2.0 study (36) in our cohort, and the fact that some medulloblastoma associated genes have only recently been described and not yet added to the standard workup for patients with SHH activated MB (19), we hypothesize that the number of undetected cases is much higher.

HIT-MED Guidance currently recommends SKK chemotherapy as initial therapy for SHH activated, low risk medulloblastomas such as DMB and MBEN in children aged 0-4/5 years (see current HIT-MED Guidance) (26, 27). SKK chemotherapy was administered in all patients initially treated in Germany (15/16) and started in the remaining patient after relocating treatment to Germany. 10/16 patients (62.5%) achieved complete remission after completing their initial

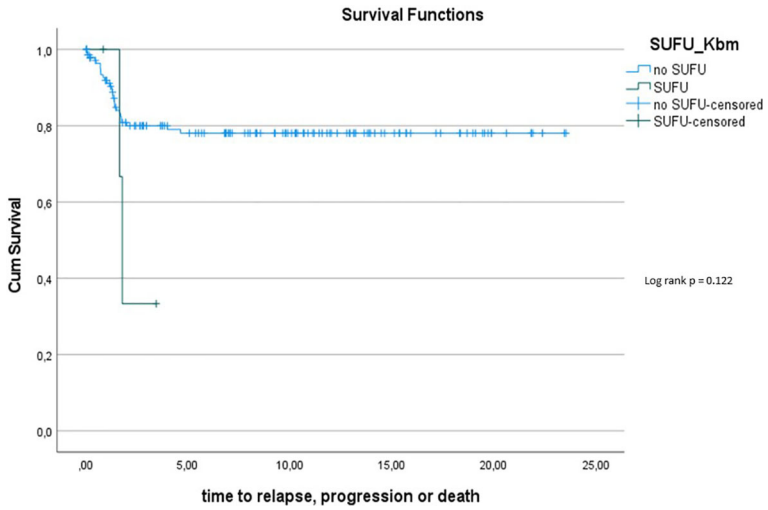

FIGURE 8 | PFS for all SHH+, MBEN/DMB <3.5 *vs. SUFU* mutated Gorlin patients.

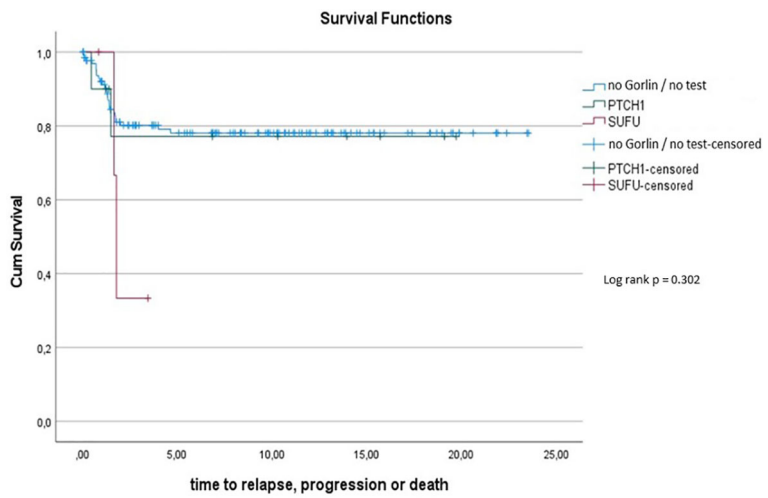

FIGURE 9 | PFS for all SHH+, MBEN/DMB <3.5 *vs. PTCH1 vs. SUFU*.

treatment regimen; the 10y-OS for all Gorlin patients was 93.3% ± 6.4%. This is in line with previously described 10y-OS from our group of 82% ± 12% for Gorlin patients (55).

Radiotherapy was not administered as part of the initial therapy in any of our Gorlin patients (0/16). This is in concordance with many radiotherapy-sparing treatment regimens for young children with medulloblastomas, potentially avoiding the devastating long-term neurological effects (26–28, 35). It was however administered later on in 2 patients (12.5%); once as part of a relapse regime and once in a patient with stable residual disease after initial R+ resection. One of the two relapsed patients terminated radiotherapy after the diagnosis of Gorlin syndrome and in one other patient radiotherapy was not administered at all during disease progression because of the genetic diagnosis (see **Figure 2**).

Overall 5/16 patients (31.3%) developed additional neoplasms (see **Figure 3**): they comprised of basal cell carcinomas, odontogenic/jaw cysts, ovarian fibromas and a meningioma. These tumors mostly developed in patients who did not receive radiation at any point. While we do not know for certain when some of these tumors appeared, some were reported before the start of the treatment of the medulloblastoma. These findings question reports that postulate a higher risk for secondary malignancies in Gorlin patients after radiotherapy and suggests a generally increased risk for such entities due to the genetic diagnosis of Gorlin syndrome and/or – possibly even more likely - after the

TABLE 2 | Patient characteristics for the Gorlin M0 Cohort (all genetically diagnosed *PTCH1* and *SUFU* associated Gorlin syndrome patients) *vs*. the Comparative M0 Cohort (all medulloblastomas (MB), SHH+, M0, <4y).

	Gorlin M0 cohort (all genetically confirmed Gorlin patients) n = 13 [this study]	Comparative M0 cohort (all MB, SHH+, M0, <4y) n = 51 [compare to Mynarek et al., J Clin Oncol., 2020]
Age [years]	0.65 – 3.41	0.29 – 3.79
Sex		
Male	7	28
Female	6	23
Histology		
DMB/MBEN	9	31
MBEN	3	18
CMB	1	2
Staging		
R0 (no rest, <1.5cm^2)	11	43
R+ (>1.5cm^2)	2	8
Initial Treatment		
SKK therapy	13	49
SKK + local RT	0	2
Trial		
HIT2000	4	27
Other	9	24

*Comparing those same two cohorts (see **Table 2**), there was also no significant difference in terms of PFS (p=0.746): 5y-PFS in the Gorlin M0 Cohort was 87.5% ± 11.7% vs. 77.7% ± 5.1% in the Comparative M0 Cohort [see **Figure 11**) (compare to (28)].*

administration of chemotherapy or radiotherapy in these mutation-prone patients (41, 58–60). Because Gorlin patients present with a generally increased risk for neoplasms of up to 100% (33), we decided to title the secondary neoplasms documented in this cohort Additional Neoplasms for accuracy (see Results).

Ideally, genetic counseling should be offered to all families of young children with DMB, MBEN or SHH-activated medulloblastoma directly after diagnosis and germline testing performed in a laboratory certified for these analyses. However, not all patients are offered this opportunity or follow these recommendations. When including patients in studies like the MNP study (36), somatic variants in tumor DNA might be identified like in our patients. These patients should then be referred to undergo genetic counseling and be tested for the germline variant. Usually in Gorlin patients, these variants will be confirmed in lymphocyte DNA, like in our patients. However, there are cases where somatic *SUFU* or *PTCH1* variants were identified in tumor DNA but could not be confirmed in the germline. If these variants appear in DNA from multiple neoplasms of the same patient or the patient presents with additional features of Gorlin syndrome, mosaicism should be considered (34, 61).

Overall survival within the Gorlin patients varied depending on mutational status. Potentially at least partially owed to the shorter follow up period, *SUFU* mutated patients had a 10y-OS of 100% while *PTCH1* mutated patients had a 10y-OS of 90%. The difference between these two groups was not statistically significant (p=0.414). However, the 5y-PFS in the *SUFU* mutated cohort was 41.7% ± 22.2%, while the 5y-PFS in the *PTCH1* mutated cohort was 88.9% ± 10.5% - even though this difference again was not statistically significant (p=0.139). This is in concordance with previous studies hinting at a reduced PFS and OS for *SUFU* mutated patients compared to *PTCH1* mutated patients or SHH activated DMB/MBEN medulloblastoma patients in general (45, 57). We hypothesize that a bigger sample size and/or longer observational period might have yielded a statistically significant difference with a less favorable outcome for *SUFU* mutated patients.

To assess this further, we compared OS and PFS of Gorlin patients to SHH activated, MBEN/DMB, younger than <3.5 years at the time of diagnosis from the registries: Neither Gorlin *vs*. the Non Gorlin/Comparative Cohort (p=0.228), nor *SUFU vs*. *PTCH1* + Non Gorlin cohort (p=0.122) nor Comparative/Non-

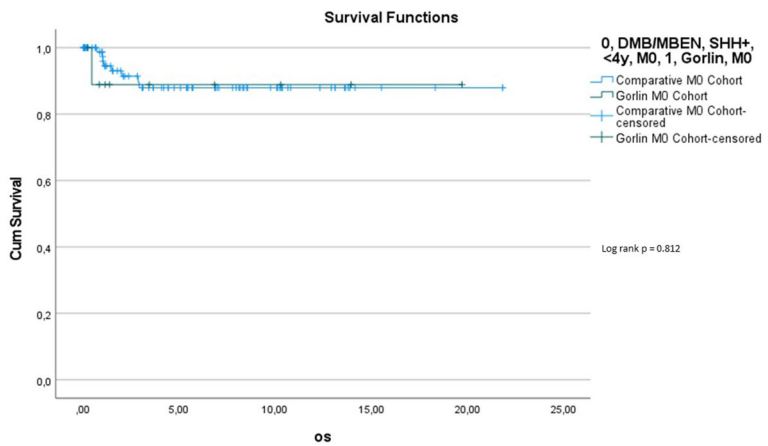

FIGURE 10 | Comparison of OS (Gorlin M0 cohort *vs*. Comparative M0 Cohort).

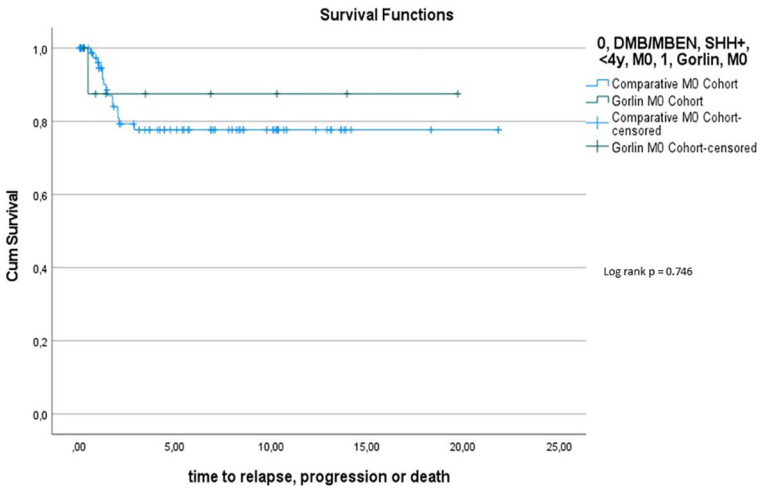

FIGURE 11 | Comparison of PFS (Gorlin M0 cohort *vs*. Comparative M0 Cohort).

Gorlin cohort *vs*. *PTCH1 vs*. *SUFU* (p=0.302) yielded significantly different results in terms of PFS and OS.

To exclude a bias owed to metastatic disease in some of the Gorlin patients in this cohort, we created a subgroup of Gorlin patients with M0 status (Gorlin M0 cohort, n = 13). To evaluate potential differences in PFS and OS for this cohort we compared these patients to the recently published SHH-activated, M0 infant medulloblastoma cohort by Mynarek et al. who also received SKK chemotherapy (Infant MB) (28). Again, there was no significant difference in terms of OS (p=0.812) or PFS (p=0.746) between these cohorts. Also, comparing non *SUFU* and *SUFU* patients in these cohorts alone, there was not significant difference between 3y-OS (92.1% ± 3.8% *vs*. 100%; p=0.623) or 3y-PFS (86.2% ± 4.9% *vs*. 75% ± 21.7%; p=0.337). After exclusion of the potential confounding variable that is metastatic disease, these findings confirm that *SUFU* mutated patients tend to present with more events over the course of time (reduced EFS/PFS), but larger numbers and longer follow up would be needed to assess for statistically significant differences between the *SUFU* and *PTCH1* versus non Gorlin MB patients.

When assessing PFS and OS we noticed the significant disparity in follow up periods for the *PTCH1* and *SUFU* mutated cohort (12.1 years *vs*. 2.58 years). We can only assume, that a longer follow up period especially for the *SUFU* mutated cohort might have altered some of the reported differences in PFS and OS to a statistically significant level. As to why the follow up for this subgroup was so much shorter, we cannot exclude the possibility that *SUFU* associated medulloblastomas represent a new tumor entity that recently rose in numbers. But more likely we assume that this is owed to the fact that *SUFU* mutations were first described in 1999 and only a few years ago added to the list of MB/Gorlin associated genes (62). Because of this timeline, a comparative prospective analysis of *PTCH1 vs*. *SUFU* associated Gorlin patients would potentially only be valid from the year 2000 on. More contradictory still, our *SUFU* patients present with a median follow up of 2.58 years only with most *SUFU* mutations identified within the last 0-4 years, allocating the least recent *SUFU* diagnosis in our cohort to the year 2014 (4 I-HIT-MED patients, 2 patients from the Interim Registry). We hypothesize that a retrospective genetic analysis of older *PTCH1* negative, SHH activated infant MBs would potentially reveal more *SUFU* associated Gorlin patients as demonstrated by Smith et al. (2014) (47). Furthermore, recently *PTCH2* and possibly also *SMO* mutations have been described as a potential cause for Gorlin syndrome associated medulloblastoma (43, 63, 64). These genes have not (yet) been implemented in routine genetic testing strategies for patients with the suspected diagnosis of Gorlin syndrome and might (partially) close the diagnostic gap in young children with SHH-activated medulloblastomas lacking germline *PTCH1* or *SUFU* mutations.

In line with previous reports, 5 patients in our cohort presented with motor and/or global developmental delay during the follow-up period (27, 60). While temporary motor delay is often reported in children with Gorlin syndrome, persisting global developmental delay is not a common finding (31). There are few affected cases in the literature, which may be caused by more complex genetic alterations, such as the 9q22.3 microdeletion encompassing the PTCH1 gene (65). However, point mutations have not commonly been associated with global developmental delay/intellectual disability (ID) (33). While developmental delay after the treatment of medullobastoma in children with Gorlin syndrome might be a secondary effect of the treatment itself, the occurrence of developmental delay before the diagnosis of the medulloblastoma is uncommon.

Interestingly, two additional dysmorphic Gorlin patients in our cohort – one harboring a *PTCH1* and the other a *SUFU* mutation - presented with developmental delay prior to the diagnosis of the medulloblastoma/the beginning of treatment. Unfortunately, follow-up neuropsychological evaluation was not available for these 2 patients, but this finding might illustrate the need to monitor the global development of Gorlin patients

closely, notwithstanding the diagnosis/treatment of a medulloblastoma.

CONCLUSION

All SHH activated medulloblastoma patients younger than 4 years of age at diagnosis – especially DMB and MBEN - should be evaluated for Gorlin syndrome and systematically undergo specific genetic testing. Taking our data and previously published data on Gorlin patients into account, we can only assume that there are many Gorlin patients out there who escaped diagnosis. Since this diagnosis affects treatment, clinical management, familial planning and strongly influences the outcome, the diagnosis of Gorlin syndrome in a patient with medulloblastoma should be made as early as possible. Effective chemotherapeutic treatment strategies aiming to avoid radiotherapy during primary treatment are available, but the optimal regimen for Gorlin patients needs to be further investigated. More retrospective and prospective international studies to assess treatment, long-term survival and secondary neoplasms of the *PTCH1* and *SUFU* mutated Gorlin subgroups are warranted.

DATA AVAILABILITY STATEMENT

The data analyzed in this study is subject to the following licenses/restrictions: Privacy restrictions (patient names, family pedigree, clinical course, etc) in HIT-MED database. Requests to access these datasets should be directed to KK, k.kloth-stachnau@uke.de or katja.kloth@gmail.com.

ETHICS STATEMENT

Ethical review and approval were not required for the study on human participants in accordance with the local legislation and institutional requirements. Written informed consent to participate in this study was provided by the participants' legal guardian/next of kin.

AUTHOR CONTRIBUTIONS

KK, SR, and MM contributed to conception and design of the study. KK, MM, DO, and SR accessed the database and generated the dataset. KK performed the statistical analysis and wrote the first draft of the manuscript. SR supervised the writing of the manuscript and the design of the study. KK, MM, DO, BB, DS, TP, MW-M, and SR provided relevant data. All authors contributed to manuscript revision, read, and approved the submitted version.

FUNDING

The HIT-MED trial office and the Neuroradiological Reference Center are supported by Deutsche Kinderkrebsstiftung.

ACKNOWLEDGMENTS

We would like to thank the patients and their families for participating in this study.

REFERENCES

1. Garber JE, Offit K. Hereditary Cancer Predisposition Syndromes. *J Clin Oncol* (2005) 23(2):276–92. doi: 10.1200/JCO.2005.10.042
2. Eng C, Hampel H, de la Chapelle A. Genetic Testing for Cancer Predisposition. *Annu Rev Med* (2001) 52:371–400. doi: 10.1146/annurev.med.52.1.371
3. Samadder NJ, Giridhar KV, Baffy N, Riegert-Johnson D, Couch FJ. Hereditary Cancer Syndromes-A Primer on Diagnosis and Management: Part 1: Breast-Ovarian Cancer Syndromes. *Mayo Clin Proc* (2019) 94(6):1084–98. doi: 10.1016/j.mayocp.2019.02.017
4. Schiffman JD, Geller JI, Mundt E, Means A, Means L, Means V. Update on Pediatric Cancer Predisposition Syndromes. *Pediatr Blood Cancer* (2013) 60 (8):1247–52. doi: 10.1002/pbc.24555
5. Ripperger T, Bielack SS, Borkhardt A, Brecht IB, Burkhardt B, Calaminus G, et al. Childhood Cancer Predisposition Syndromes-A Concise Review and Recommendations by the Cancer Predisposition Working Group of the Society for Pediatric Oncology and Hematology. *Am J Med Genet A* (2017) 173(4):1017–37. doi: 10.1002/ajmg.a.38142
6. Mitchell SG, Pencheva B, Porter CC. Germline Genetics and Childhood Cancer: Emerging Cancer Predisposition Syndromes and Psychosocial Impacts. *Curr Oncol Rep* (2019) 21(10):85. doi: 10.1007/s11912-019-0836-9
7. Parsons DW, Roy A, Yang Y, Wang T, Scollon S, Bergstrom K, et al. Diagnostic Yield of Clinical Tumor and Germline Whole-Exome Sequencing for Children With Solid Tumors. *JAMA Oncol* (2016) 2(5):616–24. doi: 10.1001/jamaoncol.2015.5699
8. Zhang J, Walsh MF, Wu G, Edmonson MN, Gruber TA, Easton J, et al. Germline Mutations in Predisposition Genes in Pediatric Cancer. *N Engl J Med* (2015) 373(24):2336–46. doi: 10.1056/NEJMoa1508054
9. Foulkes WD, Kamihara J, Evans DGR, Brugieres L, Bourdeaut F, Molenaar JJ, et al. Cancer Surveillance in Gorlin Syndrome and Rhabdoid Tumor Predisposition Syndrome. *Clin Cancer Res* (2017) 23(12):e62–7. doi: 10.1158/1078-0432.CCR-17-0595
10. Farrell CJ, Plotkin SR. Genetic Causes of Brain Tumors: Neurofibromatosis, Tuberous Sclerosis, Von Hippel-Lindau, and Other Syndromes. *Neurol Clin* (2007) 25(4):925–46, viii. doi: 10.1016/j.ncl.2007.07.008
11. Mahapatra S, Amsbaugh MJ. *Medulloblastoma*. Treasure Island (FL: StatPearls (2020).
12. Gilbertson RJ. Medulloblastoma: Signalling a Change in Treatment. *Lancet Oncol* (2004) 5(4):209–18. doi: 10.1016/S1470-2045(04)01424-X
13. DKKR. *Annual Report 2019*. Mainz: Deutsches Kinderkrebsregister (DKKR) (2019).
14. Louis DN, Perry A, Wesseling P, Brat DJ, Cree IA, Figarella-Branger D, et al. The 2021 WHO Classification of Tumors of the Central Nervous System: A Summary. *Neuro Oncol* (2021) 23(8):1231–51. doi: 10.1093/neuonc/noab106
15. Louis DN, Perry A, Reifenberger G, von Deimling A, Figarella-Branger D, Cavenee WK, et al. The 2016 World Health Organization Classification of Tumors of the Central Nervous System: A Summary. *Acta Neuropathol* (2016) 131(6):803–20. doi: 10.1007/s00401-016-1545-1
16. Waszak SM, Northcott PA, Buchhalter I, Robinson GW, Sutter C, Groebner S, et al. Spectrum and Prevalence of Genetic Predisposition in Medulloblastoma: A Retrospective Genetic Study and Prospective Validation in a Clinical Trial Cohort. *Lancet Oncol* (2018) 19(6):785–98. doi: 10.1016/S1470-2045(18) 30242-0
17. Northcott PA, Buchhalter I, Morrissy AS, Hovestadt V, Weischenfeldt J, Ehrenberger T, et al. The Whole-Genome Landscape of Medulloblastoma Subtypes. *Nature* (2017) 547(7663):311–7. doi: 10.1038/nature22973

18. Begemann M, Waszak SM, Robinson GW, Jager N, Sharma T, Knopp C, et al. Germline GPR161 Mutations Predispose to Pediatric Medulloblastoma. *J Clin Oncol* (2020) 38(1):43–50. doi: 10.1200/JCO.19.00577
19. Waszak SM, Robinson GW, Gudenas BL, Smith KS, Forget A, Kojic M, et al. Germline Elongator Mutations in Sonic Hedgehog Medulloblastoma. *Nature* (2020) 580(7803):396–401. doi: 10.1038/s41586-020-2164-5
20. Carta R, Del Baldo G, Miele E, Po A, Besharat ZM, Nazio F, et al. Cancer Predisposition Syndromes and Medulloblastoma in the Molecular Era. *Front Oncol* (2020) 10:566822. doi: 10.3389/fonc.2020.566822
21. Menyhart O, Gyorffy B. Molecular Stratifications, Biomarker Candidates and New Therapeutic Options in Current Medulloblastoma Treatment Approaches. *Cancer Metastasis Rev* (2020) 39(1):211–33. doi: 10.1007/s10555-020-09854-1
22. Smoll NR, Drummond KJ. The Incidence of Medulloblastomas and Primitive Neurectodermal Tumours in Adults and Children. *J Clin Neurosci* (2012) 19 (11):1541–4. doi: 10.1016/j.jocn.2012.04.009
23. Packer RJ, Rood BR, MacDonald TJ. Medulloblastoma: Present Concepts of Stratification Into Risk Groups. *Pediatr Neurosurg* (2003) 39(2):60–7. doi: 10.1159/000071316
24. Pui CH, Gajjar AJ, Kane JR, Qaddoumi IA, Pappo AS. Challenging Issues in Pediatric Oncology. *Nat Rev Clin Oncol* (2011) 8(9):540–9. doi: 10.1038/nrclinonc.2011.95
25. Lafay-Cousin L, Smith A, Chi SN, Wells E, Madden J, Margol A, et al. Clinical, Pathological, and Molecular Characterization of Infant Medulloblastomas Treated With Sequential High-Dose Chemotherapy. *Pediatr Blood Cancer* (2016) 63(9):1527–34. doi: 10.1002/pbc.26042
26. Rutkowski S, Bode U, Deinlein F, Ottensmeier H, Warmuth-Metz M, Soerensen N, et al. Treatment of Early Childhood Medulloblastoma by Postoperative Chemotherapy Alone. *N Engl J Med* (2005) 352(10):978–86. doi: 10.1056/NEJMoa042176
27. Rutkowski S, Gerber NU, von Hoff K, Gnekow A, Bode U, Graf N, et al. Treatment of Early Childhood Medulloblastoma by Postoperative Chemotherapy and Deferred Radiotherapy. *Neuro Oncol* (2009) 11(2):201–10. doi: 10.1215/15228517-2008-084
28. Mynarek M, von Hoff K, Pietsch T, Ottensmeier H, Warmuth-Metz M, Bison B, et al. Nonmetastatic Medulloblastoma of Early Childhood: Results From the Prospective Clinical Trial HIT-2000 and An Extended Validation Cohort. *J Clin Oncol* (2020) 38(18):2028–40. doi: 10.1200/JCO.19.03057
29. Dhall G, O'Neil SH, Ji L, Haley K, Whitaker AM, Nelson MD, et al. Excellent Outcome of Young Children With Nodular Desmoplastic Medulloblastoma Treated on "Head Start" III: A Multi-Institutional, Prospective Clinical Trial. *Neuro Oncol* (2020) 22(12):1862–72. doi: 10.1093/neuonc/noaa102
30. Garre ML, Cama A, Bagnasco F, Morana G, Giangaspero F, Brisigotti M, et al. Medulloblastoma Variants: Age-Dependent Occurrence and Relation to Gorlin Syndrome–a New Clinical Perspective. *Clin Cancer Res* (2009) 15 (7):2463–71. doi: 10.1158/1078-0432.CCR-08-2023
31. Twigg SRF, Hufnagel RB, Miller KA, Zhou Y, McGowan SJ, Taylor J, et al. A Recurrent Mosaic Mutation in SMO, Encoding the Hedgehog Signal Transducer Smoothened, Is the Major Cause of Curry-Jones Syndrome. *Am J Hum Genet* (2016) 98(6):1256–65. doi: 10.1016/j.ajhg.2016.04.007
32. Anderson DE, Taylor WB, Falls HF, Davidson RT. The Nevoid Basal Cell Carcinoma Syndrome. *Am J Hum Genet* (1967) 19(1):12–22.
33. Evans DG, Farndon PA. *Nevoid Basal Cell Carcinoma Syndrome. GeneReviews®*. Seattle (WA: University of Washington, Seattle (2002). 1993-2021.
34. Torrelo A, Hernandez-Martin A, Bueno E, Colmenero I, Rivera I, Requena L, et al. Molecular Evidence of Type 2 Mosaicism in Gorlin Syndrome. *Br J Dermatol* (2013) 169(6):1342–5. doi: 10.1111/bjd.12458
35. Lafay-Cousin L, Bouffet E, Strother D, Rudneva V, Hawkins C, Eberhart C, et al. Phase II Study of Nonmetastatic Desmoplastic Medulloblastoma in Children Younger Than 4 Years of Age: A Report of the Children's Oncology Group (Acns1221). *J Clin Oncol* (2020) 38(3):223–31. doi: 10.1200/JCO.19.00845
36. Sturm D, Sahm F, Andreiuolo F, Rode A, Grund K, Hirsch S, et al. GENE-08. The MNP 2.0 Study: Prospective Integration Of DNA Methylation Profiling In CNS Tumor Diagnostics. *Neuro-Oncol* (2019) 21(Supplement_2):ii82–ii. doi: 10.1093/neuonc/noz036.079
37. Grobner SN, Worst BC, Weischenfeldt J, Buchhalter I, Kleinheinz K, Rudneva VA, et al. The Landscape of Genomic Alterations Across Childhood Cancers. *Nature* (2018) 555(7696):321–7. doi: 10.1038/nature25480
38. Evans DG, Howard E, Giblin C, Clancy T, Spencer H, Huson SM, et al. Birth Incidence and Prevalence of Tumor-Prone Syndromes: Estimates From a UK Family Genetic Register Service. *Am J Med Genet A* (2010) 152A(2):327–32. doi: 10.1002/ajmg.a.33139
39. Spiker AM, Troxell T, Ramsey ML. *Gorlin Syndrome (Basal Cell Nevus)*. Treasure Island (FL: StatPearls (2020).
40. Gorlin RJ, Goltz RW. Multiple Nevoid Basal-Cell Epithelioma, Jaw Cysts and Bifid Rib. A Syndrome. *N Engl J Med* (1960) 262:908–12. doi: 10.1056/NEJM196005052621803
41. Hahn H, Wojnowski L, Zimmer AM, Hall J, Miller G, Zimmer A. Rhabdomyosarcomas and Radiation Hypersensitivity in a Mouse Model of Gorlin Syndrome. *Nat Med* (1998) 4(5):619–22. doi: 10.1038/nm0598-619
42. Fujii K, Ohashi H, Suzuki M, Hatsuse H, Shiohama T, Uchikawa H, et al. Frameshift Mutation in the PTCH2 Gene can Cause Nevoid Basal Cell Carcinoma Syndrome. *Fam Cancer* (2013) 12(4):611–4. doi: 10.1007/s10689-013-9623-1
43. Altaraihi M, Wadt K, Ek J, Gerdes AM, Ostergaard E. A Healthy Individual With a Homozygous PTCH2 Frameshift Variant: Are Variants of PTCH2 Associated With Nevoid Basal Cell Carcinoma Syndrome? *Hum Genome Var* (2019) 6:10. doi: 10.1038/s41439-019-0041-2
44. Kool M, Jones DT, Jager N, Northcott PA, Pugh TJ, Hovestadt V, et al. Genome Sequencing of SHH Medulloblastoma Predicts Genotype-Related Response to Smoothened Inhibition. *Cancer Cell* (2014) 25(3):393–405. doi: 10.1016/j.ccr.2014.02.004
45. Guerrini-Rousseau L, Dufour C, Varlet P, Masliah-Planchon J, Bourdeaut F, Guillaud-Bataille M, et al. Germline SUFU Mutation Carriers and Medulloblastoma: Clinical Characteristics, Cancer Risk, and Prognosis. *Neuro-Oncology* (2017) 20(8):1122–32. doi: 10.1093/neuonc/nox228
46. Guerrini-Rousseau L, Smith MJ, Kratz CP, Doergeloh B, Hirsch S, Hopman SMJ, et al. Current Recommendations for Cancer Surveillance in Gorlin Syndrome: A Report From the SIOPE Host Genome Working Group (SIOPE HGWG). *Fam Cancer* (2021) 20:317–25. doi: 10.1007/s10689-021-00247-z
47. Smith MJ, Beetz C, Williams SG, Bhaskar SS, O'Sullivan J, Anderson B, et al. Germline Mutations in SUFU Cause Gorlin Syndrome-Associated Childhood Medulloblastoma and Redefine the Risk Associated With PTCH1 Mutations. *J Clin Oncol* (2014) 32(36):4155–61. doi: 10.1200/JCO.2014.58.2569
48. Ellison DW, Dalton J, Kocak M, Nicholson SL, Fraga C, Neale G, et al. Medulloblastoma: Clinicopathological Correlates of SHH, WNT, and non-SHH/WNT Molecular Subgroups. *Acta Neuropathol* (2011) 121(3):381–96. doi: 10.1007/s00401-011-0800-8
49. Capper D, Jones DTW, Sill M, Hovestadt V, Schrimpf D, Sturm D, et al. DNA Methylation-Based Classification of Central Nervous System Tumours. *Nature* (2018) 555(7697):469–74. doi: 10.1038/nature26000
50. Pietsch T, Haberler C. Update on the Integrated Histopathological and Genetic Classification of Medulloblastoma - a Practical Diagnostic Guideline. *Clin Neuropathol* (2016) 35(6):344–52. doi: 10.5414/NP300999
51. Cavalli FMG, Remke M, Rampasek L, Peacock J, Shih DJH, Luu B, et al. Intertumoral Heterogeneity Within Medulloblastoma Subgroups. *Cancer Cell* (2017) 31(6):737–54.e6. doi: 10.1016/j.ccell.2017.05.005
52. Robinson GW, Rudneva VA, Buchhalter I, Billups CA, Waszak SM, Smith KS, et al. Risk-Adapted Therapy for Young Children With Medulloblastoma (SJYC07): Therapeutic and Molecular Outcomes From a Multicentre, Phase 2 Trial. *Lancet Oncol* (2018) 19(6):768–84. doi: 10.1016/S1470-2045(18)30204-3
53. von Bueren AO, von Hoff K, Pietsch T, Gerber NU, Warmuth-Metz M, Deinlein F, et al. Treatment of Young Children With Localized Medulloblastoma by Chemotherapy Alone: Results of the Prospective, Multicenter Trial HIT 2000 Confirming the Prognostic Impact of Histology. *Neuro Oncol* (2011) 13(6):669–79. doi: 10.1093/neuonc/nor025
54. Slavc I, Peyrl A, Chocholous M, Reisinger D, Mayr L, Azizi A, et al. MBCL-27. Response Of Recurrent Malignant Childhood CNS Tumors To A Memmat Based Metronomic Antiangiogenic Combination Therapy Varies Dependent On Tumor Type: Experience In 71 Patients. *Neuro-Oncology* (2018) 20 (suppl_2):i122–i. doi: 10.1093/neuonc/noy059.423
55. Meissner B, Mynarek M, Ole Juhnke B, von Hoff K, Pietsch T, Kortmann RD, et al. MBCL-39. Medulloblastoma In Patients With Gorlin Syndrome: Results From The Hit Study Group. *Neuro-Oncology* (2018) 20(suppl_2):i125–i. doi: 10.1093/neuonc/noy059.435

56. Malbari F, Lindsay H. Genetics of Common Pediatric Brain Tumors. *Pediatr Neurol* (2020) 104:3–12. doi: 10.1016/j.pediatrneurol.2019.08.004
57. Pietsch T, Schmidt R, Remke M, Korshunov A, Hovestadt V, Jones DT, et al. Prognostic Significance of Clinical, Histopathological, and Molecular Characteristics of Medulloblastomas in the Prospective HIT2000 Multicenter Clinical Trial Cohort. *Acta Neuropathol* (2014) 128(1):137–49. doi: 10.1007/s00401-014-1276-0
58. Robinson RG. A Second Brain Tumour and Irradiation. *J Neurol Neurosurg Psychiatry* (1978) 41(11):1005–12. doi: 10.1136/jnnp.41.11.1005
59. Packer RJ, Sutton LN, Elterman R, Lange B, Goldwein J, Nicholson HS, et al. Outcome for Children With Medulloblastoma Treated With Radiation and Cisplatin, CCNU, and Vincristine Chemotherapy. *J Neurosurg* (1994) 81 (5):690. doi: 10.3171/jns.1994.81.5.0690
60. Packer RJ, Zhou T, Holmes E, Vezina G, Gajjar A. Survival and Secondary Tumors in Children With Medulloblastoma Receiving Radiotherapy and Adjuvant Chemotherapy: Results of Children's Oncology Group Trial A9961. *Neuro-Oncology* (2012) 15(1):97–103. doi: 10.1093/neuonc/nos267
61. Evans DG, Ramsden RT, Shenton A, Gokhale C, Bowers NL, Huson SM, et al. Mosaicism in Neurofibromatosis Type 2: An Update of Risk Based on Uni/Bilaterality of Vestibular Schwannoma at Presentation and Sensitive Mutation Analysis Including Multiple Ligation-Dependent Probe Amplification. *J Med Genet* (2007) 44(7):424–8. doi: 10.1136/jmg.2006.047753
62. Taylor MD, Liu L, Raffel C, Hui CC, Mainprize TG, Zhang X, et al. Mutations in SUFU Predispose to Medulloblastoma. *Nat Genet* (2002) 31(3):306–10. doi: 10.1038/ng916
63. Epstein EH. Basal Cell Carcinomas: Attack of the Hedgehog. *Nat Rev Cancer* (2008) 8(10):743–54. doi: 10.1038/nrc2503
64. Ighilahriz M, Nikolaev S, Yurchenko AA, Battistella M, Mourah S, Jouenne F, et al. A Novel Case of Gorlin Syndrome Mosaicism Involving an SMO Gene Mutation: Clinical, Histological and Molecular Analysis of Basaloid Tumours. *Acta Derm Venereol* (2021) 101(4): adv00434. doi: 10.2340/00015555-3797
65. Muller EA, Aradhya S, Atkin JF, Carmany EP, Elliott AM, Chudley AE, et al. Microdeletion 9q22.3 Syndrome Includes Metopic Craniosynostosis, Hydrocephalus, Macrosomia, and Developmental Delay. *Am J Med Genet A* (2012) 158A(2):391–9. doi: 10.1002/ajmg.a.34216

Conflict of Interest: The authors declare that the research was conducted in the absence of any commercial or financial relationships that could be construed as a potential conflict of interest.

frontiers in Oncology

PERSPECTIVE
published: 25 February 2022
doi: 10.3389/fonc.2022.855725

Advances in Hodgkin Lymphoma: Including the Patient's Voice

Christine Moore Smith[1,2*] *and Debra L. Friedman*[1,2]

[1] Division of Pediatric Hematology/Oncology, Vanderbilt University Medical Center, Nashville, TN, United States,
[2] Vanderbilt-Ingram Cancer Center, Vanderbilt University Medical Center, Nashville, TN, United States

Since the initial treatment with radiation therapy in the 1950s, the treatment of Hodgkin lymphoma has continued to evolve, balancing cure and toxicity. This approach has resulted in low rates of relapse and death and fewer short and late toxicities from the treatments used in pursuit of cure. To achieve this balance, the field has continued to progress into an exciting era where the advent of more targeted therapies such as brentuximab vedotin, immunotherapies such as PD-1 inhibitors, and chimeric antigen receptor T-cells (CAR-T) targeted at CD30 are changing the landscape. As in the past, cooperative group and international collaborations are key to continuing to drive the science forward. Increased focus on patient-reported outcomes can further contribute to the goal of improved outcomes by examining the impact on the individual patient in the acute phase of therapy and on long-term implications for survivors. The goals of this review are to summarize recent and current clinical trials including reduction or elimination of radiation, immunotherapies and biologically-targeted agents, and discuss the use of patient-reported outcomes to help discern directions for new therapeutic regimens and more individualized evaluation of the balance of cure and toxicity.

Keywords: Hodgkin, lymphoma, patient-reported outcomes, immunotherapy, survivorship, targeted therapy, Hodgkin lymphoma (HL)

OPEN ACCESS

Edited by:
Sarah K. Tasian, Children's Hospital of Philadelphia, United States

Reviewed by:
Liora Schultz, Stanford University, United States

***Correspondence:**
Christine Moore Smith
christine.m.smith.2@vumc.org

Specialty section:
This article was submitted to Pediatric Oncology, a section of the journal Frontiers in Oncology

Received: *15 January 2022*
Accepted: *04 February 2022*
Published: *25 February 2022*

Citation:
Smith CM and Friedman DL (2022) Advances in Hodgkin Lymphoma: Including the Patient's Voice. Front. Oncol. 12:855725. doi: 10.3389/fonc.2022.855725

INTRODUCTION

Hodgkin Lymphoma (HL) is a malignant lymphoma with an impact spanning both the pediatric and adult populations. Cases occur in a bimodal distribution with peak in the adolescent and young adult (AYA) population, with varying definitions, but commonly considered to encompass the ages of 15-39 years (1–3). Within pediatrics, the incidence of HL is 12.2 per million for children under age 20, but 32 per million in ages 15-19, and highest between 20-24 years at 45 per million (4, 5).

With current treatment options, HL has a high cure rate. After the advent of successful treatment with radiotherapy (RT) and then subsequently chemotherapy, death rates from HL have declined since 1975, with an additional impressive decrease of 4% per year from 2008 to 2017. Recent data highlight excellent overall survival (OS) of 87% at 5 years across the age span and 95% for pediatric patients (1, 6). The failure rate of first-line therapies has similarly declined with 90% event free survival (EFS) in early stage disease and 80-85% EFS in advanced staged disease (7). Clinical trials have been essential in contributing to these improvements. With such high survival rates, focus over the last three decades has shifted to reducing both the acute and long-term effects of treatment while maintaining long-term EFS and OS. This focus is important as treatment of relapsed/refractory

disease requires additional exposure to toxicity through salvage regimens, RT, and potentially high dose therapy with autologous hematopoietic cell transplant (HDT/AHCT) (6).

Varied multimodal approaches to achieve these goals have been studied in clinical trials, albeit without clear consensus on the best approach. As we move forward with efficacious regimens, we continue to learn how to best incorporate, prioritize, and sequence the use of newer agents. This can be enhanced, in part, by incorporating patient-reported outcomes (PROs). This is an exciting step toward understanding the patient-level impact of regimens on EFS, OS, and tolerability of acute and long-term effects of treatment.

RISK ADAPTED THERAPY IN FRONTLINE CLINICAL TRIALS

Clinical trials in the last two decades have explored effective multiagent chemotherapy regimens for response-based risk adaptation. For patients with early responses to chemotherapy, most regimens balance curative goals with late toxicity by omitting or reducing RT. Reduction in radiation doses and fields spare normal tissues and are anticipated to decrease radiation-associated adverse long-term health effects (8). The chemotherapy backbones decreased alkylators and anthracyclines to minimize long-term adverse effects of these agents including fertility issues, secondary malignant neoplasms, and cardiotoxicity. While these have been central goals, approaches have varied somewhat in different pediatric collaborative groups including the Children's Oncology Group (COG), the St Jude-Stanford-Dana Farber Consortium, the German Paediatric Haematology-Oncology Group, and the European Network for Paediatric Hodgkin Lymphoma (EuroNet-PHL), among others. With the advent of the National Cancer Institute sponsored National Clinical Trials Network (NCTN), there is also the opportunity for further collaboration between pediatric and adult cooperative groups in the United States.

Table 1 reviews some of these more recent studies from pediatric and adult cooperative groups (9–16). The next generation of investigation builds upon these studies with incorporation of more biologically-targeted approaches.

ADVANCES IN TREATMENT WITH BRENTUXIMAB VEDOTIN

Brentuximab vedotin (Bv) is an antibody-drug conjugate that targets delivery of monomethyl auristain E to cells expressing CD30 such as the Reed Sternberg cells in classical HL.

Initially studied in the relapsed/refractory setting in ages ≥12 including adults, a study of Bv monotherapy showed efficacy with CR in 38% and some durable remissions while overall being well-tolerated (17, 18).

Pediatric and AYA regimens have combined Bv with traditional cytotoxic chemotherapy in the relapsed/refractory disease setting. For patients ≤30, COG AHOD1221 evaluated Bv with gemcitabine and reported 67% of patients achieved CR after 4 cycles when including patients meeting modern Deauville score criteria. *Ad hoc* analysis showed 1-year OS of 95% (19). Bv has also been studied with bendamustine in several trials including the pediatric and AYA populations with CR rates of 66-79% and 2 and 3-year progression free survival (PFS) of 62.6-69.8% (20–23).

In pediatrics, several studies have also incorporated Bv in frontline treatment. A single-arm trial led by the St. Jude-Stanford-Dana-Farber Consortium for ages ≤18 evaluated the safety and efficacy of Bv for high-risk patients in a backbone of A-EPA/CAPDac (Bv, etoposide, prednisone, doxorubicin, cyclophosphamide, dacarbazine). Results included 3-year EFS of 97.4%, and 35% of patients were early responders avoiding need for RT. The study highlights tolerability of Bv and effectiveness of residual node radiation (24). AHOD1331, a trial by the COG for ages 2-21, completed accrual of high-risk patients treated with a backbone of ABVE-PC (doxorubicine, bleomycin, vincristine, prednisone, cyclophosphamide) compared with Bv substitution for bleomycin. Need for involved site RT was determined by PET response. Data release and analyses are expected in the near future (25).

For frontline trials in adult patients, the ECHELON-1 trial compared the standard of ABVD (doxorubicin, bleomycin, vinblastine, dacarbazine) with A-AVD (Bv, doxorubicin, vinblastine, dacarbazine) for advanced stage disease in patients ages ≥18. The 3-year PFS was superior for A-AVD versus ABVD (83.1% versus 76%) (26, 27).

The most notable dose limiting toxicity of Bv is neuropathy which is reported subjectively by patients and has been shown to be tolerable and reversible in most trials. Reliance on the patient experience for toxicity reporting exemplifies how standardized PROs can help measure tolerability to determine which regimens best balance efficacy and toxicity (24, 27, 28).

ADVANCES IN TREATMENT WITH IMMUNE CHECKPOINT INHIBITORS

HL cells have overexpression of programmed death-1 (PD-1) ligands 1 and 2 due to alterations in the 9p24.1 locus, and PD-L1 is also expressed in tumor associated macrophages making immune checkpoint inhibitors (ICIs), specifically anti-PD-1 monoclonal antibodies, promising agents for investigation in HL (29–31). Cytotoxic T lymphocyte-associated protein 4 (CTLA-4) blockade is an alternate approach which activates peritumoral T cells to overcome T cell exhaustion in the tumor microenvironment. Ipilimumab is a monoclonal antibody targeting CTLA-4 currently being evaluated both alone and in combination as it has shown synergy with nivolumab in other cancers such as melanoma (32, 33). A number of studies first conducted among adults have demonstrated promising results in HL, and pediatric trials are now underway to ascertain if similar results can be attained in younger patients.

TABLE 1 | Recent Cooperative Group Studies.

Cooperative Group/Study	Goals	Chemotherapy and Radiotherapy	Outcomes and Notes
COG AHOD0031 (9)	Response-based risk-adaptation for reduction of RT; evaluate intensification of chemotherapy for intermediate-risk patient	ABVE-PC +/- DECA IFRT to 21 Gy based on disease at presentation if not in CR at early response assessment	EFS = 85%; OS = 97.8% For early responders, IFRT did not significantly change EFS. Chemotherapy intensification to DECA versus no DECA did not significantly change EFS for slow responders (9).
COG AHOD0431 (10)	Response-based risk-adaptation for reduction of chemotherapy and RT for low-risk patients with an integrated chemotherapy plus RT salvage regimen	*Frontline*: AVPC *Relapse*: IV + DECA IFRT to 21 Gy based on disease at presentation if not in CR at early response assessment or at relapse	If CR on FDG-PET scan (PET) after 1 cycle of chemotherapy, the 4-year EFS was 88.2% versus 68.5%. Patients with low stage mixed cellularity histology had an excellent EFS of 95.2%
COG AHOD0831 (11)	Response-based risk-adaptation for reduction of cumulative alkylators and RT in high-risk patients	ABVE-PC +/- IV IFRT to 21 Gy to initial bulky disease and sites of slow response	5-year EFS (all patients) = 79.1%; Rapid early response EFS = 83.5%; Slow early response EFS = 73.2%. EFS was below the prespecified target for the trial.
EuroNet-PHL C1 (12)	Comparison of consolidation regimens and reduction of RT; results published for intermediate and high-risk groups	OEPA + COPP vs COPDAC RT to 19.8 Gy at all initially involved tumor sites for patients with inadequate response to chemotherapy alone; additional 10 Gy boost to bulky sites or slow response	49% of intermediate and 35% of high-risk with adequate response to chemotherapy and did not have subsequent RT with 5-year EFS = 90.1%. Patients on the COPP arm had EFS of 89.9% and COPDAC 86.1%.
EuroNet-PHL C2 (13)	Evaluate intensification of chemotherapy from COPDAC-28 to DECOPDAC-21 and reduce use of RT by targeting FDG-avid sites of disease at end of chemotherapy	OEPA +/- COPDAC-28 vs DECOPDAC-21 in certain cases Randomization depending on risk group and early and late response assessments; dose ranges from 19.8 Gy to 30 Gy	Results not yet available. Notably moved toward the more modern definition of Deauville positivity of 4 and 5, which will increase the number of patients eligible for elimination of RT.
ECOG E2496 (14)	Compared chemotherapy regimens for superiority of Stanford V over ABVD	ABVD vs Stanford V RT to 36 Gy for all bulky mediastinal adenopathy; RT on Stanford V arm to 36 Gy for lesions > 5 cm or macroscopic splenic disease	No significant difference in response rate or in failure-free survival. Toxicity was reported to be similar between the two arms. The authors concluded that ABVD should remain the standard of care.
SWOG S0816 (15, 16)	Evaluate intensification of therapy if PET2 positive	ABVD +/- eBEACOPP None	PET2 was negative for 82% of patients; 5-year PFS = 76% for PET2 negative versus 66% for PET2 positive.

Recent collaborative group clinical trials with response-based risk-adjusted chemotherapy and radiotherapy (RT). ABVE-PC: doxorubicin, bleomycin, vincristine, etoposide, prednisone, cyclophosphamide; DECA: dexamethasone, etoposide, cisplatin, cytarabine; IV: vinorelbine, ifosfamide; AVPC: doxorubicin, vincristine, prednisone, cyclophosphamide; OEPA: vincristine, etoposide, prednisone, doxorubicin; COPP: cyclophosphamide, vincristine, prednisone, procarbazine; COPDAC(-28): cyclophosphamide, vincristine, prednisone, dacarbazine; DECOPDAC-21: 21 day cycle of COPDAC; ABVD: doxorubicin, bleomycin, vinblastine, dacarbazine; Stanford V: doxorubicin, vinblastine, chlormethine, vincristine, bleomycin, etoposide, prednisone; IFRT: involved field radiotherapy.

CheckMate 205 evaluated nivolumab, a PD-1 inhibitor, in several cohorts of patients ages ≥18, including relapsed/refractory disease as well as upfront with nivolumab monotherapy followed by a combination regimen of N-AVD (nivolumab, doxorubicin, vinblastine, dacarbazine). There were good overall response rates (ORR) of 71% in the relapsed/refractory cohort and 21% CR. Patients in CR had a longer median PFS (37 months) versus partial response (15 months). Upfront responses were higher with 67% achieving CR and, at time of the report, 92% PFS at a median of 9 months (31, 34–36).

KEYNOTE-087 evaluated pembrolizumab, a PD-1 inhibitor, in patients ages ≥18 with relapsed/refractory disease in multiple cohorts, with good ORR of 71.9% though only 27.6% achieved CR with a median duration of response of 16.5 months (37).

To evaluate combinations of ICIs, E4412, led by the ECOG-ACRIN Cancer Research Group, evaluated combinations of Bv with nivolumab, Bv with ipilimumab, or triplet therapy in ages ≥18 and has now expanded recruitment through the COG to include children and adolescents ≥12 with relapsed/refractory disease (38). The ipilimumab group showed 76% ORR, nivolumab 89%, and triplet therapy 82%; the PFS and OS are not yet fully reported. The triplet therapy had more adverse events than two agent combinations in the adult population, but this will remain to be seen in pediatrics and could inform which regimens are best to pursue in future trials (39, 40).

In pediatrics, the COG evaluated nivolumab as a single agent in relapsed or refractory solid tumors and lymphomas in ADVL1412 which showed 3 of 10 patients with HL, all of whom had PD-L1 expression, had responses (41).

Frontline collaborative studies now exist between pediatric and adult study groups (COG, EuroNET-PHL, NCTN, SWOG Cancer Research Network, Alliance for Clinical Trials in Oncology, ECOG-ACRIN, and NRG Oncology) to evaluate PD-1 inhibitors with chemotherapy in combined adult-pediatric populations. While open for all stages for adult patients, pediatric patients ages 3-25 can enroll on the low-risk arm of KEYNOTE-667, also known in COG as AHOD1822, evaluating the addition of pembrolizumab for patients with less than CR after 2 cycles of

ABVD (42). Led by SWOG, S1826 randomizes patients ages ≥12 with higher risk disease between A-AVD versus N-AVD (43).

As these agents are now being more widely used in both upfront and relapsed/refractory regimens, there is evidence that rechallenge with targeted agents such as Bv or ICIs can be efficacious and tolerable even if there has been progressive disease or prior dose-limiting toxicity related to the agent (39, 44, 45).

ADDITIONAL ADVANCES IN TREATMENT OF RELAPSED AND REFRACTORY DISEASE

Refractory HL occurs in up to 5-10% of cases and 10-30% of patients will experience relapse, though these numbers are lower in pediatric only trials (39). Some of the factors affecting risk stratification include time to relapse, primary refractory disease, heavy pretreatment with radiation and/or chemotherapy, extranodal disease, higher stage/risk group, anemia, and B symptoms at relapse (39). Historically, combination chemotherapy regimens were the salvage approach for relapsed and refractory disease. More information about these chemotherapy regimens can be found in reviews by Voorhees and Beaven and in the National Comprehensive Cancer Network (NCCN) Clinical Practice Guidelines for Hodgkin lymphoma and Pediatric Hodgkin lymphoma (39, 46, 47). Disease that has previously been chemotherapy responsive is a positive prognostic factor for success of such regimens for recurrent disease. However, for those with chemotherapy refractory disease, salvage regimens utilizing chemotherapy alone are likely less effective. Thus, biologically-targeted agents such Bv, ICIs, chimeric antigen receptor T-cells (CAR T), and molecular targets are exciting options for those with recurrent or refractory disease (39).

Traditionally, HDT/AHCT has been considered the standard of care for most relapsed/refractory HL. However, this approach may be challenged somewhat as new biologically-targeted agents are incorporated. The EuroNet-PHL published recommendations regarding who may benefit from HDT/AHCT versus chemotherapy/immunotherapy and/or RT alone. They propose a risk stratification based on time to relapse (primary refractory/progression, early relapse 3-12 months, or late relapse after 12 months), significant prior treatment, stage at relapse, and response to salvage therapy (7). Complete metabolic response (CMR) is also a key component for prognosis with HDT/AHCT, though this can be complicated by the use of PD-1 inhibitors that can cause FDG-avidity leading to difficulty interpreting response on PET (44). A review by Harker-Murray highlighted similar risk factors to determine the utility of HDT/AHCT (48).

A phase II study for ages ≥18 evaluated a combination of pembrolizumab with gemcitabine, vinorelbine, and liposomal doxorubicin. The regimen was efficacious in achieving CR in 95% with few toxicities allowing continuation to HDT/AHCT and maintaining remission at a median of 13.5 months (49).

In studies with combined pediatric and adult patients, targeted agents are being combined with chemotherapy. The COG study AHOD1721 evaluated Bv with nivolumab for ages 5-30. This regimen was well-tolerated with 59% in CMR after 4 cycles. For those not in CMR, 2 cycles of Bv and bendamustine were added leading to 88% of patients achieving CMR prior to consolidative therapy with HDT/AHCT off study (50, 51).

Continued maintenance therapies with or without HDT/AHCT with ICIs and Bv are another strategy with encouraging efficacy data (28, 39, 52, 53). In adults, the AETHERA trial evaluated the use of Bv in patients ages ≥18 as maintenance therapy following HDT/AHCT and demonstrated improvement in PFS (52, 53). A trial of pembrolizumab post-HDT/AHCT in patients ages 20-69 showed 82% PFS at 2 years (54). In pediatrics, Bv has also been used after HDT/AHCT in ages 16-22. Retrospective analysis showed tolerability of Bv and 100% CR in 5 patients (28).

CAR T products directed at CD30 are being evaluated for safety and efficacy with early results showing variable responses in relapsed/refractory CD30 positive lymphomas. Various co-stimulatory domains are being evaluated to improve outcomes including CD28 and CD137. Different lymphodepletion regimens affect efficacy with fludarabine leading to the best outcomes (29, 32, 45, 55, 56). A study of CD30 CAR T cells showed an encouraging ORR of 72% and CR of 59% in heavily pretreated patients ages 17-69 (57). Alternatively, CAR T directed at CD123 is under investigation given expression in 50-60% of Reed-Sternberg cells and the tumor microenvironment (29, 58, 59).

Other targeted therapies based on the biology and epidemiology of HL include JAK inhibitors, lenalidomide, everolimus, mocetinostat, panobinostat, and vorinostat (29, 58). Additionally, preclinical studies are showing the restoration of the typical B cell phenotype to retrieve CD19 expression allows for targeting by CD19 specific agents like blinatumomab or CD19 CAR T cells. Alternatively, CD20 retrieval combined with arsenic trioxide restores CD20 and allows for targeting with anti-CD20 monoclonal antibodies (29, 60).

IMPORTANCE OF PATIENT-REPORTED OUTCOMES IN FRONTLINE CARE AND SURVIVORSHIP CARE

Given the excellent disease outcomes, minimizing acute and late effects of therapy can help determine the best regimens for individual patients. Incorporation of PROs as secondary and exploratory aims in the setting of clinical trials can help inform comparison across studies based on efficacy and patient experience (61). PROs are self-reported using validated questionnaires and can encompass physical, social, and emotional impacts of disease and treatment (62). Incorporation of PRO measurement into cancer care and creation of newer tools have helped drive the field forward (61, 63–66).

Retrospectively, Johannsdottir reported 63% of Norwegian childhood lymphoma survivors treated from 1970-2000 reported psychosocial adverse health outcomes and 97% reported at least one physical adverse health outcome using the Medical Outcome Study short form-36, CTCAE version 4.0, the Hospital Anxiety and Depression Scale, and the Fatigue Questionnaire. The

majority of patients underwent combined chemotherapy and RT with a trend toward chemotherapy-only patients reporting better general health than patients undergoing combined modality or RT alone (67).

Berkman described the inclusion of PROs in phase 3 clinical trials in HL including the AYA population between 2007-2020 using the European Organization for Research and Treatment of Cancer Quality of Life Core Questionnaire (QLQ-C30). Four trials (17.4%) included PROs, but none have yet published the results (62). This is something to look forward to as studies and data mature, and, as suggested by Leblanc, we should expect PRO aims to be published with the primary results of any trial (61). The COG has endorsed and prioritized PRO inclusion in trials, demonstrating the willingness of cooperative groups to both collect and analyze the data (62).

KEYNOTE-087 reported on PROs including reports of health-related quality of life metrics as well as the response rate data showing greater than 70% of questionnaires were completed. For health-related quality of life scoring using the QLQ-C30 and the EuroQoL Five Dimensions Questionnaire, all three cohorts had similar baseline scores and improvement in both functional and symptom domains after initiation of treatment. Those with partial or complete responses had more improvement in their PRO measures than patients with stable or progressive disease (68).

There are many PRO options that can be incorporated into clinical trials, making comparisons more challenging. Standardization of PROs and comprehensive data collection can provide valuable data to assist in therapeutic decision-making for individual clinicians, individual patients, and cooperative groups planning future clinical trials. With both upfront reporting during clinical trials and follow-up in a survivorship setting, PROs can help provide a meaningful comparison of regimens regarding patient experience during and following therapy.

One example of a gap in care that could be narrowed with PROs is evaluation of psychosocial stressors. Distress in HL has been reported to exceed 30%, and recent work by Troy revealed distress levels were highest during active treatment, related to patient stress and experience of disease and therapy (65, 69). Worry and nervousness were also reported as acute psychosocial stressors (3). Addressing unmet needs as reported directly by the patient in a timely manner during therapy and in long-term follow-up can help alleviate some of the burden of the treatment experience, and these experiences may not be identified easily by other means. PROs provide standardized and validated ways to collect this data which is potentially actionable at the patient level but also by collaborative groups to better understand complications of treatment that may warrant further investigation.

The patient report of physical symptoms is also important with common symptoms being fatigue, nausea, and pain (3). Long-term health effects of HL therapy have traditionally included pulmonary fibrosis, pneumonitis, heart disease, thyroid dysfunction, chronic fatigue, neurocognitive effects, osteoporosis, and sexual dysfunction (70). Tracking of and response to patient report of these symptoms and experiences will continue to grow as a critical component of clinical trials and optimization of care. This is particularly important with regimens reducing cytotoxic chemotherapy and RT and incorporating newer agents.

With newer agents, toxicity monitoring is essential, particularly in the pediatric population. Short and long-term toxicity may differ between adult and pediatric patients. ICIs have different toxicities than traditional cytotoxic chemotherapies including autoimmune hepatitis, thyroid dysfunction, pneumonitis, colitis, rashes, fatigue, infusion reactions, pyrexia, and more rarely neurologic, renal, ocular, and pancreatic toxicity (71). Given this diverse set of toxicities, incorporation of PROs and structured follow-up of survivors can identify the prevalence and severity of adverse effects in the AYA and pediatric patient as these agents are increasingly being used.

DISCUSSION

Despite many advances, there remains lack of consensus regarding the best management of HL, and priorities differ for which strategies to evaluate next in clinical trials. Better understanding the patient experience and outcomes through collaboration, clinical trials, and the use of PROs could be an important step forward to achieve the best outcomes and therapy options.

Following patients over the last several decades allowed us to recognize the long-term health effects of curative therapeutic approaches, and subsequently long-term follow-up is essential to avoid trading one toxicity for another. Harmonization efforts for supportive care and long-term follow-up recommendations are underway and will be beneficial to provide therapy-specific and risk-adapted monitoring for toxicities and effects of therapy (2, 6, 70, 72–74). Ehrhardt makes a compelling argument to assess and consider the risk of late toxicities, converting this risk assessment into actionable data for the choice of upfront therapy (6).

Moving forward, considering toxicities in clinical decision-making, continuing to evaluate new treatments through collaborative clinical trials, and formalizing assessment of PROs can help achieve the goals to reduce toxicity and maintain high rates of cure. Continued collaborations can help standardize risk assessment, data collection, and toxicity reporting so trials can more easily be compared. This data will be invaluable when choosing a treatment for an individual patient.

DATA AVAILABILITY STATEMENT

The original contributions presented in the study are included in the article/supplementary material. Further inquiries can be directed to the corresponding author.

AUTHOR CONTRIBUTIONS

CS and DF conceptualized, drafted, reviewed, and approved the final manuscript.

REFERENCES

1. American Cancer Society. *Cancer Facts & Figures 2020*. Atlanta: American Cancer Society (2020). Available at: http://www.cancer.org/acs/groups/content/@nho/documents/document/caff2007pwsecuredpdf.pdf.
2. Flerlage JE, Metzger ML, Bhakta N. The Management of Hodgkin Lymphoma in Adolescents and Young Adults: Burden of Disease or Burden of Choice? *Blood* (2018) 132(4):376–84. doi: 10.1182/blood-2018-01-778548
3. Kahn JM, Kelly KM. Adolescent and Young Adult Hodgkin Lymphoma: Raising the Bar Through Collaborative Science and Multidisciplinary Care. *Pediatr Blood Cancer* (2018) 65(7):1–19. doi: 10.1002/pbc.27033
4. Ries L, Smith M, Gurney J, Linet M, Tamra T, Young JL, et al. *Cancer Incidence and Survival Among Children and Adolescents: United States SEER Program 1975-1995* (1999). Bethesda, MD: National Cancer Institute, SEER Program. NIH Pub. No. 9904649. Available at: https://seer.cancer.gov/archive/publications/childhood/ (Accessed January 5, 2022).
5. Howlader N, Noone A, Krapcho M, Miller D, Brest A, Yu M, et al. *Seer Cancer Statistics Review, 1975-2018*. Bethesda, MD: National Cancer Institute. Available at: https://seer.cancer.gov/csr/1975_2018/ (Accessed January 5, 2022).
6. Ehrhardt MJ, Flerlage JE, Armenian SH, Castellino SM, Hodgson DC, Hudson MM. Integration of Pediatric Hodgkin Lymphoma Treatment and Late Effects Guidelines: Seeing the Forest Beyond the Trees. *JNCCN J Natl Compr Cancer Netw* (2021) 19(6):755–64. doi: 10.6004/jnccn.2021.7042
7. Daw S, Hasenclever D, Mascarin M, Fernández-Teijeiro A, Balwierz W, Beishuizen A, et al. Risk and Response Adapted Treatment Guidelines for Managing First Relapsed and Refractory Classical Hodgkin Lymphoma in Children and Young People. Recommendations From the Euronet Pediatric Hodgkin Lymphoma Group. *HemaSphere* (2020) 4(1):e329. doi: 10.1097/HS9.0000000000000329
8. Zhou R, Ng A, Constine LS, Stovall M, Armstrong GT, Neglia JP, et al. A Comparative Evaluation of Normal Tissue Doses for Patients Receiving Radiation Therapy for Hodgkin Lymphoma on the Childhood Cancer Survivor Study and Recent Children's Oncology Group Trials. *Int J Radiat Oncol Biol Phys* (2016) 95(2):707–11. doi: 10.1016/J.IJROBP.2016.01.053
9. Friedman DL, Chen L, Wolden S, Buxton A, McCarten K, FitzGerald TJ, et al. Dose-Intensive Response-Based Chemotherapy and Radiation Therapy for Children and Adolescents With Newly Diagnosed Intermediate-Risk Hodgkin Lymphoma: A Report From the Children's Oncology Group Study AHOD0031. *J Clin Oncol* (2014) 32(32):3651–8. doi: 10.1200/JCO.2013.52.5410
10. Keller FG, Castellino SM, Chen L, Pei Q, Voss SD, McCarten KM, et al. Results of the AHOD0431 Trial of Response Adapted Therapy and a Salvage Strategy for Limited Stage, Classical Hodgkin Lymphoma: A Report From the Children's Oncology Group. *Cancer* (2018) 124(15):3210–9. doi: 10.1002/CNCR.31519
11. Kelly KM, Cole PD, Pei Q, Bush R, Roberts KB, Hodgson DC, et al. Response-Adapted Therapy for the Treatment of Children With Newly Diagnosed High Risk Hodgkin Lymphoma (AHOD0831): A Report From the Children's Oncology Group. *Br J Haematol* (2019) 187(1):39–48. doi: 10.1111/bjh.16014
12. Mauz-Körholz C, Landman-Parker J, Balwierz W, Ammann RA, Anderson RA, Attarbaschi A, et al. Response-Adapted Omission of Radiotherapy and Comparison of Consolidation Chemotherapy in Children and Adolescents With Intermediate-Stage and Advanced-Stage Classical Hodgkin Lymphoma (Euronet-PHL-C1): A Titration Study With an Open-Label, Embedded, Multinational, non-Inferiority, Randomised Controlled Trial. *Lancet Oncol* (2022) 23(1):125–37. doi: 10.1016/S1470-2045(21)00470-8
13. Mauz-Körholz C, Metzger ML, Kelly KM, Schwartz CL, Castellanos M, Dieckmann K, et al. Pediatric Hodgkin Lymphoma. *J Clin Oncol* (2015) 33(27):2975–85. doi: 10.1200/JCO.2014.59.4853
14. Gordon LI, Hong F, Fisher RI, Bartlett NL, Connors JM, Gascoyne RD, et al. Randomized Phase III Trial of ABVD Versus Stanford V With or Without Radiation Therapy in Locally Extensive and Advanced-Stage Hodgkin Lymphoma: An Intergroup Study Coordinated by the Eastern Cooperative Oncology Group (E2496). *J Clin Oncol* (2013) 31(6):684. doi: 10.1200/JCO.2012.43.4803
15. Stephens DM, Li H, Schöder H, Straus DJ, Moskowitz CH, LeBlanc M, et al. Five-Year Follow-Up of SWOG S0816: Limitations and Values of a PET-Adapted Approach With Stage III/IV Hodgkin Lymphoma. *Blood* (2019) 134(15):1238–46. doi: 10.1182/blood.2019000719
16. Press OW, Li H, Schöder H, Straus DJ, Moskowitz CH, LeBlanc M, et al. US Intergroup Trial of Response-Adapted Therapy for Stage III to IV Hodgkin Lymphoma Using Early Interim Fluorodeoxyglucose-Positron Emission Tomography Imaging: Southwest Oncology Group S0816. *J Clin Oncol* (2016) 34(17):2020–7. doi: 10.1200/JCO.2015.63.1119
17. Gopal AK, Chen R, Smith SE, Ansell SM, Rosenblatt JD, Savage KJ, et al. Durable Remissions in a Pivotal Phase 2 Study of Brentuximab Vedotin in Relapsed or Refractory Hodgkin Lymphoma. *Blood* (2015) 125(8):1236–43. doi: 10.1182/BLOOD-2014-08-595801
18. Chen R, Gopal AK, Smith SE, Ansell SM, Rosenblatt JD, Savage KJ, et al. Five-Year Survival and Durability Results of Brentuximab Vedotin in Patients With Relapsed or Refractory Hodgkin Lymphoma. *Blood* (2016) 128(12):1562–6. doi: 10.1182/BLOOD-2016-02-699850
19. Cole PD, McCarten KM, Pei Q, Spira M, Metzger ML, Drachtman RA, et al. Brentuximab Vedotin With Gemcitabine for Paediatric and Young Adult Patients With Relapsed or Refractory Hodgkin's Lymphoma (AHOD1221): A Children's Oncology Group, Multicentre Single-Arm, Phase 1–2 Trial. *Lancet Oncol* (2018) 19(9):1229–38. doi: 10.1016/S1470-2045(18)30426-1
20. LaCasce AS, Gregory Bociek R, Sawas A, Caimi P, Agura E, Matous J, et al. Brentuximab Vedotin Plus Bendamustine: A Highly Active First Salvage Regimen for Relapsed or Refractory Hodgkin Lymphoma. *Blood* (2018) 132(1):40–8. doi: 10.1182/BLOOD-2017-11-815183
21. Broccoli A, Argnani L, Botto B, Corradini P, Pinto A, Re A, et al. First Salvage Treatment With Bendamustine and Brentuximab Vedotin in Hodgkin Lymphoma: A Phase 2 Study of the Fondazione Italiana Linfomi. *Blood Cancer J* (2019) 9(12):1–8. doi: 10.1038/s41408-019-0265-x
22. Forlenza CJ, Gulati N, Mauguen A, Absalon MJ, Castellino SM, Franklin A, et al. Combination Brentuximab Vedotin and Bendamustine for Pediatric Patients With Relapsed/Refractory Hodgkin Lymphoma. *Blood Adv* (2021) 5(24):5519–24. doi: 10.1182/BLOODADVANCES.2021005268
23. O'Connor OA, Lue JK, Sawas A, Amengual JE, Deng C, Kalac M, et al. Brentuximab Vedotin Plus Bendamustine in Relapsed or Refractory Hodgkin's Lymphoma: An International, Multicentre, Single-Arm, Phase 1–2 Trial. *Lancet Oncol* (2018) 19(2):257–66. doi: 10.1016/S1470-2045(17)30912-9
24. Metzger ML, Link MP, Billett AL, Flerlage J, Lucas JT, Mandrell BN, et al. Excellent Outcome for Pediatric Patients With High-Risk Hodgkin Lymphoma Treated With Brentuximab Vedotin and Risk-Adapted Residual Node Radiation. *J Clin Oncol* (2021) 39(20):2276–83. doi: 10.1200/jco.20.03286
25. *Brentuximab Vedotin and Combination Chemotherapy in Treating Children and Young Adults With Stage IIB or Stage IIIB-IVB Hodgkin Lymphoma. Clinicaltrials.Gov Identifier: NCT02166463*. Available at: https://www.clinicaltrials.gov/ct2/show/NCT02166463 (Accessed January 2, 2022).
26. Connors JM, Jurczak W, Straus DJ, Ansell SM, Kim WS, Gallamini A, et al. Brentuximab Vedotin With Chemotherapy for Stage III or IV Hodgkin's Lymphoma. *N Engl J Med* (2018) 378(4):331–44. doi: 10.1056/NEJMoa1708984
27. Straus DJ, Długosz-Danecka M, Alekseev S, Illés Á, Picardi M, Lech-Maranda E, et al. Brentuximab Vedotin With Chemotherapy for Stage III/IV Classical Hodgkin Lymphoma: 3-Year Update of the ECHELON-1 Study. *Blood* (2020) 135(10):735–42. doi: 10.1182/BLOOD.2019003127
28. Flerlage JE, von Buttlar X, Krasin M, Triplett B, Kaste SC, Metzger ML. Brentuximab Vedotin as Consolidation After Hematopoietic Cell Transplant for Relapsed Hodgkin Lymphoma in Pediatric Patients. *Pediatr Blood Cancer* (2019) 66(12):1–2. doi: 10.1002/pbc.27962
29. Mottok A, Steidl C. Biology of Classical Hodgkin Lymphoma: Implications for Prognosis and Novel Therapies. *Blood* (2018) 131(15):1654–65. doi: 10.1182/blood-2017-09-772632
30. Chen R, Zinzani PL, Lee HJ, Armand P, Johnson NA, Brice P, et al. Pembrolizumab in Relapsed or Refractory Hodgkin Lymphoma: 2-Year Follow-Up of KEYNOTE-087. *Blood* (2019) 134(14):1144–53. doi: 10.1182/blood.2019000324
31. Ramchandren R, Domingo-Domènech E, Rueda A, Trněný M, Feldman TA, Lee HJ, et al. Nivolumab for Newly Diagnosed Advanced-Stage Classic

Hodgkin Lymphoma: Safety and Efficacy in the Phase II Checkmate 205 Study. *J Clin Oncol* (2019) 37(23):1997–2007. doi: 10.1200/JCO.19.00315
32. Matsuki E, Younes A. Checkpoint Inhibitors and Other Immune Therapies for Hodgkin and Non-Hodgkin Lymphoma. *Curr Treat Options Oncol* (2016) 17(6):31. doi: 10.1007/S11864-016-0401-9
33. Diefenbach CS, Hong F, Ambinder RF, Cohen JB, Robertson MJ, David KA, et al. Ipilimumab, Nivolumab, and Brentuximab Vedotin Combination Therapies in Patients With Relapsed or Refractory Hodgkin Lymphoma: Phase 1 Results of an Open-Label, Multicentre, Phase 1/2 Trial. *Artic Lancet Haematol* (2020) 7:660–70. doi: 10.1016/S2352-3026(20)30221-0
34. Armand P, Engert A, Younes A, Fanale M, Santoro A, Zinzani PL, et al. Nivolumab for Relapsed/Refractory Classic Hodgkin Lymphoma After Failure of Autologous Hematopoietic Cell Transplantation: Extended Follow-Up of the Multicohort Single-Arm Phase II Checkmate 205 Trial. *J Clin Oncol* (2018) 36(14):1428–39. doi: 10.1200/JCO.2017.76.0793
35. Ansell SM, Bröckelmann PJ, Keudell G, Lee HJ, Santoro A, Zinzani PL, et al. Nivolumab for Relapsed or Refractory (R/R) Classical Hodgkin Lymphoma (CHL) After Autologous Transplantation: 5-Year Overall Survival From the Phase 2 Checkmate 205 Study. *Hematol Oncol* (2021) 39(S2):122–5. doi: 10.1002/HON.74_2879
36. Younes A, Santoro A, Shipp M, Zinzani PL, Timmerman JM, Ansell S, et al. Nivolumab for Classical Hodgkin's Lymphoma After Failure of Both Autologous Stem-Cell Transplantation and Brentuximab Vedotin: A Multicentre, Multicohort, Single-Arm Phase 2 Trial. *Lancet Oncol* (2016) 17 (9):1283–94. doi: 10.1016/S1470-2045(16)30167-X
37. Chen R, Zinzani PL, Fanale MA, Armand P, Johnson NA, Brice P, et al. Phase II Study of the Efficacy and Safety of Pembrolizumab for Relapsed/Refractory Classic Hodgkin Lymphoma. *J Clin Oncol* (2017) 35(19):2125–32. doi: 10.1200/JCO.2016.72.1316
38. *Brentuximab Vedotin and Nivolumab With or Without Ipilimumab in Treating Patients With Relapsed or Refractory Hodgkin Lymphoma. Clinicaltrials.Gov Identifier: NCT01896999*. Available at: https://clinicaltrials.gov/ct2/show/NCT01896999 (Accessed January 6, 2022).
39. Voorhees TJ, Beaven AW. Therapeutic Updates for Relapsed and Refractory Classical Hodgkin Lymphoma. *Cancers (Basel)* (2020) 12(10):2887. doi: 10.3390/cancers12102887
40. Diefenbach C, Hong F, Ambinder RF, Cohen JB, Robertson M, David KA, et al. A Phase I Study With an Expansion Cohort of the Combinations of Ipilimumab, Nivolumab and Brentuximab Vedotin in Patients With Relapsed/Refractory Hodgkin Lymphoma: A Trial of the ECOG-ACRIN Research Group (E4412: Arms G-I). *Blood* (2018) 132(Supplement 1):679–9. doi: 10.1182/BLOOD-2018-99-115390
41. Davis KL, Fox E, Merchant MS, Reid JM, Kudgus RA, Liu X, et al. Nivolumab in Children and Young Adults With Relapsed or Refractory Solid Tumours or Lymphoma (ADVL1412): A Multicentre, Open-Label, Single-Arm, Phase 1-2 Trial. *Lancet Oncol* (2020) 21(4):541–50. doi: 10.1016/S1470-2045(20)30023-1
42. *Safety and Efficacy of Pembrolizumab (MK-3475) in Children and Young Adults With Classical Hodgkin Lymphoma (MK-3475-667/KEYNOTE-667). Clinicaltrials.Gov Identifier: NCT03407144*. Available at: https://clinicaltrials.gov/ct2/show/NCT03407144 (Accessed January 6, 2022).
43. *Immunotherapy (Nivolumab or Brentuximab Vedotin) Plus Combination Chemotherapy in Treating Patients With Newly Diagnosed Stage III-IV Classic Hodgkin Lymphoma. Clinicaltrials.Gov Identifier: NCT03907488*. Available at: https://www.clinicaltrials.gov/ct2/show/NCT03907488 (Accessed January 6, 2022).
44. Moskowitz AJ, Herrera AF, Beaven AW. Relapsed and Refractory Classical Hodgkin Lymphoma: Keeping Pace With Novel Agents and New Options for Salvage Therapy. *Am Soc Clin Oncol Educ B* (2019) 39):477–86. doi: 10.1200/edbk_238799
45. Othman T, Herrera A, Mei M. Emerging Therapies in Relapsed and Refractory Hodgkin Lymphoma: What Comes Next After Brentuximab Vedotin and PD-1 Inhibition? *Curr Hematol Malig Rep* (2021) 16(1):1–7. doi: 10.1007/S11899-020-00603-3
46. NCCN Guidelines, Hoppe RT, Advani RH, Ai WZ. *NCCN Clinical Practice Guidelines in Oncology: Hodgkin Lymphoma. Version 1.2022*. Available at: www.nccn.org (Accessed January 4, 2022).
47. Guidelines NCCN, Flerlage JE, SM H, Armenian S. *NCCN Clinical Practice Guidelines in Oncology: Pediatric Hodgkin Lymphoma. Version 3.2021*. Available at: www.nccn.org (Accessed January 4, 2022).
48. Harker-Murray PD, Drachtman RA, Hodgson DC, Chauvenet AR, Kelly KM, Cole PD. Stratification of Treatment Intensity in Relapsed Pediatric Hodgkin Lymphoma. *Pediatr Blood Cancer* (2014) 61(4):579–86. doi: 10.1002/pbc.24851
49. Moskowitz AJ, Shah G, Schöder H, Ganesan N, Drill E, Hancock H, et al. Phase II Trial of Pembrolizumab Plus Gemcitabine, Vinorelbine, and Liposomal Doxorubicin as Second-Line Therapy for Relapsed or Refractory Classical Hodgkin Lymphoma. *J Clin Oncol* (2021) 39(28):3109–17. doi: 10.1200/jco.21.01056
50. Harker-Murray P, Leblanc T, Mascarin M, Mauz-Körholz C, Michel G, Cooper S, et al. Response-Adapted Therapy With Nivolumab and Brentuximab Vedotin (BV), Followed by BV and Bendamustine for Suboptimal Response, in Children, Adolescents, and Young Adults With Standard-Risk Relapsed/Refractory Classical Hodgkin Lymphoma. *Blood* (2018) 132(Supplement 1):927. doi: 10.1182/BLOOD-2018-99-111279
51. Cole PD, Mauz-Körholz C, Mascarin M, Michel G, Cooper S, Beishuizen A, et al. Nivolumab and Brentuximab Vedotin (BV)-Based, Response-Adapted Treatment in Children, Adolescents, and Young Adults (CAYA) With Standard-Risk Relapsed/Refractory Classical Hodgkin Lymphoma (R/R Chl): Primary Analysis. *J Clin Oncol* (2020) 38(15_suppl):8013–3. doi: 10.1200/JCO.2020.38.15_SUPPL.8013
52. Moskowitz CH, Nademanee A, Masszi T, Agura E, Holowiecki J, Abidi MH, et al. Brentuximab Vedotin as Consolidation Therapy After Autologous Stem-Cell Transplantation in Patients With Hodgkin's Lymphoma at Risk of Relapse or Progression (AETHERA): A Randomised, Double-Blind, Placebo-Controlled, Phase 3 Trial. *Lancet* (2015) 385(9980):1853–62. doi: 10.1016/S0140-6736(15)60165-9
53. Moskowitz CH, Walewski J, Nademanee A, Masszi T, Agura E, Holowiecki J, et al. Five-Year PFS From the AETHERA Trial of Brentuximab Vedotin for Hodgkin Lymphoma at High Risk of Progression or Relapse. *Blood* (2018) 132 (25):2639–42. doi: 10.1182/blood-2018-07-861641
54. Armand P, Chen YB, Redd RA, Joyce RM, Bsat J, Jeter E, et al. PD-1 Blockade With Pembrolizumab for Classical Hodgkin Lymphoma After Autologous Stem Cell Transplantation. *Blood* (2019) 134(1):22–9. doi: 10.1182/BLOOD.2019000215
55. Brice P, de Kerviler E, Friedberg JW. Classical Hodgkin Lymphoma. *Lancet* (2021) 398(10310):1518–27. doi: 10.1016/S0140-6736(20)32207-8
56. Dahi PB, Moskowitz CH, Giralt SA, Lazarus HM. Novel Agents Positively Impact Chemotherapy and Transplantation in Hodgkin Lymphoma. *Expert Rev Hematol* (2019) 12(4):255–64. doi: 10.1080/17474086.2019.1593135
57. Ramos CA, Grover NS, Beaven AW, Lulla PD, Wu MF, Ivanova A, et al. Anti-CD30 CAR-T Cell Therapy in Relapsed and Refractory Hodgkin Lymphoma. *J Clin Oncol* (2020) 38(32):3794–804. doi: 10.1200/JCO.20.01342
58. Mehta-Shah N, Bartlett NL. Management of Relapsed/Refractory Classical Hodgkin Lymphoma in Transplant-Ineligible Patients. *Blood* (2018) 131 (15):1698–703. doi: 10.1182/blood-2017-09-772681
59. Ruella M, Klichinsky M, Kenderian SS, Shestova O, Ziober A, Kraft DO, et al. Overcoming the Immunosuppressive Tumor Microenvironment of Hodgkin Lymphoma Using Chimeric Antigen Receptor T Cells. *Cancer Discov* (2017) 7 (10):1154–67. doi: 10.1158/2159-8290.CD-16-0850
60. Du J, Neuenschwander M, Yu Y, Däbritz JH, Neuendorff NR, Schleich K, et al. Pharmacological Restoration and Therapeutic Targeting of the B-Cell Phenotype in Classical Hodgkin Lymphoma. *Blood* (2017) 129(1):71–81. doi: 10.1182/BLOOD-2016-02-700773
61. Leblanc TW. Experts on Their Own Experiences: The Rise of Patient-Reported Outcomes in Oncology Drug Trials. *Leuk Lymphoma* (2019) 60 (11):2604–5. doi: 10.1080/10428194.2019.1632446
62. Berkman AM, Murphy KM, Siembida EJ, Lau N, Geng Y, Parsons SK, et al. Inclusion of Patient-Reported Outcomes in Adolescent and Young Adult Phase III Therapeutic Trials: An Analysis of Cancer Clinical Trials Registered on Clinicaltrials.Gov. *Value Health* (2021) 24(12):1820–7. doi: 10.1016/j.jval.2021.06.012
63. Basch E. Patient-Reported Outcomes — Harnessing Patients' Voices to Improve Clinical Care. *N Engl J Med* (2017) 376(2):105–8. doi: 10.1056/nejmp1611252
64. Basch E, Barbera L, Kerrigan CL, Velikova G. Implementation of Patient-Reported Outcomes in Routine Medical Care. *Am Soc Clin Oncol Educ B* (2018) 38):122–34. doi: 10.1200/edbk_200383

65. Tarnasky AM, Troy JD, Leblanc TW. The Patient Experience of ABVD Treatment in Hodgkin Lymphoma : A Retrospective Cohort Study of Patient-Reported Distress. *Support Care Cancer* (2021) 29(9):4987–96. doi: 10.1007/s00520-021-06044-9
66. LeBlanc TW, Abernethy AP. Patient-Reported Outcomes in Cancer Care — Hearing the Patient Voice at Greater Volume. *Nat Rev Clin Oncol* (2017) 14 (12):763–72. doi: 10.1038/nrclinonc.2017.153
67. Johannsdottir IMR, Hamre H, Fossa SD, Loge JH, Drolsum L, Lund MB, et al. Adverse Health Outcomes and Associations With Self-Reported General Health in Childhood Lymphoma Survivors. *J Adolesc Young Adult Oncol* (2017) 6(3):470–6. doi: 10.1089/jayao.2017.0018
68. von Tresckow B, Fanale M, Ardeshna KM, Chen R, Meissner J, Morschhauser F, et al. Patient-Reported Outcomes in KEYNOTE-087, a Phase 2 Study of Pembrolizumab in Patients With Classical Hodgkin Lymphoma. *Leuk Lymphoma* (2019) 60(11):2705–11. doi: 10.1080/10428194.2019.1602262
69. Troy JD, Locke SC, Samsa GP, Feliciano J, Richhariya A, Leblanc TW. Patient-Reported Distress in Hodgkin Lymphoma Across the Survivorship Continuum. *Support Care Cancer* (2019) 27:2453–62. doi: 10.1007/s00520-018-4523-4
70. Frick MA, Vachani CC, Hampshire MK, Bach C, Arnold-Korzeniowski K, Metz JM, et al. Patient-Reported Survivorship Care Practices and Late Effects After Treatment of Hodgkin and non-Hodgkin Lymphoma. *JCO Clin Cancer Inform* (2018) 2):1–10. doi: 10.1200/cci.18.00015
71. Naidoo J, Page DB, Li BT, Connell LC, Schindler K, Lacouture ME, et al. Toxicities of the Anti-PD-1 and Anti-PD-L1 Immune Checkpoint Antibodies. *Ann Oncol Off J Eur Soc Med Oncol* (2015) 26(12):2375–91. doi: 10.1093/ANNONC/MDV383
72. Landier W, Bhatia S, Eshelman DA, Forte KJ, Sweeney T, Hester AL, et al. Development of Risk-Based Guidelines for Pediatric Cancer Survivors: The Children's Oncology Group Long-Term Follow-Up Guidelines From the Children's Oncology Group Late Effects Committee and Nursing Discipline. *J Clin Oncol* (2004) 22(24):4979–90. doi: 10.1200/JCO.2004.11.032
73. Kremer LC, Mulder RL, Oeffinger KC, Bhatia S, Landier W, Levitt G, et al. A Worldwide Collaboration to Harmonize Guidelines for the Long-Term Follow-Up of Childhood and Young Adult Cancer Survivors: A Report From the International Late Effects of Childhood Cancer Guideline Harmonization Group. *Pediatr Blood Cancer* (2013) 60(4):543–9. doi: 10.1002/PBC.24445
74. Bhatia S, Armenian SH, Armstrong GT, van Dulmen-den Broeder E, Hawkins MM, Kremer LC, et al. Collaborative Research in Childhood Cancer Survivorship: The Current Landscape. *J Clin Oncol* (2015) 33(27):3055. doi: 10.1200/JCO.2014.59.8052

Conflict of Interest: The authors declare that the research was conducted in the absence of any commercial or financial relationships that could be construed as a potential conflict of interest.

frontiers in Oncology

ORIGINAL RESEARCH
published: 09 March 2022
doi: 10.3389/fonc.2022.845540

Infectious Complications in Pediatric, Adolescent and Young Adult Patients Undergoing CD19-CAR T Cell Therapy

Gabriela M. Maron[1†], Diego R. Hijano[1†], Rebecca Epperly[2], Yin Su[3], Li Tang[3], Randall T. Hayden[4], Swati Naik[2], Seth E. Karol[5], Stephen Gottschalk[2], Brandon M. Triplett[2] and Aimee C. Talleur[2*]*

[1] Department of Infectious Diseases, St. Jude Children's Research Hospital, Memphis, TN, United States, [2] Department of Bone Marrow Transplantation and Cellular Therapy, St. Jude Children's Research Hospital, Memphis, TN, United States, [3] Department of Biostatistics, St. Jude Children's Research Hospital, Memphis, TN, United States, [4] Department of Pathology, St. Jude Children's Research Hospital, Memphis, TN, United States, [5] Department of Oncology, St. Jude Children's Research Hospital, Memphis, TN, United States

OPEN ACCESS

Edited by:
Sarah K. Tasian,
Children's Hospital of Philadelphia, United States

Reviewed by:
Yi Luo,
Zhejiang University, China
Muhammad Bilal Abid,
Medical College of Wisconsin, United States

***Correspondence:**
Gabriela M. Maron
Gabriela.maron@stjude.org
Aimee C. Talleur
Aimee.Talleur@stjude.org

[†]These authors have contributed equally to this work and share first authorship

Specialty section:
This article was submitted to Pediatric Oncology, a section of the journal Frontiers in Oncology

Received: 29 December 2021
Accepted: 04 February 2022
Published: 09 March 2022

Citation:
Maron GM, Hijano DR, Epperly R, Su Y, Tang L, Hayden RT, Naik S, Karol SE, Gottschalk S, Triplett BM and Talleur AC (2022) Infectious Complications in Pediatric, Adolescent and Young Adult Patients Undergoing CD19-CAR T Cell Therapy. Front. Oncol. 12:845540. doi: 10.3389/fonc.2022.845540

CD19-specific chimeric antigen receptor (CAR) T cell therapy has changed the treatment paradigm for pediatric, adolescent and young adult (AYA) patients with relapsed/refractory B-cell acute lymphoblastic leukemia (B-ALL). However, data on the associated infectious disease challenges in this patient population are scarce. Knowledge of infections presenting during treatment, and associated risk factors, is critical for pediatric cellular therapy and infectious disease specialists as we seek to formulate effective anti-infective prophylaxis, infection monitoring schemas, and empiric therapy regimens. In this work we describe our institutional experience in a cohort of 38 pediatric and AYA patients with CD19-positive malignancy treated with lymphodepleting chemotherapy (fludarabine/cyclophosphamide) followed by a single infusion of CD19-CAR T cells (total infusions, n=39), including tisagenlecleucel (n=19; CD19/4-1BB) or on an institutional clinical trial (n=20; CD19/4-1BB; NCT03573700). We demonstrate that infections were common in the 90 days post CAR T cells, with 19 (50%) patients experiencing a total of 35 infections. Most of these (73.7%) occurred early post infusion (day 0 to 28; infection density of 2.36 per 100 patient days-at-risk) compared to late post infusion (day 29 to 90; infection density 0.98 per 100 patient days-at-risk), respectively. Bacterial infections were more frequent early after CAR T cell therapy, with a predominance of bacterial blood stream infections. Viral infections occurred throughout the post infusion period and included primarily systemic reactivations and gastrointestinal pathogens. Fungal infections were rare. Pre-infusion disease burden, intensity of bridging chemotherapy, lymphopenia post lymphodepleting chemotherapy/CAR T cell infusion and development of CAR-associated hemophagocytic lymphohistiocytosis (carHLH) were all significantly associated with either infection density or time to first infection post CAR T cell infusion. A subset of patients (n=6) had subsequent CAR T cell reinfusion and did not appear to have increased risk of infectious complications. Our experience highlights the risk of infections after CD19-CAR T cell therapy, and the need

for continued investigation of infectious outcomes as we seek to improve surveillance, prophylaxis and treatment algorithms.

Keywords: chimeric antigen receptor (CAR T), infection, immunotherapy, pediatric oncology, B-cell leukemia

INTRODUCTION

CD19-targeted chimeric antigen receptor (CAR) T cell therapy has provided impressive initial response rates for pediatric and adolescent and young adult (AYA) patients with relapsed/refractory B-cell acute lymphoblastic leukemia (B-ALL) (1–5). However, with growing clinical experience, management and prevention of infectious complications have emerged as key challenges in this population (6). Prior to receiving CD19-CAR T cell therapy, patients have several potential risks factors for infection, including recent intensive therapy, active malignancy, presence of a central venous catheter, and prolonged cytopenias. These are compounded by i) receipt of lymphodepleting chemotherapy prior to CAR T cell infusion, ii) CAR T cell associated inflammation and immune mediated side effects, iii) exposure to immunomodulatory agents to treat CAR T cell-related toxicities (including high-dose corticosteroids and anti-cytokine therapies), and/or iv) anticipated on-target off-tumor effects, such as B cell aplasia (BCA) (7–11).

CD19-CAR T cell therapy studies in pediatric and AYA patients have reported infections in 36-58% of patients, with approximately 20% of patients experiencing grade 3-4 infections (4, 5, 12). In studies of adult patients, severity of cytokine release syndrome (CRS), higher doses of CAR T cells and receipt of multiple prior treatment regimens were associated with increased risk of infections (6, 10, 11, 13). CRS has also been associated with increased infectious risk in pediatric patients in the first month after infusion (6, 14), in part due to receipt of immunosuppressive medications such as corticosteroids and anti-cytokine therapies to treat CAR T cell side effects. Additionally, pediatric patients with a prior history of allogeneic hematopoietic cell transplant (AlloHCT) or immunoglobulin G (IgG) levels <400mg/dL have also been associated with increased risk of infection (14). Immune reconstitution and recovery of bone marrow function have also been identified as important factors in mitigating infections after CAR T cell therapy, though limited information is available in the pediatric setting (8, 15, 16).

Enhancing our understanding of the predictive risk factors, characteristics, timing, and duration of infections in patients receiving CD19-CAR T cells is key in guiding infectious surveillance, treatment, and prophylaxis. Here we report our institutional infectious disease experience in pediatric and AYA patients receiving CD19-CAR T cells. We describe the infectious complications experienced in this cohort and evaluate potential risk factors associated with infection.

MATERIALS AND METHODS

This is a retrospective review of patients (n=38) with relapsed and/or refractory CD19-positive malignancy who received lymphodepleting chemotherapy followed by infusion of a CD19-CAR T cell product (tisagenlecleucel or an institutional product [NCT03573700]; total infusions, n=39) at St. Jude Children's Research Hospital (St. Jude) between October 2018 – August 2021. Additionally, a subset of patients (n=6) received repeat CD19-CAR T cell infusion(s) of the same product due to recurrent malignancy or early loss of BCA. This retrospective project was approved by the St. Jude institutional review board. Written informed consent/assent was obtained from all patients and/or legal guardians to receive treatment with lymphodepletion and CAR T cell therapy, in accordance with institutional guidelines and the Declaration on Helsinki. Both CD19-CAR T cell products utilize a FMC63 svFc and 4-1BB costimulatory domain. Demographic, clinical, laboratory and treatment related data were collected from both a prospective clinical database and retrospective review of the medical record. Data was divided into three time periods: pre-CAR T cells (day -30 to day 0), early post CAR T cells (day 1 to day 28 post infusion) and late post CAR T cells (day 29 to day 90 post infusion).

Pre-CAR T Cell Infusion Variables (Day -30 to Day 0)

Patient demographics and indications for CAR T cell therapy were recorded. Prior treatment data included receipt of antigen directed therapy (CD19-CAR T cells, blinatumomab, and/or inotuzumab), prior AlloHCT and details of bridging therapy. Bridging therapy was given at the discretion of the treating provider. For this study, bridging therapy was categorized as low or high intensity. Low intensity regimens included no systemic treatment (n=5), focal radiation therapy (n=3) or receipt of systemic chemotherapy agents used during continuation/maintenance therapy for newly diagnosed B-ALL (n=14) (17). High intensity included treatment with agents not included in the low intensity definition. All available absolute neutrophil count (ANC), absolute lymphocyte count (ALC) values and IgG levels were documented. For this study, neutropenia was defined as ANC <500 cells/mm^3 and lymphopenia as ALC <300 cells/mm^3. Disease burden included morphologic blast percent from the most recent bone marrow sample, obtained post bridging therapy, when applicable, and prior to CAR T cell treatment.

CAR T Cell Infusion Related Variables

Lymphodepletion agents and dosages were recorded. All patients received a regimen containing fludarabine (Flu) and cyclophosphamide (Cy). Patients treated on trial all received Flu/Cy (cumulative doses: 75mg/m^2 and 900mg/m^2), while patients treated with tisagenlecleucel received Flu/Cy (cumulative doses: 120mg/m^2 and 1000mg/m^2, or 75mg/m^2 and 900mg/m^2) or Flu/Cy (cumulative doses: 75mg/m^2 and 900mg/m^2) with an additional agent (etoposide 500mg/m^2 or

cytarabine cumulative dose, 4000mg). Presence and severity of CAR T cell related immune side effects [CRS, neurotoxicity and CAR-associated hemophagocytic lymphohistiocytosis (carHLH) (18)] were documented, as well as receipt of immunomodulating agents (steroids, tocilizumab, siltuximab, anakinra, and/or ruxolitinib). Available post treatment ANC, ALC and IgG results were collected for up to 90 days post infusion.

Anti-Infective Prophylaxis and Infection Surveillance Post CAR T Cell Therapy

Our infection prophylaxis approach is shown in **Supplemental Table 1**. Patients received anti-infective prophylaxis for prevention of *Pneumocystis jirovecii* pneumonia (trimethoprim-sulfamethoxazole [TMP-SMX], pentamidine or atovaquone), Herpes simplex virus (HSV) for patients with positive serology or prior history of recurrent episodes of HSV infection (acyclovir or valacyclovir), and fungal disease (echinocandin during lymphodepletion, followed by an azole). Patients receiving antiviral treatment for systemic reactivation prior to CAR T cell therapy remained on the same agent (foscarnet, ganciclovir, or valganciclovir). Antiviral prophylaxis continued until 30 days post CAR T cell infusion. Antifungal prophylaxis continued for at least 30 days post infusion or until evidence of neutrophil recovery (ANC ≥ 500 for 3 consecutive measurements), whichever was longer. Patients did not receive antibacterial prophylaxis post CAR T cell infusion. Patients underwent weekly testing for cytomegalovirus (CMV), Epstein-Barr virus (EBV) and Adenovirus (ADV) by PCR in blood, as well as Aspergillus antigen. All patients had central lines at the time of CAR T cell therapy.

Definitions of Infections

Infections for which microbiology or histopathology confirmation was available were included in this study. A patient could contribute with one or more infectious episodes. Infection data was collected for the pre- and post-CAR T cell infusion periods.

Blood stream infections (BSI) were defined according to CDC criteria (19). BSIs counted as separate episodes if there was a period of at least 14 days between positive cultures, or if a different organism was identified. Polymicrobial BSI was defined as the detection of different organisms on the first day of a BSI episode. *Clostridiodes difficile* associated diarrhea (CDAD) was included in patients with gastrointestinal symptoms and identification of toxin-producing *C. difficile* by PCR. For infections in other sites, those with compatible symptoms and positive cultures were included.

Systemic viral reactivation was defined as a positive PCR result in blood above the level of detection, irrespective of the presence of symptoms. ADV colitis was reported in patients with gastrointestinal symptoms and a positive quantitative stool PCR. Respiratory viral infections included detection of a virus in a nasopharyngeal sample using the The BioFire® Respiratory 2.1 Panel, in a symptomatic patient. If more than one respiratory virus was detected in the same sample, this was counted as one episode. BK virus infection was reported in patients with hematuria and positive viral PCR in urine or blood.

Patients meeting clinical, laboratory and/or imaging criteria for invasive fungal infection (IFI) according to the European Organization for Research and Treatment of Cancer/Invasive Fungal Infections Cooperative Group and the National Institute of Allergy and Infectious Diseases Mycoses Study Group EORTC/MSG consortium definitions were included (20).

Management of Infections

Central line and peripheral blood cultures were attempted in all patients with fever, and empiric broad spectrum antibiotic therapy started. Antibiotic therapy was tailored to microbiology results as necessary. If no infectious source was identified, patients received an empiric course of broad-spectrum antibiotic (4^{th} generation cephalosporin) according to institutional guidelines. Systemic viral reactivations were monitored weekly, and therapy started if viral load exceeded institutional established threshold or end-organ disease was suspected. Antifungal prophylaxis was switched to therapy in patients who met clinical criteria for invasive fungal infection.

Statistical Analysis

The primary aim of our analysis was to describe infectious outcomes experienced by pediatric patients after CD19-CAR T cell infusion, with a focus on initial infusion. Participant data was censored at date of non-response to CAR T cells, development of recurrent detectable disease, the start of post-CAR T cell consolidative AlloHCT preparatory regimen, death or at time of last follow-up. Patients who received more than one infusion during the study period were included and reinfusion data analyzed separately from initial infusion, using descriptive statistics and summary measures.

Basic demographics, clinical information, and laboratory tests (ANC, ALC, IgG) were described using summary statistics, such as median with range and counts with percentage. Cumulative incidence plots were provided to depict the estimated probability of infections of interest in the 90 days after CAR T cell infusion, and number of patients at risk reported by week. Since a patient could die before the occurrence of infection of interest, death was defined as a competing risk. Infection rate was defined as the number of infections divided by the total person-days during the periods of interest, multiplied by 100, and was then calculated for the pre- and post-CAR T cell periods to describe infection density. A Venn diagram was used to illustrate the categories of infections patients had, either detected alone or in combination.

We applied Poisson regression to investigate the effects of pre- and post-CAR T cell therapy risk factors on post infusion infection density. The lab tests of ANC and ALC were first considered as categorial variables (yes/no) using the available data point closest to start of lymphodepletion. We then used all available ANC and ALC data points within the 30 days prior to start of lymphodepletion to define the duration of neutropenia or lymphopenia as a continuous variable. We defined the results in two ways as each captured a different dimension of the information. We considered modeling the response variable of the infections of interest within the early post CAR T cell (1-28 days), and late post CAR T cell (29-90 days) period. All factors of interest were evaluated in univariate analysis, by treating each

predictor one at a time and independently. The multivariate model only considered predictors which were statistically significant (p-value less than 0.05) in univariate analysis. A forward variable selection method at level of 0.05 was used to determine the final model. In the multivariate model building, ANC and ALC were considered either in categorical form or continuous form, but not both together.

The Fine-Gray competing risk model (21) was utilized to explore what risk factors were associated with the time to the first infection post CAR T cell therapy, with death before the occurrence of infection of interest as a competing risk. Risk factors which occurred before the first infection of interest were evaluated. ANC and ALC test results before the first infection of interest within the early post CAR T cell (1-28 days) and late post CAR T cell (29-90 days) periods were considered similarly in univariate and multivariate analyses, as in the Poisson regression above. Similarly, a multivariate model was fit with predictors which were statistically significant with (p-value less than 0.05) in the univariate analysis and a forward variable selection method at 0.05 level was used. To minimize the multicollinearity in the multivariate model, either neutropenia/lymphopenia (Yes or No) or the duration of neutropenia/lymphopenia were considered in separate models with other candidate predictors.

RESULTS

During the study period, 38 patients with relapsed and/or refractory CD19-positive malignancy received lymphodepleting chemotherapy followed by infusion of CD19-CAR T cells, for a total of 39 initial infusions. CD19-CAR T cell products included tisagenlecleucel (n=19; CD19/4-1BB) or an institutional product (n=20; CD19/4-1BB; NCT03573700). One patient received treatment with both products, with >1 year and receipt of an AlloHCT occurring in between infusions, and therefore contributed twice to initial infusions. Additionally, a subset of patients (n=6) received repeat CD19-CAR T cell infusion(s) of the same product due to recurrent malignancy or early loss of BCA. The clinical outcomes with a focus on disease response to CAR T cell therapy (22, 23), carHLH (18), and epigenetic reprograming of CAR T cells (24), have been reported elsewhere for a subset of these patients.

Pre-CAR T Cell Therapy

The demographic and clinical characteristics of patients (n=38) receiving initial CD19-CAR T cell infusions (n=39) are summarized in **Table 1**. At time of initial infusion, median age was 9.1 years (range, 1.8 – 23.6). As expected, patients were heavily pretreated, including 10 (25.6%) with prior AlloHCT and 15 (38.5%) having received CD19- and/or CD22-directed therapies. More than half of patients (56.4%) received low intensity bridging chemotherapy, including 5 patients with no systemic therapy and 3 patients that received focal RT. Pre-CAR T cell therapy, patients had a median morphologic leukemic blast percent of 5% (range, 0 – 98) (**Table 1**). Treatment included lymphodepleting chemotherapy followed by a single infusion of CAR T cells. All patients received a fludarabine (Flu) and cyclophosphamide (Cy) based chemotherapy regimen (n=30, Flu/Cy [cumulative doses, 75mg/m^2 and 900mg/m^2]; n=7, Flu/Cy [cumulative doses, 120mg/m^2 and 1000mg/m^2]; n=2, Flu/Cy [cumulative doses, 75mg/m^2 and 900mg/m^2] with etoposide [cumulative dose, 500mg/m^2] or cytarabine [cumulative dose, 4000mg]).

TABLE 1 | Demographics and treatment characteristics.

Demographics, N=38 patients	
Sex	
Female	18 (47.4)
Male	20 (52.6)
Race	
White	30 (78.9)
Black	5 (13.2)
Other (Asian, American Indian/Alaskan Native or Multiple Race)	3 (7.9)
Ethnicity	
Hispanic (Mexican/Chicano, Puerto Rican, South/Central American)	13 (34.2)
Non-Hispanic	25 (65.8)
Primary Diagnosis	
B-ALL	37 (97.4)
B-Lymphoblastic Lymphoma	1 (2.6)
Treatment Characteristics, N=39 initial infusion episodes	
Age at Infusion (median [range])	9.06 years [1.8 – 23.6]
Indication for CART	
Primary refractory	5 (12.8)
Relapsed disease	34 (87.2)
Relapse 1	17 (43.6)
Relapse ≥ 2	17 (43.6)
Pre-CART morphologic blast % (median [range])	5 [0 – 98]
Prior Therapy	
Allogeneic HCT	10 (25.6)
Antigen Directed*	15 (38.5)
Blinatumomab	12 (30.8)
Inotuzumab	5 (12.8)
CD19-CART	1 (2.5)
Bridging Chemotherapy	
High intensity	17 (43.6)
Low intensity	22 (56.4)
CRS Max Grade	
0	14 (35.9)
1-2	19 (48.7)
3-4	6 (15.4)
Neurotoxicity Max Grade	
0	30 (76.9)
1-2	5 (12.8)
3-4	4 (10.3)
carHLH	5 (12.8)
Post-CART Immunomodulatory Treatments	
Tocilizumab	13 (33.3)
Corticosteroids	5 (12.8)
Siltuximab	4 (10.2)
Anakinra	5 (12.8)
Ruxolitinib	1 (2.6)

*Numerical data are presented as the n (%) unless otherwise specified. B-ALL, B-cell acute lymphoblastic leukemia; CART, chimeric antigen receptor T-cell therapy; HCT, hematopoietic cell transplantation; CRS, cytokine release syndrome; carHLH, CAR associated hemophagocytic lymphohistiocytosis; ^morphologic blast % from most recent marrow prior to start of lymphodepleting chemotherapy; *patients may have received more than one antigen directed therapy.*

Immediately prior to the start of lymphodepleting chemotherapy, 33.3% of patients (n=13) were neutropenic (ANC <500 cells/mm^3) and 20.5% (n=8) were lymphopenic (ALC <300 cells/mm^3). When accounting for all available results within 30 days prior to start of lymphodepleting chemotherapy, 20 patients had neutropenia and lymphopenia, with a median duration of 13.5 (range, 1 – 30) and 7 (range, 1 – 30) days, respectively. Additionally, a subset of patients (n=26) had available pre-CAR T cell IgG levels, of which 23.1% were low (IgG <400 mg/dL). As expected, after CAR T cell infusion most patients experienced neutropenia and lymphopenia (**Table 2**), with a median duration of 14 (range, 1 – 69) and 11 (range, 2 – 53) days, respectively.

In the 30 days prior to CAR T cell infusion, 12 (30.8%) patients had a total of 20 infectious episodes. Most infections identified in this period were viral (n=10, 17 infectious episodes). Seven patients (41%) had systemic viral reactivations, 5 of which had a prior AlloHCT and previous history of viral reactivation. No end organ disease associated with viral reactivation was detected, and 3 received antiviral therapy while undergoing CAR T cell therapy. Only 7.7% of patients (n=3) had a bacterial infection, 2 BSIs (*A. xylosoxidans* and *S. epidermidis*) and 1 C. difficile-associated diarrhea (CDAD) (**Table 3**).

Infections Post CAR T Cell Therapy

The cumulative incidence of first infection, overall and by infection type, in the 90 days post CAR T cells are shown in **Figure 1**. The cumulative incidence of first infection was 17.9% (95% CI: 7.8-31.5%) by day 7, 25.8% (95% CI: 13.2-40.4%) by days 14 and 21, and 36.7% (95% CI: 21.6-52%) by day 28 post CAR T cell therapy. Infections were primarily bacterial (**Figure 1B**) followed by viral (**Figure 1C**), with a very low incidence of fungal infection (**Figure 1D**). Infection density in the 30 days prior to CAR T cell infusion was 1.71 per 100 days-at-risk. After CAR T cell therapy, most infections occurred early (infection density of 2.36 per 100 patient days-at-risk) compared to late post infusion (infection density 0.98 per 100 patient days-at-risk) (**Figure 2A**). The majority of patients had more than one type of infection (**Figure 2B**). Details of bacterial and viral infections are provided in **Supplemental Tables 2, 3**.

In the early post CAR T cell therapy period (day 1 – 28), 14 patients had a total of 23 infectious episodes (**Table 3**). Most infections were bacterial, with 9 patients (23.1%) contributing a total of 14 infectious episodes. This includes 9 episodes of bacteremia, 3 with gram positive and 6 with gram negative bacteria (**Figure 2C**). Most BSI episodes (78%) occurred in the setting of concurrent neutropenia. Notably, only 2 of the 9 organisms were susceptible to levofloxacin and of these, one was isolated in a non-neutropenic patient (**Supplemental Table 2**). Seven patients (17.9%) had a viral infection (n=8), most due to viral reactivation (**Supplemental Table 3**). One patient developed invasive rhinocerebral mucormycosis, identified by histopathology (**Figure 2C**). Notably, this patient had extended neutropenia pre-CAR T cell therapy, received immunomodulatory therapy for treatment of CAR-related side

TABLE 2 | Hematologic parameters pre- and post-CAR T cell therapy.

	ANC <500 cells/mm^3	ALC <300 cells/mm^3	IgG <400 mg/dL
Pre-CART Therapy (n=39)[#]			
Pre-lymphodepletion*, n (%)	13 (33.3)	8 (20.5)	6 (23.1)
Duration^, median (range);	13.5 (1 – 30)	7 (1 – 30)	–
Post-CART Therapy			
Time period, n (%)			
Days 0 – 7 (n=39)	28 (71.8)	39 (100)	5 (14.7)
Days 8 – 21 (n=39; IgG, n=32)	32 (82)	24 (61.5)	3 (8.8)
Days 22 – 63 (n=37; IgG, n=34)	15 (40.5)	14 (37.8)	16 (47.1)

*#for ANC/ALC, n=39; for IgG, n=26; *Pre-lymphodepletion, last available result prior to CART associated lymphodepleting chemotherapy; ^duration, in those with neutropenia or lymphopenia (n=20) at any time in the 30 days prior to CART infusion, the sum of days between the first value meeting defined low criteria and the first value above that criteria; CART, chimeric antigen receptor T-cell; ANC, absolute neutrophil count; ALC, absolute lymphocyte count; IgG, Immunoglobulin G.*

TABLE 3 | Infections pre- and post-CAR T cell therapy.

Type of Infection	Days -30 - 0 Pre-CART (N=39)		Days 1-28 Post CART (N=39)		Days 29-90 Post CART (N=33)	
	Total Episodes	Patients Affected	Total Episodes	Patients Affected	Total Episodes	Patients Affected
Any Infection	20	12 (30.7)	23	14 (35.9)	12	8 (24.3)
Bacterial Infections	3	3 (7.7)	14	9 (23.1)	5[+]	4 (12.2)
Bacteremia	2	2 (5.1)	9	7 (17.9)	3	3 (9.1)
Other*	1	1 (2.5)	5	3 (7.7)	3	3 (9.1)
Viral Infections	17	10 (25.6)	8	7 (17.9)	6	6 (18.2)
Systemic	11	7 (17.9)	4	4 (10.3)	1	1 (3)
Respiratory	3	3 (7.7)	1	1 (2.6)	1	1 (3)
Other*	3	3 (7.7)	3	3 (7.7)	4	4 (12.2)
Fungal Infections	0	0	1	1 (2.6)	1	1 (3)

*Numerical data are presented as the n (%). *Other infections include the following sites: skin and soft tissue, gastrointestinal, central nervous system, sinuses; +One patient had MSSA skin and bloodstream infections concomitantly.*

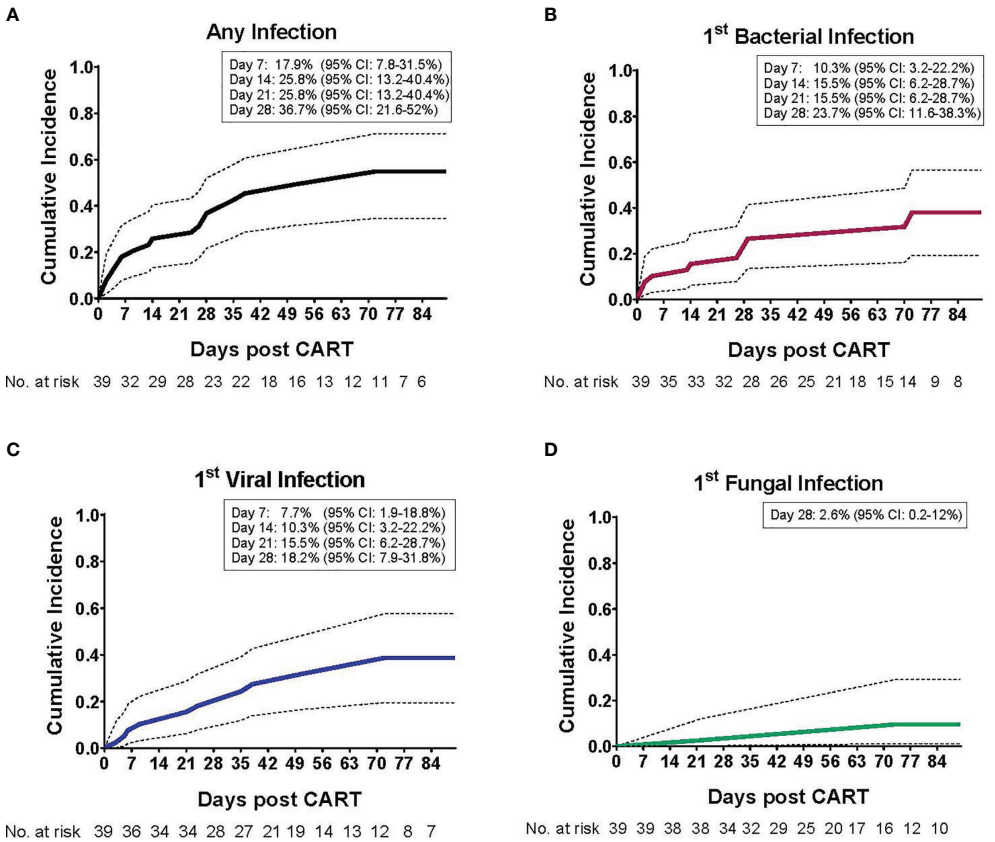

FIGURE 1 | Cumulative incidence of infections post CD19-CAR T cell therapy in pediatric and AYA patients. The cumulative incidence (CI) of infection post CD19-CAR T cell therapy, as a function of the day of infection onset, is depicted for the entire study period (day 1 – 90). **(A)** The cumulative incidence of first infection, such that each patient may contribute only once (either bacterial, viral and/or fungal infection, whichever occurred first). Most patients (73.7%) experienced their first infection within the initial 28 days post CAR T cells, with a 36.7% CI (95% confidence interval: 21.6 - 52). The cumulative incidence of first **(B)** bacterial infection, with a 23.7% CI (95% confidence interval: 11.6 – 38.3), **(C)** viral infection, with a 18.2% CI (95% confidence interval: 7.9 – 31.8), and **(D)** fungal infection, with a 2.6% CI (95% confidence interval: 0.2 – 12), by day 28 post CAR T cell infusion.

effects and only intermittently received fungal prophylaxis with an azole due to oral intolerance. No other fungal infections were found during this period (**Table 3**).

Thirty-three patients contributed data to the late post CAR T cell therapy period (day 29 – 90), with 8 patients (24.2%) experiencing a total of 12 infectious episodes. Notably, the number at risk in this period declined over time primarily due to lack of response to CAR T cell infusion or receipt of a consolidative AlloHCT. Of the 12 documented infections, 6 were viral and 5 were bacterial (3 BSIs). One episode of candidemia was identified late post CAR T cells (**Table 3**).

Post CAR T Cell Immune Mediated Side Effects and Infections

CAR T cell immune mediated side effects included CRS in 64% (n=25) of patients, neurotoxicity in 23% (n=9) and carHLH in 12.8% (n=5). Most cases were low grade, with only 15.4% of patients experiencing grade ≥3 CRS and 10.3% grade ≥3 neurotoxicity. Thirteen patients received immunomodulatory therapy, including tocilizumab (n=13), corticosteroids (n=5), siltuximab (n=4), anakinra (n=5), and/or ruxolitinib (n=1) (**Table 1**). The proportion of patients with and without infection early post CAR T cell infusion, stratified by presence and/or grade of CRS, neurotoxicity and carHLH, is shown in **Figure 3**. Eleven (44%) patients with CRS experienced at least one infectious episode. This includes 5, 6, and 1 patient(s) with at least one bacterial, viral, and fungal infection, respectively. A greater portion of patients were affected with increasing max CRS grade, with 7 of 19 (37%) patients with grade 1-2 CRS having infections, compared to 4 of 6 (67%) patients with grade 3-4 CRS (**Figure 3A**). Five (55.5%) patients with neurotoxicity and 4 (80%) patients with carHLH had at least one documented infection post CAR T cell infusion. Most infections in patients with neurotoxicity (4 of 5 patients; **Figure 3B**) and carHLH (3 of 4 patients; **Figure 3C**) were bacterial.

Outcomes Related to Infections Post CAR T Cell Therapy

Seven (17.9%) patients were admitted to the intensive care unit (ICU) after CAR T cell infusion. Three of these patients had active infections at time of ICU admission, and 2 died from

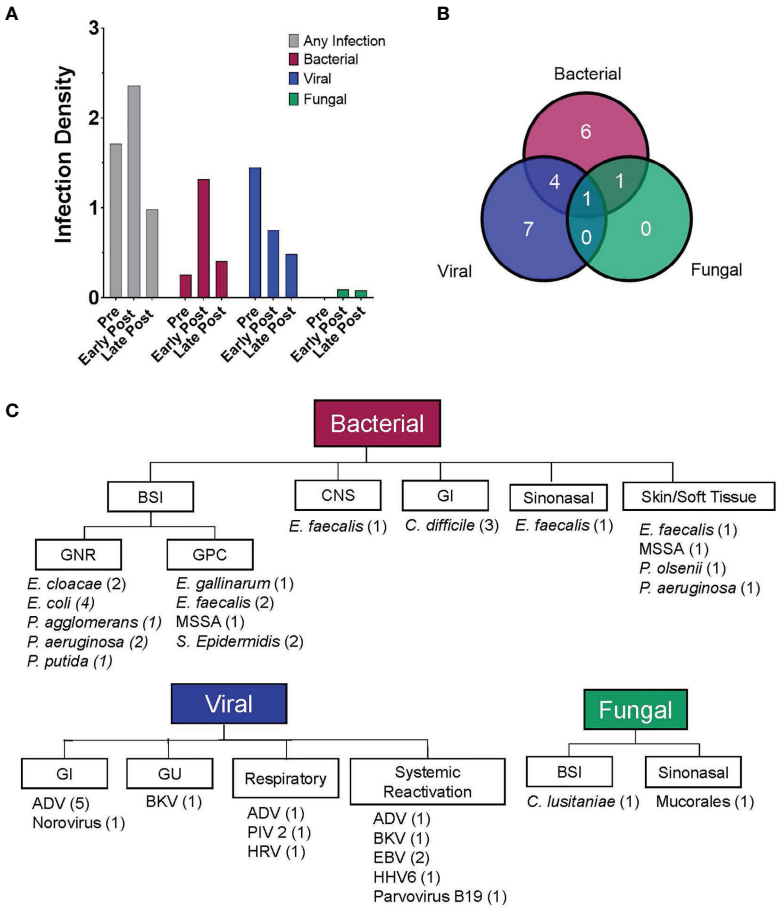

FIGURE 2 | Patients experienced a high rate of infections post CD19-CAR T cell therapy. **(A)** Bar graphs depicting the infection density per 100 days-at-risk, for any infection and by pathogen category (bacterial, viral and fungal). Data is displayed for three time periods, pre-CAR T cells (day -30 to day 0), early post CAR T cells (day 1 to day 28) and late post CAR T cells (day 29 to day 90). Infections occurred in 30.8% (infection density, 1.709), 34.2% (infection density, 2.358), and 24.2% (infection density, 0.978) of infusions, in the pre-, early post and late post CAR T cell therapy periods, respectively. **(B)** Venn diagram showing the number of patients experiencing at least one infection over the entire study period (n = 19) and depicting the types of infection experienced by each patient (bacterial, viral and/or fungal). **(C)** Flow diagram displaying details of infections experienced by pediatric and AYA patients after CD19-CAR T cell therapy (day 0 to day 90 post infusion). The figure depicts infection category, sites of infection, infectious pathogens (number of patients identified with that pathogen), for all patients after CD19-CAR T cell therapy.

infectious complications. This included 1 patient with extensive rhinocerebral mucormycosis and concomitant *E. faecalis* disseminated infection (BSI, CNS and sinonasal), and 1 patient with polymicrobial BSI with *E. faecalis* and *S. epidermidis* in the days prior to death. One additional patient had no documented infection at time of death, but postmortem examination revealed *E. faecalis* in cultures. All 3 patients that died with infection also had immune-mediated complications (CRS [n=3], neurotoxicity [n=2], carHLH [n=2]) treated with immunomodulating therapy and, in the 2 weeks prior to the last identified infection, had received a course of broad-spectrum antibiotics for documented infection or as empiric management of fever and neutropenia.

Risk Factors for Infections Post CAR T Cell Therapy

We sought to evaluate possible associations between pre- and post-CAR T cell therapy variables and infection density, within the early and late post therapy time periods. In univariate analysis, numerous variables, including duration of neutropenia pre- and post-CAR T cell therapy, intensity of bridging chemotherapy, immune mediated side effects and immunomodulatory treatment, were associated with increased infection density in the early post CAR T cell period. However, in the multivariate model, only pre-therapy disease burden (rate ratio: 1.02 [95% CI: 1.01, 1.03]; p <0.01) remained statistically significant. Conversely, in the late post CAR T cell therapy period, fewer evaluated variables were found to be associated with increased infection density in univariate analysis. However, pre-therapy lymphopenia (9.3 [2.34, 36.94]; p <0.01), carHLH (37.36 [3.56, 391.83]; p <0.01) and duration of low IgG (1.05 [1.02, 1.09]; p <0.01) were statistically significant in the multivariate model (**Table 4**).

Additionally, we investigated the impact of pre- and post-CAR T cell variables on time to first infection. In the early post CAR T cell therapy period, high intensity bridging chemotherapy

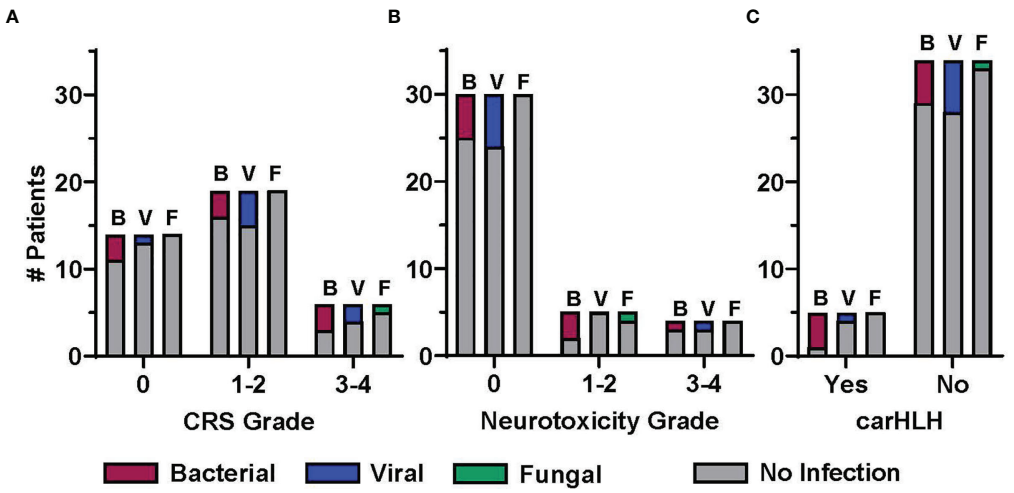

FIGURE 3 | Association between infection and post CD19-CAR T cell therapy immune mediated side effects. The proportion of patients experiencing at least one infection in the early post CAR T cell therapy period (day 1 to day 28), displayed by infection category and severity of CAR T cell therapy related immune mediated side effects (CRS, cytokine release syndrome; NTX, neurotoxicity; carHLH, CAR-associated hemophagocytic lymphohistiocytosis). Patients with at least 1 infection in a given category (B, bacterial; V, viral; F, fungal) are presented in the colored bars, with a patient contributing up to one infection per category. Patients not having an infection in the given category are accounted for in the gray bar. Distribution is by patients by highest grade **(A)** CRS and **(B)** neurotoxicity, or presence/absence of **(C)** carHLH.

TABLE 4 | Association of pre- and post-CAR T cell therapy variables with post CAR T cell therapy infection density.

Variables^	Early Post CART (day 1 to 28)		Late Post CART (day 29 to90)	
	Univariate Ratio (95% CI); *P*-value	**Adjusted Ratio (95% CI)*; *P*-value**	**Univariate Ratio (95% CI); *P*-value**	**Adjusted Ratio (95% CI)*; *P*-value**
Pre-CART variables				
ANC<500 cells/mm^3	3 (1.3, 6.93); **0.0101**		2.23 (0.71, 7.03); 0.1702	
ALC<300 cells/mm^3	0.67 (0.2, 2.24); 0.5105		5.29 (1.68, 16.66); **0.0045**	9.3 (2.34, 36.94); **0.0015**
IgG<400 mg/dL	0.22 (0.03, 1.69); 0.1471		0.44 (0.06, 3.45); 0.4354	
Duration of ANC<500 cells/mm^3	1.06 (1.02, 1.09); **0.0014**		–	
Duration of ALC<300 cells/mm^3	1.04 (1.01, 1.08); **0.022**		–	
Duration of IgG<400 mg/dL	0.88 (0.71, 1.09); 0.241		–	
Infection Pre-CART	0.96 (0.39, 2.33); 0.927		1.27 (0.38, 4.23); 0.6926	
Prior AlloHCT	0.49 (0.14, 1.64); 0.2439		2.66 (0.84, 8.38); 0.095	
Bridging chemotherapy (High vs. Low intensity)	3.92 (1.54, 9.93); **0.004**		1.42 (0.45, 4.46); 0.5523	
Pre-CART marrow blast %	1.02 (1.01, 1.03); **<0.0001**	1.02 (1.01, 1.03); **<0.0001**	1 (0.98, 1.03); 0.8288	
Post-CART variables				
CRS	2.78 (0.94, 8.16); **0.0634**		3.31 (0.73, 15.11); 0.1222	
Neurotoxicity	2.73 (1.2, 6.23); **0.0169**		–	
carHLH	3.02 (1.19, 7.65); **0.02**		9.21 (1.19, 71.33); **0.0335**	37.36 (3.56, 391.83); **0.0025**
Tocilizumab	3.37 (1.46, 7.78); **0.0045**		1.02 (0.28, 3.78); 0.9721	
Corticosteroids	4.68 (2.03, 10.81); **0.0003**		–	
Siltuximab	4.55 (1.87, 11.06); **0.0008**		–	
Anakinra	3.02 (1.19, 7.65); **0.02**		9.21 (1.19, 71.33); **0.0335**	
Duration$^{\#}$ of ANC<500 cells/mm^3	1.06 (1.02, 1.1); **0.004**		0.99 (0.95, 1.03); 0.6406	
Duration$^{\#}$ of ALC<300 cells/mm^3	1 (0.94, 1.07); 0.9315		1.01 (0.98, 1.04); 0.6485	
Duration$^{\#}$ of IgG<400 mg/dL	1 (0.87, 1.15); 0.9984		1.03 (1, 1.06); **0.0241**	1.05 (1.02, 1.09); **0.0033**

*Poisson Regression. ^variables categorized as Yes vs No, unless otherwise specified; #duration in the specified time period; *Multivariate analysis includes variables with p > 0.05 in univariate analysis. CART, chimeric antigen receptor T-cell therapy; ANC, absolute neutrophil count; ALC, absolute lymphocyte count; IgG, immunoglobulin G; AlloHCT, allogeneic hematopoietic cell transplant; CRS, cytokine release syndrome; carHLH, CAR associated hemophagocytic lymphohistiocytosis.*
Bold = statistically significant.

(rate ratio: 4.78 [95% CI: 1.41, 16.19]; $p = 0.012$) and duration of post CAR T lymphopenia (0.81 [0.7, 0.95]; $p = 0.011$) were associated with increased infection risk (**Table 5**). In the late post CAR T cell therapy period, no variables were statistically associated with time to first infection.

Infections Post Repeat CAR T Cell Infusions

After initial infusion, 6 patients received subsequent treatment with lymphodepleting chemotherapy followed by CAR T cell reinfusion. One patient contributed data for 3 reinfusions, for a total of 8 reinfusions among the 6 patients. Four patients developed infection following CAR T cell reinfusion, for a total of 12 infections. Interestingly, no patient had infection in the early post CAR T cell time period. Bacterial infections included 3 patients with a BSI (1 *Pseudomonas mendocina*, 1 Viridians Group Streptococcus [VGS], and 1 polymicrobial: VGS and *K. pneumonia*) and 3 with CDAD. Three patients had viral infections, including 2 patients with systemic reactivations and 1 with viral respiratory pathogens. No patients in this cohort had a fungal infection (**Supplemental Table 4**).

DISCUSSION

In this single institution retrospective analysis, we report on the infectious complications of 38 pediatric and AYA patients with relapsed/refractory CD19-positive malignancy, who received lymphodepleting chemotherapy followed by CD19-CAR T cell infusion. The incidence of infections post CAR T cell therapy in this cohort is similar to previous reports, with the highest number of infections occurring early post infusion (4–6, 25). Bacterial infections were the most frequent overall, typically occurring within 28 days of CAR T cell therapy and with primarily BSIs. Viral infections occurred at similar rates across the study period and included mainly systemic viral reactivations and gastrointestinal pathogens. Fungal infections were rare. Despite the small sample size and heterogenous nature of our patient population, our findings are consistent with the reported experience of other pediatric centers, demonstrating that the overall proportion and etiology of infections, as well as attributable mortality, is similar despite treatment at different centers. Given the similarities with previously published data, this work further establishes the expected infectious trends in the pediatric and AYA population, which can be used by practitioners to inform upon clinical care and decisions.

In accordance with others, most bacterial infections in our patient population presented as BSI, with organisms similar to those reported in patients receiving chemotherapy (6, 14, 25, 26). However, viral infections in our cohort were mainly due to systemic reactivations and gastrointestinal viruses, mainly ADV, with very few respiratory viruses (6, 14). This may be in part due to our routine, prospective monitoring for viral reactivations and highlights the need for such strategies. As reported by others,

TABLE 5 | Association of pre- and post-CAR T cell therapy variables with time to first infection post CAR T cell therapy.

Variables^	Early Post CART (day 1 to 28)		Late Post CART (day 29 to 90)	
	Univariate Hazard Ratio (95% CI); *P*-value	Adjusted Hazard Ratio (95% CI)*; *P*-value	Univariate Hazard Ratio (95% CI); *P*-value	Univariate Hazard Ratio (95% CI); *P*-value
Pre-CART variables				
ANC<500 cells/mm^3	1.73 (0.61, 4.89); 0.3025		2.32 (0.6, 9.01); 0.2236	
ALC<300 cells/mm^3	0.99 (0.32, 3.11); 0.9911		2.83 (0.83, 9.7); 0.0971	
IgG<400 mg/dL	0.37 (0.05, 2.69); 0.3248		0.78 (0.1, 6.18); 0.8166	
Duration of ANC<500 cells/mm^3	1.03 (0.99, 1.08); 0.1101		1.03 (0.98, 1.09); 0.2735	
Duration of ALC<300 cells/mm^3	1.02 (0.98, 1.08); 0.3278		1.03 (0.95, 1.11); 0.46	
Duration of IgG<400 mg/dL	0.92 (0.79, 1.06); 0.2547		1.01 (0.89, 1.14); 0.9361	
Infection Pre-CART	0.98 (0.3, 3.21); 0.9781		1.56 (0.4, 6.08); 0.5221	
Prior AlloHCT	0.44 (0.1, 2.01); 0.2912		0.9 (0.22, 3.64); 0.8777	
Bridging chemotherapy (High vs. Low intensity)	4.16 (1.26, 13.71); **0.0191**	4.78 (1.41, 16.19); **0.0119**	3.42 (0.89, 13.11); 0.0723	
Pre-CART marrow blast %	1.02 (1.01, 1.03); **0.0012**		1 (0.98, 1.03); 0.8571	
Post-CART variables				
CRS	1.41 (0.49, 4.07); 0.5250		4.66 (0.57, 38.15); 0.1515	
Neurotoxicity	1.76 (0.59, 5.24); 0.3064		–	
carHLH	3.24 (1.33, 7.94); **0.0099**		3.17 (0.36, 27.69); 0.2969	
Tocilizumab	1.5 (0.53, 4.29); 0.4463		1.38 (0.35, 5.38); 0.642	
Corticosteroids	2.56 (0.94, 6.97); 0.0654		–	
Siltuximab	1.08 (0.17, 7.08); 0.9347		–	
Anakinra	3.24 (1.33, 7.94); **0.0099**		3.17 (0.36, 27.69); 0.2969	
Duration# of ANC<500 cells/mm^3	0.95 (0.89, 1.02); 0.1448		0.83 (0.63, 1.08); 0.1612	
Duration# of ALC<300 cells/mm^3	0.83 (0.69, 0.99); **0.0373**		0.97 (0.91, 1.03); 0.2639	
Duration# of IgG<400 mg/dL	0.71 (0.46, 1.09); 0.1203		0.97 (0.83, 1.14); 0.7319	

*Cox proportional hazards model. ^variables categorized as Yes vs No, unless otherwise specified; #duration in the specified time period; *Multivariate analysis includes variables with p > 0.05 in univariate analysis. CART, chimeric antigen receptor T-cell therapy; ANC, absolute neutrophil count; ALC, absolute lymphocyte count; IgG, immunoglobulin G; AlloHCT, allogeneic hematopoietic cell transplant; CRS, cytokine release syndrome; carHLH, CAR associated hemophagocytic lymphohistiocytosis.*
Bold = statistically significant.

reactivation of double stranded DNA virus did not lead to end organ disease (6). While HSV and VZV have been described in children and adults after CAR T cell infusions to therapy, we did not observe any cases, likely due to the use of acyclovir prophylaxis (14). Given our data is limited to 90 days post infusion, this may influence outcomes related to viral infections. Notably, several patients had known systemic viral reactivation in the 30 days prior to CAR T cell therapy, some of which were detected as part of screening tests during pre-CAR T cell therapy evaluation. A minority of these patients required antiviral therapy, but all were monitored weekly to determine the need for preemptive therapy. Invasive fungal infection, albeit rare, carried significant morbidity and mortality, consistent with prior reports (6, 27, 28). The patient with invasive fungal infection was significantly immunosuppressed pre-therapy, and post infusion had persistent neutropenia and higher-grade CRS/neurotoxicity requiring immunomodulatory treatments, further supporting these variables as risks factor for severe infection (4, 6, 10, 11, 14). Importantly, among those patients that received repeat CD19-CAR T cell infusions, incidence of infection did not appear higher than in those with initial infusion. Larger patient cohorts are needed to evaluate this further.

We identified several factors associated with increased risk of higher infection density in the early post CAR T cell therapy period. However, in multivariate analysis only pre-CAR T cell therapy disease burden remained significant. Given the size and heterogeneity of our cohort, associated variables such as pre-CAR T cell therapy neutropenia and intensity of bridging chemotherapy may not have maintained significance, despite representing a similar patient profile to those with higher leukemia burden. Notably, receipt of high intensity bridging chemotherapy impacted time to development of first infection. Increased anti-malignancy therapies pre-CAR T cell therapy has also been reported by others as an independent risk factor for infection post CAR T cell infusions (25). In contrast to previous reports, prior AlloHCT, recent history of infections and pre-existing neutropenia were not associated with increased risk of infection (6, 14). These observations are limited due to the number and heterogeneity of patients included in this study. However, as our study includes all patients who received CD19-CAR T cell therapy at our institution, inclusive of 2 products, with a similar approach to antimicrobial prophylaxis and extended follow up to 90 days, we believe that our findings are still meaningful.

While CRS has been described as a risk factor for infection (6, 13), in our study immune mediated side effects and associated immunomodulatory treatments did not maintain statistical significance in multivariate analysis in the early post CAR T cell period. However, our limited number of patients with high grade CRS/neurotoxicity and therefore minimal use of corticosteroids may have favorably impacted infection risk. Furthermore, patients with fever received an empiric antibiotic course which may have mitigated the risk of developing infection during this high-risk period. It is therefore still prudent to have a high index of suspicion for infection in this population. Importantly, patients with carHLH did have a higher number of infections in the late post CAR T cell therapy period. This is likely since carHLH often occurs later than CRS and may require treatment with immunosuppressive agents such as anakinra and steroids (18, 29), as we saw in our patient population. The use of immunomodulatory agents to treat CAR-mediated side effects, the inflammatory response with elevated cytokines and/or the intensive supportive management in the ICU may all contribute to risk of infections in these patients (30–32). As we use such agents earlier in the course of treatment, including as prophylaxis, it will be important to continue to evaluate for impact on infectious outcomes particularly in larger patient cohorts (33–35).

Recognizing the substantial risk for infectious complication after CAR T cell therapy, we and others have developed institutional guidelines for prophylactic and empiric treatment regimens. The use of antibacterial prophylaxis in the setting of CAR T cell therapy remains controversial (7–9). While standard practice at some institutions, a recent report highlights that use of antibacterial prophylaxis may not significantly decrease rates of bacterial infection post CAR T cell therapy (25). Our data support this, as most bacterial infections in our patient cohort would not have been prevented using levofloxacin prophylaxis. Of particular importance is the use of a mold-active anti-fungal agent as soon as feasible after CAR T cell infusion, especially among those patients deemed to be at high-risk for invasive fungal infections. We also recognize that routine use and choice of prophylactic agents may impact timing and nature of post CAR T cell infectious complications. Furthermore, with the advent of new CAR T cell products and treatment of varied patient populations and disease indications, it will be important to reassess clinical management guidelines to maintain best clinical practice among different patient groups.

BCA is an expected side effect after CD19-CAR T cell therapy (3, 4, 36, 37) and recognized as a risk factor for infection (6, 8, 14). Our analysis of the possible relationship between infection and hypogammaglobulinemia is limited by the fact that, among those patients that had disease response to CAR T cell therapy, 15 proceeded to consolidative AlloHCT. Therefore, we have inadequate extended data to address this question. The role of prolonged hypogammaglobulinemia in the risk of infections beyond 90 days needs to be further addressed in larger cohorts with longer follow up periods. Specifically, several questions remain regarding the role of infections due to encapsulated bacteria, many of them immune preventable, and how BCA increases the risk and impacts revaccination in these patients. Currently, there is no evidence to guide immunization in this setting. Expert opinion, derived from knowledge on immunization after AlloHCT, established recommendations for revaccination of these patients (7, 38). However, the safety and immunogenicity of vaccines in patients undergoing CAR T cell therapy is largely unknown (7, 11, 39, 40). Prospective studies are needed to address these questions.

In conclusion, we describe the incidence and distribution of infectious complications in pediatric and AYA patients receiving CD19-CAR T cell therapy at our institution. Infections were seen throughout the first 90 days post CAR T cell infusion, with

bacterial infections being most common and occurring primarily in the early post CAR T cell therapy period. Pre-therapy disease burden, intensity of bridging chemotherapy, post CAR T cell therapy lymphopenia and development of carHLH were all significantly associated with either infection density or time to first infection. Our study adds to the growing literature and aids in defining patients at higher risk for infections after CD19-CAR T cell therapy, which is critical to the establishment of adequate protocols for infection surveillance, prophylaxis, and treatment.

DATA AVAILABILITY STATEMENT

The raw data supporting the conclusions of this article will be made available by the authors, without undue reservation.

ETHICS STATEMENT

The studies involving human participants were reviewed and approved by Institutional Review Board (IRB), St Jude Children's Research Hospital. Written informed consent from the participants' legal guardian/next of kin was not required to participate in this retrospective study in accordance with the national legislation and the institutional requirements.

AUTHOR CONTRIBUTIONS

GM, DH, RE, SN, SK, RH, SG, BT, and AT provided clinical care of patients. GM and AT performed data collection. YS and LT performed statistical analysis. GM, DH, RE, YS, LT, and AT analyzed and interpreted data. GM, DH, RE, and AT wrote the manuscript. All authors contributed to the article and approved the submitted version.

FUNDING

This work was supported by the National Institutes of Health (NIH)/National Cancer Institute grants P30CA021765 and 5P30CA021765-42, the American Society of Transplantation and Cellular Therapy (AT), the American Society of Hematology (AT), and the American Lebanese Syrian Associated Charities. The content is solely the responsibility of the authors and does not necessarily represent the official views of the NIH.

ACKNOWLEDGMENTS

We thank the staff of the clinical research office for assisting with data collection and the staff of the Departments of Infectious Diseases and Bone Marrow Transplantation and Cellular Therapy for their excellent patient care.

SUPPLEMENTARY MATERIAL

The Supplementary Material for this article can be found online at: https://www.frontiersin.org/articles/10.3389/fonc.2022.845540/full#supplementary-material

REFERENCES

1. Maude SL, Frey N, Shaw PA, Aplenc R, Barrett DM, Bunin NJ, et al. Chimeric Antigen Receptor T Cells for Sustained Remissions in Leukemia. *N Engl J Med* (2014) 371(16):1507–17. doi: 10.1056/NEJMoa1407222
2. Lee DW, Kochenderfer JN, Stetler-Stevenson M, Cui YK, Delbrook C, Feldman SA, et al. T Cells Expressing CD19 Chimeric Antigen Receptors for Acute Lymphoblastic Leukaemia in Children and Young Adults:a Phase1 Dose-Escalation Trial. *Lancet* (2015) 385(9967):517–28. doi: 10.1016/S0140-6736(14)61403-3
3. Gardner RA, Finney O, Annesley C, Brakke H, Summers C, Leger K, et al. Intent-to-Treat Leukemia Remission by CD19 CAR T Cells of Defined Formulation and Dose in Children and Young Adults. *Blood* (2017) 129 (25):3322–31. doi: 10.1182/blood-2017-02-769208
4. Maude SL, Laetsch TW, Buechner J, Rives S, Boyer M, Bittencourt H, et al. Tisagenlecleucel in Children and Young Adults With B-Cell Lymphoblastic Leukemia. *N Engl J Med* (2018) 378(5):439–48. doi: 10.1056/NEJMoa1709866
5. Curran KJ, Margossian SP, Kernan NA, Silverman LB, Williams DA, Shukla N, et al. Toxicity and Response After CD19-Specific CAR T-Cell Therapy in Pediatric/Young Adult Relapsed/Refractory B-ALL. *Blood* (2019) 134 (26):2361–8. doi: 10.1182/blood.2019001641
6. Hill JA, Li D, Hay KA, Green ML, Cherian S, Chen X, et al. Infectious Complications of CD19-Targeted Chimeric Antigen Receptor-Modified T-Cell Immunotherapy. *Blood* (2018) 131(1):121–30. doi: 10.1182/blood-2017-07-793760
7. Hill JA, Seo SK. How I Prevent Infections in Patients Receiving CD19-Targeted Chimeric Antigen Receptor T Cells for B-Cell Malignancies. *Blood* (2020) 136(8):925–35. doi: 10.1182/blood.2019004000
8. Shalabi H, Gust J, Taraseviciute A, Wolters PL, Leahy AB, Sandi C, et al. Beyond the Storm - Subacute Toxicities and Late Effects in Children Receiving CAR T Cells. *Nat Rev Clin Oncol* (2021) 18(6):363–78. doi: 10.1038/s41571-020-00456-y
9. Maus MV, Alexander S, Bishop MR, Brudno JN, Callahan C, Davila ML, et al. Society for Immunotherapy of Cancer (SITC) Clinical Practice Guideline on Immune Effector Cell-Related Adverse Events. *J Immunother Cancer* (2020) 8 (2):e001511. doi: 10.1136/jitc-2020-001511.
10. Wudhikarn K, Palomba ML, Pennisi M, Garcia-Recio M, Flynn JR, Devlin SM, et al. Infection During the First Year in Patients Treated With CD19 CAR T Cells for Diffuse Large B Cell Lymphoma. *Blood Cancer J* (2020) 10(8):79. doi: 10.1038/s41408-020-00346-7
11. Meir J, Abid MA, Abid MB. State of the CAR-T: Risk of Infections With Chimeric Antigen Receptor T-Cell Therapy and Determinants of SARS-Cov-2 Vaccine Responses. *Transplant Cell Ther* (2021) 27(12):973–87. doi: 10.1016/j.jtct.2021.09.016
12. Levine JE, Grupp SA, Pulsipher MA, Dietz AC, Rives S, Myers GD, et al. Pooled Safety Analysis of Tisagenlecleucel in Children and Young Adults With B Cell Acute Lymphoblastic Leukemia. *J Immunother Cancer* (2021) 9 (8):e002287. doi: 10.1136/jitc-2020-002287.
13. Park JH, Romero FA, Taur Y, Sadelain M, Brentjens RJ, Hohl TM, et al. Cytokine Release Syndrome Grade as a Predictive Marker for Infections in Patients With Relapsed or Refractory B-Cell Acute Lymphoblastic Leukemia Treated With Chimeric Antigen Receptor T Cells. *Clin Infect Dis* (2018) 67 (4):533–40. doi: 10.1093/cid/ciy152
14. Vora SB, Waghmare A, Englund JA, Qu P, Gardner RA, Hill JA. Infectious Complications Following CD19 Chimeric Antigen Receptor T-Cell Therapy

for Children, Adolescents, and Young Adults. *Open Forum Infect Dis* (2020) 7 (5):ofaa121. doi: 10.1093/ofid/ofaa121
15. Deya-Martinez A, Alonso-Saladrigues A, García AP, Faura A, Torrebadell M, Vlagea A, et al. Kinetics of Humoral Deficiency in CART19-Treated Children and Young Adults With Acute Lymphoblastic Leukaemia. *Bone Marrow Transplant* (2021) 56(2):376–86. doi: 10.1038/s41409-020-01027-6
16. Baird JH, Epstein DJ, Tamaresis JS, Ehlinger Z, Spiegel JY, Craig J, et al. Immune Reconstitution and Infectious Complications Following Axicabtagene Ciloleucel Therapy for Large B-Cell Lymphoma. *Blood Adv* (2021) 5(1):143–55. doi: 10.1182/bloodadvances.2020002732
17. Jeha S, Pei D, Choi J, Cheng C, Sandlund JT, Coustan-Smith E, et al. Improved CNS Control of Childhood Acute Lymphoblastic Leukemia Without Cranial Irradiation: St Jude Total Therapy Study 16. *J Clin Oncol* (2019) 37(35):3377–91. doi: 10.1200/JCO.19.01692
18. Hines MR, Keenan C, Maron Alfaro G, Cheng C, Zhou Y, Sharma A, et al. Hemophagocytic Lymphohistiocytosis-Like Toxicity (Carhlh) After CD19-Specific CAR T-Cell Therapy. *Br J Haematol* (2021) 194(4):701–7. doi: 10.1111/bjh.17662
19. N.H.S.N. Bloodstream Infection Event (Central Line-Associated Bloodstream Infection and Non-Central Line Associated Bloodstream Infection). (2022). Available at: https://www.cdc.gov/nhsn/pdfs/pscmanual/4psc_clabscurrent.pdf.
20. Donnelly JP, Chen SC, Kauffman CA, Steinbach WJ, Baddley JW, Verweij PE, et al. Revision and Update of the Consensus Definitions of Invasive Fungal Disease From the European Organization for Research and Treatment of Cancer and the Mycoses Study Group Education and Research Consortium. *Clin Infect Dis* (2020) 71(6):1367–76. doi: 10.1093/cid/ciz1008
21. Fine JP, Gray RJ. A Proportional Hazards Model for the Subdistribution of a Competing Risk. *J Am Stat Assoc* (1999) 94(446):496–509. doi: 10.1080/01621459.1999.10474144
22. Ravich JW, Huang S, Zhou Y, Brown P, Pui CH, Inaba H, et al. Impact of High Disease Burden on Survival in Pediatric Patients With B-ALL Treated With Tisagenlecleucel. *Transplant Cell Ther* (2022) 28(2):73.e1–9. doi: 10.1016/j.jtct.2021.11.019.
23. Talleur AC, Métais J-Y, Langfitt D, Mamcarz E, Crawford JC, Huang S, et al. Preferential Expansion of CD8+ CD19-CAR T Cells Post Infusion and Role of Disease Burden on Outcome in Pediatric B-ALL.
24. Zebley CC, Brown C, Mi T, Fan Y, Alli S, Boi S, et al. CD19-CAR T Cells Undergo Exhaustion DNA Methylation Programming in Patients With Acute Lymphoblastic Leukemia. *Cell Rep* (2021) 37(9):110079. doi: 10.1016/j.celrep.2021.110079
25. Mikkilineni L, Yates B, Steinberg SM, Shahani SA, Molina JC, Palmore T, et al. Infectious Complications of CAR T-Cell Therapy Across Novel Antigen Targets in the First 30 Days. *Blood Adv* (2021) 5(23):5312–22. doi: 10.1182/bloodadvances.2021004896
26. Freifeld AG, Bow EJ, Sepkowitz KA, Boeckh MJ, Ito JI, Mullen CA, et al. Clinical Practice Guideline for the Use of Antimicrobial Agents in Neutropenic Patients With Cancer: 2010 Update by the Infectious Diseases Society of America. *Clin Infect Dis* (2011) 52(4):e56–93. doi: 10.1093/cid/cir073
27. Haidar G, Dorritie K, Farah R, Bogdanovich T, Nguyen MH, Samanta P. Invasive Mold Infections After Chimeric Antigen Receptor-Modified T-Cell Therapy: A Case Series, Review of the Literature, and Implications for Prophylaxis. *Clin Infect Dis* (2020) 71(3):672–6. doi: 10.1093/cid/ciz1127
28. Garner W, Samanta P, Haidar G. Invasive Fungal Infections After Anti-CD19 Chimeric Antigen Receptor-Modified T-Cell Therapy: State of the Evidence and Future Directions. *J Fungi (Basel)* (2021) 7(2):156. doi: 10.3390/jof7020156
29. Lichtenstein DA, Schischlik F, Shao L, Steinberg SM, Yates B, Wang HW, et al. Characterization of HLH-Like Manifestations as a CRS Variant in Patients Receiving CD22 CAR T Cells. *Blood* (2021) 138(24):2469–84. doi: 10.1182/blood.2021011898
30. Brudno JN, Kochenderfer JN. Toxicities of Chimeric Antigen Receptor T Cells: Recognition and Management. *Blood* (2016) 127(26):3321–30. doi: 10.1182/blood-2016-04-703751
31. Hay KA, Hanafi LA, Li D, Gust J, Liles WC, Wurfel MM, et al. Kinetics and Biomarkers of Severe Cytokine Release Syndrome After CD19 Chimeric Antigen Receptor-Modified T-Cell Therapy. *Blood* (2017) 130(21):2295–306. doi: 10.1182/blood-2017-06-793141
32. Gutierrez C, Brown AR, Herr MM, Kadri SS, Hill B, Rajendram P, et al. The Chimeric Antigen Receptor-Intensive Care Unit (CAR-ICU) Initiative: Surveying Intensive Care Unit Practices in the Management of CAR T-Cell Associated Toxicities. *J Crit Care* (2020) 58:58–64. doi: 10.1016/j.jcrc.2020.04.008
33. Park JH, Sauter CS, Palomba ML, Shah GL, Dahi PB, Lin RJ, et al. A Phase II Study of Prophylactic Anakinra to Prevent CRS and Neurotoxicity in Patients Receiving CD19 CAR T Cell Therapy for Relapsed or Refractory Lymphoma. *Blood* (2021) 138(Supplement 1):96–6. doi: 10.1182/blood-2021-150431
34. Kadauke S, Myers RM, Li Y, Aplenc R, Baniewicz D, Barrett DM, et al. Risk-Adapted Preemptive Tocilizumab to Prevent Severe Cytokine Release Syndrome After CTL019 for Pediatric B-Cell Acute Lymphoblastic Leukemia: A Prospective Clinical Trial. *J Clin Oncol* (2021):JCO2002477. doi: 10.1200/JCO.20.02477
35. Gardner RA, Ceppi F, Rivers J, Annesley C, Summers C, Taraseviciute A, et al. Preemptive Mitigation of CD19 CAR T-Cell Cytokine Release Syndrome Without Attenuation of Antileukemic Efficacy. *Blood* (2019) 134(24):2149–58. doi: 10.1182/blood.2019001463
36. Hill JA, Giralt S, Torgerson TR, Lazarus HM. CAR-T - and a Side Order of Igg, to Go? - Immunoglobulin Replacement in Patients Receiving CAR-T Cell Therapy. *Blood Rev* (2019) 38:100596. doi: 10.1016/j.blre.2019.100596
37. Cordeiro A, Bezerra ED, Hirayama AV, Hill JA, Wu QV, Voutsinas J, et al. Late Events After Treatment With CD19-Targeted Chimeric Antigen Receptor Modified T Cells. *Biol Blood Marrow Transplant* (2020) 26(1):26–33. doi: 10.1016/j.bbmt.2019.08.003
38. Los-Arcos I, Iacoboni G, Aguilar-Guisado M, Alsina-Manrique L, Díaz de Heredia C, Fortuny-Guasch C, et al. Recommendations for Screening, Monitoring, Prevention, and Prophylaxis of Infections in Adult and Pediatric Patients Receiving CAR T-Cell Therapy: A Position Paper. *Infection* (2021) 49(2):215–31. doi: 10.1007/s15010-020-01521-5
39. Walti CS, Loes AN, Shuey K, Krantz EM, Boonyaratanakornkit J, Keane-Candib J, et al. Humoral Immunogenicity of the Seasonal Influenza Vaccine Before and After CAR-T-Cell Therapy: A Prospective Observational Study. *J Immunother Cancer* (2021) 9(10):e003428. doi: 10.1136/jitc-2021-003428
40. Bhoj VG, Arhontoulis D, Wertheim G, Capobianchi J, Callahan CA, Ellebrecht CT, et al. Persistence of Long-Lived Plasma Cells and Humoral Immunity in Individuals Responding to CD19-Directed CAR T-Cell Therapy. *Blood* (2016) 128(3):360–70. doi: 10.1182/blood-2016-01-694356

Conflict of Interest: SG consults/consulted for TESSA Therapeutics, TIDAL, Catamaran, and Novartis and is DSMB member of Immatics. SG and RE have patents/patent applications in the fields of T-cell and/or gene therapy for cancer. GM receives research funding from Astellas Inc and SymBio Pharmaceuticals Limited. DH receives research funding from Merck, AstraZeneca and Regeneron. RH serves on advisory boards for Roche Diagnostics, Quidel, Diagnostics, and Inflammatix.

The remaining authors declare that the research was conducted in the absence of any commercial or financial relationships that could be construed as a potential conflict of interest.

Publisher's Note: All claims expressed in this article are solely those of the authors and do not necessarily represent those of their affiliated organizations, or those of the publisher, the editors and the reviewers. Any product that may be evaluated in this article, or claim that may be made by its manufacturer, is not guaranteed or endorsed by the publisher.

frontiers in Oncology

ORIGINAL RESEARCH
published: 16 March 2022
doi: 10.3389/fonc.2022.828041

Multi-Faceted Effects of ST6Gal1 Expression on Precursor B-Lineage Acute Lymphoblastic Leukemia

Mingfeng Zhang[1], *Tong Qi*[1], *Lu Yang*[1], *Daniel Kolarich*[2,3] *and Nora Heisterkamp*[1]*

[1] Department of Systems Biology, Beckman Research Institute City of Hope, Duarte, CA, United States, [2] Institute for Glycomics, Griffith University, Gold Coast, QLD, Australia, [3] Australian Research Council (ARC) Centre of Excellence for Nanoscale BioPhotonics, Griffith University, Gold Coast, QLD, Australia

Normal early human B-cell development from lymphoid progenitors in the bone marrow depends on instructions from elements in that microenvironment that include stromal cells and factors secreted by these cells including the extracellular matrix. Glycosylation is thought to play a key role in such interactions. The sialyltransferase ST6Gal1, with high expression in specific hematopoietic cell types, is the only enzyme thought to catalyze the terminal addition of sialic acids in an α2-6-linkage to galactose on N-glycans in such cells. Expression of ST6Gal1 increases as B cells undergo normal B-lineage differentiation. B-cell precursor acute lymphoblastic leukemias (BCP-ALLs) with differentiation arrest at various stages of early B-cell development have widely different expression levels of *ST6GAL1* at diagnosis, with high *ST6Gal1* in some but not in other relapses. We analyzed the consequences of increasing ST6Gal1 expression in a diagnosis sample using lentiviral transduction. NSG mice transplanted with these BCP-ALL cells were monitored for survival. Compared to mice transplanted with leukemia cells expressing original ST6Gal1 levels, increased ST6Gal1 expression was associated with significantly reduced survival. A cohort of mice was also treated for 7 weeks with vincristine chemotherapy to induce remission and then allowed to relapse. Upon vincristine discontinuation, relapse was detected in both groups, but mice transplanted with ST6Gal1 overexpressing BCP-ALL cells had an increased leukemia burden and shorter survival than controls. The BCP-ALL cells with higher ST6Gal1 were more resistant to long-term vincristine treatment in an *ex vivo* tissue co-culture model with OP9 bone marrow stromal cells. Gene expression analysis using RNA-seq showed a surprisingly large number of genes with significantly differential expression, of which approximately 60% increased mRNAs, in the ST6Gal1 overexpressing BCP-ALL cells. Pathways significantly downregulated included those involved in immune cell migration. However, ST6Gal1 knockdown cells also showed increased insensitivity to chemotherapy. Our combined results point to a context-dependent effect of ST6Gal1 expression on BCP-ALL cells, which is discussed within the framework of its activity as an enzyme with many N-linked glycoprotein substrates.

Keywords: sialyltransferase, BCP-ALL, drug resistance, vincristine, microenvironment, N-linked glycan, α2-6 sialic acid

OPEN ACCESS

Edited by:
Yong-mi Kim,
Children's Hospital of Los Angeles, United States

Reviewed by:
Hisham Abdel-Azim,
University of Southern California, United States
Henrique Oliveira Duarte,
Universidade do Porto, Portugal

***Correspondence:**
Nora Heisterkamp
eheisterkamp@coh.org

Specialty section:
This article was submitted to Pediatric Oncology, a section of the journal Frontiers in Oncology

Received: *02 December 2021*
Accepted: *07 February 2022*
Published: *16 March 2022*

Citation:
Zhang M, Qi T, Yang L, Kolarich D and Heisterkamp N (2022) Multi-Faceted Effects of ST6Gal1 Expression on Precursor B-Lineage Acute Lymphoblastic Leukemia. Front. Oncol. 12:828041. doi: 10.3389/fonc.2022.828041

INTRODUCTION

B-cell precursor acute lymphoblastic leukemia (BCP-ALL) is a collective name for leukemias with differentiation arrest at various stages of early B-cell development. Owing to extensive molecular analysis including gene expression and DNA sequencing, it is possible to distinguish up to 23 different subcategories of BCP-ALL (1). However, very little is known regarding the glycome of such leukemias. Glycosylation is a dynamic and highly abundant protein post-translational modification in which glycans are attached to proteins or lipids by controlled biosynthetic pathways. Glycoproteins and glycolipids are major constituents of the cell surface glycocalyx, the major zone involved in all intercellular interactions. Glycosylation is applied by the consecutive and controlled action of numerous glycosyltransferases located in the endoplasmic reticulum and Golgi stack. Main sites of glycan attachment in glycoproteins are at serine/threonine [O-glycans] or asparagine [N-glycans] residues (2).

Sialyltransferases (ST), which attach sialic acids [Sia] as the final monosaccharide to such glycan structures, are of particular significance due to the unique biochemical properties of Sia. Sias are attached by specific sialyltransferases ST3Gal, ST6Gal/ST6GalNAc, and ST8Sia to glycoproteins in α2-3, α2-6, or α2-8 glycosidic linkages, respectively. The exact linkage has biological significance: carbohydrate-binding proteins [lectins] have evolved to recognize such specific linkages, forming the biological basis of, for example, species-restricted influenza infection (3) and specific binding by Siglecs such as the B-cell inhibitory CD22 (4). As a consequence, Sias play a crucial role in numerous signaling pathways including but not limited to those regulating Siglec signaling in innate and adaptive immunity (5).

There are only two human ST6Gal enzymes known to attach Sia onto N-glycans in an α2-6 linkage. ST6Gal2 is expressed mainly in neuronal tissues and in the thyroid gland (6), whereas ST6Gal1 is ubiquitously expressed, with highest levels in the liver and hematopoietic tissues (7). ST6Gal1 is the most intensively studied sialyltransferase in cancer. Increased ST6Gal1 expression was reported in pancreatic, prostate, breast, and ovarian cancer, and was implicated as contributing to tumor growth, metastasis, and signal transduction pathways relevant to tumorigenesis (8–15). Nonetheless, the possible active contribution of this enzyme to carcinomas is also controversial (16).

ST6Gal1 is known to sialylate many well-known cell-surface glycoproteins as demonstrated by exogenous enzymatic assays on different cell lines [HEL, HeLa and mouse lung (17–19)]. In human HEL cells, which were established from a patient with Hodgkin's disease, the 100 different substrates identified included for example CD44, numerous integrins, ICAMs, IGF1R, NOTCH1/2, and PTPRC/CD45. Since many of these glycoproteins contribute to cancer, sialylation is viewed as important from a potential diagnostic, therapeutic, and mechanistic viewpoint (20–22). ST6Gal1 also modifies the activity of the cell surface adhesion receptor PECAM1 and the store-operated calcium channel Oria1 (23, 24). Thus, increased expression of ST6Gal1 could contribute to tumorigenesis by Sia modification of many different cell surface glycoproteins, regulating cell–cell interactions and differential intracellular signaling through this route. However, the information regarding which glycoproteins are substrates of specific STs is limited because it requires analytical ability to discriminate Sia linkage in a protein-specific context.

Recently, we compared the glycome of primary B-lineage MLL-r leukemia, a subgroup of BCP-ALL, with that of normal bone marrow control CD19+CD10+ pre-B cells. Interestingly, we found increased levels of sialylated N-glycans, including α2-6 sialic acid-linked glycoconjugates, in the leukemia samples despite a downregulation of *ST6GAL1* on a transcript level (25). We considered that such higher levels of N-linked α2-6 Sia in primary BCP-ALL cells could have functional consequences, but a possible contribution of ST6Gal1 to BCP-ALL has not been examined. To test this, we here overexpressed *ST6GAL1* in a diagnosis BCP-ALL and found that in this BCP-ALL, high levels of ST6Gal1 associate with increased malignancy and large effects on the transcriptome of the cells.

RESULTS

BCP-ALL Cells Have Extensive α2,6 Sialylation With High but Varying Levels of *ST6GAL1* mRNA Expression

α2-6 sialylation can be detected by the lectin SNA. We used it to examine this specific Sia linkage in glycoproteins of a number of different PDX-derived as well as established, suspension-propagated BCP-ALL cell lines. As shown in **Figure 1A**, when used as a Western blot probe, SNA detects many glycoproteins, and/or different glycoforms of the same protein in BCP-ALL cell lines indicating that ST6Gal1 can sialylate numerous substrates in this type of leukemia. FACS analysis using SNA confirmed that there was, overall, very high representation of α2-6-linked Sia on the cell surface of such cells [for example, see **Supplementary Figure 1B**, negative controls US7, LAX57, and LAX56]. We also analyzed the relative abundance of α2-6-linked Sia using analytical glycan methods on RS4;11 as an example of a widely studied BCP-ALL suspension cell line. We found that, overall, 65% of N-linked glycans were capped by sialylation. Structures carrying Sia in α2-6-linkage were the single most abundant (>45%) modification, with fewer α2-3 Sias-containing glycans (**Figure 1B**).

These results are in agreement with our glycan analysis of primary BCP-ALL patient samples (25). We conclude that N-glycan-linked α2-6 sialylation is a very common glycan-capping modification in RS4;11 and primary BCP-ALL cells. Because ST6Gal1 is thought to be the only glycosyltransferase responsible for this modification, we examined its expression in hematopoietic cell types. As shown in **Figure 2A**, normal human hematopoietic cells differ in *ST6GAL1* expression, with relatively lower levels in myeloid, and highest levels in CD19+ B-lineage cells. CD34+ bone marrow progenitor cells also have relatively low *ST6GAL1* mRNA consistent with reports of low

Abbreviations: BCP-ALL, B-cell precursor acute lymphoblastic leukemia; GEP, gene expression profiling; rpkm, reads per kilobase million.

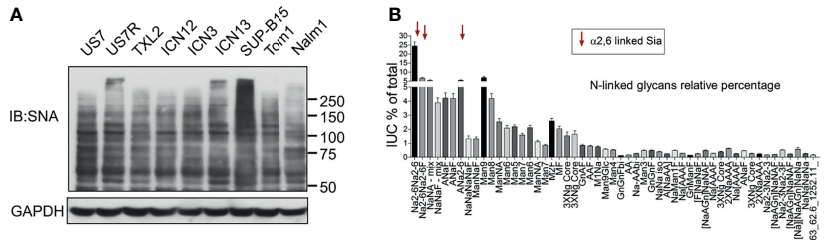

FIGURE 1 | BCP-ALL cells contain high levels of α2-6 sialylation. **(A)** Western blot of different BCP-ALL cell lines probed with SNA lectin to specifically detect α2-6-linked sialic acids on glycoproteins. GAPDH, loading control. Location of molecular weight standards to the right. **(B)** Analysis of N-glycans in RS4;11 cells as previously described (25). Combined results of 15 individual RS4;11 cell samples. Overall, more than 65% of all identified N-glycans were found to be sialylated with 7.4% in α2-3, 14.1% in α2-3/6, and 45.1% in α2-6 attachment.

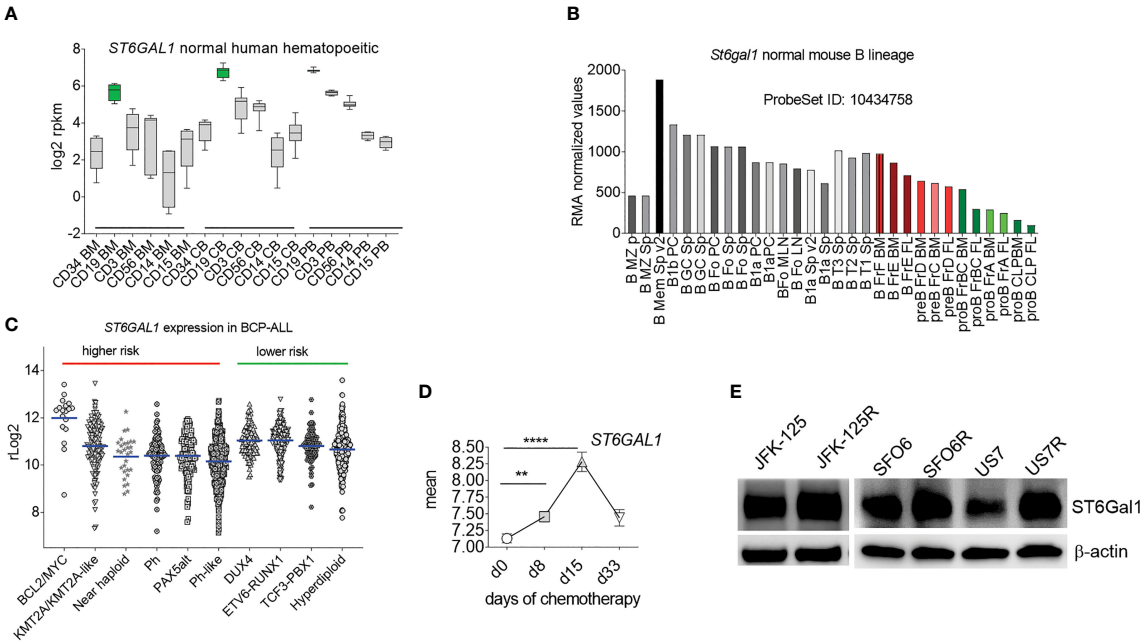

FIGURE 2 | *ST6GAL1* is highly expressed in normal and abnormal B-lineage cells. **(A)** RNA-seq-based expression levels of *ST6GAL1* in normal human hematopoietic cells (1). BM, bone marrow; CB, cord blood; PB, peripheral blood. Cells were sorted for the indicated major lineage markers [CD19: B- cells; CD3: T-cells; CD56: NK cells; CD14: myeloid/macrophage; CD15: myeloid]. Green: CD19 BM $n = 4$; CD19 CB $n = 10$; CD19 PB $n = 7$. **(B)** Normalized RMA values of *St6gal1* expression in murine hematopoietic cell types [GSE15907]. FL, fetal liver. Sp, spleen; LN, lymph node. Colored bars: B-cell developmental stages located in the bone marrow. **(C)** Scatter dot plot of rLog2 expression of *ST6GAL1* across selected subcategories of human BCP-ALL samples as indicated. Blue lines, mean values. **(D)** *ST6GAL1* RNA expression in pediatric ALL during chemotherapy treatment. Each symbol represents the mean ± SEM at an individual time point. Mean log-transformed normalized GEP values in 220 pediatric *de novo* ALL at diagnosis, day 8, day 15, and day 33 of remission–induction therapy [GSE67684]. $^{**}p < 0.01$; $^{****}p < 0.0001$. Source of expression data, see **Supplementary Table 4**. **(E)** Western blot of the indicated diagnosis and relapsed (R) samples from the same patient. β-actin, loading control.

St6gal1 expression in HSPC in mice (26). Within normal B-lineage development in the mouse (**Figure 2B**) and human (**Supplementary Figure 2**), progression from pro-B to more mature B cells correlates with increased *St6gal1* mRNA levels. However, in diagnosis human BCP-ALL samples, expression of *ST6GAL1* showed a more than 300-fold variability between the highest and lowest levels with no correlation (**Figure 2C**) between expression levels and mutation-associated risk category (27–29). In a sample set of pediatric BCP-ALL treated with induction chemotherapy over 33 days, a significant increase in expression occurred on day 15 of chemotherapy (**Figure 2D**), suggesting that *ST6GAL1* expression may additionally be regulated by inflammation as reported (30–32), which could be caused by drug treatment and/or ensuing cell death. Using Western blotting, we also measured ST6Gal1 (**Figure 2E**) in three sets of BCP-ALLs for which we had matched relapse/

diagnosis samples (**Supplementary Table 1**) and that grew in tissue co-culture. Overall, these analyses showed that *ST6GAL1* is ubiquitously expressed, but at varying levels in B-lineage cells.

Increased ST6Gal1 Expression in US7 BCP-ALL Cells Promotes More Rapid Leukemia Cell Expansion in Mice

To investigate whether or not increased ST6Gal1 expression can contribute to a more malignant phenotype in cells that initially have relatively lower expression, we transduced US7 BCP-ALL cells with a vector encoding human ST6Gal1 (**Supplementary Figure 1A**) or with the empty vector, then flow-sorted cells to obtain a homogenous population. When we compared the ability of these cells to home to the bone marrow after i.v. injection in NSG mice, no significant differences were measured (**Figure 3A**). We next transplanted the cells into NSG mice to monitor leukemia development. Based on bioluminescence (**Figures 3B, C**), mice transplanted with high ST6Gal1-expressing BCP-ALL cells showed a more rapid leukemia expansion compared to the controls and more rapid body weight loss (**Figure 3D**). Also, compared to mice transplanted with leukemia cells expressing original ST6Gal1 levels, increased ST6Gal1 expression was associated with significantly reduced survival (**Figure 3E**).

To compare the *in vivo* response to chemotherapy of these leukemia cells, we transplanted them into mice and allowed the leukemia cells to proliferate for 14 days before starting vincristine treatment. In the first weeks of treatment, based on bioluminescent imaging, chemotherapy was able to effectively control the expansion of the leukemia cells (**Figures 4A, B**, days 7–56). Treatment was discontinued after week 8, and relapse in both groups became evident about 14 days later. Based on bioluminescent imaging (**Figure 4A**, relapse; **Figure 4B**) and body weight loss (**Figure 4C**), US7 cells with increased expression of ST6Gal1 expanded and caused terminal leukemia more rapidly than the controls (**Figure 4D**). Thus, *in vivo*, increased ST6Gal1 expression allowed BCP-ALL cells to expand more rapidly than BCP-ALL cells with lower levels of ST6Gal1.

Contribution of ST6Gal1 Overexpression to Chemotherapy Resistance

In vivo, increased ST6Gal1 expression stimulated growth of BCP-ALL cells compared to cells with lower expression levels. We then examined if this could be recapitulated in a two-dimensional tissue culture model. This system makes use of co-culture with mitotically inactivated OP9 stromal cells to support growth and viability of the leukemia cells. However, under steady-state conditions, proliferation of US7-ST6Gal1 OE and EV cells was comparable (**Supplementary Figure 3A**). We also treated the cells with vincristine. As shown in **Figure 5A**, when treated with a suboptimal [non-lethal] dose of vincristine, after prolonged exposure to the drug, US7 cells with increased expression of ST6Gal1 maintained higher viable cell numbers compared to the control. Since US7 cells were from a patient at diagnosis, we also tested a second diagnosis BCP-ALL, LAX57, as well as a relapse sample, LAX56. Increased expression of ST6Gal1 in LAX57 and in LAX56 (**Supplementary Figure 1A**) also promoted resistance to vincristine, although in LAX57, the

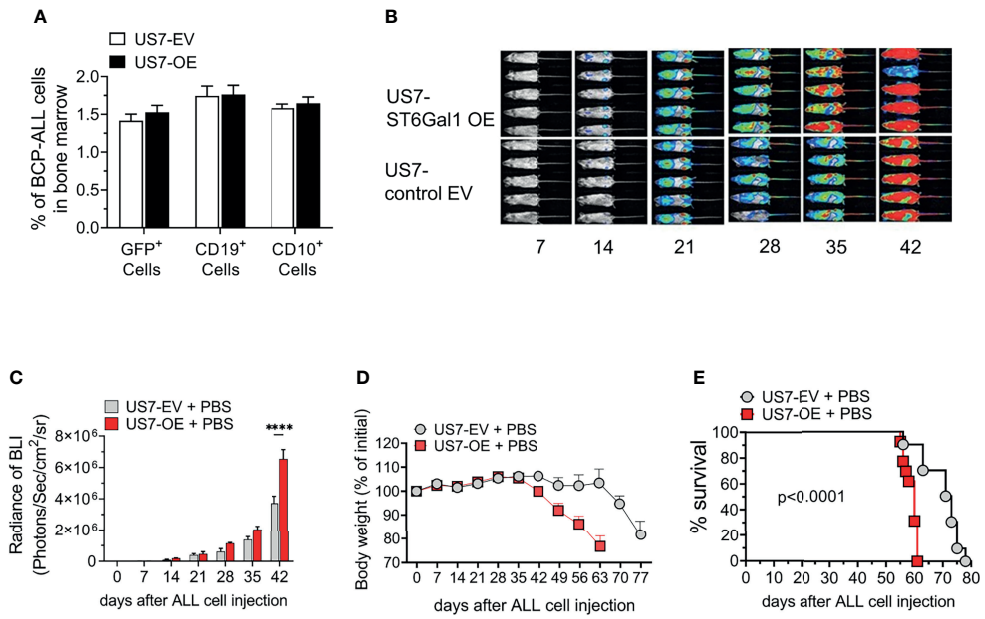

FIGURE 3 | NSG mice transplanted with US7 ST6Gal1 overexpressing ALL cells have decreased survival. **(A)** Homing of US7 ST6Gal1 OE or US7 EV leukemia cells to bone marrow of mice 16 h after i.v. injection. n = 3/group **(B, C)** Bioluminescent imaging of female cohort (n = 5/group) over time. ****$p < 0.001$, adjusted p-values, Šidák's multiple comparison test. Cells for transplant were transduced with a LV encoding luciferase. **(D)** Body weight changes and **(E)** survival of combined male and female cohorts [n = 10–13 total mice per group]. Kaplan–Meier survival curve comparing US7 control EV with US7 ST6Gal1 OE-transplanted mice. ****$p < 0.0001$, Log-rank test.

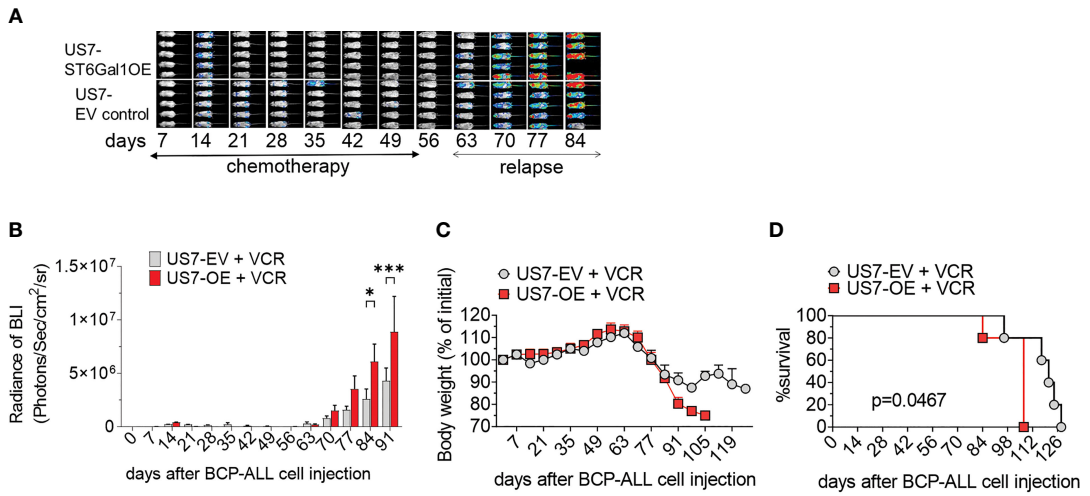

FIGURE 4 | Vincristine-induced remission and relapse of NSG mice transplanted with US7 ST6Gal1 OE or control EV cells. Female mice were transplanted with 2 × 10^6 cells on d0. Vincristine i.p. treatment was started on day 14 after transplant and was administered once per week at 0.5 mg/kg. **(A)** Bioluminescent images (BLI) of mice and **(B)** BLI quantification at weekly intervals of the two cohorts. $n = 5$ female mice/group. Two-way ANOVA, adjusted p-values, Šidák's multiple comparison test. $^*p < 0.05$; $^{***}p < 0.001$. **(C)** Body weight loss **(D)** Overall survival. $^{**}p = 0.0047$, Log-rank test.

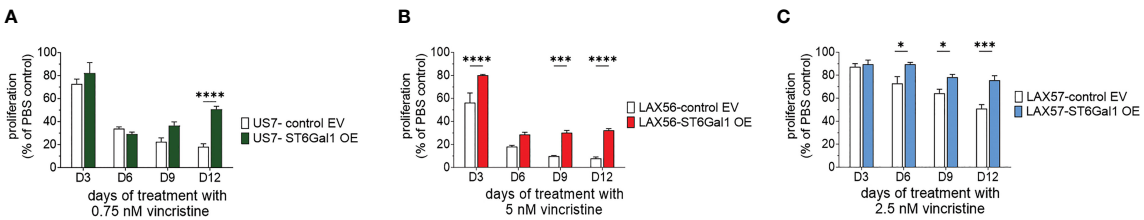

FIGURE 5 | BCP-ALLs with ST6Gal1 overexpression have a growth advantage under long-term treatment with relapse-permissive doses of vincristine. All cells were treated for 12 days while in co-culture with OP9 stromal support. Cell proliferation, measured by an assay for ATP levels, is expressed as a percentage of the PBS control at each time point. **(A–C)** US7, LAX57, and LAX56 cells as indicated and treated with 0.75 nM, 2.5 nM, or 5 nM vincristine. **(A)** Mean ± SEM of $n = 8$ replicates per time point per sample combined from two independent experiments. **(B, C)** Mean ± SEM of $n = 4$ replicates per time point per sample. Two-way ANOVA, adjusted p-values, Šidák's multiple comparison test. $^*p < 0.05$, $^{***}p < 0.001$, $^{****}p < 0.0001$.

difference with control cells was less than that in LAX56 (**Figures 5B, C**).

BCP-ALL Cells With Knockdown of ST6Gal1 Expression Also Are More Vincristine Resistant

We also reduced ST6Gal1 expression in US7 and LAX57 as diagnosis samples, and in LAX57 and JFK125R as relapses (**Supplementary Table 1**) using Cas9/CRISPR gene editing. FACS using SNA lectin was used as readout and selection method for tracking ablation of *ST6GAL1* gene function through loss of α2,6 sialylation (**Supplementary Figure 1B**). Western blotting also confirmed substantial reduction in ST6Gal1 protein levels (**Supplementary Figure 1C**). Because sialylation of the lysosomal/cell surface protein Lamp1/CD109a was reported to stimulate lysosomal exocytosis (33), we also specifically investigated the degree of α2,6 sialylation of Lamp1 in the *ST6GAL1* knockdown cells using a SNA affinity column. As shown in **Supplementary Figure 1D**, whereas Lamp1 protein isolated from wild-type cells bound to the SNA affinity column, knockdown of ST6Gal1 largely eliminated the ability of Lamp1 to be retained on the column. Thus, reduction of ST6Gal1 activity was clearly achieved in these BCP-ALLs. Steady-state growth of these cells in the absence of drug treatment was not consistently affected (**Supplementary Figure 4**). We also tested the four different BCP-ALLs with reduced ST6Gal1 levels in a long-term co-culture with OP9 cells for sensitivity to vincristine. As shown in **Figure 6**, cells expressing lower levels of ST6Gal1 were, to a varying degree, more tolerant to vincristine treatment than the matched original wild-type cells. We conclude that in *in vitro* co-culture, neither ST6Gal1 overexpression nor knockdown consistently affects steady-state proliferation of these BCP-ALL cells but changes in ST6Gal1 expression levels do reduce the ability of the cells to respond to the stress of vincristine drug treatment.

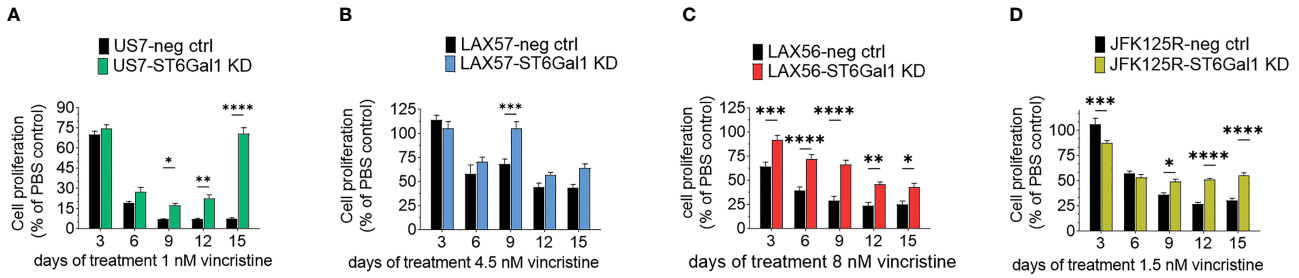

FIGURE 6 | Knockdown of ST6GAL1 expression correlates with increased resistance to vincristine. Paired sets of control BCP-ALLs and cells with ST6Gal1 knockdown were plated on mitotically inactivated OP9 cells and treated for 15 days with the indicated concentrations of vincristine. **(A, D)** Values mean ±SEM of n = 3–4 replicates per time point per sample. **(B, C)** Four to six replicates per time point per sample. Two-way ANOVA, Šidák's multiple comparison test, adjusted p-values, $^{*}p < 0.05$, $^{**}p < 0.01$; $^{***}p < 0.001$, $^{****}p < 0.0001$.

Effect of Stromal Galectin-1 on BCP-ALL Cells With ST6Gal1 Overexpression

A relatively well-described consequence of the sialylation of glycoproteins on the cell surface is to allow or inhibit the binding of lectins, a type of protein that specifically recognizes and binds to carbohydrates. Galectin-1 is such a lectin and it is inhibited in its binding to client glycoproteins by their α2-6 N-linked sialylation (34). Glycan–Galectin interactions are known to regulate B-cell function (35) and Galectin-1 plays a role in immune modulation as well as in cancer (36–38). Our previous studies had shown that inhibition of Galectin-1 using a drug, PTX008, sensitizes BCP-ALL cells to chemotherapy (39). These BCP-ALL cells endogenously produce Galectin-1 to a varying degree (39), but stromal cells can also be a source of extracellular Galectin-1 (40). Therefore, we knocked Galectin-1 out in the OP9 stromal cells used for co-culture, *via* Cas9/CRISPR (**Figure 7A**), and tested the effect on BCP-ALL cell growth and resistance to vincristine treatment in co-culture with the knockout cells. We found that wild-type and Galectin-1 knockout OP9 cells supported wild-type and ST6Gal1 OE US7 cells equally well under normal growth conditions (**Supplementary Figure 3B**), excluding a major role for stromal Galectin-1 interactions with cell surface glycoproteins that are sialylated by ST6Gal1 during normal growth. After 12 days of vincristine chemotherapy, proliferation of BCP-ALL cells with original levels of ST6Gal1 expression (EV samples **Figures 7B–D**) plated on OP9 Galectin-1 knockout stroma was comparable (LAX57 and LAX56) or enhanced (US7) (**Figures 7B, C**, compare white bars) with respect to the same cell types grown on wild-type OP9 cells. On day 12, US7 ST6Gal1 OE and LAX56 ST6Gal1 OE cultures grown on OP9 Galectin-1 knockout cells (**Figures 7B, D**) also had higher cell counts. Based on literature data, increased glycoprotein sialylation by ST6Gal1 should reduce Galectin-1 binding. Based on our PTX008 inhibitor studies (39), reduced Galectin-1 binding in turn should chemo-sensitize the BCP-ALL cells. Instead, OP9 Galectin-1 knockout cells protected BCP-ALL cells as well as, or better than, WT cells (**Figures 7B–D**). Thus, stromal-

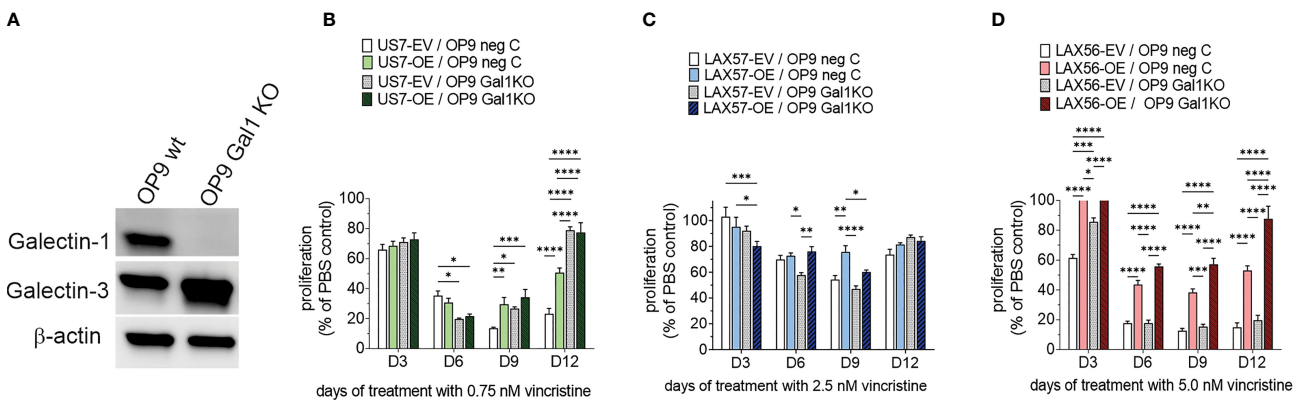

FIGURE 7 | Effect of co-culture of BCP-ALL cells on OP9 stromal cells lacking Galectin-1. **(A)** Western blot documenting loss of Galectin-1 in selected OP9 *Galectin-1* ko clone. **(B–D)** US7, LAX57, or LAX56 cells as indicated grown on control OP9 (OP9 neg C) or OP9 *Galectin-1* knockout (Gal1 KO) cells. US7, LAX57, and LAX56 were treated with 0.75, 2.5, and 5 nM vincristine. Values, mean ±SEM of n = 4 replicates per time point per sample. Two-way ANOVA, Tukey's multiple comparison test, adjusted p-values. $^{*}p < 0.05$, $^{**}p < 0.01$; $^{***}p < 0.001$, $^{****}p < 0.0001$.

produced Galectin-1 binding to α2,6 N-glycoproteins on BCP-ALL cells is not mechanistically linked to the enhanced resistance of ST6Gal1 OE cells to vincristine stress.

Increased Expression of ST6Gal1 Associates With Relatively Large Transcriptome Changes

In other types of cancer cells, ST6Gal1 expression was reported to regulate transcription [e.g., (41)]. We therefore also compared the transcriptomes of US7 ST6Gal1 OE and EV control cells. As expected, *ST6GAL1* RNA was significantly increased in the US7 ST6Gal1 OE cells (**Figure 8A** and **Supplementary Table 2**). In addition, we found differential expression of approximately 5% of all the protein-encoding genes that are expressed in these cells (**Supplementary Table 3**). Schultz et al. (42) previously reported that increased ST6Gal1 expression correlates with increased expression of the stem cell transcription factor Sox9 in colon and pancreatic cancer cell lines, conferring a stem-cell-like phenotype. However, in the BCP-ALL cells studied here, the gene expression data did not point to induction of a more stem-cell-like or primitive phenotype with increased *ST6GAL1* expression. Instead, Ingenuity Pathway Analysis of the US7 OE/EV RNA-seq data indicated "increased neoplasia" of the US7 ST6GAL1 OE cells compared to cells with baseline levels of *ST6GAL1* (**Supplementary Table 2**). We therefore compared differential gene expression in ST6Gal1 overexpressing US7 cells with that of a matched set of 10 diagnosis/relapsed BCP-ALL samples (43). Interestingly, there were 29 genes with common differential expression, of which 19 were regulated in the same direction in US7 ST6Gal1 OE cells and relapses, including VEGFA and TGFβ2 (**Supplementary Table 2**).

In terms of drug resistance in *in vitro* co-culture, we compared our data to ICN13 BCP-ALL cells that had been treated with relapse-permissive doses of vincristine while in co-culture with OP9 cells (Oliveira et al., in preparation). In that study, on d30 of drug treatment, 948 genes were differentially expressed compared to PBS-treated controls cultured for the same period of time. A comparison of the transcriptome of ST6Gal1 overexpressing US7 cells with vincristine-resistant ICN13 cells showed overlap of 78 genes with differential expression (**Supplementary Table 3**, **Supplementary Figure 5A**). However, 69 of these showed an increase in one condition (ICN13 × vincristine) and decrease in the other (ST6Gal1 overexpression), ruling out a straightforward positive correlative effect for specific genes that would account for increased *in vitro* vincristine resistance in US7 cells with increased ST6Gal1 expression.

Real-time RT/PCR was used to further validate increased mRNA levels of six selected genes in US7 ST6Gal1 OE cells. These included CD109 and BEX4, two genes that had high expression in MLL-r samples compared to normal pre-B controls (25). CD109 was of interest because increased expression correlates with worse outcome in AML and diffuse large B-cell lymphoma (44, 45). The stress pseudo-kinase TRIB3 is also implicated in acute leukemias (46, 47), and IZKF2 is a well-known transcription factor in normal and malignant hematopoietic cells (48, 49). As shown in **Figure 8B**, the analysis

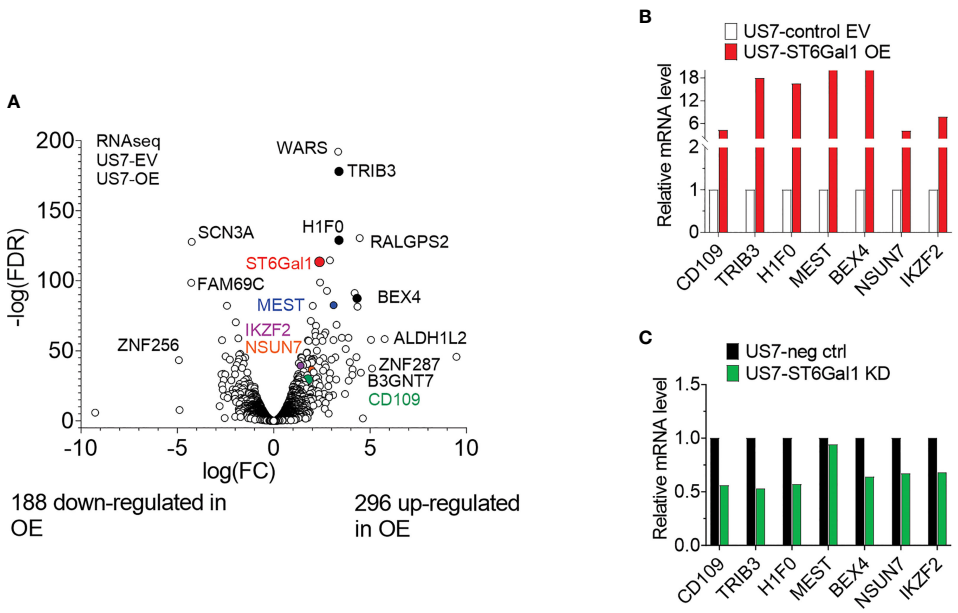

FIGURE 8 | Transcriptome of US7 cells with different levels of ST6Gal1 expression. **(A)** Volcano plot summarizing 484 differentially expressed genes (>2-fold; $p > 0.05$, rpkm cutoff = 1) in BCP-ALL cells with increased ST6Gal1 levels, with approximately 60% of protein-encoding expressed genes showing up-regulation. $n = 3$ biological replicates per RNA sample. **(B)** Real-time RT-PCR on selected genes with increased expression in the US7 ST6Gal1 OE cells. Values for the control EV samples were set as 1 and results are expressed as fold change. Note the discontinuity of the *Y*-axis. **(C)** Comparison of expression of selected genes in matched US7 control and US7 ST6Gal1 knockdown cells using real-time RT/PCR.

validated higher expression of these genes in US7 ST6Gal1 overexpressing cells. Conversely, expression of the genes was somewhat lower in ST6Gal1 knockdown US7 cells (**Figure 8C**). However, real-time RT/PCR analysis for expression of the same genes in LAX56 and LAX57 with ST6Gal1 overexpression did not yield a similar outcome (**Supplementary Figure 6A**). In addition, ST6Gal1 knockdown in two additional BCP-ALLs, ICN13 and BM41 (**Supplementary Table 1**, **Supplementary Figure 6B**) did not provide results consistent with those in US7 cells, ruling out a universal regulation of these genes by ST6Gal1 expression in BCP-ALL. Therefore, we did not find consistent changes in different BCP-ALLs in the expression of protein-encoding genes that could correlate with levels of ST6Gal1 and would explain the increased ability of ST6Gal1 overexpressing cells to proliferate in mice, and their increased resilience against vincristine stress *in vitro* co-culture.

DISCUSSION

ST6Gal1, a Non-Essential Protein With Unique Enzymatic Activity, as an Attractive Target for Treatment of Leukemias?

Although ST6Gal1 is thought to be the main enzyme responsible for the bulk of N-glycoprotein-linked α2-6 sialylation, mice with total *St6gal1* knockout are viable, with a surprisingly mild phenotype mainly manifest in immune cell function: increased inflammation, defects in dendritic cell, and myelopoiesis, as well as mature B-cell development (50–52). Also, the phenotype of mice with specific knockout of S*t6gal1* in the liver, an organ with particularly high ST6Gal1 expression, is mild (32). Thus, as a possible therapeutic target, ST6Gal1 would be attractive if increased expression is causally related to features associated with a more malignant phenotype. Indeed, as reviewed (53), numerous studies correlate ST6Gal1 overexpression with some aspects of increased malignancy in other cancers [also (41)].

A possible contribution of ST6Gal1 to hematological malignancies has been much less well-studied. The exception is multiple myeloma, in which ST6Gal1 secreted by more mature B cells in the bone marrow suppressed myeloid development (54). It is important to note in this context that normal hematopoietic progenitor stages express different levels of *ST6GAL1* mRNA, with low expression in hematopoietic stem cells, which progressively increases during maturation along the B-lineage (**Figure 2**). Thus, the varying expression levels of *ST6GAL1* in different BCP-ALL subtypes noted here may also, in part, be normal for the stage at which the cells have become arrested in their maturation.

However, we noted that *ST6GAL1* expression in the more than 20 subtypes of leukemic B cell precursors that have currently been distinguished (1) varied widely even within a specific subgroup. Accordingly, although in pediatric ALL, high *ST6GAL1* expression correlated with better relapse-free survival and relapsed samples had lower expression (**Supplementary Figures 7A, B**), in adult ALL, the overall survival probability was in fact similar [at $p = 0.37$, ns] for patients with high *ST6GAL1* (**Supplementary Figure 7D**). In addition, adult patients who achieved a complete remission had lower *ST6GAL1* mRNA than those who did not (**Supplementary Figure 7E**). Thus, in hematopoietic malignancies, there is no clear-cut correlation between *ST6GAL1* expression and clinical outcome.

Non-Concordant Phenotype of ST6Gal1 Overexpression and Knockdown in BCP-ALL Cells *In Vitro* and *In Vivo*

Frequently, the importance of a gene for a biological process is evaluated by loss-of-function and/or gain-of-function experiments; typically, this entails knockout/knockdown and overexpression. We used overexpression to investigate if increased ST6Gal1 levels in BCP-ALL contribute to a more malignant phenotype in mice. In this system, overexpression in US7 cells clearly promoted increased malignancy, in the sense that the overexpressing cells proliferated more rapidly than the cells with baseline expression, which was also seen after cessation of vincristine treatment. However, in tissue culture, there was no consistent effect of ST6Gal1 expression levels on proliferation rate. This suggests somewhat unsurprisingly that, *in vivo*, some interactions of the BCP-ALL cells with the microenvironment are not recapitulated in the tissue culture model. For example, based on the reported suppression of myeloid development by ST6Gal1 in multiple myeloma (54), it is possible that ST6Gal1 overexpressing BCP-ALL cells suppressed myeloid development in the bone marrow, which, in turn, could promote leukemia proliferation.

In contrast, in tissue culture, high ST6Gal1 contributed statistically significantly to increased drug insensitivity in three different BCP-ALLs. However, unexpectedly, in all three BCP-ALLs, ST6Gal1 knockdown also decreased responsiveness to chemotherapy, suggesting a complex contribution of ST6Gal1 to this process. Based on these findings, we posit that effects of different *ST6GAL1* expression levels in BCP-ALL are unlikely to be captured in a simple gain-of-function/loss-of-function dichotomy. We hypothesize that this could be explained by the inherent nature of the enzymatic activity of this protein, as detailed below.

Expression Levels of *ST6GAL1* mRNA May Not Correspond to Levels of N-Linked α2,6 Sialylation

There is no linear correlation between the expression of the *ST6GAL1* mRNA, and the generation of specific sialylation on glycoproteins: as with many other glycosyltransferases, ST6Gal1 does not function in 1:1 stoichiometry with client proteins since it can attach one or multiple sialic acids to a single glycoprotein. Indeed, Oswald et al. (32), who studied mice with liver-specific *St6gal1* knockout, remarked "our findings demonstrate that transcriptional changes, or lack thereof, cannot be reliably used as a surrogate for regulated changes in protein glycosylation within a cell". In addition, the sialylation of glycan structures is determined not only by ST6Gal1 protein levels but also by hypoxia (55), interactions of ST6Gal1 with the glycosyltransferase B4Galt1 (56), and metabolic flux (57, 58), which can regulate the availability of

the donor sialic acid. The existence of inherent variability in sialylation is supported by other studies in which we analyzed the glycome of US7, LAX56 and LAX57 EV, and ST6Gal1 OE cells (Oliveira et al., in preparation). In a different study, we analyzed the glycome of drug-resistant ICN13 BCP-ALL cells and found that these cells exhibit reduced overall sialylation, with a shift from α2-6- to α2-3-linked Sia without significant changes in expression of *ST6GAL1* (Oliveira et al., in preparation). These results may partly explain the inconsistent phenotypes found here associated with different ST6Gal1 expression levels.

Expression of Specific Glycoprotein Clients of ST6Gal1 N-linked α2,6 Sialylation, and the Impact of Each of These Clients on BCP-ALL Proliferation and Vincristine Resistance May Vary in Different BCP-ALL Samples

In some carcinomas, glycoproteins such as the EGFR and ErbB2 function as critical oncogenes that consistently drive the tumor phenotype. Interestingly, ST6Gal1 sialylation of these receptors was linked to sensitivity to cetuximab and trastuzumab therapeutic monoclonal antibodies (59, 60). Unfortunately, whether BCP-ALL cells of all subtypes and at different stages of treatment (diagnosis and relapse) consistently express one or more of such glycoproteins, of which the α2,6 N-linked sialylation would be critical for cell growth or drug resistance, remains unknown. Seeing that more than 350 ST6Gal1 client glycoproteins have been identified in different cell types (17–19), identification of such a putative critical glycoprotein, if there is one, is complicated. Moreover, B-lineage leukemias represent a continuum of differentiation stages and not all glycoproteins are expressed at every stage. CD75 is an example of an epitope generated by ST6Gal1 (61) which apparently is not expressed on BCP-ALL cells but is present on normal peripheral blood CD19+ B-cells (**Supplementary Figure 8**). A recent report documenting the existence of N-linked sialylated RNAs further adds to the potential complexity of ST6Gal1 involvement (62).

A Relatively Large Effect of ST6Gal1 Overexpression on Transcriptome Is Consistent With a General, Broad Effect of N-Linked α2,6 Sialylation on BCP-ALL Physiology

Apart from increased malignancy, pathway analysis of our RNA-seq data showed a correlation between increased *ST6GAL1* expression and a reduced migration and adhesion profile of the cells (**Supplementary Table 2**). We note that this correlation was unexpected in view of the lack of difference between US7 OE and EV cells in the *in vivo* bone marrow homing assay (**Figure 3A**). Moreover, the more drug-resistant phenotype of the ST6Gal1 OE cells suggests that they should have superior migration and adhesion to protective stromal cells (63, 64). However, it is consistent with the functional assay by Woodard-Grice et al. who overexpressed ST6Gal1 in acute myelogenous leukemia cell lines and found decreased α4β1-mediated VCAM1 binding (65). Thus, it is possible, based on changes in RNA expression, that other glycoproteins that can be sialylated by ST6Gal1 such as VEGFA (66) contribute to this complex phenotype.

Overall, our gene expression analysis in which we found differential expression of 484 genes in fact supports a broad effect of ST6Gal1 overexpression on the transcriptome, consistent with involvement of multiple glycoproteins and multiple downstream effects. The finding that increased ST6Gal1 expression also changes levels of mRNAs encoding its own substrate proteins adds further complexity (**Supplementary Figure 5B**). Interestingly, variability was also reported by Venturi et al. (16) who found that increased ST6Gal1 levels caused very large transcriptome changes in one but not in a different colon cancer cell line. Surprisingly, in view of the very different cell types, we found that US7 cells with ST6Gal1 overexpression had 19 genes in common (18 increased and one decreased) with the SW948 ST6Gal1 overexpressing colon cancer cells, including, among others, *ST6GAL1*, *TGFβ2*, and *CTF1*.

Conclusion

Venturi et al. (16) who investigated colon cancer cell lines stated that "changes induced by ST6Gal1 expression … are strongly cell-type specific, ruling out that the association of ST6Gal1 and malignancy is a general paradigm". Our studies support this concept, and furthermore indicate that ST6Gal1 in BCP-ALL is neither an oncogene nor a tumor suppressor. This does not exclude an important contribution of ST6Gal1 to the outcome of specific therapies such as those making use of monoclonal antibodies, as described for the EGFR and ErbB2 (59, 60). However, detailed analytical glycan studies of sialylation on CD19, CD22, or CD20 glycoproteins before and after treatment with antibodies or CAR T-cells would be needed to determine if ST6Gal1 N-linked α2,6 sialylation is a contributing factor to resistance in B-cell malignancies treated with such immune therapies.

MATERIALS AND METHODS

Cell Culture and Drug Treatment

GSE102301 describes that US7 [LAX7] and US7R [LAX7R] were obtained from a patient at diagnosis and after relapse following a standard 3-week chemotherapy regimen (vincristine, dexamethasone, L-asparaginase, and doxorubicin). JFK125/JFK125R, SF06/SF06R, and US7/US7R PDX patient-derived pre-B ALL samples have been previously described (67, 68). LAX56 and LAX57 grew directly on OP9 cells and have also been previously described (69). These BCP-ALLs are all largely stromal-dependent and were grown in co-culture with mitotically inactivated OP9 bone marrow stromal cells (ATCC CRL-2749). They were STR genotyped to confirm their identity. OP9 cells allowed to adhere overnight were treated with 10 μg/ml mitomycin C (Sigma, Cat#M4287) for 3 h in complete medium, washed, and used for co-culture with human ALL cells. Cells were co-cultured in α-MEM media supplemented with 20% FBS, 1% L-glutamine, and 100 μg/ml penicillin/streptomycin (Life

Technologies, Grand Island, NY). All cell lines used are listed in **Supplementary Table 1**. RS4;11 was obtained from the ATCC. Glycan analysis was performed as described previously (25).

For *in vitro* drug treatment, cells were plated at 0.5×10^6 cells/well in a 24-well plate with an OP9 feeder layer. Vincristine sulfate (Sigma, Cat#V8388) diluted in PBS at different concentrations was added freshly every 3 days. Each different BCP-ALL was titrated with different concentrations of vincristine to identify concentrations that would significantly inhibit proliferation but not eradicate all leukemia cells. Vincristine stocks were stored in small aliquots at −80°C. Diluted samples stored at 4°C were used within 14 days. Cell viability was determined on cells migrated into the tissue culture medium using a CellTiterGlo viability assay (Promega, Cat#G7570) according to the manufacturer's instructions.

Lentiviral Constructs and Transduction

The empty pLV411G vector was obtained from Simon Barry (70). pLV411G-ST6Gal1 was obtained from Dukka Škalamera (71). Inserts were introduced into the pLV411G vector by GateWay cloning (Invitrogen). The insert encodes the human ST6Gal1 406 amino acid isoform A, which we verified by DNA sequencing, in addition to a small C-terminal extension due to the cloning procedure. 293FT cells were cultured in high-glucose Dulbecco's modified Eagle's medium (DMEM, Gibco, Cat# 11995073) with 10% fetal bovine serum (FBS, Atlanta Biologicals, Cat# S11150H, Lot# K18135), 100 IU/ml penicillin and 100 µg/ml streptomycin (Gibco, Cat# 15070063). Lentiviral supernatant was produced by co-transfecting HEK 293FT cells with the plasmids pCD/NL-BH*DDD, pCMV-VSV-G (from AddGene), and pLV411G (with or without human *ST6GAL1*) using Lipofectamine 2000 (Invitrogen, Cat# 11-668-019) in Opti-MEM (Invitrogen) medium. The culture medium with the DNA/lipofectamine mixture was replaced after 3–4 h by DMEM medium with 10% FBS. After incubation overnight, the medium was replaced with DMEM medium containing 10% FBS and 10 mM sodium butyrate. After incubation for 6–8 h, the medium was replaced with regular growth medium. Twenty-four hours later, lentiviral supernatant was collected, filtered through a 0.45-µm filter, and loaded by centrifugation (600*g*, 30 min at 32°C) onto non-tissue culture six-well plates coated with 50 µg/ml RetroNectin (Takara). The LV backbone also encodes green fluorescent protein (GFP), which was used for flow-sorting of transductants on a BD Aria Fusion flow cytometer. LAX56 and LAX57 were transduced with the same LV vector for ST6Gal1 overexpression, but with a different empty vector control—pCL6IEGWO-GPF. All transductants were purified using flow sorting. US7 cells were also transduced with pCL6IEGWO-blasto-luc, a luciferase LV vector and selected with 8 µg/ml blasticidin, after a pilot of 4–20 µg/ml in a 6-day assay to determine a suitable selection concentration.

Cas9/CRISPR Knockout Conditions for *ST6GAL1*

For gene deletion in BCP-ALL cells, predesigned crRNAs, non-targeting control guide RNAs, trRNAs, and Cas9 protein were purchased from Integrated DNA Technologies (IDT, Coralville, Iowa). The same guide RNA against human *ST6GAL1* (IDT Hs.Cas9.ST6GAL1.1.AC; position 187072904 with the sequence CAGATGGGTCCCATACAATT AGG) was used for the different pre-B ALLs. Alt-R® CRISPR-Cas9 guide RNA for human *ST6GAL1* (crRNAs, 100 µM) and Alt-R® CRISPR-Cas9 tracrRNAs (trRNAs, 100 µM) were annealed by incubation at 95°C for 5 min. After cooling to room temperature, Alt-R® S.p. HiFi Cas9 Nuclease 3NLS (recombinant Cas9 protein, 1 µg/µl) was then added to the RNA mixture and RNA ribonucleoprotein complexes were allowed to form for 20 min. Electroporation of approximately 5×10^6 cells in Neon buffer T was performed using 3 pulses at 1, 600 V for 10 ms each on a Neon transfection system (Thermo Fisher) with the addition of 10 nmol Alt-R® Cas9 Electroporation Enhancer. Twenty-four hours after electroporation, fresh culture medium was added.

OP9 Galectin-1 Knockout

We combined two guide RNAs against mouse Galectin-1 (IDT Mm.Cas9.LGALS1.1.AA; position 78929743 with the sequence GACCTGGGGAACCGAACACC GGG and IDT Mm.Cas9.LGALS1.1AB position 78928002 with the sequence CGAACTTTGAGACATTCCCC AGG) to target Galectin-1 in OP9 cells. A total of 2×10^6 cells in Neon buffer T were electroporated using one pulse at 1,350 V for 30 ms as described above. Galectin-1 knockdown was confirmed by Western blot 72 h after electroporation. To isolate Galectin-1 knockout cells, single cells were sorted on a BD Aria Fusion around day 14 after electroporation. Single clones in 96-well plates were continuously expanded for 4 weeks with medium change weekly after the first 2 weeks of culture. Thereafter, growing clones were transferred to 24-well plates and then to 6-well plates. Galectin-1 knockout clones were verified by Western blotting and viably stored in LN_2.

Monitoring of *ST6GAL1* Gene Disruption by FACS Using SNA

Knockdown of ST6Gal1 was monitored using FACS for *Sambucus nigra* (SNA) cell surface reactivity on live cells. Careful titration of the amount of SNA lectin used for sorting was needed because exposure of the cells to high concentrations of SNA resulted in cell death. This is due to the fact that SNA I, which was obtained from Vector labs (Cat #B-1305), is a chimeric lectin composed of an A-chain with enzymatic activity and a B-chain with carbohydrate-binding activity. The A-chain encodes a ribosome-inactivating protein (72). BCP-ALL cells were blocked with human FCR blocking reagent diluted 1:100 (MACS Miltenyi Biotec, Cat#130-059-901) for 15 min at 4 °C. Cells were then incubated for 15 min at 4 °C with biotinylated SNA lectin diluted 1:100 followed by 15 min at 4 °C with streptavidin-APC diluted 1:200 (eBioscience, Cat# 17-4317-82). DAPI was added at a 1:100 dilution to distinguish dead and live cells. To enrich for *ST6GAL1* knockdown cells, we flow sorted cells on a BD Aria Fusion X20 around day 10 after electroporation. For some ALLs, electroporation with sgRNA was done twice. Using these procedures for example on day 5

after a single electroporation, there were 95.5% SNA^{med} and 0.12% SNA^{neg} cells in the LAX56 population, whereas for LAX57, this was 82.5% SNA^{med} and 1.3% SNA^{neg} cells. Repeat of the electroporation and flow sorting of the $SNA^{med/neg}$ cells failed to further yield pure SNA^{neg} populations for any of the BCP-ALLs (**Supplementary Figure 1B**).

Western Blotting

For Western blots for ST6Gal1 protein, cells were lysed in RIPA buffer with added protease and phosphatase inhibitors. We used R&D Systems human ST6Gal1 antibody diluted 1:500 (Cat#AF5924) and β-actin as loading control (Santa Cruz, 1:500, Cat#sc-47778 HRP). We also assessed the effect of ST6Gal1 ablation on Lamp1 α2,6 sialylation. BCP-ALL cells were lysed in Triton T-100 lysis buffer with glycerol at pH 7.4 (Alfa Aesar, Cat#J63866AK) and glycoproteins were captured with SNA-biotin (Vector labs Cat #B-1305). Dynabeads Streptavidin magnetic beads (Invitrogen, Cat#65801D) were used to isolate the SNA-bound glycoproteins. Proteins were separated on 4%–20% SDS-PAA gradient gels (Mini-PROTEAN® TGX Stain-Free™ Protein Gels, Bio-Rad, Cat#4568094). Lamp1 (CD109a) antibodies used at 1:1,000 dilution were from BioLegend (Cat#328602). The WB for OP9 cells used anti-Galectin-3 (BioLegend, 1:1,000, Cat#125402) or Galectin-1 (R&D Systems, 1:1,000, Cat#AF1152) antibodies. Western blotting for α2,6-sialylated proteins made use of biotinylated SNA from Vector Laboratories.

Mouse Experiments

For bone marrow homing experiments, 10^7 cells were injected *via* the tail vein into NSG mice (n = 3–4 per group). Sixteen hours later, bone marrows were analyzed by FACS for CD19, CD10, and eGFP-positive cells. Results are expressed as cell percentage in the live cell lymphocyte gate. To measure survival, non-irradiated NSG mice 8–10 weeks of age were used in all experiments. Female [n = 5 for US7/EV and n = 7 US7/OE] or male mice [n = 5 per group] were injected with 2×10^6 leukemia cells on d0. Imaging for leukemia signal was performed once per week by i.p. injection of 2.5 mg of D-luciferin in 200 µl of PBS. End points included loss of >20% initial body weight. For vincristine treatment, we used n = 5 female mice per group. Mice received six weekly vincristine treatments [0.5 mg/kg; i.p.] starting on d14. Bioluminescence signals were quantified using Aura imaging software (Spectral Instruments Imaging, LLC Tucson, AZ).

All animal experiments were conducted under an IACUC-approved institutional protocol. Methods of euthanasia were consistent with the guidelines of the American Veterinary Medical Association.

RNA Expression Analysis

RNAs were isolated from the cells by Trizol extraction. RNA-seq was performed by Novogene using an unstranded high-throughput TruSeq stranded mRNA prep kit. Analysis of the RNA-seq data was performed as previously described (25). The genome build used for analysis was hg38 and 19,862 protein-encoding genes were included in the analysis. Significantly regulated genes were defined as fold change ≥2, $p < 0.05$, and low expression filter set at rpkm <1.0. Graphs showing normalized RNA counts were generated using GraphPad Prism (v8.4.3). QIAGEN Ingenuity Pathway Analysis (IPA) version 62089861 was used to analyze results of RNA-seq for pathways with differential regulation using rpkm>1, p-values and FDR at <0.05 and logFc at −1.0 to 1.0. RNA-seq data were deposited in GEO under accession number GSE185611. Accession to all data is listed in **Supplementary Table 4**.

For real-time RT/PCR, RNA was extracted using an RNeasy Plus Mini Kit (Cat# 74134, QIAGEN). A high-capacity cDNA reverse transcription kit was from ABI (Cat# 4368814). cDNA concentrations were determined by Nanodrop. The Power SYBR™ Green PCR Master Mix was purchased from Life Technologies (Cat# 4367659). PCR was on an ABI QuantStudio 7 Flex System with 40 cycles and anneal/extend temperature set at 60°C.

Primers obtained from IDT (Integrated DNA Technologies) included the following:

Gene	Forward Primer	Reverse Primer
hCD109	AAGCCAGTGAAAGGAGACGTA	CCAGGGGAAGATAGATCCAGG
hTRIB3	AAGCGGTTGGAGTTGGATGAC	CACGATCTGGAGCAGTAGGTG
hH1F0	ACTCGCAGATCAAGTTGTCCA	GGTTCGTCGCTCTTGGCTA
hMEST	ATCGGGTGATTGCCCTTGATT	GAAAGAAGGTTGATCCTGCGG
hBEX4	AAAGAGGAACTAGCGGCAAAC	CCAAATGGCGGGATTCTTCTTC
hNSUN7	GGACTCCGTTTATGTCATGGC	CTCAGACTCGGACAAGGACC
hIKZF2	AACTACTGTGGACGAAGCTACA	CGTTTTCCCATATTCCCCGTG
hActin	CATGTACGTTGCTATCCAGGC	CTCCTTAATGTCACGCACGAT

Data Availability and Statistical Analysis

The origin and availability of the data analyzed here are summarized in **Supplementary Table 4**. Results were analyzed statistically using GraphPad Prism 8.3.1 and Excel software. The value of $p < 0.05$ was considered statistically significant. Details of biological replicate numbers and statistical tests used to analyze significance are indicated in each figure legend.

DATA AVAILABILITY STATEMENT

The datasets presented in this study can be found in online repositories. The names of the repository/repositories and accession number(s) can be found in the article/**Supplementary Material**.

ETHICS STATEMENT

The animal study was reviewed and approved by the City of Hope (COH) Institutional Animal Care and Use Committee (IACUC).

AUTHOR CONTRIBUTIONS

MZ, TQ, DK, and NH: conceptualization. LY and NH: data curation. MZ, TQ, and LY: formal analysis. NH and DK: funding acquisition. MZ and TQ: investigation. NH: project administration. NH and DK: supervision. NH: writing. All authors contributed to the article and approved the submitted version.

FUNDING

This study was partly supported in 2016/2017 by a New Idea Award from the Leukemia Lymphoma Society and NIH R01 CA172040 and CA090321 to NH. DK was supported in part by Civic Solutions Inc and is the recipient of an Australian Research Council Future Fellowship (project number FT160100344) funded by the Australian Government. Research reported in this publication included work performed in the City of Hope Small Animal Studies Core supported by the National Cancer Institute of the National Institutes of Health under award number P30CA033572. The content is solely the responsibility of the authors and does not necessarily represent the official views of the National Institutes of Health. The funders were not involved in the study design, collection, analysis, interpretation of data, the writing of this article or the decision to submit it for publication.

ACKNOWLEDGMENTS

We thank Eun Ji Joo, Chih-Ching Chou and Kathirvel Alagesan for sample preparation and glycan analysis of RS4;11 cells and SNA Western blotting. Aijun Liao is acknowledged for performing some of the cell viability assays. Helicia Paz generated the US7-pLV4111-ST6Gal1 and US7-pLV411-EV constructs. Simon Barry and Dubravka Škalamera are acknowledged for providing the empty pLV411G vector and pLV411G-ST6Gal1, respectively. Markus Muschen and Lars Klemm are acknowledged for providing JFK125/JFK125R for OP9 co-culture purposes and pCL6IEGWO-GPF; pCL6IEGWO-blasto-luc. Huimen Geng (UCSF) is acknowledged for examination of *ST6GAL1* expression for correlation with clinical outcomes in human BCP-ALL data sets.

SUPPLEMENTARY MATERIAL

The Supplementary Material for this article can be found online at: https://www.frontiersin.org/articles/10.3389/fonc.2022.828041/full#supplementary-material

Supplementary Table 2 | US7 OE EV ST6Gal1 RNA-seq data.

REFERENCES

1. Gu Z, Churchman ML, Roberts KG, Moore I, Zhou X, Nakitandwe J, et al. PAX5-Driven Subtypes of B-Progenitor Acute Lymphoblastic Leukemia. *Nat Genet* (2019) 51:296–307. doi: 10.1038/s41588-018-0315-5
2. Varki A, Kornfeld S. Historical Background and Overview. In: RA Varki, RD Cummings, JD Esko, P Stanley, GW Hart, M Aebi, AG Darvill, T Kinoshita, NH Packer, JH Prestegard, RL Schnaar, PH Seeberger, editors. *Essentials of Glycobiology*. Cold Spring Harbor (NY) (2015). p. 1–18.
3. Thompson AJ, Paulson JC. Adaptation of Influenza Viruses to Human Airway Receptors. *J Biol Chem* (2021) 296:100017. doi: 10.1074/jbc.REV120.013309
4. Meyer SJ, Linder AT, Brandl C, Nitschke L. B Cell Siglecs-News on Signaling and Its Interplay With Ligand Binding. *Front Immunol* (2018) 9:2820. doi: 10.3389/fimmu.2018.02820
5. Paulson JC, Macauley MS, Kawasaki N. Siglecs as Sensors of Self in Innate and Adaptive Immune Responses. *Ann N Y Acad Sci* (2012) 1253:37–48. doi: 10.1111/j.1749-6632.2011.06362.x
6. Lee M, Kiefel H, Lajevic MD, Macauley MS, Kawashima H, O'hara E, et al. Transcriptional Programs of Lymphoid Tissue Capillary and High Endothelium Reveal Control Mechanisms for Lymphocyte Homing. *Nat Immunol* (2014) 15:982–95. doi: 10.1038/ni.2983
7. Joshi HJ, Hansen L, Narimatsu Y, Freeze HH, Henrissat B, Bennett E, et al. Glycosyltransferase Genes That Cause Monogenic Congenital Disorders of Glycosylation Are Distinct From Glycosyltransferase Genes Associated With Complex Diseases. *Glycobiology* (2018) 28:284–94. doi: 10.1093/glycob/cwy015
8. Seales EC, Jurado GA, Brunson BA, Wakefield JK, Frost AR, Bellis SL. Hypersialylation of Beta1 Integrins, Observed in Colon Adenocarcinoma, may Contribute to Cancer Progression by Up-Regulating Cell Motility. *Cancer Res* (2005) 65:4645–52. doi: 10.1158/0008-5472.CAN-04-3117
9. Lu J, Isaji T, Im S, Fukuda T, Hashii N, Takakura D, et al. Beta-Galactoside Alpha2,6-Sialyltranferase 1 Promotes Transforming Growth Factor-Beta-Mediated Epithelial-Mesenchymal Transition. *J Biol Chem* (2014) 289:34627–41. doi: 10.1074/jbc.M114.593392
10. Lu J, Gu J. Significance of Beta-Galactoside Alpha2,6 Sialyltranferase 1 in Cancers. *Molecules* (2015) 20:7509–27. doi: 10.3390/molecules20057509
11. Wei A, Fan B, Zhao Y, Zhang H, Wang L, Yu X, et al. ST6Gal-I Overexpression Facilitates Prostate Cancer Progression via the PI3K/Akt/GSK-3beta/Beta-Catenin Signaling Pathway. *Oncotarget* (2016) 7:65374–88. doi: 10.18632/oncotarget.11699
12. Hsieh CC, Shyr YM, Liao WY, Chen TH, Wang SE, Lu PC, et al. Elevation of Beta-Galactoside Alpha2,6-Sialyltransferase 1 in a Fructoseresponsive Manner Promotes Pancreatic Cancer Metastasis. *Oncotarget* (2017) 8:7691–709. doi: 10.18632/oncotarget.13845
13. Britain CM, Holdbrooks AT, Anderson JC, Willey CD, Bellis SL. Sialylation of EGFR by the ST6Gal-I Sialyltransferase Promotes EGFR Activation and Resistance to Gefitinib-Mediated Cell Death. *J Ovarian Res* (2018) 11:12. doi: 10.1186/s13048-018-0385-0
14. Holdbrooks AT, Britain CM, Bellis SL. ST6Gal-I Sialyltransferase Promotes Tumor Necrosis Factor (TNF)-Mediated Cancer Cell Survival via Sialylation of the TNF Receptor 1 (TNFR1) Death Receptor. *J Biol Chem* (2018) 293:1610–22. doi: 10.1074/jbc.M117.801480
15. Kurz E, Chen S, Vucic E, Baptiste G, Loomis C, Agarwal P, et al. Integrated Systems-Analysis of the Murine and Human Pancreatic Cancer Glycomes Reveal a Tumor Promoting Role for ST6GAL1. *Mol Cell Proteomics* (2021) 20:100160. doi: 10.1016/j.mcpro.2021.100160
16. Venturi G, Gomes Ferreira I, Pucci M, Ferracin M, Malagolini N, Chiricolo M, et al. Impact of Sialyltransferase ST6GAL1 Overexpression on Different Colon Cancer Cell Types. *Glycobiology* (2019) 29:684–95. doi: 10.1093/glycob/cwz053
17. Sun T, Yu SH, Zhao P, Meng L, Moremen KW, Wells L, et al. One-Step Selective Exoenzymatic Labeling (SEEL) Strategy for the Biotinylation and Identification of Glycoproteins of Living Cells. *J Am Chem Soc* (2016) 138:11575–82. doi: 10.1021/jacs.6b04049
18. Yu SH, Zhao P, Sun T, Gao Z, Moremen KW, Boons GJ, et al. Selective Exo-Enzymatic Labeling Detects Increased Cell Surface Sialoglycoprotein Expression Upon Megakaryocytic Differentiation. *J Biol Chem* (2016) 291:3982–9. doi: 10.1074/jbc.M115.700369
19. Capicciotti CJ, Zong C, Sheikh MO, Sun T, Wells L, Boons GJ. Cell-Surface Glyco-Engineering by Exogenous Enzymatic Transfer Using a Bifunctional CMP-Neu5Ac Derivative. *J Am Chem Soc* (2017) 139:13342–8. doi: 10.1021/jacs.7b05358
20. Munkley J, Scott E. Targeting Aberrant Sialylation to Treat Cancer. *Medicines (Basel)* (2019) 6:1–10. doi: 10.3390/medicines6040102
21. Dobie C, Skropeta D. Insights Into the Role of Sialylation in Cancer Progression and Metastasis. *Br J Cancer* (2021) 124:76–90. doi: 10.1038/s41416-020-01126-7

22. Pietrobono S, Stecca B. Aberrant Sialylation in Cancer: Biomarker and Potential Target for Therapeutic Intervention? *Cancers (Basel)* (2021) 13:1–29. doi: 10.3390/cancers13092014
23. Lee C, Liu A, Miranda-Ribera A, Hyun SW, Lillehoj EP, Cross AS, et al. NEU1 Sialidase Regulates the Sialylation State of CD31 and Disrupts CD31-Driven Capillary-Like Tube Formation in Human Lung Microvascular Endothelia. *J Biol Chem* (2014) 289:9121–35. doi: 10.1074/jbc.M114.555888
24. Dorr K, Kilch T, Kappel S, Alansary D, Schwar G, Niemeyer BA, et al. Cell Type-Specific Glycosylation of Orai1 Modulates Store-Operated Ca2+ Entry. *Sci Signal* (2016) 9:ra25. doi: 10.1126/scisignal.aaa9913
25. Oliveira T, Zhang M, Joo EJ, Abdel-Azim H, Chen CW, Yang L, et al. Glycoproteome Remodeling in MLL-Rearranged B-Cell Precursor Acute Lymphoblastic Leukemia. *Theranostics* (2021) 11:9519–37. doi: 10.7150/thno.65398
26. Nasirikenari M, Veillon L, Collins CC, Azadi P, Lau JTY. Remodeling of Marrow Hematopoietic Stem and Progenitor Cells by Non-Self ST6Gal-1 Sialyltransferase. *J Biol Chem* (2014) 289:7178–89. doi: 10.1074/jbc.M113.508457
27. Li JF, Dai YT, Lilljebjorn H, Shen SH, Cui BW, Bai L, et al. Transcriptional Landscape of B Cell Precursor Acute Lymphoblastic Leukemia Based on an International Study of 1,223 Cases. *Proc Natl Acad Sci USA* (2018) 115:E11711–20. doi: 10.1073/pnas.1814397115
28. Paietta E, Roberts KG, Wang V, Gu Z, Buck GAN, Pei D, et al. (2021) Molecular Classification Improves Risk Assessment in Adult BCR-ABL1-Negative B-ALL. *Blood* 138:948–58. doi: 10.1182/blood.2020010144
29. Jeha S, Choi J, Roberts KG, Pei D, Coustan-Smith E, Inaba H, et al. Clinical Significance of Novel Subtypes of Acute Lymphoblastic Leukemia in the Context of Minimal Residual Disease-Directed Therapy. *Blood Cancer Discov* (2021) 2:326–37. doi: 10.1158/2643-3230.BCD-20-0229
30. Enterina JR, Jung J, Macauley MS. Coordinated Roles for Glycans in Regulating the Inhibitory Function of CD22 on B Cells. *BioMed J* (2019) 42:218–32. doi: 10.1016/j.bj.2019.07.010
31. Irons EE, Punch PR, Lau JTY. Blood-Borne ST6GAL1 Regulates Immunoglobulin Production in B Cells. *Front Immunol* (2020) 11:617. doi: 10.3389/fimmu.2020.00617
32. Oswald DM, Jones MB, Cobb BA. Modulation of Hepatocyte Sialylation Drives Spontaneous Fatty Liver Disease and Inflammation. *Glycobiology* (2020) 30:346–59. doi: 10.1093/glycob/cwz096
33. Machado E, White-Gilbertson S, Van De Vlekkert D, Janke L, Moshiach S, Campos Y, et al. Regulated Lysosomal Exocytosis Mediates Cancer Progression. *Sci Adv* (2015) 1:e1500603. doi: 10.1126/sciadv.1500603
34. Nielsen MI, Stegmayr J, Grant OC, Yang Z, Nilsson UJ, Boos I, et al. Galectin Binding to Cells and Glycoproteins With Genetically Modified Glycosylation Reveals Galectin-Glycan Specificities in a Natural Context. *J Biol Chem* (2018) 293:20249–62. doi: 10.1074/jbc.RA118.004636
35. Giovannone N, Smith LK, Treanor B, Dimitroff CJ. Galectin-Glycan Interactions as Regulators of B Cell Immunity. *Front Immunol* (2018) 9:2839. doi: 10.3389/fimmu.2018.02839
36. Sundblad V, Morosi LG, Geffner JR, Rabinovich GA. Galectin-1: A Jack-Of-All-Trades in the Resolution of Acute and Chronic Inflammation. *J Immunol* (2017) 199:3721–30. doi: 10.4049/jimmunol.1701172
37. Chou FC, Chen HY, Kuo CC, Sytwu HK. Role of Galectins in Tumors and in Clinical Immunotherapy. *Int J Mol Sci* (2018) 19:1–11. doi: 10.3390/ijms19020430
38. Martinez-Bosch N, Navarro P. Galectins in the Tumor Microenvironment: Focus on Galectin-1. *Adv Exp Med Biol* (2020) 1259:17–38. doi: 10.1007/978-3-030-43093-1_2
39. Paz H, Joo EJ, Chou CH, Fei F, Mayo KH, Abdel-Azim H, et al. Treatment of B-Cell Precursor Acute Lymphoblastic Leukemia With the Galectin-1 Inhibitor PTX008. *J Exp Clin Cancer Res* (2018) 37:67. doi: 10.1186/s13046-018-0721-7
40. Fei F, Joo EJ, Tarighat SS, Schiffer I, Paz H, Fabbri M, et al. B-Cell Precursor Acute Lymphoblastic Leukemia and Stromal Cells Communicate Through Galectin-3. *Oncotarget* (2015) 6:11378–94. doi: 10.18632/oncotarget.3409
41. Dorsett KA, Jones RB, Ankenbauer KE, Hjelmeland AB, Bellis SL. Sox2 Promotes Expression of the ST6Gal-I Glycosyltransferase in Ovarian Cancer Cells. *J Ovarian Res* (2019) 12:93. doi: 10.1186/s13048-019-0574-5
42. Schultz MJ, Holdbrooks AT, Chakraborty A, Grizzle WE, Landen CN, Buchsbaum DJ, et al. The Tumor-Associated Glycosyltransferase ST6Gal-I Regulates Stem Cell Transcription Factors and Confers a Cancer Stem Cell Phenotype. *Cancer Res* (2016) 76:3978–88. doi: 10.1158/0008-5472.CAN-15-2834
43. Meyer JA, Wang J, Hogan LE, Yang JJ, Dandekar S, Patel JP, et al. Relapse-Specific Mutations in NT5C2 in Childhood Acute Lymphoblastic Leukemia. *Nat Genet* (2013) 45:290–4. doi: 10.1038/ng.2558
44. Yokoyama M, Ichinoe M, Okina S, Sakurai Y, Nakada N, Yanagisawa N, et al. CD109, a Negative Regulator of TGF-Beta Signaling, Is a Putative Risk Marker in Diffuse Large B-Cell Lymphoma. *Int J Hematol* (2017) 105:614–22. doi: 10.1007/s12185-016-2173-1
45. Wagner S, Vadakekolathu J, Tasian SK, Altmann H, Bornhauser M, Pockley AG, et al. A Parsimonious 3-Gene Signature Predicts Clinical Outcomes in an Acute Myeloid Leukemia Multicohort Study. *Blood Adv* (2019) 3:1330–46. doi: 10.1182/bloodadvances.2018030726
46. Liang KL, Rishi L, Keeshan K. Tribbles in Acute Leukemia. *Blood* (2013) 121:4265–70. doi: 10.1182/blood-2012-12-471300
47. Choi RH, Mcconahay A, Silvestre JG, Moriscot AS, Carson JA, Koh HJ. TRB3 Regulates Skeletal Muscle Mass in Food Deprivation-Induced Atrophy. *FASEB J* (2019) 33:5654–66. doi: 10.1096/fj.201802145RR
48. Rebollo A, Schmitt C. Ikaros, Aiolos and Helios: Transcription Regulators and Lymphoid Malignancies. *Immunol Cell Biol* (2003) 81:171–5. doi: 10.1046/j.1440-1711.2003.01159.x
49. Park SM, Cho H, Thornton AM, Barlowe TS, Chou T, Chhangawala S, et al. IKZF2 Drives Leukemia Stem Cell Self-Renewal and Inhibits Myeloid Differentiation. *Cell Stem Cell* (2019) 24:153–65.e157. doi: 10.1016/j.stem.2018.10.016
50. Hennet T, Chui D, Paulson JC, Marth JD. Immune Regulation by the ST6Gal Sialyltransferase. *Proc Natl Acad Sci USA* (1998) 95:4504–9. doi: 10.1073/pnas.95.8.4504
51. Santos L, Draves KE, Boton M, Grewal PK, Marth JD, Clark EA. Dendritic Cell-Dependent Inhibition of B Cell Proliferation Requires CD22. *J Immunol* (2008) 180:4561–9. doi: 10.4049/jimmunol.180.7.4561
52. Holdbrooks AT, Ankenbauer KE, Hwang J, Bellis SL. Regulation of Inflammatory Signaling by the ST6Gal-I Sialyltransferase. *PloS One* (2020) 15:e0241850. doi: 10.1371/journal.pone.0241850
53. Garnham R, Scott E, Livermore KE, Munkley J. ST6GAL1: A Key Player in Cancer. *Oncol Lett* (2019) 18:983–9. doi: 10.3892/ol.2019.10458
54. Irons EE, Lee-Sundlov MM, Zhu Y, Neelamegham S, Hoffmeister KM, Lau JT. B Cells Suppress Medullary Granulopoiesis by an Extracellular Glycosylation-Dependent Mechanism. *Elife* (2019) 8. doi: 10.7554/eLife.47328
55. Hassinen A, Khoder-Agha F, Khosrowabadi E, Mennerich D, Harrus D, Noel M, et al. A Golgi-Associated Redox Switch Regulates Catalytic Activation and Cooperative Functioning of ST6Gal-I With B4GalT-I. *Redox Biol* (2019) 24:101182. doi: 10.1016/j.redox.2019.101182
56. Khoder-Agha F, Harrus D, Brysbaert G, Lensink MF, Harduin-Lepers A, Glumoff T, et al. Assembly of B4GALT1/ST6GAL1 Heteromers in the Golgi Membranes Involves Lateral Interactions via Highly Charged Surface Domains. *J Biol Chem* (2019) 294:14383–93. doi: 10.1074/jbc.RA119.009539
57. Saeui CT, Nairn AV, Galizzi M, Douville C, Gowda P, Park M, et al. Integration of Genetic and Metabolic Features Related to Sialic Acid Metabolism Distinguishes Human Breast Cell Subtypes. *PloS One* (2018) 13:e0195812. doi: 10.1371/journal.pone.0195812
58. Saeui CT, Cho KC, Dharmarha V, Nairn AV, Galizzi M, Shah SR, et al. Cell Line-, Protein-, and Sialoglycosite-Specific Control of Flux-Based Sialylation in Human Breast Cells: Implications for Cancer Progression. *Front Chem* (2020) 8:13. doi: 10.3389/fchem.2020.00013
59. Duarte HO, Rodrigues JG, Gomes C, Hensbergen PJ, Ederveen ALH, De Ru AH, et al. ST6Gal1 Targets the Ectodomain of ErbB2 in a Site-Specific Manner and Regulates Gastric Cancer Cell Sensitivity to Trastuzumab. *Oncogene* (2021) 40:3719–33. doi: 10.1038/s41388-021-01801-w
60. Rodrigues JG, Duarte HO, Gomes C, Balmana M, Martins AM, Hensbergen PJ, et al. Terminal Alpha2,6-Sialylation of Epidermal Growth Factor Receptor Modulates Antibody Therapy Response of Colorectal Cancer Cells. *Cell Oncol (Dordr)* (2021) 44:835–50. doi: 10.1007/s13402-021-00606-z
61. Munro S, Bast BJ, Colley KJ, Tedder TF. The B Lymphocyte Surface Antigen CD75 is Not an Alpha-2,6-Sialyltransferase But Is a Carbohydrate Antigen, the Production of Which Requires the Enzyme. *Cell* (1992) 68:1003. doi: 10.1016/0092-8674(92)90070-S

62. Flynn RA, Pedram K, Malaker SA, Batista PJ, Smith BAH, Johnson AG, et al. Small RNAs Are Modified With N-Glycans and Displayed on the Surface of Living Cells. *Cell* (2021) 184:3109–3124 e3122. doi: 10.1016/j.cell.2021.04.023
63. Sanchez VE, Nichols C, Kim HN, Gang EJ, Kim YM. Targeting PI3K Signaling in Acute Lymphoblastic Leukemia. *Int J Mol Sci* (2019) 20:1–14. doi: 10.3390/ijms20020412
64. Kim HN, Ruan Y, Ogana H, Kim YM. Cadherins, Selectins, and Integrins in CAM-DR in Leukemia. *Front Oncol* (2020) 10:592733. doi: 10.3389/fonc.2020.592733
65. Woodard-Grice AV, Mcbrayer AC, Wakefield JK, Zhuo Y, Bellis SL. Proteolytic Shedding of ST6Gal-I by BACE1 Regulates the Glycosylation and Function of Alpha4beta1 Integrins. *J Biol Chem* (2008) 283:26364–73. doi: 10.1074/jbc.M800836200
66. Munch V, Trentin L, Herzig J, Demir S, Seyfried F, Kraus JM, et al. Central Nervous System Involvement in Acute Lymphoblastic Leukemia Is Mediated by Vascular Endothelial Growth Factor. *Blood* (2017) 130:643–54. doi: 10.1182/blood-2017-03-769315
67. Pollock SB, Hu A, Mou Y, Martinko AJ, Julien O, Hornsby M, et al. Highly Multiplexed and Quantitative Cell-Surface Protein Profiling Using Genetically Barcoded Antibodies. *Proc Natl Acad Sci USA* (2018) 115:2836–41. doi: 10.1073/pnas.1721899115
68. Chan LN, Murakami MA, Robinson ME, Caeser R, Sadras T, Lee J, et al. Signalling Input From Divergent Pathways Subverts B Cell Transformation. *Nature* (2020) 583:845–51. doi: 10.1038/s41586-020-2513-4
69. George AA, Paz H, Fei F, Kirzner J, Kim YM, Heisterkamp N, et al. Phosphoflow-Based Evaluation of Mek Inhibitors as Small-Molecule Therapeutics for B-Cell Precursor Acute Lymphoblastic Leukemia. *PloS One* (2015) 10:e0137917. doi: 10.1371/journal.pone.0137917
70. Barry SC, Harder B, Brzezinski M, Flint LY, Seppen J, Osborne WR. Lentivirus Vectors Encoding Both Central Polypurine Tract and Posttranscriptional Regulatory Element Provide Enhanced Transduction and Transgene Expression. *Hum Gene Ther* (2001) 12:1103–8. doi: 10.1089/10430340175021431
71. Skalamera D, Dahmer M, Purdon AS, Wilson BM, Ranall MV, Blumenthal A, et al. Generation of a Genome Scale Lentiviral Vector Library for EF1alpha Promoter-Driven Expression of Human ORFs and Identification of Human Genes Affecting Viral Titer. *PloS One* (2012) 7:e51733. doi: 10.1371/journal.pone.0051733
72. Shang C, Chen Q, Dell A, Haslam SM, De Vos WH, Van Damme EJ. The Cytotoxicity of Elderberry Ribosome-Inactivating Proteins Is Not Solely Determined by Their Protein Translation Inhibition Activity. *PloS One* (2015) 10:e0132389. doi: 10.1371/journal.pone.0132389

Conflict of Interest: The authors declare that the research was conducted in the absence of any commercial or financial relationships that could be construed as a potential conflict of interest.

Publisher's Note: All claims expressed in this article are solely those of the authors and do not necessarily represent those of their affiliated organizations, or those of the publisher, the editors and the reviewers. Any product that may be evaluated in this article, or claim that may be made by its manufacturer, is not guaranteed or endorsed by the publisher.

frontiers | Frontiers in Oncology

ORIGINAL RESEARCH
published: 25 May 2022
doi: 10.3389/fonc.2022.864790

Bevacizumab, With Sorafenib and Cyclophosphamide Provides Clinical Benefit for Recurrent or Refractory Osseous Sarcomas in Children and Young Adults

Jessica Bodea[1]*, *Kenneth J. Caldwell*[2] *and Sara M. Federico*[1]

[1] Department of Oncology, St. Jude Children's Research Hospital, Memphis, TN, United States, [2] Johns Hopkins All Children's Hospital, Cancer and Blood Disorders Institute, St. Petersburg, FL, United States

OPEN ACCESS

Edited by:
Paraskevi Panagopoulou, Aristotle University of Thessaloniki, Greece

Reviewed by:
Sebastian Dorin Asaftei, Citta della Salute e della Scienza, Italy
Moira Garraus, Hospital Sant Joan de Déu Barcelona, Spain

***Correspondence:**
Jessica Bodea
jessie.bodea@stjude.org

Specialty section:
This article was submitted to Pediatric Oncology, a section of the journal Frontiers in Oncology

Received: *28 January 2022*
Accepted: *11 April 2022*
Published: *25 May 2022*

Citation:
Bodea J, Caldwell KJ and Federico SM (2022) Bevacizumab, With Sorafenib and Cyclophosphamide Provides Clinical Benefit for Recurrent or Refractory Osseous Sarcomas in Children and Young Adults. Front. Oncol. 12:864790. doi: 10.3389/fonc.2022.864790

Objective: Children and adolescents with recurrent and metastatic solid tumors have a poor outcome. A previous phase 1 study (ANGIO1) targeting angiogenesis with bevacizumab, sorafenib, and cyclophosphamide, demonstrated a signal of activity in a subset of patients. Here we report the results of a cohort of pediatric and young adult patients treated at the recommended phase 2 doses.

Methods: Electronic medical records of patients with refractory or recurrent solid tumors who received ANGIO1 therapy were reviewed. Treatment cycles lasted 21 days and included bevacizumab, sorafenib, and cyclophosphamide. Toxicities were assessed using Common Terminology Criteria for Adverse Events, v5.0. Responses were evaluated using Response Evaluation Criteria in Solid Tumors (RECIST1.1).

Results: Thirty-nine patients (22 male, 17 female; median age 15 years; range 1-22 years) received the treatment regimen. The most common diagnoses included bone sarcomas (n=21; 14 Ewing sarcoma, 7 osteosarcoma) and soft tissue sarcomas (n=9; 2 rhabdomyosarcoma, 3 synovial sarcoma, 2 desmoplastic small round cell tumors, and 2 high-grade sarcoma). The most common Grade 3 non-hematologic toxicities included hypertension (2, 5.4%) and hematuria (2, 5.4%). Five patients (13.5%) had a pneumothorax (3 at progressive disease, 1 post lung biopsy, and 1 spontaneous). Common Grade 3/4 hematologic toxicities were lymphopenia (19, 51%) and leukopenia (13, 35%). Sixteen patients (43.2%) developed palmar-plantar erythrodysesthesia Grade 2 or less. A total of 297 cycles were administered. Twenty-three patients required a dose reduction of cyclophosphamide, sorafenib or bevacizumab during therapy, all of whom continued to have clinical benefit following dose modification. One patient (Ewing sarcoma) achieved a complete response after 11 cycles; 2 patients (Ewing sarcoma, high grade sarcoma) achieved a partial response following cycles 2 and 4, respectively and 20 patients had stable disease as a best response.

Conclusions: Intravenous bevacizumab combined with oral sorafenib and metronomic cyclophosphamide was tolerated and required minimal supportive care or additional clinic visits. Disease stabilization for prolonged time periods was observed in greater than half of the treated patients. Patients with bone sarcoma demonstrated a signal of activity suggesting possible benefit from incorporation of the therapy as a maintenance regimen in upfront setting, or as a palliative regimen.

Keywords: pediatric sarcomas, Ewing sarcoma, osteosarcoma, sorafenib, cyclophosphamide, anti-angiogeneic therapy, bevacizumab

INTRODUCTION

Although a multitude of therapeutic advances have improved survival rates for pediatric patients with cancer (1), there is a paucity of progress for children and adolescents with recurrent and/or metastatic solid tumors. In this patient population, outcomes remain dismal (2). Thus, new therapies targeting alternative mechanisms of action are greatly needed.

Angiogenesis is critical for oncogenesis and spread of metastatic disease. Therefore, inhibition of angiogenesis is an appealing target for patients with relapsed and refractory solid tumors. The use of anti-angiogenic drugs has become a standard practice and treatment regimen for various adult cancers, including sarcomas (3, 4). Inhibition of vascular endothelial growth factors (VEGF) and platelet-derived growth factor receptors (PDGFR) impacts angiogenesis resulting in tumor suppression and may lead to tumor response (3, 5). Further, there is significant preclinical work which has shown dual inhibition of VEGF and PDGFR produces more effective tumor suppression and increases overall survival (3).

Antiangiogenic agents have been evaluated for the treatment of pediatric malignancies (6). While combining VEGF inhibitors with other chemotherapeutics is an attractive regimen, overlapping toxicities have been dose limiting. Our institution previously evaluated anti-angiogenic agents including bevacizumab (7), a VEGF-specific recombinant, humanized monoclonal antibody which binds directly to all 4 VEGF isoforms, and sorafenib tosylate (8), a multitarget kinase inhibitor of Raf-1, BRAF, FLT-3, p39a, c-Kit, VEGFR-2, VEGFR-3, and PDGFRB. These agents were combined with metronomic low dose oral cyclophosphamide, administered daily, given the oral bioavailability and decreased systemic toxicities (9–11).

This prior phase 1 dose-escalation study (NCT00665990, ANGIO1) conducted in young adults and children with relapsed and refractory solid tumors (12) identified the recommended phase 2 doses including: bevacizumab (15mg/kg/dose IV every 21 days), sorafenib (90mg/m^2/dose orally twice daily) and cyclophosphamide (50mg/m^2 orally once daily). A follow-up dose expansion cohort in patients treated at the recommended phase 2 doses demonstrated that the ANGIO1 regimen was tolerated and had a signal of activity (13). Following the closure of the clinical trial, pediatric and young adult patients have been treated with this regimen at St. Jude Children's Research Hospital. Here we report data from 39 pediatric patients, treated off study at the recommended phase 2 doses. We sought to better define the toxicities and outcomes associated to this therapeutic regimen (6–8, 12, 13).

METHODS & MATERIALS

Patient Population

This retrospective review was approved by the St. Jude Children's Research Hospital Institutional Review Board. Patients with refractory or recurrent solid tumors, who were treated as per the ANGIO1 anti-angiogenic regimen were identified through pharmaceutical records. Thirty-nine electronic medical records of patients receiving the regimen between June 2009 to July 2019 were reviewed for toxicities. Two clinicians independently reviewed all anatomic and metabolic imaging to assess for response to the therapy. Patients were excluded from the analyses if they completed less than half of the first cycle of chemotherapy or did not have complete medical records or imaging available for review.

Therapeutic Regimen

Patients received therapy, as per ANGIO1, at the recommended phase 2 doses (**Supplementary Figure 1**) (12, 13). Treatment cycle duration was 21 days and included bevacizumab (15 mg/kg, IV, day 1), sorafenib (90 mg/m^2 PO twice daily, days 1-21), and metronomic cyclophosphamide (50mg/m^2 PO daily, days 1-21). Patients were evaluated in their medical clinic by laboratory assessment and clinical monitoring on day 1 of each cycle and received IV bevacizumab in the outpatient setting. Oral cyclophosphamide and sorafenib were administered outpatient. All imaging obtained for disease evaluation at all time points was reviewed regardless of timing within a cycle of therapy. Timing of the initial disease response assessment varied by clinical provider (range 1-3 cycles).

Evaluation, Response and Toxicities

Patient demographics including age, gender, disease histology, prior systemic and radiation therapy exposure were recorded. Treatment related toxicities were collected from the electronic medical record and included laboratory assessments during the duration of therapy. Toxicities were recorded using Common Terminology Criteria for Adverse Events, v5.0. Reasons for discontinuation of therapy, number of unplanned treatment related clinic visits and/or admissions, need for transfusion(s) or other significant clinical

intervention were recorded. Dose adjustments, delay(s) in or holding of chemotherapy were reviewed. Disease response was independently evaluated by 2 reviewers using the Response Evaluation Criteria in Solid Tumors (RECIST 1.1) criteria for all available disease evaluations through the duration of treatment to determine best response.

RESULTS

Patient Characteristics

Table 1 summarizes patient characteristics. Thirty-nine patients (22 males, 17 females) received at least 1 cycle. Patients had a median age of 15 years (range 1-22 years). The most common histological diagnoses were bone sarcomas (n=21; 14 Ewing sarcoma, 7 osteosarcoma) and soft tissue sarcomas (n=9; 3 synovial sarcoma, 2 rhabdomyosarcoma, 2 desmoplastic small round cell tumors, 2 high-grade sarcoma). Additional diagnoses included rhabdoid tumor (n=3), hepatocellular carcinoma (n=2), Wilms tumor (n=2), clear cell meningioma (n=1), and neuroblastoma (n=1).

Twenty-eight patients (73.7%) had received prior radiation therapy, 14 (36.8%) of which included lung directed radiotherapy. Twenty-seven patients (71%) had lung disease at the start of the treatment regimen. Patients had received a median of 3 prior systemic therapies (range 0-6).

Two patients in the group had not received prior systemic therapy. These patients included a 20-year-old male with a sacral clear cell meningioma treated with upfront resection alone prior to receiving the therapeutic regimen and, a 15-year-old male with unresectable hepatocellular carcinoma for which other standard systemic therapy options were not available.

TABLE 1 | Baseline Characteristics.

No. Patients	**39**
Age on therapy (years)	
Median (range)	15 (1-22)
Gender, [N (%)]	
Male	22 (56%)
Female	17 (44%)
Histologic diagnosis	
Bone Sarcomas	
Ewing Sarcoma	14 (36%)
Osteosarcoma	7 (18%)
Other Solid Tumors	
Rhabdoid Tumor	3 (7%)
Synovial Sarcoma	3 (7%)
Rhabdomyosarcoma	2 (5%)
Hepatocellular Carcinoma	2 (5%)
Wilms Tumor	2 (5%)
High Grade Sarcoma	2 (5%)
Desmoplastic Small Round Cell Tumors	2 (5%)
Clear Cell Meningioma	1 (3%)
Neuroblastoma	1 (3%)
Prior therapies	
Prior systemic regimens, [median (range)]	3 (0-6)
Prior radiotherapy, [N (%)]	28 (73.7%)
Prior lung directed radiotherapy, [N (%)]	14 (36.8%)
Lung Disease at the start of regimen, [N (%)]	27 (71%)

Toxicities and Interventions of Interest

Toxicities related to therapy are summarized in **Table 2**. Thirty-seven (94.8%) of the 39 patients had laboratory evaluations for review. All 39 had clinical documentation for sufficient review of non-hematologic side effects.

The most common Grade 3/4 toxicities (n=23, 62%) were hematologic, including lymphopenia (19, 51%) and leukopenia (13, 35%). No patients experienced Grade 3/4 anemia during their treatment. Two patients (5.1%) required a platelet transfusion during the regimen, including 1 patient who was known to be platelet refractory prior to treatment initiation. One patient (2.7%) required blood transfusion for symptomatic fatigue and tachycardia. Non-hematologic toxicities greater than Grade 2 were infrequent, and included hypertension (n=2, 5.4%), nausea/vomiting, elevated lipase, weight loss, transaminitis and hyperbilirubinemia (each n=1, 2.7% respectively).

Additional treatment-related toxicities of interest included weight loss (Grade 2; n=10, 27%), palmar-plantar erythrodysesthesia (Grade 2; n=16, 43.2%), proteinuria on urine analysis of 2+ or more (n=12, 32.4%), and hematuria (n=2, 5.4%). Four patients with proteinuria and both patients with hematuria had a history of bladder involvement prior to the start of the treatment regimen. One patient with sacral clear cell meningioma had hemorrhagic cystitis resulting in removal from ANGIO1 study after 12 cycles, but then tolerated 18 cycles of therapy with the addition of oral mesna prior to developing disease progression.

Five patients (13.5%) developed a pneumothorax on therapy. Pneumothorax occurring at the time of progressive disease (n=3), following lung biopsy (n=1), and spontaneously (n=1, patient with stable disease following cycle 9). Four of the five pneumothoraces were asymptomatic Grade, and did not require intervention. One patient with pulmonary progressive disease, had a Grade 2 pneumothorax and required a chest tube placement.

TABLE 2 | Treatment Related Toxicities and Toxicities of Interest.

Grade ≥ 3 Adverse Events	**#N = 37 (%)**
Hematologic	23 (62%)
Lymphopenia	19 (51%)
Leucopenia	13 (35%)
Neutropenia	7 (19%)
Thrombocytopenia	6 (16%)
Non-Hematologic	
Hypertension	2 (5.4%)
Emesis	1 (2.7%)
Elevated Lipase	1 (2.7%)
Weight Loss	1 (2.7%)
Transaminitis	1 (2.7%)
Hyperbilirubinemia	1 (2.7%)
Toxicities of Interest	
Weight Loss Grade 2	10 (27%)
Palmar-plantar erythrodysesthesia	16 (43.2%)
Grade 2	
Urine Protein ≥ 2+ on urine analysis	12 (32.4%)
Pneumothorax ≤ Grade 2	5 (13.5%)
Hematuria ≥ Grade 2	2 (5.4%)

#Two patients from cohort not included due to unreliable complete toxicity data.

Six of the 39 patients were previously treated on the phase 1 expansion cohort but were removed from the study and received ANGIO1 therapy off study. Their removal from protocol was due to the receipt of radiation therapy (n=1), development of thrombosis (n=1), weight loss (n=2), mixed response (n=1), and increased lipase (n=1). The toxicities for the 6 patients and response of cycles completed on the phase 1 study as well as off study are included in the analysis.

Dose Modifications

Twenty-three (63.9%) patients required a dose reduction of either cyclophosphamide, sorafenib or bevacizumab during therapy. The most common reasons for dose modifications included palmar-plantar erythrodysesthesia (n=13), myelosuppression (n=8) and poor wound healing (n=7). Bevacizumab was held for upcoming surgery or radiotherapy in 3 and 2 patients respectively. Twelve patients experienced proteinuria greater than 2+ on urine analysis, and 6 of these patients experienced delay of day 1 bevacizumab while obtaining a 24-hour urine protein analysis. Formal urine protein:creatinine ratios were obtained in 4 of these patients and revealed Grade > 2 proteinuria in 3 patients. None of the patients required discontinuation of bevacizumab for this indication. Three patient's treatment regimens included the addition of oral mesna due to a prior hemorrhagic cystitis. All patients who required a dose modification or delay in therapy continued to experience a clinical response following the dose modification.

Tolerability

The majority of patients had zero unplanned hospital admissions (median 0, range 0-3) or greater than 1 clinic visit per 21-day cycle (median 0, range 0-7). A single patient experienced 7 unplanned clinic visits over the duration of 30 cycles of anti-angiogenic therapy, for nausea and recurrent urinary trat infections (sacral tumor and bladder involvement). A total of 297 cycles of therapy were administered to the 39 patients with a total of 8 hospitalizations and 33 unplanned clinic visits due to treatment related toxicities. The reasons for discontinuing therapy was progressive disease (n=34), enrollment on a phase I study (n=2), toxicities (n=2; fatigue, nausea and vomiting), and transfer to an outside hospital (n=1).

Disease Response

The best response and treatment course for patients including timing of best response, progression, and total number of cycles treated on therapy is shown in **Table 3**. **Figure 1** demonstrates the response data of all patients with osseous sarcomas and select solid tumor diagnoses who demonstrated a clinical response greater than or equal to stable disease. Unique events including breaks in therapy, disease progression, or dose adjustments are included. Description of drug dose adjustments and rationale are described in detail in **Supplementary Table 1**.

Twenty-three patients had a clinical response including 3 with a partial response or better. One patient, a 16-year-old with non-metastatic Ewing sarcoma of the right tibia treated with standard systemic chemotherapy and limb sparing surgery developed pulmonary recurrence a year and a half off therapy. The patient received 3 additional systemic therapies, surgery and whole-lung irradiation prior to the angiogenic treatment regimen. The patient achieved a complete response following 11 cycles of therapy and then developed disease progression after cycle 14, in the setting of poor compliance with oral cyclophosphamide and sorafenib. Two patients (Ewing sarcoma and high-grade glioma) achieved a partial response following cycles 2 and 4, respectively. Twenty patients had stable disease (median 8 cycles, range 1-46) of which 14 were bone sarcomas. Five of seven patients (71%) with osteosarcoma achieved stable disease and 11 of 14 patients (79%) with Ewing sarcoma achieved stable disease or better. The median duration of therapy for all patients was 4 cycles (range 1-46). The median duration of therapy for patients with bone tumors was 7 cycles (range 1-46). Progression occurred at a median time of 4 cycles (range 1-46) for the total cohort and at 6 cycles (range 2-46) for bone tumors. The median duration of days to death was 290 (35-1419) for all patients, and 385 (97-845) for patients with bone tumors.

TABLE 3 | Treatment Duration and Best Response.

Treatment Course	Median (range)
All Diagnoses	*N=39*
Cycles to best response	2 (1-11)
Cycles to progression	4 (1-46)
Cycles on therapy	4 (1-46)
Time to death (days)	290 (35-1419)
Bone Sarcomas	*N=21*
Cycles to best response	2 (1-11)
Cycles to progression	6 (2-46)
Cycles on therapy	7 (1-46)
Time to death (days)	385 (97-845)
Best Response	N (%)
All Diagnoses	*N=39*
Complete Response	1 (2.6%)
Partial Response	2 (5.1%)
Stable Disease	20 (51.3%)
Progressive Disease	16 (41%)
Bone Sarcomas	*N=21*
Complete Response	1 (4.7%)
Partial Response	1 (4.7%)
Stable Disease	14 (66.7%)
Progressive Disease	5 (23.9%)

Two patients are alive to date, including a patient with hepatocellular carcinoma and a patient with Ewing sarcoma. The patient with hepatocellular carcinoma received 2 cycles and discontinued therapy for surgical resection. The patient with Ewing sarcoma experienced multiple dose modifications throughout the course of treatment including delays and holding of medications for toxicities. Whenever the medications were delayed or held for periods of time, the patient would develop disease progression which would then resolve after ANGIO1 therapy resumed. The patient received a total of 46 cycles before developing disease progression while receiving the treatment regimen.

DISCUSSION

Angiogenesis is an important clinical target for the treatment of patients with relapsed and refractory solid tumors. This

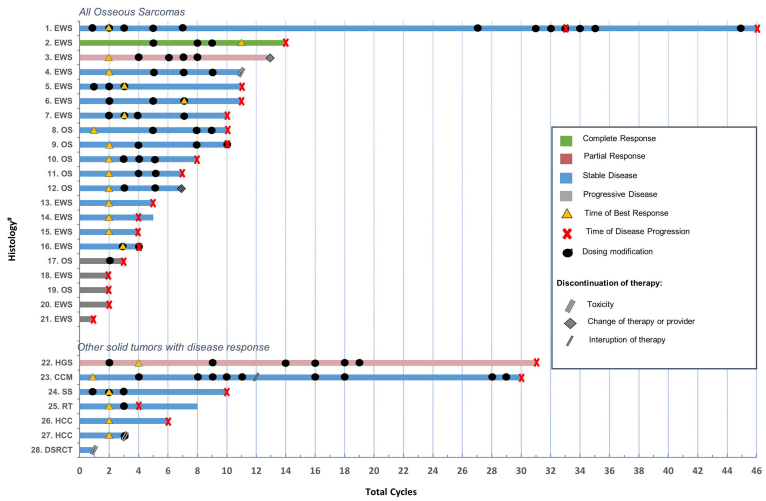

FIGURE 1 | Description of treatment duartion, clinical course, timing of dosing modifications, best response, disease progression of all osseous sarcomas and additional solid tumors with response (≥SD). *Details regarding dosing modifications and unique variables is further described for each case in **Supplementary Materials**. #EWS, Ewing sarcoma; OS, osteosarcoma; HGS, high grade sarcoma; CCM, clear cell meningioma; SS, synovial sarcoma; RT, rhabdoid tumor; HCC, hepatocellular carcinoma; DSRCT, desmoplastic small round cell tumors.

retrospective review of a cohort of 39 heavily pre-treated pediatric and young adult patients with relapsed and refractory solid tumors demonstrated that the anti-angiogenic regimen including intravenous bevacizumab and oral sorafenib combined with oral metronomic cyclophosphamide was tolerated and demonstrated clinical benefit in multiple tumors including high grade sarcoma, clear cell meningioma, synovial sarcoma, rhabdoid tumor, hepatocellular carcinoma, and desmosplastic small round cell tumor. However, particular benefit was noted in a subset of patients, most notably, those with bone tumors.

Studies evaluating anti-angiogenic therapies for the treatment of osteosarcoma and Ewing sarcoma have demonstrated variable clinical responses and need further investigation (6). Numerous agents targeting angiogenesis, including multiple tyrosine kinase inhibitors, have been evaluated for the treatment of osteosarcoma. Although bevacizumab demonstrated preclinical responses in osteosarcoma, single agent bevacizumab in the clinical setting did not increase survival (14). However, combination studies including bevacizumab have had variable results, with some studies demonstrating clinical benefit (15), and others without benefit (16, 17). Sorafenib has demonstrated activity *in vitro* and *in vivo* preclinical models of osteosarcoma with decreased tumor volume and lung metastasis following drug exposure (18). In a phase II study, single agent sorafenib led to improved progression free survival (PFS) in select patients with osteosarcoma (19, 20). In addition to sorafenib, numerous other multi-targeted tyrosine kinase inhibitors (MTKIs) have also been investigated (6). Although pazopanib demonstrated activity against osteosarcoma in preclinical studies, it failed to prevent progression in the clinical setting (21–23). Regorafenib demonstrated improved PFS in adults with osteosarcoma in two randomized control trials (24, 25) and in the CABONE study cabozantinib demonstrated a 33% longer PFS in 37% of patients with osteosarcoma (26). Numerous additional studies evaluating combinations of MTKIs with systemic chemotherapies are ongoing, yet the most effective antiangiogenic regimen have yet to be identified (6). Clinical response was demonstrated in a phase 2 trial of sorafenib and everolimus for patients with high-grade progressive osteosarcoma; however, this combination had toxic effects leading to interruptions of therapy or dose reductions in 66% of patients, highlighting the difficulty with the toxic therapeutic window (27).

While prior preclinical studies indicated that VEGF-A and PDGF were promising therapeutic targets for Ewing sarcoma, few studies evaluating antiangiogenic regimens have been conducted in this patient population. Numerous case reports and small case series have reported variable responses to therapy. Case reports using a regimen containing bevacizumab, vincristine, irinotecan, and temozolomide reported 3 patients with clinical responses including complete remission, partial response, and disease stabilization (16, 28). Another positive single case study reported prolonged remission following maintenance therapy with pazopanib in a patient with metastatic disease (29). Alternatively, other antiangiogenic regimens have produced negative responses including bevacizumab combined with gemcitabine and docetaxel (30), single agent axitinib (31) and single agent imatinib (30, 32).

Many patients experienced significant clinical benefit following administration of ANGIO1 therapy. In our treatment cohort, 16 (76.2%) of 21 patients with relapsed osseous sarcomas demonstrated a response of stable disease or better. These results are consistent with prior studies demonstrating anti-angiogenic therapeutic responses in osseous tumors (6, 7, 10). Additionally, seven patients with non-osseous disease demonstrated stable disease or better. Four of these diagnoses included synovial

sarcoma, high-grade sarcoma, desmoplastic small round cell tumor (DSRCT) and rhabdoid tumor. Although these are rare cancer diagnoses, patients with relapsed synovial sarcoma have demonstrated prolonged response when treated with pazopanib as a single agent (33). Additionally, some patients with DSRCT and non-rhabdomyosarcoma soft tissue sarcomas have demonstrated partial response and disease stabilization, to anti-angiogenic therapy (34, 35). DSRCT has also been shown to demonstrate clinical response when pazopanib is used in combination with other systemic drugs such as vincristine and irinotecan (35).

The final 3 patients who demonstrated clinical benefit in the cohort included 2 with hepatocellular carcinoma (HCC) and one with a clear cell meningioma. HCC tumors are known to be hypervascular and have dysregulated angiogenic pathways (36). In the adult setting, one trial demonstrated an increased survival of 2.8 months over placebo when using single agent sorafenib in patients with advanced HCC (36, 37). Further, regorafenib has been utilized in patients with HCC who have failed or progressed while on treatment with sorafenib and has demonstrated survival benefit to those patients (38, 39).

The 39 patients who received the antiangiogenic regimen required minimal supportive care, with many patients experiencing prolonged periods of disease stabilization. Although more than half of the patient required dose reductions for toxicity, patients did not experience unexpected hospital admissions, clinic visits, or increased transfusions. While the most common toxicities experienced by patients were hematologic, importantly these patients did not require significant transfusions or admissions for febrile neutropenia. Thirty-four of 39 patients had zero hospital admissions while receiving the therapeutic regimen. Approximately half of the patients only required one clinic visit every 21 days to receive the IV bevacizumab. Furthermore, of the 19 patients that had an unplanned visit, 11 required only 1 extra clinic visit throughout the total duration of treatment.

Clinically significant non-hematologic toxicities were rare, most commonly including palmar-plantar erythrodysesthesia and pneumothorax. Those experiencing palmar-plantar erythrodysesthesiadid not have interference with their daily functioning and all had improved symptoms with dose modifications or treatment with emollients. Although pneumothorax was previously described in the phase 1 of this regimen as a common occurrence in 25% of patients (13, 40), the rate of pneumothorax in this cohort was lower at 12.8% and most frequently occurred at the time of disease progression (n=3). The significance of this is unclear due to several study limitations, including sample size, numerous cancer diagnoses and variable prior treatment regimens. Further evaluation will be necessary and would be best evaluated in a randomized trial.

There are numerous clinical applications of this treatment regimen that may benefit patients going forward. First, the clinical benefit of stable disease or better in conjunction with manageable toxicities and a decreased need of frequent medical visits makes this an appealing palliative regimen. Additionally, for patients who reside in countries with limited access to supportive care, this therapeutic treatment may be beneficial when compared to the side effect profiles of cytotoxic chemotherapeutic regimens (6). Finally, the signal of activity demonstrated in bone sarcomas suggests that it may be beneficial in if incorporated in an upfront regimen, either in combination with other cytotoxic chemotherapies or as a maintenance regimen, such as that currently done as standard of care with neuroblastoma and rhabdomyosarcoma (41, 42). Further studies with larger sample sizes and randomized controls need to be conducted for all anti-angiogenic regimens in the future to best evaluate the utility of the therapies being studied, as well as determine the best therapeutic schedule.

DATA AVAILABILITY STATEMENT

The original contributions presented in the study are included in the article/**Supplementary Material**. Further inquiries can be directed to the corresponding author.

ETHICS STATEMENT

The studies involving human participants were reviewed and approved by the St. Jude Children's Research Hospital Institutional Review Board. Written informed consent from the participants' legal guardian/next of kin was not required to participate in this study in accordance with the national legislation and the institutional requirements.

AUTHOR CONTRIBUTIONS

JB, SF, and KC contributed to conception and of the study. JB organized the database and performed the statistical analysis. JB wrote the first draft of the manuscript. JB and SF wrote sections of the manuscript. All authors contributed to manuscript revision, read, and approved the submitted version.

FUNDING

This research was supported by St. Jude Children's Research Hospital. Supported in part by Cancer Center Grant CA23099 and Cancer Center Support CORE Grant P30 CA 21765 from the National Cancer Institute and by the American Lebanese Syrian Associated Charities.

SUPPLEMENTARY MATERIAL

The Supplementary Material for this article can be found online at: https://www.frontiersin.org/articles/10.3389/fonc.2022.864790/full#supplementary-material

REFERENCES

1. Smith MA, Altekruse SF, Adamson PC, Reaman GH, Seibel NL. Declining Childhood and Adolescent Cancer Mortality. *Cancer* (2014) 120(16):2497–506. doi: 10.1002/cncr.28748
2. Perkins SM, Shinohara ET, DeWees T, Frangoul H. Outcome for Children With Metastatic Solid Tumors Over the Last Four Decades. *PloS One* (2014) 9 (7):e100396. doi: 10.1371/journal.pone.0100396
3. Yang JC, Haworth L, Sherry RM, Hwu P, Schwartzentruber DJ, Topalian SL, et al. A Randomized Trial of Bevacizumab, an Anti-Vascular Endothelial Growth Factor Antibody, for Metastatic Renal Cancer. *N Engl J Med* (2003) 349(5):427– 34. doi: 10.1056/NEJMoa021491
4. Pujade-Lauraine E, Hilpert F, Weber B, Reuss A, Poveda A, Kristensen G, et al. Bevacizumab Combined With Chemotherapy for Platinum-Resistant Recurrent Ovarian Cancer: The AURELIA Open-Label Randomized Phase III Trial. *J Clin Oncol* (2014) 32(13):1302–8. doi: 10.1200/JCO.2013.51.4489
5. Hurwitz H, Fehrenbacher L, Novotny W, Cartwright T, Hainsworth J, Heim W, et al. Bevacizumab Plus Irinotecan, Fluorouracil, and Leucovorin for Metastatic Colorectal Cancer. *N Engl J Med* (2004) 350(23):2335–42. doi: 10.1056/NEJMoa032691
6. Ollauri-Ibáñez C, Astigarraga I. Use of Antiangiogenic Therapies in Pediatric Solid Tumors. *Cancers (Basel)* (2021) 13(2):253. doi: 10.3390/cancers13020253
7. Glade Bender JL, Adamson PC, Reid JM, Xu L, Baruchel S, Shaked Y, et al. Phase I Trial and Pharmacokinetic Study of Bevacizumab in Pediatric Patients With Refractory Solid Tumors: A Children's Oncology Group Study. *J Clin Oncol* (2008) 26:399–405. doi: 10.1200/JCO.2007.11.9230
8. Widemann BC, Kim A, Fox E, Baruchel S, Adamson PC, Ingle AM, et al. A Phase I Trial And Pharmacokinetic Study of Sorafenib In Children With Refractory Solid Tumors or Leukemias: A Children's Oncology Group Phase I Consortium Report. *Clin Cancer Res.* (2012) 18(21):6011–22. doi: 10.1158/1078-0432.CCR-11-3284
9. Bolis G, Bortolozzi G, Carinelli G, D'Incalci M, Gramellini F, Morasca L, et al. Low-Dose Cyclophosphamide Versus Adriamycin Plus Cyclophosphamide in Advanced Ovarian Cancer. A Randomized Clinical Study. *Cancer Chemother Pharmacol* (1980) 4:129–32. doi: 10.1007/BF00254034
10. Casanova M, Ferrari A, Bisogno G, Merks JH, De Salvo GL, Meazza C, et al. Vinorelbine and Low Dose Cyclophosphamide in the Treatment of Pediatric Sarcomas: Pilot Study for the Upcoming European Rhabdomyosarcoma Protocol. *Cancer* (2004) 101:1664–71. doi: 10.1002/cncr.20544
11. Kieran MW, Turner CD, Rubin JB, Chi SN, Zimmerman MA, Chordas C, et al. A Feasibility Trial of Antiangiogenic (Metronomic) Chemotherapy in Pediatric Patients With Recurrent or Progressive Cancer. *J Pediatr Hematol Oncol* (2005) 27:573–81. doi: 10.1097/01.mph.0000183863.10792.d4
12. Navid F, Baker SD, McCarville MB, Stewart CF, Billups CA, Wu J, et al. Phase I and Clinical Pharmacology Study of Bevacizumab, Sorafenib, and Low-Dose Cyclophosphamide in Children and Young Adults With Refractory/Recurrent Solid Tumors. *Clin Cancer Res* (2013) 19(1):236–46. doi: 10.1158/1078-0432.CCR-12-1897
13. Federico SM, Caldwell KJ, McCarville MB, Daryani VM, Stewart CF, Mao S, et al. Phase I Expansion Cohort to Evaluate the Combination of Bevacizumab, Sorafenib and Low-Dose Cyclophosphamide in Children and Young Adults With Refractory or Recurrent Solid Tumours. *Eur J Cancer (Oxf Engl 1990)* (2020) 132:35–42. doi: 10.1016/j.ejca.2020.03.010
14. Danieau G, Morice S, Rédini F, Verrecchia F, Royer B.B.-L.B.-L. New Insights About the Wnt/β-Catenin Signaling Pathway in Primary Bone Tumors and Their Microenvironment: A Promising Target to Develop Therapeutic Strategies? *Int J Mol Sci* (2019) 20:3751. doi: 10.3390/ijms20153751
15. Kuo C, Kent PM, Logan AD, Tamulonis KB, Dalton KL, Batus M, et al. Docetaxel, Bevacizumab, and Gemcitabine for Very High Risk Sarcomas in Adolescents and Young Adults: A Single-Center Experience. *Pediatr Blood Cancer* (2017) 64:e26265. doi: 10.1002/pbc.26265
16. Venkatramani R, Malogolowkin M, Davidson TB, May W, Sposto R, Mascarenhas L. A Phase I Study of Vincristine, Irinotecan, Temozolomide and Bevacizumab (Vitb) in Pediatric Patients With Relapsed Solid Tumors. *PloS One* (2013) 8:e68416. doi: 10.1371/journal.pone.0068416
17. Subbiah V, Wagner MJ, McGuire MF, Sarwari NM, Devarajan E, Lewis VO, et al. Personalized Comprehensive Molecular Profiling of High-Risk Osteosarcoma: Implications and Limitations for Precision Medicine. *Oncotarget* (2015) 6:40642–54. doi: 10.18632/oncotarget.5841
18. Pignochino Y, Grignani G, Cavalloni G, Motta M, Tapparo M, Bruno S, et al. Sorafenib Blocks Tumour Growth, Angiogenesis and Metastatic Potential in Preclinical Models of Osteosarcoma Through a Mechanism Potentially Involving the Inhibition of ERK1/2, MCL-1 and Ezrin Pathways. *Mol Cancer* (2009) 8:118. doi: 10.1186/1476-4598-8-118
19. Grignani G, Palmerini E, Dileo P, Asaftei SD, D'Ambrosio L, Pignochino Y, et al. A Phase II Trial of Sorafenib in Relapsed and Unresectable High-Grade Osteosarcoma After Failure of Standard Multimodal Therapy: An Italian Sarcoma Group Study. *Ann Oncol* (2012) 23(2):508–16. doi: 10.1093/annonc/mdr151
20. Raciborska A, Bilska K. Sorafenib in Patients With Progressed and Refractory Bone Tumors. *Med Oncol* (2018) 35(10):126. doi: 10.1007/s12032-018-1180-x
21. Penel-Page M, Ray-Coquard I, Larcade J, Girodet M, Bouclier L, Rogasik M, et al. Off-Label Use of Targeted Therapies in Osteosarcomas: Data From the French Registry OUTC's (Observatoire De L'Utilisation Des Thérapies Ciblées Dans Les Sarcomes). *BMC Cancer* (2015) 15:854. doi: 10.1186/s12885-015-1894-5
22. Umeda K, Kato I, Saida S, Okamoto T, Adachi S. Pazopanib for Second Recurrence of Osteosarcoma in Pediatric Patients. *Pediatr Int* (2017) 59:937–8. doi: 10.1111/ped.13307
23. Czarnecka AM, Synoradzki K, Firlej W, Bartnik E, Sobczuk P, Fiedorowicz M, et al. Molecular Biology of Osteosarcoma. *Cancers* (2020) 12:2130. doi: 10.3390/cancers12082130
24. Duffaud F, Mir O, Boudou-Rouquette P, Piperno-Neumann S, Penel N, Bompas E, et al. Efficacy and Safety of Regorafenib in Adult Patients With Metastatic Osteosarcoma: A Non-Comparative, Randomised, Double-Blind, Placebo-Controlled, Phase 2 Study. *Lancet Oncol* (2019) 20(1):120–33. doi: 10.1016/S1470-2045(18)30742-3
25. Davis LE, Bolejack V, Ryan CW, Ganjoo KN, Loggers ET, Chawla S, et al. Randomized Double-Blind Phase II Study of Regorafenib in Patients With Metastatic Osteosarcoma. *J Clin Oncol* (2019) 37(16):1424–31. doi: 10.1200/JCO.18.02374
26. Italiano A, Mir O, Mathoulin-Pelissier S, Penel N, Piperno-Neumann S, Bompas E, et al. Cabozantinib in Patients With Advanced Ewing Sarcoma or Osteosarcoma (CABONE): A Multicentre, Single-Arm, Phase 2 Trial. *Lancet Oncol* (2020) 21(3):446–55. doi: 10.1016/S1470-2045(19)30825-3
27. Grignani G, Palmerini E, Ferraresi V, D'Ambrosio L, Bertulli R, Asaftei SD, et al. Sorafenib and Everolimus for Patients With Unresectable High-Grade Osteosarcoma Progressing After Standard Treatment: A Non-Randomised Phase 2 Clinical Trial. *Lancet Oncol* (2015) 16(1):98–107. doi: 10.1016/S1470-2045(14)71136-2
28. Wagner L, Turpin B, Nagarajan R, Weiss BD, Cripe T, Geller J. Pilot Study of Vincristine, Oral Irinotecan, and Temozolomide (VOIT Regimen) Combined With Bevacizumab in Pediatric Patients With Recurrent Solid Tumors or Brain Tumors. *Pediatr Blood Cancer* (2013) 60:1447–51. doi: 10.1002/pbc.24547
29. Wachtel M, Schäfer BW. Targets for Cancer Therapy in Childhood Sarcomas. *Cancer Treat Rev* (2010) 36:318–27. doi: 10.1016/j.ctrv.2010.02.007
30. Bond M, Bernstein ML, Pappo A, Schultz KR, Krailo M, Blaney SM, et al. A Phase II Study of Imatinib Mesylate in Children With Refractory or Relapsed Solid Tumors: A Children's Oncology Group Study. *Pediatr Blood Cancer* (2007) 50:254–8. doi: 10.1002/pbc.21132
31. Geller J, Fox E, Turpin BK, Goldstein SL, Liu X, Minard CG, et al. A Study of Axitinib, a VEGF Receptor Tyrosine Kinase Inhibitor, in Children and Adolescents With Recurrent or Refractory Solid Tumors: A Children's Oncology Group Phase 1 and Pilot Consortium Trial (ADVL1315). *Cancer* (2018) 124:4548–55. doi: 10.1002/cncr.31725
32. Tamura A, Yamamoto N, Nino N, Ichikawa T, Nakatani N, Nakamura S, et al. Pazopanib Maintenance Therapy After Tandem High-Dose Chemotherapy for Disseminated Ewing Sarcoma. *Int Cancer Conf J* (2019) 8:95–100. doi: 10.1007/s13691-019-00362-w
33. Casanova M, Basso E, Magni C, Bergamaschi L, Chiaravalli S, Carta R, et al. Response to Pazopanib in Two Pediatric Patients With Pretreated Relapsing Synovial Sarcoma. *Tumor* (2017) 103:e1–3. doi: 10.5301/tj.5000548
34. Menegaz BA, Cuglievan B, Benson J, Camacho P, Lamhamedi-Cherradi S, Leung CH, et al. Clinical Activity of Pazopanib in Patients With Advanced

Desmoplastic Small Round Cell Tumor. *Oncology* (2018) 23:360–6. doi: 10.1634/theoncologist.2017-0408
35. Russo I, di Paolo V, Crocoli A, Mastronuzzi A, Serra A, di Paolo PL, et al. A Chart Review on the Feasibility and Safety of the Vincristine Irinotecan Pazopanib (VIPaz) Association in Children and Adolescents With Resistant or Relapsed Sarcomas. *Front Oncol* (2020) 10:1228. doi: 10.3389/fonc.2020.01228
36. Morse MA, Sun W, Kim R, He AR, Abada PB, Mynderse M, et al. The Role of Angiogenesis in Hepatocellular Carcinoma. *Clin Cancer Res* (2019) 25 (3):912–20. doi: 10.1158/1078-0432.CCR-18-1254
37. Llovet JM, Ricci S, Mazzaferro V, Hilgard P, Gane E, Blanc JF, et al. Sorafenib in Advanced Hepatocellular Carcinoma. *N Engl J Med* (2008) 359(4):378–90. doi: 10.1056/NEJMoa0708857
38. Bender JG, Lee A, Reid JM, Baruchel S, Roberts T, Voss SD, et al. Phase I Pharmacokinetic and Pharmacodynamic Study of Pazopanib in Children With Soft Tissue Sarcoma and Other Refractory Solid Tumors: A Children's Oncology Group Phase I Consortium Report. *J Clin Oncol* (2013) 31:3034–43. doi: 10.1200/JCO.2012.47.0914
39. Okada K, Nakano Y, Yamasaki K, Nitani C, Fujisaki H, Hara J. Sorafenib Treatment in Children With Relapsed and Refractory Neuroblastoma: An Experience of Four Cases. *Cancer Med* (2016) 5:1947–9. doi: 10.1002/cam4.784
40. Interiano RB, McCarville MB, Wu J, Davidoff AM, Sandoval J, Navid F. Pneumothorax as a Complication of Combination Antiangiogenic Therapy in Children and Young Adults With Refractory/Recurrent Solid Tumors. *J Pediatr Surg* (2015) 50(9):1484–9. doi: 10.1016/j.jpedsurg.2015.01.005
41. Bisogno G, De Salvo GL, Bergeron C, Gallego Melcón S, Merks JH, Kelsey A, et al. Vinorelbine and Continuous Low-Dose Cyclophosphamide as Maintenance Chemotherapy in Patients With High-Risk Rhabdomyosarcoma (RMS 2005): A Multicentre, Open-Label, Randomised, Phase 3 Trial. *Lancet Oncol* (2019) 20(11):1566–75. doi: 10.1016/S1470-2045(19)30617-5
42. McGinty L, Kolesar J. Dinutuximab for Maintenance Therapy in Pediatric Neuroblastoma. *Am J Health Syst Pharm* (2017) 74(8):563–7. doi: 10.2146/ajhp160228

Conflict of Interest: The authors declare that the research was conducted in the absence of any commercial or financial relationships that could be construed as a potential conflict of interest.

Publisher's Note: All claims expressed in this article are solely those of the authors and do not necessarily represent those of their affiliated organizations, or those of the publisher, the editors and the reviewers. Any product that may be evaluated in this article, or claim that may be made by its manufacturer, is not guaranteed or endorsed by the publisher.

frontiers | Frontiers in Oncology

REVIEW
published: 08 June 2022
doi: 10.3389/fonc.2022.854973

Murine Models of Acute Myeloid Leukemia

Kristen J. Kurtz[1†], *Shannon E. Conneely*[1†], *Madeleine O'Keefe*[1], *Katharina Wohlan*[2] *and Rachel E. Rau*[1*]

[1] Department of Pediatrics, Baylor College of Medicine, Texas Children's Hospital, Houston, TX, United States,
[2] Department of Molecular and Cellular Biology, Baylor College of Medicine, Houston, TX, United States

Acute myeloid leukemia (AML) is a phenotypically and genetically heterogeneous hematologic malignancy. Extensive sequencing efforts have mapped the genomic landscape of adult and pediatric AML revealing a number of biologically and prognostically relevant driver lesions. Beyond identifying recurrent genetic aberrations, it is of critical importance to fully delineate the complex mechanisms by which they contribute to the initiation and evolution of disease to ultimately facilitate the development of targeted therapies. Towards these aims, murine models of AML are indispensable research tools. The rapid evolution of genetic engineering techniques over the past 20 years has greatly advanced the use of murine models to mirror specific genetic subtypes of human AML, define cell-intrinsic and extrinsic disease mechanisms, study the interaction between co-occurring genetic lesions, and test novel therapeutic approaches. This review summarizes the mouse model systems that have been developed to recapitulate the most common genomic subtypes of AML. We will discuss the strengths and weaknesses of varying modeling strategies, highlight major discoveries emanating from these model systems, and outline future opportunities to leverage emerging technologies for mechanistic and preclinical investigations.

Keywords: acute myeloid leukemia, AML, transgenic mouse, genetically engineered mice (GEM), core binding factor acute myeloid leukemia, KMT2a (MLL) rearrangements, NUP98 fusion, patient-derived xenograft (PDX)

OPEN ACCESS

Edited by:
Paraskevi Panagopoulou, Aristotle University of Thessaloniki, Greece

Reviewed by:
Stefan Heinrichs, Essen University Hospital, Germany
Ilaria Iacobucci, St. Jude Children's Research Hospital, United States

****Correspondence:***
Rachel E. Rau
Rachel.rau@bcm.edu

[†]These authors have contributed equally to this work and share first authorship

Specialty section:
This article was submitted to Pediatric Oncology, a section of the journal Frontiers in Oncology

Received: *14 January 2022*
Accepted: *16 May 2022*
Published: *08 June 2022*

Citation:
Kurtz KJ, Conneely SE, O'Keefe M, Wohlan K and Rau RE (2022) Murine Models of Acute Myeloid Leukemia. Front. Oncol. 12:854973. doi: 10.3389/fonc.2022.854973

1 INTRODUCTION

Acute myeloid leukemia (AML) is a heterogeneous hematologic malignancy. The heterogeneity of AML has been understood for as long as the disease has been described and led to efforts to categorize the disease into similarly behaving subgroups (1). The earliest divisions were based on microscopic visualization. Perhaps the most well-known is the French-American-British classification system, first outlined in 1976. This system divided AML into eight subtypes based on morphology and cytochemical properties of leukemic blasts.

Advances in chromosome banding visualization techniques in the 1970s allowed for the first identification of genetic changes associated with AML. Several common, non-random cytogenetic abnormalities were found to correlate with clinical behavior, morphology, and patient outcomes with high predictability (2). These patterns included: favorable survival with inv (16) and t (8;21), increased early hemorrhage with t (15;17), and correlation of the poor-prognosis monosomy 5/7 or

del 5q/7q with history of previous malignancy or carcinogenic exposures. Though not known at the time if these changes were drivers of or resulting from leukemia, these correlations provided some of the earliest evidence that the clinical heterogeneity of AML may be explained by underlying genetic heterogeneity.

It is now understood that approximately 55% of adult AML and 75% of pediatric AML is driven by a cytogenetic aberration (3–5). Presently, assessment of cytogenetic abnormalities is performed by karyotyping and fluorescent *in situ* hybridization for specific recurrent rearrangements of clinical significance (6). There are currently seven subclasses of AML that are defined by their translocations or inversions as defined by the World Health Organization (7). The most common are the same that were first identified in the 1970s. Now known as core binding factor (CBF) leukemias, those with t(8;21)(q22;q22) with resulting *RUNX1-RUNX1T1* fusion (formerly *AML1*-ETO) and inv(16)(p13q22)/t(16;16)(p13;q22) with resulting *CBFB-MYH11* fusion gene carry favorable prognoses. CBF AML is more prevalent in the pediatric population, estimated at 20-25% compared to 13% of AML in adults (4, 6). Acute promyelocytic leukemia (APL) defined by t(15;17) (q24;21) and resulting in a *PML-RARA* fusion comprises about 13% of adult and 10% of pediatric AML cases (4, 6). APL is associated with severe, sometimes life-threatening, coagulopathy at presentation. Prompt treatment with all-*trans* retinoic acid is critical to preventing early death during this high-risk time. With early recognition and treatment, survival is excellent for patients with APL, with long term remission rates as high as 85-90% (6). Monosomy 5/7 or del 5q/7q are rare and typically confer poor prognosis. Though estimated to represent only 4% of adult AML, *KMT2A* rearrangements (*KMT2A*r) are found in 20% of pediatric AML and are especially common in the infant population (4). The prognosis of *KMT2A*r AML depends on the fusion partner, over 100 of which have been identified, but is often poor (8).

In addition to cytogenetic abnormalities, extensive sequencing efforts have revealed driving gene mutations in nearly all cases of AML (6, 9–13). The mutational landscape of pediatric AML differs from that in adults, and though mutational burden increases with age overall AML has one of the lowest mutational rates amongst malignancies (13, 14). In adults the most commonly mutated genes include *fms-like tyrosine kinase* 3 (*FLT3)*, *nucleophosmin 1* (*NPM1)*, and *DNA methyltransferase 3A* (*DNMT3A)*, each occurring in approximately one third of patients (10, 12, 13, 15). While *FLT3* mutations also occur in about 30% of pediatric AML cases, *NPM1* is seen in only 10% of pediatric patients and *DNMT3A* mutations are almost never identified (13, 16–18). Along with *FLT3*, other signaling pathway-affecting mutations such as Ras pathway mutations (*NRAS, KRAS, HRAS, NF1, CBL* and *PTPN11)* and *KIT* are some of the most common in pediatric AML, and less commonly seen in adults (6, 10, 12, 13).

Many mutations have prognostic implications, and some may represent therapeutic targets. For example, *FLT3* mutations most often confer poor prognosis, depending on the allelic fraction and co-occurring mutations. Importantly, *FLT3* is a targetable tyrosine kinase receptor. The addition of *FLT3*-targeting tyrosine kinase inhibitors has significantly improved the outcome of these patients (3). *DNMT3A*, along with other methylation associated genes including *TET2*, *IDH1*, and *IDH2*, have been associated with poor prognosis in adults but are infrequently found in children (16). Each newly identified driver mutation presents the opportunity for targeted treatment with Food and Drug Administration approval of IDH inhibitors as a recent example.

Our understanding of the genomic landscape of AML continues to expand. Ongoing investigations are focused on co-occurring mutations and their effects on patient outcomes and responses to treatment. Much has been uncovered over the last several decades, and much remains to be discovered. To adequately address these remaining questions, in addition to rigorous clinical investigations of large, uniformly-treated patient populations, the availability of faithful model systems will be essential. While not all encompassing, here we will review several recent murine models selected for their relevance to human AML, with similar genetic lesions modeled, characteristic disease phenotypes, and that have advanced AML research over the last several decades. Additionally, we have included papers that highlight a spectrum of techniques used to generate murine model systems to allow for comparison of the advantages and disadvantages of each strategy that may aid in selecting the appropriate model system to address a specific research question.

2 HISTORY OF MOUSE MODELING HEMATOLOGIC MALIGNANCY

The goals of biomedical research of leukemia include predicting disease behavior to subclassify and risk stratify and developing or refining therapies to achieve the best efficacy. Animal models of human disease are vital to understanding disease pathogenesis and development of novel therapeutic strategies. The mouse (*Mus musculus*) is the most widely used animal model of human disease because of its genetic and physiologic similarity to humans. Humans and mice share approximately 80% of their genes with conservation of tissue-specific gene expression across species (19, 20). They also have remarkably similar organ systems. Other advantages to murine model systems include their small size, short lifespan, and rapid breeding, making them ideal models for scientific research. Murine hematopoiesis has been well-characterized over the years such that the similarities and differences to human hematopoiesis can be considered when creating and interpreting mouse models of leukemia.

When using murine models, it is crucial that each model be validated and evaluated for its similarities and potential differences to human disease. Some mouse strains harbor characteristic background lesions or are prone to diseases that are related to mouse biology rather than the model of human disease they are meant to represent. These details must be teased out so as not to attribute unrelated sequelae to the model of human disease. Differences in the human and murine genome as well as differences in hematopoiesis, aging and general development may impact the evolution and behavior of

leukemia within the mouse model and must be considered. There are innate differences in hematopoiesis between humans and mice that may influence interpretation of mouse models. For example, mice exhibit lymphocyte predominance in the circulating leukocyte population while humans exhibit neutrophil predominance (21). There may also be subtle differences in the hematopoietic niche that affect leukemia development and progression that are unidentified and should be considered when interpreting results from mouse models.

The earliest mouse models of leukemia were created *via* exposure to external carcinogens. These included carcinogenic chemicals, irradiation, and viruses. The first transplantable leukemic mouse cell lines (L1210 and p388) were isolated from DBA/2 mice following exposure to 3-methylcholantrene (22, 23). These mouse models were highly valuable for exploring drug efficacy and developing strategies to overcome drug resistance (24). However, such chemically induced models can be inefficient and imprecise when used to recapitulate a specific malignant process and more often resulted in lymphoblastic rather than myeloid leukemia (25–27). Once the link between radiation and leukemia was established from observational studies involving individuals exposed to excessive radiation from nuclear attacks, the RF mouse model of myeloid leukemia was created *via* exposure to ionizing radiation (28). While this method effectively mirrored an actual environmental trigger and subsequent leukemic process to establish this causal relationship, there was a 6–8-month latency to leukemia onset and a low incidence of leukemia in the exposed mice, rendering it inefficient to create a robust cohort of leukemic mice for further study. Alternatively, viruses have been used to induce a more efficient animal model of leukemia. Murine leukemia viruses (MuLV) are retroviruses that have been used to induce myeloid leukemias in mice with a relatively short latency since the 1950s (29–31). Virally-induced mouse models of AML led to important discoveries of previously unknown oncogenes and the underlying pathogenesis of leukemia (32–34).

Gene editing has recently revolutionized the way in which mouse models of leukemia are generated. Advancements during the 1970-80s introduced techniques that allowed scientists to deliver engineered genetic material into the murine genome, thus creating transgenic mouse models. As advancements in high-throughput sequencing led to a wealth of new data on the genetic underpinnings of hematologic malignancy, gene editing paved the way for novel animal models of these newly defined genetic subtypes of disease. This led to more precise models that better mimicked the progression and behavior of subgroups of human leukemias. These techniques were first used to introduce proto-oncogenes under the control of a constitutively activated promoter to define their role in leukemogenesis in the 1980s (35, 36). Since then, the field of gene editing has advanced significantly to allow for a variety of constitutive and inducible models that can be integrated to more precisely recapitulate leukemogenesis.

3 MOUSE MODELS OF AML FUSIONS

Classic cytogenetic rearrangements found in AML are associated with the generation of fusion genes which demonstrate altered function compared to their wild-type components (**Table 1**). Here, we will review murine models used to study these classic fusion genes as well as newly described fusion genes not identified *via* standard cytogenetic testing.

4 Core Binding Factor Leukemias

CBF AML encompasses patients with t(8;21) or inv(16) cytogenetic rearrangements or their associated fusion genes, *RUNX1-RUNX1T1* and *CBFB-MYH11*, respectively (54). The chimeric proteins which result from CBF AML fusion genes function as dominant negative inhibitors of the CBF transcription factor, composed of RUNX1 and CBFβ, which are essential for normal myeloid cell development. The CBF

TABLE 1 | Mouse models of fusion genes.

Fusion Gene	Year	Expression	Mechanism	Phenotype	References
RUNX1-RUNX1T1	2006	Constitutive	Retrovirus	9a isoform: AML	(37)
	2001	Constitutive	Germline - *Mrp8* promoter (myeloid specific)	AML, T-ALL after ENU treatment	(38)
	2013	Inducible	Tet-On	MDS	(39)
	2021	Inducible	eR1-CreER^{T2}	AML, MPD	(40)
CBFB-MYH11	2006	Inducible	Mx1-Cre	AML	(41)
KMT2A-MLLT3	1996	Constitutive	Germline	AML	(42)
	2000	Inducible	Lmo2-Cre	AML	(43)
	2013	Constitutive	Retrovirus	AML (Transduced LSKs > GMP)	(44)
	2016	Inducible	Retrovirus	AML	(45)
MLL-PTD	2012	Constitutive	Germline	AML (if *FLT3*-ITD mutated)	(46)
KMT2A-MLLT1	2013	Inducible	CreER	ALL	(47)
	2014	Inducible	Tet-On	ALL	(48)
NUP98-NSD1	2020	Constitutive	Retrovirus	AML	(49)
Other *NUP98* fusions	2020	Inducible	Tet-On Retrovirus	AML	(50)
PML-RARA	1997	Constitutive	Germline – *Ctsg* promoter (myeloid specific)	AML – long latency	(51)
	1999	Constitutive	Retrovirus	Differentiation blockade, enhanced self-renewal	(52)
	2003	Constitutive	Germline – *Mrp8* promoter (myeloid specific)	AML	(53)

AML, acute myeloid leukemia; ENU, N-ethyl-N-nitrosurea; GMP, granulocyte-macrophage progenitor; ITD, internal tandem duplication; LSK, Lin$^-$Sca1$^+$Kit$^+$; MDS, myelodysplastic syndrome; MPD, myeloproliferative disease; PTD, partial tandem duplication; T-ALL, T-acute lymphoblastic leukemia.

AML fusion genes are associated with a favorable prognosis and share a common pathogenic mechanism, though *RUNX1-RUNX1T1* and *CBFB-MYH11* driven leukemias are distinct from one another.

Pioneering work from the labs of Drs. Dong Er Zhang, Nancy Speck and others have generated various murine model systems that have enhanced our understanding of this common AML fusion. Initial attempts to model t (8;21) AML utilized a germline knock-in of the *RUNX1-RUNX1T1* fusion gene (55). However, embryonic expression of RUNX1-RUNX1T1proved to be embryonic lethal due to central nervous system hemorrhage and failed hematopoiesis. While this method failed to create a model of t (8;21) leukemia, these early studies helped to establish the role of *RUNX1-RUNX1T1* as an inhibitor of normal RUNX1 function and highlighted the need for alternative murine models with delayed *RUNX1-RUNX1T1* expression.

Current murine models of t (8;21) AML rely on delayed introduction or expression of the *RUNX1-RUNX1T1* fusion through various means (**Figure 1**). One method utilizes retroviral transduction to introduce constitutive expression of *RUNX1-RUNX1T1* from a retroviral vector incorporated into the DNA of a cell of interest. Retroviral expression of the full length 752 amino acid protein in murine hematopoietic stem cells (HSCs) failed to produce leukemia or signs of altered hematopoiesis when transplanted into lethally irradiated recipient mice, however, and led to the conclusion that *RUNX1-RUNX1T1* alone is insufficient for leukemogenesis (56). Yan et al. subsequently identified a splice variant which generates a 575 amino acid protein, termed RUNX1-RUNX1T19a, that is variably expressed in human AML and generates leukemia when transduced into murine fetal liver cells (37). All mice transplanted with RUNX1-RUNX1T19a expressing cells developed leukemia within 16 weeks of transplant. As this is the only retroviral model to establish a t (8;21)-like AML without the addition of cooperating mutations, it is commonly used for *in vivo* modeling of *RUNX1-RUNX1T1* driven disease, though the full-length construct remains the preferred model for *in vitro* experiments.

Transgenic models in which *RUNX1-RUNX1T1* is transcribed in mice only in the presence of specific drivers have also been developed. One example is the *MRP8-AE* mouse in which *RUNX1-RUNX1T1* is expressed in myeloid cells under control of the *MRP8* promoter (38). Consistent with results from retroviral models, these mice remain healthy during their lifetime unless secondary mutations are induced with the alkylating agent *N*-ethyl-*N*-nitrosourea. However, only 55% of leukemia generated *via* this method was AML, while the remaining 45% was T-cell acute leukemia. A recent study published by Abdallah et al. used a model in which the *RUNX1-RUNX1T1* downstream of a lox-stop-lox cassette was knocked-in to the ROSA26 locus such that Cre mediated recombination leads to excision of the stop codon and induced expression of the knocked-in fusion gene in HSCs at varying ages (40). They demonstrated that earlier expression of *RUNX1-RUNX1T1*, as early as postnatal day 3, resulted in a higher AML penetrance and lower incidence of non-AML disease compared to mice where *RUNX1-RUNX1T1* expression was induced at 8-16 weeks of age. This is the only transgenic

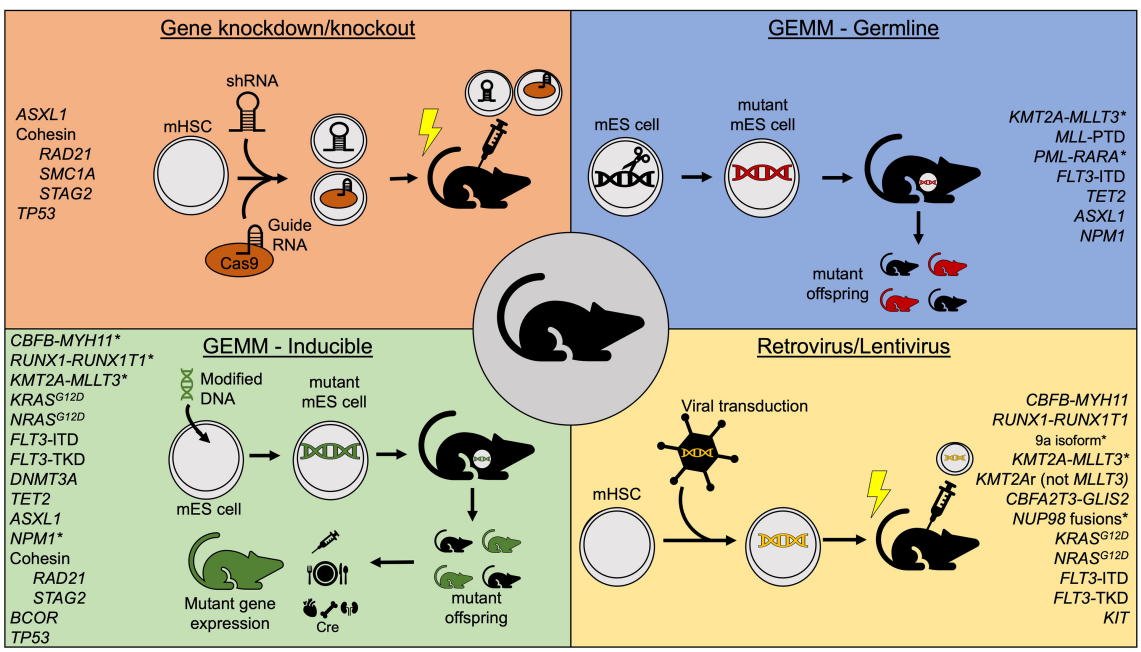

FIGURE 1 | Summary of commonly used mouse model methods to study acute myeloid leukemia. *Indicates models that independently generate leukemia without cooperating mutations. GEMM, Genetically-engineered mouse model; mHSC, murine hematopoietic stem cell; mES, murine embryonic stem cell; shRNA, short hairpin RNA.

model and full-length isoform to consistently produce AML in the absence of other mutations. An alternative model uses a 'tet-On' method to express *RUNX1-RUNX1T1* [ROSA26-iM2-tetrO-GFP/TgPtet-AML1-ETO (*R26/AE*)] (39). *R26/AE* mice that also carry a reverse tetracycline transactivator *(rtTa*) gene will express *RUNX1-RUNX1T1* from a tetracycline-responsive promoter when exposed to doxycycline in their food or water. However, transplantation of bone marrow from *R26/AE rtTa*$^{+/-}$ mice into wild-type recipients is required to isolate expression to hematopoietic cells. Prolonged expression of *RUNX1-RUNX1T1* in this system led to expansion of myeloid progenitor cells and produced myelodysplastic syndrome (MDS) with peripheral blasts without overt leukemia.

Similar to the effects of *RUNX1-RUNX1T1* expression in embryos, germline knock-in of *CBFB-MYH11* is embryonic lethal due to multiple fetal hemorrhages and failed hematopoiesis (57). However, early models showed that induced expression of *CBFB-MYH11* in the hematopoietic system could independently induce leukemia in mice. This was robustly demonstrated by *Kuo* et al. who developed a conditional knock-in of the *Cbfb-Myh11* gene *(CBFB*^{56M}*)* (41). Following induction of Cre recombinase expression in *Mx1-Cre*$^{+}$ *CBFB*^{56M} mice with polyinosinic: polycytidilic acid (pIpC), the fusion gene is knocked in to the native *Cbfb* locus. Treated mice develop AML 11-21 weeks following the fusion gene restoration. This model has been used extensively to characterize inv (16) AML, cooperating mutations, and essential partners in leukemogenesis.

3.2 *KMT2A* Fusions

*KMT2A*r AML poses a particular challenge for mouse modeling strategies, as over 100 different fusion genes are known to partner with *KMT2A* as a result of 11q23 rearrangements (58). Over 90% of *KMT2A*r AML is caused by 9 specific fusions, and the frequency of these fusions varies with patient age. Thus, established murine models represent only the most common *KMT2A* fusions.

KMT2A-MLLT3 (formerly *MLL-AF9)* fusions are the most common KMT2A rearrangement in AML and account for 25-40% of *KMT2A*r AML across all age groups (58). Murine models have all demonstrated that *KMT2A-MLLT3* is a potent oncogene with the ability to induce leukemic transformation. Early studies produced genetically engineered germline *Kmt2a-MLLT3* mutants in which the fusion is expressed in all cells throughout development (42). Although this model did lead to development of AML, or less commonly acute lymphoid leukemia, there are known effects of *Kmt2a* haploinsufficiency during murine development that cannot be controlled using this method, such as anemia, thrombocytopenia, and decreased B-cells (59). Thus, a *Cre-loxP* system was introduced such that intrachromosomal recombination of *Kmt2a and Mllt3* could be induced *via* Cre-mediated recombination (43). Although effective in generating AML when *Kmt2a-Mllt3* recombination was induced in primitive progenitor cells *via* progenitor-specific Cre, *Lmo2-Cre*, off-target expression of Cre recombinases poses concerns regarding specificity for cellular populations of interest (60). This is particularly true in *KMT2A*r AML, where cell of origin can dictate the resultant type of leukemia and gene expression pattern (44).

To restrict expression of *KMT2A-MLLT3* to specific stem and progenitor populations and study the differing effects on each, retroviral transduction of isolated bone marrow stem/progenitor cells with *KMT2A-MLLT3* followed by transplantation has become a popular model. Lineage^{-}Sca-1^{+}Kit^{+} (LSK) cells expressing *KMT2A-MLLT3* are more potent inducers of leukemic transformation than *KMT2A-MLLT3* expressing granulocyte-macrophage progenitors (44). Interestingly, leukemia generated from transduced LSK cells is also more chemoresistant than that originating from granulocyte-macrophage progenitors, is more highly methylated, and carries a gene expression signature associated with poor prognosis in patients with AML (44). Selection of appropriate cell population for retroviral transduction and attendant gene expression is therefore integral to the interpretation of results from *KMT2A*r models and relating them to human AML. One concern regarding retroviral transduction is the possibility of supraphysiologic expression of *KMT2A-MLLT3* which may significantly impact study results. Recently, doxycycline-inducible genetic *KMT2A-MLLT3* models have helped to address these concerns. These models demonstrate dose-dependent expression of *KMT2A-MLLT3* resulting in 10-20-fold lower protein amounts compared to retroviral transduction models, allowing improved control over fusion gene expression (45). As with retroviral models, cells of interest can be isolated and transplanted into recipients, though expression of *KMT2A-MLLT3* can be induced before or after transplantation. These studies have confirmed effects of *KMT2A-MLLT3* expression on different stem and progenitor populations identified from studies using retroviral transduction and demonstrate their utility in future mouse modeling of *KMT2A-MLLT3* AML.

As *KMT2A-MLLT3* is the most common *KMT2A*r fusion gene in AML, it is also the most studied. After *KMT2A-MLLT3*, the next most common fusion partners are *MLLT10, ELL, AFDN, MLLT1*, and *SEPT6* (58). Murine models of these *KMT2A* fusions depend primarily on retroviral transduction of murine HSCs or human hematopoietic cells isolated from cord blood (61–63). As an alternative, immortalized murine cells lines expressing *KMT2A-MLL10* and *KMT2A-ELL* have been created which engraft into syngeneic recipients and cause disease (64, 65). In addition to recurrent *KMT2A* fusions, partial tandem duplications (PTD) of *KMT2A* are also common in adult AML while nearly absent from infant and pediatric cases (58). A germline knock-in model of *Kmt2a*-PTD exists but requires cooperating mutations, such as a *Flt3* internal tandem duplication (ITD), to produce disease (46). Transgenic mouse models of *KMT2A-MLLT1* have also been created and characterized including one which utilizes Cre recombination to induce expression of *KMT2A-MLLT1* and the other with doxycycline-inducible expression of *KMT2A-MLLT1* (47, 66). However, *KMT2A-MLLT1* fusions are much more common in ALL and occur rarely in AML, limiting the use of these models in AML research. Finally, CRISPR/Cas9-mediated genome editing has been used to create a model of *Kmt2a-Mllt3* AML *via* dual

single-guide RNAs simultaneous targeting the breakpoint cluster region of *Kmt2a* and *Mllt3* (67). Unique to *KMT2A*r AML, close attention must be paid to the model system and cell of origin in studying *KMT2A*r disease, as similar *KMT2A* fusions can be found across hematologic malignancies, and selection of methods will have profound effects on the resulting disease.

The development of these varying murine models of *KMT2A*r AML have helped identify potential novel therapeutic strategies for this poor prognosis subset of AML. These include Dr. Katherine Bernt and colleagues' identification of the histone 3, lysine 79 methylase, DOT1L, as a critical dependency and therapeutic vulnerability in *KMT2A*r AML (48). Other investigations have revealed preclinical efficacy of BET bromodomain inhibitors in *KMT2A*r AML (68). Perhaps the most exciting, pioneering work by Dr. Jolanta Grembecka and colleagues has led to the development and validation of inhibitors of the MENIN-MLL interaction as highly promising agents for the treatment of *KMT2A*r leukemias (69). Results from these seminal investigations have led to early phase clinical trials and ultimately could result in meaningful improvements in outcomes for patients with *KMT2A*r AML.

3.4 *NUP98* Fusions

While relatively uncommon in AML, *NUP98* gene fusions carry a dismal prognosis even with stem cell transplant. Thus, establishment of mouse models is a high priority to identify novel treatments for this chemoresistant AML. Retroviral models of *NUP98* fusions have served as the predominant mouse models to date. Mohanty et al. showed that retroviral transduction of *NUP98-NSD1*, the most common *NUP98* fusion in pediatric AML, into murine HSCs followed by transplantation independently produced AML with a median survival of 250 days post-transplant with significant disease acceleration when $NRAS^{G12D}$ is co-expressed. Furthermore, the authors found that upregulation of *Hox* genes, specifically *Hoxa7, Hoxa9*, and *Hoxa10* was a major contributor to disease development, while other studies have demonstrated a dependence on interaction between NUP98-NSD1 and SMARCA5 for leukemic transformation (49, 70). A separate study introduced three different AML-specific *NUP98* fusions (*NUP98-NSD1, NUP98-KDM5A*, and *NUP98-DDX10)* into murine fetal liver cells *via* retrovirus with doxycycline-inducible expression of the fusion gene tagged with GFP (50). Following transplantation into recipient mice and induction with doxycycline, all 3 tested *NUP98* fusions rapidly produced leukemia. This also identified *cyclin-dependent kinase 6* (*CDK6)* as an integral disease driver and that pharmacologic inhibition of *CDK6* could prolong survival in these mice. Interestingly, *CDK6* is also an important driver in *KMT2A*r AML (71). Other murine-based models of *NUP98* fusions suggest that NUP98 fusion proteins interact with MLL1, suggesting a common link between these two genetic AML subtypes (72). *Ex vivo* drug sensitivity assays have also been performed using retroviral transduction models, identifying BRD2/4 inhibitors, topoisomerase II inhibitors, and gemcitabine as effective in *NUP98-KDM5A* AML (73). Finally, Heikamp et al. recently used retroviral transduction of murine hematopoietic cells with *NUP98-HOXA9* or *NUP98-KDM5A* followed by transplantation to generate pre-clinical models which they used to define MENIN-MLL1 inhibition as a potential new treatment strategy for this refractory disease (74). It is important to note that, like *KMT2A*r AML, the cell of origin of gene expression significantly impacts disease phenotype. *NUP98-KDM5A* is often associated with acute erythroid or megakaryoblastic leukemia in patients, but when expressed in mouse HSPCs then transplanted into syngeneic recipients leads to an AML-like myeloid phenotype with blasts expressing the mature myeloid markers, Cd11b and Gr1in transplant models (50, 75).

3.4 *CBFA2T3-GLIS2*

Recent human studies have identified a *CBFA2T3-GLIS2* fusion, resulting from inv (16) (p13.3q24.3), in 27% of pediatric acute megakaryoblastic leukemia (76). This fusion is found in 2% of pediatric AML cases overall but has an event-free survival of less than 20%. As this is both a new and rare entity, murine models have been limited thus far. Retroviral transduction has been used to introduce the fusion into murine HSCs for *in vitro* experiments, which demonstrated increased self-renewal of *CBFA2T3-GLIS2*-expressing cells. However, *in vivo* experiments using these same methods fail to develop leukemia (77). Patient-derived xenografts (PDXs) have been the only method to successfully induce *CBFA2T3-GLIS2*-driven disease and have been the model of choice (78).

3.5 *PML-RARA*

APL, characterized by the *PML-RARA* gene fusion, is a unique disease entity that requires vastly different treatment than standard AML and has significantly superior outcomes. Murine models have been integral to understanding the pathophysiology of APL and critical tools for the development of current targeted treatment strategies. Retroviral transduction models used to express *PML-RARA* in hematopoietic cells demonstrate increased cellular self-renewal and differentiation blockade but fail to generate leukemia when transplanted into recipient mice (52). Transgenic models have therefore become preferred with multiple models available, each with slightly different features. The earliest transgenic models expressed *PML-RARA* under control of sequences that regulate the expression of the human cathepsin G gene in myeloid cells, though leukemia penetrance was low at 30% and disease latency was prolonged (51). This model was improved upon with *PML-RARA* under control of the murine cathepsin G (*MRP8*) promoter, yielding higher expression of the fusion product and 90% leukemia penetrance with continued prolonged disease latency (53). This *MRP8-PML/RARA* model is the predominant model currently used in APL research. However, while AML does occur, differentiation arrest characteristic of APL varies and is less pronounced than in human correlates. Prior efforts have attempted to improve on this model by selectively expressing the fusion in promyelocytes to mimic the suspected origin cell population in human APL but fail to induce leukemia or demonstrate enhanced self-renewal properties of *PML-RARA*-expressing cells despite a distinct gene expression signature (79).

4 MUTATIONS THAT ACTIVATE SIGNAL TRANSDUCTION PATHWAYS

Mutation profiling studies have subsequently identified activating mutations in genes involved in signal transduction pathways as commonly mutated in both adult and pediatric AML and key targetable lesions (**Table 2**). These mutations generally occur at hotspot locations within the gene and are thus ideal to recapitulate with murine models that mimic activation of these pathways. Here we will review the murine models currently used to study these activating mutations.

4.1 Ras Pathway

The Rat Sarcoma virus (Ras) family of genes represents critical regulators of cell proliferation and differentiation and is mutated across a variety of cancers. Activating mutations in Ras family genes including *NRAS, KRAS, NF1, PTPN11* and *CBL* occur in up to 50% of pediatric AML but are less common in adult AML. The predominant model used to study *KRAS* mutations is used in both hematologic and solid malignancies and was originally developed by Dr. Erica Jackson and colleagues as a model for lung cancer (98). This model has lox-stop-lox $Kras^{G12D}$ knocked into the native *Kras* locus leading to expression of mutant *Kras* following Cre recombination. When combined with tissue-specific Cre drivers, the mutation is expressed only in the tissue of interest. Induction of $Kras^{G12D}$ expression in the hematopoietic system *via Mx1-Cre* leads to a rapid and highly penetrant myeloproliferative disease (MPD) but not overt AML (80). Concurrent homozygous loss of *Dnmt3a* cooperates with $Kras^{G12D}$ to accelerate disease progression and leads to development of AML in approximately 30% of mice, though heterozygous loss of *Dnmt3a* had no effect (82). $Kras^{G12D}$ also cooperates with *PML-RARA* to produce malignancy consistent with APL with a short latency of only 37 days (83). Despite the ability to target specific cell populations with tissue-specific Cre drivers, this model has also been used in transplantation experiments where induced bone marrow from primary transgenic mice is transplanted into recipient mice along with supportive bone marrow (81). Interestingly, transplant recipients predominantly develop T-cell leukemia or lymphoma and occasionally juvenile myelomonocytic leukemia in contrast to the MPD described above, thus limiting the use of transplant models to study AML biology (81).

NRAS is another Ras pathway gene that is commonly mutated in AML. As with *KRAS* mutations, *NRAS* mutations are activating mutations that have been modeled using genetic mouse models. When expressed in the hematopoietic system, $Nras^{G12D}$ alone induces a MPD similar to $Kras^{G12D}$ but with significantly longer disease latency and lower penetrance (86). However, $Nras^{G12D}$ cooperates with heterozygous loss of *Dnmt3a* to promote AML development in one third of induced mice (82). As *DNMT3A* mutations are predominantly heterozygous in human disease, this may represent a more biologically relevant model of AML.

Retroviral transduction models of Ras mutants have also been employed to study cooperating mutations in AML. Zhao et al. used co-transduction of $KRAS^{G12D}$ or $NRAS^{G12D}$ and *RUNX1-RUNX1T1* followed by transplantation to demonstrate cooperation between activating Ras mutations and *RUNX1-RUNX1T1* in leukemogenesis (84). Retroviral expression of either $KRAS^{G12D}$ or $NRAS^{G12D}$ alone did not induce leukemia or an identified MPD, yet both cooperated with *RUNX1-RUNX1T1* to accelerate development of AML with *NRAS* serving as a more potent inducer of disease in this context.

TABLE 2 | Mouse models of signal transduction pathways.

Gene Mutation	Year	Expression	Mechanism	Phenotype	References
$Kras^{G12D}$	2004	Inducible	Mx1-Cre	MPD	(80)
	2009	Inducible	Mx1-Cre then transplant	T-ALL/lymphoma, JMML	(81)
+$Dnmt3a^{-/-}$	2015	Inducible	Mx1-Cre	MPD, AML	(82)
+*PML-RARA*	2006	Inducible	Mx1-Cre	APL	(83)
+*RUNX-RUNX1T1*	2014	Constitutive	Retrovirus	AML	(84)
$Nras^{G12D}$	2013	Inducible	Mx1-Cre	MPD	(85)
+$Dnmt3a^{+/-}$	2015	Inducible	Mx1-Cre	MPD/AML	(82)
+*RUNX1-RUNX1T1*	2014	Constitutive	Retrovirus	AML	(86)
KIT	2011	Constitutive	Retrovirus	MPD	(85)
+*CBFB-MYH11*	2012	Constitutive	Retrovirus	Accelerated AML	(87)
+*RUNX1-RUNX1T1*	2011	Inducible	Retrovirus	AML	(85)
FLT3-ITD	2005	Constitutive	Retrovirus	MPD	(88)
	2005	Constitutive	Germline – *Vav* promoter (hematopoietic specific)	MPD	(89)
	2007	Constitutive	Germline	CMML (AML if combined with *KMT2A*-PTD, *Npm1c*, *Dnmt3a, RUNX1-RUNX1T1)*	(46, 90–93)
	2008	Inducible	Mx1-Cre	MPD (AML if combined with *Npm1c* or *WT1*)	(94–96)
FLT3-TKD	2005	Constitutive	Retrovirus	ALL	(88)
D835Y	2014	Constitutive	Germline	MPD	(97)

AML, acute myeloid leukemia; APL, acute promyelocytic leukemia; CMML, chronic myelomonocytic leukemia; JMML, juvenile myelomonocytic leukemia; ITD, internal tandem duplication; MPD, myeloproliferative disease; T-ALL, T-acute lymphoblastic leukemia; TKD, tyrosine kinase domain.

Retroviral expression of $NRAS^{G12D}$ has also been shown to cooperate with loss of *Dnmt3a* in mouse models to generate AML (99). Retroviral expression of Ras mutants may therefore serve as a reasonable method when transplantation models using AML-specific drivers are preferred.

4.2 *KIT*

Tyrosine protein kinase KIT, encoded by the gene *KIT (formerly c-KIT)*, is a proto-oncogene which plays a critical role in signaling pathways that promote cellular proliferation, particularly within HSCs. Activating mutations in *KIT* have been found at several gene loci in patients with AML, and such mutations occur in nearly 40% of patients with CBF AML (100). These mutations are predominantly found in exons 8 and 17 with amino acids D816 and N822 serving as recurrent mutation hotspots. As with other tyrosine kinase activating mutations, studies have shown that activating mutations in *KIT* are not sufficient to cause leukemia but cooperate with other driver mutations to transform leukemic cells. Retroviral transduction of the two recurrent exon 17 *KIT* mutant genes into *CBFB-MYH11*-expressing bone marrow cells shortened survival of transplant recipients compared to those which expressed wild-type *KIT* (87). In a model of t (8;21) AML in which retrovirus expression *KIT* N822 and *RUNX1-RUNX1T1* were co-transduced, expression of the *KIT* mutant alone led to MPD, but overt leukemia was observed when KIT^{N822} was expressed in conjunction with *RUNX1-RUNX1T1* (85).

4.3 *FLT3*

FLT3 is a commonly mutated gene in AML, leading this receptor tyrosine kinase to be constitutively active driving uninhibited cell growth. Internal tandem duplications (*FLT3*-ITD) of the juxtamembrane domain encompass a majority of *FLT3* mutations, though activating mutations in the tyrosine kinase domain (*FLT3*-TKD) also occur (10, 13). Early retroviral transduction models of both *FLT3*-ITD and *FLT3*-TKD mutations revealed that expression of these activating mutations lead to distinctly different disease phenotypes (88). Transplantation of *FLT3*-ITD expressing bone marrow led to MPD, whereas transplantation of *FLT3*-TKD expressing cells led to a lymphoid disease with longer latency, consistent with the finding that TKD mutations are more common in acute lymphoblastic leukemia than AML (101). In addition, these studies revealed that *FLT3*-ITD mutations, and not *FLT3*-TKD, lead to activation of STAT5 signaling.

Several transgenic models of *FLT3*-ITD have been developed, each with slightly different advantages, though they predominantly produce MPD. First, a transgenic model expressing *FLT3*-ITD under the control of the hematopoietic-specific *Vav* promoter was created by the lab of Dr. D. Gary Gilliland which developed MPD at 6-12 months (89). Subsequently, the same group developed a model in which a humanized ITD is knocked into the native murine *Flt3* gene (90). This model minimizes the effects of gene overexpression on disease phenotype inherent to retroviral transduction or use of heterologous promoters, as expression levels of FLT3 in both wild-type and mutant forms have a significant impact on disease. In the absence of cooperating mutations, this model leads to the development of chronic myelomonocytic leukemia (CMML) and not AML. However, when used in combination with other common AML lesions, such as *KMT2A*-PTD, *Npm1c* mutation, *Dnmt3a* deletion, and *RUNX1-RUNX1T1*, expression of *Flt3*-ITD is capable of producing AML, though with relatively long latency (46, 91–93). A similar model in which an 18-base pair ITD was knocked into the juxtamembrane domain of native *Flt3* gene was also developed by Dr. Li in the lab of Dr. Donald Small. This model is characterized by the development of MPD with a median survival of 10 months (94), and cooperates with other common AML mutations, including *NPM1c* and mutant *Wt1*, to generate AML or accelerate the MPD disease process (95, 96).

FLT3-TKD mutations also occur in AML but are less common and not as strongly associated with prognosis compared to ITD mutations. Plasmids conferring the expression of various *FLT3*-TKD mutants have been developed but are predominantly used to transform cell lines, and murine models of *FLT3*-TKD mutants are lacking (97, 102, 103). Dr. Emily Bailey and colleagues previously generated a knock-in of the most common TKD mutant, D835Y, which developed predominantly MPD but with a longer latency than ITD models (104). Thus, new murine models which cover the spectrum of relevant *FLT3* aberrations are needed to adequately study this common mutation in AML.

5 MUTATIONS THAT AFFECT TRANSCRIPTION FACTORS OR EPIGENETIC MODIFIERS

Genomic landscape studies have revealed critical epigenetic modifiers that are frequently mutated in myeloid malignancies (**Table 3**). Here we will review data from some of the best characterized murine models of these epigenetic modifier mutations.

5.1 *DNMT3A*

DNA methyltransferase 3A (DNMT3A) is a *de novo* DNA methyltransferase that methylates cytosine moieties of CpG dinucleotides (127). HSCs frequently acquire *DNMT3A* mutations which act as pre-leukemic lesions and in turn lead to clonal hematopoiesis which, in some cases, ultimately progresses to leukemia. Up to 22% of adult *de novo* AML cases (128, 129) and 10% of MDS (105, 130) harbor somatic mutations in *DNMT3A*, most occurring at arginine 882 (R882) in the DNMT3A methyltransferase domain. Since *DNMT3A* variants were first reported in AML in 2010, a variety of mouse modeling techniques have been used to clarify the role of *DNMT3A* in HSCs and the precise role that loss of function of *DNMT3A* plays in leukemogenesis.

In 2011, the lab of Dr. Margaret Goodell reported the effects of *Dnmt3a* deficiency *in vivo* using an inducible *Dnmt3a* knock-out (KO) murine model (131). Transgenic animals carrying hematopoietic tissue-specific *Mx1-Cre* were crossed with mice

TABLE 3 | Mouse models of epigenetic regulators.

Genemutation	Year	Expression	Mechanism	Phenotype	References
Dnmt3a (KO)	2011	Inducible	Mx1-Cre	Enhanced self-renewal	(105)
	2015	Inducible	Mx1-Cre	MDS, AML, ALL	(99)
	2015	Inducible	Mx1-Cre	MDS, AML, MDS/MPN	(106)
Dnmt3a^{R882}	2016	Inducible	Mx1-Cre	HSPC expansion, myeloid bias, AML when combined with FLT3+Npm1c	(107)
	2019	Inducible	Mx1-Cre	AML on serial transplant co-expressed with Npm1c	(108)
Dnmt3a (KO)	2017	Inducible	Mx1-Cre	ALL, AML	(92)
+ Flt3		Inducible	Retrovirus		
Dnmt3a (KO)	2016	Inducible	Mx1-Cre	ALL, AML	(109)
+ Tet2		Constitutive			
Dnmt3a (KO)	2020	Inducible	Mx1-Cre	AML	(110)
+ Idh2		Inducible	Retrovirus		
Tet2 (KO)	2011	Inducible	Mx1-Cre	CMML-like	(111, 112)
	2011	Constitutive		Increased BM cellularity and HSPC expansion	(113)
	2011	Constitutive		CMML, MPN, MDS (low penetrance)	(114)
	2012	Constitutive		Mild myeloproliferation	(115)
Tet2 (KO)	2018	Inducible	Mx1-Cre	CMML	(116)
+ NRAS		Inducible	Mx1-Cre		
Tet2 (KO)	2018	Constitutive		MPN	(117)
+ KIT		Inducible	Mx1-Cre		
Asxl1 (KO)	2013	Inducible	Mx1- and Vav- Cre	MDS	(118)
	2014	Constitutive		MDS, some CMML	(119)
Asxl1 (mut)	2018	Inducible	Vav-Cre	Mild anemia	(120)
	2021	Constitutive		Mild splenomegaly	(121)
Smc3	2015	Inducible	Mx1-Cre	None (shortened latency of AML when added to Flt3-ITD)	(122)
Smc1a	2015	Inducible	rtTAs	MPN-like	(123)
Bcor	2017	Inducible	CreER	T-ALL	(124)
	2019	Inducible	CreER	AML if combined with *Kras*^{G12D}	(125)
	2021	Inducible	Mx1-Cre	(erythroid) AML	(126)

AML, acute myeloid leukemia; BM, bone marrow; CMML, chronic myelomonocytic leukemia; HSPC, hematopoietic stem/progenitor cell; ITD, internal tandem duplication; KO, knock-out; MDS, myelodysplastic syndrome; MPD, myeloproliferative disease; MPN, myeloproliferative neoplasm; PTD, partial tandem duplication; T-ALL, T-acute lymphoblastic leukemia.

carrying *loxP*-flanked copies of *Dnmt3a*, and *Dnmt3a* loss was then induced *via* serial intraperitoneal injections of pIpC. In competitive transplant experiments, equal parts purified HSCs from non-induced *Dnmt3a*$^{fl/fl}$ and wild-type mice were transplanted into primary recipients followed by induced deletion of *Dnmt3a*. They found no difference in the represented proportion of HSCs before or after *Dnmt3a* deletion was induced in primary recipients. However, in secondary competitive transplants, there was a significant increase in *Dnmt3a*-null HSCs compared to wild-type, demonstrating that loss of *Dnmt3a* led to enhanced stem cell self-renewal. No mice developed MPD or overt leukemia suggesting that additional cooperating mutations are necessary for leukemogenesis.

Similar inducible models have since been used in non-competitive transplants resulting in a variety of hematologic malignancies, including MDS, AML, primary myelofibrosis, and T- and B-cell acute lymphoblastic lymphoma. Dr. Allison Mayle and colleagues demonstrated that with non-competitive transplantation of *Dnmt3a*-null bone marrow, all transplanted mice died between 200- and 400-days post-transplant from a variety of hematologic malignancies (99). Challen et al. reported similar findings of bone marrow failure resulting in death with 100% penetrance following transplantation of *Dnmt3a*-null whole bone marrow into sublethally irradiated mice (132). The majority of moribund mice met diagnostic criteria for MDS with 2/15 mice developing frank AML and 4/25 developing an intermediate MDS/myeloproliferative neoplasm. This inducible *Dnmt3a* KO model has also been combined with a variety of murine models harboring genetic lesions of genes that are commonly co-mutated in human *DNMT3A*-mutant AML, including *FLT3*, *TET2*, *IDH2*, and *KIT*, identifying critical cooperative mechanisms that drive leukemogenesis (92, 106, 109, 110).

In AML, the most common *DNMT3A* mutation affects amino acid R882 (*DNMT3A*^{R882}) in the methyltransferase domain. *DNMT3A*^{R882} encodes a mutant protein that is hypomorphic and exerts a dominant negative effect, interfering with wild-type *DNMT3A* function resulting in severely reduced cellular methyltransferase activity (133, 134). Several inducible models have been created to specifically replicate *DNMT3A*^{R882} and elucidate the precise role of this dominant negative acting mutant in leukemogenesis. Dr. Olga Guryanova and colleagues utilized a model in which mutant *Dnmt3a*^{R878H} (the mouse homolog to *DNMT3A*^{R882H}) is expressed from the endogenous *Dnmt3a* locus. To do so, they replaced endogenous *Dnmt3a* exon 23 with a *Lox-Stop-Lox* cassette followed by exon 23 and 24 with the point mutation affecting amino acid R878. In this model, prior to Cre recombination, the modified allele functions as a null allele, and after Cre recombination leads to expression of the mutant mRNA and protein. When *Dnmt3a*^{R878} is conditionally expressed in the hematopoietic system by induction of the hematopoietic-specific *Mx-Cre* by pIpC injections, hematopoietic stem/progenitor cell expansion and myeloid bias

in differentiation were observed, but no overt leukemia (107). They were able to create a fully penetrant and robust model of AML *via* co-expression of $Dnmt3a^{R878H}$, $Flt3^{ITD}$ and $Npm1^{c}$. The lab of Dr. Jennifer Trowbridge recently created a similar conditional model of $Dnmt3a^{R878H}$ (108). However, an advantage of the Trowbridge model over that used by Guryanova is that prior to Cre-mediated recombination, wild-type *Dnmt3a* is expressed from the modified allele whereas the modified allele in the Guryanova model is null prior to recombination. This strategy eliminates the possible confounding impact of constitutive haploinsufficiency of *Dnmt3a* in the hematopoietic system prior to recombination.

Our group recently used CRISPR/Cas9-mediated gene editing of murine embryonic stem cells to create constitutive models germline *Dnmt3a* lesions that have been previously described in patients with the rare overgrowth, intellectual disability syndrome, Tatton-Brown-Rahman syndrome. We found that each model recapitulated the distinct growth, behavioral and hematologic phenotypes observed in their human counterparts including increased risk of hematologic malignancy (135). Dr. Amanda Smith in the lab of Dr. Timothy Ley similarly found that a germline $Dnmt3a^{R878}$ model also recapitulated the features of TBRS including risk of hematologic malignancy development (136). These and additional models that recapitulate specific point mutations observed in human disease will help us establish the connection between alterations in *DNMT3A* function and pathogenesis.

Further development of mouse models that utilize inducible gene deletion strategies to incorporate mutations that are known to co-occur with *DNMT3A* in human disease will help to further define the role of DNMT3A in leukemic transformation and more closely mirror the natural disease process.

5.2 *TET2*

TET2 is a member of the TET family of proteins with dioxygenase enzymatic activity resulting in oxidation of the methyl group at the 5-position of cytosine. The precise effect of *TET2*'s action has not been proven, but it is hypothesized that this modified locus prevents *DNMT1*-mediated methylation during DNA replication, thus leading to passive loss of DNA methylation. Loss of function *TET2* mutations are among the most common drivers of clonal hematopoiesis and have been detected in 10-20% of *de novo* AML (137) and up to 50% of cases of CMML (138). As one of the most prevalent mutations affecting hematopoiesis, the development of faithful murine models of *TET2* loss has been pursued by several research groups.

Multiple *Tet2* KO mouse models have been created, all demonstrating expansion of the HSC compartment following ablation of *Tet2* expression secondary to increased self-renewal capacity (111–115). In 2011, Moral-Crusio et al. developed a novel conditional *Tet2* KO murine model that resulted in MPD (111). This group utilized homologous recombination to introduce two *loxP* sites flanking exon 3 of *Tet2* in embryonic stem cells that were then injected into blastocysts. The resulting mice ($Tet2^{fl/fl}$) were then crossed with transgenic *Vav*-Cre mice, resulting in *Tet2* deletion in the hematopoietic system *in utero*, leading to the development of a CMML-like disease by 20 weeks of life with monocyte–predominant leukocytosis and splenomegaly.

Another group developed a novel constitutive model *via* construction of a *Tet2*-targeting vector that disrupted the endogenous ATG start codon, leading to silencing of *Tet2* gene expression (114). The resultant mice with germline deletion of *Tet2* are viable and fertile but develop a CMML-like disease with leukocytosis, neutrophilia and monocytosis along with increased bone marrow cellularity, splenomegaly, and moderate liver enlargement. Approximately one-third of the $Tet2^{-/-}$ mice died within a year due to myeloid malignancy. These mice exhibited two distinct phenotypes: one with a population of erythroblasts infiltrating hematopoietic organs and the other with an aberrant population of mature myeloid cells including myeloblasts, monocytes/macrophages and neutrophils. Both malignant myeloid phenotypes caused massive hepatosplenomegaly and anemia.

These models of *Tet2* loss have proven useful for studies of collaborative leukemogenesis. A number of labs have conducted important studies combining *Tet2* deletion with other lesions that frequently co-occur in human AML, such as *Dnmt3a* as previously mentioned, *NRAS* and *KIT* (109, 116, 117). These models are crucial for clarifying the interplay between cooperative mutations providing models that closely mirror human disease.

5.3 *ASXL1*

Additional sex comb-like 1 (ASXL1) is a polycomb group protein that interacts with BAP1 and PRC2 to remodel chromatin thus regulate gene expression. *ASXL1* mutations have been reported in 5-11% of *de novo* AML (139–141). These mutations occur with increased frequency among older patients and are frequently detected in clonal hematopoiesis (140).

Abdel-Wahab et al. developed a novel murine model of *Asxl1* knockdown *via* retroviral transduction to introduce short hairpin RNA (shRNA) constructs into mouse bone marrow cells that were then transplanted into lethally irradiated recipient mice (142). They found that knockdown of *Asxl1* in a mouse expressing the oncogene $Nras^{G12D}$ accelerated the expected MPD, resulting in more severe symptoms of anemia and organomegaly as well as decreased lifespan. The same group then created a conditional KO model *via* insertion of two *loxP* sites flanking exons 5-10 of *Asxl1* (118). They crossed $Asxl1^{fl/fl}$ mice with transgenic mice harboring various tissue-specific Cre recombinase systems. *Ella-Cre*$^{+}$ $Asxl^{fl/fl}$ mice had germline deletion of *Asxl1* and resulted in 100% embryonic lethality. Heterozygous germline deletion of *Asxl1* led to viable embryos at expected Mendelian ratios, though 35% of these mice exhibited craniofacial dysmorphism. Hematopoietic-specific deletion of *Asxl1* using either *Mx1-Cre* or *Vav-Cre* resulted in MDS with progressive anemia and leukopenia compared with littermate controls. They observed morphological dysplasia of peripheral myeloid cells and erythroid precursors with bone marrow hypocellularity.

A constitutive *Asxl1*-null murine model was created by Wang et al. the following year (119). This group replaced part of *Asxl1*

exon 1 with *nlacZ/nGFP* reporter to disrupt the endogenous ATG and inhibit transcription of *Asxl1*. They used this technique to generate both *Asxl1*$^{+/-}$ and *Asxl1*$^{-/-}$ mice to compare the effects of haploinsufficiency versus complete loss of *Asxl1*. Complete loss of *Asxl1* resulted in an estimated 80% embryonic lethality, similar to the high rate observed in the inducible germline model that was previously published. Of the *Asxl1*-null mice, 80% that survived to birth died within the first day of life, and the remainder survived for 18-42 days. Surviving mice exhibited cytopenias and myeloid dysplasia, consistent with MDS-like disease. Interestingly, heterozygous deletion of *Asxl1* was also sufficient for development of a similar MDS-like disease. The disease phenotype became increasingly severe with age in *Asxl*$^{+/-}$ mice with worsening cytopenias and dysplasia, and progressed to a CMML-like disease in 22% (4 of 18 mice).

An alternative approach was taken to better mimic the truncating mutations that typically occur in human disease. A conditional knock-in mouse model was created by introducing a floxed mutant *Asxl1* allele *via* homologous recombination to mimic p.E635RfsX15 that is well-described in human disease (120). These mice were crossed with transgenic *Vav-Cre* mice in which recombination occurs in the hematopoietic system. Modest anemia was observed along with skewing of hematopoietic bone marrow population toward megakaryocyte progenitors and away from erythrocyte progenitors, but no frank MDS or AML was observed. However, when the authors incorporated concurrent expression of a mutant form of *RUNX1* into their mouse model, they found that co-expression of these two mutations led to development of frank MDS/AML with a short latency period following induced expression of the mutations (median survival of 160 days). They also performed retroviral insertional mutagenesis and found that all mice in this experimental cohort developed AML within a 1.5-year observation period.

Another knock-in model was recently created using CRISPR/Cas9 to introduce the most common MDS-associated mutation in humans, *ASXL1*^{G643W}, into murine embryonic stem cells resulting in expression of a truncated ASXL1 protein, mirroring that which occurs in humans (121, 143). This solo model again produced only mild impacts on hematopoiesis with skewing towards the myeloid lineage and mild splenomegaly. However, combination with an inducible model of *Cepba* haploinsufficiency drove the development of AML. Together these findings demonstrate the utility of a mouse model of *Asxl1* that recapitulates the pre-leukemic effect of this lesion and can be used to study its interaction with cooperating mutations in the progression to leukemia.

5.4 Cohesin Complex

The cohesin complex is a ring-like structure made up of various protein components including SMC1, SMC3, RAD21, and STAG1/2. Cohesin mediates the approximation of DNA fragments and plays a crucial role in sister chromatid cohesion, homologous recombination, and DNA looping. In turn, cohesin regulates gene expression *via* the approximation of distal enhancers and promoters. Somatic cohesin mutations have been identified in 12% of myeloid malignancies and often co-occur with genetic lesions such as t (8;21) and mutations in genes such as *TET2*, *NPM1*, and *ASXL1* (144, 145). Cohesin mutations are mutually exclusive, suggesting that reduction of one component leads to insufficiency of the entire complex. Therefore, the specific cohesin gene targeted in various murine models should not affect the disease. It is believed that cohesin's vital role in sister chromatid cohesion makes complete cohesin loss incompatible with life. This hypothesis has been supported by the universally lethal effect of homozygous *Rad21* deletion in mice (146).

Two groups published mouse models of cohesin loss in 2015 using different genetic engineering techniques. Viny et al. (122) created a conditional knock-out model in which exon 4 is flanked by loxP sites. When crossed with transgenic *Mx1*-Cre mice, they induced complete loss of SMC3 in hematopoietic tissues *via* pIpC injections. Biallelic loss of *Smc3* resulted in 100% lethality within 11 days of Cre recombinase activation due to CNS hemorrhage and multiorgan failure. They then created a model of conditional *Smc3* haploinsufficiency *via* Cre-mediated deletion of a single *Smc3* allele in hematopoietic tissues and found a resultant increase in self-renewal capacity of HSCs. Alone, *Smc3* haploinsufficiency did not lead to phenotypic changes suggestive of MDS or leukemia, but the addition of *Flt3*-ITD expression within the mouse model of cohesin insufficiency led to AML with shortened latency compared to *Flt3*-ITD alone.

Alternatively, Mullenders et al. introduced shRNA to silence expression of cohesin components in a mouse model (123). They introduced a GFP transgene that housed a single copy of their engineered shRNA downstream of a tetracycline (Tet)-responsive element and crossed them with rtTA-transgenic animals to create an inducible and reversible model of cohesin knockdown. shRNAs were engineered to knockdown three of the core cohesin proteins, *Rad21*, *Smc1a* and *Stag2*. Mice were exposed to doxycycline starting at 6 weeks of age to induce shRNA expression. *Rad21* $^{(shRNA/+)}$, *Smc1a* $^{(shRNA/+)}$, *Stag2* $^{(shRNA/+)}$ mice all demonstrated a skewing toward the myeloid lineages. Interestingly, *Smc1a*-targeting shRNA expression resulted in a significant decrease in all core cohesin proteins rather than just in SMC1A. Over time, a subset of these cohesin knockdown mice developed a myeloproliferative neoplasm-like phenotype characterized by blood and bone marrow myeloid hyperplasia, hypocellular bone marrow, and splenomegaly.

shRNA knockdown and Cre recombinase-mediated deletion remain popular methods of modeling cohesin loss, particularly in novel models that combine cohesin insufficiency with other gene mutations to mirror leukemogenesis in humans. Both strategies effectively reduce gene expression and can be induced at specific timepoints to elucidate the precise order of acquisition that is hypothesized to occur in subsets of leukemia.

5.5 *BCOR*

BCOR is a tumor suppressor gene that encodes the transcription repressor BCL6 corepressor (BCOR). Over the past decade mutations in *BCOR* have been identified in 3.4-5% of cytogenetically normal AML in adults and 1.2% of pediatric AML (147–150). In 2017, Tanaka et al. created a transgenic

mouse model using tamoxifen-inducible *Cre-ERT* in the ROSA26 locus to delete exon 4 of *Bcor* resulting in a truncated protein that lacks the BCL6 binding site (124). HSCs harvested from this model exhibited impaired repopulating capabilities. Half of their cohort developed T lymphoblastic leukemia but they did not observe development of myeloid malignancy.

Dr. Kelly and colleagues similarly generated a model in which exons 9 and 10 of the murine *Bcor* gene is flanked by *loxP* sites. When crossed to mice with transgenic *HSC-SCL-Cre-ER*^{T} recombinase, Cre activation by tamoxifen injections lead to deletion of exons 9 and 10 of *Bcor* (termed *Bcor*$^{\Delta E9\text{-}10}$) specifically in HSCs, resulting in low level expression of a truncated protein that lacks the C-terminal PCGF Ub-like fold discriminator domain (125). *Bcor*$^{\Delta E9\text{-}10}$ mice did not exhibit an abnormal hematopoietic phenotype but did demonstrate expansion of the myeloid progenitor compartment. The authors then found that combination of *Bcor*$^{\Delta E9\text{-}10}$ and *Kras*^{G12D} results in a highly penetrant model of myeloid leukemia with significantly decreased survival compared to leukemia resulting from *Kras*^{G12D} alone.

Findings from recent *Bcor*-mutated murine models of AML have established a strong role for *Bcor* in the development of acute erythroid leukemia (AEL). Drs. Brunangelo Falini, Margaret Goodell, and colleagues collaborated to generate a double *Dnmt3a*$^{-/-}$ and *Bcor*$^{-/-}$ mouse model (126). They first created conditional *Bcor* knockout in which exons 8-10 are flanked by *loxP* sites crossed with transgenic *Mx1-Cre* to induce *Bcor* knock out in the hematopoietic system. These mice were then mated with others carrying two floxed *Dnmt3a* alleles and induced full knockout of both genes, which resulted in a fully penetrant and lethal AEL. They then used this model to demonstrate the efficacy of the demethylating agent decitabine, which exhibited better control of tumor burden than cytarabine alone. Dr. Charles Mullighan and colleagues used multiplex genome editing in HSPCs that were transplanted into primary recipient mice and similarly found that co-occurrence of mutations in *Bcor* and *Trp53* strongly promoted development of AEL (73).

These existing murine models recapitulate what is observed in humans and will help to better understand the precise role of *BCOR* loss as it cooperates with leukemogenic mutations in other cellular pathways as well as the role it plays in therapeutic response.

6 OTHER RECURRENT AML MUTATIONS

There are several recurrently mutated genes that do not fall into the specific categories discussed above which have distinct roles in leukemia pathophysiology. These mutations will be reviewed below.

6.1 *NPM1*

Mutations of the gene *NPM1* are among the most common mutations in adult AML, found in up to 35% of patients (15). While less common in childhood AML (8-10%), like in adults, *NPM1*-mutant AML is generally associated with a favorable prognosis, co-occurrence with *FLT3*-ITD mutations, and *HOX* gene overexpression (18). NPM1 is a molecular chaperone with roles in centrosome duplication, ribosome biogenesis, and stress-induced regulation of P53 (151). In its wild-type state, NPM1 shuttles rapidly between the nucleus and cytoplasm, and predominantly localizes to the nucleoli. In AML, frameshift mutations of *NPM1* lead to its aberrant cytoplasmic localization, thus the common designation, NPMc+ (15). Given the prevalence of *NPM1* mutations in AML, there has been much interest in generating murine models with which to study the biology of *NPM1*-mutant AML.

In 2010, researchers from the lab of Dr. Pier Paolo Pandolfi published their work developing and characterizing a murine model in which mutant *NPM1* was transgenically expressed under the control of the *hMRP8* promoter, resulting in overexpression of mutant NPM1 in myeloid progenitors. These mice developed myeloproliferation in the bone marrow and spleens but did not develop overt AML (152). This model was later crossed to mice with a heterozygous germline *Flt3*-ITD mutation, demonstrating cooperativity between these commonly co-occurring lesions (96). In 2012, another group developed a model in which they knocked-in TCTG into murine *Npm1* exon 11, similar to the most common frameshift mutation found in human AML. While the resultant mutant protein differed slightly from human NPMc+ protein, the group still found excess cytoplasmic expression. This strategy led to an incompletely penetrant MPD, but like the transgenic model from the Pandolfi group, did not develop AML (153). Around this same time, Vassiliou et al. developed the first conditional NPMc+ model, by knocking-in a 'humanized' exon 11 frameshift mutation (the most common mutation in AML) just downstream of murine exon 11. They also knocked-in *loxP* sites flanking murine exon 11, such that Cre-mediated recombination leads to excision of the native exon 11 and exclusive expression of humanized mutant *Npm1c*. As expected, when induced in the hematopoietic system by pIpC activation of *Mx1*-Cre, the mutant protein localized predominantly to the cytoplasm. Expression of mutant NPM1c led to Hox gene overexpression, enhanced stem cell self-renewal and myeloid skewing with ~1/3 of the mice developing a delayed onset AML (154). When crossed to mice constitutively expressing *Flt3*-ITD mutation, mice with induced *Npm1c* expression developed a rapid onset AML, confirming molecular synergy (155). This model has also proved useful for pre-clinical investigations including studies demonstrating the therapeutic potential of inhibitors of the MENIN-MLL interaction for the treatment of NPMc+ AML (156).

More recently, the lab of Dr. Jennifer Trowbridge designed a humanized, inducible *Npm1c* mutation similar to that developed by Vassiliou et al., but instead of a Cre-inducible system, utilized an Flp-recombinase inducible system. They crossed these mice with transgenic mice in which the tamoxifen-inducible FlpoER is knocked into the *Gt* (*ROSA) 26Sor* locus. This strategy allowed for the sequential induction of both a Cre-inducible *Dnmt3a*^{R878} mutation (see DNMT3A section above) and the FLP-inducible

expression of *Npm1c*. A potential disadvantage of this strategy is that because *FlpoER* is knocked into the *Rosa26* locus it is expressed ubiquitously; to isolate the hematologic effects of these combined mutations, hematopoietic transplantation was necessary. In isolation, induction of the *Npm1c* mutation in the hematopoietic system led to a low penetrance MPD but no overt AML. However, when induction of *Npm1c* was preceded by induction of the *Dnmt3a* mutation, the mice developed a highly penetrant MDS and/or MPD. Interestingly, the disease latency was inversely correlated with the length of time between induction of the *Dnmt3a* mutation and the *Npm1c* mutation (i.e., the longer the mouse had expression of mutant *Dnmt3a* prior to induction of *Npm1c* expression, the shorter the disease latency) (108).

6.2 *TP53*

Greater than 50% of human cancers carry mutations in the well-established tumor suppressor gene *TP53* (157). Interestingly *TP53* mutations are only detected in less than 10% of *de novo* AML but confer high risk disease with an extremely poor prognosis (10, 158). Creation of a mouse model of *TP53*-mutant AML is important for further therapeutic development in this traditionally hard to treat subset. Isolated mutations in *Trp53* have proven insufficient to induce leukemogenesis in mouse models but can be combined with commonly co-occurring mutations to generate models of myeloid leukemia that can be used to define the role of cooperative mutations and provide an environment for the development of new therapeutic targets and strategies.

Several transgenic mouse models have shown that *Trp53* cooperates with other genetic aberrations to hasten the development of AML. In the development of these AML models it was important to utilize non-germline methods to reduce p53 expression as *Trp53* null mice are prone to developing T cell malignancies. Stoddart et al. created a novel model of therapy-related AML using a *Trp53*-targeting shRNA to knock down expression of p53 in bone marrow cells harvested from transgenic mice harboring heterozygous loss of *Erg1* and *Apc*, two genes located on the long arm of chromosome 5, and thus lost in AML with 5q deletion (159). While they were successful in generating a novel model that may mirror the behavior of therapy-related AML, the low penetrance of disease (17%) likely indicates that additional genes lost with 5q deletion play an important role in the transformation to AML. This is supported by work done by Yang et al., who recently generated dual transgenic mice with Gilliland *Flt3*-ITD knock-in model and either heterozygous or homozygous *Trp53* deletion (160). Heterozygous *Trp53* knockout significantly increased the penetrance and lethality of myeloid leukemia compared to *Flt3*-ITD alone, and homozygous *Trp53* knockout led to a further decrease in median survival.

Additional models have been created to recapitulate the common co-occurrence of mutations in *TP53* and Ras family genes and determine their cooperative roles in leukemogenesis. *Zhou* et al. found that *Trp53* depletion accelerated AML development in mice expressing $Kras^{G12D}$ (161). Members of Dr. Jing Zhang's lab then created a conditional transgenic model of AML using *Mx1*-Cre to induce homozygous loss of *Trp53* in the hematopoietic system and concurrently induce expression of the oncogenic $Nras^{G12D}$ (162). They used RNA sequencing to define the transcriptome of the leukemic cells and determined that *Trp53* loss cooperated with mutant *Nras* within the megakaryocyte-erythroid progenitors to result in AML.

Together, these findings have shown the utility of generating mouse models of *Trp53*-mutant AML to advance our understanding of and develop new treatment strategies for this aggressive subcategory of AML.

7 PATIENT DERIVED XENOGRAFTS

The murine models of AML discussed above are essential tools to study leukemia development and unfold molecular mechanisms related to the disease. Despite sophisticated advancements in transgenic mouse modeling, there are differences in the murine and human leukemic phenotype that require humanized models to better understand nuances of human disease. *Ex vivo* models with human AML blasts have been developed for these purposes but are limited due to the missing interaction of the human AML blasts with the bone marrow microenvironment which plays an important role in leukemia development and therapeutic response. Here we review patient derived xenograft models that have been developed and improved over time to overcome these limitations.

The development of immunocompromised mouse models was essential for the study of patient-derived tumors and preclinical discovery of new compounds for cancer treatment (**Table 4**). The first immunodeficient mouse model was described in 1966 by Flanagan (163). These nude athymic (nu/nu) mice were T-cell-deficient due to a homozygous *Foxn1* mutation and enabled the study of human cancer in mice (164). However, this model has its limitations for studying AML since the intact murine B- and natural killer (NK)-cell populations lead to poor human AML engraftment (165). The severe combined immune deficiency (SCID) phenotype was first described in C.B-17 mice in 1983, caused by a homozygous mutation in the *Scid* gene (scid/scid). The SCID immunodeficient mouse model proved superior to nude mice for *in vivo* studies of human cancers (166). The *Scid* mutation affects the VDJ recombinase system and results in a lack of mature T- and B-lymphocytes. In the early 1990s, multiple groups showed the engraftment of human myeloid leukemia cell lines and patient AML cells in SCID mice, indicating that this PDX model is a useful tool for studying AML. However, the SCID model still had technical limitations as some human AMLs failed to engraft without exogenous cytokine treatment (167–169). Reports by Carrol et al. and Riggs et al. suggested that this mouse model is "leaky" as mice showed the presence of mature lymphocytes, likely explaining the relative engraftment barrier (180, 181).

Throughout the years more severe immunodeficient mouse models have been developed to improve engraftment, including

the non-obese diabetic NOD/SCID (NOD/LtSz-scid/scid) mouse. SCID mice were backcrossed onto the NOD/Lt strain background resulting in a strain that is deficient in B- and T-lymphocytes and shows reduced NK-cell and macrophage activity (170). In contrast to SCID mice, normal human bone marrow cells and patient-derived AML cells can be engrafted with much higher efficiency in NOD/SCID mice using fewer cells (171, 172, 182, 183). A robust engraftment of primitive $CD34^+CD38^-$ leukemic progenitors, also known as NOD/SCID leukemia-initiating cells (NOD/SL-IC) or leukemic stem cells (LSC), was observed in NOD/SCID mice. Serial transplantation of LSCs and their potential to differentiate into leukemic blasts provides the opportunity to study those leukemia initiating clones more closely and identify potential drugs against them. However, while the NOD/SCID xenograft model has shown efficient engraftment for high-risk AML cases, it is still limited by poor engraftment for favorable and intermediate-risk AML (173).

The introduction of a deletion of the *interleukin 2 (IL2) receptor gamma chain* (*Il2rγ*) gene led to an even more immune compromised mouse model, the NOD-scid Il2rγnull (NSG) mouse, that improved engraftment of patient AML cells regardless of the French-American-British classification or cytogenetic features (174). Better engraftment and longer lifespan (>16 months) made NSG mice the preferred immunodeficient model for AML research over NOD/SCID mice. Studies in NSG mice showed that human LSCs can home to the bone marrow niche of the mouse resulting in quiescent LSC that are resistant to chemotherapy (184). Those features of the NSG PDX model that recapitulates human AML facilitate the study of chemotherapy resistance conferring mechanisms. The use of NSG PDX models has also led to a better understanding of the heterogeneity of leukemia-initiating cells (LIC) as reports identified the existence of not only $CD34^+CD38^-$ LIC cells but also $CD34^+CD38^+$ and even $CD34^-$ populations capable of initiating AML (185, 186).

Over time more strains have been developed to overcome the limitations of the previous models. Wunderlich et al. generated a mouse strain that transgenically expresses the human cytokines stem cell factor (SCF), GM-CSF, and IL-3 (SGM3) in the NOD/SCID background (175). Usage of NOD/LtSz-scid IL2RG–SGM3 mice (NSGS) led to superior engraftment of AML cells compared to other strains (175, 176). Even AML samples from favorable risk groups like CBF AML, *NPM1*-mutated/*FLT3* wild type, or *CEBPA*-mutated AML, that are difficult to engraft in previous immunocompromised strains, were capable of engrafting in NSGS mice (175, 176).

An even more advanced immunodeficient mouse strain was developed by Dr. Flavell and colleagues (177). MISTRG mice are $Rag2^-$ and IL2rγ-deficient, with genes for four human cytokines (hM-CSF, hIL-3, hGM-CSF, and hTPO) knocked-in to their respective mouse loci. Because they are under the control of their endogenous promoters, they are expressed at physiologic levels as opposed to the supraphysiologic levels in NSGS mice. The MISTRG mice also express human SIRPa which binds to human CD47 and results in inhibition of phagocytosis of human cells and hence supports better engraftment (178). Ellegast et al. reported successful engraftment of *NPM1* mutated and inv (16) AML samples using this advanced mouse model (179). They also reported an important role for M-CSF expression in mice using MSTRG (knock-in for only hMCSF and hTPO) as an important factor for inv (16) AML engraftment. The successful engraftment of t (8;21) AML cells in MISTRG mice that leads to leukemia has not yet been shown.

The development of new immune compromised mouse models over the last few decades has led to increasingly efficient engraftment of human AML samples. This gave rise to new insights into AML hierarchy, genetic and functional characteristics of human AML, and the option for drug testing on human AML cells in an *in vivo* model. Yet, there are still challenges that need to be addressed in the future such as efficient engraftment of less aggressive AML subtypes. Recently, it has been shown by Reinisch et al. that establishing a human bone marrow niche in the mouse by transplanting human bone marrow-mesenchymal stem cell (MSC)-derived ossicles results in robust and superior engraftment of human AML samples (187). In another study, hMSC were seeded in a gelatin-based porous scaffold and cultured *in vitro* (188). Before implanting the scaffolds into NSG mice, patient-derived AML cells were pre-seeded into the scaffold. This method led to successful engraftment of AML samples that failed to engraft in NSG mice after intravenous injection of the leukemic cells. This approach has also been tested for other stromal cell types like endothelial cells and osteoblasts. Since there is crosstalk between

TABLE 4 | Mouse models available for patient-derived xenografts of AML.

Mouse Strain	Common Abbreviation	Immune system	Cytokines expressed	Engraftment of AML			References
				High-Risk	Intermediate Risk	FavorableRisk	
nude athymic	nude	T-cell deficient	–	–	–	–	(163–165)
C.B-17 SCID	SCID	no functional T- and B-cells	–	+	–	–	(166–169)
NOD/LtSz-scid/scid	NOD/SCID	T- and B-cell deficient, reduced NK and macrophage activity	–	++	–	–	(170–173)
NOD-scid $Il2r\gamma^{null}$	NSG	no functional T-, B- and NK cells	–	+++	++	+	(174)
NSG–SGM3	NSGS	no functional T-, B- and NK cells	hIL-3, hGM-CSF, hCSF	++++	++++	++	(175, 176)
MISTRG	–	no functional T-, B- and NK cells	hM-CSF, hIL-3, hGM-CSF, hTPO	++++	++++	+++	(177–179)

leukemia cells and the bone marrow niche, these kinds of models help to study the leukemia bone marrow microenvironment and possible cell-extrinsic mechanisms that may contribute to chemotherapy resistance.

Another xenograft mouse model to study leukemia has been developed using isolated human CD34+ hematopoietic cells from healthy donors that are transduced with a viral vector expressing system or have been genetically engineered which are then transplanted into immunodeficient mice. Wei et al. used the retroviral transduction method to express the KMT2A-MLLT3 fusion protein in human CD34+ cord blood (huCB) cells resulting in indefinite proliferation of the cells *in vivo* and *in vitro* (189). Transplanting the KMT2A-MLLT3 expressing cells into different immunodeficient mouse models led to AML in NSGS mice and AML, B-ALL or mixed lineage leukemia in NSG and NSG beta 2 microglobulin (NS-B2M) mice showing that the immune microenvironment plays an important role in leukemia development. In this approach both copies of the wild-type *KMT2A* gene are present which is not found in *KMT2A*r leukemias resulting in unknown regulatory effects by the wild-type protein. Dr. Corinna Buechele and colleagues used transcription activator-like effector nucleases (TALENs) gene editing tool to introduce DNA double strand breaks at known breakpoint cluster regions in the *KMT2A* gene and nucleofected with DNA templates with KMT2A homology flanking the sites targeted by TALENs, fusion partner (*MLLT3 or MLLT1*) cDNA, and a fluorescent tag. The strategy resulting in the expression of the designed KMT2A fusion proteins in huCB cells (190). The model was sufficient to initiate leukemia in NSG mice and recapitulated many clinical features of *KMT2A*r leukemias. A model for AML with t(6;9)(p22;q34) was successfully established by transplanting human CD34+ cells transduced with the *DEK-NUP214* fusion gene into NSGS mice resulting in AML development and showing phenotypic and genetic features of human t(6;9) AML (191). Genetic alteration of human CD34+ hematopoietic cells and transplantation into immunodeficient mice provides a humanized mouse model to study the leukemic potential of mutations and chromosomal aberrations found in AML without the potential confounding effects of the co-occurring mutations inherent to human AML cell lines and primary patient samples.

8 CONCLUSION

For AML, like many other human diseases, mouse models are indispensable research tools. Genetically engineered models of common AML driver lesions have provided invaluable insight into disease mechanisms, led to identification of therapeutic targets, and enhanced our understanding of the intricate interactions between collaborating genetic and epigenetic events. Engraftment of human AML cells into immunocompromised mice has expanded our understanding of tumor heterogeneity, shaped the definition of the leukemia initiating cell and allowed for critical pre-clinical investigations of promising novel therapeutics.

Over just the last few years, research employing murine models of AML has resulted in several highly significant advancements in the field. For example, we have learned that not just the combination of mutations matter in the genesis of AML, but the order of mutation acquisition, the age at which the mutations are acquired, and even the length of time between collaborating mutations critically impacts disease development (40, 116). Additionally, efforts to develop mouse models of rare genetic disease entities, such as *NUP98*-rearranged and *BCOR* mutant AML have shed new mechanistic light on previously poorly understood genetic drivers and revealed novel therapeutic vulnerabilities (49, 50, 72, 74, 126). Further, ongoing improvements in immunodeficient mouse strains coupled with efficient genome engineering tools have allowed for not only the engraftment of virtually all subsets of human AML cells into mice, but also for the transformation of normal human hematopoietic cells into leukemic cells capable of engraftment into immunocompromised mice (177, 187, 189–191).

While undeniably powerful, limitations of murine models still must be acknowledged including potential differences in murine and human biology, differences in the malignancies that develop in mice compared to humans, and remaining challenges in engraftment of certain human leukemias into immunodeficient murine recipients. However, with numerous labs around the world working to optimize existing and generate new and relevant murine models, the field will undoubtedly continue to advance, paving the way for ongoing improvements in the care of patients with AML.

AUTHOR CONTRIBUTIONS

RR, SC, KK and MO'K participated in the conception and content planning for the review. KK and SC contributed equally to the composition of the manuscript. MO'K, KW and RR contributed substantially to the fabrication of the paper. RR reviewed and edited the manuscript as last author. All authors contributed to the article and approved the submitted version.

FUNDING

KK was supported by CPRIT RP210027 - Baylor College of Medicine Comprehensive Cancer Training Program. SC was supported by the St. Baldrick's Foundation and Children's Cancer Research Fund.

REFERENCES

1. Sakurai M, Sandberg AA. Prognosis of Acute Myeloblastic Leukemia: Chromosomal Correlation. *Blood* (1973) 41(1):93–104. doi: 10.1182/blood.V41.1.93.93
2. Keating MJ, Cork A, Broach Y, Smith T, Walters RS, McCredie KB, et al. Toward a Clinically Relevant Cytogenetic Classification of Acute Myelogenous Leukemia. *Leuk Res* (1987) 11(2):119–33. doi: 10.1016/0145-2126(87)90017-8
3. Voso MT, De Bellis E, Ottone T. Diagnosis and Classification of AML: WHO 2016. In: *Acute Myeloid Leukemia*. Cham: Springer (2021). p. [23–54].
4. Quessada J, Cuccuini W, Saultier P, Loosveld M, Harrison CJ, Lafage-Pochitaloff M. Cytogenetics of Pediatric Acute Myeloid Leukemia: A Review of the Current Knowledge. *Genes (Basel)* (2021) 12(6):924. doi: 10.3390/genes12060924
5. Creutzig U, Zimmermann M, Reinhardt D, Rasche M, von Neuhoff C, Alpermann T, et al. Changes in Cytogenetics and Molecular Genetics in Acute Myeloid Leukemia From Childhood to Adult Age Groups. *Cancer* (2016) 122(24):3821–30. doi: 10.1002/cncr.30220
6. Ley TJ, Miller C, Ding L, Raphael BJ, Mungall AJ, Robertson A, et al. Genomic and Epigenomic Landscapes of Adult *De Novo* Acute Myeloid Leukemia. *N Engl J Med* (2013) 368(22):2059–74. doi: 10.1056/NEJMoa1301689
7. Arber DA, Orazi A, Hasserjian R, Thiele J, Borowitz MJ, Le Beau MM, et al. The 2016 Revision to the World Health Organization Classification of Myeloid Neoplasms and Acute Leukemia. *Blood* (2016) 127(20):2391–405. doi: 10.1182/blood-2016-03-643544
8. Balgobind BV, Raimondi SC, Harbott J, Zimmermann M, Alonzo TA, Auvrignon A, et al. Novel Prognostic Subgroups in Childhood 11q23/MLL-Rearranged Acute Myeloid Leukemia: Results of an International Retrospective Study. *Blood* (2009) 114(12):2489–96. doi: 10.1182/blood-2009-04-215152
9. Moarii M, Papaemmanuil E. Classification and Risk Assessment in AML: Integrating Cytogenetics and Molecular Profiling. *Hematol Am Soc Hematol Educ Program* (2017) 2017(1):37–44. doi: 10.1182/asheducation-2017.1.37
10. Papaemmanuil E, Gerstung M, Bullinger L, Gaidzik VI, Paschka P, Roberts ND, et al. Genomic Classification and Prognosis in Acute Myeloid Leukemia. *N Engl J Med* (2016) 374(23):2209–21. doi: 10.1056/NEJMoa1516192
11. Chen X, Zhu H, Qiao C, Zhao S, Liu L, Wang Y, et al. Next-Generation Sequencing Reveals Gene Mutations Landscape and Clonal Evolution in Patients With Acute Myeloid Leukemia. *Hematology* (2021) 26(1):111–22. doi: 10.1080/16078454.2020.1858610
12. Tyner JW, Tognon CE, Bottomly D, Wilmot B, Kurtz SE, Savage SL, et al. Functional Genomic Landscape of Acute Myeloid Leukaemia. *Nature* (2018) 562(7728):526–31. doi: 10.1038/s41586-018-0623-z
13. Bolouri H, Farrar JE, Triche T, Ries RE, Lim EL, Alonzo TA, et al. Publisher Correction: The Molecular Landscape of Pediatric Acute Myeloid Leukemia Reveals Recurrent Structural Alterations and Age-Specific Mutational Interactions. *Nat Med* (2019) 25(3):530. doi: 10.1038/s41591-019-0369-7
14. Conneely SE, Rau RE. The Genomics of Acute Myeloid Leukemia in Children. *Cancer Metastasis Rev* (2020) 39(1):189–209. doi: 10.1007/s10555-020-09846-1
15. Falini B, Mecucci C, Tiacci E, Alcalay M, Rosati R, Pasqualucci L, et al. Cytoplasmic Nucleophosmin in Acute Myelogenous Leukemia With a Normal Karyotype. *N Engl J Med* (2005) 352(3):254–66. doi: 10.1056/NEJMoa041974
16. Ho PA, Kutny MA, Alonzo TA, Gerbing RB, Joaquin J, Raimondi SC, et al. Leukemic Mutations in the Methylation-Associated Genes DNMT3A and IDH2 are Rare Events in Pediatric AML: A Report From the Children's Oncology Group. *Pediatr Blood Cancer* (2011) 57(2):204–9. doi: 10.1002/pbc.23179
17. Juhl-Christensen C, Ommen HB, Aggerholm A, Lausen B, Kjeldsen E, Hasle H, et al. Genetic and Epigenetic Similarities and Differences Between Childhood and Adult AML. *Pediatr Blood Cancer* (2012) 58(4):525–31. doi: 10.1002/pbc.23397
18. Brown P, McIntyre E, Rau R, Meshinchi S, Lacayo N, Dahl G, et al. The Incidence and Clinical Significance of Nucleophosmin Mutations in Childhood AML. *Blood* (2007) 110(3):979–85. doi: 10.1182/blood-2007-02-076604
19. Waterston RH, Lindblad-Toh K, Birney E, Rogers J, Abril JF, Agarwal P, et al. Initial Sequencing and Comparative Analysis of the Mouse Genome. *Nature* (2002) 420(6915):520–62. doi: 10.1038/nature01262
20. Zheng-Bradley X, Rung J, Parkinson H, Brazma A. Large Scale Comparison of Global Gene Expression Patterns in Human and Mouse. *Genome Biol* (2010) 11(12):R124. doi: 10.1186/gb-2010-11-12-r124
21. O'Connell KE, Mikkola AM, Stepanek AM, Vernet A, Hall CD, Sun CC, et al. Practical Murine Hematopathology: A Comparative Review and Implications for Research. *Comp Med* (2015) 65(2):96–113.
22. LW L, Taormina V, Boyle PJ. Response of Acute Lymphocytic Leukemias to the Purine Antagonist 6-Mercaptopurine. *Ann N Y Acad Sci* (1954) 60 (2):244–50. doi: 10.1111/j.1749-6632.1954.tb40015.x
23. Skipper HE, Perry S. Kinetics of Normal and Leukemic Leukocyte Populations and Relevance to Chemotherapy. *Cancer Res* (1970) 30 (6):1883–97.
24. Skipper HE, Schabel FM, Wilcox WS. Experimental Evaluation of Potential Anticancer Agents. XXI. Scheduling of Arabinosylcytosine to Take Advantage of Its S-Phase Specificity Against Leukemia Cells. *Cancer Chemother Rep* (1967) 51(3):125–65.
25. Casazza AM, Pratesi G, Giuliani F, Di Marco A. Antileukemic Activity of 4-Demethoxydaunorubicin in Mice. *Tumori* (1980) 66(5):549–64. doi: 10.1177/030089168006600503
26. Law LW, Dunn TB. Observations on the Effect of a Folic-Acid Antagonist on Transplantable Lymphoid Leukemias in Mice. *J Natl Cancer Inst* (1949) 10 (1):179–92.
27. Kawasaki Y, Hirabayashi Y, Kaneko T, Kanno J, Kodama Y, Matsushima Y, et al. Benzene-Induced Hematopoietic Neoplasms Including Myeloid Leukemia in Trp53-Deficient C57BL/6 and C3H/He Mice. *Toxicol Sci* (2009) 110(2):293–306. doi: 10.1093/toxsci/kfp107
28. Furth J, Seibold H, Rathbone R. Experimental Studies on Lymphomatosis of Mice. *Am J Cancer* (1933) 19(3):521–604.
29. Gross L. "Spontaneous" Leukemia Developing in C3H Mice Following Inoculation in Infancy, With AK-Leukemic Extracts, or AK-Embrvos. *Proc Soc Exp Biol Med* (1951) 76(1):27–32.
30. Siegler R, Rich MA. Pathogenesis of Virus-Induced Myeloid Leukemia in Mice. *J Natl Cancer Inst* (1967) 38(1):31–50.
31. McGarry MP, Steeves RA, Eckner RJ, Mirand EA, Trudel PJ. Isolation of a Myelogenous Leukemia-Inducing Virus From Mice Infected With the Friend Virus Complex. *Int J Cancer* (1974) 13(6):867–78. doi: 10.1002/ijc.2910130614
32. Bedigian HG, Johnson DA, Jenkins NA, Copeland NG, Evans R. Spontaneous and Induced Leukemias of Myeloid Origin in Recombinant Inbred BXH Mice. *J Virol* (1984) 51(3):586–94. doi: 10.1128/jvi.51.3.586-594.1984
33. Copeland NG, Buchberg AM, Gilbert DJ, Jenkins NA. Recombinant Inbred Mouse Strains: Models for Studying the Molecular Genetic Basis of Myeloid Tumorigenesis. *Curr Top Microbiol Immunol* (1989) 149:45–57. doi: 10.1007/978-3-642-74623-9_4
34. Li J, Shen H, Himmel KL, Dupuy AJ, Largaespada DA, Nakamura T, et al. Leukaemia Disease Genes: Large-Scale Cloning and Pathway Predictions. *Nat Genet* (1999) 23(3):348–53. doi: 10.1038/15531
35. Adams JM, Harris AW, Pinkert CA, Corcoran LM, Alexander WS, Cory S, et al. The C-Myc Oncogene Driven by Immunoglobulin Enhancers Induces Lymphoid Malignancy in Transgenic Mice. *Nature* (1985) 318(6046):533–8. doi: 10.1038/318533a0
36. Schmidt EV, Pattengale PK, Weir L, Leder P. Transgenic Mice Bearing the Human C-Myc Gene Activated by an Immunoglobulin Enhancer: A Pre-B-Cell Lymphoma Model. *Proc Natl Acad Sci USA* (1988) 85(16):6047–51. doi: 10.1073/pnas.85.16.6047
37. Yan M, Kanbe E, Peterson LF, Boyapati A, Miao Y, Wang Y, et al. A Previously Unidentified Alternatively Spliced Isoform of T(8;21) Transcript Promotes Leukemogenesis. *Nat Med* (2006) 12(8):945–9. doi: 10.1038/nm1443

38. Yuan Y, Zhou L, Miyamoto T, Iwasaki H, Harakawa N, Hetherington CJ, et al. AML1-ETO Expression Is Directly Involved in the Development of Acute Myeloid Leukemia in the Presence of Additional Mutations. *Proc Natl Acad Sci U S A* (2001) 98(18):10398–403. doi: 10.1073/pnas.171321298
39. Cabezas-Wallscheid N, Eichwald V, de Graaf J, Löwer M, Lehr HA, Kreft A, et al. Instruction of Haematopoietic Lineage Choices, Evolution of Transcriptional Landscapes and Cancer Stem Cell Hierarchies Derived From an AML1-ETO Mouse Model. *EMBO Mol Med* (2013) 5(12):1804–20. doi: 10.1002/emmm.201302661
40. Abdallah MG, Niibori-Nambu A, Morii M, Yokomizo T, Ideue T, Kubota S, et al. RUNX1-ETO (RUNX1-RUNX1T1) Induces Myeloid Leukemia in Mice in an Age-Dependent Manner. *Leukemia* (2021) 35(10):2983–8. doi: 10.1038/s41375-021-01268-4
41. Kuo YH, Landrette SF, Heilman SA, Perrat PN, Garrett L, Liu PP, et al. Cbf Beta-SMMHC Induces Distinct Abnormal Myeloid Progenitors Able to Develop Acute Myeloid Leukemia. *Cancer Cell* (2006) 9(1):57–68. doi: 10.1016/j.ccr.2005.12.014
42. Corral J, Lavenir I, Impey H, Warren AJ, Forster A, Larson TA, et al. An Mll-AF9 Fusion Gene Made by Homologous Recombination Causes Acute Leukemia in Chimeric Mice: A Method to Create Fusion Oncogenes. *Cell* (1996) 85(6):853–61. doi: 10.1016/S0092-8674(00)81269-6
43. Collins EC, Pannell R, Simpson EM, Forster A, Rabbitts TH. Inter-Chromosomal Recombination of Mll and Af9 Genes Mediated by cre-loxP in Mouse Development. *EMBO Rep* (2000) 1(2):127–32. doi: 10.1093/embo-reports/kvd021
44. Krivtsov AV, Figueroa ME, Sinha AU, Stubbs MC, Feng Z, Valk PJ, et al. Cell of Origin Determines Clinically Relevant Subtypes of MLL-Rearranged AML. *Leukemia* (2013) 27(4):852–60. doi: 10.1038/leu.2012.363
45. Stavropoulou V, Kaspar S, Brault L, Sanders MA, Juge S, Morettini S, et al. MLL-AF9 Expression in Hematopoietic Stem Cells Drives a Highly Invasive AML Expressing EMT-Related Genes Linked to Poor Outcome. *Cancer Cell* (2016) 30(1):43–58. doi: 10.1016/j.ccell.2016.05.011
46. Zorko NA, Bernot KM, Whitman SP, Siebenaler RF, Ahmed EH, Marcucci GG, et al. Mll Partial Tandem Duplication and Flt3 Internal Tandem Duplication in a Double Knock-in Mouse Recapitulates Features of Counterpart Human Acute Myeloid Leukemias. *Blood* (2012) 120 (5):1130–6. doi: 10.1182/blood-2012-03-415067
47. Ono R, Masuya M, Nakajima H, Enomoto Y, Miyata E, Nakamura A, et al. Plzf Drives MLL-Fusion-Mediated Leukemogenesis Specifically in Long-Term Hematopoietic Stem Cells. *Blood* (2013) 122(7):1271–83. doi: 10.1182/blood-2012-09-456665
48. Bernt KM, Zhu N, Sinha AU, Vempati S, Faber J, Krivtsov AV, et al. MLL-Rearranged Leukemia is Dependent on Aberrant H3K79 Methylation by DOT1L. *Cancer Cell* (2011) 20(1):66–78. doi: 10.1016/j.ccr.2011.06.010
49. Mohanty S, Jyotsana N, Sharma A, Kloos A, Gabdoulline R, Othman B, et al. Targeted Inhibition of the NUP98-NSD1 Fusion Oncogene in Acute Myeloid Leukemia. *Cancers (Basel)* (2020) 12(10):2766. doi: 10.3390/cancers12102766
50. Schmoellerl J, Barbosa IAM, Eder T, Brandstoetter T, Schmidt L, Maurer B, et al. CDK6 is an Essential Direct Target of NUP98 Fusion Proteins in Acute Myeloid Leukemia. *Blood* (2020) 136(4):387–400. doi: 10.1182/blood.2019003267
51. Grisolano JL, Wesselschmidt RL, Pelicci PG, Ley TJ. Altered Myeloid Development and Acute Leukemia in Transgenic Mice Expressing PML-RAR Alpha Under Control of Cathepsin G Regulatory Sequences. *Blood* (1997) 89(2):376–87. doi: 10.1182/blood.V89.2.376
52. Du C, Redner RL, Cooke MP, Lavau C. Overexpression of Wild-Type Retinoic Acid Receptor Alpha (RARalpha) Recapitulates Retinoic Acid-Sensitive Transformation of Primary Myeloid Progenitors by Acute Promyelocytic Leukemia RARalpha-Fusion Genes. *Blood* (1999) 94 (2):793–802. doi: 10.1182/blood.V94.2.793
53. Westervelt P, Lane AA, Pollock JL, Oldfather K, Holt MS, Zimonjic DB, et al. High-Penetrance Mouse Model of Acute Promyelocytic Leukemia With Very Low Levels of PML-RARalpha Expression. *Blood* (2003) 102(5):1857–65. doi: 10.1182/blood-2002-12-3779
54. Speck NA, Gilliland DG. Core-Binding Factors in Haematopoiesis and Leukaemia. *Nat Rev Cancer* (2002) 2(7):502–13. doi: 10.1038/nrc840
55. Yergeau DA, Hetherington CJ, Wang Q, Zhang P, Sharpe AH, Binder M, et al. Embryonic Lethality and Impairment of Haematopoiesis in Mice Heterozygous for an AML1-ETO Fusion Gene. *Nat Genet* (1997) 15(3):303–6. doi: 10.1038/ng0397-303
56. Downing JR. The Core-Binding Factor Leukemias: Lessons Learned From Murine Models. *Curr Opin Genet Dev* (2003) 13(1):48–54. doi: 10.1016/S0959-437X(02)00018-7
57. Castilla LH, Wijmenga C, Wang Q, Stacy T, Speck NA, Eckhaus M, et al. Failure of Embryonic Hematopoiesis and Lethal Hemorrhages in Mouse Embryos Heterozygous for a Knocked-in Leukemia Gene CBFB-Myh11. *Cell* (1996) 87(4):687–96. doi: 10.1016/S0092-8674(00)81388-4
58. Meyer C, Burmeister T, Gröger D, Tsaur G, Fechina L, Renneville A, et al. The MLL Recombinome of Acute Leukemias in 2017. *Leukemia* (2018) 32 (2):273–84. doi: 10.1038/leu.2017.213
59. Hess JL, Yu BD, Li B, Hanson R, Korsmeyer SJ. Defects in Yolk Sac Hematopoiesis in Mll-Null Embryos. *Blood* (1997) 90(5):1799–806. doi: 10.1182/blood.V90.5.1799
60. Drynan LF, Pannell R, Forster A, Chan NM, Cano F, Daser A, et al. Mll Fusions Generated by Cre-loxP-Mediated *De Novo* Translocations can Induce Lineage Reassignment in Tumorigenesis. *EMBO J* (2005) 24 (17):3136–46. doi: 10.1038/sj.emboj.7600760
61. Chen L, Deshpande AJ, Banka D, Bernt KM, Dias S, Buske C, et al. Abrogation of MLL-AF10 and CALM-AF10-Mediated Transformation Through Genetic Inactivation or Pharmacological Inhibition of the H3K79 Methyltransferase Dot1l. *Leukemia* (2013) 27(4):813–22. doi: 10.1038/leu.2012.327
62. Moriya K, Suzuki M, Watanabe Y, Takahashi T, Aoki Y, Uchiyama T, et al. Development of a Multi-Step Leukemogenesis Model of MLL-Rearranged Leukemia Using Humanized Mice. *PLoS One* (2012) 7(6):e37892. doi: 10.1371/journal.pone.0037892
63. Deshpande AJ, Chen L, Fazio M, Sinha AU, Bernt KM, Banka D, et al. Leukemic Transformation by the MLL-AF6 Fusion Oncogene Requires the H3K79 Methyltransferase Dot1l. *Blood* (2013) 121(13):2533–41. doi: 10.1182/blood-2012-11-465120
64. Fu JF, Hsu CL, Shih LY. MLL/AF10(OM-LZ)-Immortalized Cells Expressed Cytokines and Induced Host Cell Proliferation in a Mouse Bone Marrow Transplantation Model. *Int J Cancer* (2010) 126(7):1621–9. doi: 10.1002/ijc.24867
65. Li Z, Luo RT, Mi S, Sun M, Chen P, Bao J, et al. Consistent Deregulation of Gene Expression Between Human and Murine MLL Rearrangement Leukemias. *Cancer Res* (2009) 69(3):1109–16. doi: 10.1158/0008-5472.CAN-08-3381
66. Ugale A, Norddahl GL, Wahlestedt M, Säwén P, Jaako P, Pronk CJ, et al. Hematopoietic Stem Cells are Intrinsically Protected Against MLL-ENL-Mediated Transformation. *Cell Rep* (2014) 9(4):1246–55. doi: 10.1016/j.celrep.2014.10.036
67. Sarrou E, Richmond L, Carmody RJ, Gibson B, Keeshan K. CRISPR Gene Editing of Murine Blood Stem and Progenitor Cells Induces MLL-AF9 Chromosomal Translocation and MLL-AF9 Leukaemogenesis. *Int J Mol Sci* (2020) 21(12):4266. doi: 10.3390/ijms21124266
68. Dawson MA, Prinjha RK, Dittmann A, Giotopoulos G, Bantscheff M, Chan WI, et al. Inhibition of BET Recruitment to Chromatin as an Effective Treatment for MLL-Fusion Leukaemia. *Nature* (2011) 478(7370):529–33. doi: 10.1038/nature10509
69. Grembecka J, He S, Shi A, Purohit T, Muntean AG, Sorenson RJ, et al. Menin-MLL Inhibitors Reverse Oncogenic Activity of MLL Fusion Proteins in Leukemia. *Nat Chem Biol* (2012) 8(3):277–84. doi: 10.1038/nchembio.773
70. Jevtic Z, Matafora V, Casagrande F, Santoro F, Minucci S, Garre' M, et al. SMARCA5 Interacts With NUP98-NSD1 Oncofusion Protein and Sustains Hematopoietic Cells Transformation. *J Exp Clin Cancer Res* (2022) 41(1):34. doi: 10.1186/s13046-022-02248-x
71. Placke T, Faber K, Nonami A, Putwain SL, Salih HR, Heidel FH, et al. Requirement for CDK6 in MLL-Rearranged Acute Myeloid Leukemia. *Blood* (2014) 124(1):13–23. doi: 10.1182/blood-2014-02-558114
72. Xu H, Valerio DG, Eisold ME, Sinha A, Koche RP, Hu W, et al. NUP98 Fusion Proteins Interact With the NSL and MLL1 Complexes to Drive Leukemogenesis. *Cancer Cell* (2016) 30(6):863–78. doi: 10.1016/j.ccell.2016.10.019

73. Iacobucci I, Qu C, Varotto E, Janke LJ, Yang X, Seth A, et al. Modeling and Targeting of Erythroleukemia by Hematopoietic Genome Editing. *Blood* (2021) 137(12):1628–40. doi: 10.1182/blood.2020009103
74. Heikamp EB, Henrich JA, Perner F, Wong EM, Hatton C, Wen Y, et al. The Menin-MLL1 Interaction is a Molecular Dependency in NUP98-Rearranged AML. *Blood* (2021) 139(6):894-906. doi: 10.1182/blood.2021012806
75. Iacobucci I, Wen J, Meggendorfer M, Choi JK, Shi L, Pounds SB, et al. Genomic Subtyping and Therapeutic Targeting of Acute Erythroleukemia. *Nat Genet* (2019) 51(4):694–704. doi: 10.1038/s41588-019-0375-1
76. Gruber TA, Larson Gedman A, Zhang J, Koss CS, Marada S, Ta HQ, et al. An Inv(16)(p13.3q24.3)-Encoded CBFA2T3-GLIS2 Fusion Protein Defines an Aggressive Subtype of Pediatric Acute Megakaryoblastic Leukemia. *Cancer Cell* (2012) 22(5):683–97. doi: 10.1016/j.ccr.2012.10.007
77. Dang J, Nance S, Ma J, Cheng J, Walsh MP, Vogel P, et al. AMKL Chimeric Transcription Factors are Potent Inducers of Leukemia. *Leukemia* (2017) 31 (10):2228–34. doi: 10.1038/leu.2017.51
78. Thiollier C, Lopez CK, Gerby B, Ignacimouttou C, Poglio S, Duffourd Y, et al. Characterization of Novel Genomic Alterations and Therapeutic Approaches Using Acute Megakaryoblastic Leukemia Xenograft Models. *J Exp Med* (2012) 209(11):2017–31. doi: 10.1084/jem.20121343
79. Wartman LD, Welch JS, Uy GL, Klco JM, Lamprecht T, Varghese N, et al. Expression and Function of PML-RARA in the Hematopoietic Progenitor Cells of Ctsg-PML-RARA Mice. *PLoS One* (2012) 7(10):e46529. doi: 10.1371/journal.pone.0046529
80. Chan IT, Kutok JL, Williams IR, Cohen S, Kelly L, Shigematsu H, et al. Conditional Expression of Oncogenic K-Ras From its Endogenous Promoter Induces a Myeloproliferative Disease. *J Clin Invest* (2004) 113(4):528–38. doi: 10.1172/JCI20476
81. Zhang J, Wang J, Liu Y, Sidik H, Young KH, Lodish HF, et al. Oncogenic Kras-Induced Leukemogeneis: Hematopoietic Stem Cells as the Initial Target and Lineage-Specific Progenitors as the Potential Targets for Final Leukemic Transformation. *Blood* (2009) 113(6):1304–14. doi: 10.1182/blood-2008-01-134262
82. Chang YI, You X, Kong G, Ranheim EA, Wang J, Du J, et al. Loss of Dnmt3a and Endogenous Kras(G12D/+) Cooperate to Regulate Hematopoietic Stem and Progenitor Cell Functions in Leukemogenesis. *Leukemia* (2015) 29 (9):1847–56. doi: 10.1038/leu.2015.85
83. Chan IT, Kutok JL, Williams IR, Cohen S, Moore S, Shigematsu H, et al. Oncogenic K-Ras Cooperates With PML-RAR Alpha to Induce an Acute Promyelocytic Leukemia-Like Disease. *Blood* (2006) 108(5):1708–15. doi: 10.1182/blood-2006-04-015040
84. Zhao S, Zhang Y, Sha K, Tang Q, Yang X, Yu C, et al. KRAS (G12D) Cooperates With AML1/ETO to Initiate a Mouse Model Mimicking Human Acute Myeloid Leukemia. *Cell Physiol Biochem* (2014) 33(1):78–87. doi: 10.1159/000356651
85. Wang YY, Zhao LJ, Wu CF, Liu P, Shi L, Liang Y, et al. C-KIT Mutation Cooperates With Full-Length AML1-ETO to Induce Acute Myeloid Leukemia in Mice. *Proc Natl Acad Sci U S A* (2011) 108(6):2450–5. doi: 10.1073/pnas.1019625108
86. Wang J, Kong G, Liu Y, Du J, Chang YI, Tey SR, et al. Nras(G12D/+) Promotes Leukemogenesis by Aberrantly Regulating Hematopoietic Stem Cell Functions. *Blood* (2013) 121(26):5203–7. doi: 10.1182/blood-2012-12-475863
87. Zhao L, Melenhorst JJ, Alemu L, Kirby M, Anderson S, Kench M, et al. KIT With D816 Mutations Cooperates With CBFB-MYH11 for Leukemogenesis in Mice. *Blood* (2012) 119(6):1511–21. doi: 10.1182/blood-2011-02-338210
88. Grundler R, Miething C, Thiede C, Peschel C, Duyster J. FLT3-ITD and Tyrosine Kinase Domain Mutants Induce 2 Distinct Phenotypes in a Murine Bone Marrow Transplantation Model. *Blood* (2005) 105(12):4792–9. doi: 10.1182/blood-2004-11-4430
89. Lee BH, Williams IR, Anastasiadou E, Boulton CL, Joseph SW, Amaral SM, et al. FLT3 Internal Tandem Duplication Mutations Induce Myeloproliferative or Lymphoid Disease in a Transgenic Mouse Model. *Oncogene* (2005) 24(53):7882–92. doi: 10.1038/sj.onc.1208933
90. Lee BH, Tothova Z, Levine RL, Anderson K, Buza-Vidas N, Cullen DE, et al. FLT3 Mutations Confer Enhanced Proliferation and Survival Properties to Multipotent Progenitors in a Murine Model of Chronic Myelomonocytic Leukemia. *Cancer Cell* (2007) 12(4):367–80. doi: 10.1016/j.ccr.2007.08.031
91. Yun H, Narayan N, Vohra S, Giotopoulos G, Mupo A, Madrigal P, et al. Mutational Synergy During Leukemia Induction Remodels Chromatin Accessibility, Histone Modifications and Three-Dimensional DNA Topology to Alter Gene Expression. *Nat Genet* (2021) 53(10):1443–55. doi: 10.1038/s41588-021-00925-9
92. Yang L, Rodriguez B, Mayle A, Park HJ, Lin X, Luo M, et al. DNMT3A Loss Drives Enhancer Hypomethylation in FLT3-ITD-Associated Leukemias. *Cancer Cell* (2016) 29(6):922–34. doi: 10.1016/j.ccell.2016.05.003
93. Schessl C, Rawat VP, Cusan M, Deshpande A, Kohl TM, Rosten PM, et al. The AML1-ETO Fusion Gene and the FLT3 Length Mutation Collaborate in Inducing Acute Leukemia in Mice. *J Clin Invest* (2005) 115(8):2159–68. doi: 10.1172/JCI24225
94. Li L, Piloto O, Nguyen HB, Greenberg K, Takamiya K, Racke F, et al. Knock-In of an Internal Tandem Duplication Mutation Into Murine FLT3 Confers Myeloproliferative Disease in a Mouse Model. *Blood* (2008) 111(7):3849–58. doi: 10.1182/blood-2007-08-109942
95. Annesley CE, Rabik C, Duffield AS, Rau RE, Magoon D, Li L, et al. Knock-In of the. *Oncotarget* (2018) 9(82):35313–26. doi: 10.18632/oncotarget.26238
96. Rau R, Magoon D, Greenblatt S, Li L, Annesley C, Duffield AS, et al. NPMc+ Cooperates With Flt3/ITD Mutations to Cause Acute Leukemia Recapitulating Human Disease. *Exp Hematol* (2014) 42(2):101–13.e5. doi: 10.1016/j.exphem.2013.10.005
97. Lee HK, Kim HW, Lee IY, Lee J, Jung DS, Lee SY, et al. G-749, a Novel FLT3 Kinase Inhibitor, can Overcome Drug Resistance for the Treatment of Acute Myeloid Leukemia. *Blood* (2014) 123(14):2209–19. doi: 10.1182/blood-2013-04-493916
98. Jackson EL, Willis N, Mercer K, Bronson RT, Crowley D, Montoya R, et al. Analysis of Lung Tumor Initiation and Progression Using Conditional Expression of Oncogenic K-Ras. *Genes Dev* (2001) 15(24):3243–8. doi: 10.1101/gad.943001
99. Mayle A, Yang L, Rodriguez B, Zhou T, Chang E, Curry CV, et al. Dnmt3a Loss Predisposes Murine Hematopoietic Stem Cells to Malignant Transformation. *Blood* (2015) 125(4):629–38. doi: 10.1182/blood-2014-08-594648
100. Duployez N, Marceau-Renaut A, Boissel N, Petit A, Bucci M, Geffroy S, et al. Comprehensive Mutational Profiling of Core Binding Factor Acute Myeloid Leukemia. *Blood* (2016) 127(20):2451–9. doi: 10.1182/blood-2015-12-688705
101. Armstrong SA, Mabon ME, Silverman LB, Li A, Gribben JG, Fox EA, et al. FLT3 Mutations in Childhood Acute Lymphoblastic Leukemia. *Blood* (2004) 103(9):3544–6. doi: 10.1182/blood-2003-07-2441
102. Yu Z, Du J, Hui H, Kan S, Huo T, Zhao K, et al. LT-171-861, a Novel FLT3 Inhibitor, Shows Excellent Preclinical Efficacy for the Treatment of FLT3 Mutant Acute Myeloid Leukemia. *Theranostics* (2021) 11(1):93–106. doi: 10.7150/thno.46593
103. Janke H, Pastore F, Schumacher D, Herold T, Hopfner KP, Schneider S, et al. Activating FLT3 Mutants Show Distinct Gain-of-Function Phenotypes *In Vitro* and a Characteristic Signaling Pathway Profile Associated With Prognosis in Acute Myeloid Leukemia. *PloS One* (2014) 9(3):e89560. doi: 10.1371/journal.pone.0089560
104. Bailey E, Li L, Duffield AS, Ma HS, Huso DL, Small D. FLT3/D835Y Mutation Knock-in Mice Display Less Aggressive Disease Compared With FLT3/internal Tandem Duplication (ITD) Mice. *Proc Natl Acad Sci U S A* (2013) 110(52):21113–8. doi: 10.1073/pnas.1310559110
105. Xu F, Wu LY, He Q, Wu D, Zhang Z, Song LX, et al. Exploration of the Role of Gene Mutations in Myelodysplastic Syndromes Through a Sequencing Design Involving a Small Number of Target Genes. *Sci Rep* (2017) 7:43113. doi: 10.1038/srep43113
106. Celik H, Mallaney C, Kothari A, Ostrander EL, Eultgen E, Martens A, et al. Enforced Differentiation of Dnmt3a-Null Bone Marrow Leads to Failure With C-Kit Mutations Driving Leukemic Transformation. *Blood* (2015) 125 (4):619–28. doi: 10.1182/blood-2014-08-594564
107. Guryanova OA, Shank K, Spitzer B, Luciani L, Koche RP, Garrett-Bakelman FE, et al. DNMT3A Mutations Promote Anthracycline Resistance in Acute Myeloid Leukemia *via* Impaired Nucleosome Remodeling. *Nat Med* (2016) 22(12):1488–95. doi: 10.1038/nm.4210
108. Loberg MA, Bell RK, Goodwin LO, Eudy E, Miles LA, SanMiguel JM, et al. Sequentially Inducible Mouse Models Reveal That Npm1 Mutation Causes

Malignant Transformation of Dnmt3a-Mutant Clonal Hematopoiesis. *Leukemia* (2019) 33(7):1635–49. doi: 10.1038/s41375-018-0368-6
109. Zhang X, Su J, Jeong M, Ko M, Huang Y, Park HJ, et al. DNMT3A and TET2 Compete and Cooperate to Repress Lineage-Specific Transcription Factors in Hematopoietic Stem Cells. *Nat Genet* (2016) 48(9):1014–23. doi: 10.1038/ng.3610
110. Zhang X, Wang X, Wang XQD, Su J, Putluri N, Zhou T, et al. Dnmt3a Loss and Idh2 Neomorphic Mutations Mutually Potentiate Malignant Hematopoiesis. *Blood* (2020) 135(11):845–56. doi: 10.1182/blood.2019003330
111. Moran-Crusio K, Reavie L, Shih A, Abdel-Wahab O, Ndiaye-Lobry D, Lobry C, et al. Tet2 Loss Leads to Increased Hematopoietic Stem Cell Self-Renewal and Myeloid Transformation. *Cancer Cell* (2011) 20(1):11–24. doi: 10.1016/j.ccr.2011.06.001
112. Quivoron C, Couronné L, Della Valle V, Lopez CK, Plo I, Wagner-Ballon O, et al. TET2 Inactivation Results in Pleiotropic Hematopoietic Abnormalities in Mouse and is a Recurrent Event During Human Lymphomagenesis. *Cancer Cell* (2011) 20(1):25–38. doi: 10.1016/j.ccr.2011.06.003
113. Ko M, Bandukwala HS, An J, Lamperti ED, Thompson EC, Hastie R, et al. Ten-Eleven-Translocation 2 (TET2) Negatively Regulates Homeostasis and Differentiation of Hematopoietic Stem Cells in Mice. *Proc Natl Acad Sci U S A* (2011) 108(35):14566–71. doi: 10.1073/pnas.1112317108
114. Li Z, Cai X, Cai CL, Wang J, Zhang W, Petersen BE, et al. Deletion of Tet2 in Mice Leads to Dysregulated Hematopoietic Stem Cells and Subsequent Development of Myeloid Malignancies. *Blood* (2011) 118(17):4509–18. doi: 10.1182/blood-2010-12-325241
115. Kunimoto H, Fukuchi Y, Sakurai M, Sadahira K, Ikeda Y, Okamoto S, et al. Tet2 Disruption Leads to Enhanced Self-Renewal and Altered Differentiation of Fetal Liver Hematopoietic Stem Cells. *Sci Rep* (2012) 2:273. doi: 10.1038/srep00273
116. Kunimoto H, Meydan C, Nazir A, Whitfield J, Shank K, Rapaport F, et al. Cooperative Epigenetic Remodeling by TET2 Loss and NRAS Mutation Drives Myeloid Transformation and MEK Inhibitor Sensitivity. *Cancer Cell* (2018) 33(1):44–59.e8. doi: 10.1016/j.ccell.2017.11.012
117. Palam LR, Mali RS, Ramdas B, Srivatsan SN, Visconte V, Tiu RV, et al. Loss of Epigenetic Regulator TET2 and Oncogenic KIT Regulate Myeloid Cell Transformation *via* PI3K Pathway. *JCI Insight* (2018) 3(4):e94679. doi: 10.1172/jci.insight.94679
118. Abdel-Wahab O, Gao J, Adli M, Dey A, Trimarchi T, Chung YR, et al. Deletion of Asxl1 Results in Myelodysplasia and Severe Developmental Defects In Vivo. *J Exp Med* (2013) 210(12):2641–59. doi: 10.1084/jem.20131141
119. Wang J, Li Z, He Y, Pan F, Chen S, Rhodes S, et al. Loss of Asxl1 Leads to Myelodysplastic Syndrome-Like Disease in Mice. *Blood* (2014) 123(4):541–53. doi: 10.1182/blood-2013-05-500272
120. Nagase R, Inoue D, Pastore A, Fujino T, Hou HA, Yamasaki N, et al. Expression of Mutant Asxl1 Perturbs Hematopoiesis and Promotes Susceptibility to Leukemic Transformation. *J Exp Med* (2018) 215(6):1729–47. doi: 10.1084/jem.20171151
121. D'Altri T, Wilhelmson AS, Schuster MB, Wenzel A, Kalvisa A, Pundhir S, et al. The ASXL1-G643W Variant Accelerates the Development of CEBPA Mutant Acute Myeloid Leukemia. *Haematologica* (2021) 106(4):1000–7. doi: 10.3324/haematol.2019.235150
122. Viny AD, Ott CJ, Spitzer B, Rivas M, Meydan C, Papalexi E, et al. Dose-Dependent Role of the Cohesin Complex in Normal and Malignant Hematopoiesis. *J Exp Med* (2015) 212(11):1819–32. doi: 10.1084/jem.20151317
123. Mullenders J, Aranda-Orgilles B, Lhoumaud P, Keller M, Pae J, Wang K, et al. Cohesin Loss Alters Adult Hematopoietic Stem Cell Homeostasis, Leading to Myeloproliferative Neoplasms. *J Exp Med* (2015) 212(11):1833–50. doi: 10.1084/jem.20151323
124. Tanaka T, Nakajima-Takagi Y, Aoyama K, Tara S, Oshima M, Saraya A, et al. Internal Deletion of BCOR Reveals a Tumor Suppressor Function for BCOR in T Lymphocyte Malignancies. *J Exp Med* (2017) 214(10):2901–13. doi: 10.1084/jem.20170167
125. Kelly MJ, So J, Rogers AJ, Gregory G, Li J, Zethoven M, et al. Bcor Loss Perturbs Myeloid Differentiation and Promotes Leukaemogenesis. *Nat Commun* (2019) 10(1):1347. doi: 10.1038/s41467-019-09250-6
126. Sportoletti P, Sorcini D, Guzman AG, Reyes JM, Stella A, Marra A, et al. Bcor Deficiency Perturbs Erythro-Megakaryopoiesis and Cooperates With Dnmt3a Loss in Acute Erythroid Leukemia Onset in Mice. *Leukemia* (2021) 35(7):1949–63. doi: 10.1038/s41375-020-01075-3
127. Butler JS, Dent SY. The Role of Chromatin Modifiers in Normal and Malignant Hematopoiesis. *Blood* (2013) 121(16):3076–84. doi: 10.1182/blood-2012-10-451237
128. Ley TJ, Ding L, Walter MJ, McLellan MD, Lamprecht T, Larson DE, et al. DNMT3A Mutations in Acute Myeloid Leukemia. *N Engl J Med* (2010) 363(25):2424–33. doi: 10.1056/NEJMoa1005143
129. Yan XJ, Xu J, Gu ZH, Pan CM, Lu G, Shen Y, et al. Exome Sequencing Identifies Somatic Mutations of DNA Methyltransferase Gene DNMT3A in Acute Monocytic Leukemia. *Nat Genet* (2011) 43(4):309–15. doi: 10.1038/ng.788
130. Walter MJ, Ding L, Shen D, Shao J, Grillot M, McLellan M, et al. Recurrent DNMT3A Mutations in Patients With Myelodysplastic Syndromes. *Leukemia* (2011) 25(7):1153–8. doi: 10.1038/leu.2011.44
131. Challen GA, Sun D, Jeong M, Luo M, Jelinek J, Berg JS, et al. Dnmt3a is Essential for Hematopoietic Stem Cell Differentiation. *Nat Genet* (2011) 44(1):23–31. doi: 10.1182/blood.V118.21.386.386
132. Challen GA, Sun D, Mayle A, Jeong M, Luo M, Rodriguez B, et al. Dnmt3a and Dnmt3b Have Overlapping and Distinct Functions in Hematopoietic Stem Cells. *Cell Stem Cell* (2014) 15(3):350–64. doi: 10.1016/j.stem.2014.06.018
133. Kim SJ, Zhao H, Hardikar S, Singh AK, Goodell MA, Chen T. A DNMT3A Mutation Common in AML Exhibits Dominant-Negative Effects in Murine ES Cells. *Blood* (2013) 122(25):4086–9. doi: 10.1182/blood-2013-02-483487
134. Russler-Germain DA, Spencer DH, Young MA, Lamprecht TL, Miller CA, Fulton R, et al. The R882H DNMT3A Mutation Associated With AML Dominantly Inhibits Wild-Type DNMT3A by Blocking its Ability to Form Active Tetramers. *Cancer Cell* (2014) 25(4):442–54. doi: 10.1016/j.ccr.2014.02.010
135. Tovy A, Rosas C, Gaikwad AS, Medrano G, Zhang L, Reyes JM, et al. Perturbed Hematopoiesis in Individuals With Germline DNMT3A Overgrowth Tatton-Brown-Rahman Syndrome. *Haematologica* (2021) 107(4):887-98. doi: 10.3324/haematol.2021.278990
136. Smith AM, LaValle TA, Shinawi M, Ramakrishnan SM, Abel HJ, Hill CA, et al. Functional and Epigenetic Phenotypes of Humans and Mice With DNMT3A Overgrowth Syndrome. *Nat Commun* (2021) 12(1):4549. doi: 10.1038/s41467-021-24800-7
137. Delhommeau F, Dupont S, Della Valle V, James C, Trannoy S, Massé A, et al. Mutation in TET2 in Myeloid Cancers. *N Engl J Med* (2009) 360(22):2289–301. doi: 10.1056/NEJMoa0810069
138. Kosmider O, Gelsi-Boyer V, Ciudad M, Racoeur C, Jooste V, Vey N, et al. TET2 Gene Mutation Is a Frequent and Adverse Event in Chronic Myelomonocytic Leukemia. *Haematologica* (2009) 94(12):1676–81. doi: 10.3324/haematol.2009.011205
139. Pratcorona M, Abbas S, Sanders MA, Koenders JE, Kavelaars FG, Erpelinck-Verschueren CA, et al. Acquired Mutations in ASXL1 in Acute Myeloid Leukemia: Prevalence and Prognostic Value. *Haematologica* (2012) 97(3):388–92. doi: 10.3324/haematol.2011.051532
140. Paschka P, Schlenk RF, Gaidzik VI, Herzig JK, Aulitzky T, Bullinger L, et al. ASXL1 Mutations in Younger Adult Patients With Acute Myeloid Leukemia: A Study by the German-Austrian Acute Myeloid Leukemia Study Group. *Haematologica* (2015) 100(3):324–30. doi: 10.3324/haematol.2014.114157
141. Metzeler KH, Herold T, Rothenberg-Thurley M, Amler S, Sauerland MC, Görlich D, et al. Spectrum and Prognostic Relevance of Driver Gene Mutations in Acute Myeloid Leukemia. *Blood* (2016) 128(5):686–98. doi: 10.1182/blood-2016-01-693879
142. Abdel-Wahab O, Adli M, LaFave LM, Gao J, Hricik T, Shih AH, et al. ASXL1 Mutations Promote Myeloid Transformation Through Loss of PRC2-Mediated Gene Repression. *Cancer Cell* (2012) 22(2):180–93. doi: 10.1016/j.ccr.2012.06.032
143. Chou WC, Huang HH, Hou HA, Chen CY, Tang JL, Yao M, et al. Distinct Clinical and Biological Features of *De Novo* Acute Myeloid Leukemia With Additional Sex Comb-Like 1 (ASXL1) Mutations. *Blood* (2010) 116(20):4086–94. doi: 10.1182/blood-2010-05-283291

144. Thota S, Viny AD, Makishima H, Spitzer B, Radivoyevitch T, Przychodzen B, et al. Genetic Alterations of the Cohesin Complex Genes in Myeloid Malignancies. *Blood* (2014) 124(11):1790–8. doi: 10.1182/blood-2014-04-567057
145. Thol F, Bollin R, Gehlhaar M, Walter C, Dugas M, Suchanek KJ, et al. Mutations in the Cohesin Complex in Acute Myeloid Leukemia: Clinical and Prognostic Implications. *Blood* (2014) 123(6):914–20. doi: 10.1182/blood-2013-07-518746
146. Xu H, Balakrishnan K, Malaterre J, Beasley M, Yan Y, Essers J, et al. Rad21-Cohesin Haploinsufficiency Impedes DNA Repair and Enhances Gastrointestinal Radiosensitivity in Mice. *PLoS One* (2010) 5(8):e12112. doi: 10.1371/journal.pone.0012112
147. de Rooij JD, van den Heuvel-Eibrink MM, Hermkens MC, Verboon LJ, Arentsen-Peters ST, Fornerod M, et al. BCOR and BCORL1 Mutations in Pediatric Acute Myeloid Leukemia. *Haematologica* (2015) 100(5):e194–5. doi: 10.3324/haematol.2014.117796
148. Terada K, Yamaguchi H, Ueki T, Usuki K, Kobayashi Y, Tajika K, et al. Usefulness of BCOR Gene Mutation as a Prognostic Factor in Acute Myeloid Leukemia With Intermediate Cytogenetic Prognosis. *Genes Chromosomes Cancer* (2018) 57(8):401–8. doi: 10.1002/gcc.22542
149. Grossmann V, Tiacci E, Holmes AB, Kohlmann A, Martelli MP, Kern W, et al. Whole-Exome Sequencing Identifies Somatic Mutations of BCOR in Acute Myeloid Leukemia With Normal Karyotype. *Blood* (2011) 118 (23):6153–63. doi: 10.1182/blood-2011-07-365320
150. Shiba N, Yoshida K, Shiraishi Y, Okuno Y, Yamato G, Hara Y, et al. Whole-Exome Sequencing Reveals the Spectrum of Gene Mutations and the Clonal Evolution Patterns in Paediatric Acute Myeloid Leukaemia. *Br J Haematol* (2016) 175(3):476–89. doi: 10.1111/bjh.14247
151. Rau R, Brown P. Nucleophosmin (NPM1) Mutations in Adult and Childhood Acute Myeloid Leukaemia: Towards Definition of a New Leukaemia Entity. *Hematol Oncol* (2009) 27(4):171–81. doi: 10.1002/hon.904
152. Cheng K, Sportoletti P, Ito K, Clohessy JG, Teruya-Feldstein J, Kutok JL, et al. The Cytoplasmic NPM Mutant Induces Myeloproliferation in a Transgenic Mouse Model. *Blood* (2010) 115(16):3341–5. doi: 10.1182/blood-2009-03-208587
153. Chou SH, Ko BS, Chiou JS, Hsu YC, Tsai MH, Chiu YC, et al. A Knock-in Npm1 Mutation in Mice Results in Myeloproliferation and Implies a Perturbation in Hematopoietic Microenvironment. *PLoS One* (2012) 7(11): e49769. doi: 10.1371/journal.pone.0049769
154. Vassiliou GS, Cooper JL, Rad R, Li J, Rice S, Uren A, et al. Mutant Nucleophosmin and Cooperating Pathways Drive Leukemia Initiation and Progression in Mice. *Nat Genet* (2011) 43(5):470–5. doi: 10.1038/ng.796
155. Mupo A, Celani L, Dovey O, Cooper JL, Grove C, Rad R, et al. A Powerful Molecular Synergy Between Mutant Nucleophosmin and Flt3-ITD Drives Acute Myeloid Leukemia in Mice. *Leukemia* (2013) 27(9):1917–20. doi: 10.1038/leu.2013.77
156. Kühn MW, Song E, Feng Z, Sinha A, Chen CW, Deshpande AJ, et al. Targeting Chromatin Regulators Inhibits Leukemogenic Gene Expression in NPM1 Mutant Leukemia. *Cancer Discov* (2016) 6(10):1166–81. doi: 10.1158/2159-8290.CD-16-0237
157. Kastenhuber ER, Lowe SW. Putting P53 in Context. *Cell* (2017) 170(6):1062–78. doi: 10.1016/j.cell.2017.08.028
158. Barbosa K, Li S, Adams PD, Deshpande AJ. The Role of TP53 in Acute Myeloid Leukemia: Challenges and Opportunities. *Genes Chromosomes Cancer* (2019) 58(12):875–88. doi: 10.1002/gcc.22796
159. Stoddart A, Fernald AA, Wang J, Davis EM, Karrison T, Anastasi J, et al. Haploinsufficiency of Del(5q) Genes, Egr1 and Apc, Cooperate With Tp53 Loss to Induce Acute Myeloid Leukemia in Mice. *Blood* (2014) 123(7):1069–78. doi: 10.1182/blood-2013-07-517953
160. Yang M, Pan Z, Huang K, Büsche G, Liu H, Göhring G, et al. A Unique Role of P53 Haploinsufficiency or Loss in the Development of Acute Myeloid Leukemia With FLT3-ITD Mutation. *Leukemia* (2022) 36(3):675–86. doi: 10.1038/s41375-021-01452-6
161. Zhao Z, Zuber J, Diaz-Flores E, Lintault L, Kogan SC, Shannon K, et al. P53 Loss Promotes Acute Myeloid Leukemia by Enabling Aberrant Self-Renewal. *Genes Dev* (2010) 24(13):1389–402. doi: 10.1101/gad.1940710
162. Zhang J, Kong G, Rajagopalan A, Lu L, Song J, Hussaini M, et al. P53-/- Synergizes With Enhanced NrasG12D Signaling to Transform Megakaryocyte-Erythroid Progenitors in Acute Myeloid Leukemia. *Blood* (2017) 129(3):358–70. doi: 10.1182/blood-2016-06-719237
163. Flanagan SP. 'Nude', A New Hairless Gene With Pleiotropic Effects in the Mouse. *Genet Res* (1966) 8(3):295–309. doi: 10.1017/s0016672300010168
164. Pantelouris EM. Absence of Thymus in a Mouse Mutant. *Nature* (1968) 217 (5126):370–1. doi: 10.1038/217370a0
165. Nara N, Miyamoto T. Direct and Serial Transplantation of Human Acute Myeloid Leukaemia Into Nude Mice. *Br J Cancer* (1982) 45(5):778–82. doi: 10.1038/bjc.1982.120
166. Bosma GC, Custer RP, Bosma MJ. A Severe Combined Immunodeficiency Mutation in the Mouse. *Nature* (1983) 301(5900):527–30. doi: 10.1038/301527a0
167. Cesano A, Hoxie JA, Lange B, Nowell PC, Bishop J, Santoli D. The Severe Combined Immunodeficient (SCID) Mouse as a Model for Human Myeloid Leukemias. *Oncogene* (1992) 7(5):827–36.
168. Sawyers CL, Gishizky ML, Quan S, Golde DW, Witte ON. Propagation of Human Blastic Myeloid Leukemias in the SCID Mouse. *Blood* (1992) 79 (8):2089–98. doi: 10.1182/blood.V79.8.2089.2089
169. Lapidot T, Sirard C, Vormoor J, Murdoch B, Hoang T, Caceres-Cortes J, et al. A Cell Initiating Human Acute Myeloid Leukaemia After Transplantation Into SCID Mice. *Nature* (1994) 367(6464):645–8. doi: 10.1038/367645a0
170. Shultz LD, Schweitzer PA, Christianson SW, Gott B, Schweitzer IB, Tennent B, et al. Multiple Defects in Innate and Adaptive Immunologic Function in NOD/LtSz-Scid Mice. *J Immunol* (1995) 154(1):180–91.
171. Bonnet D, Dick JE. Human Acute Myeloid Leukemia is Organized as a Hierarchy That Originates From a Primitive Hematopoietic Cell. *Nat Med* (1997) 3(7):730–7. doi: 10.1038/nm0797-730
172. Ailles LE, Gerhard B, Kawagoe H, Hogge DE. Growth Characteristics of Acute Myelogenous Leukemia Progenitors That Initiate Malignant Hematopoiesis in Nonobese Diabetic/Severe Combined Immunodeficient Mice. *Blood* (1999) 94 (5):1761–72. doi: 10.1182/blood.V94.5.1761.417k23_1761_1772
173. Pearce DJ, Taussig D, Zibara K, Smith LL, Ridler CM, Preudhomme C, et al. AML Engraftment in the NOD/SCID Assay Reflects the Outcome of AML: Implications for Our Understanding of the Heterogeneity of AML. *Blood* (2006) 107(3):1166–73. doi: 10.1182/blood-2005-06-2325
174. Sanchez PV, Perry RL, Sarry JE, Perl AE, Murphy K, Swider CR, et al. A Robust Xenotransplantation Model for Acute Myeloid Leukemia. *Leukemia* (2009) 23(11):2109–17. doi: 10.1038/leu.2009.143
175. Wunderlich M, Chou FS, Link KA, Mizukawa B, Perry RL, Carroll M, et al. AML Xenograft Efficiency is Significantly Improved in NOD/SCID-IL2RG Mice Constitutively Expressing Human SCF, GM-CSF and IL-3. *Leukemia* (2010) 24(10):1785–8. doi: 10.1038/leu.2010.158
176. Krevvata M, Shan X, Zhou C, Dos Santos C, Habineza Ndikuyeze G, Secreto A, et al. Cytokines Increase Engraftment of Human Acute Myeloid Leukemia Cells in Immunocompromised Mice But Not Engraftment of Human Myelodysplastic Syndrome Cells. *Haematologica* (2018) 103(6):959–71. doi: 10.3324/haematol.2017.183202
177. Rongvaux A, Willinger T, Martinek J, Strowig T, Gearty SV, Teichmann LL, et al. Development and Function of Human Innate Immune Cells in a Humanized Mouse Model. *Nat Biotechnol* (2014) 32(4):364–72. doi: 10.1038/nbt.2858
178. Strowig T, Rongvaux A, Rathinam C, Takizawa H, Borsotti C, Philbrick W, et al. Transgenic Expression of Human Signal Regulatory Protein Alpha in Rag2-/-Gamma(C)-/- Mice Improves Engraftment of Human Hematopoietic Cells in Humanized Mice. *Proc Natl Acad Sci U S A* (2011) 108(32):13218–23. doi: 10.1073/pnas.1109769108
179. Ellegast JM, Rauch PJ, Kovtonyuk LV, Müller R, Wagner U, Saito Y, et al. Inv (16) and NPM1mut AMLs Engraft Human Cytokine Knock-in Mice. *Blood* (2016) 128(17):2130–4. doi: 10.1182/blood-2015-12-689356
180. Carroll AM, Hardy RR, Bosma MJ. Occurrence of Mature B (IgM+, B220+) and T (CD3+) Lymphocytes in Scid Mice. *J Immunol* (1989) 143(4):1087–93.
181. Riggs JE, Stowers RS, Mosier DE. Adoptive Transfer of Neonatal T Lymphocytes Rescues Immunoglobulin Production in Mice With Severe Combined Immune Deficiency. *J Exp Med* (1991) 173(1):265–8. doi: 10.1084/jem.173.1.265
182. Pflumio F, Izac B, Katz A, Shultz LD, Vainchenker W, Coulombel L. Phenotype and Function of Human Hematopoietic Cells Engrafting Immune-Deficient CB17-Severe Combined Immunodeficiency Mice and

Nonobese Diabetic-Severe Combined Immunodeficiency Mice After Transplantation of Human Cord Blood Mononuclear Cells. *Blood* (1996) 88(10):3731–40. doi: 10.1182/blood.V88.10.3731.bloodjournal88103731

183. Wang JC, Doedens M, Dick JE. Primitive Human Hematopoietic Cells are Enriched in Cord Blood Compared With Adult Bone Marrow or Mobilized Peripheral Blood as Measured by the Quantitative *In Vivo* SCID-Repopulating Cell Assay. *Blood* (1997) 89(11):3919–24. doi: 10.1182/blood.V89.11.3919
184. Ishikawa F, Yoshida S, Saito Y, Hijikata A, Kitamura H, Tanaka S, et al. Chemotherapy-Resistant Human AML Stem Cells Home to and Engraft Within the Bone-Marrow Endosteal Region. *Nat Biotechnol* (2007) 25 (11):1315–21. doi: 10.1038/nbt1350
185. Taussig DC, Miraki-Moud F, Anjos-Afonso F, Pearce DJ, Allen K, Ridler C, et al. Anti-CD38 Antibody-Mediated Clearance of Human Repopulating Cells Masks the Heterogeneity of Leukemia-Initiating Cells. *Blood* (2008) 112 (3):568–75. doi: 10.1182/blood-2007-10-118331
186. Taussig DC, Vargaftig J, Miraki-Moud F, Griessinger E, Sharrock K, Luke T, et al. Leukemia-Initiating Cells From Some Acute Myeloid Leukemia Patients With Mutated Nucleophosmin Reside in the CD34(-) Fraction. *Blood* (2010) 115(10):1976–84. doi: 10.1182/blood-2009-02-206565
187. Reinisch A, Thomas D, Corces MR, Zhang X, Gratzinger D, Hong WJ, et al. A Humanized Bone Marrow Ossicle Xenotransplantation Model Enables Improved Engraftment of Healthy and Leukemic Human Hematopoietic Cells. *Nat Med* (2016) 22(7):812–21. doi: 10.1038/nm.4103
188. Abarrategi A, Foster K, Hamilton A, Mian SA, Passaro D, Gribben J, et al. Versatile Humanized Niche Model Enables Study of Normal and Malignant Human Hematopoiesis. *J Clin Invest* (2017) 127(2):543–8. doi: 10.1172/JCI89364
189. Wei J, Wunderlich M, Fox C, Alvarez S, Cigudosa JC, Wilhelm JS, et al. Microenvironment Determines Lineage Fate in a Human Model of MLL-AF9 Leukemia. *Cancer Cell* (2008) 13(6):483–95. doi: 10.1016/j.ccr.2008.04.020
190. Buechele C, Breese EH, Schneidawind D, Lin CH, Jeong J, Duque-Afonso J, et al. MLL Leukemia Induction by Genome Editing of Human CD34+ Hematopoietic Cells. *Blood* (2015) 126(14):1683–94. doi: 10.1182/blood-2015-05-646398
191. Qin H, Malek S, Cowell JK, Ren M. Transformation of Human CD34+ Hematopoietic Progenitor Cells With DEK-NUP214 Induces AML in an Immunocompromised Mouse Model. *Oncogene* (2016) 35(43):5686–91. doi: 10.1038/onc.2016.118

Conflict of Interest: The authors declare that the research was conducted in the absence of any commercial or financial relationships that could be construed as a potential conflict of interest.

Publisher's Note: All claims expressed in this article are solely those of the authors and do not necessarily represent those of their affiliated organizations, or those of the publisher, the editors and the reviewers. Any product that may be evaluated in this article, or claim that may be made by its manufacturer, is not guaranteed or endorsed by the publisher.

frontiers | Frontiers in Oncology

ORIGINAL RESEARCH
published: 23 June 2022
doi: 10.3389/fonc.2022.874317

An Integrated Analysis of Clinical, Genomic, and Imaging Features Reveals Predictors of Neurocognitive Outcomes in a Longitudinal Cohort of Pediatric Cancer Survivors, Enriched with CNS Tumors (Rad ART Pro)

Cassie Kline[1,2,3†], Schuyler Stoller[2†], Lennox Byer[4], David Samuel[5], Janine M. Lupo[6], Melanie A. Morrison[6], Andreas M. Rauschecker[6], Pierre Nedelec[6], Walter Faig[7], Dena B. Dubal[8], Heather J. Fullerton[2,3] and Sabine Mueller[2,3,9]*

[1] Division of Oncology, Department of Pediatrics, Children's Hospital of Philadelphia, University of Pennsylvania Perelman School of Medicine, Philadelphia, PA, United States, [2] Division of Child Neurology, Department of Neurology, University of California, San Francisco, United States, [3] Department of Pediatrics, University of California, San Francisco, San Francisco, CA, United States, [4] UCSF School of Medicine, University of California, San Francisco, United States, [5] Division of Pediatric Hematology/Oncology, Valley Children's Hospital, Madera, CA, United States, [6] Department of Radiology and Biomedical Imaging, University of California, San Francisco, United States, [7] Children's Hospital of Philadelphia, Philadelphia, PA, United States, [8] Department of Neurology, University of California, San Francisco, CA, United States, [9] Department of Neurological Surgery, University of California, San Francisco, CA, United States

Background: Neurocognitive deficits in pediatric cancer survivors occur frequently; however, individual outcomes are unpredictable. We investigate clinical, genetic, and imaging predictors of neurocognition in pediatric cancer survivors, with a focus on survivors of central nervous system (CNS) tumors exposed to radiation.

Methods: One hundred eighteen patients with benign or malignant cancers (median diagnosis age: 7; 32% embryonal CNS tumors) were selected from an existing multi-institutional cohort (RadART Pro) if they had: 1) neurocognitive evaluation; 2) available DNA; 3) standard imaging. Utilizing RadART Pro, we collected clinical history, genomic sequencing, CNS imaging, and neurocognitive outcomes. We performed single nucleotide polymorphism (SNP) genotyping for candidate genes associated with neurocognition: *COMT*, *BDNF*, *KIBRA*, *APOE*, *KLOTHO.* Longitudinal neurocognitive testing were performed using validated computer-based CogState batteries. The imaging cohort was made of patients with available iron-sensitive (n = 28) and/or T2 FLAIR (n = 41) sequences. Cerebral microbleeds (CMB) were identified using a semi-automated algorithm. Volume of T2 FLAIR white matter lesions (WML) was measured using an automated method based on a convolutional neural network. Summary statistics were performed for patient characteristics, neurocognitive assessments, and imaging. Linear mixed effects and hierarchical models assessed patient characteristics and SNP

OPEN ACCESS

Edited by:
Paraskevi Panagopoulou, Aristotle University of Thessaloniki, Greece

Reviewed by:
Maura Massimino, National Cancer Institute Foundation (IRCCS), Italy
Carsten Friedrich, University Children's Hospital, Germany

***Correspondence:**
Sabine Mueller
sabine.mueller@ucsf.edu

†These authors have contributed equally to this work

Specialty section:
This article was submitted to Pediatric Oncology, a section of the journal Frontiers in Oncology

Received: *11 February 2022*
Accepted: *16 May 2022*
Published: *23 June 2022*

Citation:
Kline C, Stoller S, Byer L, Samuel D, Lupo JM, Morrison MA, Rauschecker AM, Nedelec P, Faig W, Dubal DB, Fullerton HJ and Mueller S (2022) An Integrated Analysis of Clinical, Genomic, and Imaging Reveals Predictors of Neurocognitive Outcomes in a Longitudinal Cohort of Pediatric Cancer Survivors, Enriched With CNS Tumors (Rad ART Pro). Front. Oncol. 12:874317. doi: 10.3389/fonc.2022.874317

relationship with neurocognition over time. Nested case-control analysis was performed to compare candidate gene carriers to non-carriers.

Results: CMB presence at baseline correlated with worse performance in 3 of 7 domains, including executive function. Higher baseline WML volumes correlated with worse performance in executive function and verbal learning. No candidate gene reliably predicted neurocognitive outcomes; however, *APOE ϵ4* carriers trended toward worse neurocognitive function over time compared to other candidate genes and carried the highest odds of low neurocognitive performance across all domains (odds ratio 2.85, *P*=0.002). Hydrocephalus and seizures at diagnosis were the clinical characteristics most frequently associated with worse performance in neurocognitive domains (5 of 7 domains). Overall, executive function and verbal learning were the most frequently negatively impacted neurocognitive domains.

Conclusion: Presence of CMB, *APOE ϵ4* carrier status, hydrocephalus, and seizures correlate with worse neurocognitive outcomes in pediatric cancer survivors, enriched with CNS tumors exposed to radiation. Ongoing research is underway to verify trends in larger cohorts.

Keywords: pediatric cancer survivors, Apo E4, neurocognition, late effects, radiation

INTRODUCTION

Pediatric cancer survivors, particularly survivors of central nervous system (CNS) tumors, suffer from a range of late effects related to their tumor diagnosis and therapies, often leading to long-term negative impacts on quality of life (1, 2). Arguably, one of the most challenging late effects seen in this population is neurocognitive impairment (3–5). This is especially true after exposure to CNS radiation. Adults that survive childhood CNS tumors have lower intelligence quotients (IQs) and neurocognitive deficits specific to a variety of domains such as attention, processing speed, and executive function that worsen over time (6–10). Although neurocognitive outcomes for pediatric CNS tumor survivors show poorer neurocognitive functioning when compared to population means and normal matched controls (4, 11, 12), there remains great variability among individuals (7, 13). It is well supported that certain interventions such as cranial radiation therapy (14), particularly in the youngest patients, negatively impact neurocognition. Other clinical characteristics such as young age, hydrocephalus, and seizure disorder at diagnosis have also shown inverse relationships with later neurocognitive aptitude (15, 16).

Across adult literature, limited pediatric literature, and in preclinical models for aging and dementia, there are several candidate genes linked to neurocognitive outcomes. Within these genes, there are single nucleotide polymorphisms (SNPs) that correlate with neurocognitive performance. In aging adult populations, catechol-O-methyltransferase (*COMT*, rs4680); brain-derived neurotrophic factor (*BDNF*, rs6265); kidney and brain expressed protein (*KIBRA*, rs17070145); apolipoprotein E (*APOE*, rs429358, rs7412); and klotho (*KL*, rs9536314, rs95270025) each carry allelic variants that can be beneficial or detrimental to neurocognition (17–19). *APOE*, *BDNF*, and *COMT* candidate genes have demonstrated influence on neurocognition in oncology populations, though limited data exists specific to pediatric cancer and CNS tumor populations (20, 21). Confirmation of the role of such genetic predictors on neurocognitive outcomes in pediatric cancer survivors, particularly those with CNS tumors, could help personalize cancer therapy with the potential to limit neurocognitive injury and refine follow-up care. Further, at diagnosis, identification of predictors would help families make treatment-related decisions; prepare families for potentially significant, long-term impacts on their child's life; and identify children at greatest risk.

In addition to genetic correlates, radiographic and radiogenomic signatures of neurocognitive outcomes would augment our understanding of which patients are at greatest risk of neurocognitive injury and who may benefit from early educational or cognitive interventions. Patients who undergo cranial radiation are at risk of developing cerebral microbleeds (CMB), which associate with higher doses of radiation, volume of radiation field, longer follow up, and age (22–26). High resolution 7T MRI studies have reported as high as 100% prevalence in CMB detection after 1 year following radiation therapy (27, 28) CMB presence in the frontal lobe associates with worse performance in executive functioning in the RadART cohort (29). Similarly, white matter lesions (WML), as measured by T2 FLAIR sequences on MR imaging, are an established neuroimaging marker of chronic effects of pediatric cancer therapy, such as radiation. The risk of accumulating

Abbreviations: APOE4, apolipoprotein E (*APOE*, rs429358, rs7412); BDNF, brain-derived neurotrophic factor (*BDNF*, rs6265); COMT, catechol-O-methyltransferase (*COMT*, rs4680); CMBs, cerebral microbleeds; KIBRA, kidney and brain expressed protein (*KIBRA*, rs17070145); WML, white matter lesions.

WMLs is increased by younger age at diagnosis, hydrocephalus, methotrexate exposure, and treatment with radiation. Further, higher dose and volume of irradiated tissue impact the accumulation of WMLs (22, 23, 25, 30), which ultimately correlate with negative effects on intelligent quotient (IQ) and cognitive domains such as processing speed (31, 32).

In the current study, we assessed the impact of clinical characteristics, CMB and WML, and cognition-related genes (*COMT*, *BDNF*, *KIBRA*, *APOE*, and *KLOTHO*) on neurocognitive outcomes in a cohort of pediatric cancer survivors, enriched with CNS tumors, using an established multi-institutional cohort (Rad ART Pro) (29, 33). We hypothesize certain clinical characteristics, extent of CMB and WML, and genetic variants related to cognition will augment prediction of neurocognitive outcomes in survivors of CNS tumors. Our long-term aim is to improve anticipatory guidance, contribute to treatment stratification, and improve protective interventions for this high-risk population.

METHODS

Patient Population

The patient population included in this study was selected from a cohort of patients who were previously enrolled in a multicenter, longitudinal cohort investigating radiation-induced arteriopathy, RadART Pro. The study collects clinical characteristics, DNA samples from peripheral blood collections, imaging, and neurocognitive performance outcomes in pediatric cancer survivors (29, 33). The cohort is enriched with patients with CNS tumors previously exposed to radiation therapy. Initial inclusion criteria for enrollment into RadART Pro were: 1) prior diagnosis of cancer, 2) previous exposure to radiation of the brain and/or neck, 3) age ≤ 21 years at time of radiation exposure, 4) anticipated survival > 1 year post-radiation. In 2015, the study expanded to include a comparison group of pediatric brain tumor patients that did not receive radiation therapy. For this group, diagnosis of a brain tumor must have occurred at age ≤ 21 years. Patients were recruited from four sites, including UCSF Benioff Children's Hospital – San Francisco and Oakland sites (San Francisco, CA; Oakland, CA); Valley Children's Hospital (Madera, CA); and St, Louis Children's Hospital (St. Louis, MO). The institutional review boards of all participating sites of the RadART Pro study approved the protocol and procedures for that study. Informed consent was obtained from all patients prior to participation.

To be included in the integrated analyses in the current work, patients must have had at least candidate gene sequencing and one timepoint of neurocognitive testing.

Genotyping

SNP genotyping for *COMT*, *BDNF*, *KIBRA*, *APOE*, and *KLOTHO* was performed for each patient (**Supplemental Table 1**). Amplified product was sequenced in both directions with PCR primers using the Sanger method (Quintara Biosciences, Berkeley, CA). The complete sequencing protocol is included in the **Supplemental Methods** section.

Neurocognitive Testing

Neurocognitive assessments were completed for all patients at an initial visit and regular follow-up intervals (about yearly) using computer-based CogState testing. CogState has been validated for patients 5 years and older, across a variety of populations, including the CNS tumor population (34–36). The CogState battery used in our study included the following tests: Identification test (IDN; attention), Continuous Paired Associate Learning test (CPAL; paired associate learning), Detection test (DET; psychomotor function), Groton Maze Learning test (GML; executive function), International Shopping List test (ISL and ISRL; verbal learning and verbal memory), and One Back test (ONB; working memory). All tests were administered by trained clinical research associates during standard of care clinic visits and under appropriate test-taking environments. Scores were collected for each test and converted to z-scores based on age-normed population means. For younger ages, some tests lacked sufficient population norms (e.g. age 5 to 9 years for the Groton Maze Learning, International Shopping List, and Continuous Paired Associate Learning tests). In these instances, z-scores were derived from age-matched comparisons within the patient cohort itself, as per vendor guidance.

Initial neurocognitive screens were typically conducted following completion of tumor-directed therapy for the primary diagnosis. Subsequent screens were completed at standard of care clinic visits for regular tumor surveillance. Due to the nature of this study opening several years after some patients completed therapy, initial testing occurred at variable post-therapy time points for individual patients. A continuous variable, "time from radiation" was used in all models to address the heterogeneity in timing of initial testing and follow-up. This variable reflected the time in years from end of cranial radiation therapy to the follow-up time point being tested.

Imaging

Participants enrolled in RadART Pro were followed prospectively with structural and cerebrovascular brain imaging, as available. Imaging interval and acquisition parameters were based on institutional standards for routine clinical care and tumor surveillance. All imaging was performed on 1.5 and 3T scanners. Iron-sensitive imaging and T2 FLAIR sequences were acquired following primary therapy completion and within 180 days of the date of neurocognitive assessment.

Iron-sensitive imaging including T2*-weighted gradient echo sequences or susceptibility-weighted imaging (SWI; a technique that combines T2* magnitude and phase images to further enhance susceptibility contrast) were collected to detect, segment, and quantify CMBs using MATLAB-based semi-automated CMB detection and segmentation (37). CMBs were defined as hypointense foci that were present on consecutive, axial slices exceeding a threshold degree of radial symmetry (38). CMB candidates were excluded if in close proximity to perpendicular vessels or the tumor cavity. A single reader (LB) reviewed CMB candidates to determine if the segmented lesions were true CMBs or false positives. Segmented CMBs were

counted and the cumulative CMB aggregate volume (mm^3) was calculated.

T2-weighted fluid-attenuated inversion-recovery (FLAIR) sequences were collected across study sites, with inter-site variability in two-dimensional and three-dimensional acquisitions. A previously described convolutional neural network with 3D U-net architecture (39, 40) was trained to identify abnormal FLAIR signal attributable to prior radiation, excluding abnormal FLAIR signal attributable to post-surgical changes or treated tumor tissue. Training data consisted of 246 expert manual segmentations of target FLAIR signal, which were initially segmented by a research specialist with several years of brain MRI segmentation experience and modified or verified by a board-certified neuroradiologist with 4 years of post-residency experience. Training data were independent of test data, noting that 9 of the MRIs used for training were from patients that were also included in the test set, but from MRIs obtained in different years from those in the test set. Training hyperparameters included a kernel size of 3 x 3 x 3, cross-entropy loss function, and an Adam optimizer with learning rate of 1 x 10−4, implemented in TensorFlow 2 (https://www.tensorflow.org) using the Python programming language. The network was trained for 110 epochs, with a batch size of 37 3D patches (96 x 96 x 96 mm each). The implementation was on a DGX-2 AI server (version 4.5.0; NVIDIA). The fully trained U-net was then applied to the patients in our cohort with available FLAIR sequences and neurocognitive assessments to detect and segment areas of abnormal FLAIR signal attributable to radiation treatment, and the volume of this abnormality was quantified.

Statistical Analysis

Clinical, genomic, and imaging variables were defined as follows: time from radiation (continuous variable), age at diagnosis (continuous variable), presence of hydrocephalus at diagnosis (binary variable), presence of seizures at diagnosis (binary variable), chemotherapy exposure (binary variable), radiation exposure (binary variable), gender (binary variable), tumor type (categorical variable), tumor location (categorical variable), presence of CMB at baseline (binary variable), and WML volume at baseline (continuous variable). Radiation was included as a binary variable to accommodate patients for which we did not have details on radiation dose. Across each model and statistical comparison, neurocognitive outcomes were evaluated per neurocognitive domain tested.

Summary statistics for patient characteristics, neurocognitive assessments, and imaging variables are presented as frequencies and percentages for categorical measures and median and interquartile range (IQR) for continuous variables. Neurocognitive outcomes are plotted over time with trajectories stratified by SNP carrier status (heterozygous or homozygous [carrier] vs non-carrier). Linear mixed effects models with time from radiation were used to assess the significance of SNP carriers on neurocognitive outcomes over time. The association of patient characteristics on neurocognitive outcomes were evaluated similarly. Characteristics significantly associated with most neurocognitive assessments were included in adjusted models considering SNP carrier status effect on outcome measures. Baseline association of imaging variables with patient characteristics, neurocognitive assessments, and SNP carrier status were evaluated by Chi-Square or Fisher's exact tests, Wilcoxon rank-sum or Kruskal-Wallis tests, or Spearman correlation as appropriate. Hierarchical modeling with the addition of baseline CMB presence and WML volume to our adjusted models is used to assess longitudinal effect. All inference was conducted with significance level 0.05. All analyses were figures are generated in R 4.1.2.

Nested case-control analysis was done to compare candidate gene carriers (cases) and non-carriers (controls). Odds ratios were calculated to compare the prevalence of carriers and non-carriers in the lowest and highest performers on neurocognitive testing. Scores that were at least one standard deviation above or below the mean were considered high and low performers, respectively.

RESULTS

Cohort Descriptions

Overall Cohort

Within the full RadART Pro cohort (n=447), 118 patients met criteria for completion of both candidate sequencing and at least one timepoint of neurocognitive testing (n=57 males; median age at diagnosis 7 years [IQR 4, 11]; **Table 1** and **Figure 1**). A total of 28 patients in this cohort had available iron-sensitive imaging sequences for assessment of CMBs and 41 patients had T2 FLAIR imaging for assessment of WMLs. These subcohorts are described in detail below.

Embryonal tumors were the most frequent tumor diagnosis (n=38, 32%) with cerebellum/posterior fossa being the most common primary tumor location (n=35, 30%). Most patients (n=100, 85%) were treated with radiation therapy. Median time from cranial radiation therapy to time of initial neurocognitive testing was 3.9 years (IQR 2.1, 6.5) and median age at time of initial neurocognitive testing was 13 years (IQR 9.0, 18). Median time from diagnosis to initial neurocognitive testing was 5.0 years (IQR 3.0, 8.0; **Table 2**).

CMB Subcohort

Of the 28 patients with available iron-sensitive imaging, 17 were male (61%; median age of diagnosis was 5 years [IQR 3, 8]; **Table 1**). Embryonal tumors were the most frequent tumor diagnosis (n = 11, 39%) with cerebellum/posterior fossa as the most common primary tumor location (n=9, 32%). Most patients (n=26, 93%) were treated with radiation therapy. Median age at initial neurocognitive assessment was 13 years (IQR 9, 15) and median time from diagnosis to initial neurocognitive testing was 6.5 (IQR 4.0, 9.0; **Table 2**). In patients previously treated with radiation therapy, median time from radiation therapy to initial neurocognitive testing was 4.5 years (IQR 2.5, 6.5). At least one CMB was detected in 10 patients (36%) at the time of initial neurocognitive assessment. Among those with at least one CMB, the median number of CMBs was

TABLE 1 | Summary of patient demographics, tumor characteristics, and baseline clinical symptoms across each subcohort by column.

Characteristics	Overall (n=118)	CMBs (n=28)	White matter changes (n=41)
Age at diagnosis, years (median [IQR])			
Diagnosis	7 (4, 11)	5.0 (3, 8)	7 (3, 10)
Gender, n (%)			
Male	67 (57)	17 (61)	21 (51)
Race, n (%)			
American Indian or Alaska Native	1 (1)	0 (0)	0 (0)
Asian	12 (10)	3 (11)	7 (17)
Black or African American	4 (3)	1 (4)	2 (5)
Multiracial	5 (4)	3 (11)	0 (0)
Native Hawaiian or Other Pacific Islander	1 (1)	0 (0)	0 (0)
Unknown	13 (11)	2 (7)	3 (7)
White	82 (70)	19 (68)	29 (71)
Ethnicity, n (%)			
Hispanic or Latino	30 (25)	2 (7)	8 (20)
Not Hispanic or Latino	88 (75)	26 (93)	33 (80)
Tumor Type, n (%)			
Embryonal tumors	38 (32)	11 (39)	19 (46)
Hematologic Malignancy	21 (18)	0 (0)	1 (2)
Low-grade glioma	16 (14)	6 (21)	6 (15)
NOS	13 (11)	4 (14)	5 (12)
Ependymal tumors	8 (7)	1 (4)	4 (10)
Solid tumors (extra-CNS)	8 (7)	0 (0)	0 (0)
Germ cell tumors	7 (6)	2 (7)	5 (12)
High-grade glioma	7 (6)	4 (14)	1 (2)
Tumor Location, n (%)			
Cerebellum/Posterior fossa	35 (30)	9 (32)	17 (41)
Extra-CNS	31 (26)	0 (0)	1 (2)
Midline	21 (18)	8 (29)	12 (29)
Lobar	14 (12)	6 (21)	4 (10)
NOS	6 (5)	2 (7)	1 (2)
Multifocal	5 (4)	2 (7)	3 (7)
Optic nerves	5 (4)	1 (4)	3 (7)
Radiation therapy exposure, n (%)	100 (85)	26 (93)	36 (88)
Hydrocephalus at diagnosis, n (%)	40 (34)	13 (46)	18 (44)
Seizures at diagnosis, n (%)	14 (12)	2 (7)	6 (15)

Details of each cohort are provided, including demographics of patients and diagnoses and treatment details. CMBs, cerebral microbleeds; IQR, interquartile range; WMLs, white matter lesions; NOS, not otherwise specified.

5.0 (IQR 4.0, 5.0) and the median total volume of CMBs was 120 mm^3 (**Figure 2**). Neither the age at diagnosis nor the time from radiation significantly differed between the CMB-present and CMB-absent groups.

WML Subcohort

Of the 41 patients with available T2 FLAIR imaging, 21 were male (51%; median age of diagnosis was 7 years [IQR 3. 10]; **Table 1**). Embryonal tumors were the most frequent tumor diagnosis (n = 19, 46%) with cerebellum/posterior fossa as the most common primary tumor location (n=17, 41%). Most patients (n=36, 88%) were treated with radiation therapy. Median age at initial neurocognitive assessment was 12 years (IQR 9, 17 and median time from diagnosis to initial neurocognitive testing was 6.0 years (IQR 3.0, 8.0; **Table 2**). In patients previously treated with radiation therapy, median time from radiation therapy to initial neurocognitive testing was 4.3 years (IQR 1.5, 6.4). Most patients (n=39; 95%) had measurable WML volumes identified by the convolutional neural network, of which the median volume was 1400 mm^3 (IQR 349, 4590; **Figure 3**).

Prevalence of Candidate Genes

Each genetic variant was present at varying prevalence across the cohorts, with the largest difference in candidate gene carrier proportion being 32% and 46% for BDNF rs6265 in the CMB and WML cohorts, respectively (**Supplemental Table 2**). For the subset of 118 total patients, sequencing was unsuccessful for individual two alleles of interest (*APOE*: n=9; *BDNF*: n=1).

Clinical, Genomic, and Imaging Effects on Neurocognitive Outcomes

We initially performed bivariate analyses to identify isolated associations between clinical, genomic, and imaging characteristics with neurocognitive outcomes and inclusive of time to radiation as a variable. Based on statistical significance in bivariate analyses, we then determined which variables would be used in a hierarchical analysis to identify contributions of multiple variables on each neurocognitive domain tested.

Clinical characteristics

Hydrocephalus and seizures were the most common clinical characteristics associated with worse neurocognitive outcome.

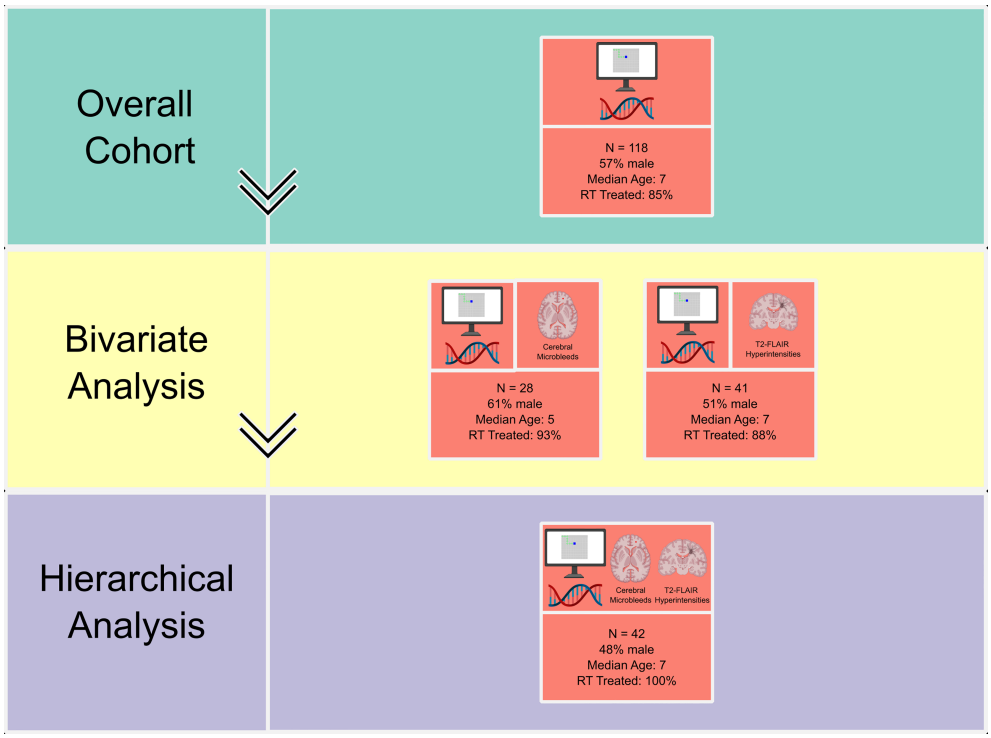

FIGURE 1 | Diagram of modalities investigated and bivariate and multivariate analyses with individual subcohort size and characteristics. Diagram details delineate data type at each level of analysis: neurocognitive assessments (computer screen), candidate gene sequencing (double helix), and imaging (CMBs as axial view, FLAIR WML as coronal view). RT, radiation therapy. Created with BioRender.com.

These were each associated with 5 of 7 domains tested, including verbal learning, verbal memory, working memory, attention, and executive function (**Table 3**). Of tumor diagnoses, germ cell tumors associated with the highest number of affected domains (3 of 7), including verbal learning, working memory, and executive function. Age at diagnosis associated with worse performance in attention (P=0.03) and time from radiation associated with worse performance in verbal learning (P=0.03).

Genomic Characteristics

No candidate gene reliably predicted neurocognitive outcomes at a statistically significant level. However, compared to non-carriers, *APOE ϵ4* carriers demonstrated worsening neurocognitive performance over time across all domains, albeit in a small cohort in later years of analysis (**Figure 4**). No other genetic variants demonstrated obvious trends on neurocognitive outcomes over time (**Supplemental Figures 1**–**4**). In the nested case-control candidate gene analyses comparing proportion of *APOE ϵ4 carrier and non-carriers within the highest and lowest performers in neurocognitive testing*, *APOE ϵ4* carriers had the greatest odds of being among the poorest performers across all neurocognitive domains at all time points tested (Odds ratio [OR] 2.85, P=0.002), *BDNF* carriers showed the lowest odds, (OR 0.52, P=0.001), and *COMT* did not reach statistical significance (**Table 4**).

No candidate gene was found to correlate with CMBs or WML volume at baseline assessment.

Imaging Characteristics

The impact of baseline CMBs and WML volume on neurocognition was evaluated independently and in

TABLE 2 | Time of initial neurocognitive assessments in relationship to patient diagnosis and radiation by subcohort.

Temporal characteristics at baseline Cogstate testing	Overall Cohort n = 118	CMBs n = 28	WMLs n = 41
Age, years [median (IQR)]	13 (9, 18)	13 (9,15)	12 (9, 17)
Time from diagnosis, years [median (IQR)]	5.0 (3.0, 8.0)	6.5 (4.0, 9.0)	6.0 (3.0, 8.0)
Time from radiation therapy, years [median (IQR)]	3.9 (2.1, 6.5)	4.5 (2.5, 6.5)	4.3 (1.5, 6.4)

Table describes age at time of Cogstate neurocognitive testing, time from diagnosis to testing, and time from radiation to testing. IQR, interquartile range; CMBs, cerebral microbleeds; WMLs, white matter lesions.

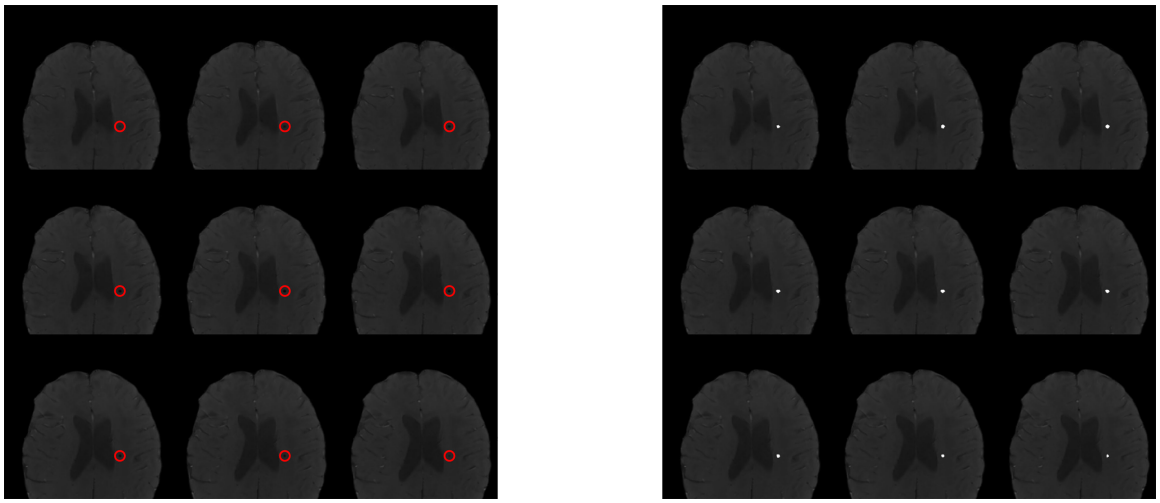

FIGURE 2 | Visual representation of CMB analysis. Imaging inclusive of semi-automated lesion segmentation iron-sensitive sequence analysis. Left panel shows sequence without segmentation label with manually insertion of red circle outlining area of known cerebral microbleed. Right panel displays with semi-automated insertion of white circle overlying area of cerebral microbleed identified on segmentation.

combination. The presence of CMBs at time of initial neurocognitive assessment associated with worse performance in psychomotor function, executive function, verbal learning with median z-scores across each domain of -1.84 (P=0.01), -1.75 (P=0.02), and -0.77 (P=0.03), respectively. The impact of volume of WMLs at time of initial neurocognitive assessment was evaluated using Spearman correlation coefficients. Higher baseline WML volumes trended with worse performance in executive function (P=0.05) and verbal learning (P=0.06), but these did not reach statistical significance.

Hierarchical Cluster Analysis

While we recognize limitations of our cohort size, we sought to preliminarily explore interactions of possible neurocognitive predictors. Based on statistical significance from bivariate analyses combined with prior work to suspect association with neurocognitive outcome (i.e. time from radiation), we performed hierarchical analyses across each candidate gene and neurocognitive outcome. The first model incorporated candidate gene carrier status, hydrocephalus, seizures, tumor type and time from radiation, and the second model added CMB and WML volume at baseline.

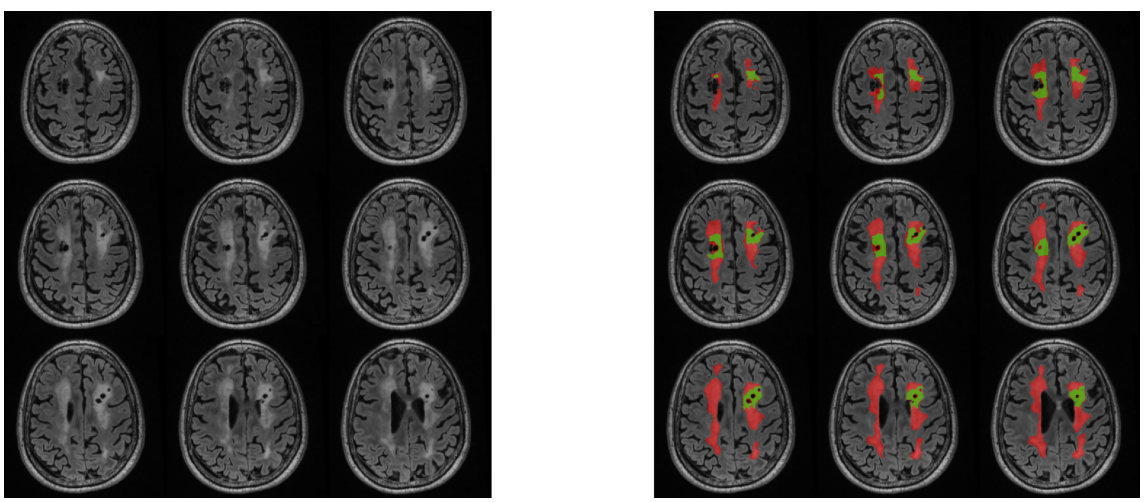

FIGURE 3 | Visual representation of WML analysis. Imaging inclusive of manual T2-FLAIR white matter lesion segmentations with RT-induced (red) and non-RT-induced (green) labeling. RT, radiation therapy.

TABLE 3 | Patient and imaging characteristics associated with domains of neurocognitive outcomes.

Neurocognitive Domain	Hydrocephalus n = 118	Seizures n = 118	Time from RT n =100	CMBs n= 28	WML volume n = 41
Executive functioning (GML)	(0.05)	0.0009	0.16	0.02	(0.05)
Verbal learning (ISL)	0.0002	0.003	0.03	0.03	0.06
Working memory (ONB)	0.0005	0.03	0.85	0.13	0.31
Attention (IDN)	0.02	0.01	0.89	0.13	0.49
Verbal memory (ISRL)	0.0001	0.002	0.39	0.10	0.77
Psychomotor functioning (DET)	(0.05)	0.19	0.30	0.01	0.51
Paired associate learning (CPAL)	0.15	0.76	0.77	0.36	0.19

Patient clinical characteristics, baseline CMB, and baseline WML volume (top row) associations with neurocognitive outcomes (left column) in bivariate analysis with inclusion of time from radiation. Cells contain statistically significant P-values (P < 0.05). Three comparisons reach borderline association indicated by parentheses (P = 0.05). Clinical characteristics analyzed and not displayed in table include age at diagnosis, chemotherapy exposure, and tumor location. RT, radiation therapy; CMBs, cerebral microbleeds; WML, white matter lesion.

Across the models without imaging findings, hydrocephalus or seizures at baseline continued to be the most prevalent characteristics associated with negative neurocognitive outcomes. No candidate gene demonstrated significant association once other characteristics were considered. Across these models, verbal learning, memory, working memory, executive function were consistently significantly impacted, most frequently in association with baseline hydrocephalus or seizures (P<0.05). In contrast, paired associate learning, psychomotor function, and attention were not significantly impacted across the variables tested.

DISCUSSION

As children complete therapy and enter long-term surveillance, identification of those at high-risk of neurocognitive injury based on genomics and/or radiographic imaging could lead to more aggressive and earlier neurocognitive and educational intervention. Our study sought to broaden understanding of predictors of neurocognitive outcomes in pediatric cancer survivors. Compared to adult populations, few studies exist that investigate genetic predictors for neurocognition in long-term survivors (17, 18, 41–43). *COMT* has been investigated in childhood brain tumor survivors, where Met/Val heterozygotes outperform Met/Met and Val/Val homozygotes (rs4680; Val158Met) (44). And, a common polymorphism in *BDNF*, Val66Met, shows valine homozygosity associates with higher IQs, processing speed, and memory in adults (17), but lacks demonstrated impact on neurocognitive function in adult CNS tumor survivors (20). In other adult studies, heterozygosity for the *KL* haplotype, KL-VS (Phe352Val and Cys370Ser), leads to improved cognition, executive function, and larger brain

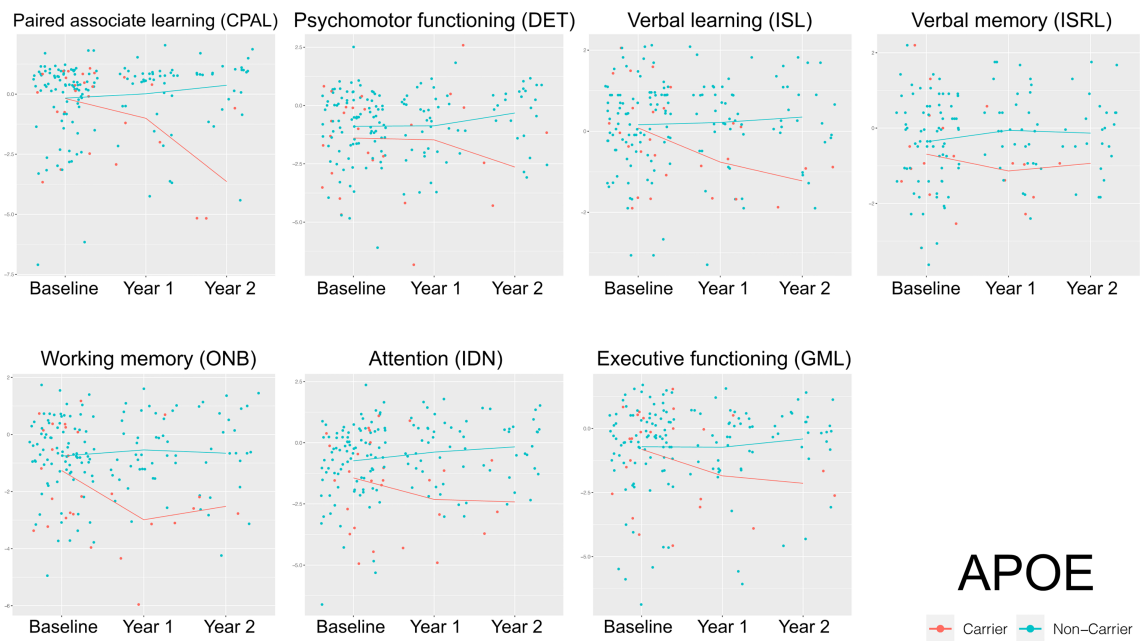

FIGURE 4 | Longitudinal impact of *APOE ϵ4* carrier status across each neurocognitive domain tested at baseline, Year 1, and Year 2 of enrollment. Trajectory of *APOE ϵ4* carrier versus non-carrier mean performance across each neurocognitive domain from initial neurocognitive testing (baseline) to timepoint 3 of neurocognitive testing (Year 2). Blue line=non-carrier, red line=carrier.

TABLE 4 | Prevalence of candidate gene carriers among high and low performers of neurocognitive assessments for timepoints 1 to 3 of testing.

Candidate gene (allele of interest)	High performers, n (% overall)	Low performers, n (% overall)	Odds ratio (95% CI)	*P*-Value
APOE	11 (6)	75 (43)	2.85 (1.46, 5.57)	0.002
BDNF	69 (13)	127 (24)	0.53 (0.36, 0.78)	0.001
COMT	79 (10)	241 (30)	1.31 (0.90, 1.90)	0.16
KIBRA	103 (10)	328 (33)	1.97 (1.28, 3.05)	0.002
KLOTHO	19 (6)	107 (34)	2.47 (1.45, 4.20)	0.0008

Candidate gene alleles of interest (left column) carrier status with associated prevalence among high (>1 SD from mean) and low performers (<1 SD from mean) across any neurocognitive domain at all timepoints of testing. Odds ratio with 95% confidence interval indicates increased (APOE, KIBRA, KLOTHO) versus decreased risk (BDNF) of being among low performers. Last column contains statistically significant P-value (P < 0.05).

volumes in aging adults and transgenic mouse models (18, 43, 45). Meanwhile, in healthy children, *APOE ϵ4* homozygotes have shown poorer executive function, memory, and attention, and a potential relationship to smaller hippocampal volumes (46). Further, *APOE ϵ4* has been linked to poorer neurocognition, memory, and executive function in adult CNS tumor patients (19, 47, 48) and was linked to tau-mediated neuroinflammation and neurodegeneration, independent of amyloid-ß deposition (19, 49).

Although no single gene was a reliable predictor across all tested neurocognitive domains in our cohort, *APOE ϵ4* carrier status most robustly associated with neurocognitive worsening over time. Other candidate genes, *COMT, BDNF, KIBRA* and *KLOTHO*, demonstrated mixed impact on neurocognitive outcomes and sometimes unexpected impact, such as the apparent protective effect of *BDNF* Val66Met. We recognize that we did not explore all possible SNP possibilities that may play a role across these genes and explored only SNPs of interest, which may inform future analyses of this cohort. Further, the cohort of patients with the SNPs of interest remained small overall and warrants study in a larger population. Additionally, we did not fully explore circulating peripheral protein levels, which may inform genotype: phenotype relationships. For example, high circulating levels of BDNF negatively correlate with neurocognitive function (50), while elevated klotho levels correlate with improved cognitive (43, 45). A next iteration of our work will be to correlate protein levels with genotype, which is currently under way for cerebrospinal and blood collections from our cohort.

We previously demonstrated that the presence of CMBs is associated with poor neurocognitive outcomes in pediatric CNS tumor survivors (28, 29). Of particular interest to the current work is that CMBs also associate with Alzheimer's disease (29, 51) and *APOE ϵ4* has been linked directly to CMBs in non-demented elderly patients, as well as neurovascular disease, decreased neuronal repair, and increased brain atrophy (52, 53). Given the role of *APOE ϵ4* across broad pathophysiologic processes, it is possible that radiation injury in the setting of *APOE ϵ4* exacerbates underlying predisposition to multifactorial neurocognitive injury. This would support our preliminary *APOE ϵ4* signal as a biomarker of neurocognitive outcomes in our patient cohort, which again was enriched with patients that previously received CNS radiation. Although our findings include a limited sample size, we feel they confirm that future exploration should explore volumetric analyses, white matter changes based on DTI sequences, and in larger patient numbers.

From a clinical standpoint, our work supported previous reports identifying hydrocephalus and seizures at baseline as predictors of worse cognitive function (2, 6, 8, 54–58). In our cohort, across both bivariate and multivariate analyses, hydrocephalus and seizures reliably correlated with worse performance across several domains, including executive function. Of interest was that age at diagnosis and time from radiation did not reliably correlate with worse outcomes as in Morrison et al. (28), while germ cell tumors seem to most commonly correlated with worse outcomes albeit in overall small numbers. The lack of impact from age and time could be in part due distinctions in analyses, including our use of age as a continuous variable compared to other analyses using age cut-offs as binary or categorical variables (56, 59–61). Additionally, from a longitudinal perspective, it is possible that because our patients were commonly already five or more years from diagnosis, we see a decreased impact on rate of change (i.e. patients entered the study at an already lower baseline performance). In contrast, the contribution of the germ cell diagnosis could be reflective of the radiation field in these tumors and overlap with critical structures like the hippocampus (12, 57–59), but the validity of finding related to germ cell tumors require verification in larger patient numbers.

The strengths of our study arise from the diversity of the patient population and long-term follow-up, typically spanning over five years. Our cohort included several different tumor types and tumor locations, as well as patients across a range of ages and demographics. By pooling of patients from four separate sites across California and Missouri, we capture a broad and diverse patient population from multiple socioeconomic backgrounds, races, and ethnicities. The longitudinal time points of follow-up also strengthen our findings, as neurocognitive injury in pediatric brain tumor survivors worsens over time and becomes more impacting as patients age (2, 62). Lastly, the consistency of the neurocognitive measurements and analyses among each gene solidified the comparison between genes, more so than if the genes had been evaluated in separate studies. In contrast, the main shortfalls of our study arise from non-standardized follow-up periods, late timepoints to initial neurocognitive testing, and overall small cohort size for multivariate analyses. First, there was a limited number of patients that had reliable follow-up and a cohort of patients with missing treatment details. This was both a result of not yet reaching the assigned time point of follow up, but also due to patients being lost to follow-up and in recent years and clinical

research restrictions imposed by the COVID-19 pandemic. Unfortunately, this contributed to missingness within the hierarchical analysis, inclusive of imaging variables, and thus limited these models. Future studies will need to expand the cohort size to accommodate the number of variables. Second, the follow-up intervals are not uniform throughout the cohort. This was driven by the neurocognitive tests being given as part of standard of care clinic visits and follow-up appointments being patient-dependent. We attempted to address this in our statistical analysis by including time from radiation as a continuous variable. Additionally, the patient population, although diverse, predominantly included patients with embryonal tumors reflecting the fact that medulloblastoma is the most common malignant pediatric CNS tumor. Further, we did not delineate dose of radiation or type of chemotherapy and only included these as binary variables in this initial review. Lastly, we recognize the nature of our investigation does not utilize reliable change indices as has been previously proposed for longitudinal neuropsychological testing (63) and the derivation of some normative values for the youngest patients within our cohort can be considered a shortcoming of this study, as this normalization may skew z-scores to higher performance than if compared to healthy populations alone. On the other hand, given that all testing was analyzed in the same manner across all genetic variants, we feel the reliability of the comparison across the genes remains intact and we would not expect the trend differences between the genes to be impacted by practiced learning or developmental changes within age groups over time.

In summary, our work shows that CMBs, WMLs, *APOE ϵ4* carrier status, hydrocephalus and/or seizures at baseline may serve as markers for long-term cognitive dysfunction in pediatric cancer survivors, especially in patients with CNS tumors previously treated with radiation. Work is actively underway to expand the preliminary findings in this report and to include additional retrospective and prospective genetic and imaging studies for this target population.

DATA AVAILABILITY STATEMENT

The raw data supporting the conclusions of this article will be made available by the authors, without undue reservation.

ETHICS STATEMENT

The studies involving human participants were reviewed and approved by UCSF Benioff Children's Hospital – San Francisco and Oakland sites (San Francisco, CA; Oakland, CA); Valley Children's Hospital (Madera, CA); and Washington University School of Medicine, St, Louis (St. Louis, MO).Written informed consent to participate in this study was provided by all participants and/or participants' legal guardian.

AUTHOR CONTRIBUTIONS

CK, SM, HF contributed to conception and design of the study. DS recruited and enrolled participants on to the study. WF, SS performed the statistical analysis with review done by CK. LB, JL, MM, AR, PN performed imaging data analysis. CK, SS wrote first draft of the manuscript. JL, MM, AR, PN, WF contributed to specific sections of the manuscript. CK, SS, WF created all figures and tables. All authors reviewed and provided feedback to manuscript first draft. CK, SS completed the manuscript final revision. All authors contributed to the article and approved the submitted version.

FUNDING

This work was supported by a donation from the LaRoche family (HF, SM).

ACKNOWLEDGMENTS

The authors would like to thank all participants for their time to contribute to the study. We would like to thank Quintara Biosciences for completing the SNP genotyping and assisting with the supplementary methods section as well as Adrian Schembri and Paul Maruff at CogState, Ltd. for assistance in organizing and interpreting scores from neurocognitive testing.

SUPPLEMENTARY MATERIAL

The Supplementary Material for this article can be found online at: https://www.frontiersin.org/articles/10.3389/fonc.2022.874317/full#supplementary-material

Supplementary Figure 1 | Longitudinal impact of *BDNF* carrier status across each neurocognitive domain tested at baseline, Year 1, and Year 2 of enrollment. Trajectory of *BDNF* carrier versus non-carrier performance across each neurocognitive domain from initial neurocognitive testing (baseline) to timepoint 3 of neurocognitive testing (Year 2). Blue line=non-carrier, red line=carrier.

Supplementary Figure 2 | Longitudinal impact of *COMT* carrier status across each neurocognitive domain tested at baseline, Year 1, and Year 2 of enrollment. Trajectory of *COMT* carrier versus non-carrier performance across each neurocognitive domain from initial neurocognitive testing (baseline) to timepoint 3 of neurocognitive testing (Year 2). Blue line=non-carrier, red line=carrier.

Supplementary Figure 3 | Longitudinal impact of *KIBRA* carrier status across each neurocognitive domain tested at baseline, Year 1, and Year 2 of enrollment. Trajectory of *KIBRA* carrier versus non-carrier performance across each neurocognitive domain from initial neurocognitive testing (baseline) to timepoint 3 of neurocognitive testing (Year 2). Blue line=non-carrier, red line=carrier.

Supplementary Figure 4 | Longitudinal impact of *KL-VS* carrier status across each neurocognitive domain tested at baseline, Year 1, and Year 2 of enrollment. Trajectory of *KL-VS* carrier versus non-carrier performance across each neurocognitive domain from initial neurocognitive testing (baseline) to timepoint 3 of neurocognitive testing (Year 2). Blue line=non-carrier, red line=carrier.

Supplementary Table 1 | Description of candidate gene SNPs of interest and anticipated impact on neurocognitive outcome. Candidate gene alleles sequenced and expected effects on neurocognitive outcomes

Supplementary Table 2 | Prevalence of candidate gene SNPs of interest across each investigated subcohort. Candidate gene allele frequencies by cohort across each row.

REFERENCES

1. Macartney G, Harrison MB, Vandenkerkhof E, Stacey D, Mccarthy P. Quality of Life and Symptoms in Pediatric Brain Tumor Survivors: A Systematic Review. *J Pediatr Oncol Nurs* (2014) 31:65–77. doi: 10.1177/1043454213520191
2. Roddy E, Mueller S. Late Effects of Treatment of Pediatric Central Nervous System Tumors. *J Child Neurol* (2016) 31:237–54. doi: 10.1177/0883073815587944
3. Kiehna EN, Mulhern RK, Li C, Xiong X, Merchant TE. Changes in Attentional Performance of Children and Young Adults With Localized Primary Brain Tumors After Conformal Radiation Therapy. *J Clin Oncol* (2006) 24:5283–90. doi: 10.1200/JCO.2005.03.8547
4. Pietila S, Korpela R, Lenko HL, Haapasalo H, Alalantela R, Nieminen P, et al. Neurological Outcome of Childhood Brain Tumor Survivors. *J Neurooncol* (2012) 108:153–61. doi: 10.1007/s11060-012-0816-5
5. Sato I, Higuchi A, Yanagisawa T, Murayama S, Kumabe T, Sugiyama K, et al. Impact of Late Effects on Health-Related Quality of Life in Survivors of Pediatric Brain Tumors: Motility Disturbance of Limb(s), Seizure, Ocular/Visual Impairment, Endocrine Abnormality, and Higher Brain Dysfunction. *Cancer Nurs* (2014) 37:E1–E14. doi: 10.1097/NCC.0000000000000110
6. Robinson KE, Kuttesch JF, Champion JE, Andreotti CF, Hipp DW, Bettis A, et al. A Quantitative Meta-Analysis of Neurocognitive Sequelae in Survivors of Pediatric Brain Tumors. *Pediatr Blood Cancer* (2010) 55:525–31. doi: 10.1002/pbc.22568
7. Lafay-Cousin L, Fay-Mcclymont T, Johnston D, Fryer C, Scheinemann K, Fleming A, et al. Neurocognitive Evaluation of Long Term Survivors of Atypical Teratoid Rhabdoid Tumors (ATRT): The Canadian Registry Experience. *Pediatr Blood Cancer* (2015) 62:1265–9. doi: 10.1002/pbc.25441
8. Lassaletta A, Bouffet E, Mabbott D, Kulkarni AV. Functional and Neuropsychological Late Outcomes in Posterior Fossa Tumors in Children. *Childs Nerv Syst* (2015) 31:1877–90. doi: 10.1007/s00381-015-2829-9
9. Liu F, Scantlebury N, Tabori U, Bouffet E, Laughlin S, Strother D, et al. White Matter Compromise Predicts Poor Intellectual Outcome in Survivors of Pediatric Low-Grade Glioma. *Neuro Oncol* (2015) 17:604–13. doi: 10.1093/neuonc/nou306
10. Fay-Mcclymont TB, Ploetz DM, Mabbott D, Walsh K, Smith A, Chi SN, et al. Long-Term Neuropsychological Follow-Up of Young Children With Medulloblastoma Treated With Sequential High-Dose Chemotherapy and Irradiation Sparing Approach. *J Neurooncol* (2017) 133:119–28. doi: 10.1007/s11060-017-2409-9
11. Mulhern RK, White HA, Glass JO, Kun LE, Leigh L, Thompson SJ, et al. Attentional Functioning and White Matter Integrity Among Survivors of Malignant Brain Tumors of Childhood. *J Int Neuropsychol Soc* (2004) 10:180–9. doi: 10.1017/S135561770410204X
12. Nagel BJ, Delis DC, Palmer SL, Reeves C, Gajjar A, Mulhern RK. Early Patterns of Verbal Memory Impairment in Children Treated for Medulloblastoma. *Neuropsychology* (2006) 20:105–12. doi: 10.1037/0894-4105.20.1.105
13. Beebe DW, Ris MD, Armstrong FD, Fontanesi J, Mulhern R, Holmes E, et al. Cognitive and Adaptive Outcome in Low-Grade Pediatric Cerebellar Astrocytomas: Evidence of Diminished Cognitive and Adaptive Functioning in National Collaborative Research Studies (CCG 9891/POG 9130). *J Clin Oncol* (2005) 23:5198–204. doi: 10.1200/JCO.2005.06.117
14. Silber JH, Radcliffe J, Peckham V, Perilongo G, Kishnani P, Fridman M, et al. Whole-Brain Irradiation and Decline in Intelligence: The Influence of Dose and Age on IQ Score. *J Clin Oncol* (1992) 10:1390–6. doi: 10.1200/JCO.1992.10.9.1390
15. Reimers TS, Ehrenfels S, Mortensen EL, Schmiegelow M, Sonderkaer S, Carstensen H, et al. Cognitive Deficits in Long-Term Survivors of Childhood Brain Tumors: Identification of Predictive Factors. *Med Pediatr Oncol* (2003) 40:26–34. doi: 10.1002/mpo.10211
16. Chow EJ, Chen Y, Hudson MM, Feijen E, Kremer LC, Border WL, et al. Prediction of Ischemic Heart Disease and Stroke in Survivors of Childhood Cancer. *J Clin Oncol* (2018) 36:44–52. doi: 10.1200/JCO.2017.74.8673
17. Papenberg G, Salami A, Persson J, Lindenberger U, Backman L. Genetics and Functional Imaging: Effects of APOE, BDNF, COMT, and KIBRA in Aging. *Neuropsychol Rev* (2015) 25:47–62. doi: 10.1007/s11065-015-9279-8
18. Yokoyama JS, Sturm VE, Bonham LW, Klein E, Arfanakis K, Yu L, et al. Variation in Longevity Gene KLOTHO is Associated With Greater Cortical Volumes. *Ann Clin Transl Neurol* (2015) 2:215–30. doi: 10.1002/acn3.161
19. Correa DD, Kryza-Lacombe M, Zhou X, Baser RE, Beattie BJ, Beiene Z, et al. A Pilot Study of Neuropsychological Functions, APOE and Amyloid Imaging in Patients With Gliomas. *J Neurooncol* (2018) 136:613–22. doi: 10.1007/s11060-017-2692-5
20. Correa DD, Satagopan J, Cheung K, Arora AK, Kryza-Lacombe M, Xu Y, et al. COMT, BDNF, and DTNBP1 Polymorphisms and Cognitive Functions in Patients With Brain Tumors. *Neuro Oncol* (2016) 18:1425–33. doi: 10.1093/neuonc/now057
21. Correa DD, Satagopan J, Martin A, Braun E, Kryza-Lacombe M, Cheung K, et al. Genetic Variants and Cognitive Functions in Patients With Brain Tumors. *Neuro Oncol* (2019) 21:1297–309. doi: 10.1093/neuonc/noz094
22. Lupo JM, Chuang CF, Chang SM, Barani IJ, Jimenez B, Hess CP, et al. 7-Tesla Susceptibility-Weighted Imaging to Assess the Effects of Radiotherapy on Normal-Appearing Brain in Patients With Glioma. *Int J Radiat Oncol Biol Phys* (2012) 82:e493–500. doi: 10.1016/j.ijrobp.2011.05.046
23. Lupo JM, Molinaro AM, Essock-Burns E, Butowski N, Chang SM, Cha S, et al. The Effects of Anti-Angiogenic Therapy on the Formation of Radiation-Induced Microbleeds in Normal Brain Tissue of Patients With Glioma. *Neuro Oncol* (2016) 18:87–95. doi: 10.1093/neuonc/nov128
24. Passos J, Nzwalo H, Valente M, Marques J, Azevedo A, Netto E, et al. Microbleeds and Cavernomas After Radiotherapy for Paediatric Primary Brain Tumours. *J Neurol Sci* (2017) 372:413–6. doi: 10.1016/j.jns.2016.11.005
25. Wahl M, Anwar M, Hess CP, Chang SM, Lupo JM. Relationship Between Radiation Dose and Microbleed Formation in Patients With Malignant Glioma. *Radiat Oncol* (2017) 12:126. doi: 10.1186/s13014-017-0861-5
26. Klos J, Van Laar PJ, Sinnige PF, Enting RH, Kramer MCA, van der Weide HL, et al. Quantifying Effects of Radiotherapy-Induced Microvascular Injury; Review of Established and Emerging Brain MRI Techniques. *Radiother Oncol* (2019) 140:41–53. doi: 10.1016/j.radonc.2019.05.020
27. Morrison MA, Hess CP, Clarke JL, Butowski N, Chang SM, Molinaro AM, et al. Risk Factors of Radiotherapy-Induced Cerebral Microbleeds and Serial Analysis of Their Size Compared With White Matter Changes: A 7t MRI Study in 113 Adult Patients With Brain Tumors. *J Magn Reson Imaging* (2019) 50:868–77. doi: 10.1002/jmri.26651
28. Morrison MA, Mueller S, Felton E, Jakary A, Stoller S, Avadiappan S, et al. Rate of Radiation-Induced Microbleed Formation on 7T MRI Relates to Cognitive Impairment in Young Patients Treated With Radiation Therapy for a Brain Tumor. *Radiother Oncol* (2021) 154:145–53. doi: 10.1016/j.radonc.2020.09.028
29. Roddy E, Sear K, Felton E, Tamrazi B, Gauvain K, Torkildson J, et al. Presence of Cerebral Microbleeds is Associated With Worse Executive Function in Pediatric Brain Tumor Survivors. *Neuro Oncol* (2016) 18:1548–58. doi: 10.1093/neuonc/now082.02
30. Partap S, Russo S, Esfahani B, Yeom K, Mazewski C, Embry L, et al. A Review of Chronic Leukoencephalopathy Among Survivors of Childhood Cancer. *Pediatr Neurol* (2019) 101:2–10. doi: 10.1016/j.pediatrneurol.2019.03.006
31. Fouladi M, Chintagumpala M, Laningham FH, Ashley D, Kellie SJ, Langston JW, et al. White Matter Lesions Detected by Magnetic Resonance Imaging After Radiotherapy and High-Dose Chemotherapy in Children With Medulloblastoma or Primitive Neuroectodermal Tumor. *J Clin Oncol* (2004) 22:4551–60. doi: 10.1200/JCO.2004.03.058
32. Aleksonis HA, Krishnamurthy LC, King TZ. White Matter Hyperintensity Volumes are Related to Processing Speed in Long-Term Survivors of Childhood Cerebellar Tumors. *J Neurooncol* (2021) 154:63–72. doi: 10.1007/s11060-021-03799-3

33. Nordstrom M, Felton E, Sear K, Tamrazi B, Torkildson J, Gauvain K, et al. Large Vessel Arteriopathy After Cranial Radiation Therapy in Pediatric Brain Tumor Survivors. *J Child Neurol* (2018) 33:359–66. doi: 10.1177/0883073818756729
34. Bangirana P, Sikorskii A, Giordani B, Nakasujja N, Boivin MJ. Validation of the CogState Battery for Rapid Neurocognitive Assessment in Ugandan School Age Children. *Child Adolesc Psychiatry Ment Health* (2015) 9:38. doi: 10.1186/s13034-015-0063-6
35. Cromer JA, Harel BT, Yu K, Valadka JS, Brunwin JW, Crawford CD, et al. Comparison of Cognitive Performance on the Cogstate Brief Battery When Taken In-Clinic, In-Group, and Unsupervised. *Clin Neuropsychol* (2015) 29:542–58. doi: 10.1080/13854046.2015.1054437
36. Heitzer AM, Ashford JM, Harel BT, Schembri A, Swain MA, Wallace J, et al. Computerized Assessment of Cognitive Impairment Among Children Undergoing Radiation Therapy for Medulloblastoma. *J Neurooncol* (2019) 141:403–11. doi: 10.1007/s11060-018-03046-2
37. Morrison MA, Payabvash S, Chen Y, Avadiappan S, Shah M, Zou X, et al. A User-Guided Tool for Semi-Automated Cerebral Microbleed Detection and Volume Segmentation: Evaluating Vascular Injury and Data Labelling for Machine Learning. *NeuroImage: Clin* (2018) 20:498–505. doi: 10.1016/j.nicl.2018.08.002
38. Bian W, Hess CP, Chang SM, Nelson SJ, Lupo JM. Computer-Aided Detection of Radiation-Induced Cerebral Microbleeds on Susceptibility-Weighted MR Images. *NeuroImage Clin* (2013) 2:282–90. doi: 10.1016/j.nicl.2013.01.012
39. Duong MT, Rudie JD, Wang J, Xie L, Mohan S, Gee JC, et al. Convolutional Neural Network for Automated FLAIR Lesion Segmentation on Clinical Brain MR Imaging. *AJNR Am J Neuroradiol* (2019) 40:1282–90. doi: 10.3174/ajnr.A6138
40. Rauschecker AM, Gleason TJ, Nedelec P, Duong MT, Weiss DA, Calabrese E, et al. Interinstitutional Portability of a Deep Learning Brain MRI Lesion Segmentation Algorithm. *Radiol Artif Intell* (2021) 4. doi: 10.1148/ryai.2021200152
41. Arking DE, Krebsova A, Macek MSR, Macek MJr., Arking A, Mian IS, et al. Association of Human Aging With a Functional Variant of Klotho. *Proc Natl Acad Sci USA* (2002) 99:856–61. doi: 10.1073/pnas.022484299
42. Duce JA, Podvin S, Hollander W, Kipling D, Rosene DL, Abraham CR. Gene Profile Analysis Implicates Klotho as an Important Contributor to Aging Changes in Brain White Matter of the Rhesus Monkey. *Glia* (2008) 56:106–17. doi: 10.1002/glia.20593
43. Dubal DB, Yokoyama JS, Zhu L, Broestl L, Worden K, Wang D, et al. Life Extension Factor Klotho Enhances Cognition. *Cell Rep* (2014) 7:1065–76. doi: 10.1016/j.celrep.2014.03.076
44. Howarth RA, Adamson AM, Ashford JM, Merchant TE, Ogg RJ, Schulenberg SE, et al. Investigating the Relationship Between COMT Polymorphisms and Working Memory Performance Among Childhood Brain Tumor Survivors. *Pediatr Blood Cancer* (2014) 61:40–5. doi: 10.1002/pbc.24649
45. Dubal DB, Zhu L, Sanchez PE, Worden K, Broestl L, Johnson E, et al. Life Extension Factor Klotho Prevents Mortality and Enhances Cognition in hAPP Transgenic Mice. *J Neurosci* (2015) 35:2358–71. doi: 10.1523/JNEUROSCI.5791-12.2015
46. Chang L, Douet V, Bloss C, Lee K, Pritchett A, Jernigan TL, et al. Gray Matter Maturation and Cognition in Children With Different APOE Epsilon Genotypes. *Neurology* (2016) 87:585–94. doi: 10.1212/WNL.0000000000002939
47. Correa DD, Deangelis LM, Shi W, Thaler HT, Lin M, Abrey LE. Cognitive Functions in Low-Grade Gliomas: Disease and Treatment Effects. *J Neurooncol* (2007) 81:175–84. doi: 10.1007/s11060-006-9212-3
48. Correa DD, Satagopan J, Baser RE, Cheung K, Richards E, Lin M, et al. APOE Polymorphisms and Cognitive Functions in Patients With Brain Tumors. *Neurology* (2014) 83:320–7. doi: 10.1212/WNL.0000000000000617
49. Arking DE, Becker DM, Yanek LR, Fallin D, Judge DP, Moy TF, et al. KLOTHO Allele Status and the Risk of Early-Onset Occult Coronary Artery Disease. *Am J Hum Genet* (2003) 72:1154–61. doi: 10.1086/375035
50. Yeom CW, Park YJ, Choi SW, Bhang SY. Association of Peripheral BDNF Level With Cognition, Attention and Behavior in Preschool Children. *Child Adolesc Psychiatry Ment Health* (2016) 10:10. doi: 10.1186/s13034-016-0097-4
51. De Reuck J, Deramecourt V, Cordonnier C, Leys D, Pasquier F, Maurage CA. Prevalence of Small Cerebral Bleeds in Patients With a Neurodegenerative Dementia: A Neuropathological Study. *J Neurol Sci* (2011) 300:63–6. doi: 10.1016/j.jns.2010.09.031
52. Liu CC, Liu CC, Kanekiyo T, Xu H, Bu G. Apolipoprotein E and Alzheimer Disease: Risk, Mechanisms and Therapy. *Nat Rev Neurol* (2013) 9:106–18. doi: 10.1038/nrneurol.2012.263
53. Graff-Radford J, Simino J, Kantarci K, Mosley TH Jr, Griswold ME, Windham BG, et al. Neuroimaging Correlates of Cerebral Microbleeds: The ARIC Study (Atherosclerosis Risk in Communities). *Stroke* (2017) 48:2964–72. doi: 10.1161/STROKEAHA.117.018336
54. Nathan PC, Patel SK, Dilley K, Goldsby R, Harvey J, Jacobsen C, et al. Guidelines for Identification of, Advocacy for, and Intervention in Neurocognitive Problems in Survivors of Childhood Cancer: A Report From the Children's Oncology Group. *Arch Pediatr Adolesc Med* (2007) 161:798–806. doi: 10.1001/archpedi.161.8.798
55. Ellenberg L, Liu Q, Gioia G, Yasui Y, Packer RJ, Mertens A, et al. Neurocognitive Status in Long-Term Survivors of Childhood CNS Malignancies: A Report From the Childhood Cancer Survivor Study. *Neuropsychology* (2009) 23:705–17. doi: 10.1037/a0016674
56. Duffner PK. Risk Factors for Cognitive Decline in Children Treated for Brain Tumors. *Eur J Paediatr Neurol* (2010) 14:106–15. doi: 10.1016/j.ejpn.2009.10.005
57. Kline CN, Mueller S. Neurocognitive Outcomes in Children With Brain Tumors. *Semin Neurol* (2020) 40:315–21. doi: 10.1055/s-0040-1708867
58. Tsang DS, Kim L, Liu ZA, Janzen L, Khandwala M, Bouffet E, et al. Intellectual Changes After Radiation for Children With Brain Tumors: Which Brain Structures are Most Important? *Neuro Oncol* (2021) 23:487–97. doi: 10.1093/neuonc/noaa217
59. Greenberger BA, Pulsifer MB, Ebb DH, Macdonald SM, Jones RM, Butler WE, et al. Clinical Outcomes and Late Endocrine, Neurocognitive, and Visual Profiles of Proton Radiation for Pediatric Low-Grade Gliomas. *Int J Radiat Oncol Biol Phys* (2014) 89:1060–8. doi: 10.1016/j.ijrobp.2014.04.053
60. Pulsifer MB, Sethi RV, Kuhlthau KA, Macdonald SM, Tarbell NJ, Yock TI. Early Cognitive Outcomes Following Proton Radiation in Pediatric Patients With Brain and Central Nervous System Tumors. *Int J Radiat Oncol Biol Phys* (2015) 93:400–7. doi: 10.1016/j.ijrobp.2015.06.012
61. Michalski JM, Janss AJ, Vezina LG, Smith KS, Billups CA, Burger PC, et al. Children's Oncology Group Phase III Trial of Reduced-Dose and Reduced-Volume Radiotherapy With Chemotherapy for Newly Diagnosed Average-Risk Medulloblastoma. *J Clin Oncol* (2021) 39:2685–97. doi: 10.1200/JCO.20.02730
62. Mulhern RK, Merchant TE, Gajjar A, Reddick WE, Kun LE. Late Neurocognitive Sequelae in Survivors of Brain Tumours in Childhood. *Lancet Oncol* (2004) 5:399–408. doi: 10.1016/S1470-2045(04)01507-4
63. Gavett BE, Ashendorf L, Gurnani AS. Reliable Change on Neuropsychological Tests in the Uniform Data Set. *J Int Neuropsychol Soc* (2015) 21:558–67. doi: 10.1017/S1355617715000582

Conflict of Interest: The authors declare that the research was conducted in the absence of any commercial or financial relationships that could be construed as a potential conflict of interest.

Publisher's Note: All claims expressed in this article are solely those of the authors and do not necessarily represent those of their affiliated organizations, or those of the publisher, the editors and the reviewers. Any product that may be evaluated in this article, or claim that may be made by its manufacturer, is not guaranteed or endorsed by the publisher.

Frontiers in Oncology

Advances knowledge of carcinogenesis and tumor progression for better treatment and management

The third most-cited oncology journal, which highlights research in carcinogenesis and tumor progression, bridging the gap between basic research and applications to imrpove diagnosis, therapeutics and management strategies.

Discover the latest Research Topics

See more →

Frontiers

Avenue du Tribunal-Fédéral 34
1005 Lausanne, Switzerland
frontiersin.org

Contact us

+41 (0)21 510 17 00
frontiersin.org/about/contact